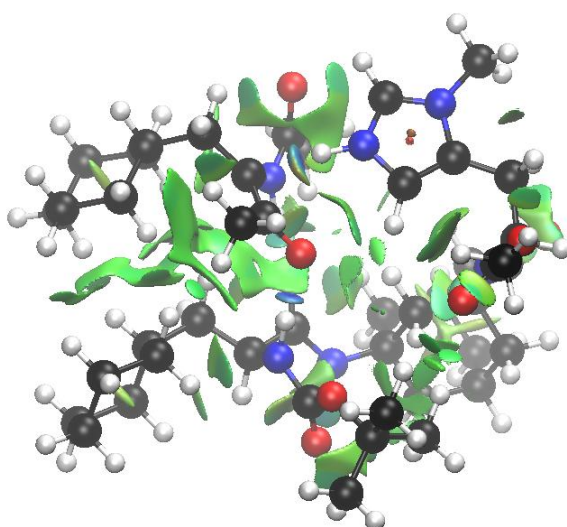


New Frontiers in Peptide Catalysis

Multicatalysis, Challenging Reactions, and the Importance of Dispersion Interactions



Dissertation zur Erlangung des Doktorgrades der
Naturwissenschaftlichen Fachbereiche
(Fachbereich 08 – Biologie und Chemie)
der Justus-Liebig-Universität Gießen

vorgelegt von

Raffael Christoph Wende

aus Aßlar

Gießen 2016

Die vorliegende Arbeit wurde in der Zeit von März 2011 bis Juni 2016 am Institut für Organische Chemie der Justus-Liebig-Universität Gießen unter Anleitung von Herrn Prof. Dr. Peter R. Schreiner, Ph.D. angefertigt.

Mein aufrichtiger Dank gebührt meinem Doktorvater, Herrn Prof. Dr. Peter R. Schreiner, für die Vergabe dieses interessanten und aktuellen Forschungsthemas, die gewährte Freiheit bei dessen Bearbeitung, sowie die vielen anregenden und lehrreichen Diskussionen.

für Lena, Nele, Carlotta und Janne

„So eine Arbeit wird eigentlich nie fertig, man muss sie für fertig erklären, wenn man nach Zeit und Umständen das möglichste getan hat.“

– Johann Wolfgang von Goethe –

Eidesstattlich Erklärung nach §17 der Promotionsordnung

„Ich erkläre: Ich habe die vorgelegte Dissertation selbständig und ohne unerlaubte fremde Hilfe und nur mit den Hilfen angefertigt, die ich in der Dissertation angegeben habe. Alle Textstellen, die wörtlich oder sinngemäß aus veröffentlichten Schriften entnommen sind, und alle Angaben, die auf mündlichen Auskünften beruhen, sind als solche kenntlich gemacht. Bei den von mir durchgeführten und in der Dissertation erwähnten Untersuchungen habe ich die Grundsätze guter wissenschaftlicher Praxis, wie sie in der „Satzung der Justus-Liebig-Universität Giessen zur Sicherung guter wissenschaftlicher Praxis“ niedergelegt sind, eingehalten.“

Ort, Datum

Unterschrift

Table of Contents

Publications in Peer Reviewed Journals	1
Motivation and Research Objectives	3
Summary	5
Zusammenfassung	9
Chapter I – Evolution of Asymmetric Organocatalysis: Multi- and Retrocatalysis ...	13
1. Introduction	17
2. Multicatalysis – A Survey	19
2.1 <i>Taxonomy of One-Pot Reactions Using Multiple Catalysts</i>	19
2.2 <i>Reaction Efficiency and Sustainability Aspects of Multicatalysis</i>	22
3. Secondary Amine Catalysts	25
3.1 <i>The Beginnings of Organomulticatalysis – Merging Iminium and Enamine Catalysis</i>	25
3.2 <i>Combinations of Secondary Amine Catalysts with Brønsted Acids and Bases</i>	37
3.3 <i>Miscellaneous Combinations with Secondary Amines</i>	43
4. N-Heterocyclic Carbene Catalysts	47
4.1 <i>Combinations with Secondary Amine Catalysts</i>	47
4.2 <i>Miscellaneous Combinations with N-Heterocyclic Carbenes</i>	59
5. Thiourea Catalysts	62
5.1 <i>Combinations of Thioureas with Secondary Amine Catalysts</i>	62
5.2 <i>Combination of Thiourea Catalysts with Brønsted Acids and Bases</i>	65
6. Non-Natural Oligopeptides for Acyl Transfer Reactions	70
7. Multicatalyst Approaches	72
7.1 <i>Miscellaneous Examples of Oligopeptide Catalyzed Reactions</i>	74
8. Conclusions	76

Chapter II – Lipophilic Oligopeptides for Chemo- and Enantioselective

Acyl Transfer Reactions onto Alcohols	85
1. Introduction	86
2. Results and Discussion	89
2.1 Catalyst Screening Using the Acylative KR of <i>trans</i> -Cyclohexane-1,2-diol as Test Reaction	89
2.2 Substrate Scope for Peptide 12b-Catalyzed Acylations	94
2.3 Chemoselectivity of 12b	97
2.4 Mechanistic Model for the Enantioselective Acylation with 12b	99
2.5 Alternative Electrophiles in Group Transfer Reactions Catalyzed via Peptide 12b	101
3. Conclusion and Outlook	107
4. Experimental Section	108
4.1 Availability and Characterization of the Catalysts	108
4.2 Chiral-GC Properties and Characterization Data of the Alcohols	114
4.3 Procedure for the Competitive Catalytic Run with Alcohols 1, 41, 42, and 43	124
4.4 Description of the Preparative Kinetic Resolution Experiment of (\pm)-1 with Boc ₂ O	126
4.5 Sulfonylation of <i>rac</i> -1 Using 12b as Catalyst	127
4.6 Sulfonylation Test Reactions	127
4.7 Competition Experiment with Different Electrophiles	129
5. References	130

Chapter III – En Route to Multicatalysis: Kinetic Resolution of <i>trans</i>-Cyclo- alkane-1,2-diols via Oxidative Esterification	137
Chapter IV – Functionality, Effectiveness, and Mechanistic Evaluation of a Multicatalyst-Promoted Reaction Sequence by Electrospray Ionization Mass Spectrometry	147
1. Introduction	148
2. Results and Discussion	149
3. Conclusion	154
4. Experimental Section	154
5. References	156
Chapter V – Towards the Multicatalytic Synthesis of 2-Deoxygalactosides: Peptide-Catalyzed Regioselective Acetylation	161
1. Introduction	162
2. Results and Discussion	164
3. Conclusions and Outlook	177
4. Experimental Section	178
4.1 <i>Synthesis of Mono- and Diacetylated Carbohydrate Derivatives for Elucidation of Product Distribution and Conversion</i>	179
4.2 <i>Availability of Catalysts</i>	182
4.3 <i>Description of Catalytic Experiments</i>	189
4.4 <i>Computational Details</i>	190
4.5 <i>NMR Spectra</i>	197
5. References	204

Chapter VI – The Enantioselective Dakin–West Reaction	207
1. The Enantioselective Dakin–West Reaction	210
1.1 References	216
2. Supporting Information	218
2.1 General Remarks	218
2.2 Starting Materials and Reaction Intermediates	219
2.2.1 Synthesis of starting materials	219
2.2.2 Synthesis of possible reaction intermediates	225
2.3 Synthesis of Racemic Products	228
2.4 Availability of Catalysts	240
2.5 Catalytic Experiments	254
2.5.1 Reaction optimization	254
2.5.2 Catalyst screening	257
2.5.3 Preparative enantioselective Dakin–West reaction	259
2.6 Mechanistic Investigations	262
2.6.1 Computational details	262
2.6.2 Additionally performed reactions towards the investigation of the enantioselective decarboxylative protonation	266
2.7 NMR Spectra	269
2.8 References	307
Chapter VII – Unpublished Results	309
1. The Importance of Side-Chain Interactions	311
2. Binding of the Transient Enolate	314
3. Synthesis of Protease Inhibitor Warheads	318
4. Enantioselective Decarboxylative Protonation and the Acetylation of <i>In Situ</i> Formed Azlactones	320
5. Conclusions and Outlook	324
6. Experimental Section	326
6.1 General Remarks	326

6.2	<i>Availability of Starting Materials</i>	327
6.3	<i>Synthesis of Racemic Products</i>	332
6.4	<i>Opening of C-Acetylated Azlactones with Different Nucleophiles</i>	337
6.5	<i>Availability of Catalysts</i>	342
6.6	<i>Procedures for Catalytic Experiments</i>	343
6.7	<i>Energies and Cartesian Coordinates for Computed Structures</i>	344
6.8	<i>NMR Spectra</i>	355
7.	References	371
Acknowledgement		373

Publications in Peer Reviewed Journals

Raffael C. Wende, Alexander Seitz, Dominik Niedek, Sören M. M. Schuler, Christine Hofmann, Jonathan Becker, Peter R. Schreiner, The Enantioselective Dakin–West Reaction, *Angew. Chem. Int. Ed.* **2016**, *55*, 2719–2723; *Angew. Chem.* **2016**, *128*, 2769–2773.

M. Wasim Alachraf, Raffael C. Wende, Sören M. M. Schuler, Peter R. Schreiner, Wolfgang Schrader, Functionality, Effectiveness, and Mechanistic Evaluation of a Multicatalyst-Promoted Reaction Sequence by Electrospray Ionization Mass Spectrometry, *Chem.–Eur. J.* **2015**, *21*, 16203–16208.

Christine Hofmann, Sören M. M. Schuler, Raffael C. Wende, Peter R. Schreiner, En Route to Multicatalysis: Kinetic Resolution of *trans*-Cycloalkane-1,2-diols *via* Oxidative Esterification, *Chem. Commun.* **2014**, *50*, 1221–1223.

Christian E. Müller, Daniela Zell, Radim Hrdina, Raffael C. Wende, Lukas Wanka, Sören M. M. Schuler, P. R. Schreiner, Lipophilic Oligopeptides for Chemo- and Enantioselective Acyl Transfer Reactions onto Alcohols, *J. Org. Chem.* **2013**, *78*, 8465–8484.

Raffael C. Wende, Peter R. Schreiner, Evolution of Asymmetric Organocatalysis: Multi- and Retrocatalysis, *Green Chem.* **2012**, *14*, 1821–1849.

Radim Hrdina, Christian E. Müller, Raffael C. Wende, Lukas Wanka, Peter R. Schreiner, Enantiomerically Enriched *trans*-Diols from Alkenes in One Pot: A Multicatalyst Approach, *Chem. Commun.* **2012**, *48*, 2498–2500.

Christian E. Müller, Radim Hrdina, Raffael C. Wende, Peter R. Schreiner, A Multicatalyst System for the One-Pot Desymmetrization/Oxidation of *meso*-1,2-Alkane Diols, *Chem.–Eur. J.* **2011**, *17*, 6309–6314.

Radim Hrdina, Christian E. Müller, Raffael C. Wende, Katharina M. Lippert, Mario Benassi, Bernhard Spengler, Peter R. Schreiner, Silicon–(Thio)urea Lewis Acid Catalysis, *J. Am. Chem. Soc.* **2011**, *133*, 7624–7627.

Christian M. Kleiner, Luise Horst, Christian Würtele, Raffael Wende, Peter R. Schreiner, Isolation of the key intermediates in the catalyst-free conversion of oxiranes to thiiranes in water at ambient temperature, *Org. Biomol. Chem.* **2009**, *7*, 1397–1403.

Motivation and Research Objectives

Nature's biosynthetic machinery undeniably is a paragon in terms of efficiency, reactivity as well as selectivity and consequently has fascinated and challenged alike generations of chemists. This extraordinary effectiveness often relies on the direct coupling of concurrent reaction steps, thus allowing the assembly of complex molecules from readily available starting materials. Mammalian fatty acid synthase as a representative model is an outstanding example for this assembly line approach (Figure 1). This multienzyme complex catalyzes all necessary reaction steps of fatty acid biosynthesis consisting of a transesterification and a number of consecutive reduction, elimination, and condensation steps (Figure 1; see: T. Maier, S. Jenni, N. Ban, *Science* **2006**, *311*, 1258–1262 and M. Leibundgut, T. Maier, S. Jenni, N. Ban, *Curr. Opin. Struct. Biol.* **2008**, *18*, 714–725).

The development and application of novel, efficacious catalysts to achieve the performance of enzymes is an unambiguously important issue at the forefront of synthetic organic chemistry. Consequently, the application of small organic molecules for the acceleration of chemical reactions, *i.e.*, organocatalysis, was a milestone in the field of catalysis. In the early days of asymmetric organocatalysis, chemists delved into the *chiral pool* making use of, *e.g.*, simple amino acids as chiral catalysts. Various different catalyst types were subsequently developed and laid the foundation for this nowadays vibrant area of research. Later, the abovementioned principles of biosynthesis were also applied to catalysis, enabling the synthesis of complex molecular frameworks from simple starting materials (see Chapter I). However, the possibilities of using distinct organocatalysts for one-pot reactions still are limited, due to compatibility issues, the proper reaction sequence, or regio- and chemoselectivity, amongst other difficulties, that become apparent with an increasing number of catalyzed steps. Therefore, most examples rely on the combination of only two catalysts.

The application of oligopeptides as catalysts in order to mimic the performance of enzymes is a particularly elegant approach to asymmetric chemical synthesis. Arguably, such catalysts can be seen as “minimal” artificial enzymes as they often rely on comparable activation modes, reaction types as well as catalyst–substrate interactions (*e.g.*, hydrogen bonding, electrostatic or dispersion interactions). The diversity of available amino acids (natural and synthetic), well-established coupling techniques, and the ease of modification makes peptides ideally suited for the design of potent catalysts. Moreover, the possible incorporation of orthogonal (*i.e.*, independent) catalytic moieties into a single peptide backbone may not only overcome some of the potential problems discussed above, but even lead to enhanced reactivities and selectivities. Indeed, such *multicatalysts* have now been realized.

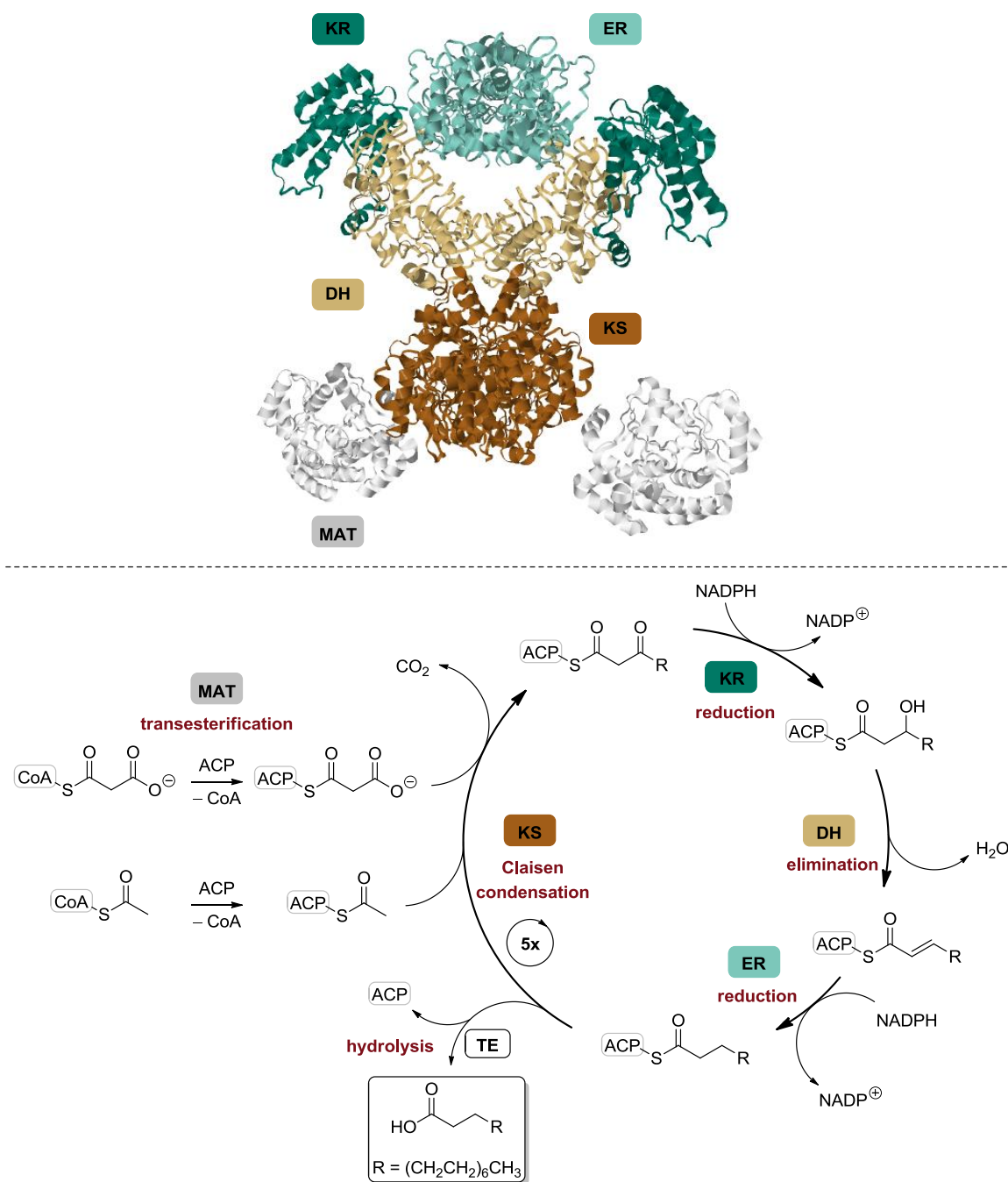


Figure 1. Top: Crystal structure of mammalian fatty acid synthase as ribbon representation; the structure was obtained from the RCSB Protein Data Bank (PDB code: 2CF2) and was generated with JSmol. Bottom: Complete catalytic cycle for fatty acid biosynthesis. CoA = coenzyme A; ACP = acyl carrier protein; NADPH = nicotinamide adenine dinucleotide phosphate; TE = thioesterase.

The research presented in this doctoral thesis is dedicated to the development of synthetic oligopeptides and their application in enantioselective concurrent “assembly line” approaches and as catalysts for demanding reactions.

Summary

Chapter I

Published as: R. C. Wende and P. R. Schreiner, *Green Chem.* **2012**, *14*, 1821–1849

The first part of this thesis is a Critical Review on mult catalysis that is used as a general introduction to this rapidly growing field of research. We define the different types of one-pot reactions employing multiple catalysts, introduce the concept of *retrocatalysis* and discuss the significant advantages and potential problems associated with mult catalysis. Reactions using combinations of secondary amines, *N*-heterocyclic carbenes and thiourea catalysts, amongst others, are presented. Finally, we introduce our previous achievements in mult catalysis and disclose the development of the first peptidic mult catalyst.

Chapter II

Published as: C. E. Müller, D. Zell, R. Hrdina, R. C. Wende, L. Wanka, S. M. M. Schuler, P. R. Schreiner, *J. Org. Chem.* **2013**, *78*, 8465–8484

This chapter serves as an introduction to peptide catalysis in general and gives detailed insights into our catalyst design concept. The oligopeptide presented herein, was previously developed in our group but recently provided the basis for further developments, such as mult catalytic reactions and the expansion to the first organic mult catalysts (also see Chapter I).

From a library of various peptides Boc-L-Pmh-^AGly-L-Cha-L-Phe-OMe was identified as an remarkably efficient catalyst for the kinetic resolution of *trans*-cycloalkane-1,2-diols. The *ee* values are typically >99% (for the remaining diols) corresponding to *S*-values >50. Whereas the catalyst is also highly selective for the desymmetrization of *meso*-alkane-1,2-diols other substrates, *e.g.*, 1,3-diols, provide only low selectivities. The extraordinary chemoselectivity of the peptide is also revealed by competition experiments. Thus, this small tetrapeptide already shows a behavior that may be compared with enzymes. Moreover, computational investigations on complexes of the acylium ion of the catalyst with the fast reacting enantiomer of *trans*-cyclohexan-1,2-diol were performed. The exceptionally high selectivities are made possible by the interplay of the aminoadamantane carboxylic acid that forms a dynamic binding pocket as well as by attractive dispersion interactions of the cyclohexyl residue with the substrate.

Chapter III

Published as: C. Hofmann, S. M. M. Schuler, R. C. Wende, P. R. Schreiner, *Chem. Commun.* **2014**, 50, 1221–1223

A multicyclic enantioselective oxidative esterification is reported. The combination of TEMPO as oxidation catalyst and *p*-nitrobenzoic acid as additive allows the oxidation of a variety of aldehydes to their mixed anhydrides. These are enantioselectively transferred by the peptide catalyst described in Chapter II onto *trans*-cycloalkane-1,2-diols with up to 94% *ee* for the recovered diol and 93% *ee* for the corresponding acylated derivative. The reaction progress and the formation of the mixed as well as symmetric anhydrides was followed by NMR spectroscopy. The reaction could also be performed with our previously developed multicyclic (see Chapter I) instead of the two individual catalysts.

Chapter IV

Published as: M. W. Alachraf, R. C. Wende, S. M. M. Schuler, P. R. Schreiner, W. Schrader, *Chem.–Eur. J.* **2015**, 21, 16203–16208

In cooperation with Prof. Dr. Wolfgang Schrader a multicyclic incorporating π -methyl histidine and a diacid as catalytic moieties was studied by high-resolution mass spectrometry. The peptide was previously used for a one-pot epoxidation/hydrolysis/kinetic resolution sequence starting from simple alkenes and affording enantiomerically enriched *trans*-cycloalkane-1,2-diols (see Chapter I). Although the selectivities are synthetically useful (64 – 99% *ee* for the remaining diol) they can not compete with the selectivities achieved with the corresponding tetrapeptide alone. All important intermediates have been identified and characterized. It was found that the epoxidation step also leads to a partial oxidation of the imidazole moiety and consequently to a reduced catalytic performance of the multicyclic.

Chapter V

Unpublished results

We envisaged the development of a multicatalytic reaction sequence for the synthesis of 2-deoxygalactosides. Our approach is based on the partial protection of carbohydrates that may subsequently act as glycosyl donors. We identified Boc-D-Pmh-^AGly-L-Val-L-Phe-OMe to be a highly regioselective catalyst in the acetylation of methyl 4,6-*O*-benzylidene- α -D-glucopyranoside. In comparison to simple *N*-methylimidazole, which mostly leads to the acetylation of the 3-hydroxy group on the substrate (2-OAc/3-OAc/diacetylated: 22:70:8; 93% conversion), the peptide preferentially gives the 2-acetylated product (2-OAc/3-OAc/diacetylated: 85:9:6; >95% conversion). Thus, this catalyst is not simply enhancing but completely overriding the inherent reactivity of the substrate.

Chapter VI

Published as: R. C. Wende, A. Seitz, D. Niedek, S. M. M. Schuler, C. Hofmann, J. Becker, P. R. Schreiner, *Angew. Chem. Int. Ed.* **2016**, 55, 2719–2723; *Angew. Chem.* **2016**, 128, 2769–2773

The Dakin–West reaction is one of the most viable methods for the preparation of α -acylamido ketones directly from the corresponding primary α -amino acids. Although this reaction was known for decades no enantioselective variant has been reported previously. We found that the complexity of the mechanism of the reaction requires the separation of the two crucial steps: the acetylation of the azlactone intermediate and the final decarboxylation step. Under optimized reaction conditions the Pmh-containing peptide catalysts act as a Lewis base in the first step and as a Brønsted base in a final enantioselective decarboxylative protonation. With the best-working catalyst selectivities with up to 58% *ee* were achieved with good yields. Two of the obtained products were recrystallized once to achieve up to 84% *ee*. Importantly, computational investigations further proved the importance of dispersion interactions in the enantioselectivity determining reaction step.

Chapter VII

Unpublished results

The last chapter describes further experiments regarding the enantioselective Dakin–West reaction. Computational and experimental investigations were performed to provide further evidence for attractive dispersion interactions and to give insights how the selectivities could be enhanced. Leucine derivatives with diverse protecting groups and different anhydrides were explored. Although the previously observed selectivities could not be increased, the performed experiments support our proposal for substrate-binding by the catalyst in the stereochemistry determining reaction step. Moreover, a potential synthesis of protease inhibitors applying the Dakin–West reaction is reported. Both important reaction steps, the enantioselective decarboxylative protonation and the acetylation of the azlactone, are studied individually and may lead to additional developments.

Zusammenfassung

Kapitel I

Veröffentlicht als: R. C. Wende and P. R. Schreiner, *Green Chem.* **2012**, *14*, 1821–1849

Der erste Teil der vorliegenden Doktorarbeit ist eine kritische Übersicht zur Multikatalyse und dient als Einleitung in dieses sich schnell entwickelnde Forschungsfeld. Wir definieren die verschiedenen Typen von Eintopfreaktionen mit mehreren Katalysatoren, stellen das Konzept der *Retrokatalyse* vor, und diskutieren die signifikanten Vorteile und potentiellen Probleme, welche mit der Multikatalyse assoziiert werden. Kombinationen von sekundären Amininen, *N*-heterocyclischen Carbenen und Thioharnstoffkatalysatoren, neben weiteren anderen, werden präsentiert. Schließlich stellen wir unsere bisherigen Erfolge in der Multikatalyse und die Entwicklung des ersten peptidbasierten Multikatalysators vor.

Kapitel II

Veröffentlicht als: C. E. Müller, D. Zell, R. Hrdina, R. C. Wende, L. Wanka, S. M. M. Schuler, P. R. Schreiner, *J. Org. Chem.* **2013**, *78*, 8465–8484

Dieses Kapitel dient als generelle Einleitung in die Peptidkatalyse und gewährt einen detaillierten Einblick in unser Konzept des Katalysatordesigns. Das hier präsentierte Oligopeptid wurde zuvor in unserer Arbeitsgruppe entwickelt und bildete jüngst die Basis für weitere Entwicklungen, wie multikatalytische Reaktionen und die Weiterentwicklung des ersten peptidischen Multikatalysators (siehe auch Kapitel I).

Aus einer Bibliothek unterschiedlicher Peptide wurde Boc-L-Pmh-^AGly-L-Cha-L-Phe-OMe als bemerkenswert effizienter Katalysator für die kinetische Racematspaltung von *trans*-Cycloalkan-1,2-diolen identifiziert. Die Enantiomerenüberschüsse liegen typischerweise bei >99% (für das verbliebene Diol), was sich in *S*-Werten >50 äußert. Obwohl der Katalysator auch hochselektiv für die Desymmetrisierung von *meso*-Alkan-1,2-diolen ist, werden für andere Substrate, z.B. 1,3-Diole, nur geringe Selektivitäten erhalten. Die außergewöhnliche Chemoselektivität dieses Peptides wird zudem durch Konkurrenzexperimente offenbart. Dieses kleine Tetrapeptid zeigt somit bereits ein Verhalten, welches mit dem von Enzymen vergleichbar ist. Zudem wurden computerchemische Untersuchungen der Komplexe des Katalysator Acyliumions mit dem schnell reagierenden Enantiomer von *trans*-Cyclohexan-1,2-diol durchgeführt. Die außerordentlich hohen Selektivitäten werden durch das Zusammenspiel der Aminoadamantan-

carbonsäure, welche eine dynamische Bindungstasche ausbildet, und attraktive Dispersionswechselwirkungen des Cyclohexylrestes mit dem Substrat ermöglicht.

Kapitel III

Veröffentlicht als: C. Hofmann, S. M. M. Schuler, R. C. Wende, P. R. Schreiner, *Chem. Commun.* **2014**, 50, 1221–1223

Eine multikatalytische enantioselektive oxidative Veresterung wird beschrieben. Die Kombination von TEMPO als Oxidationskatalysator und *p*-Nitrobenzoesäure als Additiv erlauben die Oxidation einer Reihe von Aldehyden zu den entsprechenden gemischten Anhydriden. Diese werden enantioselektiv durch den in Kapitel II beschriebenen Katalysator auf *trans*-Cycloalkan-1,2-diole mit bis zu 94% *ee* für das zurückgewonnene Diol und 93% *ee* für das entsprechende acylierte Derivat übertragen. Der Reaktionsverlauf und die Bildung des gemischten und symmetrischen Anhydrides wurden NMR-spektroskopisch verfolgt. Zudem konnte die Reaktion auch mit unserem zuvor entwickelten Multikatalysator (siehe Kapitel I), anstelle der beiden individuellen Katalysatoren, durchgeführt werden.

Kapitel IV

Veröffentlicht als: M. W. Alachraf, R. C. Wende, S. M. M. Schuler, P. R. Schreiner, W. Schrader, *Chem.–Eur. J.* **2015**, 21, 16203–16208

In Kooperation mit Prof. Dr. Wolfgang Schrader wurde ein mit π -Methylhistidin und einer Disäure bestückter Multikatalysator mithilfe von hochauflösender Massenspektrometrie untersucht. Das Peptid wurde zuvor für eine Reaktionssequenz bestehend aus Epoxidierung, Hydrolyse und kinetischer Racematspaltung verwendet, welche es erlaubt enantiomerenangereicherte *trans*-Cycloalkan-1,2-diole ausgehend von einfachen Alkenen zu erhalten (siehe Kapitel I). Obwohl synthetisch akzeptable Selektivitäten (64 – 99% *ee* für das verbleibende Diol) beobachtet werden, reichen diese nicht an die Werte heran, die bei Verwendung des entsprechenden Tetrapeptides alleine erhalten werden. Alle wichtigen Intermediate wurden identifiziert und charakterisiert. Es konnte gezeigt werden, dass der Epoxidierungsschritt teilweise auch zu einer Oxidation des Imidazols und folglich zu einer herabgesetzten katalytischen Aktivität des Multikatalysators führt.

Kapitel V

Unveröffentlichte Ergebnisse

Wir fassten die Entwicklung einer multikatalytischen Reaktionssequenz für die Synthese von 2-Deoxygalaktosiden ins Auge. Unser Ansatz basiert hierbei auf der partiellen Schützung von Kohlenhydraten, welche anschließend als Glykosyldonor fungieren könnten. Boc-D-Pmh-^AGly-L-Val-L-Phe-OMe wurde als Katalysator für die regioselektive Acetylierung von Methyl-4,6-*O*-benzyliden- α -D-glucopyranosid identifiziert. Im Vergleich zu einfachem *N*-Methylimidazol, welches hauptsächlich zur Acetylierung der 3-Hydroxygruppe des Substrates führt (2-OAc/3-OAc/diacetyliert: 22:70:8; 93% Umsatz), wird mit dem Peptid überwiegend das 2-acetylierte Produkt gebildet (2-OAc/3-OAc/diacetyliert: 85:9:6; >95% Umsatz). Somit verstärkt dieser Katalysator nicht einfach die inhärente Reaktivität des Substrates, sondern setzt sich vollständig über diese hinweg.

Kapitel VI

Veröffentlicht als: R. C. Wende, A. Seitz, D. Niedek, S. M. M. Schuler, C. Hofmann, J. Becker, P. R. Schreiner, *Angew. Chem. Int. Ed.* **2016**, 55, 2719–2723; *Angew. Chem.* **2016**, 128, 2769–2773

Die Dakin–West–Reaktion ist eine der brauchbarsten Methoden zur Darstellung von α -Acylamidoketonen ausgehend von den entsprechenden primären α -Aminosäuren. Obwohl diese Reaktion seit Jahrzehnten bekannt ist, wurde zuvor keine enantioselective Variante beschrieben. Wir fanden, dass die Komplexität des Reaktionsmechanismus eine Trennung der beiden entscheidenden Schritte erfordert: der Acetylierung des intermediär gebildeten Azlactons und des abschließenden Decarboxylierungsschrittes. Unter optimierten Reaktionsbedingungen fungieren die Pmh-enthaltenden Peptidkatalysatoren als eine Lewisbase im ersten Schritt und als eine Brønstedbase in der finalen enantioselectiven decarboxylativen Protonierung. Mit dem besten Katalysator konnten Selektivitäten von bis zu 58% *ee* bei guten Ausbeuten erzielt werden. Durch einfache Umkristallisation von zwei der erhaltenen Produkte konnten die Selektivitäten auf bis zu 84% *ee* gesteigert werden. Durch computerchemische Untersuchungen konnte auch hier die Bedeutung von Dispersionswechselwirkungen für den enantioselectivitätsbestimmenden Reaktionsschritt nachgewiesen werden.

Kapitel VII

Unveröffentlichte Ergebnisse

Im letzten Kapitel werden weitere Experimente zur Dakin–West–Reaktion vorgestellt. Computerchemische und experimentelle Untersuchungen wurden durchgeführt um attraktive Dispersionwechselwirkungen nachzuweisen und einen Einblick zu erhalten, wie die Selektivitäten verstärkt werden könnten. Leucin-Derivate mit diversen Schutzgruppen und unterschiedliche Anhydride wurden untersucht. Obwohl die zuvor beobachteten Selektivitäten nicht weiter erhöht werden konnten, stützen die durchgeführten Experimente unsere vorgeschlagene Bindung des Substrates durch den Katalysator im selektivitätsbestimmenden Reaktionsschritt. Zudem wird die Anwendung der Dakin–West–Reaktion für eine potentielle Synthese von Proteaseinhibitoren vorgestellt. Die beiden entscheidenden Reaktionsschritte, die enantioselektive decarboxylative Protonierung und die Acetylierung der Azlactone, werden separat untersucht und könnten zu weiteren Entwicklungen führen.

– Chapter I –

Evolution of Asymmetric Organocatalysis: Multi- and Retrocatalysis

Raffael C. Wende and Peter R. Schreiner, *Green Chem.* **2012**, *14*, 1821–1849



“Reproduced from *Green Chemistry* **2012**, *14*, 1821–1849 with permission from The Royal Society of Chemistry.”

Abstract

The evolution of organocatalysis led to various valuable approaches, such as multicomponent as well as domino and tandem reactions. Recently, organomulticatalysis, *i.e.*, the modular combination of distinct organocatalysts enabling consecutive reactions to be performed in one pot, has become a powerful tool in organic synthesis. It allows the construction of complex molecules from simple and readily available starting materials, thereby maximizing reaction efficiency and sustainability. A logical extension of conventional multicatalysis is a multicatalyst, *i.e.*, a catalyst backbone equipped with independent, orthogonally reactive catalytic moieties. Herein we highlight the impressive advantages of asymmetric organomulticatalysis, examine its development, and present detailed reactions based on the catalyst classes employed, ranging from the very beginnings to the latest multicatalyst systems.

1. Introduction

The development of resource-efficient and sustainable chemical methodologies and processes has become one of the most important goals of synthetic organic chemistry in the 21st century. Various attempts were undertaken to minimize the adverse environmental impact and maximize the efficiency of chemical reactions. As one of numerous advances, multicatalysis, *i.e.*, the modular combination of distinct catalysts for consecutive transformations in a single flask, emerged as a highly valuable tool for the construction of complex molecular frameworks from simple and readily available starting materials.^[1]

Since its fundamental “renaissance” organocatalysis became a vibrant area of research and grew rapidly to become a pillar in organic synthesis.^[2] Further developments mainly focused on novel catalyst classes and activation modes, and their use in iterative single step operations.^[2] Simultaneously, multistep processes, such as domino/cascade and tandem reactions,^[3-5] as well as asymmetric multicomponent reactions^[6] gained increasing attention and have soon been adopted to organocatalysis.^[5,7-9] Multicatalysis may condense the operational simplicity and synthetic efficiency provided by the aforementioned concepts to allow the rapid synthesis of even complex molecules in one pot syntheses.^[10-12] However, this concept only recently started flourishing in the field of organocatalysis.^[1] An approach that is even rarer and a logical extension of conventional multicatalysis is a multicatalyst^[13] (‘assembly line’ approach), *i.e.*, an arbitrary catalyst backbone equipped with independently reactive catalytic moieties, which are separated by an appropriate spacer (Figure 1). The design of a multicatalyst system hinges on the concept of *retrosynthesis* for assembling complex molecules. Whereas in retrosynthesis the target structure is disassembled into synthons (as equivalents for starting materials or intermediates) and steps, the development of a multicatalyst relies on the judicious choice of

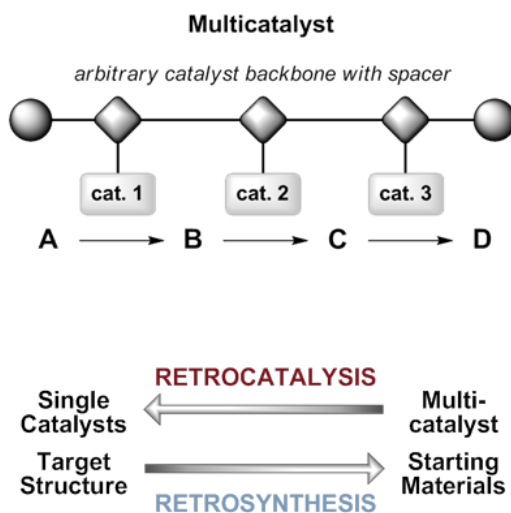


Figure 1. Schematic representation of a multicatalyst and the concept of retrocatalysis.

catalytic moieties that can be brought together in a single catalyst structure. Such a multicatalyst should then be able to allow the synthesis of the target structure from simple starting materials in a sequence of highly chemoselective reactions in one pot. This systematic strategy toward reverse catalyst design is therefore complementary to *retrosynthesis* (a target structure oriented approach) and may therefore be labelled as *retrocatalysis* (a reaction step oriented approach)^[14] to emphasize their close conceptional relationship (Figure 1).

The main challenge in the development of multicatalytic reactions is to ensure compatibility of reactants, intermediates and catalysts throughout the whole reaction sequence. Many organocatalytic reactions are nowadays well understood. Their underlying activation modes, reaction pathways and intermediates have been precisely elucidated, experimentally^[15] as well as theoretically,^[16] for a variety of reactions, allowing reasonable predictability for the realization of *organomulticatalysis* (indicating that the reaction is purely organocatalyzed). In order to circumvent compatibility problems, the following strategies have been adopted: the use of obviously compatible catalysts, sequential addition of catalysts, and the site-isolation or phase-separation of catalysts. Additional challenges appear in the case of a multicatalyst. The choice of a proper catalyst backbone should allow easy preparation, alteration as well as modification. Moreover, appropriate spacers may be crucial for the separation of the catalytically active moieties. The envisioned multicatalyst must be compatible with all required reaction conditions and intermediates.

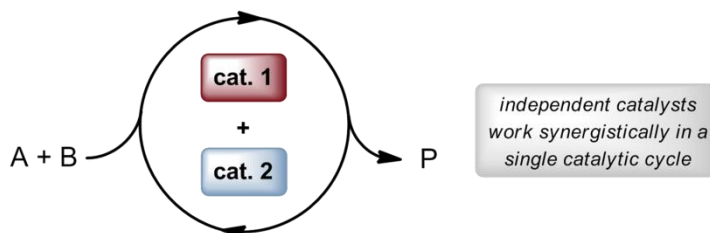
Interestingly, many examples of multicatalysis have not been recognized as such. Amongst other things, this may be due to the following reasons: not taking into account simple achiral Brønsted acids and bases as organocatalysts and inconsistent terminology (many multicatalytic reactions are lost amidst publications dealing with domino or tandem reactions). For this reason we will first define the prevalent types of one-pot organocatalysis employing multiple steps, illustrated with selected examples, before examining the advantages of multicatalysis and discussing representative examples.

2. Multicatalysis – A Survey

2.1 Taxonomy of One-Pot Reactions Using Multiple Catalysts

There are many examples of one-pot reactions where multiple organocatalysts are employed,^[10,11,17] and these have been termed cooperative catalysis,^[18] multifunctional catalysts,^[19] and dual catalysis.^[20] For simplicity, we schematically depict the catalytic cycles for a general reaction of two starting materials (A and B) affording a product (P). As evident from this simplified picture, multicatalysis should be clearly distinguished from cooperative catalysis where neither catalyst one nor catalyst two are sufficient to perform a desired reaction individually, and only a combination of both catalysts (sharing a single catalytic cycle) leads to a significant increase in the reaction rate (Figure 2).^[18]

Cooperative catalysis



representative example:

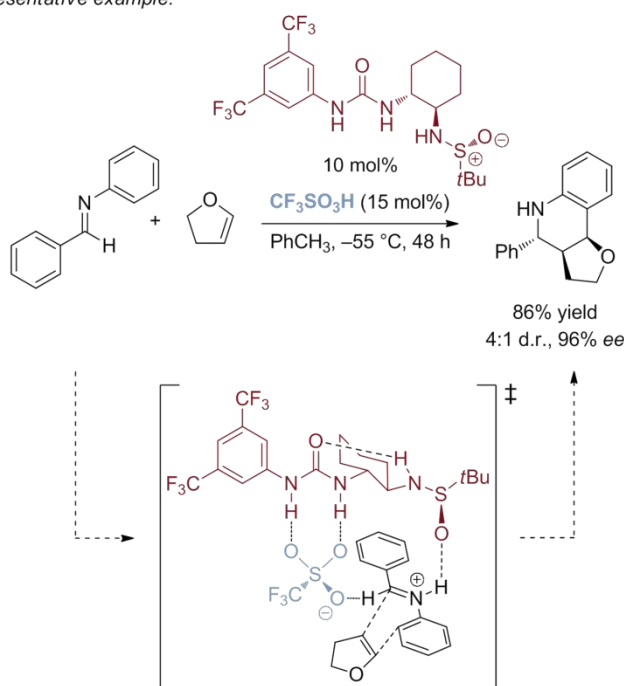


Figure 2. The concept of cooperative catalysis taking the co-catalyzed asymmetric Povarov reaction as an example; see ref. 18c and 18d.

Moreover, multicatalysis and especially a multicatalyst (compare Figure 1) are different from multifunctional catalysts^[19] (Figure 3), and dual catalyst systems^[20] (Figure 4). In the case of a multifunctional catalyst one catalytic functionality mutually enhances the activity of another catalytically active center on the same catalyst *via* the separate activation of multiple reaction partners (mostly a nucleophile and an electrophile).^[19] The types of catalysts which are able in simultaneously activating two reactants are manifold, ranging from, *e.g.*, proline^[21] to cinchona alkaloid derivatives^[22-23] and bifunctional (thio)urea derivatives^[24] (such as Takemoto's catalyst; Figure 3),^[25] and proved their efficiency in a variety of reactions.^[19,21-25]

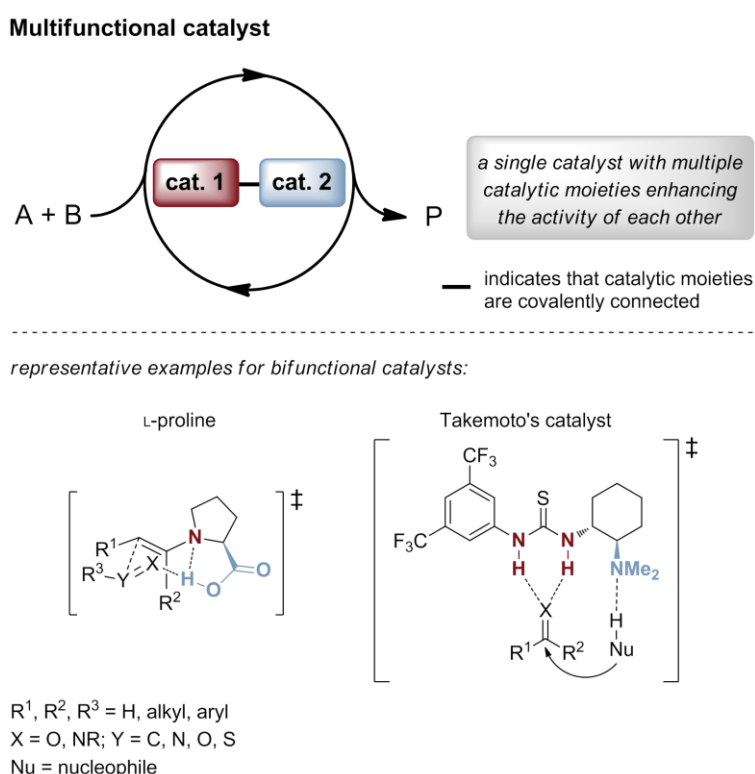
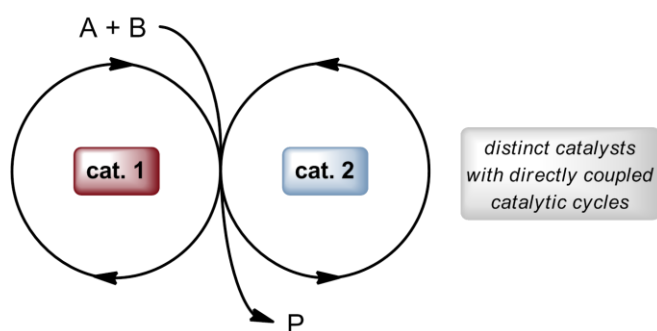


Figure 3. The concept of a multifunctional catalyst taking proline and Takemoto's catalyst as representative examples; see ref. 21 and 25.

The third type of catalysis that should be distinguished from multicatalysis is dual catalysis (Figure 4).^[20] It should be mentioned that dual catalysis is inconsistently used and may lead to confusion as it is indeed used for multicatalytic reactions in some cases. Very recently, Allen and MacMillan defined synergistic catalysis as the simultaneous activation of an electrophile and a nucleophile by independent catalysts in directly coupled catalytic cycles.^[26] Indeed, the same is true for dual catalysis. From our point of view synergistic catalysis is a better terminology for reactions wherein two directly coupled catalytic cycles lead to the formation of a product (see example in Figure 4).

Dual catalysis / Synergistic catalysis



representative example:

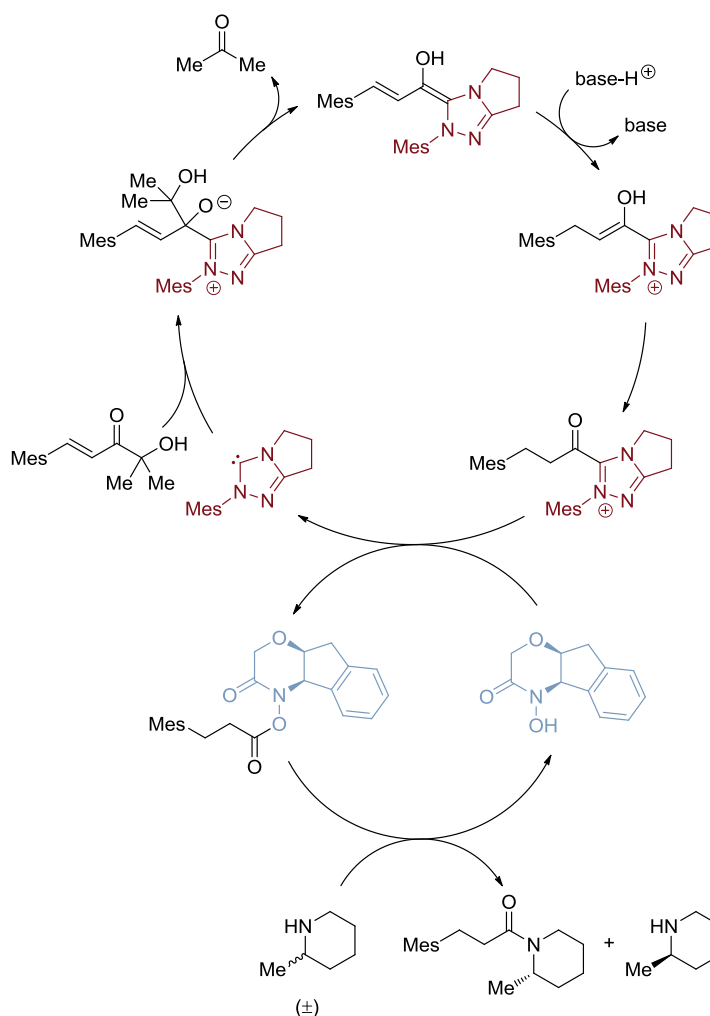
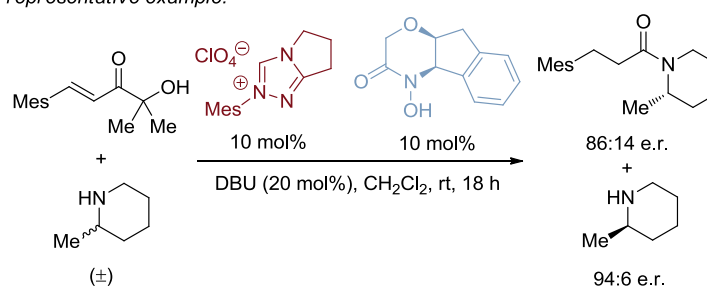


Figure 4. The concept of dual catalysis/synergistic catalysis taking the kinetic resolution of cyclic amines as an example; see ref. 20c. DBU = 1,8-diazabicyclo[5.4.0]undec-7-ene; Mes = mesityl (2,4,6-trimethylphenyl).

For clarity, the term multicational should be solely used for combinations of distinct catalysts to perform consecutive reactions, whereby the starting materials (A and B) react to form an intermediate (IM) in a first catalytic cycle (Figure 5). Subsequently, this intermediate is converted to the final product (P) by another independent catalyst (or catalytic moiety in the case of a multicational) without intermittent work-up and purification procedures (Figure 5). Based on the way of their execution, multicational reactions employing two (or more) catalysts can be further categorized. For instance, the term sequential (multi)catalysis^[4,11] is typically used to describe multicational reactions that rely on the addition of another catalyst or reagent (C, Figure 5), or an intermittent alteration of reaction conditions (*e.g.*, solvent, temperature) to initiate a subsequent catalytic cycle. Tandem catalysis^[4] or relay catalysis,^[11] respectively, refer to a multicational reaction whereby the product formed in the first catalytic cycle is directly fed into a subsequent one without a change in the reaction conditions. Moreover each of the employed catalysts may independently allow for domino/cascade or tandem reactions. Therefore, we recommend using the comprehensive expression organomulticational for the overall reaction and more specific terms only for the distinct reactions.

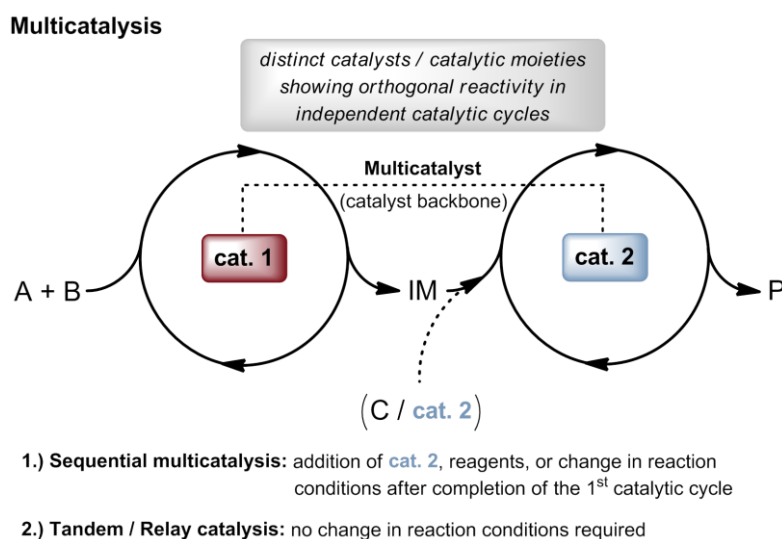


Figure 5. Possible types of multicational.

2.2 Reaction Efficiency and Sustainability Aspects of Multicational

What are the benefits of multicational reactions relative to well-established traditional synthetic strategies and domino reactions, and how do they contribute to an environmentally benign chemistry? These questions can be answered when considering multicational in the context of GreenChemistry^[27-30] and its Twelve Principles,^[27,31] taking into account the Environmental factor (*E*-factor),^[32] as well as the concepts of atom economy,^[33] step economy,^[34] and redox

economy^[35] as key parameters.^[36] However, the rapid increase in reaction efficiency and sustainability from the ‘stop-and-go’ to multicatalysis is based on some simple considerations.

Catalysis is a key to sustainability and is superior compared to the use of stoichiometric amounts of reagents.^[28] Organocatalysis often circumvents many of the drawbacks usually associated with transition-metal catalysis and biocatalysis. Organocatalysts are usually non-toxic, readily available (either commercially or derived from natural sources), and in many cases allow reactions under mild conditions. They are robust catalysts, *e.g.*, tolerate air and moisture, and are compatible with a large variety of functional groups. One-pot multistep reaction sequences, may they be promoted by a single organocatalyst or of multicatalytic nature, avoid costly and time-consuming, intermittent work-up and purification steps, thus preventing yield losses, saving energy, time and effort, and reducing waste (indeed, most waste originates from work-up and purification procedures in the form of solvents, drying, and separation agents). As a consequence, considerably lower *E*-factors, which is the mass ratio of generated waste to desired product, can be achieved. Moreover, the mentioned functional group tolerance of organocatalysts may permit protecting-group free syntheses^[37] and avoid other unnecessary functional group conversions (*e.g.*, non-strategic oxidation and reduction steps), thus leading to high step^[34] as well as redox economy.^[35] Recently, pot economy^[38] has been suggested with the ultimate goal of performing entire multistep syntheses in a single reaction vessel. Multicatalysis also appreciably broadens the spectrum of applicable substrates and achievable transformations when employing independent catalysts with orthogonal reactivity. Hence, it may be more easily combined with multicomponent reactions^[6,9,6] leading to overall high atom economy,^[33] which is defined as the ratio of the molecular weight of desired product to the sum of molecular weights of the reactants. Equilibrium reactions can be driven to completeness, avoiding the use of excess reagents, and possible side-reactions can be circumvented by direct consumption of reactive intermediates in a concurrent catalytic cycle. This is especially important in cases where potentially toxic or unstable intermediates are formed; these can be directly converted into safer or lower energy species, thus lowering the risks of transportation, storage, and handling. An additional factor for high reaction efficiency in catalysis undoubtedly is selectivity,^[39] namely chemo-, regio- or stereoselectivity (in cases where any other than the desired isomers can be regarded as waste). Multicatalysis may not only improve the reactivity, but lead to an amplification of stereoselectivity due to synergistic effects or to an enantioenrichment in subsequent catalytic cycles when a set of chiral catalysts is used.^[5] Moreover, it provides an elegant approach to attain products with the desired stereochemistry depending on the configuration of the catalysts employed.^[5]

Further advantages may be offered by a multicatalyst: the close proximity of the catalytic moieties ensures higher local concentrations of the formed intermediates at the common catalyst backbone for consecutive reactions (if the reaction rates are such that each subsequent reaction

comes is faster). This leads to an efficient feeding of the intermediates into the next catalytic cycle, therefore, improving reactivity and material-balance.

This *Critical Review* examines and highlights the impressive developments and advances of asymmetric organocatalyzed mult catalysis (at least one chiral catalyst is used) with the focus on different organocatalyst classes. At the beginning of each chapter we will provide a short introduction in the common activation modes and reaction types discussed herein. The reactions presented are classified depending on the different catalyst classes employed and their specific activation modes. In particular, these are:

- Secondary amines – enamine/iminium activation
- *N*-heterocyclic carbenes – Umpolung
- Thiourea derivatives – hydrogen bonding
- Non-natural oligopeptides – acyl transfer reactions

Wherever necessary for a better understanding we will present mechanistic details for selected transformations. We cover only enantioselective approaches; diastereoselective reactions are not included. Multicatalysis employing metal catalysts,^[1,4,11,13,40] multienzymatic reactions,^[41-42] as well as combinations of metal-, bio-, and organocatalysis^[1,4,11,42-43] are beyond the scope of this review and have been covered elsewhere.

3. Secondary Amine Catalysts

3.1 The Beginnings of Organomulticatalysis – Merging Iminium and Enamine Catalysis

Chiral secondary amines are commonly employed as organocatalysts as these are in most cases readily available and show remarkable performance in a variety of carbonyl functionalizations *via* iminium ion (LUMO lowering) and enamine (HOMO raising) catalysis.^[44] Both activation modes have been elegantly combined in asymmetric domino reactions, which now constitute possibly one of the most applied one-pot multistep approaches in organocatalysis.^[7,44e] This strategy is outlined in Figure 6: an α,β -unsaturated aldehyde (or ketone) is activated by a secondary amine catalyst, reversibly forming an iminium ion that is able to undergo a conjugate addition of a nucleophile (Nu). The enamine intermediate formed as a result of the first reaction step enables a consecutive reaction with an electrophile (E) to afford the α,β -disubstituted aldehyde usually containing two newly formed stereogenic centers.

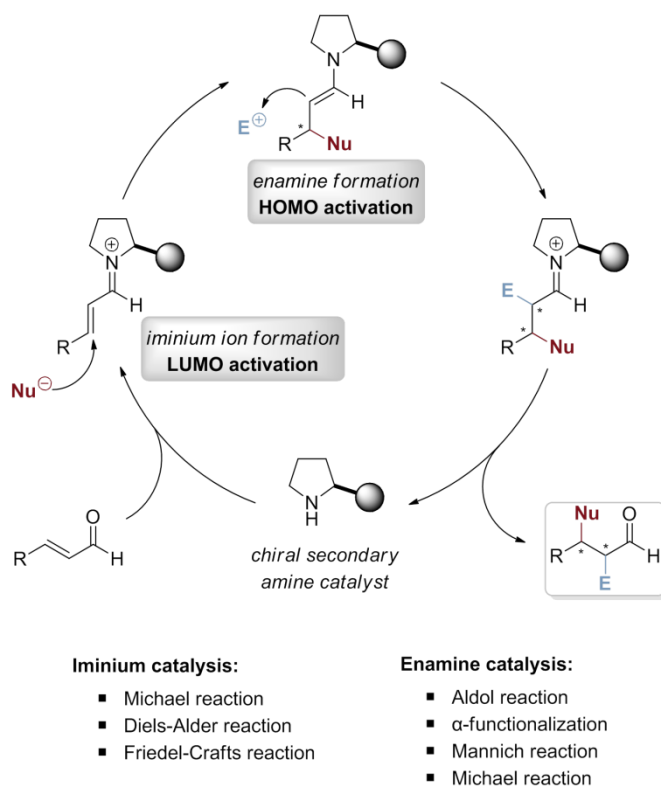
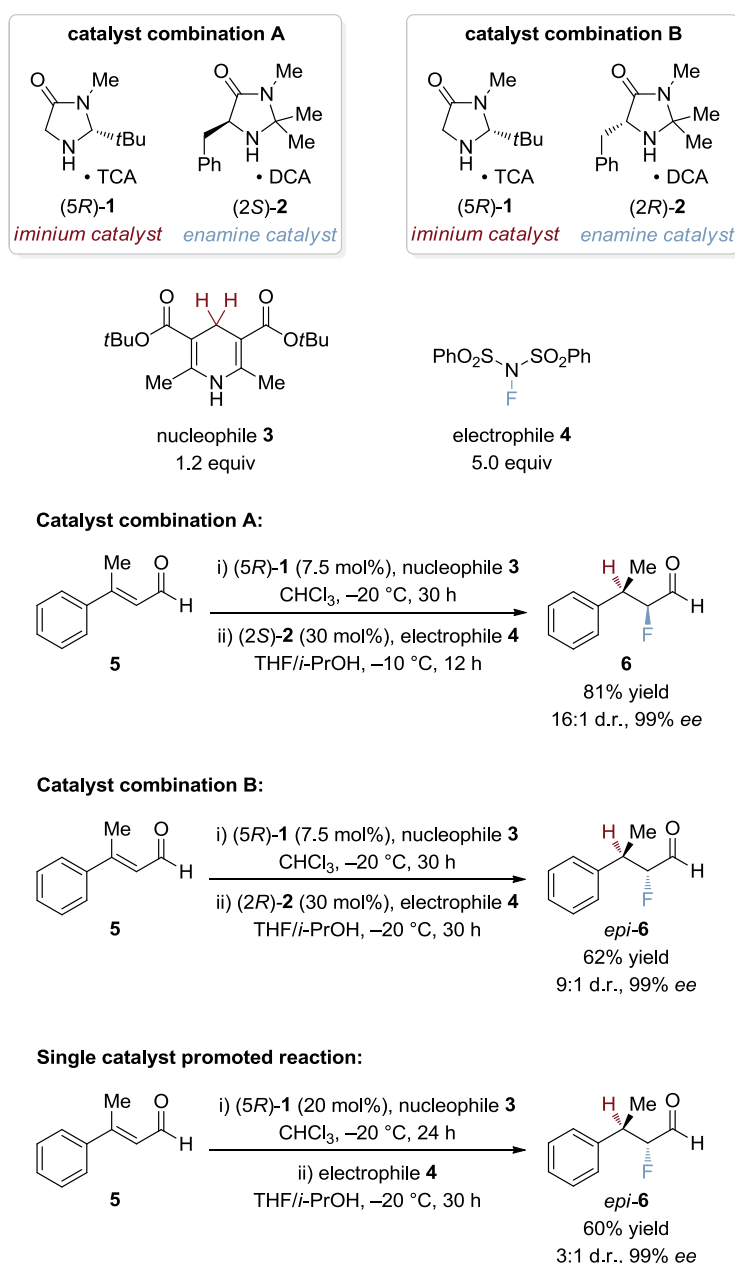


Figure 6. Simplified general mechanism for a secondary amine catalyzed domino reaction and prevalent reaction types. R = alkyl, aryl; Nu = nucleophile; E = electrophile.

The way to secondary amine-catalyzed multicatalytic reactions was paved by MacMillan *et al.* in 2005, as they realized that two discrete imidazolidinones, **1** and **2**, respectively, can be combined to enforce cycle-specific selectivities (Scheme 1).^[45] To the best of our knowledge this was the

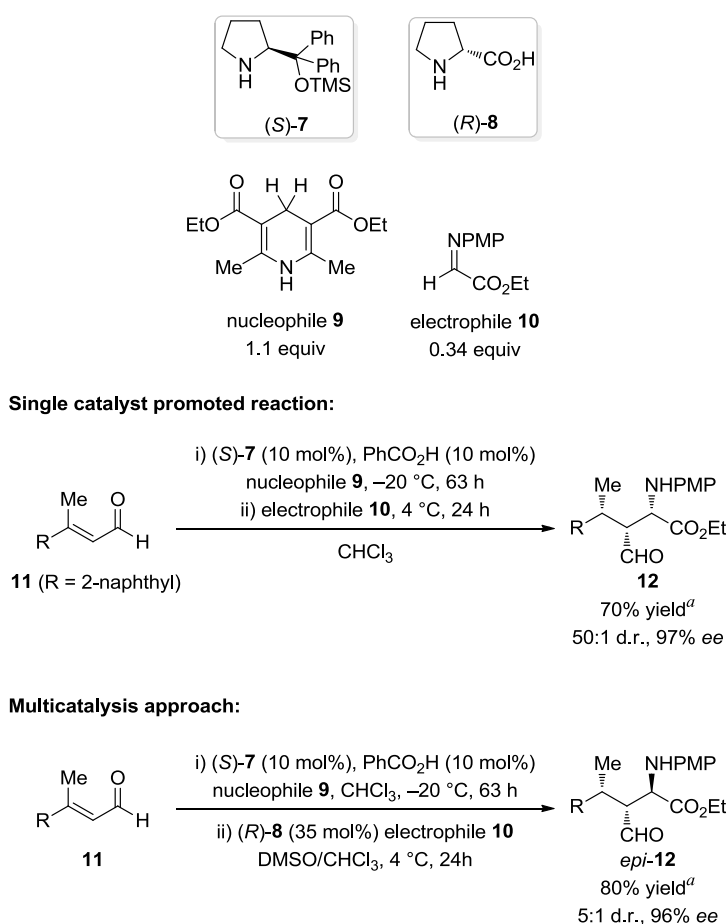
earliest example of asymmetric multicatalysis employing two chiral organocatalysts. The transfer hydrogenation reaction^[46] with Hantzsch ester **3** as organic hydride source in conjunction with direct α -fluorination using *N*-fluorodibenzenesulfonamide (NFSI; **4**) as electrophile allowed the formal asymmetric addition of HF across β -methylcinnamaldehyde (**5**; Scheme 1). This multicatalytic reaction sequence showed for the first time one of the advantages of the multicatalysis approach, namely the easy modulation to provide the required diastereo- and enantioselectivity *via* the judicious choice of the enantiomeric forms of the secondary amine catalysts. For example, catalyst combination A, with iminium catalyst (5*R*)-**1** and enamine catalyst (2*S*)-**2**, gives access to the *anti*-diastereomer **6** in 16:1 d.r. with 99% *ee*. Employing



Scheme 1. Cycle-specific catalysis for the transfer hydrogenation/ α -fluorination of β -methylcinnamaldehyde (**5**).

catalyst combination B, with enamine catalyst (2*R*)-**2**, provides a direct entry to the *syn*-addition product *epi*-**6** in 9:1 d.r. and 99% *ee*, respectively (Scheme 1). When (5*R*)-**1** was used for both iminium and enamine activation the *syn*-addition product *epi*-**6** was obtained with a diminished diastereomeric ratio of 3:1 (Scheme 1).^[45] This result clearly demonstrates that multicatalysis may not only allow controlling the diastereo- and enantioselectivity of the final product it may also significantly enhance stereoinduction.

Soon after MacMillan's pioneering work^[45] related reactions comprising the sequential iminium-enamine activation by distinct secondary amines have been published. For example, a similar procedure for a reductive Mannich-type reaction was reported by Córdova *et al.* (Scheme 2).^[47]

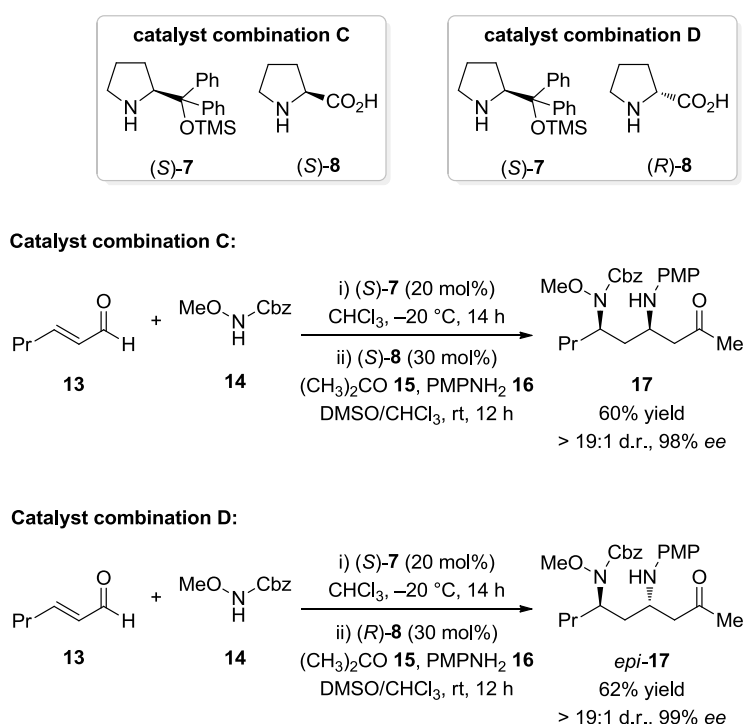


Scheme 2. Enantioselective reductive Mannich-type reaction reported by Córdova. ^a Yield of isolated product based on *N*-PMP-protected α -iminoglyoxylate (**10**).

Instead of imidazolidinone (5*R*)-**1** used by MacMillan, they applied the Jørgensen–Hayashi catalyst^[48] ((S)-**7**; TMS = trimethylsilyl) with benzoic acid as co-catalyst, which proved to be more reactive in the transfer hydrogenation step under the applied conditions. The reactions gave the corresponding amino acid derivatives, such as **12**, in good yields and excellent stereo-selectivities using Hantzsch ester **9**, *para*-methoxyphenyl (PMP)-protected α -iminoglyoxylate

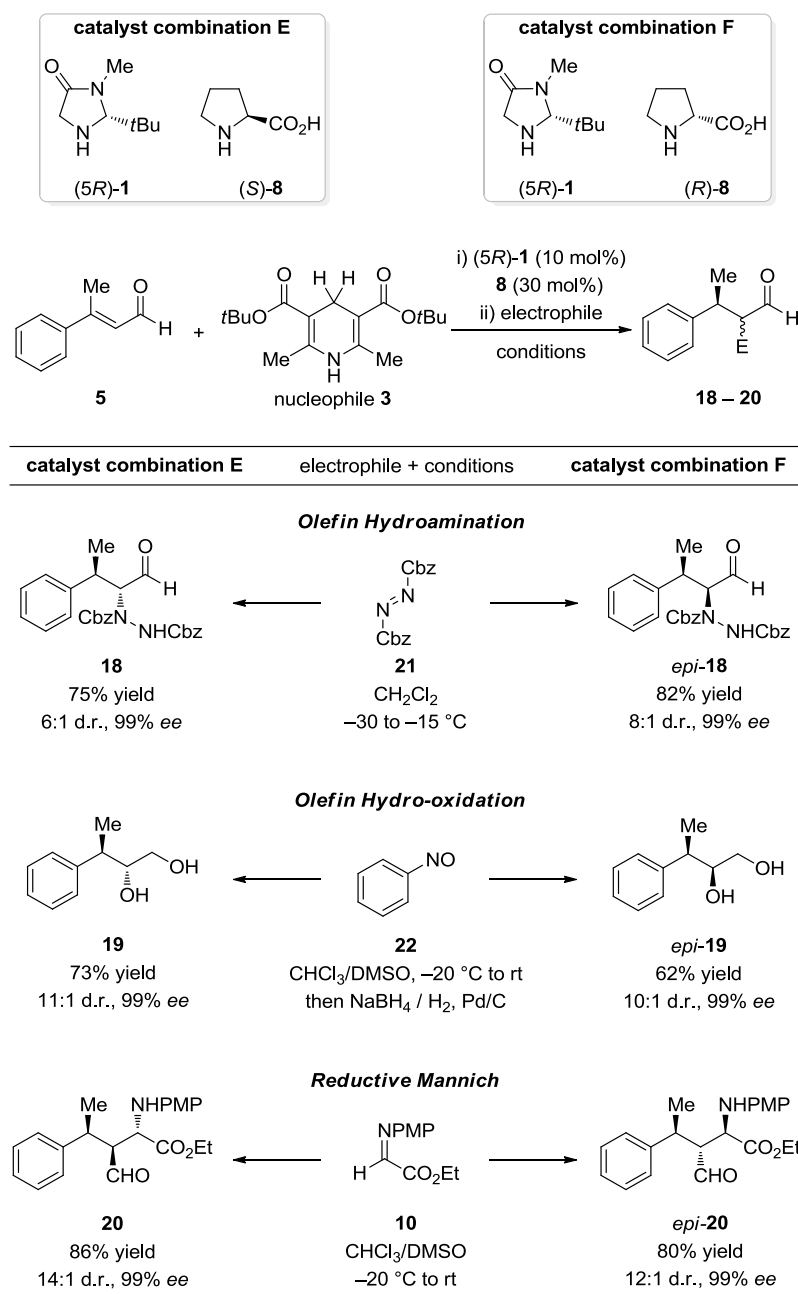
(**10**), α,β -unsaturated aldehyde **11**, and (*S*)-**7** as catalyst for both reaction steps (Scheme 2). By analogy to the reactions reported by MacMillan *et al.*,^[45] the sequential addition of D-proline ((*R*)-**8**) and electrophile **10** in the second reaction step altered the diastereoselectivity: the *syn*-product *epi*-**12** was obtained instead of the *anti*-isomer **12**, albeit with significantly diminished selectivity (5:1 instead of 50:1 d.r.; Scheme 2).

Later, the same group reported the cycle-specific four-component reaction of (*E*)-hex-2-enal (**13**), benzyl methoxycarbamate (**14**; Cbz = benzyloxycarbonyl), acetone (**15**) and *p*-anisidine (**16**) under mult catalysis conditions, which gives direct access to the chiral, orthogonally protected diamine derivatives **17** and *epi*-**17** through an asymmetric aza-Michael/Mannich reaction cascade catalyzed by (*S*)-**7**, and (*S*)-**8** or (*R*)-**8** (Scheme 3).^[49] The subsequent (*S*)-**8** catalyzed Mannich reaction thereby kinetically resolved the β -amino aldehyde intermediate (96% *ee*) to give the diamine products **17** with 98% *ee* (for catalyst combination C) and *epi*-**17** with 99% *ee* (for catalyst combination D), respectively, in good yields and high diastereomeric ratios (> 19:1 d.r. in both cases).



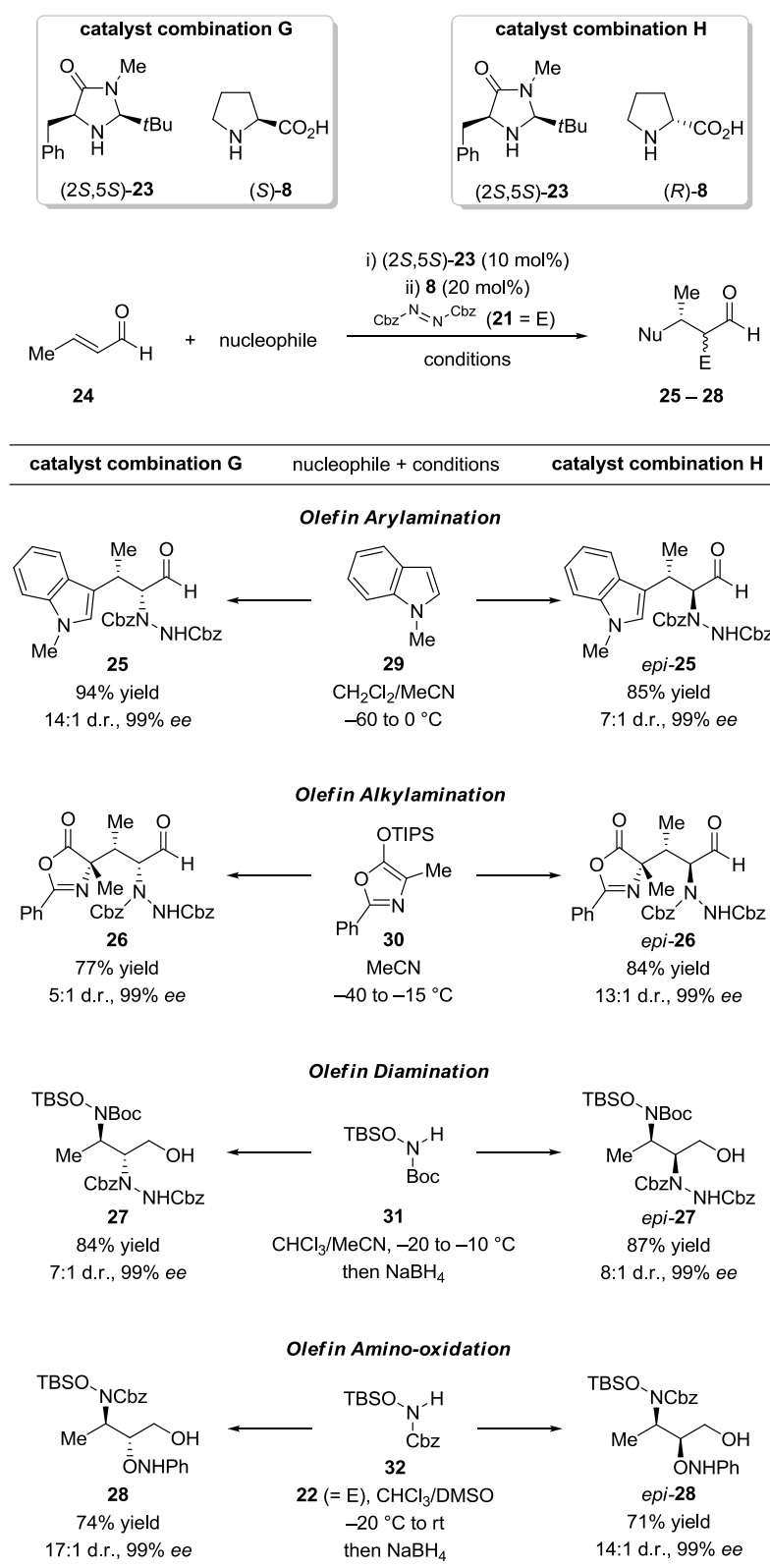
Scheme 3. Aza-Michael/Mannich reaction cascade for the synthesis of orthogonally protected diamine derivatives.

In order to expand their cycle-specific mult catalysis approach to a variety of other transformations, MacMillan and co-workers investigated imidazolidinones (*5R*)-**1** and (*2S,5S*)-**23** as iminium catalysts and either (*S*)-**8** or (*R*)-**8** as enamine catalyst (Scheme 4 and Scheme 5).^[50]



Scheme 4. Cycle-specific reaction cascades employing Hantzsch ester **3** as hydride nucleophile and different electrophiles. (5*R*)-**1** was used as its corresponding TCA salt. E = electrophile.

While imidazolidinones are principally able to serve as iminium *and* enamine catalysts, they are not capable of participating in bifunctional enamine catalysis (in which activation of the electrophile is performed by the same amine catalyst). In contrast, bifunctional activation is a standard mode of activation for proline **8** (due to its acid functionality; compare Figure 3),^[21] but this catalyst is generally ineffective as iminium catalyst particularly with enals or enones. Owing to this orthogonal reactivity, the combination of (5*R*)-**1** or (2*S*,5*S*)-**23** with **8** enabled a broader spectrum of valuable transformations by using different electrophiles (Scheme 4) and nucleophiles (Scheme 5).^[50] For example, a combination of (5*R*)-**1** and (S)-**8** as catalysts (catalyst combination E), β-methylcinnamaldehyde (**5**), Hantzsch ester **3** as nucleophile and dibenzyl-



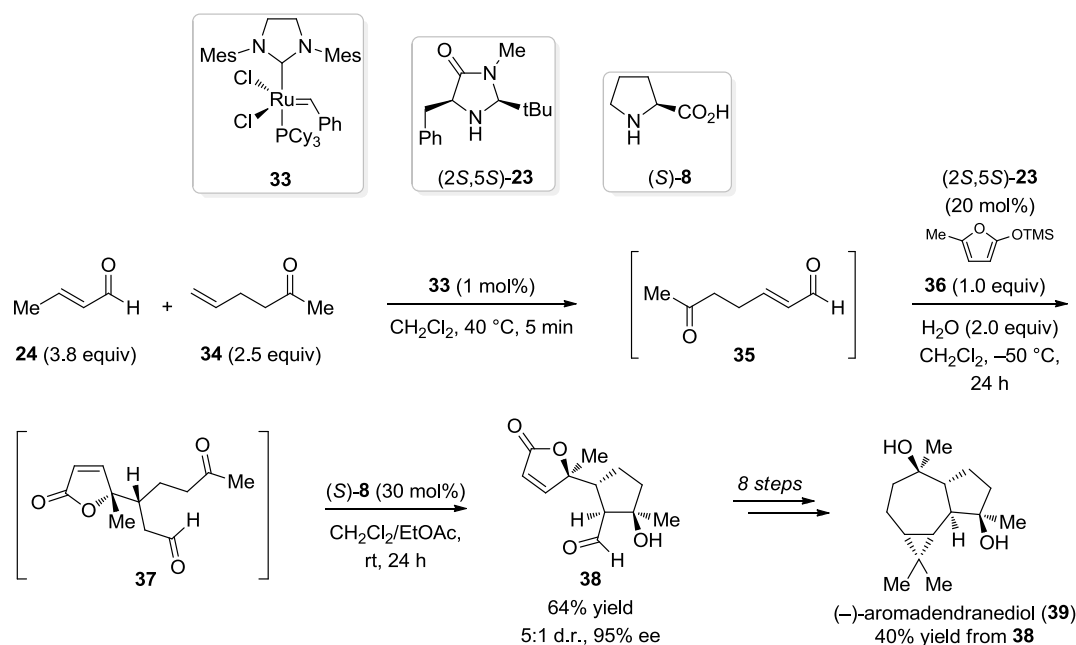
Scheme 5. Cycle-specific reaction cascades employing dibenzylazodicarboxylate (**21**) or nitrosobenzene (**22**) as electrophiles and different nucleophiles. (2S,5S)-**23** was used as its corresponding TCA or TFA salt. E = electrophile; Nu = nucleophile.

azodicarboxylate (**21**) as aza-Michael acceptor afforded the desired hydroamination product **18** (6:1 *anti/syn*, 99% *ee*). As expected, the combination of (5*R*)-**1** and (*R*)-**8** (catalyst combination F) led to an inversion in diastereoselectivity furnishing *epi*-**18** (8:1 *syn/anti*, 99% *ee*). Employing nitrosobenzene **22** as electrophile provided the hydro-oxidation products **19** (11:1 *anti/syn*, and 99% *ee* with catalyst combination E) and *epi*-**19** (10:1 *syn/anti* and 99% *ee* with catalyst combination F). Moreover, a reductive Mannich reaction cascade, similar to the one reported by Córdova^[47] (compare Scheme 2) using *N*-PMP-protected α -iminoglyoxylate (**10**) as electrophile could be realized. The corresponding products were obtained in high yields, diastereomeric ratios and excellent enantiomeric excess (**20**: 14:1 d.r., 99% *ee*; *epi*-**20**: 80% yield, 12:1 d.r., 99% *ee*).

The same methodology was applicable for a variety of nucleophiles, using a combination of imidazolidinone (2*S*,5*S*)-**23** and both enantiomeric forms of proline **8** as catalysts, crotonaldehyde (**24**) as enal substrate and dibenzylazodicarboxylate (**21**) as electrophilic reagent (Scheme 5).^[50] With 1-methylindole (**29**) as π -nucleophile the corresponding arylamination products were obtained (**25**: 14:1 *syn/anti*, 99% *ee* with catalyst combination G; *epi*-**25**: 7:1 *anti/syn*, 99% *ee* with catalyst combination H). An alkylamination reaction cascade with silyloxazazole **30** (TIPS = triisopropylsilyl) as nucleophile afforded the desired product **26** with three contiguous stereogenic centers (5:1 d.r. and 99% *ee*) for catalyst combination G, whereas catalyst combination H gave the corresponding *anti*-isomer *epi*-**26** (13:1 d.r., 99% *ee*). The cycle-specific reaction was also applicable to olefin diamination and amino-oxidation reactions. Employing *N*-Boc-protected silyloxycarbamate (**31**; Boc = *tert*-butoxycarbonyl, TBS = *tert*-butyl dimethylsilyl) in conjunction with dibenzylazodicarboxylate (**21**) afforded the diamination products **27** (7:1 *anti/syn*, 99% *ee* with catalyst combination G) and *epi*-**27** (8:1 *syn/anti*, 99% *ee* with catalyst combination H). A related Cbz-protected amine nucleophile **32** and nitrosobenzene (**22**) as electrophile formed the amino-oxidation products with excellent diastereo- and enantioselectivities (catalyst combination G for **28**: 17:1 *anti/syn*, 99% *ee*; catalyst combination H for *epi*-**28**: 14:1 *syn/anti*, 99% *ee*).

In order to further demonstrate its viability, MacMillan *et al.* applied their multicatalysis system in combination with a metal-catalyzed olefin cross-metathesis to a triple cascade reaction for the synthesis of an intermediate of the natural product (–)-aromadendranediol^[51] (**37**; Scheme 6). Thus, the use of Grubbs' second generation catalyst **33**, 5-hexene-2-one (**34**) and crotonaldehyde (**24**) allowed the formation of ketoenal **35** in the first step. The sequential addition of imidazolidinone catalyst (2*S*,5*S*)-**23** and silyloxyfuranyl **36** as nucleophile led to the formation of intermediate **37** through an iminium-activated Mukaiyama-Michael reaction. Upon addition of (*S*)-**8** as enamine-catalyst, intermediate **37** underwent a diastereoselective intramolecular aldol reaction furnishing the complex key intermediate **38** (64% yield, 5:1 d.r., 95% *ee*), which already contains four of the six required stereogenic centers and 12 of the 15 necessary carbon atoms.

The synthesis of (–)-aromadendranediol (**39**) could then be accomplished in eight further linear steps with 40% overall yield (starting from **38**). For comparison, a previously reported synthesis starting from enantiomerically pure (+)-spathulenol afforded (–)-aromadendranediol (**39**) in only 13% total yield over three steps.^[51a] Although we will exclusively focus on organocatalyzed reactions in the following, we show this example because it beautifully demonstrates the applicability of organomulticatalysis in the total synthesis of complex natural products.

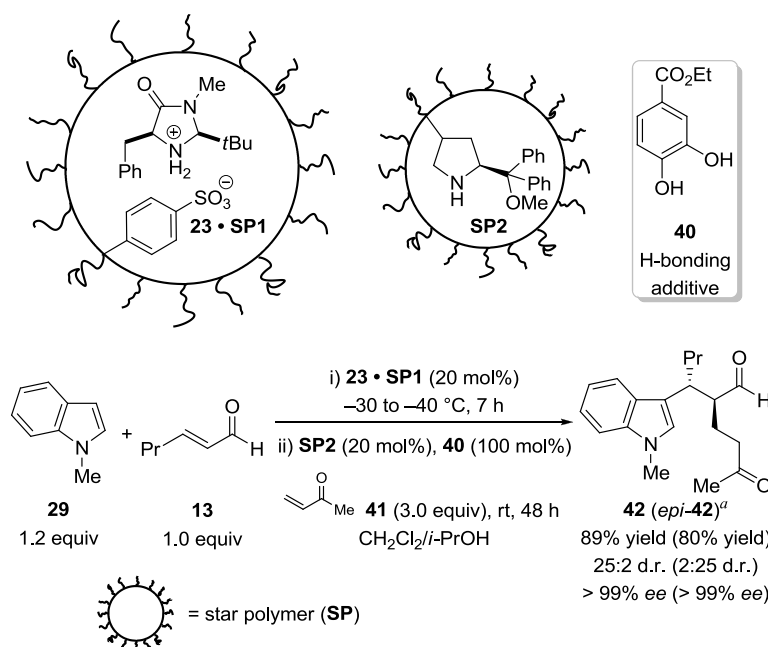


Scheme 6. Multicatalysis approach for the preparation of key intermediate **38** in the total synthesis of the natural product (–)-aromadendranediol (**39**). Catalyst (2*S*,5*S*)-**23** was used as its corresponding 2,4-dinitrobenzoic acid salt. Cy = cyclohexyl; Mes = mesityl (2,4,6-trimethylphenyl).

Note that although Hantzsch esters (as well as analogues thereof and, *e.g.*, benzothiazolines or benzoimidazolines) suffer from poor atom economy they are the hydride source of choice in organocatalysis.^[46] Metal-free transfer hydrogenations with Hantzsch esters proceed under mild reaction conditions and are compatible with various functional groups, making them ideal for domino, tandem, and multicatalytic reactions.^[46]

In 2008, Fréchet and co-workers reported the combination of non-interpenetrating star polymers **SP1** and **SP2** with core-confined catalysts, and hydrogen bonding additive **40** (Scheme 7).^[52] This site-isolation approach allowed the use of otherwise incompatible catalysts, circumventing undesired catalyst interactions. Indeed, small molecule reagents are able to freely diffuse to the core of the star polymers, allowing catalysis to take place. For example, the addition of imidazolidinone (2*S*,5*S*)-**23** to star polymer **SP1** resulted in the formation of salt (2*S*,5*S*)-**23** • **SP1**, which acts as iminium catalyst, thus enabling the conjugate addition of 1-methylindole (**29**) to (*E*)-hex-2-enal (**13**). Addition of **SP2**, methylvinyl ketone (**41**) and **40**

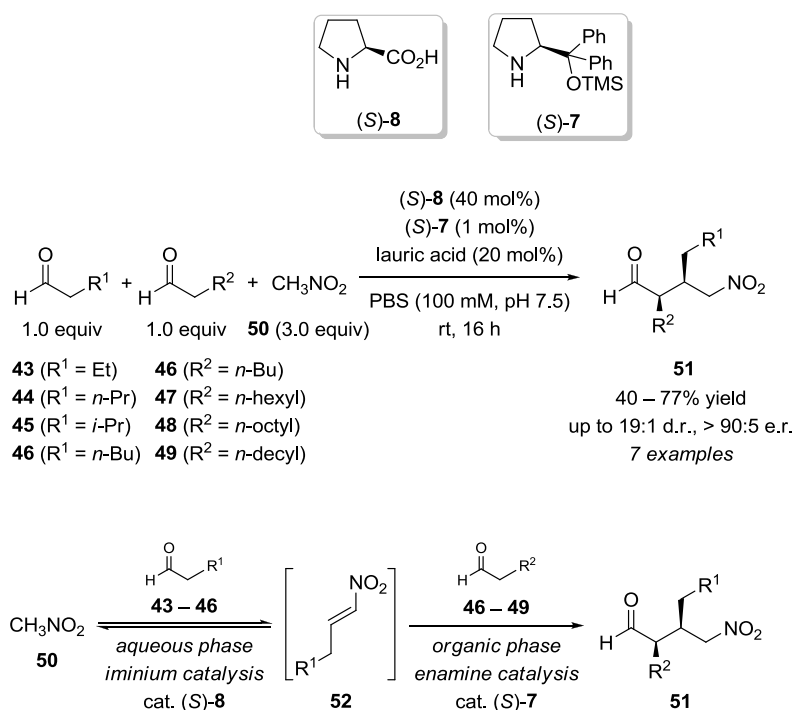
(which was expected to activate the relatively unreactive Michael acceptor **41**) afforded the desired indole derivative **42** with high yield and excellent stereoselectivity (89% yield, 25:2 d.r., > 99% *ee*) through the second Michael reaction. When star polymer **SP1** was replaced with *para*-toluenesulfonic acid and/or **SP2** with the analogues free secondary amine catalyst no desired product was observed. Only traces of product formed when linear polymer analogues of **SP1** and **SP2** were used. Additionally, the use of (2*R*,5*R*)-**23** as iminium catalyst afforded the other diastereomer *epi*-**42** (80% yield, 2:25 d.r., > 99% *ee*) similar to the aforementioned examples.



Scheme 7. Combination of iminium, enamine and H-bonding catalysis using non-interpenetrating starpolymer catalysts (2*S*,5*S*)-**23** • **SP1** and **SP2** for the one-pot synthesis of indole derivative **42**. ^a Values in parentheses indicate reaction using (2*R*,5*R*)-**23** as iminium catalyst.

Later, the same group reported a mult catalysis reaction in aqueous buffer, enabling the polarity-directed, chemoselective formation of desired cross-cascade products.^[53] Employing (*S*)-**8** and (*S*)-**7** as catalysts, this biphasic reaction allowed the differentiation of two aldehydes with similar chemical reactivity based on their different polarity to form a major cross-cascade product **51** (Scheme 8). Preliminary studies indicated that the success of this reaction is based on some special requirements. Hence, the first amine catalyst (*S*)-**8**, dissolves well in the aqueous phase, but poor in organic solvents. The other amine catalyst (*S*)-**7**, in conjunction with lauric acid as hydrophobic acid co-catalyst, shows a greater miscibility with the organic phase rather than water (even slightly water-miscible organic acids turned out to be problematic because they lower the pH of the aqueous phase and therefore slow down the condensation reaction). Moreover, (*S*)-**8** is an efficient catalyst for the condensation reaction, but a poor catalyst for the conjugate addition under aqueous conditions. In sharp contrast, diphenylprolinol (*S*)-**7** is

inefficient in the condensation reaction, but an efficient and highly enantioselective catalyst for the conjugate addition of aldehydes to nitroalkenes. On the basis of these requirements, Fréchet and co-workers succeeded in the development of a biphasic reaction facilitating the selective activation of the two aldehydes. In aqueous phase, the use of a large amount of (*S*)-**8** (40 mol%, respectively) efficiently catalyzes the reversible condensation of the less hydrophobic aldehydes **43** – **46** ($R^1 = \text{Et}$, *n*-Pr, *i*-Pr, *n*-Bu) and nitromethane (**50**). In the organic phase, the use of only 1 mol% of catalyst (*S*)-**7** slows down the addition reaction, so that the aldehydes **43** – **46** are readily consumed in the condensation step, suppressing the addition of the more hydrophobic aldehydes **46** – **49** ($R^2 = n\text{-Bu}$, *n*-hexyl, *n*-octyl, *n*-decyl) to the nitroalkene intermediate **52**, thus avoiding the formation of undesired by-products. Consequently, the aldehydes **46** – **49** survive the condensation step and react with the nitroalkene intermediate **52** in the organic phase to give exclusively **51**. Indeed, only traces of by-products could be detected. This approach sheds light on the cycle-specific activation of reagents as well as intermediates based on physical (polarity) rather than chemical properties.



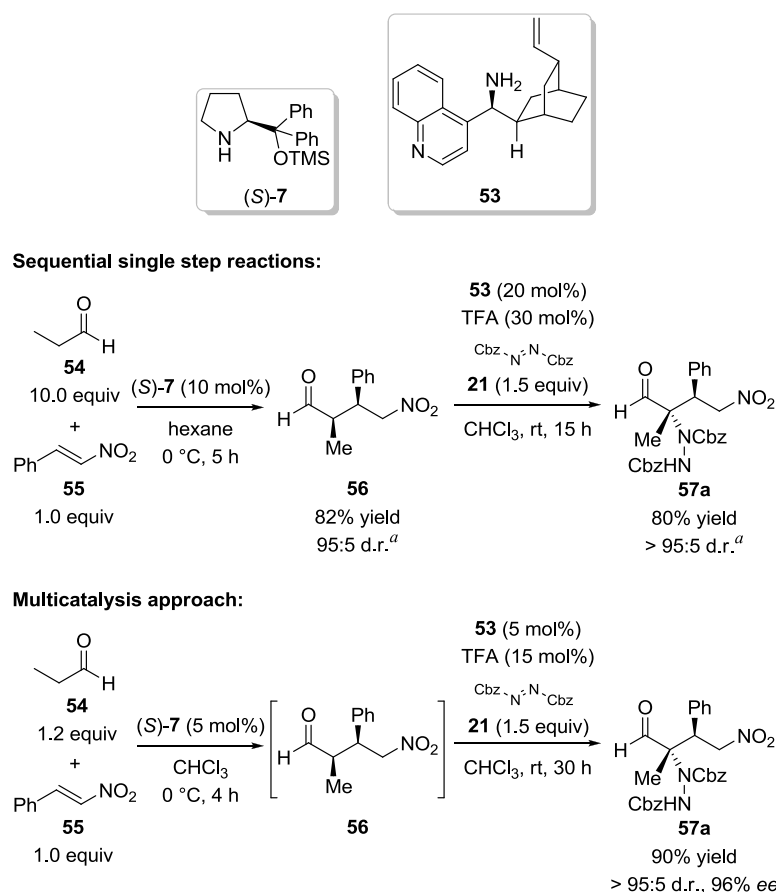
Scheme 8. Biphasic polarity-directed reaction in aqueous buffer employing two aldehydes with similar reactivity but different polarity.

Contrary to the above examples, Moreau and Greck envisaged a multicatalytic reaction comprising two consecutive enamine cycles, based on two previously developed reactions, a Michael addition of aldehydes to β -nitrostyrene (**55**)^[48b] and a Michael addition/ α -amination cascade reaction,^[54] respectively (Scheme 9 and Table 1).^[55] Indeed, the combination of (*S*)-**7** and 9-amino(9-deoxy)*epi*-cinchonine (**53**; 5 mol% for both), propionaldehyde (**54**), nitrostyrene

(**55**), and electrophilic dibenzylazodicarboxylate (**21**) afforded the desired α -hydrazino aldehyde **57a** (80% yield, >95:5 d.r., 96% *ee*). When both reactions were performed independently, 10 mol% of **7** and a tenfold excess of aldehyde **54** (instead of 1.2 equivalents) were necessary to afford the intermittent Michael addition product **56** (82% yield, 95:5 d.r.) in the first reaction (Scheme 9). The second reaction, using the previously reported conditions^[54] (20 mol% **53**, 30 mol% TFA, 1.5 equivalents of **21**), gave the expected product **57a** in 80% yield (66% yield overall) and in >95:5 d.r. Various other nitroalkenes **58** bearing electron-rich (**57b** and **57c**; Table 1, entries 2 and 3) and electron-deficient aryl groups (**57d–57h**; entries 4–8) with different substitution pattern (*i.e.*, *para*- or *meta*-substituted) could be used under the optimized conditions, affording the corresponding products **57** as a single diastereomer with good yields (73 – 85%) and high enantioselectivities (96 – 98% *ee*).

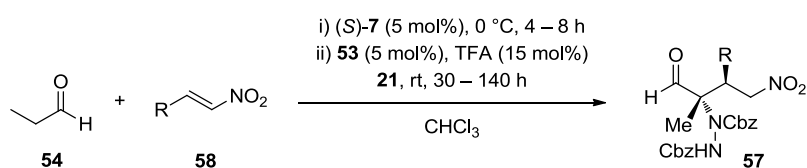
Very recently, the combination of Jørgensen's TMS-protected diarylprolinol (*S*)-**59**^[56] and (*S*)-**8** was reported by the group of Díez to participate in the sequential Michael/Morita-Baylis-Hillman with concomitant Knoevenagel condensation reaction cascade of Nazarov reagent **60** with α,β -unsaturated aldehydes leading to 2-alkylidene cyclohexanones **65** (Scheme 10).^[57] The success of the reaction was based on the combination of the two amine catalysts (*S*)-**59** and (*S*)-**8**. For example, using only (*S*)-**59** gave the Michael addition product as a mixture of diastereomers (*syn/anti* 1:1), but did not afford any cyclization product. The same was observed when (*S*)-**7** was used as catalyst; with MacMillan's imidazolidinone (2*S*,5*S*)-**23** only starting material could be detected. When (*S*)-**8** was applied for the total reaction the desired products **65** formed with reasonable diastereomeric ratio (*E/Z* = 2:1) and yields, but no enantioselectivity could be achieved under these conditions. In contrast, the conjugate addition reaction of **60** with α,β -unsaturated aldehydes **13** and **61–64** catalyzed by (*S*)-**59** and sequential addition of (*S*)-**8** after consumption of the starting material afforded the cyclized products **65** (*E/Z* = 2:1 in all cases) with moderate to good yields and high enantiomeric ratios (41 – 77% yield; up to 98:2 e.r.). However, the reaction did not proceed with aryl aldehydes.^[57]

As the scope of secondary amines is limited to carbonyl compounds the combination of these catalysts with other organocatalysts is highly desirable to provide a way to reactions otherwise not attainable.



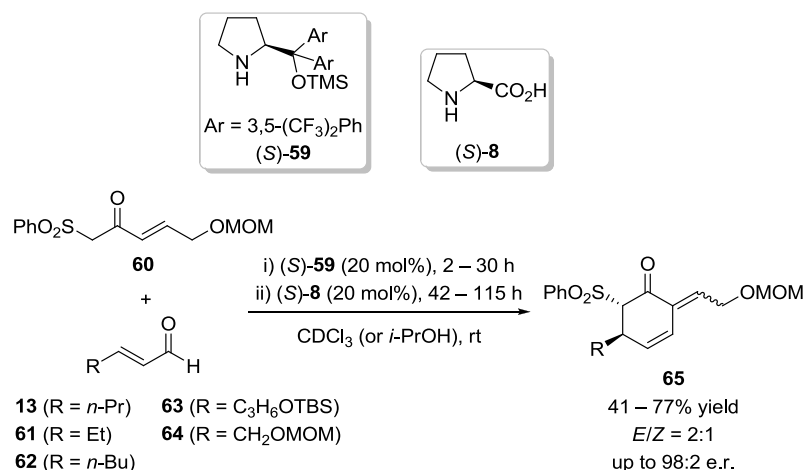
Scheme 9. Comparison of the sequential preparation and the one-pot multicatalytic synthesis of product **57a**. ^a No enantiomeric excess given.

Table 1. Michael addition/ α -amination reaction sequence through double enamine activation. Table corresponds to Scheme 9.



Entry	R	Product	Yield (%)	ee (%)
1	Ph	57a	90	96
2	1-naphthyl	57b	73	96
3	4-MePh	57c	85	96
4	4-MeOPh	57d	85	97
5	4-ClPh	57e	85	98
6	4-FPh	57f	81	97
7	3-ClPh	57g	85	98
8 ^a	3-MeOPh	57h	76	96

^a 10 mol% of (S)-7 were used.



Scheme 10. Michael/Morita-Baylis-Hillman/Knoevenagel condensation reaction sequence for the preparation of 2-alkylidene cyclohexanones **65**. MOM = methoxymethyl.

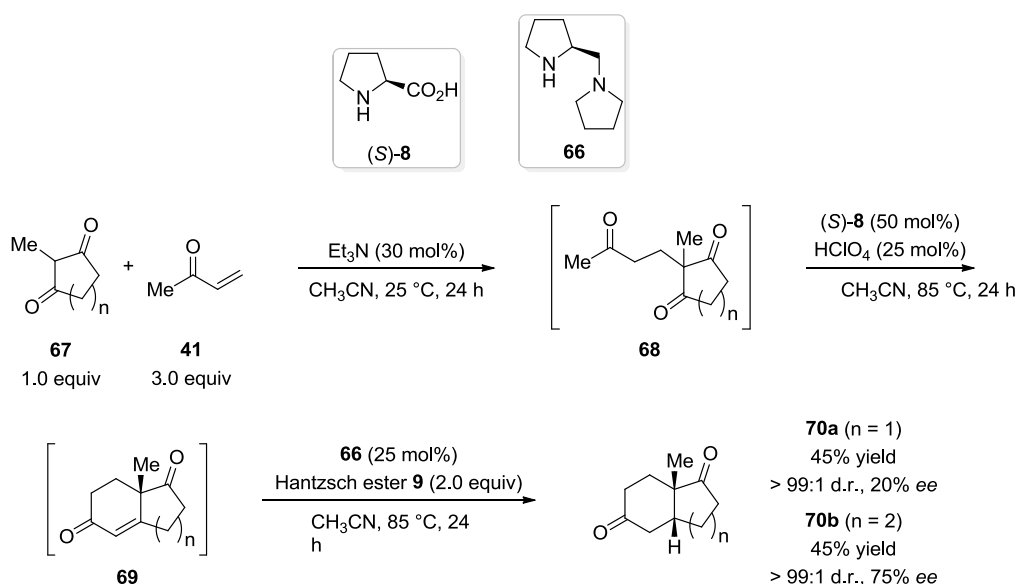
3.2 Combinations of Secondary Amine Catalysts with Brønsted Acids and Bases

During the last few years, the group of Ramachary reported a variety of multicomponent reactions and multicomponent catalysis providing direct access to a variety of valuable compounds (most of them being achiral), such as agrochemicals, fine chemicals, as well as pharmaceutical drugs, drug intermediates, and building blocks for the synthesis of natural products.^[58] However, as already mentioned above we focus on asymmetric organocatalyzed variants here.

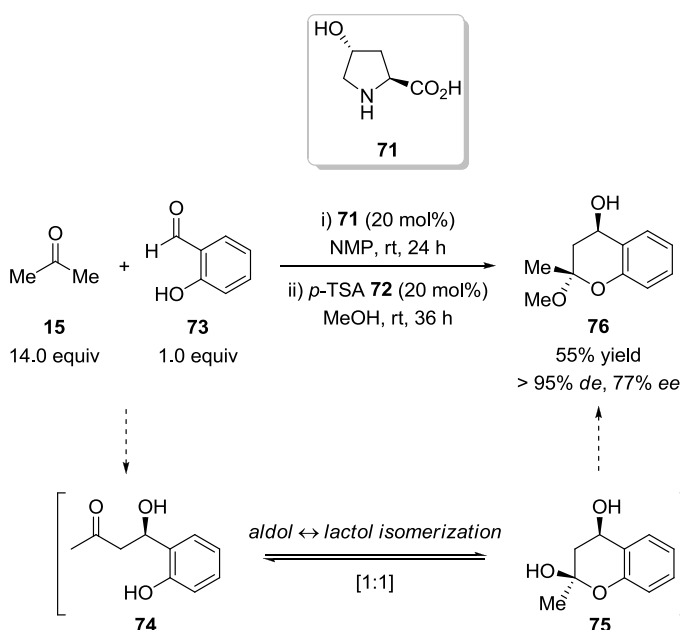
After the successful demonstration of the one-pot asymmetric syntheses of the Wieland-Miescher^[59] and Hajos-Parrish^[60] ketones and their analogues *via* a three-component reductive alkylation and Robinson annulation,^[61,62] Ramachary *et al.* investigated the one-pot asymmetric synthesis of the corresponding hydrogenated derivatives by combining three components and four catalysts, triethylamine, **(S)-8**, perchloric acid, and **(S)-1-(2-pyrrolidinyl-methyl)pyrrolidine** (**66**), respectively (Scheme 11).^[63] Therefore, they suggested a triethylamine-catalyzed regio-selective Michael reaction of diketones **67** and methylvinyl ketone (**41**) followed by a Robinson annulation of intermediate Michael adducts **68** through amino acid/Brønsted acid catalysis furnishing the chiral Wieland-Miescher and Hajos-Parrish ketones **69** ($n = 1, 2$). Final iminium activated stereoselective hydrogenation of the respective intermediates **69** with Hantzsch ester **9** and diamine catalyst **66** would then lead to hydrogenated Hajos-Parrish ketone **70a** or Wieland-Miescher ketone **70b**. Indeed, the sequential combination of **67** and **41** with Hantzsch ester **9** and catalytic amounts of triethylamine, **(S)-8**, perchloric acid, and **66** afforded the hydrogenated Wieland-Miescher ketone **70b** in 45% yield with >99% d.r. and 75% *ee*. However, the hydrogenated Hajos-Parrish ketone **70a** was obtained in 45% yield and >99% d.r., but only 20% *ee* (the corresponding **(S)-8** catalyzed two-component reaction affords the intermediate Hajos-

Parrish ketone (**69**, $n = 1$) with 86% *ee*).^[62] This was proposed to be because of the involvement of triethylamine in the transition state of the (*S*)-**8** promoted intramolecular aldol reaction.^[63]

Another mult catalysis reaction was reported by the same group, combining amino catalysis and Brønsted acid catalysis for the synthesis of a chiral chromane **76** (Scheme 12).^[64] The *trans*-4-



Scheme 11. Asymmetric synthesis of hydrogenated Hajos-Parrish ketone **70a** and Wieland-Miescher ketone **70b** through the one-pot combination of three components and four catalysts reported by Ramachary.



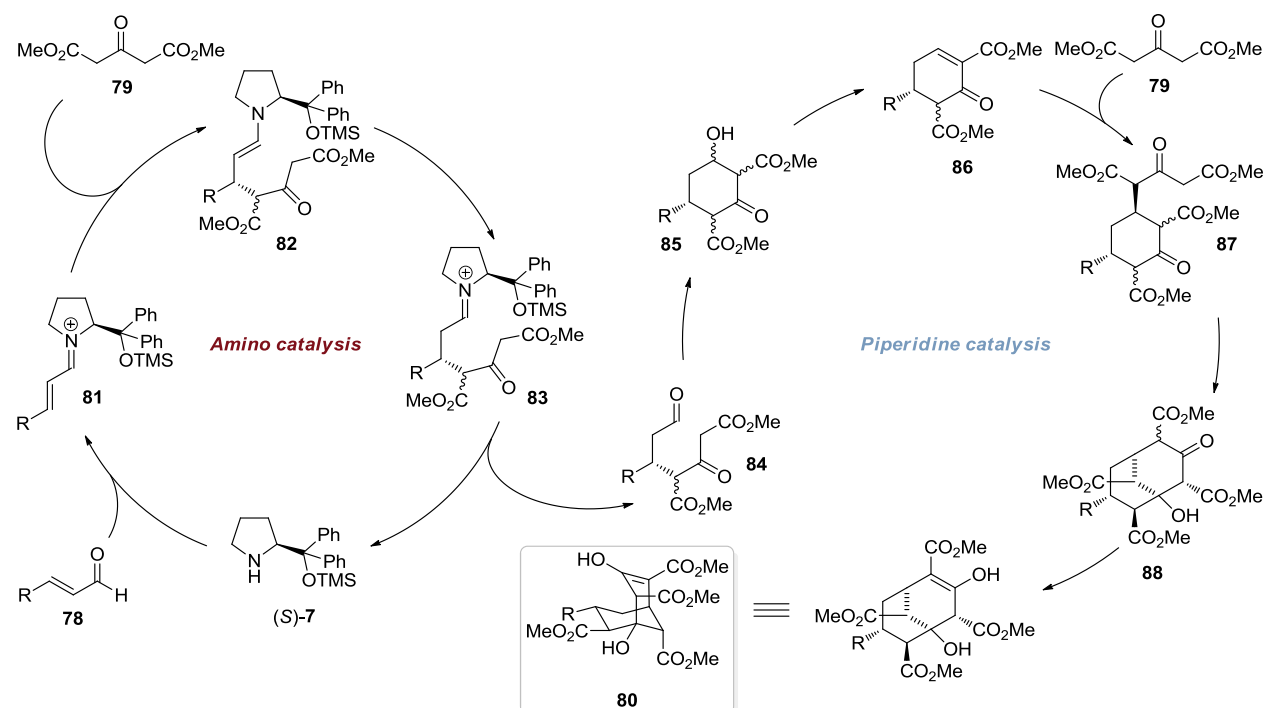
Scheme 12. Multicatalytic synthesis of chromane derivatives reported by Ramachary. NMP = *N*-methylpyrrolidinone.

hydroxy-L-proline (**71**) catalyzed reaction of acetone (**15**) and 2-hydroxybenzaldehyde (**73**) via Barbas-List aldol reaction gave intermediate **74** which is in a fast dynamic equilibrium with its lactol form **75**. Subsequent treatment with *para*-toluenesulfonic acid (*p*-TSA; **72**) in methanol selectively afforded the chiral *trans*-2-methoxy-2-methylchroman-4-ol (**76**) in 55% yield with >95% *de* and 77% *ee* (Scheme 12).^[64]

An impressive example of stereocontrol was reported by Jørgensen *et al.* employing (*S*)-**7** and piperidine (**77**) as catalysts for the formation of complex chiral bicyclo[3.3.1]non-2-enes **80**, starting from simple α,β -unsaturated aldehydes **78** and dimethyl 3-oxopentanedioate (**79**; Table 2).^[65] Four new carbon–carbon bonds formed, affording the desired product **80** bearing six stereogenic centers with excellent diastereo- and enantioselectivity (up to >99:1 d.r. and 96% *ee*) out of 64 theoretically possible stereoisomers. Jørgensen and co-workers proposed the following mechanism for the formation of the six stereogenic centers in **80** (Scheme 13).^[65] The reaction is initiated by standard iminium ion catalysis by diphenylprolinol silylether (*S*)-**7** with

Table 2. Asymmetric two-component reaction for the formation of bicyclo[3.3.1]non-2-enes.

Entry	R	Product	Yield (%)	d.r.	<i>ee</i> (%)
1	Et	80a	48	>99:1	94
2	<i>i</i> -Pr	80b	65	>99:1	96
3	<i>n</i> -heptyl	80c	69	88:12	95
4	EtO ₂ C	80d	38	>99:1	89
5	(<i>Z</i>)-hex-3-enyl	80e	51	94:6	94
6	Ph	80f	70	>99:1	93
7	4-MeOPh	80g	93	92:8	91
8	2-furyl	80h	86	94:6	90
9	2-BrPh	80i	86	>99:1	96

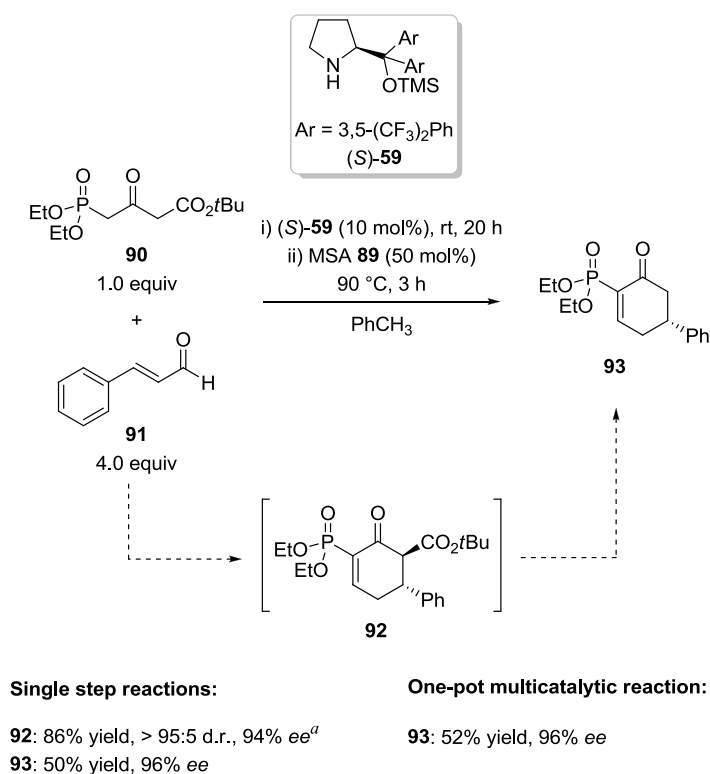


Scheme 13. Mechanistic proposal for the formation of bicyclo[3.3.1]non-2-enes **80**.

enals **78** generating **81**, which is nucleophilically attacked at the β -carbon atom by dimethyl 3-oxopentanedioate (**79**), thus leading to enamine **82**. Formation of iminium ion intermediate **83** and subsequent hydrolysis releases **84** with the first two stereogenic centers. In the second cyclization reaction of intermediate **84** with its second activated methylene functionality leads to **85** which, after elimination of water, gives intermediate **86**. The cyclization step is possibly preceded by hydrolysis of secondary amine catalyst (*S*)-**7**, however, this could not be clarified. Conjugate addition with a second molecule of **79** leads to **87** (the stereoinduction in this step arises from steric hindrance of the former created stereogenic center bearing R).^[65] Final ring closure between the last free activated methylene and the central ketone furnishes product **88**. Due to strong intramolecular hydrogen bonding, tautomeric equilibration leads to the more stable aldehydes **78**. For example, aliphatic aldehydes (**80a** – **80c**; Table 2, entries 1 – 3), esters (**80d**; entry 4), and olefins (**80e**; entry 5) were applicable. Superior yields were achieved employing aromatic compounds, *e.g.*, *para*- and *ortho*-substituted phenyls (**80g** and **80i**; entries 7 and 9) or heteroaromatic substituents, such as furyl (**80h**; entry 8). Importantly, the products **80** could be purified by crystallization after completion of the reaction, thus avoiding waste-generating chromatographic steps.^[65]

One year later, the same group reported an organocatalytic Michael/Knoevenagel domino reaction for the synthesis of optically active 3-diethoxyphosphoryl-2-oxocyclohex-3-ene-carboxylates.^[66] In order to demonstrate the synthetic feasibility of these products, Jørgensen *et al.* performed consecutive reactions, one of it being multicatalytic. Hence, Jørgensen and co-workers envisioned a hydrolysis/decarboxylation reaction as an entry to 5-substituted

2-diethoxyphosphorylcyclohex-2-enones, such as **90** (Scheme 14). In this example, the (*S*)-**59** catalyzed domino Michael/Knoevenagel condensation reaction of 4-diethoxyphosphoryl-3-oxobutanoate (**90**) and cinnamaldehyde (**91**) afforded *tert*-butyl-2-oxocyclohex-3-carboxylate (**92**). Subsequent methanesulfonic acid (MSA; **89**) catalyzed hydrolysis/decarboxylation then gave the target compound 2-diethoxyphosphoryl-5-phenylcyclohex-2-enone (**93**) in 52% yield and 96% *ee*. The stepwise synthesis yielded **93** in slightly lower yield (43% over two steps) and same enantiomeric excess.^[66] However, the one-pot synthesis avoids intermediate work-up, isolation, and purification of **92**, thus is more time-cost-efficient.

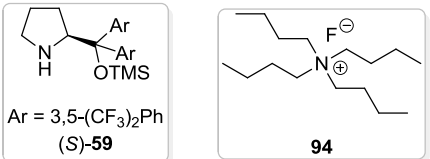


Scheme 14. Stepwise and multicatalytic synthesis of 2-diethoxyphosphoryl-5-phenylcyclohex-2-enone **93**. ^a First reaction was performed in dichloromethane.

In the same year, García Ruano and Alemán reported the successful combination of amino catalysis and fluoride catalysis using (*S*)-**59** and *n*-tetrabutylammonium fluoride (TBAF; **94**) for the synthesis of pentasubstituted cyclohexanes **96** (Table 3).^[67] The reaction proceeds *via* a Michael addition of diketones **95** to α,β -unsaturated aldehydes **78** promoted by (*S*)-**59**. Subsequent addition of nitromethane (**50**) and TBAF (**94**) leads to the generation of a nitromethane anion (by fluoride) which first reacts with the Michael adduct in an intermolecular Henry reaction, thus affording a nitroalcohol intermediate. This subsequently undergoes a second, intramolecular Henry reaction catalyzed by **94** to give the densely functionalized cyclohexanes **96** with high stereoselectivities (>98:2 d.r., 92 to >99% *ee*) although in only moderate yields (35 – 57%). The stereochemical outcome of the reaction was proposed to be due

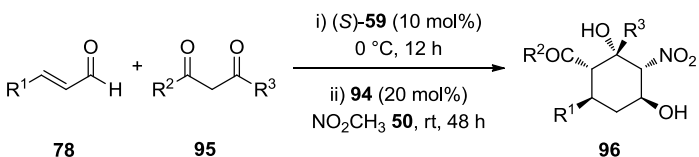
to the reversibility of the two Henry reactions, leading to the thermodynamically favoured (equatorial arrangement of all substituents except the hydroxyl group that is intramolecularly associated to the nitro group) instead of the kinetically favoured product. Therefore, the enantioselectivity is defined by amine catalyst (*S*)-**59** in the first step (employing (*R*)-**59** as amine catalyst afforded the enantiomer *ent*-**96b**; Table 3, entry 4). When other fluoride sources were used instead of **94** the corresponding product was isolated with decreased enantioselectivity, possibly due to a retro-Michael side-reaction.^[67]

Table 3. Combination of amino and fluoride catalysis for the synthesis of cyclohexane derivatives with five contiguous stereogenic centers.



Ar = 3,5-(CF₃)₂Ph
(*S*)-**59**

94



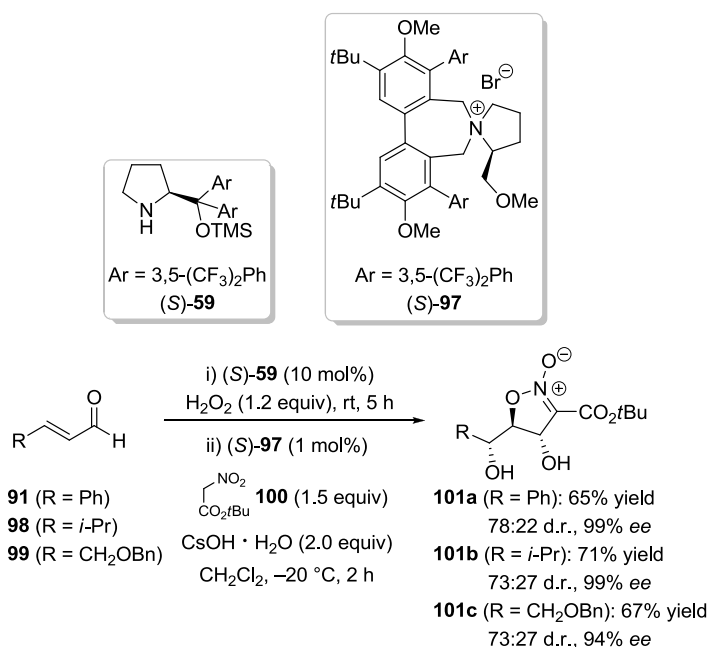
78 **95** **96**

Entry	R ¹	R ²	R ³	Product	Yield (%)	d.r.	ee (%)
1 ^a	Et	Ph	Ph	96a	45	>98:2	99
2 ^a	Me	Ph	Ph	96b	55	>98:2	>99
3 ^{a,b}	Me	Ph	Ph	96b	47	>98:2	99
4 ^c	Me	Ph	Ph	<i>ent</i> - 96b	57	>98:2	>99
5	<i>n</i> -Pr	Ph	Ph	96c	46	>98:2	92
6	<i>n</i> -pentyl	Ph	Ph	96d	40	>98:2	>99
7	<i>n</i> -nonyl	Ph	Ph	96e	40	>98:2	92
8	<i>n</i> -Bu	Ph	Ph	96f	43	>98:2	92
9	<i>n</i> -hexyl	Ph	Ph	96g	42	>98:2	>99
10	(<i>Z</i>)-hex-3-enyl	Ph	Ph	96h	42	>98:2	94
11	C ₂ H ₄ Ph	Ph	Ph	96i	46	>98:2	>99
12	Me	PMP	PMP	96j	35	>98:2	98
13	Me	Ph	Me	96k	44	>98:2	98
14	Et	Ph	Me	96l	47	>98:2	94
15 ^c	Ph	Ph	Ph	96m	—	—	—

^a First step was performed at rt for 4 h; second step was performed for 18 h. ^b Preparative experiment on 2.0 mmol scale. ^c (*R*)-**59** was used.

3.3 Miscellaneous Combinations with Secondary Amines

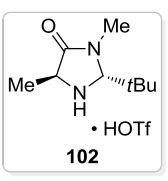
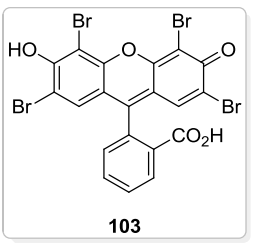
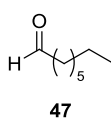
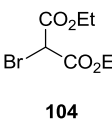
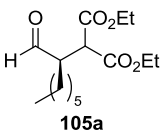
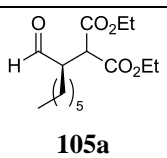
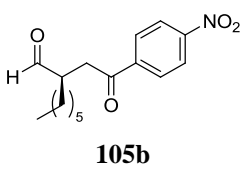
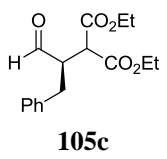
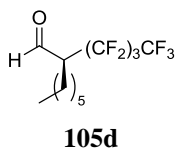
In 2009, Jørgensen and coworkers reported the combination of prolinol (*S*)-**59** and chiral Lygo-type ammonium salt (*S*)-**97**^[68] as phase-transfer catalyst^[69] for a novel one-pot synthesis of 4,5-substituted isoxazoline-*N*-oxides **101** (Scheme 15).^[70] The reaction is initiated by the asymmetric epoxidation of α,β -unsaturated aldehydes by hydrogen peroxide through iminium catalysis, followed by a base-mediated intermolecular Henry reaction with nitroacetate **100** under phase-transfer conditions. Consecutive intramolecular S_N2 -like *O*-alkylation then affords the isoxazoline-*N*-oxides **101**. Aromatic, aliphatic and functionalized aldehydes **91**, **98**, and **99** were applicable providing the desired products **101** in good yields (65 – 71%) and diastereomeric ratios (up to 78:22 d.r.), and excellent enantioselectivities (99% *ee*). These products are only a few reaction steps from highly valuable synthetic targets. For instance, **101c** could be readily converted into a β,γ,δ -trihydroxylated α -amino acid derivative.^[70]



Scheme 15. Merging amino and phase-transfer catalysis for the synthesis of isoxazoline *N*-oxides.

The concept of photoredox catalysis was first disclosed by MacMillan through the combination of organometallic complexes and secondary amine catalysts.^[71] However, the applied ruthenium and iridium salts are expensive and potentially toxic, which represents a major drawback of these catalysts. A metal-free, organocatalytic photoredox reaction was presented recently by Zeitler *et al.* using MacMillan's imidazolidinone **102**^[71] in conjunction with readily available, inexpensive xanthene dye eosin Y (**103**) as photosensitizer (Table 4).^[72] The reaction gave the desired products **105** with good yield and high enantioselectivities. However, the selectivities showed to be temperature dependent (Table 4, entries 1, 4, and 5). For instance, at room temperature **105a**

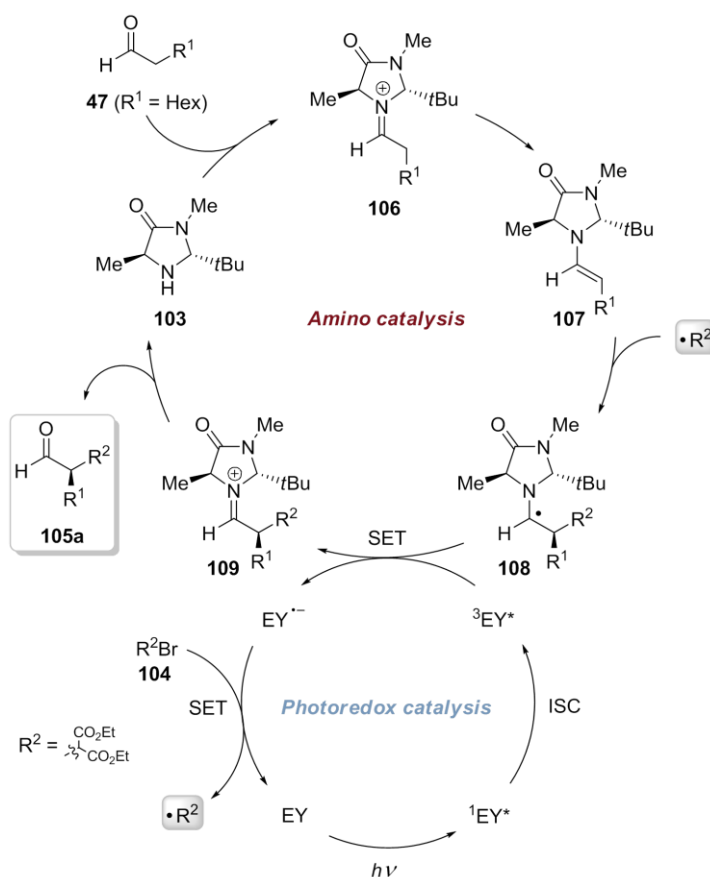
Table 4. Metal-free, asymmetric organophotoredox catalysis with visible light.

<div style="display: flex; justify-content: space-around; align-items: center;"> <div style="text-align: center;">  <p>102</p> </div> <div style="text-align: center;">  <p>103</p> </div> </div>				
<p style="text-align: center;"> 102 (20 mol%), 103 (0.5 mol%) lutidine (2.0 equiv) $h\nu$ (λ = 530 nm, LED) DMF, rt, 18 h </p>				
<div style="display: flex; align-items: center; justify-content: center;"> <div style="text-align: center;">  <p>47</p> </div> <div style="margin: 0 10px;">+</div> <div style="text-align: center;">  <p>104</p> </div> <div style="margin-left: 20px;"> \longrightarrow </div> <div style="text-align: center;">  <p>105a</p> </div> </div>				
Entry	Conditions	Product	Yield (%)	ee (%)
1	as shown above	 <p>105a</p>	63	77
2	23 W fluorescent bulb was used instead of LED	105a	78	80
3	23 W fluorescent bulb and [Ru(bpy) ₃]Cl ₂ were used instead of LED	105a	75	76
4	reaction was performed at 0 °C	105a	70	81
5	reaction was performed at –5 °C	105a	85	88
6 ^a	sunlight; reaction performed at ≈ 30 °C	105a	77	76
7 ^b	reaction was performed at 5 °C	 <p>105b</p>	82	95
8 ^c	as described above	 <p>105c</p>	76	86
9 ^d	reaction was performed at –15 °C	 <p>105d</p>	56	96

^a Full conversion after 4 h. ^b *para*-nitrophenacyl bromide was used instead of diethyl bromomalonate (**104**).

^c Phenylpropionaldehyde was used instead of octanal (**47**). ^d 1-Iodoperfluorobutane was used instead of diethyl bromomalonate (**104**).

was isolated with 77% *ee* (Table 4, entry 1) whereas a decrease of the reaction temperature to -5°C led to an increase of the enantioselectivity to 88% *ee* (entry 5). Conducting the reaction under direct sunlight led to faster conversion (4 h) but again decreased enantioselectivity, possibly due to the higher reaction temperature (approximately 30°C ; entry 6). The methodology was also applicable to the stereoselective addition of nitrophenacyl (**105b**; entry 7) and polyfluorinated alkyl substituents (**105d**; entry 9) which showed superior selectivities up to 96% *ee*. Additionally, an example was presented using phenylpropionaldehyde instead of diethyl bromomalonate (**104**). Although the mechanism of this reaction is not yet fully understood (initially irradiated samples which were kept in the dark showed an increase in yield), a possible reaction path is depicted in Scheme 16. Thus, eosin Y (**103**; EY) is excited with visible light to its singlet state ($^1\text{EY}^*$) which in turn converts to its more stable triplet state ($^3\text{EY}^*$) through intersystem crossing (ISC). Simultaneously, the amino catalysis cycle is initiated by the formation of iminium ion **106**, consequently generating enamine **107**. Addition of the electron-deficient alkyl radical to **107** gives amino radical **108**, which is subsequently oxidized to iminium species **109** thereby providing the necessary electron for the reductive quenching of the dyes excited state ($^3\text{EY}^*$) through single-electron transfer (SET). The thus generated radical anion ($\text{EY}^{\bullet-}$) in turn acts as a reductant to furnish the alkyl radical by SET with the alkyl halide.



Scheme 16. Proposed mechanism for the organophotoredox catalysis reported by Zeitler *et al.*

According to the proposed reaction pathway a catalytic amount of **108** has to be present as the initial electron reservoir.^[72] This type of reaction is at the border to a dual or synergistic catalysis reaction as the two catalytic cycles are directly coupled.^[26] However, the radical produced in the photoredox cycle independently enters the next cycle.

4. N-Heterocyclic Carbene Catalysts

N-heterocyclic carbenes (NHCs) are versatile organocatalysts^[8,73] due to their ability to render aldehydes nucleophilic, hence inverting their classical reactivity (“Umpolung”).^[74] The nucleophilic addition of a carbene to an aldehyde leads to the formation of a tetrahedral intermediate which undergoes proton transfer to a nucleophilic enaminol, commonly referred to as the Breslow intermediate.^[75] This can act as an acyl anion equivalent (d^1 -synthon), allowing reactions with electrophiles to take place. Depending on the kind of electrophilic component utilized, either benzoin condensation (the electrophile is an alkyl/aryl aldehyde or ketone) or Stetter reaction (the electrophile is an α,β -unsaturated aldehyde or ketone) takes place (Figure 7).^[8,73] In the case of aldehydes bearing a leaving group at the α -position the enaminol can undergo an intramolecular redox reaction (extended Umpolung).^[8,73b,e,f] The elimination of the leaving group generates an enol and after isomerization an activated carboxylate, which is prone to nucleophilic attack.

4.1 Combinations with Secondary Amine Catalysts

Apart from the mentioned combinations of secondary amines with other organocatalysts, multicatalytic reactions employing combinations of chiral secondary amine catalysts and NHCs have begun growing rapidly in the last years. Due to their inherently Lewis basic nature these two catalyst classes can be combined in one pot; both act on carbonyl compounds but show complementary reactivities.

The approach of asymmetric amino and heterocyclic carbene catalysis (AHCC) was first demonstrated in 2007 by Córdova *et al.* for epoxidation–esterification, cyclopropanation–esterification, and aziridination–esterification reactions (Scheme 17).^[76] Employing diphenylprolinol silylether (*S*)-**7** and thiazolium salt **110**^[77] (Bn = benzyl) as catalysts, and hydrogen peroxide, diethylbromomalonate (**104**), or Cbz-protected carbamate **117** enabled the enantioselective synthesis of β -hydroxy esters **113** (up to 82% yield, 95% *ee*), β -malonate esters **116** (up to 74% yield, 97% *ee*), and β -amino ester derivative **118** (41% yield, 61% *ee*) from various readily available α,β -unsaturated aldehydes through the intermediacy of the corresponding 2,3-epoxy, cyclopropyl, and 2,3-aziridine aldehydes (Scheme 17).^[76] Although very useful chiral molecules were accessible by this approach, the reactions suffered from relatively high catalyst loadings of 10 – 20 mol% for amine catalyst (*S*)-**7** and up to 40 mol% for carbene catalyst **110**.

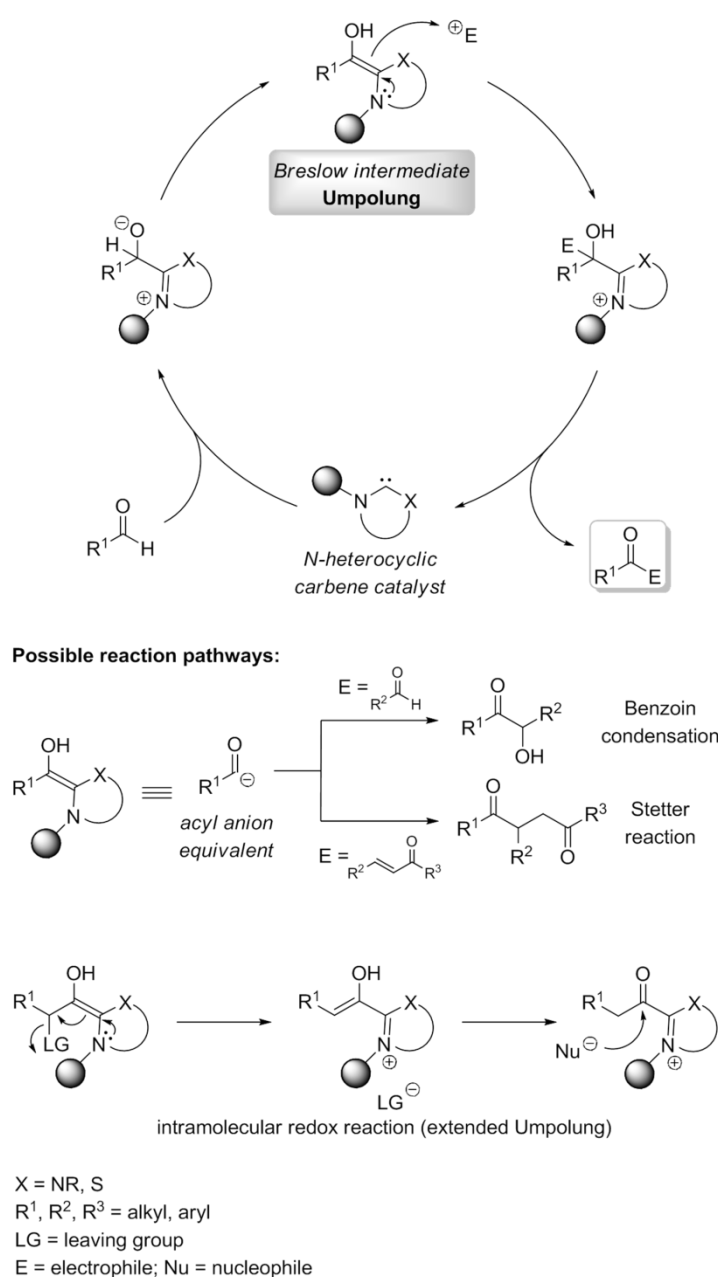
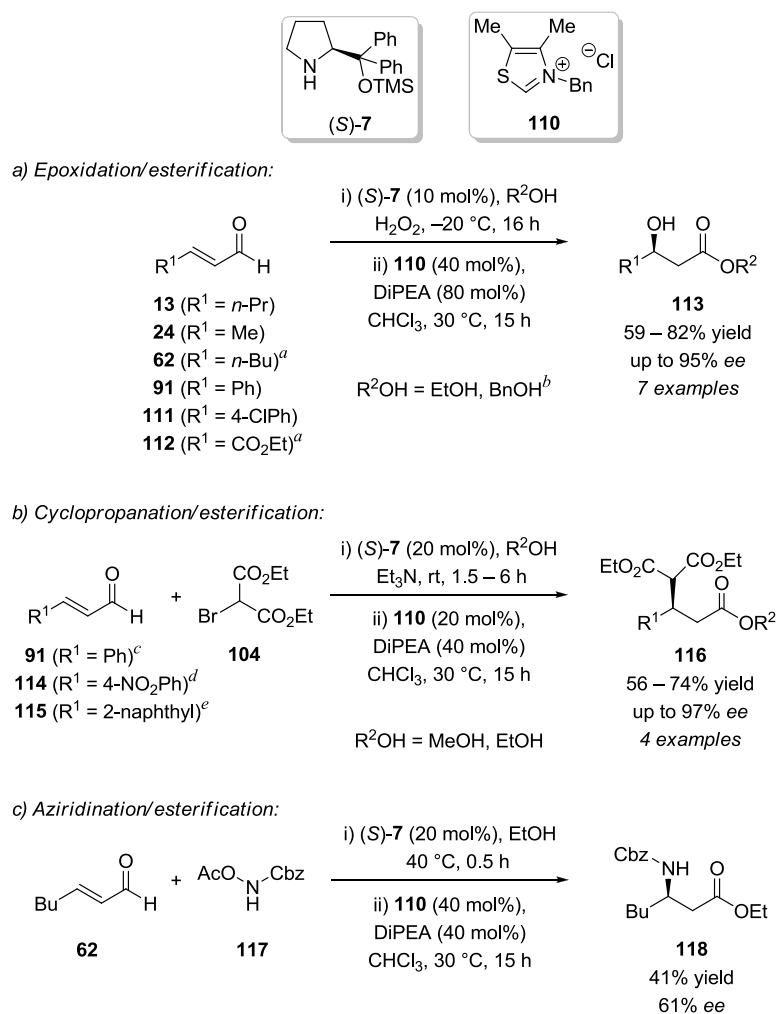


Figure 7. General representation of *N*-heterocyclic carbene catalysis and reactions important in the context of this publication.

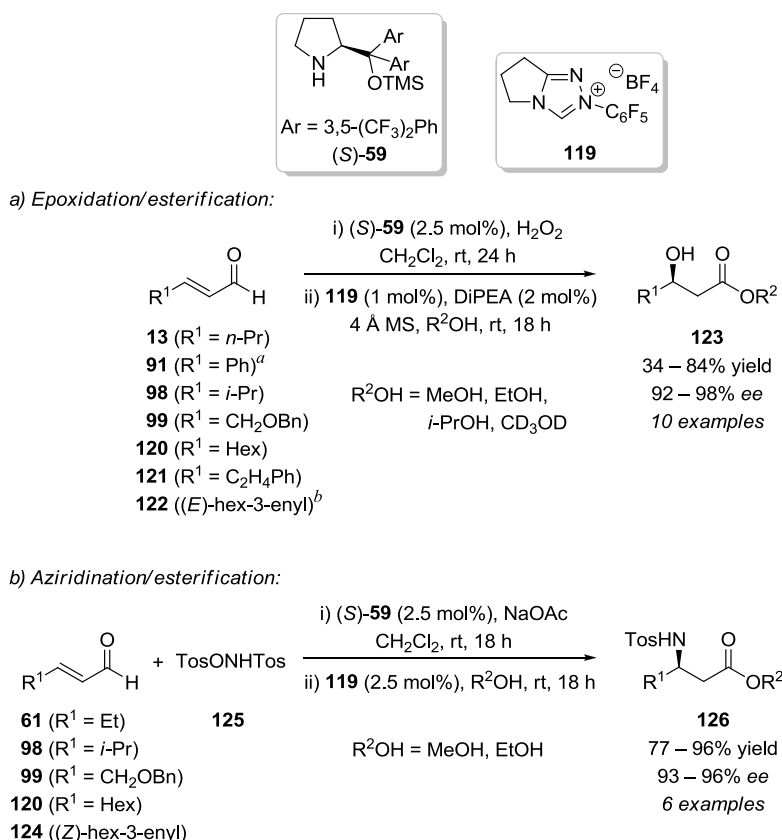
By employing (*S*)-**59** and Rovis *et al.*'s *N*-heterocyclic carbene catalyst precursor **119**^[78] Jørgensen and co-workers could employ drastically lower catalyst loadings (2.5 mol% of amine catalyst (*S*)-**59** and down to 1 mol% for the carbene **119**) for similar transformations, thus significantly improving the efficiency and sustainability of these reactions (Scheme 18).^[79] The addition of 4 Å molecular sieves to remove excess water from the epoxidation step that competes as nucleophile with the alcohols in the final esterification step proved to be crucial to achieve high yields. Linear and γ -branched, as well as functionalized α,β -unsaturated aldehydes provided the β -hydroxylated esters in good yields and enantioselectivities (up to 84% yield, 98% *ee*). However, cinnamaldehyde (**91**) as the enal component required higher catalyst loading of (*S*)-**59** (10 mol%) for the epoxidation step (Scheme 18). Various alcohols were applicable as nucleo-

philes (*i*-PrOH gave only poor yields due to increased steric bulk and reduced nucleophilicity; for **124** used as enal: 34% yield). Moreover, employing different enals and **125** (Tos = 4-toluenesulfonyl (tosyl)) significantly higher yields and enantioselectivities compared to the previously reported procedure could be achieved for the preparation of β -amino esters **126**.^[80] The active carbene catalyst was generated by remaining NaOAc from the aziridination step, thus avoiding the addition of Hünig's base for the second reaction. Note, however, that the carbamate **117** used by Córdova is more environmentally friendly and atom economy is better compared to **125** due to the release of acetate instead of tosylate. Both epoxidation–esterification as well as aziridination–esterification were additionally tested employing the commercially available citral **127** as enal substrate under the developed conditions (Scheme 19). Starting from a 1:1 (*E/Z*) mixture in **127** the intermediate 2,3-epoxy aldehyde **128a** and aziridine aldehyde **128b** formed in 3:1 diastereomeric ratio, due to possible isomerisation during the reaction. Subsequent ring-



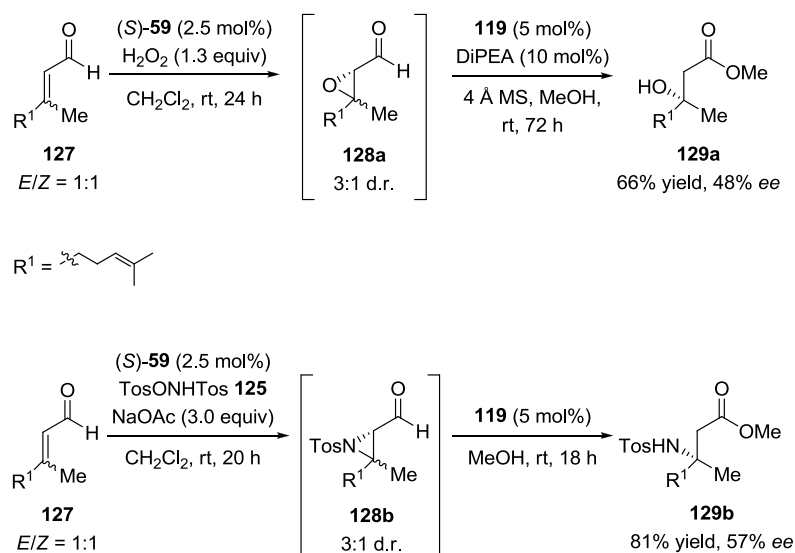
Scheme 17. AHCC catalysis for the synthesis of β -substituted esters reported by Córdova. ^a Epoxidation was performed at 4°C for 6 h; ^b BnOH was added after completion of the epoxidation; ^c 30 mol% **110** were used for the esterification with MeOH; ^d Cyclopropanation was performed for 1.5 h; ^e Cyclopropanation was performed at 4°C for 6 h.

opening gave the desired products **129** bearing tertiary hydroxyl or amino moieties, however, with moderate enantioselectivities (the significant amount of the minor diastereomers **128a** and **128b** possibly leads to the formation of the wrong enantiomer; **129a**: 66% yield, 48% *ee*; **129b**: 81% yield, 57% *ee*).^[79]

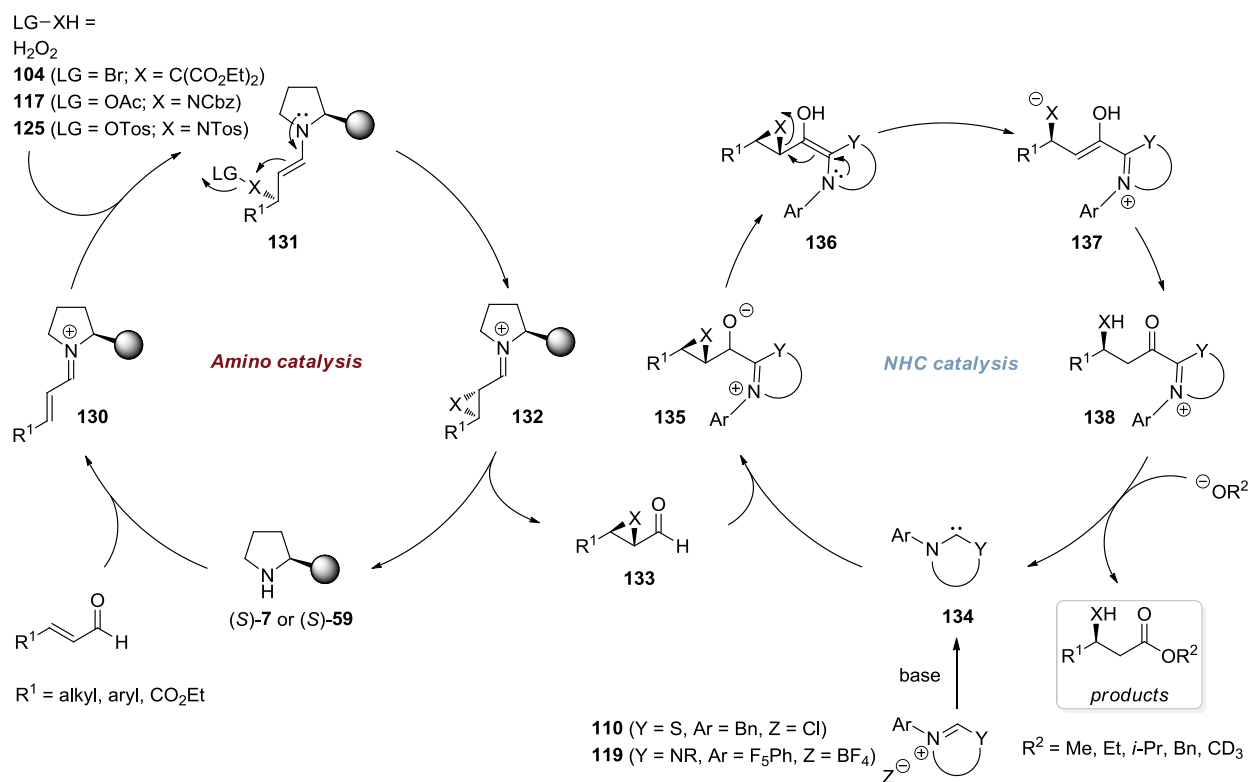


Scheme 18. AHCC catalysis for the synthesis of β -substituted esters reported by Jørgensen. ^a 10 mol% **(S)-59** were used; 5 h for epoxidation. ^b 2.5 mol% **(R)-59**, 2 mol% **119**, and 4 mol% DiPEA were used.

A generalized mechanistic picture for the mentioned combinations of amino and *N*-heterocyclic carbene catalysis is presented in Scheme 20. The reaction is initiated through the reversible formation of an iminium ion **130** allowing the conjugate addition of the *O*-, *C*-, or *N*-nucleophiles to the β -carbon at the *Re* face generating the chiral enamine intermediate **131** (similarly to the examples described above for combinations of secondary amines). In the next step, **131** performs an intramolecular 3-*exo*-tet cyclization from its *Re* face under release of the leaving group forming **132**. This cyclization step is irreversible and governs the stereoselective outcome of the overall reaction. Hydrolysis gives the corresponding epoxide, cyclopropyl, or aziridine aldehydes **133**. After *in situ* generation of the NHC **134** from its corresponding precatalyst, it nucleophilically attacks the carbonyl carbon of **133**, thus forming the zwitterionic species **135**. Subsequent generation of the Breslow intermediate **136**, and following intramolecular redox reaction leads to the activated carboxylate **138** via intermediate **137**. Final transesterification with an alcohol as nucleophile releases the carbene catalyst and gives the corresponding products (compare Figure 7).

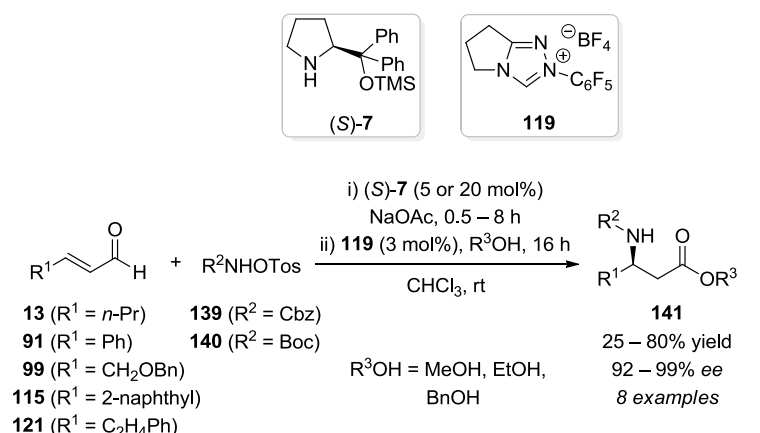


Scheme 19. AHCC reactions for the preparation of β -substituted esters bearing a quaternary carbon center.

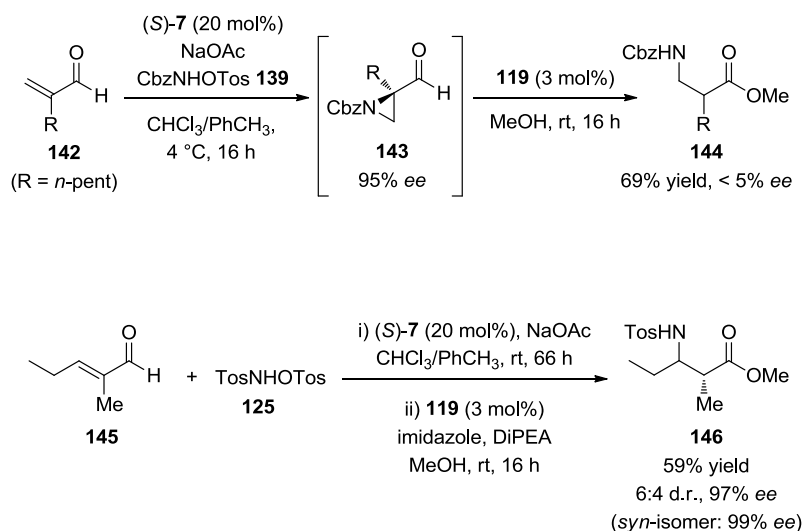


Scheme 20. Possible general mechanistic picture for the AHCC reactions shown in Schemes 17 and 18, and Scheme 15 (secondary amine catalyzed epoxidation step only).

In 2011, Córdova *et al.* reported a related enantioselective AHCC three-component reaction of α,β -unsaturated aldehydes, tosylated hydroxycarbamates **139** and **140**, and different alcohols yielding Cbz- or Boc-protected β -amino acid ester derivatives **141** (Scheme 21).^[81] Similarly to Jørgensen's work, the use of (*S*)-**7** and **119** as catalysts afforded various β -amino acid ester derivatives **141** in moderate to good yields (up to 80% yield) with 92 – 99% *ee*. When aromaticenals such as **91** or **115** were used the corresponding products were obtained with significantly lower yield (25 – 54% yield) although with excellent stereoselectivities (94 – 99% *ee*) due to a base-catalyzed rearrangement side-reaction. According to the mechanistic picture provided in Scheme 20 the use of α -substituted enal **142** formed the intermediate aziridine **143** with high 95% *ee* (Scheme 22). Subsequent ring-opening/esterification afforded nearly racemic β^2 amino acid ester **144** in 69% yield. However, employing enal **145** the corresponding product **146** was isolated in 59% yield with low diastereoselectivity, albeit with excellent enantioselectivity for both isomers (*anti*-isomer: 97%; *syn*-isomer: 99% *ee*) as shown in Scheme 22.



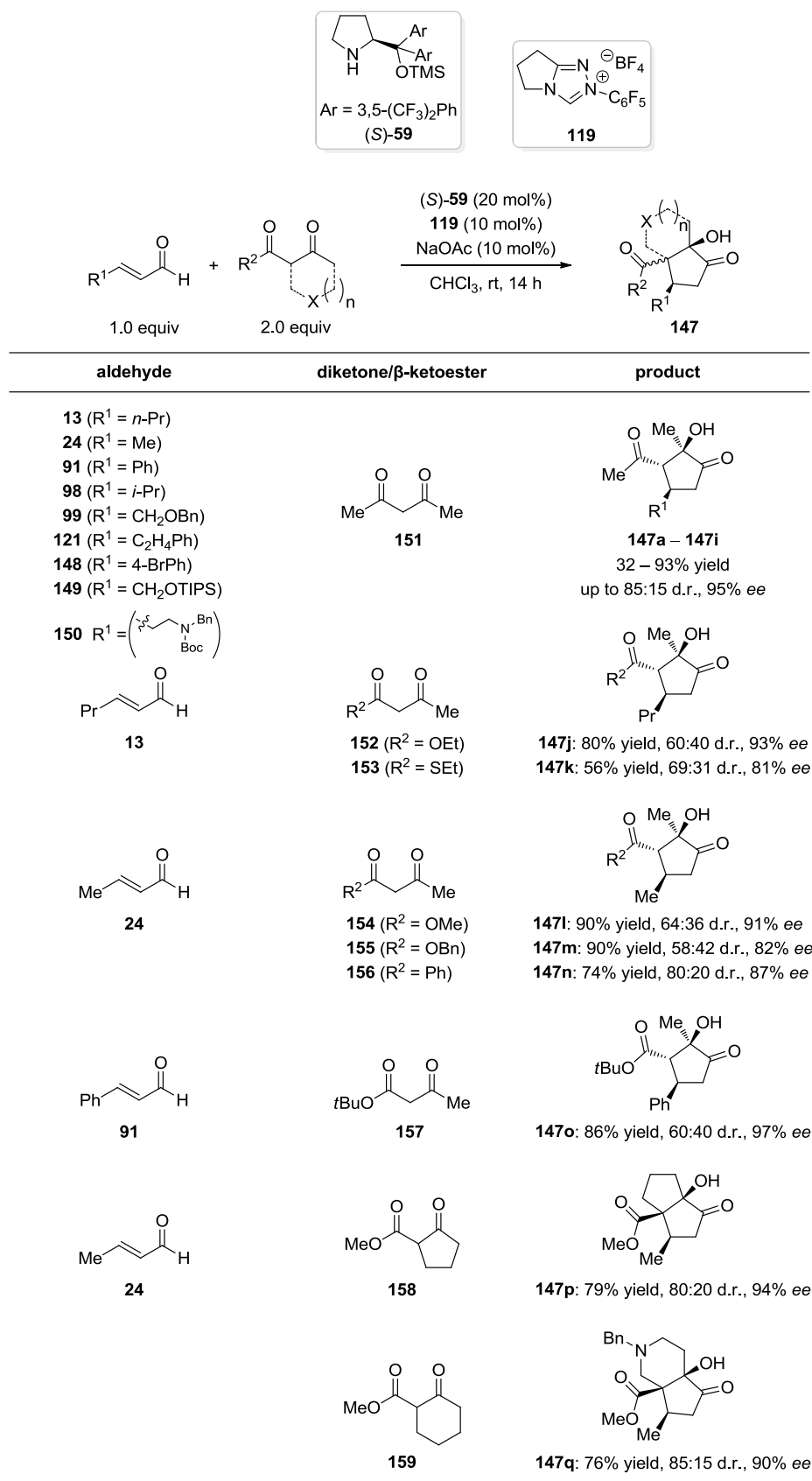
Scheme 21. AHCC reactions for the enantioselective synthesis of protected β -amino acid ester derivatives.



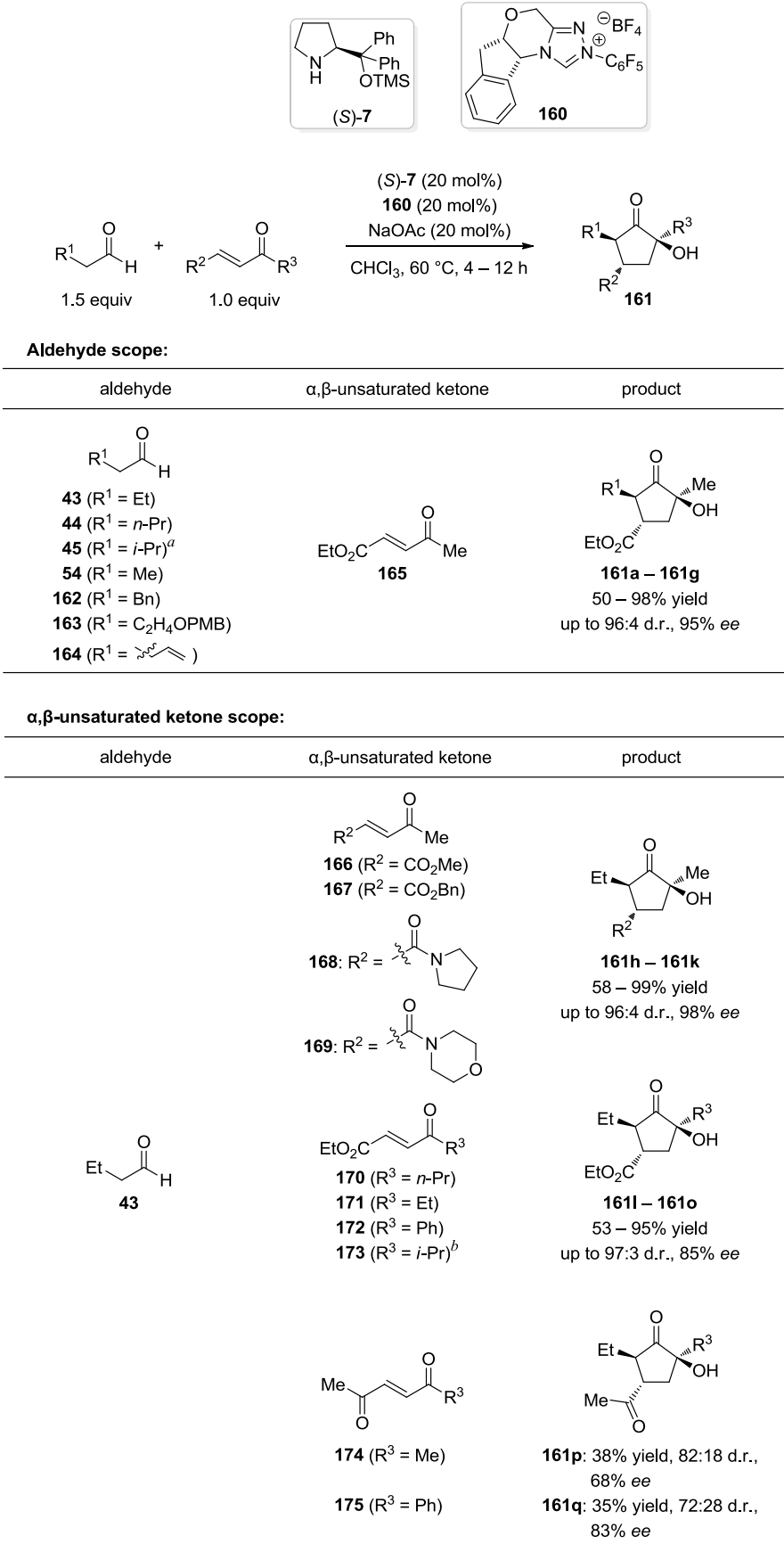
Scheme 22. AHCC reactions for the preparation of α,β -substituted amino acid ester derivatives.

In 2009, Lathrop and Rovis demonstrated another example of AHCC for the realization of a Michael addition/cross-benzoin reaction (Scheme 23).^[82] This multicyclic tandem reaction enabled the synthesis of highly functionalized cyclopentanones **147** containing three stereogenic centers (including a quaternary stereogenic center) from readily available starting materials. By using silyl-protected prolinol catalyst (*S*)-**59**, asymmetric conjugate addition of α,β -unsaturated aldehydes to β -dicarbonyl compounds **151** – **159** was induced *via* iminium activation. The following carbene **119** catalyzed intramolecular benzoin condensation produced the densely substituted cyclopentanones **147** in high yields and enantioselectivities, however, with only moderate diastereoselectivities (Scheme 23). The reaction showed a broad scope with respect to the aldehyde and the β -dicarbonyl starting materials leading to a variety of possible products, while branched aliphatic aldehydes (such as **98**) gave considerably lower yields. For example, bicyclic products **147p** and **147q** could be obtained using β -ketoesters **158** or **159**. Mechanistic investigations revealed that the performance of iminium catalyst (*S*)-**59** and carbene **119** in a tandem reaction is crucial for the high yield and selectivity of this reaction. When the transformation is performed in stepwise manner the intermediate aldehydes probably undergo retro-Michael reaction in the presence of (*S*)-**59** and are prone to epimerization during purification by column chromatography.^[82] As a consequence, the desired products **147** are obtained in lower yield and significantly lower enantioselectivity (46% yield, 58% *ee* for two sequential reactions), showing the sharp contrast to the yield and enantioselectivity of the one-pot tandem reaction (93% yield, 86% *ee*). When the two steps are combined into a tandem reaction, the carbene catalyst **119** effectively suppresses the retro-Michael reaction by direct consumption of the intermediate aldehyde in the following benzoin reaction, hence achieving the high enantioselectivity (Scheme 23). This work further emphasizes one of the advantages of multiple catalysts promoted asymmetric tandem reactions: the fast consumption of intermediates in a concurrent catalytic cycle allows catalysts to work synergistically, thereby suppressing side reactions.

The orthogonal reactivity of secondary amines and *N*-heterocyclic carbenes for the asymmetric synthesis of highly functionalized cyclopentanones was shown with another example by Ozboya and Rovis in 2011 (Scheme 24).^[83] In contrast to the previous work which relied on iminium catalysis as the first step, this reaction was initiated by enamine activation using secondary amine catalyst **7** followed by direct benzoin condensation catalyzed by chiral triazolium catalyst precursor **160**.^[78,84] Aliphatic aldehydes and various α,β -unsaturated ketones provided the desired products in good yield and high enantio- and diastereoselectivity. Employing isovaleraldehyde (**45**) competitively formed the corresponding Stetter product in a 1:1 ratio with the desired product **161c**. However, the sequential addition of **160** after complete formation of the corresponding intermediate avoided the formation of the side-product, thus affording **161c** (98% yield, 96:4:<1:<1 d.r., 88% *ee*). Aldehydes **163** and **164**, and α,β -unsaturated ketones **167** **173** bearing sterically more demanding substituents were also applicable but usually required



Scheme 23. AHCC tandem reaction for the synthesis of cyclopentanone derivatives reported by Lathrop and Rovis. Diastereomeric ratios are shown for major diastereomer : sum of three possible minor diastereomers.

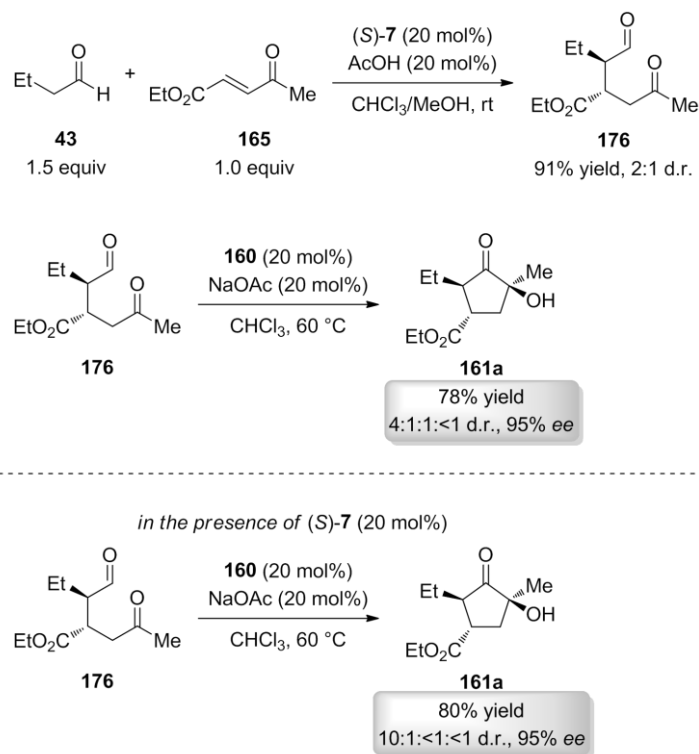


Scheme 24. AHCC tandem reaction for the synthesis of cyclopentanone derivatives reported by Ozboya and Rovis. Diastereomeric ratios are shown for major diastereomer : sum of three possible minor diastereomers. PMB = *para*-methoxybenzyl. ^a Catalyst **160** was added after complete consumption of starting material. ^b Carbene precatalyst **119** was used instead of **160**.

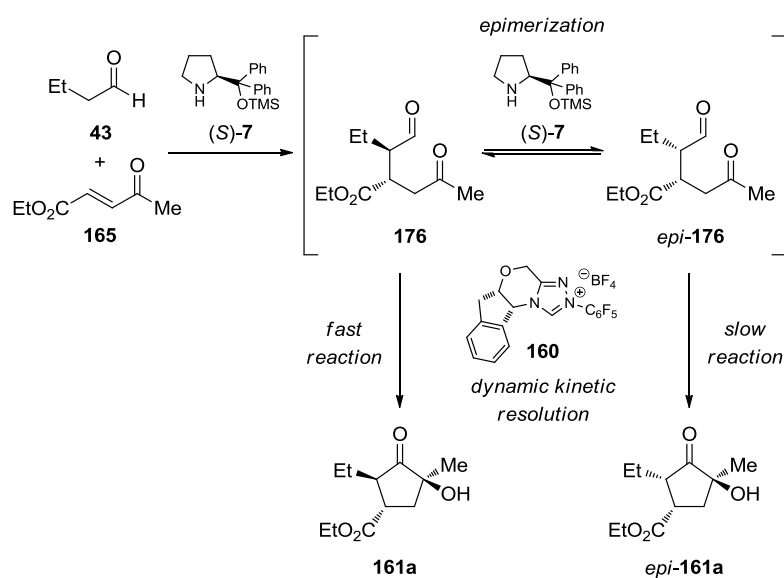
and longer reaction times and led to lower yields. When, for example, **173** was used as enone the intramolecular benzoin reaction could only be accomplished using smaller achiral carbene catalyst **119**, however with diminished enantioselectivity (51% *ee*). Diketones **174** and **175** gave the corresponding products **161p** and **161q** in considerably lower yields. Additional mechanistic investigations again showed that the one-pot tandem reaction leads to better selectivities compared to the single step reactions *via* a dynamic kinetic resolution of intermediate **176** by chiral NHC **160** (Schemes 25 and 26). Control experiments revealed that when prepared from butyraldehyde (**43**) and enone **165** with catalyst(*S*)-**7** and catalytic acetic acid the corresponding intermediate aldehyde **176** formed in 91% yield with only 2:1 diastereomeric ratio. The consecutive benzoin reaction afforded **161a** in comparable yield and enantioselectivity to the multicatalytic one-pot reaction, but in lower diastereomeric ratio (78% yield, 4:1:1:<1 d.r., 95% *ee* for two consecutive reactions; 87% yield, 19:1:<1:<1 d.r., 95% *ee* for the tandem reaction). Indeed, in the presence of (*S*)-**7** the diastereo-selectivity of the final product could be significantly improved (10:1:<1:<1 d.r.; Scheme 25). Thus, the secondary amine catalyst (*S*)-**7** possibly epimerizes the α -position of the intermediate aldehyde **176**, leading to *epi*-**176**, and the chiral triazolium catalyst **160** preferentially reacts with intermediate **176** instead of *epi*-**176** to form the enantioenriched product **161a** (Scheme 26).

In the same year, Enders *et al.* employed (*S*)-**59** and **119** for the sequential multicatalytic Michael addition/cross-benzoin reaction of α,β -unsaturated aldehydes and β -oxo sulfones **178** – **189** for the preparation of polysubstituted cyclopentanones **177** (Scheme 27).^[85] Hence, they first applied the conditions reported previously for the reaction of β -dicarbonyl compounds with enals by Lathrop and Rovis.^[82] Under these conditions (compare Scheme 23) the reaction of crotonaldehyde (**24**, 1.0 equivalents) with phenylsulfonylacetone (**178**, 2.0 equivalents) afforded mainly two of the four possible diastereomers of **177b** in high yield and enantioselectivity, however, in an only moderate diastereomeric ratio (85% yield, 63:37 d.r., 88% *ee*). After re-optimization of reaction conditions the desired product **177b** could be obtained in quantitative yield while stereoselectivity was retained. With these conditions at hand, Enders and co-workers studied the scope of the reaction. A wide range of different sulfones **179** – **189** was applicable using **24** as aldehyde component to generate cyclopentanones **177d** – **177k** in 70 – 96% yield, in most cases as a single diastereomer (99:1 d.r.), and with up to 97% *ee*. Interestingly, the benzoin condensation proceeded with *cis*-selectivity (contrary to the reactions reported by Rovis; compare Scheme 23)^[82] when sulfones bearing an aromatic moiety were employed. Using α -substituted α -(phenylsulfonyl)ketones as nucleophiles significantly decreased the reaction rate and the yield. For instance, the cyclic sulfone **187** formed product **177l** in 53% yield even when the reaction time was prolonged to three days with moderate selectivities (67:33 d.r.), whereas **188** gave **177m** in only 20% yield, albeit with very good stereoselectivity (99:1 d.r., 91% *ee*). When acyclic **189** was used as sulfone component the desired product was not produced. Similarly to the reactions reported by Rovis and co-workers,^[83] Enders observed epimerization

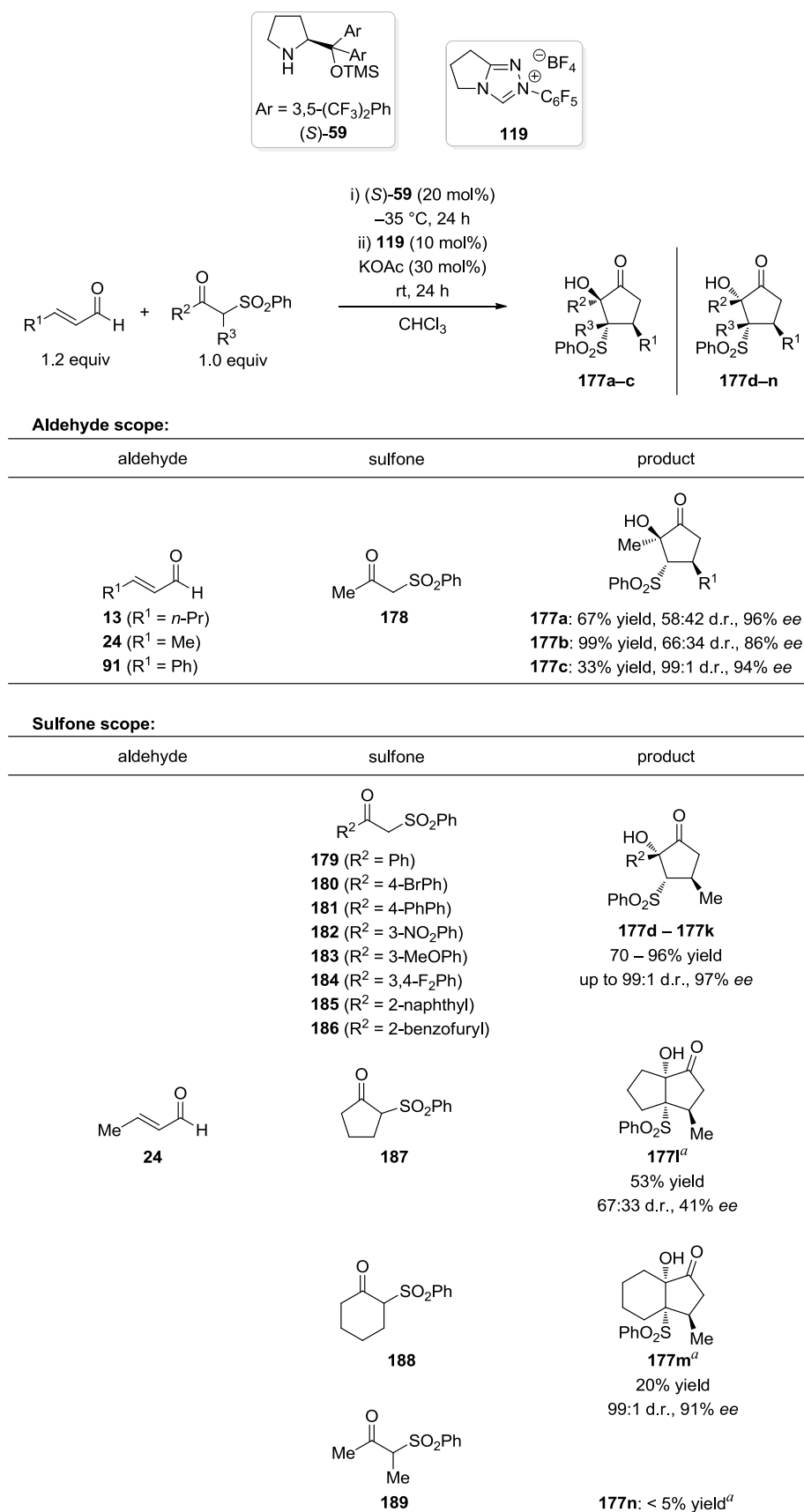
of the corresponding Michael adduct. Hence, the achieved diastereoselectivities result from the preference of one of the diastereomers to react with the carbene catalyst (also compare Scheme 26).



Scheme 25. Single step reactions for the preparation of **161a**.

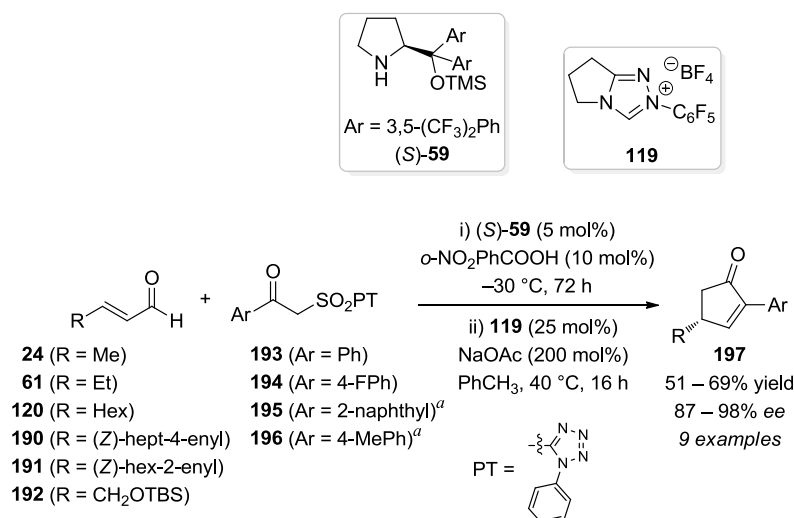


Scheme 26. Mechanistical proposal for the observed reaction outcome in the multicatalytic synthesis of **161a**.



Scheme 27. AHCC cascade reactions for the synthesis of cyclopentanone derivatives reported by Enders. Diastereomeric ratios are shown for major diastereomer : sum of three possible minor diastereomers. ^a First reaction was prolonged to 3 d.

Encouraged by the previous reports by Rovis (Scheme 23)^[82] and Enders (Scheme 27),^[85] Jørgensen *et al.* envisioned an AHCC reaction sequence for the formation of optically active 2,4-disubstituted cyclopent-2-enones (Scheme 28).^[86] Similar to the previous reports the reaction is initiated by an iminium activated Michael addition of sulfones **204** – **207** to α,β -unsaturated aldehydes employing (*S*)-**59**. The successive NHC **119** catalyzed benzoin reaction subsequently leads to a Smiles rearrangement,^[87] thus affording the desired 2,4-disubstituted cyclopentan-2-enones **197** (Scheme 28). Various aliphatic aldehydes (**24**, **61** and **120**), olefinic aldehydes (**190** and **291**), and the aldehyde **192** bearing a TBS-protected alcohol were used affording the corresponding products in 51 – 69% yield and enantioselectivities up to 98%. Nucleophiles bearing an aliphatic ketone substituent were found to be inapplicable, presumably because of the formation of a stable pyranose intermediate.^[86,88]

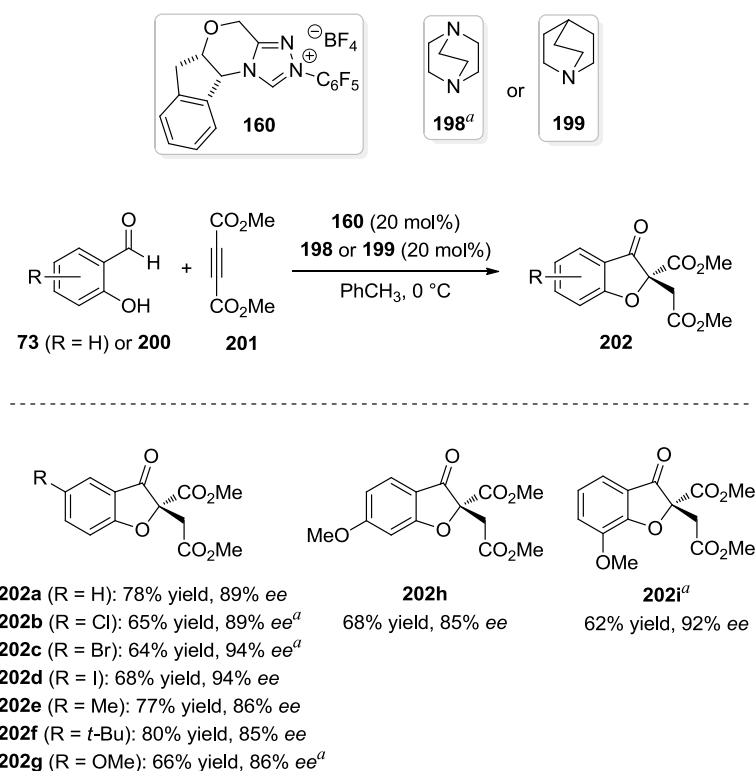


Scheme 28. AHCC cascade reactions for the synthesis of cyclopentenone derivatives. ^a 10 mol% (*S*)-**59** and 20 mol% *o*-NO₂PhCOOH were used.

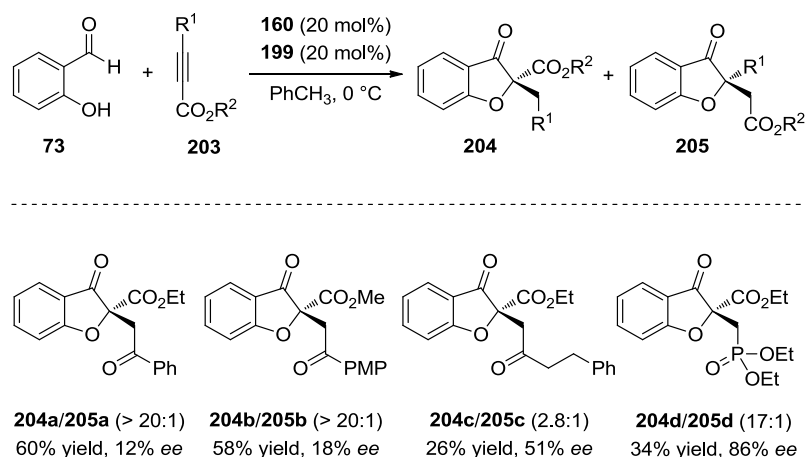
4.2 Miscellaneous Combinations with *N*-Heterocyclic Carbenes

In 2010, Lathrop and Rovis reported an asymmetric Michael/Stetter tandem reaction for the synthesis of valuable benzofuranones from readily available starting materials (Scheme 29).^[89] Based on other preliminary studies which showed that 1,4-diazabicyclo[2.2.2]octane (DABCO, **198**) allows the addition of amine and oxygen nucleophiles to dimethyl acetylenedicarboxylate (DMAD; **201**)^[90] the authors envisioned the combination of **160** and a tertiary amine, such as

DABCO (**198**) or quinuclidine (**199**), acting as both nucleophilic catalyst for the Michael addition and as base for the deprotonation of the carbene precatalyst. The combination of both catalysts should then allow performing a tandem Michael/Stetter reaction (Scheme 29). Indeed, the combination of **160**, and **198** or **199**, respectively, facilitated the reaction of salicylaldehydes **73** or **200** with different substitution pattern, and DMAD (**201**) to furnish the desired products **202**. Interestingly, the tertiary amine (**198** or **199**) *not* the carbene **160** acts as nucleophilic catalyst for the Michael reaction although both are present from the outset of the reaction, which was confirmed by control experiments.^[89] Further investigations indicated that the enantioselectivity of the reaction is possibly enhanced by traces of strong hydrogen bonding donors, such as catechols,^[91] derived from Dakin-oxidation of salicylaldehydes. When the reaction was performed stepwisely the final products were isolated in good yields, however, in lower and more uniform enantioselectivities. Contrary, addition of a salicylaldehyde or a catechol slightly improved the selectivity of the Stetter reaction.^[91] Unsymmetrical alkynes **203** were tested as Michael acceptors as well (Scheme 30) under the developed reaction conditions. Thus, reaction of salicylaldehyde (**73**) with two different ketoalkynoates regioselectively afforded the products **204a** and **204b** in moderate yields and poor enantioselectivities. The use of a less electrophilic alkyne resulted in higher enantioselectivity for product **204c** (51% *ee*), but low regioselectivity (**204c**/**205c**: 2.8:1). Interestingly, the minor regioisomer **205c** formed with appreciably higher enantioselectivity (89% *ee*). Employing a phosphonate ester as alkyne component afforded **204d** in low yield and with better selectivity.^[89]

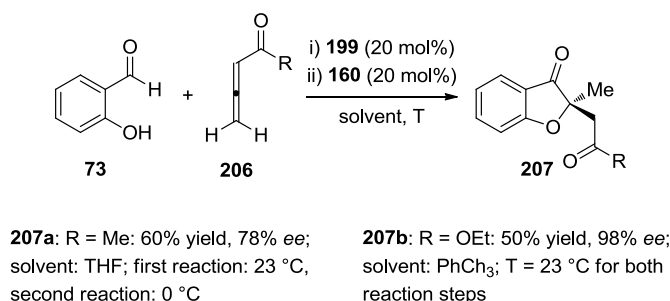


Scheme 29. Michael/Stetter tandem reaction of different salicylaldehydes with DMAD (**201**). ^a **198** was used.



Scheme 30. Michael/Stetter tandem reaction of salicylaldehyde (**73**) with unsymmetrical alkynes **203**.

In order to achieve better yields and high regio- and enantioselectivities, Lathrop and Rovis examined the reaction of salicylaldehyde (**73**) with alkynes bearing a single electron-withdrawing group^[89,92] (the thus-generated intermediate aldehydes have been used previously in the Stetter reaction affording the corresponding products in high enantioselectivity). However, an initial attempt resulted in the isolation of starting materials only. As the Stetter reaction is significantly influenced by olefin geometry (*E*-isomers react with higher yield and enantioselectivity) the authors performed the reaction sequence with allenates **206** (Scheme 31).^[89] These starting materials (as well as **201**) formed the intermediate aldehydes with high *E*-selectivity, whereas ketoalkynoates gave mixtures of *E* and *Z* isomers. Thus, employing **73** and **206** in a sequential multicatalytic reaction afforded the desired products **207** in reasonable yields and with up to 98% ee (Scheme 31).



Scheme 31. Michael/Stetter tandem reaction of salicylaldehyde (**73**) with activated allenates **206**.

5. Thiourea Catalysts

During the last decade, thiourea derivatives have received great attention and have displayed their efficiency as hydrogen-bonding organocatalysts^[22,24,93] and anion-receptors.^[94] In hydrogen bonding catalysis the interaction between the catalyst and an electrophilic substrate generally results in the LUMO activation of the latter, thus allowing nucleophilic attack (Figure 8). Therefore, the combination of thioureas with other catalysts allows additional valuable transformations.

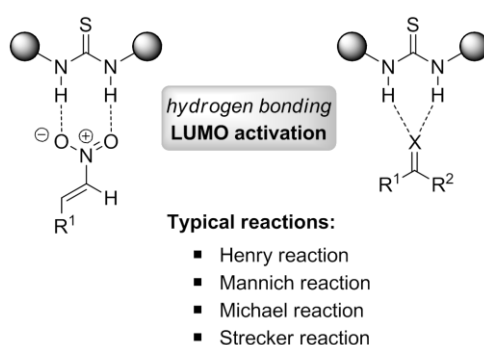
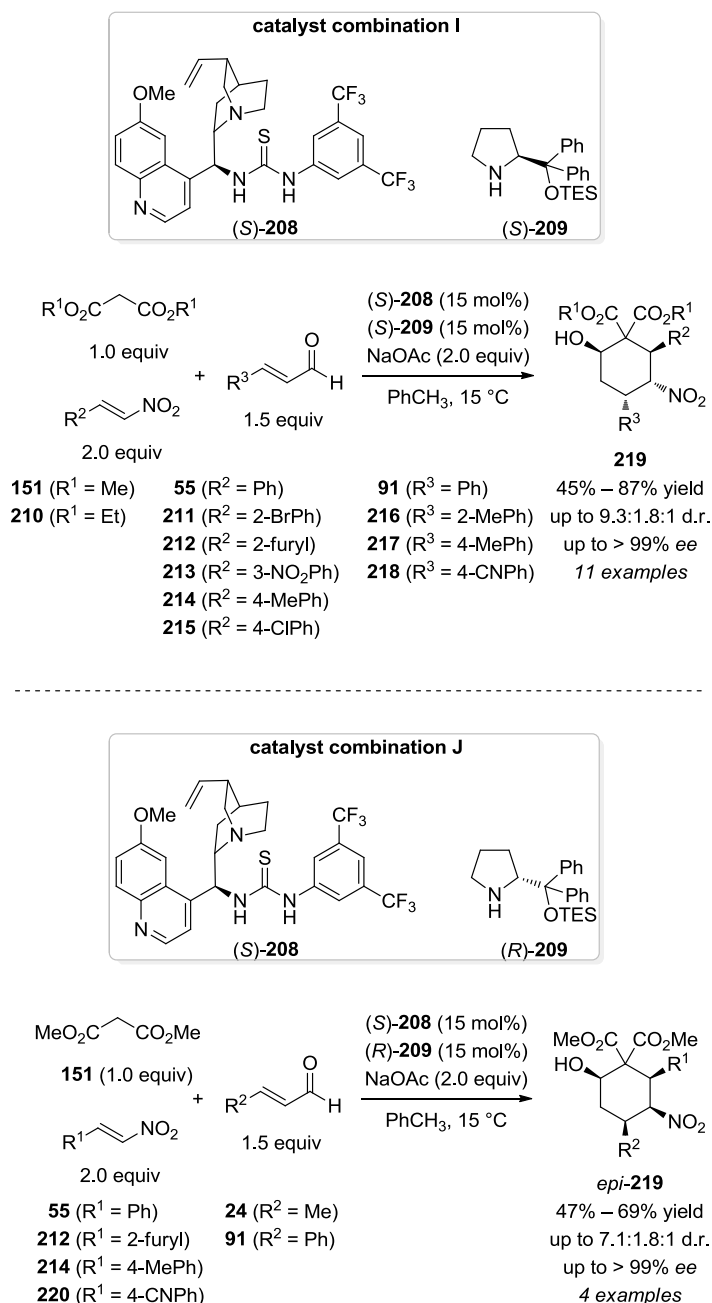


Figure 8. Hydrogen bonding catalysis. $R^1, R^2 = \text{H, alkyl, aryl}$; $X = \text{O, NR}$.

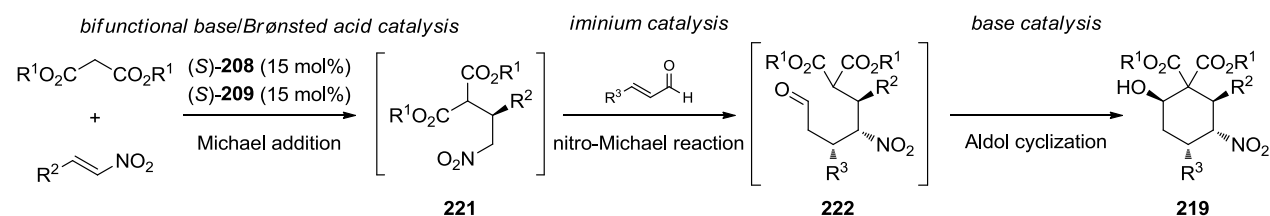
5.1 Combinations of Thioureas with Secondary Amine Catalysts

In 2009, Dixon *et al.* combined bifunctional thiourea (*S*)-**208** and either secondary amine (*S*)-**209** (catalyst combination I) or (*R*)-**209** (catalyst combination J) for a three-component tandem reaction comprising malonate esters, nitroolefins and α,β -unsaturated aldehydes to form polysubstituted cyclohexanes **219** (Scheme 32).^[95] The reaction was applicable for a wide range of starting materials, leading to a broad product scope. Thus, the products **219** were formed with catalyst combination I (45 – 87% yield, 9.3:1.8:1 d.r., up to >99% *ee*). Four additional examples were reported using catalyst combination J (with (*R*)-**209**) and dimethylmalonate ester **151** under variation of the nitroalkene and enal component affording *epi*-**219** (47 – 69% yield, 7.1:1.8:1 d.r., up to >99% *ee*). The reaction has been suggested to proceed *via* bifunctional activation of malonate esters and nitroalkene through base and Brønsted acid catalysis by (*S*)-**208** leading to stereoselective Michael addition (Scheme 33). The thus formed Michael adduct **221** subsequently undergoes a regioselective nitro-Michael reaction to the enal under iminium activation with secondary amine (*S*)-**209** producing **222**. This intermediate undergoes a base-promoted

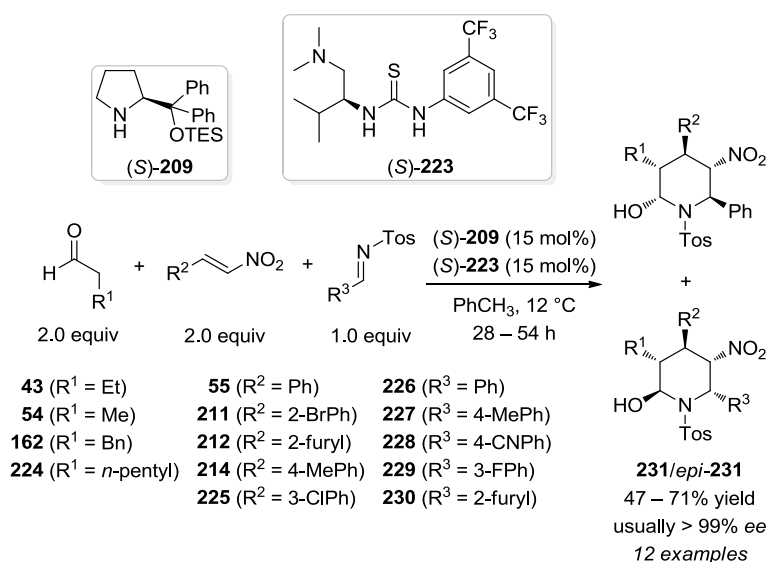
aldol cyclization to generate the desired product **219**. Control experiments suggested that the iminium catalyzed nitro-Michael addition is also base-promoted, and therefore that both catalysts work cooperatively. Moreover, there are putative matched and mismatched combinations of catalysts and reaction intermediates and an amplification of enantioselectivity for the matching cases.



Scheme 32. Combination of bifunctional thiourea and amino catalysis reported by Dixon. TES = triethylsilyl.



One year later, Dixon and Xu reported a similar bifunctional thiourea (*S*)-**223**/secondary amine (*S*)-**209** catalyzed tandem reaction (Scheme 34). Different aldehydes, nitroolefins, and tosyl-protected imines **226** – **230** were employed producing the fully substituted piperidines **231** or *epi*-**231** in moderate to good yields (47 – 71%) and excellent enantioselectivities, usually >99% *ee*.^[96] The reaction is initiated by the Michael addition of enamine activated aldehydes with cooperatively hydrogen-bonding activated nitroalkenes. Following thiourea (*S*)-**223** catalyzed nitro-Michael reaction of the corresponding Michael adducts and the imines through bifunctional base/Brønsted acid catalysis gives the substituted aminoaldehyde, and final cyclization leads to the *N*-tosyl protected hemiaminals **231** and *epi*-**231**.

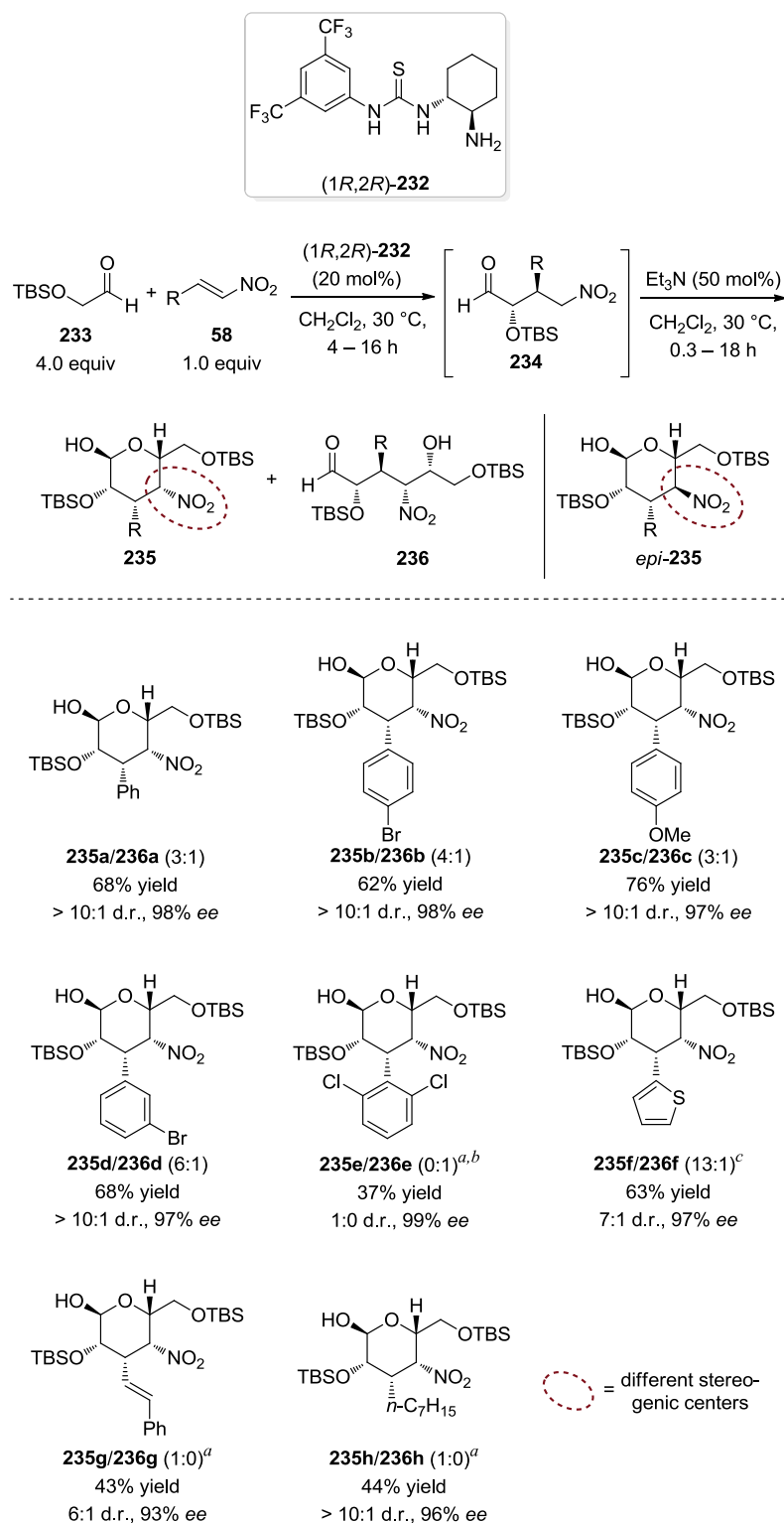


Scheme 34. Synthesis of fully substituted piperidines *via* the merger of enamine and bifunctional base/Brønsted acid catalysis. TES = triethylsilyl.

5.2 Combination of Thiourea Catalysts with Brønsted Acids and Bases

In 2010, Barbas *et al.* reported the organocatalytic synthesis of carbohydrate derivatives through sequential Michael/Henry reactions employing thiourea (1*R*,2*R*)-**232** and either triethylamine or 1,8-diazabicyclo[5.4.0]undec-7-ene (DBU, **237**; Schemes 35 and 36).^[97,98] The (1*R*,2*R*)-**232** with remaining aldehyde **233** affording 3,4-dideoxy-D-talose derivative **235a** in 68% yield with 98% *ee*, which is in equilibrium with its open form **236a** in solution due to a 1,3-diaxial interaction between the nitro group and the alkoxy substituent. Indeed, only small amounts of the D-*manno*-isomer *epi*-**235a** formed (Scheme 35). Other nitrostyrenes with both electron-withdrawing and electron-donating groups on the aromatic ring were used affording the desired products **235b** – **235d** in good yields and high enantioselectivities (62 – 67% yield, up to 98% *ee*). Heteroaromatic substituents could be introduced as shown for **235f**. However, **236e** was present only in the open form and required an equimolar amount of triethylamine for the Henry reaction to proceed. Nitroalkenes bearing smaller substituents afforded products **235g** and **235h** exclusively as their cyclized form. The use of DBU (**237**) as base catalyst under otherwise identical conditions led to a complete epimerization at the stereogenic center bearing the nitro group thus afforded the corresponding 3,4-dideoxy-D-mannose derivatives *epi*-**235** (Scheme 36; only the cyclized form was observed).^[97] Except for 2,6-dichloronitrostyrene all previously tested nitroolefins were applicable affording products *epi*-**235** via the *anti*-Michael/*syn*-Henry/epimerization reaction sequence. To increase the utility of the reaction other aldehydes were tested as acceptors for the Henry reaction. For example, the use of glyoxylate **244** gave carbohydrate derivatives **245** and *epi*-**245** in moderate yield but high enantioselectivity (98% *ee*) under the developed conditions (Scheme 37). Moreover, the group disclosed an example for an intermolecular *syn*-Michael/Henry reaction sequence (Scheme 38). The *syn*-Michael reaction was accomplished using isovaleraldehyde (**99**), β -nitrostyrene (**55**), and diphenylprolinol silyl ether (*S*)-**7** as first catalyst. The sequential addition of *para*-nitrobenzaldehyde (**246**) and triethylamine produced **247** in 77% yield and excellent 99% *ee* as a 4:1 mixture of the corresponding α/β -isomers. The reactions presented in Schemes 35 – 37 are good examples testifying that even simple catalysts such as triethylamine and DBU (**237**) may provide a direct entry to different diastereomeric forms of a desired product.

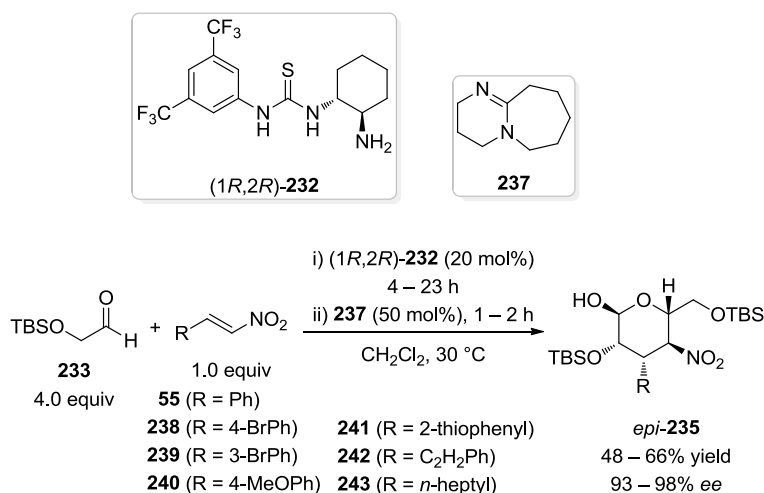
In 2011, Enders *et al.* reported the one-pot combination of thiourea catalyst (1*S*,2*S*)-**248** and *p*-TSA (**72**) for a Michael/hemiacetalization/dehydration reaction sequence assembling 4-nitromethyl-4*H*-chromenes **258** (Scheme 39).^[99] Different nitroalkene phenols **249** – **254** were applied with various β -keto esters affording the desired products **258** in high yield and enantioselectivity. When *ortho*-substituted nitroalkene phenols **253** and **254** were used a change in the configuration was observed. However, the corresponding 4*H*-chromenes were formed with excellent enantiomeric excess (99% *ee* in both cases).^[99,100]



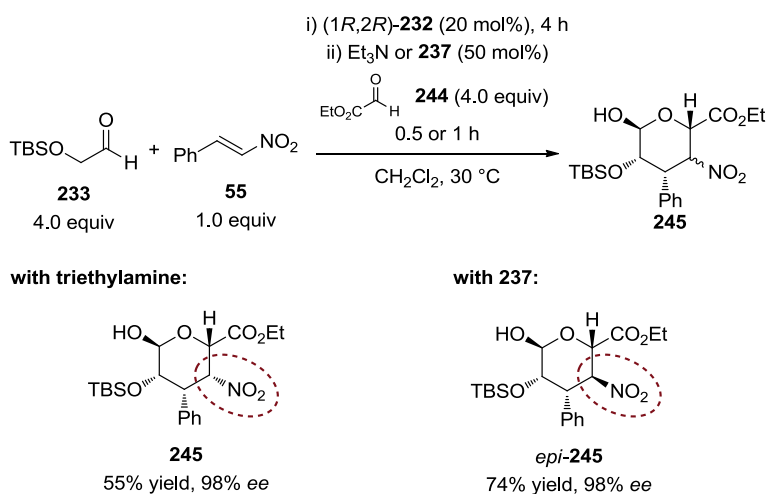
Scheme 35. Sequential Michael/Henry reaction for the synthesis of 3,4-dideoxy-D-talose derivatives **235**.

^a Reaction performed with 50 mol% (1R,2R)-**232**. ^b 100 mol% triethylamine used. ^c 30 mol% triethylamine used.

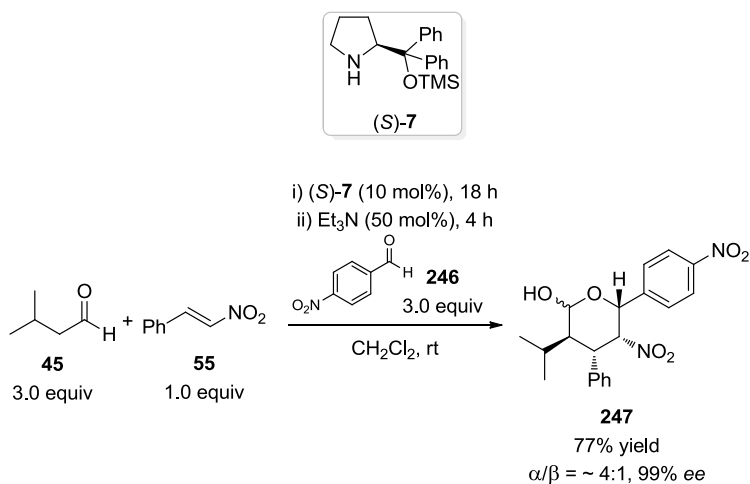
Very recently, the combination of thiourea (1S,2S)-**259** with *N*-Boc-protected glycine (**260**) as acid additive, and chiral phosphoric acid **261** was reported to promote the α -alkylation and two consecutive Friedel-Crafts alkylations of aldehydes and indol derivatives affording enantio-merically enriched cyclopenta[*b*]-indoles **263** (Scheme 40).^[101] The reaction showed a very



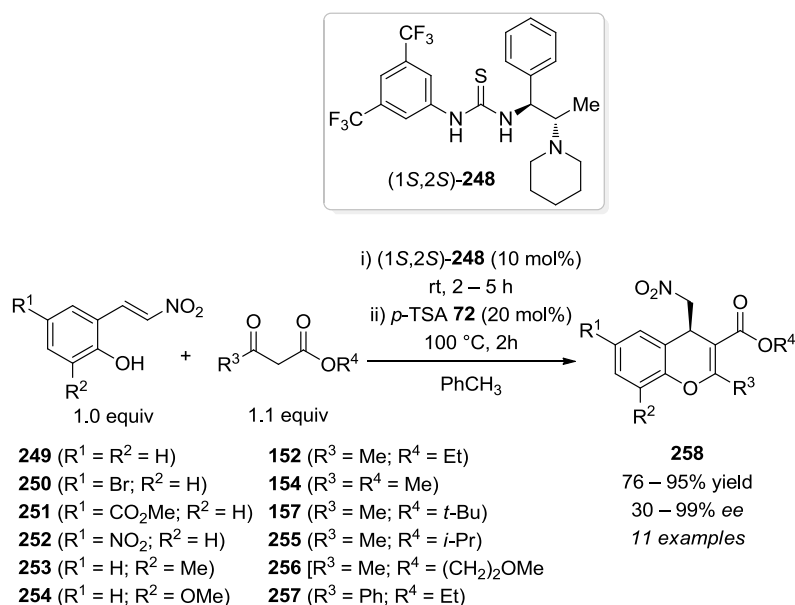
Scheme 36. Sequential Michael/Henry reaction for the synthesis of 3,4-dideoxy-D-mannose derivatives *epi*-**235**.
^a Reaction was performed with 50 mol% (1*R*,2*R*)-**232**.



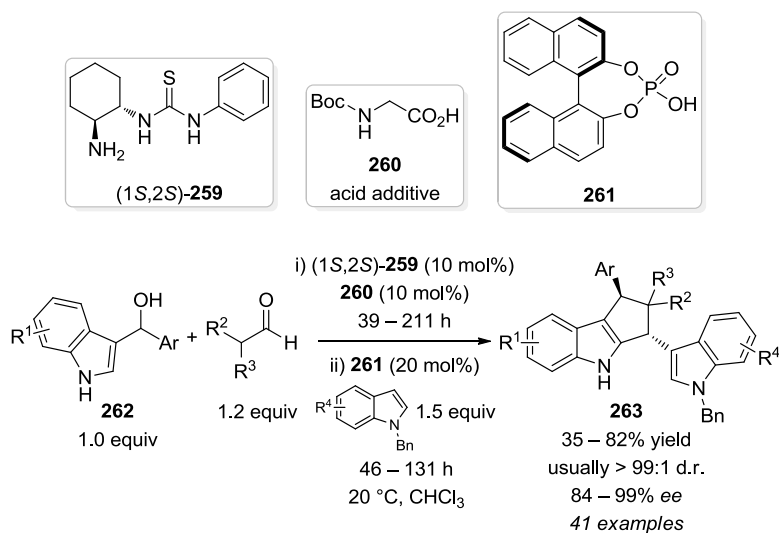
Scheme 37. Sequential Michael/Henry reaction for the synthesis of carbohydrate derivatives **245** and *epi*-**245**.



Scheme 38. Sequential *syn*-Michael/Henry reaction for the synthesis of carbohydrate derivative **247**.



Scheme 39. Michael/hemiacetalization/dehydration reaction sequence for the synthesis of 4-nitromethyl-4H-chromenes.



262	aldehydes	indole derivatives
Ar = Ph, 2-FPh, 3-FPh, 4-FPh, 2-ClPh, 4-ClPh, 2-BrPh, 4-BrPh, 4-CNPh, 4-CF ₃ Ph, 4- <i>t</i> -BuPh, 2-MeOPh, 3-MeOPh, 4-MeOPh, 3-MePh, 4-MePh, 1-naphthyl, 2-naphthyl	44 (R ² = H, R ³ = <i>n</i> -Pr) 46 (R ² = H, R ³ = <i>n</i> -Bu) 264 (R ² = R ³ = Me) 265 (–(CH ₂) ₅ –) 266 (R ² = Me, R ³ = Et)	267 (R ⁴ = H) 268 (R ⁴ = 6-F) 269 (R ⁴ = 5-Cl) 270 (R ⁴ = 5-Me) 271 (R ⁴ = 6-Me) 272 (R ⁴ = 7-Me)

R¹ = H, 6-F, 5-Cl, 5-Br, 5-MeO, 5-Me, 6-Me, 7-Me

Scheme 40. Synthesis of cyclopenta[*b*]indoles **263** via α -alkylation and two consecutive Friedel-Crafts alkylations.

broad scope with respect to the 3-indolylmethanol compounds **262**, the indole derivatives, and the aldehydes. The corresponding products were usually formed as a single diastereomer, with moderate to good yields and high enantioselectivities. Importantly, the multicomponent reaction afforded the desired product in higher yield compared to two separate reactions (70% instead of 58% overall yield for **263a**; Ar = Ph, R¹ = R⁴ = H, R² = R³ = Me).

6. Non-Natural Oligopeptides for Acyl Transfer Reactions

Synthetic oligopeptides proved to be versatile and efficient catalysts in a variety of chemical transformations.^[102-103] Well-established solution-phase and (automated) solid-phase peptide synthesis (SPPS) protocols, and the commercial availability of most natural as well as non-natural amino acids allow the easy and efficient assembly of these types of catalysts. The modular build-up of the oligopeptide catalysts ensures their rapid variation and modification. Moreover, oligopeptides are particularly attractive from an environmental point of view as they should be biodegradable.

Oligopeptides bearing nucleophilic catalytic moieties, such as *N*-alkylimidazoles, showed to be highly efficient catalysts in the kinetic resolution of racemic substrates as well as the desymmetrization of *meso* compounds through acyl group transfer.^[104] Thus, the nucleophilic catalyst forms an acylium cation salt with the corresponding counterion^[105] with an acyl donor (*e.g.*, acetic anhydride or acetyl chloride; Figure 9).^[104] This acylium ion allows transferring the acetyl group onto a nucleophile (*e.g.*, alcohol, amine, thiol) affording the product. Depending on the pK_a -values of the protonated imidazole and the counterion (X in Figure 9) the addition of base may be necessary to prevent catalyst protonation and deactivation.^[104]

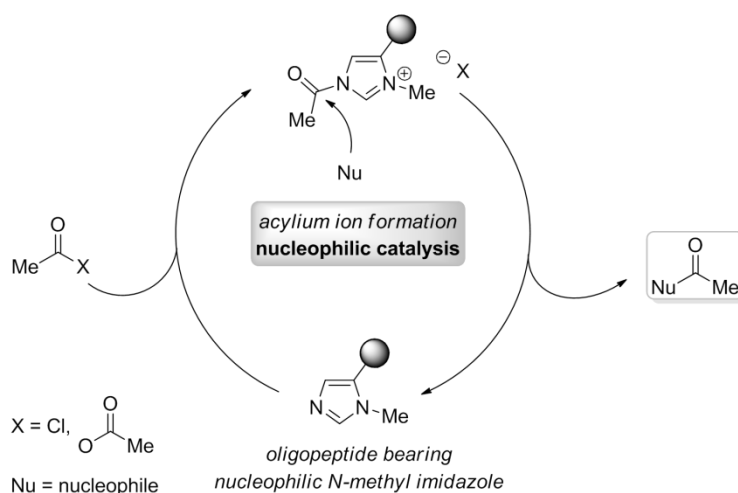
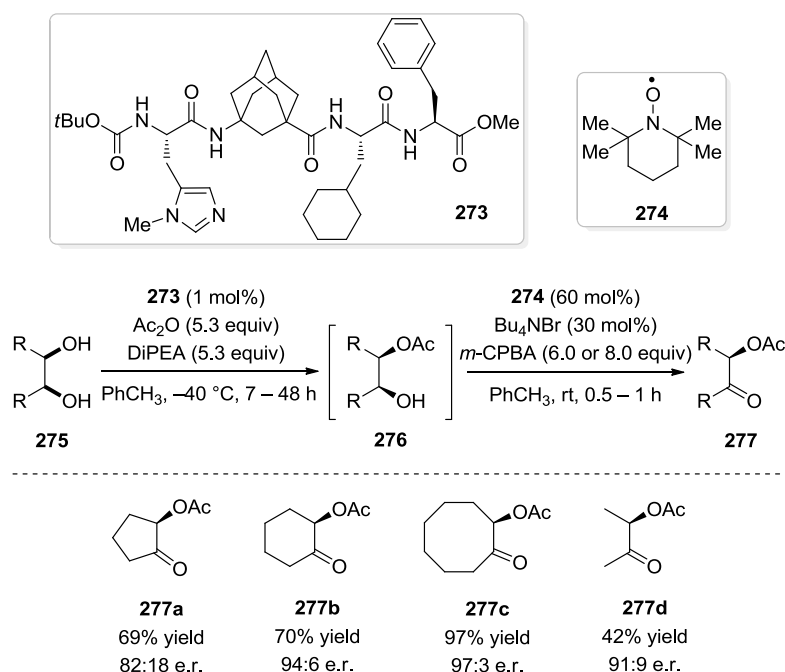


Figure 9. General representation for acyl transfer reactions with *N*-methylimidazole derivatives.

In 2008, Müller *et al.* introduced tetrapeptide **273** (Boc-L-Pmh-^AGly-L-Cha-L-Phe-OMe)^[106] equipped with π -methyl histidine (Pmh) as catalytic moiety. The incorporation of a rigid non-natural γ -amino adamantane carboxylic acid (^AGly)^[107] into the backbone led to a more lipophilic and structurally less flexible oligopeptide.^[106] Hence, this approach did not follow conventional design principles for oligopeptide catalysts which usually emphasize the importance of secondary structures (stabilized by intramolecular hydrogen bonding) for activity and selectivity.^[102] Catalyst **273** was first applied for the acylative kinetic resolution^[104] of

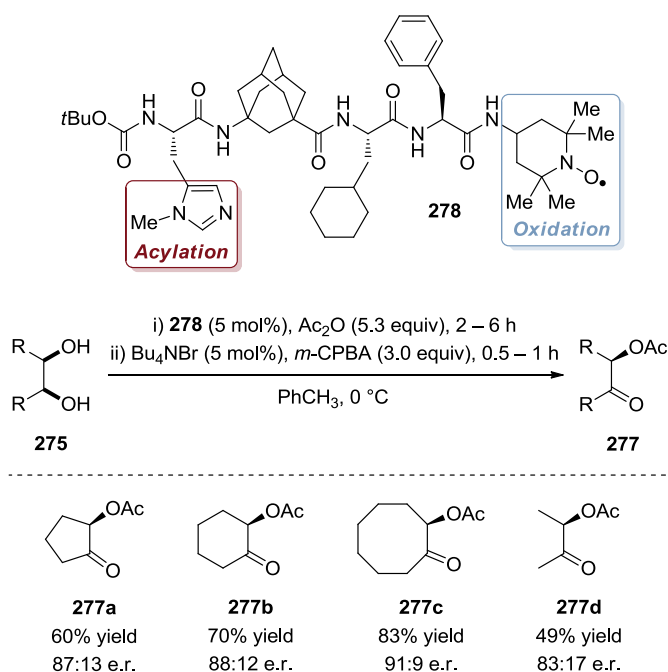
racemic *trans*-cycloalkane-1,2-diols, a substance class previously challenging to resolve, achieving >99% *ee* for the remaining diol enantiomers and *S*-values^[108] of typically >50.^[106,109] Later, oligopeptide **273** was applied for the desymmetrization^[104] of *meso*-alkane-1,2-diols **275**.^[110] Owing to racemization of the monoacetylated products **276** through intramolecular transesterification during work-up, Müller *et al.* envisioned the direct one-pot oxidation^[111] of intermediate **276** using TEMPO (2,2,6,6-tetramethylpiperidin-1-oxyl; **274**) which then would lead to the valuable enantiomerically enriched α -acetoxy ketones **277** (Scheme 41). Under optimized conditions, the desymmetrization was performed using only 1 mol% **272**, acetic anhydride and Hünig's base (5.3 equivalents each). The sequential addition of TEMPO (**274**; 60 mol%), tetrabutylammonium bromide (30 mol%) and *meta*-chloroperbenzoic acid (*m*-CPBA, 6.0 or 8.0 equivalents) as co-oxidant then initiated the second catalytic cycle. Thus, the corresponding α -acetoxy ketones **277** were afforded with moderate to excellent yields and high enantiomeric ratios (up to 97% yield and 97:3 d.r. for **277c**).



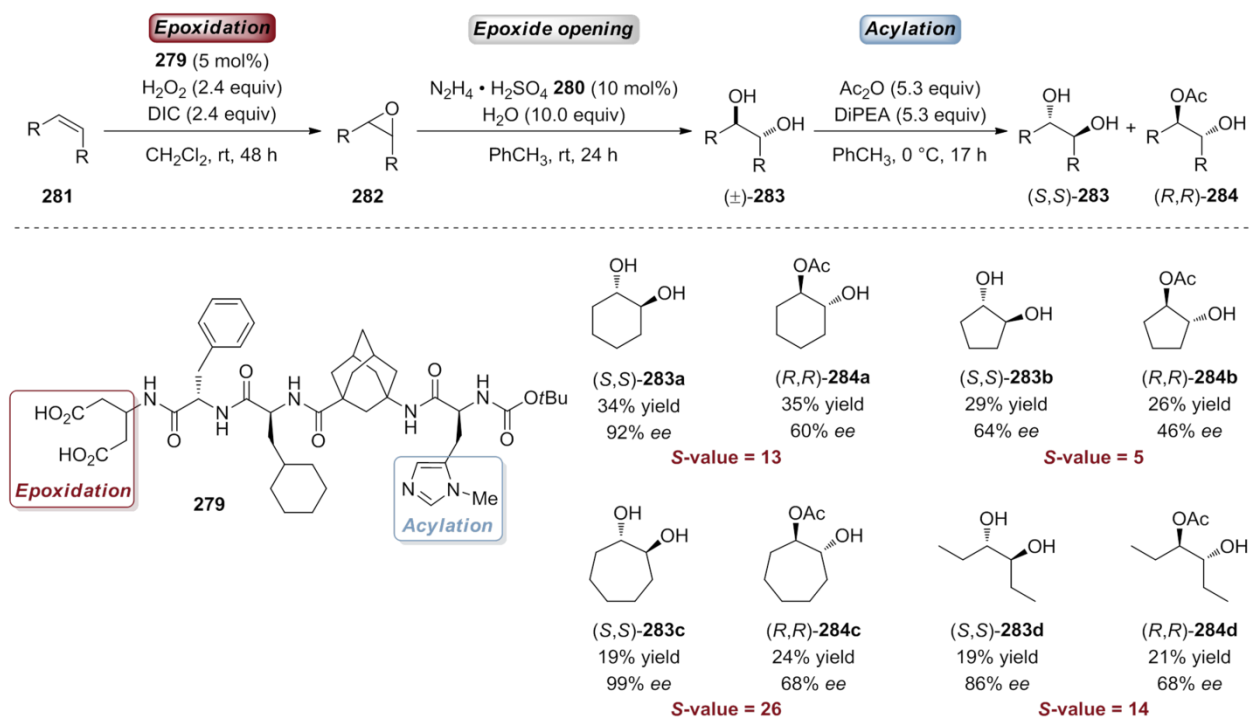
Scheme 41. Oligopeptide **273** catalyzed desymmetrization of *meso*-alkane-1,2-diols and one-pot TEMPO (**274**) oxidation.

7. Multicatalyst Approaches

Inspired by their sequential multicatalysis approach (Scheme 41),^[110] Müller *et al.* envisioned a multicatalyst system to perform the entire reaction sequence (Scheme 42). Indeed, by replacing the C-terminal methyl ester group of peptide **273** with a TEMPO-amide functionality they obtained the first member of organic multicatalysts **278** (Boc-L-Pmh-^AGly-L-Cha-L-Phe-NH-TEMPO), bearing two orthogonal catalytic moieties (Scheme 42).^[13,112] Remarkably, this proof-of-principle study revealed that the multicatalyst **278** shows an increased oxidation activity compared to TEMPO itself. As a result, the amounts of *m*-CPBA (3.0 instead of up to 8.0 equivalents) and tetrabutylammonium bromide (5 mol% instead of 30 mol%) could be significantly reduced. Moreover, 5 mol% of multicatalyst **278** and, therefore, only 5 mol% of TEMPO-analogue (instead of 60 mol% TEMPO), were sufficient to perform the second reaction at 0 °C without affecting the reaction time. The desymmetrization step showed only a slight decrease in selectivity compared to the two-catalyst approach. Indeed, a molecular force-field analysis revealed that the conformation of peptide **278** is not affected upon introduction of the TEMPO moiety, therefore maintaining selectivity.



Scheme 42. Oligopeptide based multicatalyst **278** for the one-pot desymmetrization and subsequent oxidation of *meso*-alkane-1,2-diols.

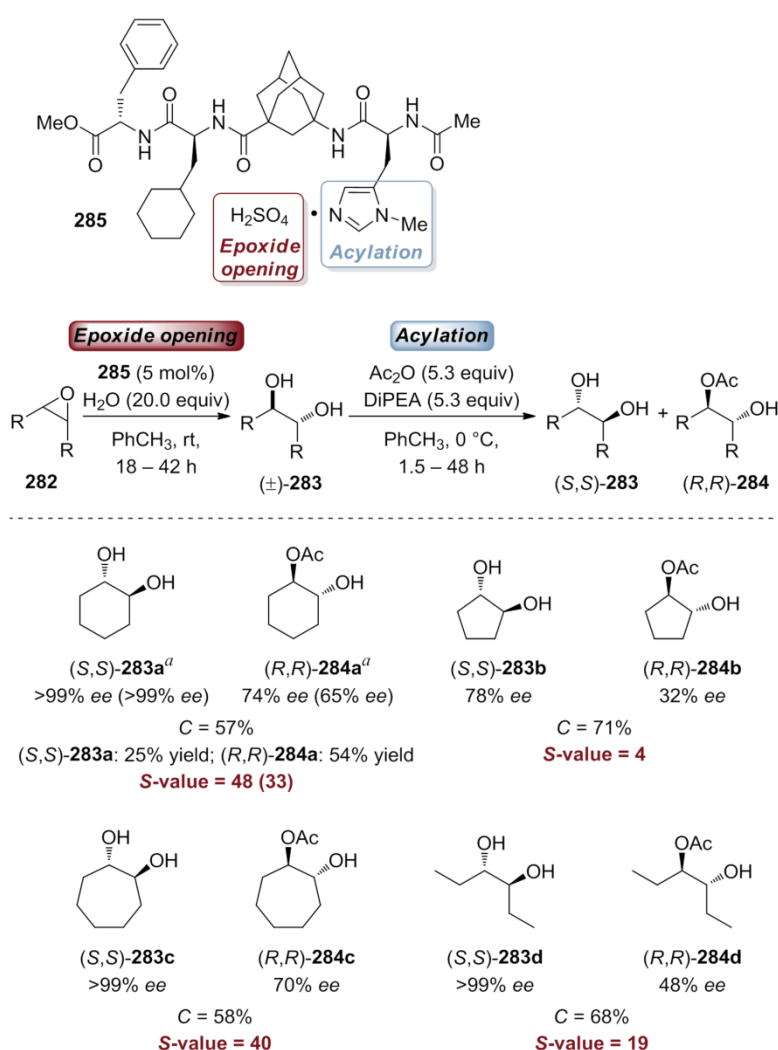


Scheme 43. Performance of multicatalyst **279** in conjunction with catalyst **280** for the three-step one-pot synthesis of enantiomerically enriched *trans*-1,2-alkanediols (*S,S*)-**283** and monoacetylated *trans*-1,2-diols (*R,R*)-**284**.

Applying the concept of *retrocatalysis*, the same group developed a new peptide-based multicatalyst (Scheme 43) bearing β -aspartate and π -methyl histidine (Pmh) as catalytic moieties (step oriented approach; see introduction).^[113] Multicatalyst **279** in conjunction with hydrazinium sulfate (**280**) enabled the synthesis of enantiomerically enriched *trans*-1,2-alkanediols (*S,S*)-**283** and monoacetylated diols (*R,R*)-**284** employing simple symmetrical alkenes **281**, hydrogen peroxide, water, and acetic anhydride. Hence, the epoxidation of alkenes **281** catalyzed by the aspartate moiety^[114] proceeds *via* intramolecular anhydride formation using *N,N'*-diisopropyl carbodiimide (DIC) as dehydrating agent. Anhydride cleavage by hydrogen peroxide generates the catalytically active monoperacid that enables the epoxidation to **282**. Addition of **280** as additional Brønsted acid catalyst, water, and toluene (the epoxide opening proceeds slower in polar solvents) for the subsequent epoxide hydrolysis produces racemic *trans*-1,2-alkanediol (\pm)-**283**. Final kinetic resolution through acylation by multicatalyst **279** completes the reaction sequence and affords the corresponding enantiomerically enriched diols (*S,S*)-**283** and monoacetylated diols (*R,R*)-**284** with moderate to good yields (the maximum would be 50%) and *S*-values up to 26 (corresponding to 99% *ee* for (*S,S*)-**283c** and 68% *ee* for (*R,R*)-**284c**). Due to protonation of the basic histidine residue by the bisulfate the addition of Hünig's base is necessary for the acylation step.

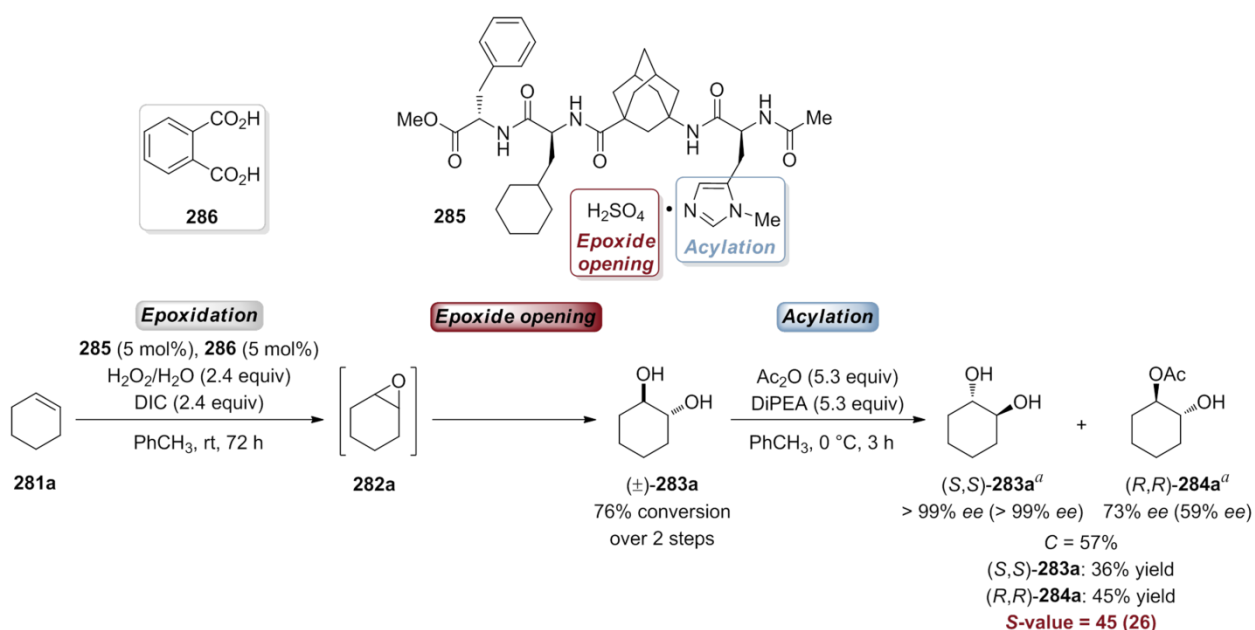
7.1 Miscellaneous Examples of Oligopeptide Catalyzed Reactions

Two related reaction sequences were reported in the same publication.^[113] Preparing the bisulfate salt **285** as an analogue of oligopeptide **280** (due to its acid lability the Boc-protecting group was exchanged by an acetyl group) allowed for the epoxide opening (Scheme 44). Addition of Hünig's base in the next step releases the acylation catalyst, thus enables the subsequent kinetic resolution of (\pm)-**283**. The corresponding *trans*-1,2-alkanediols (*S,S*)-**283** were produced with excellent enantioselectivities (usually >99% *ee*, except for (*S,S*)-**283b**). Thereby, the mono-acetylated products (*R,R*)-**284** formed with good enantioselectivities (up to 74% *ee* for (*R,R*)-**284a**) leading to *S*-values of up to 48 (at 57% conversion). Indeed, **285** is not a multicatalyst in that sense. Referring to the terminology of Fogg and dos Santos^[4] this example can be labelled as assisted tandem reaction. However, this reaction sequence was further expanded using phthalic acid (**286**) as additional epoxidation catalyst and peptide salt **285** as catalyst for the subsequent



Scheme 44. Performance of peptide salt **285** in an epoxide hydrolysis/kinetic resolution reaction sequence.

^a Values in parentheses indicate a preparative experiment on 1.0 mmol scale.



Scheme 45. Performance of peptide salt **285** in conjunction with phthalic acid (**286**) in the epoxidation/epoxide hydrolysis/kinetic resolution reaction sequence. ^a Values in parentheses indicate a preparative experiment on 1.0 mmol scale.

reaction steps (Scheme 45). Starting from cyclohexene (**281a**) this three-step reaction sequence furnished (*S,S*)-**283a** and (*R,R*)-**284a** with >99% *ee* and 73% *ee*, respectively, corresponding to an excellent *S*-value of 45 (an experiment at preparative scale gave a *S*-value of 26; Scheme 45).

8. Conclusions

In only one decade, the field of organocatalysis, an area ideally suited for green chemistry approaches, has seen tremendous progress. The development of new catalyst classes with orthogonal reactivities and their implementation in one-pot multistep processes led to considerable increase of reaction efficiency, selectivity, and sustainability.

From the beginning organomulticatalysis provided a powerful tool for the synthesis of complex molecules with increased efficiency and diminished effort. The prevalent organocatalyst classes and their specific activation modes, secondary amine catalysts, *N*-heterocyclic carbenes, thiourea derivatives, as well as synthetic oligopeptides equipped with nucleophilic π -methyl imidazole, respectively, have been applied in conjunction with other catalysts. As for any other rapidly developing discipline it is difficult to forecast what the future of multicatalysis will look like but it is clear that this concept is likely to meet many of the demands that will become increasingly important in the future, *e.g.*, reaction and resource-efficiency as well as sustainability. Organomulticatalysis is therefore likely to become one of the prevailing methodologies in organic synthesis. As there are so many different organocatalysts, the number of theoretically possible combinations seems to be limitless, and we have only begun recently to explore its potential. Most reactions discussed herein utilize only a very limited number of catalytically active moieties (mainly two) so that the main developments are in expanding the number of catalyzed reaction steps that can be carried out in one pot.

Oligopeptides offer an excellent platform for the development of novel multicatalysts. Applying the complementary strategies of *retrosynthesis* and *retrocatalysis*, a reasonable but yet elusive goal would be to enable entire syntheses of highly complex molecules (*e.g.*, natural products) by one-pot multicatalyst systems. A clear testament to the potential and importance of this approach has recently been made by Anastas and Eghbali: “*If the same catalyst could be used for various independent reactions or achieve an entire synthesis in one pot, it will bring chemistry to a new level as more complex molecules could be made with higher material and energy efficiency*”.^[29]

9. Notes and References

- [1] For general reviews on multicatalysis, see: a) L. M. Ambrosini, T. H. Lambert, *ChemCatChem* **2010**, *2*, 1373–1380; b) J. Zhou, *Chem.–Asian J.* **2010**, *5*, 422–434.
- [2] For selected authoritative reviews covering the field of asymmetric organocatalysis, see: a) A. Berkessel, H. Gröger, *Asymmetric Organocatalysis: From Biomimetic Concepts to Applications in Asymmetric Synthesis*, Wiley-VCH, Weinheim, **2005**; b) J. Seayad, B. List, *Org. Biomol. Chem.* **2005**, *3*, 719–724; c) P. I. Dalko, *Enantioselective Organocatalysis: Reactions and Experimental Procedures*, Wiley-VCH, Weinheim, **2007**; d) R. M. de Figueiredo, M. Christmann, *Eur. J. Org. Chem.* **2007**, 2575–2600; e) M. J. Gaunt, C. C. C. Johansson, A. McNally, N. T. Vo, *Drug Discovery Today* **2007**, *12*, 8–27; f) H. Pellissier, *Tetrahedron* **2007**, *63*, 9267–9331; g) D. W. C. MacMillan, *Nature* **2008**, *455*, 304–308; h) E. Marqués-López, R. P. Herrera, M. Christmann, *Nat. Prod. Rep.* **2010**, *27*, 1138–1167; i) A. Moyano, R. Rios, *Chem. Rev.* **2011**, *111*, 4703–4832; j) F. Giacalone, M. Gruttadauria, P. Agrigento, R. Noto, *Chem. Soc. Rev.* **2012**, *41*, 2406–2447.
- [3] a) L. F. Tietze, *Chem. Rev.* **1996**, *96*, 115–136; b) K. C. Nicolaou, T. Montagnon, S. A. Snyder, *Chem. Commun.* **2003**, 551–564; c) J.-C. Wasilke, S. J. Obrey, R. T. Baker, G. C. Bazan, *Chem. Rev.* **2005**, *105*, 1001–1020; d) H. C. Guo, J. A. Ma, *Angew. Chem. Int. Ed.* **2006**, *45*, 354–366; e) K. C. Nicolaou, D. J. Edmonds, P. G. Bulger, *Angew. Chem. Int. Ed.* **2006**, *45*, 7134–7186; f) L. F. Tietze, G. Brasche, K. Gericke, *Domino Reactions in Organic Synthesis*, Wiley-VCH, Weinheim, **2006**; g) C. J. Chapman, C. G. Frost, *Synthesis* **2007**, 1–21; h) K. C. Nicolaou, J. S. Chen, *Chem. Soc. Rev.* **2009**, *38*, 2993–3009.
- [4] For a general classification of cascade/domino and tandem reactions, see: D. E. Fogg, E. N. dos Santos, *Coord. Chem. Rev.* **2004**, *248*, 2365–2379.
- [5] A. M. Walji, D. W. C. MacMillan, *Synlett* **2007**, 1477–1489.
- [6] For selected general reviews on multicomponent reactions, see: a) D. J. Ramón, M. Yus, *Angew. Chem. Int. Ed.* **2005**, *44*, 1602–1634; b) J. Zhu, H. Bienaymé, *Multicomponent Reactions*, Wiley-VCH, Weinheim, **2005**; c) E. Ruijter, R. Scheffelaar, R. V. A. Orru, *Angew. Chem. Int. Ed.* **2011**, *50*, 6234–6246.
- [7] For recent reviews on organocatalytic cascade/domino reactions, see: a) D. Enders, C. Grondal, M. R. M. Hüttl, *Angew. Chem. Int. Ed.* **2007**, *46*, 1570–1581; b) X. Yu, W. Wang, *Org. Biomol. Chem.* **2008**, *6*, 2037–2046; c) A.-N. Alba, X. Companyó, M. Viciano, R. Rios, *Curr. Org. Chem.* **2009**, *13*, 1432–1474; d) C. Grondal, M. Jeanty, D. Enders, *Nat. Chem.* **2010**, *2*, 167–178; e) B. Westermann, M. Ayaz, S. S. van Berkel, *Angew. Chem. Int. Ed.* **2010**, *49*, 846–849; f) H. Pellissier, *Adv. Synth. Catal.* **2012**, *354*, 237–294.
- [8] For *N*-heterocyclic carbene catalyzed domino reactions, see: A. Grossmann, D. Enders, *Angew. Chem. Int. Ed.* **2012**, *51*, 314–325.
- [9] For a review on asymmetric organocatalytic multicomponent reactions, see: G. Guillena, D. J. Ramón, M. Yus, *Tetrahedron: Asymmetry* **2007**, *18*, 693–700.
- [10] For a general classification and overview of organocatalytic one-pot reactions, see: Ł. Albrecht, H. Jiang, K. A. Jørgensen, *Angew. Chem. Int. Ed.* **2011**, *50*, 8492–8509.
- [11] N. T. Patil, V. S. Shinde, B. Gajula, *Org. Biomol. Chem.* **2012**, *10*, 211–224.
- [12] For a recent highlight on one-pot syntheses, see: C. Vaxelaire, P. Winter, M. Christmann, *Angew. Chem. Int. Ed.* **2011**, *50*, 3605–3607.
- [13] For multicatalyst approaches employing heterodimetallic complexes, see for example: a) A. Zanardi, R. Corberán, J. A. Mata, E. Peris, *Organometallics* **2008**, *27*, 3570–3576; b) A. Zanardi, J. A. Mata, E. Peris, *J. Am. Chem. Soc.* **2009**, *131*, 14531–14537; c) A. Zanardi, J. A. Mata, E. Peris, *Chem.–Eur. J.* **2010**, *16*, 10502–10506; d) A. Zanardi, J. A. Mata, E. Peris, *Chem.–Eur. J.* **2010**, *16*, 13109–13115.
- [14] The expression *retrocatalysis* was first mentioned in context with the development of a multicatalyst in ref. 113.
- [15] a) W. Schrader, P. P. Handayani, C. Burstein, F. Glorius, *Chem. Commun.* **2007**, 716–718; b) G. W. Amarante, M. Benassi, H. M. S. Milagre, A. A. C. Braga, F. Maseras, M. N. Eberlin, F. Coelho, *Chem.–Eur. J.* **2009**, *15*, 12460–12469; c) W. Schrader, P. P. Handayani, J. Zhou, B. List, *Angew. Chem. Int. Ed.* **2009**, *48*, 1463–1466; d) A. Berkessel, S. Elfert, K. Etzenbach-Effers, J. H. Teles, *Angew. Chem. Int. Ed.*

- 2010, 49, 7120–7124; e) D. A. Bock, C. W. Lehmann, B. List, *Proc. Natl. Acad. Sci. U.S.A.* **2010**, 107, 20636–20641; f) O. V. Maltsev, A. O. Chizhov, S. G. Zlotin, *Chem.–Eur. J.* **2011**, 17, 6109–6117; g) M. W. Alachraf, P. P. Handayani, M. R. M. Hüttel, C. Grondal, D. Enders, W. Schrader, *Org. Biomol. Chem.* **2011**, 9, 1047–1053; h) J. Mahatthananchai, P. Zheng, J. W. Bode, *Angew. Chem. Int. Ed.* **2011**, 50, 1673–1677; i) M. B. Schmid, K. Zeitler, R. M. Gschwind, *J. Am. Chem. Soc.* **2011**, 133, 7065–7074; j) M. B. Schmid, K. Zeitler, R. M. Gschwind, *J. Org. Chem.* **2011**, 76, 3005–3015; k) G. Tárkányi, P. Király, T. Soós, S. Varga, *Chem.–Eur. J.* **2012**, 18, 1918–1922.
- [16] P. H.-Y. Cheong, C. Y. Legault, J. M. Um, N. Çelebi-Ölçüm, K. N. Houk, *Chem. Rev.* **2011**, 111, 5042–5137.
- [17] S. Piovesana, D. M. Scarpino Schietroma, M. Bella, *Angew. Chem. Int. Ed.* **2011**, 50, 6216–6232.
- [18] For selected publications on cooperative organocatalysis, see: a) T. Weil, M. Kotke, C. M. Kleiner, P. R. Schreiner, *Org. Lett.* **2008**, 10, 1513–1516; b) R. S. Klausen, E. N. Jacobsen, *Org. Lett.* **2009**, 11, 887–890; c) P. R. Schreiner, *Science* **2010**, 327, 965–966; d) H. Xu, S. J. Zuend, M. G. Woll, Y. Tao, E. N. Jacobsen, *Science* **2010**, 327, 986–990; e) K. Yoshida, T. Inokuma, K. Takasu, Y. Takemoto, *Synlett* **2010**, 1865–1869; f) G. Bergonzini, S. Vera, P. Melchiorre, *Angew. Chem. Int. Ed.* **2010**, 49, 9685–9688; g) S. Číhalová, P. Dziedzic, A. Córdova, J. Veselý, *Adv. Synth. Catal.* **2011**, 353, 1096–1108; h) S. Lin, L. Deiana, G.-L. Zhao, J. Sun, A. Córdova, *Angew. Chem. Int. Ed.* **2011**, 50, 7624–7630; i) Z. Zhang, K. M. Lippert, H. Hausmann, M. Kotke, P. R. Schreiner, *J. Org. Chem.* **2011**, 76, 9764–9776; j) X. Zhao, D. A. DiRocco, T. Rovis, *J. Am. Chem. Soc.* **2011**, 133, 12466–12469.
- [19] For selected publications on organocatalysis with bifunctional and multifunctional organocatalysts, see: a) A. Berkessel, F. Cleemann, S. Mukherjee, T. N. Müller, J. Lex, *Angew. Chem. Int. Ed.* **2005**, 44, 807–811; b) A. Berkessel, S. Mukherjee, F. Cleemann, T. N. Müller, J. Lex, *Chem. Commun.* **2005**, 1898–1900; c) B. Vakulya, S. Varga, A. Csampai, T. Soós, *Org. Lett.* **2005**, 7, 1967–1969; d) J. Lubkoll, H. Wennemers, *Angew. Chem. Int. Ed.* **2007**, 46, 6841–6844; e) S. J. Zuend, E. N. Jacobsen, *J. Am. Chem. Soc.* **2007**, 129, 15872–15883; f) Y.-Q. Fang, E. N. Jacobsen, *J. Am. Chem. Soc.* **2008**, 130, 5660–5661; g) C. Rabalakos, W. D. Wulff, *J. Am. Chem. Soc.* **2008**, 130, 13524–13525; h) P. Galzerano, G. Bencivenni, F. Pesciaoli, A. Mazzanti, B. Giannichi, L. Sambri, G. Bartoli, P. Melchiorre, *Chem.–Eur. J.* **2009**, 15, 7846–7849; i) J.-M. Garnier, F. Liu, *Org. Biomol. Chem.* **2009**, 7, 1272–1275; j) H. Huang, F. Yu, Z. Jin, W. Li, W. Wu, X. Liang, J. Ye, *Chem. Commun.* **2010**, 46, 5957–5959; k) V. N. Wakchaure, B. List, *Angew. Chem. Int. Ed.* **2010**, 49, 4136–4139; l) Y. Wei, M. Shi, *Acc. Chem. Res.* **2010**, 43, 1005–1018; m) J. Alemán, A. Parra, H. Jiang, K. A. Jørgensen, *Chem.–Eur. J.* **2011**, 17, 6890–6899; n) W.-Y. Siau, J. Wang, *Catal. Sci. Technol.* **2011**, 1, 1298–1310; o) B. Tan, N. R. Candeias, C. F. Barbas III, *Nat. Chem.* **2011**, 3, 473–477; p) Z. Zhang, G. Jakab, P. R. Schreiner, *Synlett* **2011**, 1262–1264; q) X. Jiang, X. Shi, S. Wang, T. Sun, Y. Cao, R. Wang, *Angew. Chem. Int. Ed.* **2012**, 51, 2084–2087; r) C. Palacio, S. J. Connon, *Chem. Commun.* **2012**, 48, 2849–2851.
- [20] For selected different examples of dual catalysis, see: a) C. E. Aroyan, M. M. Vasbinder, S. J. Miller, *Org. Lett.* **2005**, 7, 3849–3851; b) H. U. Vora, T. Rovis, *J. Am. Chem. Soc.* **2007**, 129, 13796–13797; c) M. Binanzer, S.-Y. Hsieh, J. W. Bode, *J. Am. Chem. Soc.* **2011**, 133, 19698–19701; d) N. Z. Burns, M. R. Witten, E. N. Jacobsen, *J. Am. Chem. Soc.* **2011**, 133, 14578–14581; e) C. K. De, N. Mittal, D. Seidel, *J. Am. Chem. Soc.* **2011**, 133, 16802–16805; f) S. Iwahana, H. Iida, E. Yashima, *Chem.–Eur. J.* **2011**, 17, 8009–8013; g) H. Rahaman, Á. Madarász, I. Pápai, P. M. Pihko, *Angew. Chem. Int. Ed.* **2011**, 50, 6123–6127.
- [21] a) B. List, *Tetrahedron* **2002**, 58, 5573–5590; b) S. K. Panday, *Tetrahedron: Asymmetry* **2011**, 22, 1817–1847.
- [22] S. J. Connon, *Chem. Commun.* **2008**, 2499–2510.
- [23] a) S. H. McCooey, S. J. Connon, *Angew. Chem. Int. Ed.* **2005**, 44, 6367–6370; b) T. Marcelli, J. H. van Maarseveen, H. Hiemstra, *Angew. Chem. Int. Ed.* **2006**, 45, 7496–7504; c) T. Marcelli, H. Hiemstra, *Synthesis* **2010**, 1229–1279.
- [24] a) Y. Takemoto, *Org. Biomol. Chem.* **2005**, 3, 4299–4306; b) S. J. Connon, *Chem.–Eur. J.* **2006**, 12, 5418–5427; c) M. Kotke, P. R. Schreiner, in *Hydrogen Bonding in Organic Synthesis* (Ed.: P. M. Pihko), Wiley-VCH, Weinheim, **2009**, pp. 141–351; d) S. J. Connon, *Synlett* **2009**, 354–376; e) Y. Takemoto, *Chem. Pharm. Bull.* **2010**, 58, 593–601; f) K. Hof, K. M. Lippert, P. R. Schreiner, in *Science of Synthesis*

- *Asymmetric Organocatalysis 2 – Brønsted Base and Acid Catalysts, and Additional Topics* (Ed.: K. Maruoka), Thieme, Stuttgart, NY, **2011**, pp. 297–402.
- [25] T. Okino, Y. Hoashi, Y. Takemoto, *J. Am. Chem. Soc.* **2003**, *125*, 12672–12673.
- [26] A. E. Allen, D. W. C. MacMillan, *Chem. Sci.* **2012**, *3*, 633–658.
- [27] a) P. T. Anastas, J. C. Warner, *Green Chemistry: Theory and Practice*, Oxford University Press, New York, **1998**; b) P. T. Anastas, M. M. Kirchhoff, *Acc. Chem. Res.* **2002**, *35*, 686–694.
- [28] R. A. Sheldon, I. W. C. E. Arends, U. Hanefeld, *Green Chemistry and Catalysis*, Wiley-VCH, Weinheim, **2007**.
- [29] P. Anastas, N. Eghbali, *Chem. Soc. Rev.* **2010**, *39*, 301–312.
- [30] R. A. Sheldon, *Chem. Soc. Rev.* **2012**, *41*, 1437–1451.
- [31] The twelve principles of Green Chemistry were more recently captured in the mnemonic 'PRODUCTIVELY': S. L. Y. Tang, R. L. Smith, M. Poliakoff, *Green Chem.* **2005**, *7*, 761–762.
- [32] a) R. A. Sheldon, *Chem. Ind. (London)* **1992**, 903–906; b) R. A. Sheldon, *Green Chem.* **2007**, *9*, 1273–1283.
- [33] a) B. M. Trost, *Science* **1991**, *254*, 1471–1477; b) B. M. Trost, *Angew. Chem. Int. Ed.* **1995**, *34*, 259–281.
- [34] a) P. A. Wender, S. T. Handy, D. L. Wright, *Chem. Ind. (London)* **1997**, 765–769; b) P. A. Wender, V. A. Verma, T. J. Paxton, T. H. Pillow, *Acc. Chem. Res.* **2008**, *41*, 40–49.
- [35] N. Z. Burns, P. S. Baran, R. W. Hoffmann, *Angew. Chem. Int. Ed.* **2009**, *48*, 2854–2867.
- [36] T. Newhouse, P. S. Baran, R. W. Hoffmann, *Chem. Soc. Rev.* **2009**, *38*, 3010–3021.
- [37] a) R. W. Hoffmann, *Synthesis* **2006**, 3531–3541; b) I. S. Young, P. S. Baran, *Nat. Chem.* **2009**, *1*, 193–205.
- [38] P. A. Clarke, S. Santos, W. H. C. Martin, *Green Chem.* **2007**, *9*, 438–440.
- [39] B. M. Trost, *Science* **1983**, *219*, 245–250.
- [40] For a review on multicatalysis employing transition-metal catalysts, see: a) J. M. Lee, Y. Na, H. Han, S. Chang, *Chem. Soc. Rev.* **2004**, *33*, 302–312. For a recent highlight, see: b) A. Duschek, S. F. Kirsch, *Angew. Chem. Int. Ed.* **2008**, *47*, 5703–5705.
- [41] For selected recent reviews on multienzymatic reactions, see: a) F. Lopez-Gallego, C. Schmidt-Dannert, *Curr. Opin. Chem. Biol.* **2010**, *14*, 174–183; b) E. Ricca, B. Brucher, J. H. Schrittwieser, *Adv. Synth. Catal.* **2011**, *353*, 2239–2262; c) P. A. Santacoloma, G. Sin, K. V. Gernaey, J. M. Woodley, *Org. Proc. Res. Dev.* **2011**, *15*, 203–212.
- [42] A. Bruggink, R. Schoevaart, T. Kieboom, *Org. Proc. Res. Dev.* **2003**, *7*, 622–640.
- [43] For selected reviews and highlights on combined organo-metal multicatalysis, see: a) Z. Shao, H. Zhang, *Chem. Soc. Rev.* **2009**, *38*, 2745–2755; b) A. S. K. Hashmi, C. Hubbert, *Angew. Chem. Int. Ed.* **2010**, *49*, 1010–1012; c) M. Rueping, R. M. Koenigs, I. Atodiresei, *Chem.–Eur. J.* **2010**, *16*, 9350–9365; d) C. Zhong, X. Shi, *Eur. J. Org. Chem.* **2010**, 2999–3025. For selected recent examples, see: e) J. Alemán, V. del Solar, C. Martín-Santos, L. Cubo, C. Navarro Ranninger, *J. Org. Chem.* **2011**, *76*, 7287–7293; f) I. Ibrahim, S. Santoro, F. Himo, A. Córdova, *Adv. Synth. Catal.* **2011**, *353*, 245–252; g) C. C. J. Loh, J. Badorrek, G. Raabe, D. Enders, *Chem.–Eur. J.* **2011**, *17*, 13409–13414; h) S. Lin, G.-L. Zhao, L. Deiana, J. Sun, Q. Zhang, H. Leijonmarck, A. Córdova, *Chem.–Eur. J.* **2011**, *16*, 13930–13934; i) A. Quintard, A. Alexakis, *Adv. Synth. Catal.* **2011**, *352*, 1856–1860; j) A. Quintard, A. Alexakis, C. Mazet, *Angew. Chem. Int. Ed.* **2011**, *50*, 2354–2358; k) L. Ren, T. Lei, J.-X. Ye, L.-Z. Gong, *Angew. Chem. Int. Ed.* **2012**, *51*, 771–774; l) M. Rueping, J. Dufour, M. S. Maji, *Chem. Commun.* **2012**, *48*, 3406–3408. For combinations of enzymes and metal catalysts, see: m) O. Pàmies, J.-E. Bäckvall, *Chem. Rev.* **2003**, *103*, 3247–3262; n) J. H. Lee, K. Han, M.-J. Kim, J. Park, *Eur. J. Org. Chem.* **2010**, 999–1015.
- [44] For recent reviews on aminocatalysis, see: a) B. List, *Chem. Commun.* **2006**, 819–824; b) A. Erkkilä, I. Majander, P. M. Pihko, *Chem. Rev.* **2007**, *107*, 5416–5470; c) S. Mukherjee, J. W. Yang, S. Hoffmann, B. List, *Chem. Rev.* **2007**, *107*, 5471–5569; d) P. Melchiorre, M. Marigo, A. Carlone, G. Bartoli, *Angew. Chem. Int. Ed.* **2008**, *47*, 6138–6171; e) S. Bertelsen, K. A. Jørgensen, *Chem. Soc. Rev.* **2009**, *38*, 2178–2189; f) J. B. Brazier, N. C. O. Tomkinson, *Top. Curr. Chem.* **2010**, *291*, 281–347; g) P. M. Pihko, I. Majander, A. Erkkilä, *Top. Curr. Chem.* **2010**, *291*, 29–75; h) M. Nielsen, D. Worgull, T. Zweifel, B. Gschwend, S. Bertelsen, K. A. Jørgensen, *Chem. Commun.* **2011**, *47*, 632–649.
- [45] Y. Huang, A. M. Walji, C. H. Larsen, D. W. C. MacMillan, *J. Am. Chem. Soc.* **2005**, *127*, 15051–15053.

- [46] For selected reviews on metal-free transfer hydrogenation reactions, see: a) S. G. Ouellet, A. M. Walji, D. W. C. Macmillan, *Acc. Chem. Res.* **2007**, *40*, 1327–1339; b) M. Rueping, J. Dufour, F. R. Schoepke, *Green Chem.* **2011**, *13*, 1084–1105.
- [47] G.-L. Zhao, A. Córdova, *Tetrahedron Lett.* **2006**, *47*, 7417–7421.
- [48] a) M. Marigo, T. C. Wabnitz, D. Fielenbach, K. A. Jørgensen, *Angew. Chem. Int. Ed.* **2005**, *44*, 794–797; b) Y. Hayashi, H. Gotoh, T. Hayashi, M. Shoji, *Angew. Chem. Int. Ed.* **2005**, *44*, 4212–4215.
- [49] J. Vesely, I. Ibrahim, R. Rios, G.-L. Zhao, Y. Xu, A. Córdova, *Tetrahedron Lett.* **2007**, *48*, 2193–2198.
- [50] B. Simmons, A. M. Walji, D. W. C. MacMillan, *Angew. Chem. Int. Ed.* **2009**, *48*, 4349–4353.
- [51] (–)-Aromadendranediol is a sesquiterpene, isolated from the marine coral *Sinularia mayi* and from the leaves of the Amazonian tree *Xylopia brasiliensis*; see: a) C. M. Beechan, C. Djerassi, H. Eggert, *Tetrahedron* **1978**, *34*, 2503–2508; b) I. C. Moreira, J. H. G. Lago, M. C. M. Young, N. F. Roque, *J. Braz. Chem. Soc.* **2003**, *14*, 828–831.
- [52] Y. Chi, S. T. Scroggins, J. M. J. Fréchet, *J. Am. Chem. Soc.* **2008**, *130*, 6322–6323.
- [53] S. T. Scroggins, Y. Chi, J. M. J. Fréchet, *Angew. Chem. Int. Ed.* **2010**, *49*, 2393–2396.
- [54] P. Galzerano, F. Pesciaioli, A. Mazzanti, G. Bartoli, P. Melchiorre, *Angew. Chem. Int. Ed.* **2009**, *48*, 7892–7894.
- [55] A. Desmarchelier, J. Marrot, X. Moreau, C. Greck, *Org. Biomol. Chem.* **2011**, *9*, 994–997.
- [56] J. Franzén, M. Marigo, D. Fielenbach, T. C. Wabnitz, A. Kjærsgaard, K. A. Jørgensen, *J. Am. Chem. Soc.* **2005**, *127*, 18296–18304.
- [57] J. Peña, A. B. Antón, R. F. Moro, I. S. Marcos, N. M. Garrido, D. Díez, *Tetrahedron* **2011**, *67*, 8331–8337.
- [58] For a comprehensive review on multicatalysis and multicomponent reactions developed by the Ramachary group, see: D. B. Ramachary, S. Jain, *Org. Biomol. Chem.* **2011**, *9*, 1277–1300.
- [59] U. Eder, G. Sauer, R. Wiechert, *Angew. Chem. Int. Ed.* **1971**, *10*, 496–497.
- [60] Z. G. Hajos, D. R. Parrish, *J. Org. Chem.* **1974**, *39*, 1615–1621.
- [61] D. B. Ramachary, M. Kishor, *J. Org. Chem.* **2007**, *72*, 5056–5068.
- [62] D. B. Ramachary, M. Kishor, *Org. Biomol. Chem.* **2008**, *6*, 4176–4187.
- [63] D. B. Ramachary, R. Sakthidevi, *Org. Biomol. Chem.* **2008**, *6*, 2488–2492.
- [64] D. B. Ramachary, R. Sakthidevi, *Chem.–Eur. J.* **2009**, *15*, 4516–4522.
- [65] S. Bertelsen, R. L. Johansen, K. A. Jørgensen, *Chem. Commun.* **2008**, 3016–3018.
- [66] Ł. Albrecht, B. Richter, C. Vila, H. Krawczyk, K. A. Jørgensen, *Chem.–Eur. J.* **2009**, *15*, 3093–3102.
- [67] J. L. García Ruano, V. Marcos, J. Antonio Suanzes, L. Marzo, J. Alemán, *Chem.–Eur. J.* **2009**, *15*, 6576–6580.
- [68] B. Lygo, B. Allbutt, S. R. James, *Tetrahedron Lett.* **2003**, *44*, 5629–5632.
- [69] T. Ooi, K. Maruoka, *Angew. Chem. Int. Ed.* **2007**, *46*, 4222–4266.
- [70] H. Jiang, P. Elsner, K. L. Jensen, A. Falcicchio, V. Marcos, K. A. Jørgensen, *Angew. Chem. Int. Ed.* **2009**, *48*, 6844–6848.
- [71] a) D. A. Nicewicz, D. W. C. MacMillan, *Science* **2008**, *322*, 77–80; b) D. A. Nagib, M. E. Scott, D. W. C. MacMillan, *J. Am. Chem. Soc.* **2009**, *131*, 10875–10877; c) H.-W. Shih, M. N. Vander Wal, R. L. Grange, D. W. C. MacMillan, *J. Am. Chem. Soc.* **2010**, *132*, 13600–13603.
- [72] M. Neumann, S. Földner, B. König, K. Zeitler, *Angew. Chem. Int. Ed.* **2011**, *50*, 951–954.
- [73] a) D. Enders, T. Balensiefer, *Acc. Chem. Res.* **2004**, *37*, 534–541; b) K. Zeitler, *Angew. Chem. Int. Ed.* **2005**, *44*, 7506–7510; c) D. Enders, O. Niemeier, A. Henseler, *Chem. Rev.* **2007**, *107*, 5606–5655; d) N. Marion, S. Díez-González, S. P. Nolan, *Angew. Chem. Int. Ed.* **2007**, *46*, 2988–3000; e) A. T. Biju, N. Kuhl, F. Glorius, *Acc. Chem. Res.* **2011**, *44*, 1182–1195; f) V. Nair, R. S. Menon, A. T. Biju, C. R. Sinu, R. R. Paul, A. Jose, V. Sreekumar, *Chem. Soc. Rev.* **2011**, *40*, 5336–5346.
- [74] D. Seebach, *Angew. Chem. Int. Ed.* **1979**, *18*, 239–258.
- [75] R. Breslow, *J. Am. Chem. Soc.* **1958**, *80*, 3719–3726.
- [76] G.-L. Zhao, A. Córdova, *Tetrahedron Lett.* **2007**, *48*, 5976–5980.
- [77] K. Y.-K. Chow, J. W. Bode, *J. Am. Chem. Soc.* **2004**, *126*, 8126–8127.
- [78] M. S. Kerr, J. R. de Alaniz, T. Rovis, *J. Org. Chem.* **2005**, *70*, 5725–5728.
- [79] H. Jiang, B. Gschwend, Ł. Albrecht, K. A. Jørgensen, *Org. Lett.* **2010**, *12*, 5052–5055.

- [80] Very recently, Jørgensen and co-workers reported the enantioselective one-pot synthesis of γ -nitroesters by a Michael addition/oxidative esterification of α,β -unsaturated aldehydes employing (*S*)-**7** and *N*-bromosuccinimide (NBS). The desired γ -nitroesters were formed in good yields (54 – 78%) and high enantioselectivities (93 – 96% *ee*). However, overstoichiometric amounts (1.5 or 3.0 equivalents) of NBS were necessary to perform the oxidative esterification step; see: K. L. Jensen, P. H. Poulsen, B. S. Donslund, F. Morana, K. A. Jørgensen, *Org. Lett.* **2012**, *14*, 1516–1519.
- [81] L. Deiana, P. Dziedzic, G.-L. Zhao, J. Vesely, I. Ibrahim, R. Rios, J. Sun, A. Córdova, *Chem.–Eur. J.* **2011**, *17*, 7904–7917.
- [82] S. P. Lathrop, T. Rovis, *J. Am. Chem. Soc.* **2009**, *131*, 13628–13630.
- [83] K. E. Ozboya, T. Rovis, *Chem. Sci.* **2011**, *2*, 1835–1838.
- [84] M. S. Kerr, T. Rovis, *J. Am. Chem. Soc.* **2004**, *126*, 8876–8877.
- [85] D. Enders, A. Grossmann, H. Huang, G. Raabe, *Eur. J. Org. Chem.* **2011**, 4298–4301.
- [86] C. B. Jacobsen, K. L. Jensen, J. Udmark, K. A. Jørgensen, *Org. Lett.* **2011**, *13*, 4790–4793.
- [87] L. A. Warren, S. Smiles, *J. Chem. Soc.* **1930**, 1327–1331.
- [88] An example for a multicatalytic asymmetric Diels-Alder/cross-benzoin reaction sequence was reported by Melchiorre *et al.* during the revision of this manuscript. The use of (*S*)-**7** and **119** as catalyst pair enabled the synthesis of densely functionalized *trans*-fused tetracyclic products in moderate to good yields (40 – 66%) and with high stereoselectivities (up to 8:1 d.r., 97 – 99% *ee*); see: Y. Liu, M. Nappi, E. C. Escudero-Adán, P. Melchiorre, *Org. Lett.* **2012**, *14*, 1310–1313.
- [89] C. M. Filloux, S. P. Lathrop, T. Rovis, *Proc. Natl. Acad. Sci. U.S.A.* **2010**, *107*, 20666–20671.
- [90] a) M.-J. Fan, G.-Q. Li, L.-H. Li, S.-D. Yang, Y.-M. Liang, *Synthesis* **2006**, 2286–2292; b) M.-J. Fan, G.-Q. Li, Y.-M. Liang, *Tetrahedron* **2006**, *62*, 6782–6791.
- [91] The observation that catechols enhance the catalytic efficiency of *N*-heterocyclic carbenes in Stetter reactions was confirmed recently; see: D. A. DiRocco, T. Rovis, *J. Am. Chem. Soc.* **2011**, *133*, 10402–10405.
- [92] Related non-asymmetric multicatalytic variants were reported recently: a) M. Padmanaban, A. T. Biju, F. Glorius, *Org. Lett.* **2011**, *13*, 5624–5627; b) J. F. Franz, P. J. W. Fuchs, K. Zeitler, *Tetrahedron Lett.* **2011**, *52*, 6952–6956.
- [93] For selected reviews and highlights on hydrogen bonding in organocatalysis, see: a) P. R. Schreiner, *Chem. Soc. Rev.* **2003**, *32*, 289–296; b) P. M. Pihko, *Angew. Chem. Int. Ed.* **2004**, *43*, 2062–2064; c) M. S. Taylor, E. N. Jacobsen, *Angew. Chem. Int. Ed.* **2006**, *45*, 1520–1543; d) A. G. Doyle, E. N. Jacobsen, *Chem. Rev.* **2007**, *107*, 5713–5743; e) X. Yu, W. Wang, *Chem.–Asian J.* **2008**, *3*, 516–532.
- [94] a) Z. Zhang, P. R. Schreiner, *Chem. Soc. Rev.* **2009**, *38*, 1187–1198; b) A.-F. Li, J.-H. Wang, F. Wang, Y.-B. Jiang, *Chem. Soc. Rev.* **2010**, *39*, 3729–3745. For selected examples, see: c) M. Kotke, P. R. Schreiner, *Tetrahedron* **2006**, *62*, 434–439; d) M. Kotke, P. R. Schreiner, *Synthesis* **2007**, 779–790.
- [95] Y. Wang, R.-G. Han, Y.-L. Zhao, S. Yang, P.-F. Xu, D. J. Dixon, *Angew. Chem. Int. Ed.* **2009**, *48*, 9834–9838.
- [96] Y. Wang, D.-F. Yu, Y.-Z. Liu, H. Wei, Y.-C. Luo, D. J. Dixon, P.-F. Xu, *Chem.–Eur. J.* **2010**, *16*, 3922–3925.
- [97] H. Uehara, R. Imashiro, G. Hernández-Torres, C. F. Barbas III, *Proc. Natl. Acad. Sci. U.S.A.* **2010**, *107*, 20672–20677.
- [98] A variant for the synthesis of iminosugar derivatives has been published by Barbas and co-workers employing (1*R*,2*R*)-**232** and *N,N,N',N'*-tetramethylguanidine (TMG) in conjunction with acetic acid as co-catalyst. The (1*R*,2*R*)-**232** catalyzed *anti*-Michael reaction of **233** with various nitrostyrenes **58** and subsequent TMG and acetic acid promoted intermolecular *anti*-aza-Henry reaction with tosyl-protected imine **226** provided the desired products in up to 69% yield and with high stereoselectivities (up to 10:1 d.r. and 99% *ee*). However, the use of substoichiometric amounts of base did not form the desired products in reasonable yields; see: R. Imashiro, H. Uehara, C. F. Barbas III, *Org. Lett.* **2010**, *12*, 5250–5253.
- [99] D. Enders, G. Urbanietz, G. Raabe, *Synthesis* **2011**, 1905–1911.
- [100] During the revision of this manuscript Enders *et al.* reported a multicatalytic Michael/lactonization reaction sequence employing thiourea derivative (*S*)-**208** and *p*-TSA (**72**) for the asymmetric synthesis of functionalized chromans: D. Enders, G. Urbanietz, R. Hahn, G. Raabe, *Synthesis* **2012**, 773–782.

- [101] B. Xu, Z.-L. Guo, W.-Y. Jin, Z.-P. Wang, Y.-G. Peng, Q.-X. Guo, *Angew. Chem. Int. Ed.* **2012**, *51*, 1059–1062.
- [102] For selected reviews on organocatalysis with oligopeptides, see: a) E. R. Jarvo, S. J. Miller, *Tetrahedron* **2002**, *58*, 2481–2495; b) S. J. Miller, *Acc. Chem. Res.* **2004**, *37*, 601–610; c) E. A. C. Davie, S. M. Mennen, Y. Xu, S. J. Miller, *Chem. Rev.* **2007**, *107*, 5759–5812.
- [103] For a recent highlight on asymmetric catalysis employing synthetic peptides, see: H. Wennemers, *Chem. Commun.* **2011**, *47*, 12036–12041.
- [104] For a recent review on organocatalyzed kinetic resolution and desymmetrization reactions through acyl transfer, see: C. E. Müller, P. R. Schreiner, *Angew. Chem. Int. Ed.* **2011**, *50*, 6012–6042.
- [105] V. Lutz, J. Glatthaar, C. Würtele, M. Serafin, H. Hausmann, P. R. Schreiner, *Chem.–Eur. J.* **2009**, *15*, 8548–8557.
- [106] a) C. E. Müller, L. Wanka, K. Jewell, P. R. Schreiner, *Angew. Chem. Int. Ed.* **2008**, *47*, 6180–6183; b) R. Hrdina, C. E. Müller, P. R. Schreiner, *Chem. Commun.* **2010**, *46*, 2689–2690.
- [107] L. Wanka, C. Cabrele, M. Vanejews, P. R. Schreiner, *Eur. J. Org. Chem.* **2007**, 1474–1490.
- [108] H. B. Kagan, J. C. Fiaud, *Top. Stereochem.* **1988**, *18*, 249–330.
- [109] The hypothesis that tetrapeptide **273** does not form a stable secondary structure which is stabilized by intramolecular hydrogen bonding and the stereochemical outcome of the reaction was confirmed by Shinisha and Sunoj using ONIOM computations: C. B. Shinisha, R. B. Sunoj, *Org. Lett.* **2009**, *11*, 3242–3245.
- [110] C. E. Müller, D. Zell, P. R. Schreiner, *Chem.–Eur. J.* **2009**, *15*, 9647–9650.
- [111] R. A. Sheldon, I. Arends, *Adv. Synth. Catal.* **2004**, *346*, 1051–1071.
- [112] C. E. Müller, R. Hrdina, R. C. Wende, P. R. Schreiner, *Chem.–Eur. J.* **2011**, *17*, 6309–6314.
- [113] R. Hrdina, C. E. Müller, R. C. Wende, L. Wanka, P. R. Schreiner, *Chem. Commun.* **2012**, *48*, 2498–2500.
- [114] G. Peris, C. E. Jakobsche, S. J. Miller, *J. Am. Chem. Soc.* **2007**, *129*, 8710–8711.

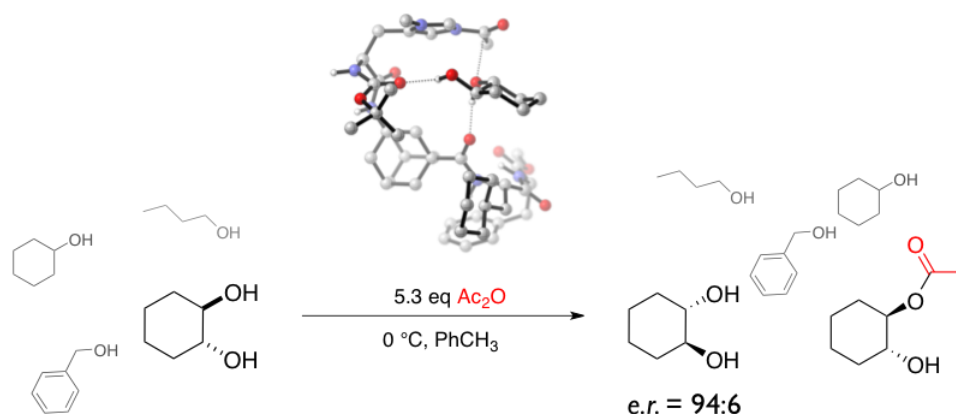
Acknowledgements

We gratefully acknowledge financial support by the Deutsche Forschungsgemeinschaft (SPP1179 Organocatalysis). R. C. W. thanks Christian E. Müller for fruitful discussions.

- Chapter II -

Lipophilic Oligopeptides for Chemo- and Enantioselective Acyl Transfer Reactions onto Alcohols

Christian E. Müller,[#] Daniela Zell,[#] Radim Hrdina, Raffael C. Wende, Lukas Wanka, Sören M. M. Schuler, and Peter R. Schreiner, *J. Org. Chem.* **2013**, 78, 8465–8484



Abstract

Inspired by the extraordinary selectivities of acylases, we envisioned the use of lipophilic oligopeptidic organocatalysts for the acylative kinetic resolution/desymmetrization of *rac*- and *meso*-cycloalkane-1,2-diols. Here we describe in a full account the discovery and development process from the theoretical concept to the final catalyst, including scope and limitations. Competition experiments with various alcohols and electrophiles show the full potential of the employed oligopeptides. Additionally, we utilized NMR and IR-spectroscopic methods as well as computations to shed light on the factors responsible for the selectivity. The catalyst system can be readily modified to a mult catalyst by adding other catalytically active amino acids to the peptide backbone, enabling the stereoselective one-pot synthesis of complex molecules from simple starting materials.

"Reprinted with permission from *The Journal of Organic Chemistry* **2013**, 78, 8465–8484. Copyright 2013 American Chemical Society."

1. Introduction

Stereoselective acylations of chiral or prochiral alcohols are common reactions both in nature and in chemistry. Enzymes can be used for the acylative resolution and desymmetrization of a broad range of secondary alcohols (*e.g.*, cyclic *meso*-1,2- and 1,3-diols, 2,5-hexanediols, 1,4-cyclooctanediols, and acylation of natural products like vitamin C, alkaloids, and hydrocortisone).^[1-5] Though enzymatic acylations are highly chemo- and enantioselective, these approaches are often expensive and require stringent reaction conditions and long reaction times, and typically just one enantiomer of the product can be obtained. Also, there is a variety of substrates that cannot be resolved effectively by enzymes (*e.g.*, *trans*-cyclohexane-1,2-diol and primary alcohols).^[6] Hence, in the past 20 years, various organic and organometallic catalysts (*e.g.*, amidines,^[7] vicinal diamines,^[8,9] *N*-alkylimidazoles,^[10-14] phosphines,^[15,16] phosphinites,^[17,18] Cu-complexes^[19-21] and 4-aminopyridine derivatives^[22,23]^[24,25] were successfully applied in kinetic resolutions (KRs),^[26,27] desymmetrizations,^[28] and dynamic kinetic resolutions (DKR)^[29,30] of alcohols, amines, and thiols (Figure 1).

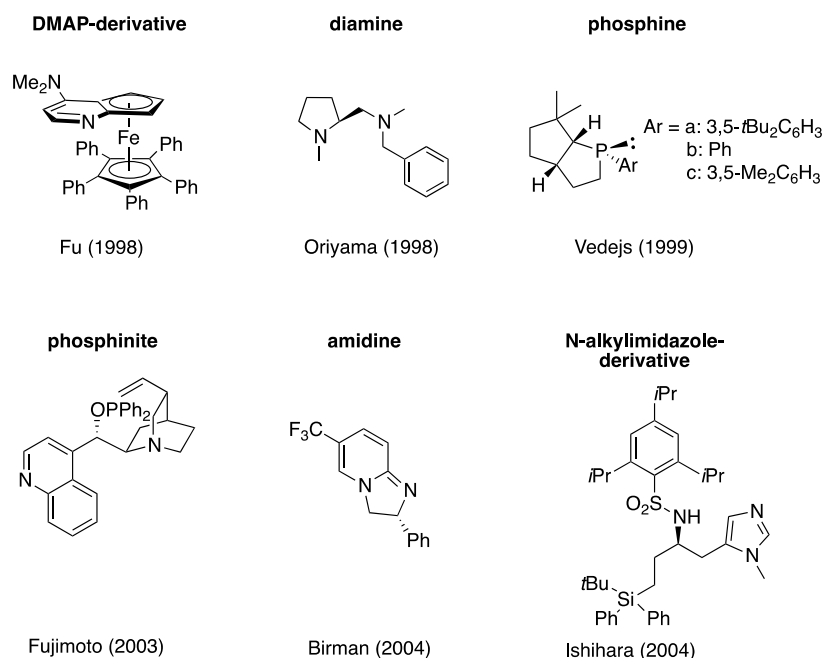


Figure 1. Nonpeptidic organocatalysts capable of selective acyl transfer.

The application of oligopeptides as catalysts for enantioselective transformations has been neglected for a surprisingly long time, though many approaches were inspired by nature.^[31,32] Only at the end of the last century did chemists realize the capacity of oligopeptides as active catalysts due to their high diversity and their well-established syntheses based on the coupling of readily available enantiopure amino acids.^[31-33] Early prominent examples are the cyclic dipeptides (diketopiperazines) introduced by Inoue in 1981 for the enantioselective

hydrocyanation of benzaldehydes^[34-38] and the homooligomers of Juliá and Colonna that proved to be highly efficient in epoxidation reactions.^[39-42] Wennemers *et al.* discovered that short proline containing oligopeptides display significantly higher reactivity at comparable enantioselectivities in aldol reactions compared to proline itself, which emphasizes the importance of the peptide backbone (Figure 2).^[43-45]

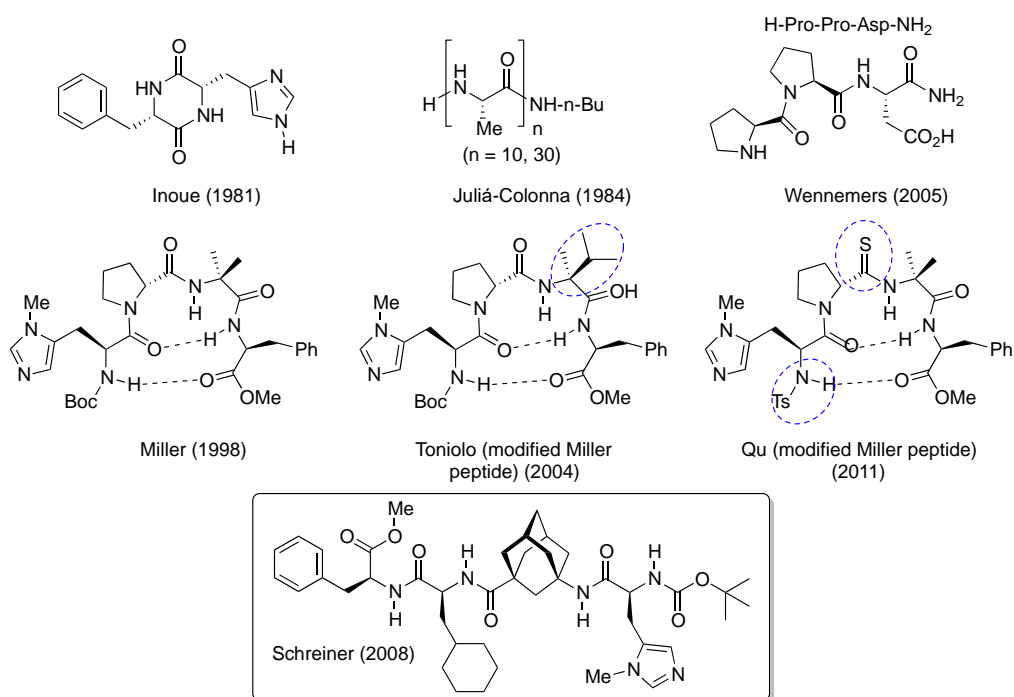


Figure 2. Peptide-based catalysts for enantioselective reactions.

Acyl transfer as part of nature's reaction portfolio is one of the most prominent examples for the use of short non-natural peptide catalysts for enantioselective transformations.^[24,25,31] In 1998, Miller and co-workers introduced *N*-alkylimidazole containing peptides (π -methyl histidine derivatives performed best) as acylation catalysts, which proved to be highly selective in various KRs and desymmetrizations.^[31,46-49] Especially the KR of racemic *trans*-2-*N*-acetamidocyclohexanol using such peptides was intensively studied and led to the conclusion that a stable yet slightly flexible secondary structure based on intramolecular H-bonding is responsible for the high enantioselectivities (Figure 2).^[31,46,49-51] Several attempts were made to improve the selectivities of these peptides by modifying the motifs that are responsible for the formation of a secondary structure (see the peptides of Toniolo^[52] and Qu^[53] in Figure 2). Though nonpeptidic catalysts were successfully utilized in natural product synthesis of, *e.g.*, epothilone, (–)-baclofen (with Fu's planar chiral ferrocenyl-DMAP derivative),^[54] lobeline (with Birman's amidine-based catalysts),^[55] and biotin (with Deng's modified cinchona alkaloid catalyst),^[56] peptidic approaches may offer chemoselective acylations of complex polyols bearing compounds (*e.g.*, vancomycin^[57] and erythromycin A^[58]) and even carbohydrates.^[59]

In 2008 our group introduced a highly efficient tetrapeptide catalyst for the KR of *trans*-cycloalkane-1,2-diols via acyl transfer (Figure 2).^[25,60] In contrast to the established peptide design concepts focusing on secondary structure formation, our approach utilizes a highly lipophilic, structurally less flexible, non-natural adamantane γ -amino acid (^AGly in our shorthand notation) in the center of the peptide. We envisioned that the more flexible amino acids at the *N*- and the *C*-terminus of the peptide would form a “dynamic pocket” like an active site in an enzyme and enable selective acyl transfer. The incorporation of additional lipophilic amino acids would allow the use of nonpolar organic solvents.

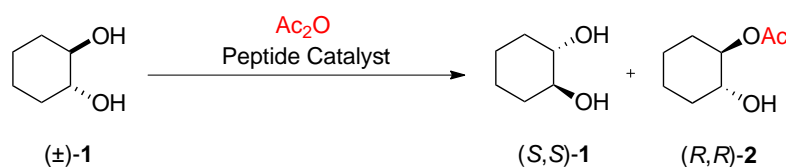
The KR of cyclic chiral *trans*-cycloalkane-1,2-diols via acyl transfer was chosen as the test reaction, because no synthetically useful approach for this class of substrates was reported. Additionally, natural products bearing vicinal diols are frequently found (*e.g.*, in steroids, flavonoids, carbohydrates, and pharmaceuticals), and therefore a highly chemoselective peptide would be quite useful.^[61] Monoacetylation of *trans*-cycloalkane-1,2-diols utilizing enzymes (*Pseudomonas* lipases) displayed low activities as well as selectivities.^[6] In the case of metal catalytic approaches for the KR of *trans*-cycloalkane-1,2-diols, only selective benzoyl transfers utilizing 0.5 equiv of benzoyl chloride with lower selectivities (*S* = 14 to 22) compared to our approach (*S* > 50) were reported by Onomura (2003),^[19] Reiser (2005),^[20] and Pfaltz (2006).^[21,62] This is one of the rare cases where a chemical method is significantly more efficient than an enzymatic approach. Later the same peptide or similar peptidic catalysts were successfully applied to selective single- and multicatalytic transformations.^[25,63-68]

The identification of such highly enantioselective catalysts is still a formidable challenge and mostly relies on trial and error or extensive screening experiments, because the chemical recognition processes of catalyst and substrate are usually hardly predictable.^[32] Here we report a full investigation of our oligopeptide catalyst platform, including catalyst screenings, substrate scope, and chemoselectivity, and present a structural mechanistic model for enantioselective acylations. Additionally, the peptide-catalyzed transfer of various other electrophiles will be described.

2. Results and Discussion

2.1 Catalyst Screening Using the Acylative KR of *trans*-Cyclohexane-1,2-diol as Test Reaction

A large variety of peptide catalysts was synthesized via automated solid phase peptide synthesis (SPPS) using a Fmoc-strategy; additionally, the chosen peptides were prepared in solution in larger quantities utilizing Boc-strategy. The crude peptides were initially characterized using ESI-MS; purified peptides were characterized by NMR, IR, ESI-MS, and ESI-HRMS (for detailed experimental procedures and analytical data, see Experimental Section and Supporting Information). All peptide catalysts were tested in the KR of racemic *trans*-cyclohexane-1,2-diol **1** (Scheme 1) with acetic anhydride. Addition of a base is not required, because the generated acetic acid ($pK_a = 4.74$) is comparably weak and in equilibrium with the methylimidazolium ion ($pK_a = 7.3$);^[69] always a small amount of unprotonated catalyst is available.



Scheme 1. KR of *trans*-cyclohexane-1,2-diol **1** as test reaction.

We started our search for a new highly lipophilic peptide by using Boc- π -methyl histidine methylester **3** (Figure 3) as a catalyst to determine whether the acyl transfer onto **1** under our chosen reaction conditions (in toluene; no auxiliary base) is generally possible.^[70] The ability to perform the KR in a nonpolar solvent in the absence of base simplifies the purification of the product. The *ee* values and yields for our test reaction (Table 1) with **3** were low. Additionally, we tested **4** introduced by Snapper and Hoveyda in 2006 (**4** showed excellent selectivities in the silylation of racemic and *meso*-1,2-diols) in the acylative KR of *rac*-**1**, but only low selectivity was observed.^[71] Our design concept focused on the ^AGly moiety as a sterically demanding and structure-determining spacer that should lead to lipophilic peptides soluble in organic solvents. At first we synthesized various tri-, tetra-, and pentapeptides and placed the rigid ^AGly in the center of the molecule (Figure 3). We hoped separating the more flexible amino acids on the C- and N-terminus of the peptide would enable the formation of a chiral environment (*e.g.*, “a pocket”, *vide infra*). Several different catalytically active histidine moieties were tested: Boc-L-histidine for peptide **5**; Boc-L-(τ -Bzl)-histidine for **7**, **8**, and **9**; and Boc-L-(π -Me)-histidine for **6**, **10**, **11**, and **12a**.

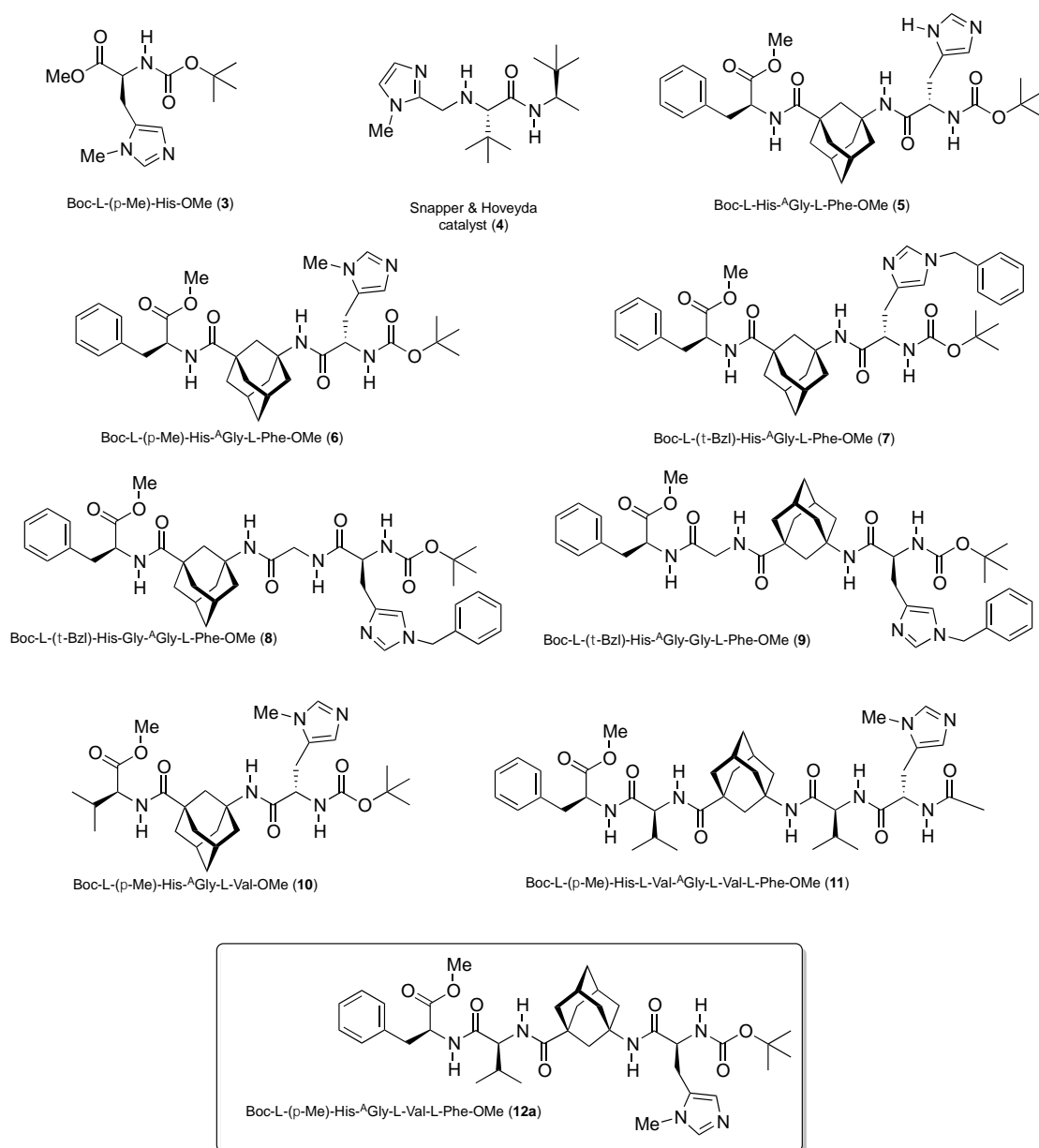


Figure 3. Starting sequences for the search of a selective acyl transfer catalyst.

The results for **3–12a** as applied to the KR of *rac*-**1** are summarized in Table 1. A comparison of the tripeptides **5–7** having the same peptidic backbone bearing a histidine (**5**), π -methyl histidine (**6**) and a τ -benzyl-histidine moiety (**7**) shows that Boc-L-(π -Me)-histidine is the catalytically most active histidine derivative. Tripeptidic and tetrapeptidic structures produced high yields but moderate selectivities; pentapeptides showed only low selectivities and activities and were not investigated further. Tetrapeptide **12a** was the most selective catalyst and was used as the reference structure for further modifications.

In contrast to enzymes, whose catalytically active sites often only exist in one stereoisomeric form, we readily synthesized *ent*-**12b** (all amino acids D-configured), and as expected, were able to acetylate *S,S*-**1** with the opposite selectivity. Switching the positions of L-Val and π -Me-His

(**13**) or L-Val and ^AGly (**17**) lowered the selectivities for the KR of *rac*-**1** compared to **12a**. Hence, it is important that ^AGly is in direct neighborhood to the catalytically active His-moiety.

Table 1. KR of *trans*-Diol (\pm)-**1** with Peptide Catalysts **3–12a**

Entry ^a	Cat.	<i>t</i> (h)	Yield (%) ^c of (<i>R,R</i>)- 2	<i>er</i> ^c of (<i>R,R</i>)- 2
1 ^b	3	15	2	46:54
2 ^d	4	4	11	44:56
3	5	42	4	76:24
4	6	18	48	69:31
5	7	210	10	54:46
6	8	210	10	58:42
7 ^b	9	210	5	53:47
8 ^b	10	15	1	75:25
9	11	15	7	50:50
10	12a	18	43	73:27

^a All reactions were performed at 0 °C in a mixture of 2.25 mL of toluene and 0.85 mL of CHCl₃ with 1 equiv (43.6 mg, 0.375 mmol) of racemic substrate **1**, 0.5 equiv of acetic anhydride, and 1 mol% of catalyst. ^b Reaction was performed at –20 °C with 0.1 equiv of acetic anhydride. Without catalyst, no conversions could be observed. ^c Yields and enantiomeric ratios were determined by chiral GC analysis using an internal calibration. ^d Reaction was performed at 0 °C in 4.5 mL of toluene with 1 equiv of racemic substrate **1** (0.025 mmol, 2.9 mg), 5.3 equiv of acetic anhydride, and 2 mol% of catalyst in toluene.

Next we focused on changing the configuration of Val, Boc-(π -Me)-His (**14** and **15**) and of both amino acids (**16**). The best *er* values were obtained for peptides containing homoconfigured Val and His (matched situation for **12a,b**, *ent*-**12b**, and **16**). The mismatched configuration of either Val or π -Me-His (**14** and **15**) decreases the selectivity for the KR of *rac*-**1** dramatically (Figure 4).

The catalytic efficiency of **12a** and the results presented in Table 2 encouraged further variations. The use of Boc-L-(π -Me)-His-^AGly-L-Cha-L-Phe-OMe (**12b**) as catalyst gave the highest *ee* in the KR of *rac*-**1**. Indeed, **12b** is the most efficient catalyst for the KR of *trans*-cycloalkane-1,2-diols to date.^[25,60] Though having identified a capable catalyst for the selective acylation of *rac*-**1** the role of the C-terminal amino acid was investigated by using the Boc-L-(π -Me)-His-^AGly-L-Leu-L-R motif (Table 3) in order to obtain mechanistic insights into the substrate recognition process by the catalyst.

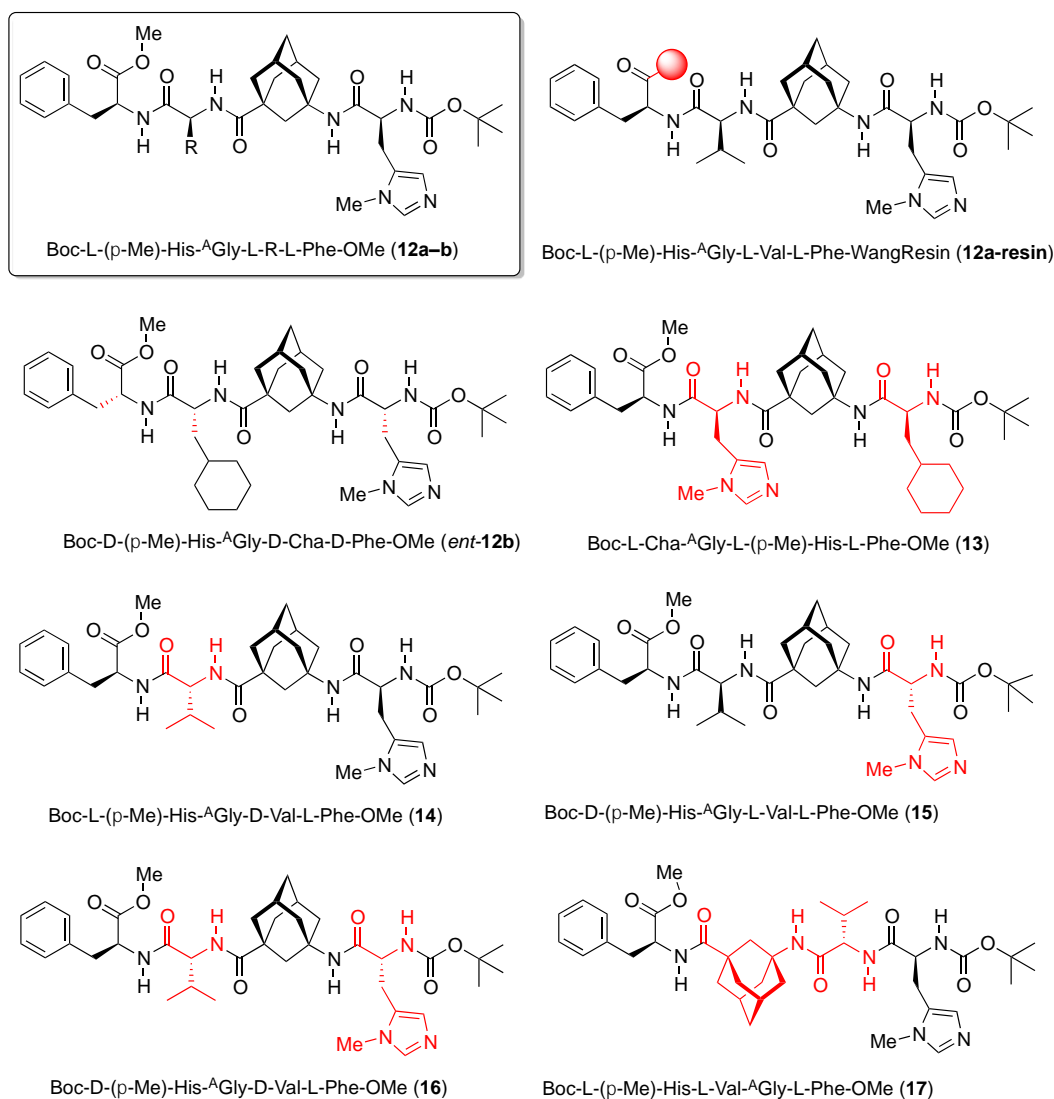


Figure 4. Variation of peptide catalysts. Structural changes of the peptides compared to **12a** and **12b** are drawn in red.

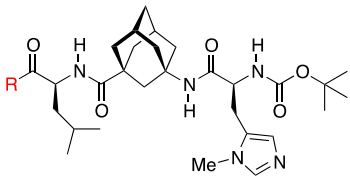
Peptide catalyst **21** with C-terminal L-Cha proved to be the most selective, but generally all tested peptides showed high selectivities. This finding implies that the C-terminal amino acid in the tetrapeptide does not strongly affect the selectivity of the peptide, and other catalytically active amino acids may be attached and therefore offer their application in multicatalytic approaches.^[65,67,68]

Table 2. Screening of the KR of (±)-**1** with peptide catalysts **12–17**.

Entry ^a	Cat.	R	Yield (%) ^c of (<i>R,R</i>)- 2	<i>er</i> ^c of (<i>R,R</i>)- 2
1	12a ^d	Val	9.9	85:15
2 ^b	12a-resin ^[72]	Val	10.2	63:37
3 ^d	<i>ent</i> - 12b	Cha	57	12:88
4	12b	Cha	8.3	88:12
5 ^d	13	—	35	57:43
6	14	—	9.8	60:40
7	15	—	8.1	46:54
8	16	—	10.5	21:79
9	17	—	5.4	67:33

^aAll reactions were performed at −20 °C for 15 h in a mixture of toluene and CHCl₃ with 1 equiv of racemic substrate **1**, 0.1 equiv of acetic anhydride, and 1 mol% of catalyst (raw product, after resin cleavage and evaporating of the solvents; without further purification). Without catalyst, no conversions were observed. ^b Reaction was performed for 24 h. ^c Yields and *er* values were determined by chiral GC analysis using an internal calibration. ^d All reactions were performed at 0 °C in 4.5 mL of toluene with 1 equiv of racemic substrate **1** (0.025 mmol, 2.9 mg), 5.3 equiv of acetic anhydride, and 2 mol% of catalyst.

Table 3. Screening of the KR of (±)-**1** with peptide catalysts **18–21** and **12c**. Investigation of the role of the C-terminal amino acid.



Boc-L-(π -Me)-His-AGly-L-Leu-R

Entry ^a	Cat.	R-	Yield (%) ^b of (<i>R,R</i>)- 2	<i>er</i> ^b of (<i>R,R</i>)- 2
1	18	L-Ala-OMe	2.0	86:14
2	19	L-Val-OMe	1.6	84:16
3	20	L-Leu-OMe	4.9	87:13
4	21	L-Cha-OMe	5.1	89:11
5	12c	L-Phe-OMe	12.7	86:14

^aAll reactions were performed at −20 °C for 15 h in a mixture of toluene and CHCl₃ with 1 equiv of racemic substrate **1**, 0.1 equiv of acetic anhydride, and 1 mol% of catalyst (raw product, after resin cleavage and evaporating of the solvents; without further purification) **18–21** and **12c**. Without catalyst, no conversions were observed.

^b Yields and enantiomer ratios were determined by chiral GC analysis using an internal calibration.

2.2 Substrate Scope for Peptide 12b-Catalyzed Acylations

In contrast to the selective esterification of 1,2-diols such as **1** (the second OH-group is important as an internal H-bond donor), other biomimetic approaches mostly require monoacetylated 1,2-diols or monoacetylated 1,2-aminoalcohols to achieve high selectivities.^[10-12,14,46] In these cases the additional H-bond acceptor of the acyl group serves as a docking position. Therefore acylation catalyst **12b** was tested in the KR of racemic **2**, **22**, and **23** (Figure 5). The latter substrate was successfully used by Miller *et al.*,^[31,46,48,50] in our hands, Miller's catalyst also led to excellent selectivities in the KR of *rac*-**23** (90% *ee* for **23**, 86% *ee* for the diacetylated aminoalcohol, *S* = 41 at *C* = 51%, 24 h at 0 °C).^[60] As expected, **12b** proved to be unselective in these three cases showing the complementarity to Miller's catalyst (Figure 2); this emphasizes the importance of the second hydrogen bond donor in the enantiodifferentiating step with **12b**.

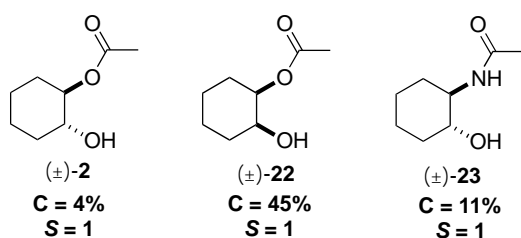


Figure 5. KR of the racemic monoacetylated substrates **2**, **22**, and **23**.

The enantioseparation of racemic secondary monoalcohols is another challenging field for acylative KRs. The KR of racemic 1-phenylethanol (**24**) via organocatalytic acyl transfer is one of the most common test reactions in this area (efficient methods often take advantage of selective π - π interactions between substrate and catalyst)^[24,25,73] and was therefore chosen as a test reaction for **12b** as well. Catalyst **12b** promoted this reaction but showed no enantioselectivity (Figure 6).^[74] The KR of other racemic secondary alcohols like *exo*-norborneol (**25**) and *rac*-**26** via acylative KR with catalyst **12b** also led to low selectivities (Figure 6).

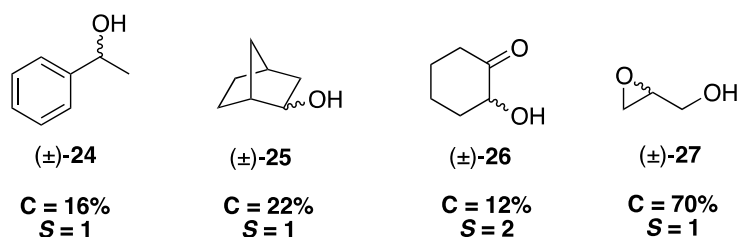
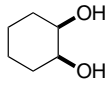
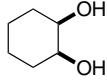
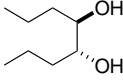
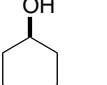
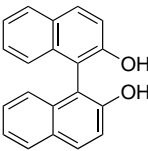
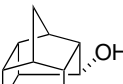
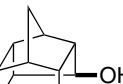
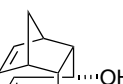
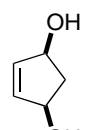
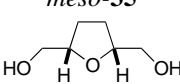


Figure 6. Testing the KR of the racemic monoalcohols **24**–**27** with catalyst **12b**.

Table 4. Testing the KR and Desymmetrization of Diols **28–36** with **12b**.

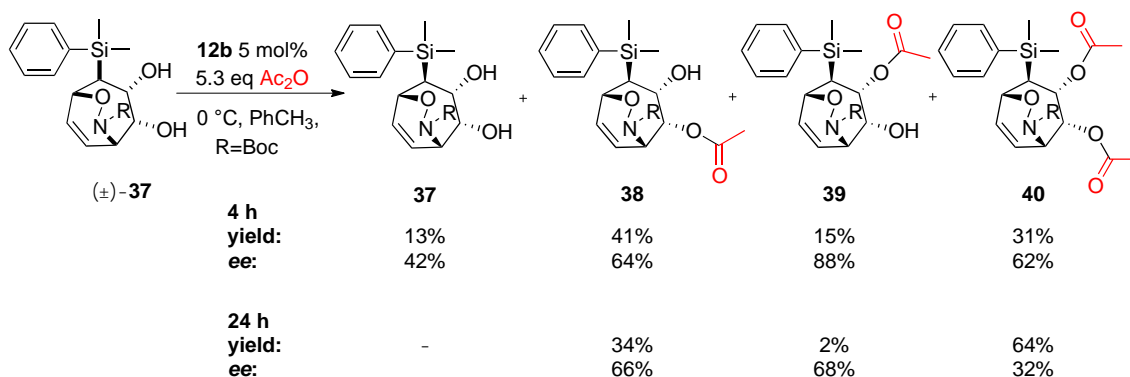
Entry ^a	Diol	<i>t</i> (h)	<i>T</i> (°C)	<i>C</i> (%) ^b	<i>ee</i> (%) ^c remaining diol	<i>ee</i> (%) ^c monoacetylated diol	<i>S</i> ^b
1	 <i>meso</i> - 28	24	0	88	—	74	—
2	 <i>meso</i> - 28	48	−40	99	—	88	—
3	 (±)- 29	8	0	61	95	65	16
4	 (±)- 30	24	0	6	—	11	1
5 ^e	 (±)- 31	24	0	60	50	33	3
6	 (±)- 32	24	0	5	—	1	1
7 ^d	 <i>meso</i> - 33	6	0	90	—	5	—
8 ^d	 <i>meso</i> - 34	5	0	2	—	11	—
9	 <i>meso</i> - 35	24	−20	63	—	4	—
10 ^d	 <i>meso</i> - 36	5	0	99	—	39	—

^a Reaction conditions: 1 equiv of diol in toluene, 5.3 equiv of Ac₂O, and 2 mol% of catalyst **12b** (purified via HPLC). Without catalyst, no conversions were observed. ^b *S*-values and conversions determined using the procedure of Kagan and Fiaud.^[77] ^c *ee* values were determined by chiral GC analysis or chiral HPLC. ^d Reaction conditions: 1 equiv of diol in toluene, 5.3 equiv of Ac₂O, 2 mol% of catalyst **12b** and 5.3 equiv of DiPEA. ^e Reaction conditions: 1 equiv of diol in toluene, 0.6 equiv of Ac₂O, and 2 mol% of catalyst (purified via HPLC) **12b**.

Nonenzymatic examples of KR or desymmetrizations of primary alcohols are rare, because no second functional group, which is usually required to achieve chemical recognition by the catalyst, is close to the hydroxyl group.^[75,76] As expected the selectivity of **12b** in the KR of racemic **27** was low (Figure 6), despite significant activity. This finding again implies that the second vicinal OH-group is key for the acylation selectivity.

As the mechanism of action (vide infra) for **12b** in acylative KRs requires a second hydrogen bond donor, a broader range of *meso*- and *rac*-1,2-diols **28–37** (Table 4/Scheme 2) was investigated.

The desymmetrization of *meso*-cyclohexane-1,2-diol (**28**) (Table 4) utilizing **12b** was tested under standard conditions (5.3 equiv of Ac₂O, toluene), and an *ee* of 74% was observed. However, the reaction was slightly more selective with base (5.3 equiv of DIPEA; *ee* = 88%). Noncyclic analogues like **29** can also be resolved with an *S*-value of 16; apparently **12b** is not only efficient for cyclic vicinal diols. 1,3-, 1,4- and 1,5-diols are also synthetically useful substrates and were therefore tested in the acylative KR with **12b**. Racemic 1,3-diol *rac*-**30** was only poorly resolved, and after 24 h, only 6% of the monoacetylated product was observed. To our delight, moderate selectivities were achieved in the **12b**-catalyzed KR of non-vicinal 1,1'-binaphthyl-2,2'-diol *rac*-**31** (*S* = 3). Enzymatic^[78] and chemical approaches^[79] were reported for the resolution of *rac*-**31**; the nonenzymatic methods are based on inclusion complexes^[80] or salt formation.^[81] Both enantiomers can be obtained in high yields and excellent *ee* values (>99%).^[80, 82] To the best of our knowledge, no catalytic, nonenzymatic approaches for the acylative KR of *rac*-**31** are known to date. This is the first example for catalyst **12b** displaying moderate selectivity for a substrate class different from 1,2-diols (Table 4). It is also worth mentioning that the KR of **31** with catalyst **12b** and acetic anhydride proceeded rapidly (4 h) under optimal conditions (5.3 equiv of Ac₂O, 0 °C), and the diol was completely converted to the corresponding monoacetylated (64%) and diacetylated (36%) products. Therefore the amount of acetic anhydride was reduced to 0.6 equiv of Ac₂O, which led to a conversion of 43% after 4 h (stirring overnight yielded 60% of monoacetylated product with 33% *ee*), and no diacetylated product was observed. This indicates that the KR of *rac*-**31** is even faster than for our reference diol **1**. In contrast, **12b** proved to be inactive and unselective for **32** and **34** and only moderately active but rather unselective in the desymmetrization experiments with the *meso*-diol **33** (Table 4). An explanation might be the rather rigid structure of **32**, **33**, and **34** and the steric demand of the substrates, as well as the absence of intramolecular hydrogen bonds. Peptide **12b** showed higher activity for the desymmetrization of *meso*-1,3-diol **35** but provided no selectivity. Surprisingly, high activity and moderate selectivity was observed for the desymmetrization of 1,5-diol **36**.^[83]

Scheme 2. KR of *rac*-**37** utilizing **12b**.

Landais *et al.* reported an efficient 10-step synthesis of aminocycloheptitols *via* desymmetrization/functionalization of 7-silylcycloheptatrienes.^[84] Further functionalization of the 7-silylcycloheptatrienes gave racemic products. Hence, we investigated the selective acetylation of *rac*-**37** by **12b** because it appeared as an excellent stereochemical test case.

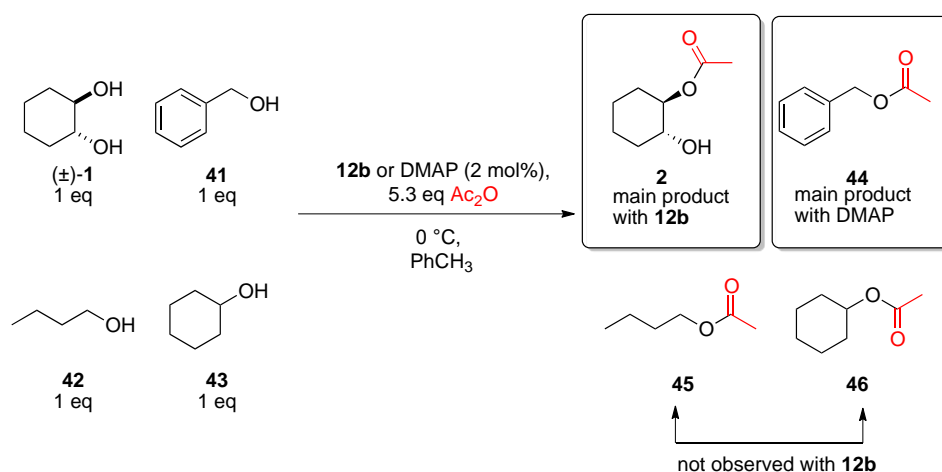
The KR of diol *rac*-**37** is rather challenging because of the complex structure (five stereogenic centers) and the potential formation of two product regioisomers **38** and **39**. In principle catalyst **12b** is capable of differentiating between both enantiomeric forms by preferring the acylation of the *R,R*-enantiomer (configuration of the hydroxyl-groups). The highest *ee*, but rather low yield (yield = 15%), was observed for the monoacetylated regioisomer **39**. The selectivity for **38** was lower, but the yield was good (yield = 41%) (Scheme 2). We suggest that the high selectivity but lower reactivity of **39** is due to the high steric demand of the dimethylphenylsilyl group in the proximity to the acetylated hydroxyl group. In contrast to all other KR experiments, we found a large amount of diacetylated product **40**.

2.3 Chemoselectivity of **12b**

The outstanding performance of catalyst **12b** for vicinal diols implies high chemoselectivity, which underlines the close relationship to natural catalysts, *e.g.*, enzymes. Of course, high chemoselectivity is often undesirable in synthetic chemistry, which normally strives for broad substrate scope. However, highly chemoselective catalytic processes are a stringent requirement for one-pot reactions, wherein various chemicals are present in the reaction mixture. This is typically the case for domino,^[85] tandem,^[85-87] or cascade^[86,87] reactions and becomes even more important for multicatalytic reactions.^[63,64,67,68,88] Additionally, this approach could be a useful tool for the site-selective acylation of, *e.g.*, polyols.

We performed competition experiments for the acetylation of chemically different alcohols with **12b** to investigate the chemoselectivity of our best catalyst. For comparison we performed the same experiments with 4-dimethylaminopyridine (DMAP) in parallel. Initial studies showed that **12b** is capable of transferring acyl groups selectively to the (*R,R*)-enantiomer of *trans*-cycloalkane-1,2-diol **1** out of a mixture of alcohols **41–43** (Table 5). We used the optimized standard reaction conditions for the KR. The reaction was quenched after 1 h and was analyzed by GC. In the presence of **12b** only esters **2** and **44** were observed. Ester **2** proved to be the main product; the e.r. of the remaining diol (94% (*S,S*)-**1** and 6% (*R,R*)-**1**) indicates that indeed (*R,R*)-**1** is by far the most reactive compound in the mixture. In contrast, DMAP led to the formation of the esters **2**, **44**, and **45** with **44** being the main product. After 2 h all of the (*R,R*)-**1** enantiomer had been acetylated by **12b**, and the catalyst showed higher activity toward **41** than to (*S,S*)-**1**. The reactivities for the acetylation of (*S,S*)-**1** and **43** by **12b** were comparable.

Table 5. Yields (via GC/MS) of **2**, **44**, **45**, and **46** obtained in the competitive acetylation reaction.



Entry	Cat.	<i>t</i> (h)	Yield (%) of 2	Yield (%) of 44	Yield (%) of 45	Yield (%) of 46
1	12b	1	59	traces	-	-
2	DMAP	1	traces	22	traces	-
3	12b	2	65	15	traces	-
4	DMAP	2	31	36	13	-
5	12b	5	72	32	traces	-
6	DMAP	5	59	68	20	-

Catalyst **12b** can also differentiate between *cis*- and *trans*-cyclohexane-1,2-diol; the acetylation of a 1:1 mixture of **1** and **28** resulted in a ratio of 84:16 (**2/28**) after 3 h. In contrast, DMAP proved to be less active and showed only a marginal preference for the *trans*-diol. The results for **12b** (Table 6) are remarkable because both diols should have comparable nucleophilicities and

differ only in the configuration of one OH group. We conclude that stronger hydrogen-bond interactions between (*R,R*)-**1** and **12b** compared to (*S,S*)-, (*R,S*)-, and (*S,R*)-**1** and **12b** are responsible for (*R,R*)-**1** preferential acetylation. The structure of (*R,R*)-**1** seems to fit perfectly into the “pocket” formed by **12b**. This extraordinary high chemo- and enantioselectivity is an astonishing feature for a small molecule.

Table 6. Concurrent and competitive acetylation of *trans*-diol (\pm)-**1** and *meso*-diol **28** with catalyst **12b** and DMAP.

$(\pm)\text{-1}$ (1 eq) + meso-28 (1 eq) $\xrightarrow[-20\text{ }^{\circ}\text{C, PhCH}_3]{\text{12b or DMAP (2 mol\%), 5.3 eq Ac}_2\text{O}}$ **2** + **22**

Entry ^a	Cat.	<i>t</i> (h)	Yield (%) 2 ^b	<i>er</i> ^b 2	Yield (%) 28 ^b	Ratio 2:28 ^b
1	12b	1.5	23	94:6	3	87:13
2	DMAP	1.5	5	50:50	4	56:44
3	12b	3	31	91:9	6	84:16
4	DMAP	3	9	50:50	7	56:44
5 ^b	12b	4.5	36	85:15	11	77:23
6	DMAP	4.5	15	50:50	12	55:44
6	12b	7.5	38	80:20	15	72:28
7 ^b	DMAP	22	20	50:50	16	55:44

^a Reactions performed at $-20\text{ }^{\circ}\text{C}$ in 4.5 mL of toluene with 1 equiv of racemic substrate **1** (0.025 mmol, 2.9 mg) and *meso* substrate **28** (0.025 mmol, 2.9 mg), 5.3 equiv of acetic anhydride, and 2 mol% **12b** or DMAP. Without catalyst, no conversions were observed. ^b Yield, *er*, values, and the **2:28** ratios were determined by chiral GC analysis.

2.4 Mechanistic Model for the Enantioselective Acylation with **12b**

For a better understanding of the chemical recognition process of the substrate by the catalyst responsible for the selectivity, we attempted NMR polarization transfer^[89] and IR studies^[90] at variable temperatures with **12b**, but we found no evidence for a secondary structure at rt (see Supporting Information for spectroscopic data). We also investigated the possibility of a structure-forming element at the stage of the acylium ion, and therefore NMR spectra of the acylium ion were measured at rt in CDCl_3 , but again no unusual NOEs indicating a secondary structure were observed.

In 2009 Sunoj et al. performed ONIOM computations at the B3LYP/6-31G(*d*):PM3 level that yielded transition structures for the **12b**-catalyzed acyl transfer onto (*R,R*)- and (*S,S*)-**1**.^[91] These computations nicely explain the observed high enantioselectivities by an energy difference of 4.5 kcal mol⁻¹ between the two transition states. Nevertheless, Sunoj's computations could not properly estimate the influence of hydrophobic R-groups in the *i* + 2 position on the selectivity, because the B3LYP/6-31G(*d*):PM3 level of theory does not include dispersion interactions.

Hence, we applied a molecular dynamics search for low-lying conformations of the catalyst/acylium ion adduct and (*R,R*)-**1** using the Merck molecular force field (MMFF)^[92] and reoptimized the lowest-lying conformation at M06-2X/6-31+G(*d,p*), which was parametrized to take into account dispersion interactions.^[93,94] The acetylated catalyst **12b** generates a chiral environment around the substrate (Figure 7, right and left). Irrespective of the starting geometry, the most favorable conformer always placed the cyclohexyl group in **12b** in close proximity to **1** (Figure 7). This arrangement helps rationalize why more hydrophobic R-groups provide higher *ee* values, as they enhance the London dispersion interactions with the substrate (Figure 7, right).^[95,96]

The two geometrically nearest C=O groups apparently provide hydrogen bonding acceptors (Figure 7) needed for chiral recognition of the diols. The model also emphasizes that the ^AGly building block provides a scaffold that separates both ends of the peptide and also holds the centers governing recognition and stereochemistry in place. It seems that *rac*-**1**, as well as the acylium ion adduct have to be present to structure the “active site” of the peptide by dispersion (Figure 7, right) and hydrogen-bonding interactions in a rather dynamic binding event.

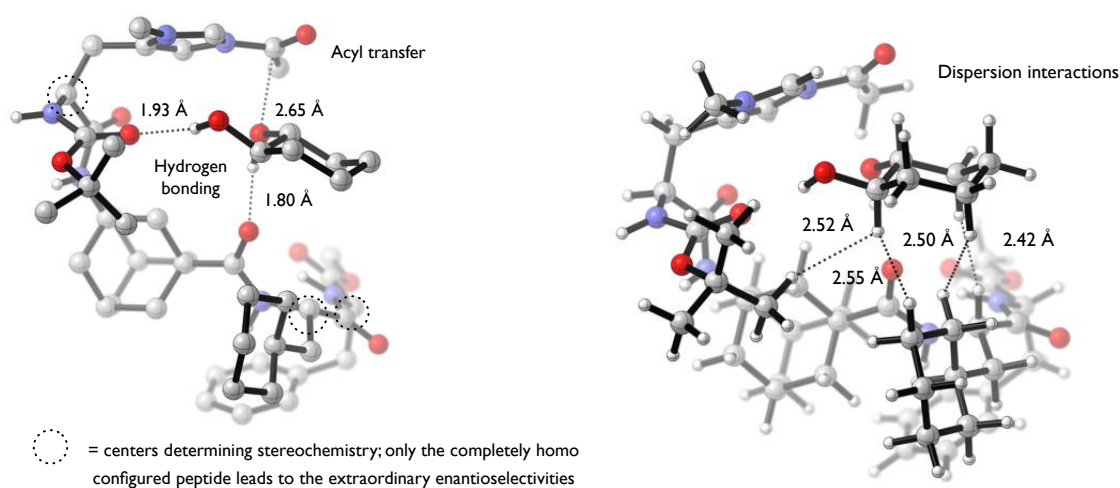


Figure 7. Left: M06-2X/6-31+G(*d,p*)^[93,94] optimized structure for the enantioselective acetylation of *trans*-cyclohexane-1,2-diol **1** in the “pocket” of the acetylated catalyst. Hydrogen atoms on the catalyst are omitted for clarity. C = gray, N = blue, O = red.^[97] Right: dispersion interactions of substrate and catalyst as judged by the typical van der Waals contacts.

2.5 Alternative Electrophiles in Group Transfer Reactions Catalyzed via Peptide **12b**

In addition to acetic anhydride, we tested a range of electrophiles in KRs and desymmetrization experiments. First of all, we investigated the role of the electrophile by determining the activity and selectivity of **12b** in the KR of *rac*-**1** using various acyl donors (Table 7). All anhydrides reacted with **1** to give the corresponding monoesters in good yields. In contrast, vinyl acetate as electrophile, which is often used in combination with enzymes, provided no conversion. Acetyl chloride gave only 5% of the monoacetylated product after 4 h and resulted in no enantioselectivity, neither for the starting material nor for the product (the background reaction led to similar conversions in the same time). Even addition of base to avoid the protonation of the catalysts only slightly increased the selectivity and reactivity. The finding that acyl chlorides, though they generally have higher carbonyl reactivities than anhydrides, are less reactive in acetyl transfer reactions catalyzed by the nucleophilic catalysts (DMAP) is common.^[98-103] The importance of the counterion for the deprotonation of the alcohol was computationally confirmed by Zipse *et al.*^[102-104] The counterion effects were experimentally analyzed by Lutz *et al.* in their X-ray, NMR- and IR-spectroscopic investigation of *N*-acetyl-DMAP salts.^[104] Surprisingly no evidence for the formation of a “tight” ion pair for the *N*-acetylpyridinium chloride was found, but in the case of *N*-acetylpyridinium acetate the analysis of the X-ray data, as well as the computations, confirmed the existence of a “tight” ion pair. Under our reaction conditions with no additional base the proton transfer has to be accomplished by the counterion, and therefore acetic anhydride reacts faster. The reaction with acetic or isobutyric anhydride proved to be fast compared to the sterically more hindered benzoic and pivalic anhydrides (Table 7). The use of acetic anhydride and isobutyric anhydride led to high selectivities ($S > 50$ for acetic anhydride, $S = 41$ for isobutyric anhydride), whereas for benzoic anhydride ($S = 8$) and pivalic anhydride ($S = 5$), only moderate selectivities were observed.

The direct use of acids as electrophiles in acylation reactions was realized by using peptide **12b** and carbodiimides (DI) for the activation and in situ formation of the anhydrides from carboxylic acid precursor; this constitutes the first enantioselective Steglich esterification.^[66]

Other electrophiles such as di-*tert*-butyl dicarbonate (Boc_2O), diphenylchlorophosphate, and various benzenesulfonyl chlorides were also used as electrophiles in the KR of (\pm) -**1** with **12b**. Miller *et al.* reported the selective sulfonylation (benzenesulfonyl chlorides)^[105] and phosphorylation (diphenylchlorophosphate)^[31, 106, 107] mediated by π -(Me)-histidine containing peptides and achieved an *ee* of 98% in 65% yield for the phosphorylation of a *meso*-inositol derivative. The selective sulfonylation of various functionalized *meso*-1,3-diols was accomplished in high yields and good selectivities (yield up to 76%; *er* up to 97:3).^[105] The reactivity of Boc_2O toward alcohols and diols in the presence of 4-(dimethylamino)pyridine (DMAP) and *N*-methyl-

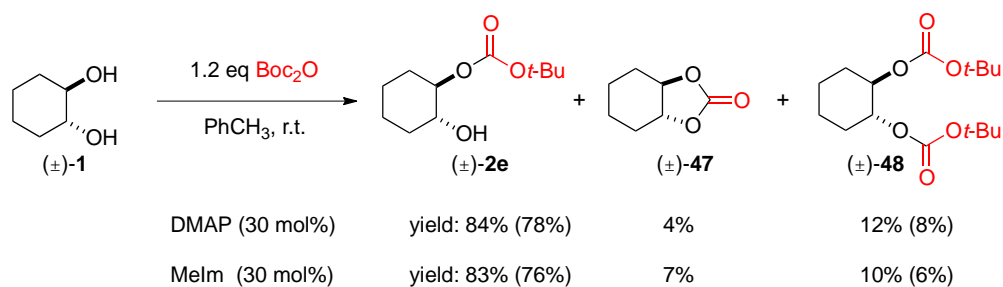
imidazole (MeIm) has been reported by Hassner et al.^[108] The transfer of the Boc-group onto *rac*-**1** was tested utilizing 30 mol% DMAP (30 mol% *N*-methylimidazole) and 1.2 equiv of Boc₂O (Scheme 3).

Table 7. KR of *trans*-diol (\pm)-**1** with peptide catalyst **12b** using various acyl donors.

<div style="text-align: center;"> </div>						
Entry ^a	Electrophile	Ester	<i>C</i> (%) ^b	<i>ee</i> (%) ^c (<i>R,R</i>)- 2	<i>ee</i> (%) ^c (<i>S,S</i>)- 1	<i>S</i> ^b
1		2	57	75	>99	>50
2		2b	59	71	>99	41
3		2c	2	64	2	5
4		2d	5	76	4	8
5		2	5	—	—	1
6 ^d		2	27	12	32	2.2
7		2	—	—	—	—

^a All reactions were performed at 0 °C in 4.5 mL of toluene, 1 equiv of racemic substrate **1** (0.025 mmol, 2.9 mg), 5.3 equiv of the electrophile, and 2 mol% of catalyst **12b** (purified via HPLC). Without catalyst, no conversions were observed. ^b *S*-values and conversions determined using the procedure of Kagan and Fiaud.^[77] ^c *ee* values were determined by chiral GC analysis. ^d The reactions were performed at 0 °C in 4.5 mL of toluene, 1 equiv of racemic substrate **1** (0.025 mmol, 2.9 mg), 5.3 equiv of the electrophile, 2 mol% of catalyst **12b** and 5.3 equiv of DIPEA.

While the monoacetylated diol (*R,R*)-**2** is the only product of the acetylation reaction, the reaction with Boc₂O is more complex, and three products were obtained by the DMAP- and MeIm-catalyzed reaction (Scheme 3). Therefore the KR of *rac*-**1** with Boc₂O required optimization (Table 8).



Scheme 3. Reaction of DMAP and MeIm with **Boc₂O** and Diol **rac-1** Leading to **O-Boc-2e**, **O,O**-di-Boc-product **48** and the cyclic carbonate **47**. Yields were determined *via* GC–MS; yields of isolated products are given in parentheses.

Table 8. KR of *trans*-cyclohexane-1,2-diol **1** with **Boc₂O** using various reaction conditions.

Entry ^a	Cat. 12b (mol%)	<i>t</i> (h)	<i>C</i> (%)	Boc₂O (eq)	<i>er</i> (<i>S,S</i>)- 1 ^c	<i>er</i> (<i>R,R</i>)- 2e ^c	<i>er</i> (<i>R,R</i>)- 47 ^e	<i>S</i> ^d
1	2	58	30	1	80:20	15:85	17:83	10.3
2	2	58	30	2	64:36	18:82	17:83	6.3
3	2	36	60	5.3	95:5	18:82	22:78	11.7
4	2	16	58	10	83:17	24:76	28:72	6.2
5	5	16	50	5	80:20	20:80	20:80	7.2
6	10	21	54	2	87:13	18:82	–	9.6
7	5	102	50	2	86:14	14:86	–	12.8
8 ^b	10	192	50	2	76:24	24:76	traces	5.2

^a All reactions were performed in 4.5 mL of dry toluene at rt. ^b This reaction was carried out at 0 °C in 4.5 mL of dry toluene. ^c Yields and enantiomer ratios were determined by chiral GC analysis. ^d *S*-values (selectivity factors) determined by the method of Kagan and Fiaud.^[77]

In principle, the enantioselective transfer of the Boc-group with **12b** is possible, but the reaction requires conditions different from those of the acylation reaction. While the acetylation reactions are most efficient using a large excess of **Ac₂O** (5.3 equiv) at low temperature (0 °C), the transfer of the Boc-group works best at rt, with 2 equiv of **Boc₂O** and 5 mol% of **12b**.

The generation of the *O*-Boc protected diol **2e** is catalyzed by **12b**, whereas the formation of the cyclic carbonate **47** only occurs in the presence of a strong base. The reaction mechanism implies that the formation of the *tert*-butoxide during the catalytic cycle probably removes the proton from the second alcohol functionality and therefore promotes cyclization to the cyclic carbonate **47** (Figure 8).^[108] Evidence for this proposal comes from the finding that **2e** does not cyclize to **47** in solution even in the presence of catalyst **12b**. In contrast, addition of Boc_2O to the solution gives only the cyclic carbonate **47**.

Using less Boc_2O minimized the formation of *tert*-butoxide, and the rate of cyclization of **2e** decreased. A catalyst loading of 5 mol% and higher temperature accelerates the reaction and avoids the generation of **47**.

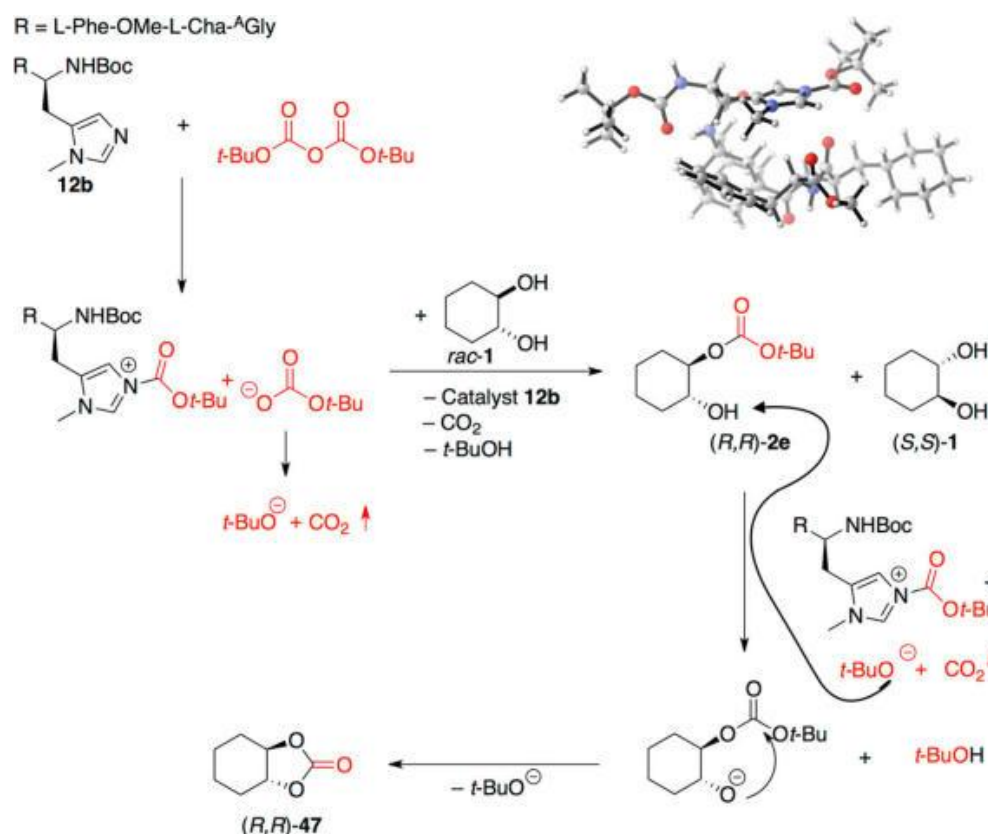


Figure 8. Proposed mechanism of the KR of *trans*-cyclohexane-1,2-diol with Boc_2O and the reoptimized (M06-2X/6-31+G(*d,p*)) structure of the catalyst/*tert*-butoxycarbonylium adduct.

Although sulfonylation reactions are widely used in organic synthesis, catalytic asymmetric sulfonyl transfer reactions are rare.^[105,109] The KR of *trans*-cyclohexane-1,2-diol with various benzenesulfonyl chlorides were therefore examined. Much to our dismay, *p*-Cl- and *p*-CH₃-benzenesulfonyl chlorides gave no reaction, while *p*-nitrobenzenesulfonyl chloride unselectively

provided 14% of the monosulfonylated-*trans*-1,2-cyclohexanediol and 8% of the disulfonylated-*trans*-1,2-cyclohexanediol after 24 h at rt.

Phosphoryl group transfer plays an important role in natural processes like cell signaling pathways. Histidine containing kinases transfer the phosphoryl group to other nucleophiles. Miller et al. successfully applied a histidine-containing peptide catalyst in the asymmetric phosphorylation of myoinositol.^[31,106,107] The phosphorylation of *trans*-cyclohexane-1,2-diol mediated by **12b** utilizing POCl(OPh)₂ under optimized reaction conditions (10 mol % **12b**, 1 equiv of POCl(OPh)₂, 1 equiv of Et₃N, rt, PhCH₃), unfortunately, yielded only 40% of the monophosphorylated product.

Table 9. Competitive functionalization of *rac*-**1** with **12b** and DMAP.

Entry	Cat.	<i>t</i> (h)	<i>C</i> (%)	<i>er</i> (%) of 1 ^c	<i>er</i> (%) of 2 ^c	<i>S</i>
1 ^a	12b	1	48	85:15	13:87	14
2 ^b	DMAP	1	16	50:50	50:50	-
3 ^a	12b	2	50	86:14	14:86	13
4 ^b	DMAP	2	18	50:50	50:50	-
5 ^a	12b	3	53	90:10	15:85	14
6 ^b	DMAP	3	20	50:50	50:50	-
7 ^d	12b	1	51	93:7	8:92	32

^a *S*-values and conversions *C* determined using the procedure of Kagan and Fiaud.^[77] ^b Conversions were determined by GC–MS analysis. ^c e.r. values were determined by chiral GC analysis. ^d Reaction was performed with 5.3 equiv of Ac₂O in absence of other electrophiles.

To test again the chemoselectivity (this time for the electrophile), we performed a competition experiment using different electrophiles (Ac_2O , $\text{POCl}(\text{OPh})_2$ or $\text{POCl}(\text{OEt})_2$ and $p\text{-NO}_2\text{-SO}_2\text{Cl}$) for the functionalization of *rac*-**1**. The progress of the reaction was monitored via GC–MS and TLC. For reasons of comparability, **12b** and DMAP were used as catalysts in parallel runs (Table 9).

After 1 h, **12b** converted nearly consumed all of (*R,R*)-**1** ($C = 48\%$). The DMAP-catalyzed reaction is slower and only provided 16% yield after 1 h. Under optimized reaction conditions, only **2** was observed with both catalysts. K_2CO_3 was used as base to avoid protonation of the catalyst. The selectivity of the competitive functionalization experiment ($S = 14$) is lower compared to the acylation experiment ($S = 32$) but still good. These results show the capability of **12b** to chemoselectively acylate *rac*-**1** even in the presence of other good electrophiles.

3. Conclusion and Outlook

We identified the highly chemo- and enantioselective peptide catalyst **12b** for acyl transfer onto racemic alkane-1,2-diols. In contrast to common peptide design approaches, **12b** does not display a preferred secondary structure but instead recognizes the diols in a dynamic binding event of the acylium cation complex involving hydrogen bonding and dispersion interactions.

Anhydrides proved to be the most efficient acyl source. Competitive experiments for substrates and electrophiles show extraordinary chemoselectivity for cyclic *trans*-alkane-1,2-diols as the substrate and acetic anhydride as the electrophile. Such a narrow substrate scope is usually only observed for enzymes or generally much larger molecules utilized as catalysts. It is therefore a rather surprising finding that a short oligopeptide such as **12b** mimics the behavior of structures that are typically by orders of magnitude more complex, but with the advantage that both substrate enantiomers can selectively be acetylated.

Such exquisite chemoselectivity is the basis for multicatalytic approaches that are now being realized. These provide high potential for rapidly reaching molecular complexity from simple starting materials in one pot, not requiring protective group chemistry.

4. Experimental Section

General Methods. Unless otherwise noted, all chemicals were purchased commercially at the highest purity grade available. Acetic anhydride, acetyl chloride, diphenylchlorophosphate and diethylchloro-phosphate were distilled prior use and stored under argon. Potassium *tert*-butylate and K_2CO_3 were dried at 200 °C under a vacuum and stored under argon. DBU, Et_3N , and DIPEA were distilled and dried prior use. All catalytic reactions were carried out under argon atmosphere employing oven- and flame-dried glassware. All solvents were distilled prior use and dried by standard laboratory protocols. 1H and ^{13}C NMR spectra were recorded on 600, 400, and 200 MHz spectrometers using TMS as an internal standard with chemical shifts given in ppm relative to TMS (δ = 0.00 ppm) or the respective solvent peaks. Two-dimensional NMR experiments were recorded on 600 or 400 MHz spectrometers using apparatus standard pulse sequences and parameters. ESI mass spectra were recorded using methanol solutions of the respective compounds. High resolution ESI mass spectrometry (ESI-TOF) was performed using methanol/water solution of the respective compounds, and MS/HRMS were recorded on a sector field spectrometer (EI-sector field). Analytical thin-layer chromatography (TLC) was performed using precoated polyester sheets Polygram SIL G/UV₂₅₄ Machery-Nagel, 0.2 mm silica gel with fluorescent indicator. Visualization was accomplished by irradiation with UV lamp and/or molybdophosphoric acid solution (5% $H_3[P(Mo_3O_{10})_4]$ in ethanol). Flash column chromatography and filtration was performed using Merck silica gel 60 Å (0.040–0.063 mm).

4.1 Availability and Characterization of the Catalysts

General Procedure I: HBTU/HOBt-Mediated Peptide Coupling on Solid Support. All peptides were prepared employing standard solid phase peptide synthesis techniques (SPPS), utilizing Fmoc-protected amino acids. 2-(1*H*-Benzotriazole-1-yl)-1,1,3,3-tetramethyluronium hexafluorophosphate (HBTU) was used as the coupling agent and 1-hydroxybenzotriazole (HOBt) as a racemization suppressant. Couplings: 1 equiv of the amino acid on solid support was shaken twice with 2 equiv of amino acid, 2 equiv of HOBt, 2 equiv of HBTU, and 4 equiv of DIPEA in DMF for 30 min. Fmoc-L-Phe-Wang resin was used as solid support and swollen in DMF for 30 min prior to first Fmoc-cleavage.

General Procedure II: Fmoc-Cleavage on Solid Support. Cleavage of *N*-terminal Fmoc-protective groups was accomplished by shaking the solid phase supported peptide twice in 25% piperidine in DMF (25 min). Prior to the next coupling step, the resin was washed 5 times with

DMF, DCM and DMF. For storing, the resin should be washed 5 times with DMF, DCM and diethyl ether and kept in a refrigerator until use.

General Procedure III: Peptide Cleavage from the Resin. Peptides were cleaved from their resins as methyl esters by shaking the functionalized resin twice for 2 days with methanol/Et₃N/THF (9:1:1). The resin was filtered off and washed several times with chloroform. The collected solutions were concentrated under reduced pressure and purified via flash silica gel chromatography eluting with chloroform/methanol (95:5).

General Procedure IV: EDC/HOBt-Mediated Peptide Coupling in Solution. The same equivalents of *N*-protected amino acids or peptide fragments, 1.1 equiv of 1-(3-dimethylaminopropyl)-3-ethylcarbodiimide hydrochloride (EDC), 1.1 equiv of HOBt and 1.1 equiv of Et₃N were dissolved in DCM and stirred for 12 h at rt. The reaction mixture was diluted with EtOAc and extracted with 0.5 M citric acid (4×) and saturated NaHCO₃ solution. The solvent was removed under reduced pressure, and the crude product was dried in a desiccator over paraffin wax and P₂O₅.

General Procedure V: Cleavage of the –O^tBu-Protecting Group (Boc). The Boc-protected peptide was dissolved in a solution of HCl in 1,4-dioxane (4.0 M) and stirred for 1 h. The excess of HCl was removed by bubbling argon through the solution. After evaporation of the solvent under reduced pressure, the deprotected peptide was coupled without further purification.

The peptides were characterized via electrospray mass spectrometry and used in the screening experiments without further purification. Peptides of interest were purified via HPLC or silica flash gel chromatography. Standard procedures for the solid phase Fmoc-based peptide synthesis as well as the Boc-based solution phase peptide chemistry can also be found in previous publications.^[61,68,69,71] The general procedure for the catalytic reactions can be found in the literature.^[61,68,69] *S*-values and conversions were calculated according to Kagan's equations.^[77] The enantiomeric excess values for the esters and recovered unreacted alcohols were determined by chiral stationary phase HPLC or chiral GC.

Boc-L-(π -Me)-His-OMe (3). Amino acid **3** is a byproduct occurring during the Wang resin cleavage of the *N*-terminal Boc-L-(π -Me)-histidine peptides. The methyl esters can be purified and isolated via HPLC. The crude product was purified by preparative HPLC (eluent: TBME/CH₃OH 93:7) UV-detector λ = 254 nm, E_{max} = 2.56; refractometer; Column *l* = 250 mm, *d* = 8 mm, LiChrosorb Diol (7 μ m, Merck); retention time (**3**) = 6.50 min. ¹H NMR (400 MHz, CDCl₃): δ /ppm = 7.32 [s, 1 H, H_{Ar}, CH (His)]; 6.71 [s, 1 H, H_{Ar}, CH (His)]; 5.19 [d, 1 H, *J* = 7.3 Hz, NH], 4.52–4.40 [m, 1 H, H_α]; 3.67 (s, 3 H, OCH₃); 3.51 (s, 3 H, NCH₃); 3.11–2.91 [m, 2 H, H_β]; 1.35 [s, 9 H, C(CH₃)₃]. ¹³C NMR (100 MHz, CDCl₃): δ /ppm = 171.6 (C=O); 155.0 (C=O); 138.3; 128.2; 126.4; 80.2; 53.0; 52.5; 31.3; 28.2; 26.8. IR (KBr): $\tilde{\nu}$ /cm^{−1} = 2978; 1746; 1709; 1507; 1438; 1367; 1290; 1253; 1217; 1200; 1167. HRMS (ESI-TOF) *m/z*: [M + H]⁺ calcd for C₁₃H₂₂N₃O₄⁺ 284.1605, found 284.1610.

Hoveyda's Catalyst: (−)-(S)-N-((R)-3,3-Dimethylbutan-2-yl)-3,3-dimethyl-2-((1-methyl-1*H*-imidazol-2-yl)methylamino)butanamide (4). Catalyst **4** was purchased and used without further purification.

Boc-L-His-^AGly-L-Phe-OMe (5). For preparation and analytics, see Ph.D. thesis of Lukas Wanka.^[110]

Boc-L-(π -Me)-His-^AGly-L-Phe-OMe (6) and Boc-L-(τ -Bzl)-His-^AGly-L-Phe-OMe (7). Analytical data of peptide **6** and **7** were identical to those reported in literature.^[111]

Boc-L-(τ -Bzl)-His-Gly-^AGly-L-Phe-OMe (8). Peptide **8** was synthesized using standard Fmoc-coupling procedures. ESI-MS: *m/z* = 741.4 [M + H]⁺ (calcd *m/z* = 741.4); *m/z* = 763.4 [M + Na]⁺ (calcd *m/z* = 763.4); *m/z* = 1481.2 [2M + H]⁺ (calcd *m/z* = 1481.8); *m/z* = 1503.2 [2M + Na]⁺ (calcd *m/z* = 1503.8).

Boc-L-(τ -Bzl)-His-^AGly-Gly-L-Phe-OMe (9). Peptide **9** was synthesized using standard Fmoc-coupling procedures. ESI-MS: *m/z* = 741.5 [M + H]⁺ (calcd *m/z* = 741.4); *m/z* = 763.4 [M + Na]⁺

(calcd m/z = 763.4); m/z = 1481.3 $[2M + H]^+$ (calcd m/z = 1481.8); m/z = 1503.3 $[2M + Na]^+$ (calcd m/z = 1503.8).

Boc-L-(π -Me)-His-^AGly-L-Val-OMe (10). Peptide **10** was synthesized using standard Fmoc-coupling procedures. ESI-MS: m/z = 560.3 $[M + H]^+$ (calcd m/z = 560.3); m/z = 582.3 $[M + Na]^+$ (calcd m/z = 582.3); m/z = 1141.1 $[2M + Na]^+$ (calcd m/z = 1141.7).

Boc-L-(π -Me)-His-L-Val-^AGly-L-Val-L-Phe-OMe (11). Peptide **11** was synthesized using standard Fmoc-coupling procedures. ESI-MS: m/z = 806.5 $[M + H]^+$ (calcd m/z = 806.5); m/z = 828.4 $[M + Na]^+$ (calcd m/z = 828.5); m/z = 1633.3 $[2M + Na]^+$ (calcd m/z = 1633.9).

Boc-L-(π -Me)-His-^AGly-L-Val-L-Phe-OMe (12a) and Boc-L-(π -Me)-His-^AGly-L-Cha-L-Phe-OMe (12b). Synthesis and analytical data can be found in the literature.^[60]

Boc-L-(π -Me)-His-^AGly-L-Val-L-Phe-WangResin (12a-resin). No characterization possible; **12a-resin** was characterized by cleaving the peptide from the peptide loaded resin. A small amount of loaded resin **12a** was used for the catalytic experiments.

Boc-D-(π -Me)-His-^AGly-D-Cha-D-Phe-OMe (*ent*-12b). The crude product was purified by preparative HPLC (eluent: TBME/CH₃OH 90:10) UV-detector λ = 254 nm, E_{\max} = 2.56; refractometer; column l = 250 mm, d = 8 mm, LiChrosorb Diol (7 μ m, Merck); retention time (*ent*-12b) = 6.60 min. 176 mg (0.23 mmol; 77%) of *ent*-12b were isolated as colorless solid. ¹H NMR (400 MHz, CDCl₃): δ /ppm = 7.34 [s, 1 H, H_{Ar}, CH (His)]; 7.25–7.14 [m, 3 H, H_{Ar} (Phe)]; 7.09–7.01 [m, 2 H, H_{Ar} (Phe)]; 6.78 [s, 1 H, H_{Ar}, CH (His)]; 6.45 [d, J = 7.8 Hz, 1 H, NH]; 5.92 [d, J = 7.9 Hz, 1 H, NH]; 5.69 [s, 1 H, NH]; 5.09 [d, J = 8.2 Hz, 1 H, NH]; 4.78–4.69 [m, 1 H, H_a]; 4.43–4.31 [m, 1 H, H_a]; 4.16–3.99 [m, 1 H, H_a]; 3.64 (s, 3 H, OCH₃); 3.53 (s, 3 H, NCH₃); 3.09–2.96 [m, 2 H, H_β]; 2.96–2.89 [m, 2 H, H_β]; 2.13 [s, 2 H, adamantane]; 1.95–1.77 [m, 6 H, adamantane + Cha]; 1.71–1.49 [m, 12 H, adamantane + Cha]; 1.44–1.38 [m, 1 H, Cha]; 1.37 [s, 9 H, C(CH₃)₃]; 1.23–0.98 [m, 4 H, Cha]; 0.92–0.71 [m, 2 H, Cha]. ¹³C NMR (100 MHz, CDCl₃):

δ/ppm = 176.3 (C=O); 171.8 (C=O); 171.6 (C=O); 169.7 (C=O), 155.4 (C=O); 138.3; 135.7; 129.2; 128.6; 128.3; 127.2; 80.5; 54.4; 53.2; 52.3; 50.7; 42.5; 42.1; 40.3; 40.3; 39.5; 38.2; 38.0; 37.8; 35.1; 34.2; 33.5; 32.7; 31.5; 29.1; 29.1; 28.3; 26.8; 26.3; 26.1; 26.1. ESI-MS: m/z = 761.6 $[\text{M} + \text{H}]^+$ (calcd m/z = 761.5); m/z = 783.5 $[\text{M} + \text{Na}]^+$ (calcd m/z = 783.4); m/z = 1543.3 $[2\text{M} + \text{Na}]^+$ (calcd m/z = 1543.9). HRMS (ESI-TOF) m/z : $[\text{M} + \text{H}]^+$ calcd for $\text{C}_{42}\text{H}_{61}\text{N}_6\text{O}_7^+$ 761.4596, found 761.4610. IR (KBr): $\tilde{\nu}/\text{cm}^{-1}$ = 3313; 2922; 2853; 1747; 1665; 1509; 1450; 1366; 1248; 1169.

Boc-L-Cha-^AGly-L-(π -Me)-His-L-Phe-OMe (13). Peptide **13** was synthesized using standard Fmoc-coupling strategy. 184 mg (0.24 mmol; 80%) of **13** were isolated as colorless solid. ^1H NMR (400 MHz, CDCl_3): δ/ppm = 7.58 [s, 1 H, H_{Ar} , CH (His)], 7.25–7.13 [m, 3 H, H_{Ar} (Phe)], 7.00 [d, 2 H, J = 8 Hz, H_{Ar} (Phe)], 6.82 [s, 1 H, H_{Ar} , CH (His)], 6.39 [d, 1 H, J = 8 Hz, NH (Phe)], 5.89 [s, 1 H, NH (Cha)], 4.88 [s, 1 H, NH (^AGly)], 4.65 [q, 1 H, J = 7.2 Hz, H_α (Phe)], 4.51 [q, 1 H, J = 7.2 Hz, H_α (Cha)], 3.98–3.89 [m, 2 H, H_α (His) + NH (His)], 3.64 [s, 3 H, OCH_3], 3.60 [s, 3 H, NCH_3], 3.10–3.01 [m, 1 H, H_β (Phe)], 3.00–2.91 [m, 3 H, H_β (His) + H_β (Phe)], 2.17–2.09 [m, 2 H, adamantane], 2.03–1.78 [m, 7 H, adamantane + Cha], 1.75–1.50 [m, 12 H, adamantane + Cha], 1.38 [s, 9 H, $\text{C}(\text{CH}_3)$], 1.27–1.01 [m, 4 H, Cha], 0.97–0.74 [m, 2 H, Cha]. ^{13}C NMR (100 MHz, CDCl_3): δ/ppm = 176.7 (C=O); 171.9 (C=O); 171.5 (C=O); 170.2 (C=O); 155.8 (C=O); 137.9, 135.8, 129.1, 128.6, 127.6, 127.1, 77.2, 53.8, 52.5, 52.0, 51.7, 42.6, 42.4, 40.5, 40.3, 39.9, 38.1, 37.9, 37.5, 35.2, 34.1, 33.7, 32.7, 32.0, 39.1, 28.3, 26.6, 26.4, 26.3, 26.1. ESI-MS: m/z = 761.3 $[\text{M} + \text{H}]^+$ (calcd m/z = 761.5). HRMS (ESI-TOF) m/z : $[\text{M} + \text{H}]^+$ calcd for $\text{C}_{42}\text{H}_{61}\text{N}_6\text{O}_7^+$ 761.4596, found 761.4575.

Boc-L-(π -Me)-His-^AGly-D-Val-L-Phe-OMe (14). Peptide **14** was synthesized using standard Fmoc-coupling strategy. The crude product was purified by preparative HPLC (eluent: TBME/ CH_3OH 90:10) UV-detector λ = 254 nm, E_{max} = 2.56; refractometer; column l = 250 mm, d = 8 mm, LiChrosorb Diol (7 μm , Merck); retention time (**14**) = 4.20 min. 193 mg (0.27 mmol; 91%) of **14** were isolated as colorless solid. ^1H NMR (400 MHz, CDCl_3): δ/ppm = 7.38 [s, 1 H, H_{Ar} , CH (His)]; 7.31–7.20 [m, 3 H, H_{Ar} (Phe)]; 7.17–7.11 [m, 2 H, H_{Ar} (Phe)]; 7.00 [bs, 1 H, NH]; 6.83 [s, 1 H, H_{Ar} , CH (His)]; 6.35 [bs, 1 H, NH]; 6.27 [d, 1 H, J = 8.4 Hz, NH]; 5.31 [d, 1 H, J = 6.4 Hz, NH]; 4.91–4.84 [m, 1 H, H_α]; 4.35 [dd, J_1 = 8.0 Hz, J_2 = 5.7 Hz, 1 H, H_α]; 4.32–4.24 [m, 1 H, H_α]; 3.70 (s, 3 H, OCH_3); 3.56 (s, 3 H, NCH_3); 3.22–3.14 [m, 1 H, H_β]; 3.05–2.95 [m, 3 H, H_β]; 2.23–1.55 (m, 14 H, adamantane); 2.16–2.08 [m, 1 H, H_β]; 1.42 (s, 9 H, $\text{C}(\text{CH}_3)_3$); 0.77 [d, 3 H, J = 6.8 Hz, H_γ (Val)]; 0.69 [d, 3 H, J = 6.8 Hz, H_γ (Val)]. ^{13}C NMR (100 MHz, CDCl_3): δ/ppm = 176.4 (C=O); 171.7 (C=O); 171.0 (C=O); 169.7 (C=O), 155.4 (C=O); 138.2;

136.0; 129.1; 128.6; 128.4; 127.1; 80.2; 57.3; 54.2; 53.2; 52.4; 52.3; 42.7; 42.7; 40.0; 38.5; 38.1; 38.1; 35.0; 31.5; 31.4; 29.1; 29.1; 28.3; 27.2; 19.3; 17.5. ESI-MS: $m/z = 707.4$ $[M + H]^+$ (calcd $m/z = 707.4$); $m/z = 729.3$ $[M + Na]^+$ (calcd $m/z = 729.4$); $m/z = 1413.1$ $[2M + H]^+$ (calcd $m/z = 1413.8$). HRMS (ESI-TOF) m/z : $[M + H]^+$ calcd for $C_{38}H_{55}N_6O_7^+$ 707.4127, found 707.4140. IR (KBr): $\tilde{\nu}/\text{cm}^{-1} = 3312$; 2912; 1745; 1661; 1509; 1455; 1367; 1248; 1169.

Boc-D-(π -Me)-His-^AGly-L-Val-L-Phe-OMe (15). Peptide **15** was synthesized using standard Fmoc-based SPPS strategy. ESI-MS: $m/z = 707.4$ $[M + H]^+$ (calcd $m/z = 707.4$); $m/z = 729.4$ $[M + Na]^+$ (calcd $m/z = 729.4$); $m/z = 1435.0$ $[2M + Na]^+$ (calcd $m/z = 1435.8$).

Boc-D-(π -Me)-His-^AGly-D-Val-L-Phe-OMe (16). Peptide **16** was synthesized using standard Fmoc-based SPPS strategy. ESI-MS: $m/z = 707.5$ $[M + H]^+$ (calcd $m/z = 707.4$); $m/z = 729.4$ $[M + Na]^+$ (calcd $m/z = 729.4$); $m/z = 745.3$ $[M + K]^+$ (calcd $m/z = 745.4$); $m/z = 1435.1$ $[2M + Na]^+$ (calcd $m/z = 1435.8$).

Boc-L-(π -Me)-His-L-Val-^AGly-L-Phe-OMe (17). Peptide **17** was synthesized using standard Fmoc-based SPPS strategy. ESI-MS: $m/z = 707.4$ $[M + H]^+$ (calcd $m/z = 707.4$); $m/z = 729.3$ $[M + Na]^+$ (calcd $m/z = 729.4$); $m/z = 1435.1$ $[2M + Na]^+$ (calcd $m/z = 1435.8$).

Boc-L-(π -Me)-His-^AGly-L-Leu-L-Ala-OMe (18). Peptide **18** was synthesized using standard Fmoc-based SPPS strategy. ESI-MS: $m/z = 645.4$ $[M + H]^+$ (calcd $m/z = 645.4$); $m/z = 667.4$ $[M + Na]^+$ (calcd $m/z = 667.4$).

Boc-L-(π -Me)-His-^AGly-L-Leu-L-Val-OMe (19). Peptide **19** was synthesized using standard Fmoc-based SPPS strategy. ESI-MS: $m/z = 673.4$ $[M + H]^+$ (calcd $m/z = 673.4$); $m/z = 695.4$ $[M + Na]^+$ (calcd $m/z = 695.4$).

Boc-L-(π -Me)-His-^AGly-L-Leu-L-Leu-OMe (20). Peptide **20** was synthesized using standard Fmoc-based SPPS strategy. ESI-MS: $m/z = 687.4$ $[M + H]^+$ (calcd $m/z = 687.4$); $m/z = 709.3$ $[M + Na]^+$ (calcd $m/z = 709.4$); $m/z = 1395.1$ $[2M + Na]^+$ (calcd $m/z = 1395.9$).

Boc-L-(π -Me)-His-^AGly-L-Leu-L-Cha-OMe (21). Peptide **21** was synthesized using standard Fmoc-based SPPS strategy. ESI-MS: $m/z = 727.5$ $[M + H]^+$ (calcd $m/z = 727.5$); $m/z = 749.4$ $[M + Na]^+$ (calcd $m/z = 749.5$); $m/z = 1475.3$ $[2M + Na]^+$ (calcd $m/z = 1475.9$).

4.2 Chiral-GC Properties and Characterization Data of the Alcohols

***trans*-Cyclohexane-1,2-diol (1).** Alcohol **1** is commercially available. The GC retention times and characterization of **1** can be found in the literature.^[60]

***trans*-1-Acetoxycyclohexan-2-ol (2).** The GC retention times, the availability, as well as the characterization of **2a** can be found in the literature.^[60]

***trans*-1,2-Diacetoxycyclohexane.** Enantiomers of *trans*-1,2-diacetoxycyclohexane were separated by chiral GC employing a 30 m FS-Hydrodex β -6TBDM column (Macherey Nagel). T (Injector + Detector) = 250 °C. Splitflow = 80 mL/min. Precolumn pressure = 0.8 bar. Conditions: 140 °C isothermal. Retention times: $t_{R,1} = 8.2$ min; $t_{R,2} = 8.5$ min. The analytical data were in accordance with the literature.^[112]

2-Hydroxycyclohexyl isobutyrate (2b), 2-Hydroxycyclohexyl pivalate (2c), and 2-Hydroxycyclohexyl benzoate (2d). The GC retention times, the proof of the GC retention time, as well as the characterization of **2b**, **2c**, and **2d** can be found in the literature.^[66]

***tert*-Butyl-2-hydroxycyclohexyl carbonate (2e).** Enantiomers of the mono-*tert*-butoxycarbonylated product **2e** were separated by chiral GC employing a 30 m FS-Hydrodex β -6TBDM column (Macherey Nagel). T (Injector + Detector) = 250 °C. Splitflow = 80 mL/min. Precolumn pressure = 0.8 bar. Conditions: 100–250 °C, 2 °C/min. Retention times: $t_{R,1}$ = 27.6 min; $t_{R,2}$ = 27.4 min. NMR data are in accordance with the literature.^[119]

***cis*-1-Acetoxycyclohexane-2-ol (22).** The GC retention times, the availability, as well as the characterization of **22** can be found in the literature.^[65,67]

***cis*-1,2-Diacetoxycyclohexane.** The GC retention time, the availability, as well as the characterization of diacetylated **22** can be found in the literature.^[65,67]

***trans*-2-Acetamidocyclohexane-1-ol (23).** Enantiomers of alcohol **23** were separated by chiral GC employing a 30 m Chiraldex G-TA column (Astech). T (Injector + Detector) = 250 °C. Splitflow = 80 mL/min. Precolumn pressure = 0.8 bar. Conditions: 130–180 °C, 2 °C/min. Retention times: $t_{R,1}$ = 25.0 min; $t_{R,2}$ = 25.8 min.

Racemic *trans*-2-amino-cyclohexan-1-ol hydrochloride (purchased and used without further purification) (0.904 g, 6.0 mmol) was treated with 0.3 M NaOH in ethanol (0.24 g in 20 mL) and stirred for 1 h at rt. Then the precipitate (NaCl) was filtered off. The ethanol was removed in vacuo, and the remaining solid was treated with 30 mL of CHCl₃ for 10 min. The precipitate was again filtered off, and the removal of the solvent in vacuo gave 0.586 g (5.1 mmol) of *trans*-2-amino-cyclohexan-1-ol as colorless powder. Analytical data of the *trans*-2-amino-cyclohexan-1-ol were essentially identical to those reported in the literature.^[113]

Racemic *trans*-2-amino-cyclohexan-1-ol (0.691 g, 6.0 mmol) was treated with acetic anhydride (742 μ L, 8 mmol) in the presence of DMAP (0.147 g, 1.2 mmol) in 25 mL of CHCl₃, and the resulting solution was stirred for 8 h at rt (25 °C). CHCl₃ was then removed in vacuo, and the monoacetylated product ((\pm)-**23**) was purified by silica flash gel chromatography (EtOAc/MeOH 75:25, R_f (**23**) = 0.44). Isolated racemic (\pm)-**23** (0.359 g, 2.3 mmol) was characterized and then subjected to the GC assay described above to prove the origin of the GC signals. Analytical data of the monoacetylated amino alcohol **23** were essentially identical to those reported in the literature.^[47,114]

***trans*-1-Acetoxy-2-acetamidocyclohexane.** Retention times: $t_{R,1} = 19.5$ min; $t_{R,2} = 19.8$ min. Analytical data of the diacetylated amino alcohol were essentially identical to those reported in literature.^[47,114]

1-Phenylethanol (24). Racemic 1-phenylethanol **24** was purchased and used without further purification. Enantiomers of alcohol **24** were separated by chiral GC employing a 30 m FS-Hydrodex β -6TBDM column (Macherey Nagel). T (Injector + Detector) = 250 °C. Splitflow = 80 mL/min. Precolumn pressure = 0.8 bar. Conditions: 100–135 °C, 1 °C/min. Retention times: $t_{R,1} = 18.6$ min; $t_{R,2} = 19.5$ min.

1-Phenyl-1-acetoxyethane. Retention times: $t_{R,1} = 13.1$ min; $t_{R,2} = 14.7$ min. The racemic acylated compound was purchased and used to prove the GC retention times.

***exo*-Bicyclo[2.2.1]heptan-2-ol (*exo*-norborneol) (25).** Racemic bicyclo[2.2.1]heptan-2-ol **25** was purchased and used without further purification. Enantiomers of alcohol **25** were separated by chiral GC employing a 30 m FS-Hydrodex β -6TBDM column (Macherey Nagel). T (Injector + Detector) = 250 °C. Splitflow = 80 mL/min. Precolumn pressure = 0.8 bar. Conditions: 80–160 °C, 2 °C/min. Retention times: $t_{R,1} = 20.9$ min; $t_{R,2} = 21.3$ min.

***exo*-2-Acetoxybicyclo[2.2.1]heptanes.** Enantiomers of the acetate of **25** were not separated by chiral GC under these conditions. Retention time: $t_R = 16.8$. The product was not isolated; a mixture of monoacylated and diacylated product were synthesized via DMAP catalysis. The products were not separated because the GC signals could clearly be allocated.

2-Hydroxycyclohexanone (26). 2-Hydroxycyclohexanone **26** was purchased as dimer (in solution the racemic monomer is formed) and used without further purification. Enantiomers of alcohol **26** were separated by chiral GC employing a 30 m FS-Hydrodex β -6TBDM column (Macherey Nagel). T (Injector + Detector) = 250 °C. Splitflow = 80 mL/min. Precolumn pressure = 0.8 bar. Conditions: 80–160 °C, 2 °C/min. Retention times: $t_{R,1} = 8.1$ min; $t_{R,2} = 8.4$ min.

2-Acetoxycyclohexanone. The GC retention times as well as the characterization can be found in the literature.^[65]

2-Oxiranylmethanol (27). Racemic 2-oxiranylmethanol **27** was purchased and used without further purification. Enantiomers of alcohol **27** were separated by chiral GC employing a 30 m FS-Hydrodex γ -TBDAC column (Macherey Nagel). T (Injector + Detector) = 250 °C. Splitflow = 80 mL/min. Precolumn pressure = 0.8 bar. Conditions: 60 °C isothermal for 3 min; then 60–100 °C, 2 °C/min. Retention times: $t_{R,1}$ = 10.8 min; $t_{R,2}$ = 10.9 min.

2-Oxiranylmethyl acetate. Retention times: $t_{R,1}$ = 17.1 min; $t_{R,2}$ = 17.5 min. Analytical data and synthesis of the acetate were identical to those reported in the literature.^[115]

cis-Cyclohexane-1,2-diol (28). Alcohol **28** is commercially available. The GC retention time and characterization of **28** can be found in the literature.^[65,67]

trans-Octane-4,5-diol (29). Enantiomers of **29** were separated by chiral GC employing a 30 m FS-Hydrodex β -TBDAC column (Macherey Nagel). T (Injector + Detector) = 250 °C. Splitflow = 80 mL/min. Precolumn pressure = 0.8 bar. Conditions: 100 °C–160 °C, 2 °C/min. Retention times: $t_{R,1}$ = 21.1 min; $t_{R,2}$ = 21.4 min. Synthesis of the alcohol: To a mixture of 4-octene oxide (1 mmol, 126 mg) in toluene (100 μ L), trifluoroacetic acid (1 mmol, 77 μ L) was added. After stirring for 24 h at rt, water (2 mmol, 36 μ L, 2.0 equiv) and DIPEA (5.3 mmol, 0.9 mL, 5.3 equiv) were added, and the reaction mixture was stirred for additional 24 h. Chromatography on silica gel in EtOAc as mobile phase afforded diol (\pm)-**29**. Analytical data of the diol ((\pm)-**29**) were identical to those reported in the literature.^[116]

trans-4-Acetoxyoctane-5-ol. Retention times: $t_{R,1}$ = 15.6 min; $t_{R,2}$ = 16.2 min. Racemic *trans*-octane-3,4-diol ((\pm)-**29**) (0.3 mmol) was treated with acetic anhydride (37 μ L, 0.4 mmol) in the presence of DMAP (7.3 mg, 0.06 mmol) in 2 mL of dichloromethane, and the resulting solution was stirred for 3 h at rt (25 °C). Dichloromethane was then removed in vacuo, and the monoacylated product was purified by silica flash gel chromatography (EtOAc). Isolated racemic acetylated **29** was analytically characterized and then subjected to the GC assay

described above to prove the origin of the GC signals. Analytical data of the monoacylated product were identical to those reported in the literature.^[117]

***trans*-Cyclohexane-1,3-diol (30).** Racemic *trans*-cyclohexane-1,3-diol **30** was purchased and used without further purification. Enantiomers of diol **30** were separated by chiral GC employing a 30 m FS-Hydrodex β -6TBDM column (Macherey Nagel). *T* (Injector + Detector) = 250 °C. Splitflow = 80 mL/min. Precolumn pressure = 0.8 bar. Conditions: 60 °C isothermal for 2 min; then 60–140 °C, 1 °C/min. Retention times: $t_{R,1}$ = 53.5 min; $t_{R,2}$ = 54.3 min.

***trans*-3-Cyclohexane-1-ol.** Retention times: $t_{R,1}$ = 51.1 min; $t_{R,2}$ = 51.9 min. *trans*-Diol **30** (0.118 g, 1.0 mmol) was treated with acetic anhydride (95 μ L, 1.0 mmol) in the presence of DMAP (0.019 g, 0.15 mmol) in 10 mL of DCM, and the resulting solution was stirred overnight at rt (25 °C). DCM was then removed in vacuo, and the monoacetylated product was purified by silica flash gel chromatography (EtOAc, R_f = 0.46). Isolated racemic monoacetylated **30** (0.082 g, 0.7 mmol; 70%) was characterized and then subjected to the GC assay described above to prove the origin of the GC signals.^[118] Additionally 0.035 g of the diacylated diol (EtOAc, R_f = 0.63; 18 mmol; 18%) were obtained. The NMR data are in accordance with the literature.^[118]

[1,1'-Binaphthalene]-2,2'-diol (Binaphthol) (31). Racemic [1,1'-binaphthalene]-2,2'-diol (Binaphthol) (**31**) was purchased and used without further purification. Enantiomers of diol **31** were separated by using HPLC employing a 25 cm, d = 0.46 cm Chiralpak IB column (Daicel). Eluent: Hexane/Isopropanol 95:5; flow = 1 mL/min; UV-detector λ = 254 nm. Retention times: $t_{R,1}$ = 32.7 min; $t_{R,2}$ = 35.0 min.

2'-Hydroxy-[1,1'-binaphthalen]-2-yl acetate. Retention times: $t_{R,1}$ = 14.1 min; $t_{R,2}$ = 16.0 min. Monoacetylated **31** was not isolated; a mixture of monoacetylated and diacylated product was synthesized via DMAP catalysis. The products were not separated because the HPLC-signals could clearly be allocated.

Octahydro-1,5,4-(epipropane[1,1,3]triyl)pentalene-2,8-diol (32). Racemic **32** was purchased from the University Lodz and used without further purification. Enantiomers of diol **32** were separated by chiral GC employing a 30 m FS-Hydrodex β -6TBDM column (Macherey Nagel). T (Injector + Detector) = 250 °C. Splitflow = 80 mL/min. Precolumn pressure = 0.8 bar. Conditions: 180 °C isothermal. Retention times: $t_{R,1}$ = 35.8 min; $t_{R,2}$ = 37.9 min.

8-Hydroxyoctahydro-1,5,4-(epipropane[1,1,3]triyl)pentalen-2-yl acetate. Retention times: $t_{R,1}$ = 20.7 min; $t_{R,2}$ = 21.4 min. Racemic diol **32** (0.089 g, 0.5 mmol) was treated with acetic anhydride (66 μ L, 0.7 mmol) in the presence of DMAP (0.012 g, 0.1 mmol) in 20 mL of Et₂O, and the resulting solution was stirred overnight at rt (25 °C). Et₂O was then removed in vacuo, and the monoacetylated product was purified by silica flash gel chromatography (EtOAc, R_f = 0.49). Isolated racemic monoacetylated product (0.051 g, 0.23 mmol; 46%) was characterized and then subjected to the GC assay described above to prove the origin of the GC signals. ¹H NMR (600 MHz, CDCl₃): δ /ppm = 4.71–4.68 [m, 1 H]; 4.68–4.65 [m, 1 H]; 2.81–2.76 [m, 1 H]; 2.76–2.71 [m, 2 H]; 2.60–2.46 [m, 3 H]; 2.38–2.33 [m, 2 H]; 2.04 [s, 3 H, CH₃]; 1.73 [d, 1 H, J = 10.6 Hz]; 1.37 [bs, 1 H, OH]; 1.34 [d, 1 H, J = 11.0 Hz]. ¹³C NMR (150 MHz, CDCl₃): δ /ppm = 170.3 (C=O); 74.5; 73.1; 48.9; 44.5; 44.1; 43.0; 42.1; 40.6; 38.8; 36.2; 34.9; 21.4. HRMS (EI-sector field) m/z : [M]⁺ calcd for C₁₃H₁₆O₃⁺ 220.109, found 220.109. IR (KBr): $\tilde{\nu}$ /cm⁻¹ = 3320; 2974; 2954; 2864; 1740; 1730; 1370; 1276; 1249; 1238; 1095; 1043.

Octahydro-1H-2,4,1-(epiethane[1,1,2]triyl)cyclobuta[cd]pentalene-5,7-diyl diacetate. Retention times: $t_{R,1}$ = 17.0 min; $t_{R,2}$ = 17.3 min. Racemic diol **32** (0.089 g, 0.5 mmol) was treated with acetic anhydride (66 μ L, 0.7 mmol) in the presence of DMAP (0.012 g, 0.1 mmol) in 20 mL of Et₂O, and the resulting solution was stirred overnight at rt (25 °C). Et₂O was then removed in vacuo, and the diacetylated product was purified by silica flash gel chromatography (EtOAc, R_f = 0.58). Isolated racemic diacetylated **32** (0.020 g, 0.08 mmol; 16%) was characterized and then subjected to the GC assay described above to prove the origin of the GC signals. ¹H NMR (600 MHz, CDCl₃): δ /ppm = 5.52 [s, 1 H]; 4.64 [t, 1 H, J = 3.9 Hz]; 2.79–2.74 [m, 1 H]; 2.68–2.64 [m, 1 H]; 2.62–2.57 [m, 2 H]; 2.50–2.43 [m, 2 H]; 2.41–2.36 [m, 1 H]; 2.33–2.88 [m, 1 H]; 2.01 [s, 3 H, CH₃]; 1.92 [s, 3 H, CH₃]; 1.65 [d, 1 H, J = 10.8 Hz]; 1.26 [d, 1 H, J = 10.7 Hz]. ¹³C NMR (150 MHz, CDCl₃): δ /ppm = 170.8 (C=O); 170.8 (C=O); 77.3; 74.1; 46.3; 45.1; 44.3; 43.0; 40.9; 39.5; 38.9; 36.4; 35.0; 21.5; 21.5. HRMS (EI-sector field) m/z : [M]⁺ calcd for C₁₅H₁₈O₄⁺ 262.121, found 262.122. IR (KBr): $\tilde{\nu}$ /cm⁻¹ = 2973; 2867; 1740; 1377; 1363; 1275; 1238; 1100; 1047; 1016.

Octahydro-1*H*-2,4,1-(epiethane[1,1,2]triyl)cyclobuta[*cd*]pentalene-5,7-diol (33). *meso*-**33** was purchased from the University Lodz and used without further purification. Achiral diol **33** was separated from the other compounds of the reaction mixture using chiral GC employing a 30 m FS-Hydrodex β -6TBDM column (Macherey Nagel). *T* (Injector + Detector) = 250 °C. Splitflow = 80 mL/min. Precolumn pressure = 0.8 bar. Conditions: 100–250 °C, 5 °C/min. Retention time: t_R = 28.4 min.

7-Hydroxyoctahydro-1*H*-2,4,1-(epiethane[1,1,2]triyl)cyclobuta[*cd*]pentalen-5-yl acetate. Enantiomers of the monoacetate of **33** were separated by chiral GC employing a 30 m FS-Hydrodex β -6TBDM column (Macherey Nagel). *T* (Injector + Detector) = 250 °C. Splitflow = 80 mL/min. Precolumn pressure = 0.8 bar. Conditions: 140 °C isothermal for 55 min; then 140–250 °C, 20 °C/min and then 250 °C for 5 min. Retention times: $t_{R,1}$ = 58.9 min; $t_{R,2}$ = 59.1 min. *Preparation:* *meso*-Diol **33** (0.089 g, 0.5 mmol) was treated with acetic anhydride (66 μ L, 0.7 mmol) in the presence of DMAP (0.012 g, 0.1 mmol) in 20 mL of Et₂O, and the resulting solution was stirred overnight at rt (25 °C). Et₂O was then removed in vacuo, and the monoacetylated product was purified by silica flash gel chromatography (EtOAc/hexane 1:1, R_f = 0.30). Isolated racemic monoacetylated **33** (0.099 g, 0.45 mmol; 90%) was characterized and then subjected to the GC assay described above to prove the origin of the GC signals. ¹H NMR (400 MHz, CDCl₃): δ /ppm = 4.89 [t, 1 H, J = 3.8 Hz]; 4.18 [d, 1 H, J = 12.4 Hz]; 3.76 [td, 1 H, J_1 = 12.4 Hz, J_2 = 3.4 Hz]; 2.84–2.76 [m, 1 H]; 2.72–2.58 [m, 3 H]; 2.53–2.47 [m, 1 H]; 2.45–2.33 [m, 3 H]; 2.11 [s, 3 H, CH₃]; 1.69 [d, 1 H, J = 10.7 Hz]; 1.11 [d, 1 H, J = 10.8 Hz]. ¹³C NMR (100 MHz, CDCl₃): δ /ppm = 169.3 (C=O); 73.0; 72.0; 45.4; 43.0; 43.0; 42.5; 39.7; 39.2; 38.1; 35.6; 34.3; 21.4. HRMS (EI-sector field) m/z : [M]⁺ calcd for C₁₃H₁₆O₃⁺ 220.110, found 220.110. IR (KBr): $\tilde{\nu}$ /cm⁻¹ = 3545; 2964; 2864; 1744; 1436; 1368; 1311; 1268; 1224; 1150; 1098; 1077; 1038.

7-Hydroxyoctahydro-1*H*-2,4,1-(epiethane[1,1,2]triyl)cyclobuta[*cd*]pentalen-5-yl diacetate. The achiral diacetate of **33** was separated from the other compounds of the reaction mixture using chiral GC employing a 30 m FS-Hydrodex β -6TBDM column (Macherey Nagel). *T* (Injector + Detector) = 250 °C. Splitflow = 80 mL/min. Precolumn pressure = 0.8 bar. Conditions: 100–250 °C, 5 °C/min. Retention time: t_R = 25.7 min. *Preparation:* *meso*-Diol **33** (0.089 g, 0.5 mmol) was treated with acetic anhydride (66 μ L, 0.7 mmol) in the presence of DMAP (0.012 g, 0.1 mmol) in 20 mL of Et₂O, and the resulting solution was stirred overnight at rt (25 °C). Et₂O was then removed in vacuo, and the diacetylated product was purified by silica flash gel chromatography (EtOAc/hexane 1:1, R_f = 0.41). Isolated diacetylated **33** (0.010 g, (0.04 mmol; 8%) was characterized and then subjected to the GC assay described above to prove the origin of the GC signals. ¹H NMR (400 MHz, CDCl₃): δ /ppm = 4.58–4.53 [m, 2 H]; 2.82–

2.71 [m, 2 H]; 2.62–2.51 [m, 2 H]; 2.45 [s, 2 H]; 2.39–2.30 [m, 2 H]; 2.00 [s, 6 H, CH₃]; 1.62 [d, 1 H, *J* = 10.8 Hz]; 1.06 [d, 1 H, *J* = 10.8 Hz]. ¹³C NMR (100 MHz, CDCl₃): δ/ppm = 171.1 (C=O); 72.2; 43.0; 42.2; 39.2; 35.3; 34.1; 21.6. HRMS (EI-sector field) *m/z*: [M]⁺ calcd for C₁₅H₁₈O₄⁺ 262.121, found 262.124. IR (KBr): $\tilde{\nu}/\text{cm}^{-1}$ = 2969; 2942; 2927; 2858; 1728; 1449; 1438; 1374; 1366; 1305; 1269; 1245; 1165; 1095; 1076; 1067; 1053; 1017.

1,4,4a,5,8,8a-Hexahydro-1,4-methanonaphthalene-5,8-diol (34). *meso*-**34** was purchased from the University Lodz and used without further purification. Achiral diol **34** was separated from the other compounds of the reaction mixture using chiral GC employing a 30 m FS-Hydrodex β-6TBDM column (Macherey Nagel). *T* (Injector + Detector) = 250 °C. Splitflow = 80 mL/min. Precolumn pressure = 0.8 bar. Conditions: 100–250 °C, 5 °C/min. Retention time: *t*_R = 23.1 min.

8-Hydroxy-1,4,4a,5,8,8a-hexahydro-1,4-methanonaphthalen-5-yl acetate. Retention times: *t*_{R,1} = 22.5 min; *t*_{R,2} = 22.7 min. *Preparation:* *meso*-Diol **34** (0.089 g, 0.5 mmol) was treated with acetic anhydride (66 μL, 0.7 mmol) in the presence of DMAP (0.012 g, 0.1 mmol) in 20 mL of Et₂O, and the resulting solution was stirred overnight at rt (25 °C). Et₂O was then removed in vacuo, and the monoacetylated product was purified by silica flash gel chromatography (EtOAc/hexane 1:1, *R*_f = 0.29). Isolated racemic monoacetylated **34** (0.037 g, 0.18 mmol; 36%) was characterized and then subjected to the GC assay described above to prove the origin of the GC signals. ¹H NMR (400 MHz, CDCl₃): δ/ppm = 5.88 [dd, 1 H, *J*₁ = 5.5 Hz, *J*₂ = 2.8 Hz]; 5.81 [dd, 1 H, *J*₁ = 5.5 Hz, *J*₂ = 2.8 Hz]; 5.49–5.43 [m, 1 H]; 5.40–5.34 [m, 1 H]; 5.32–5.26 [m, 1 H]; 4.52–4.43 [m, 1 H]; 3.09–2.98 [m, 2 H]; 2.89–2.80 [m, 2 H]; 2.12 [s, 3 H, CH₃]; 1.90 [s, 1 H]; 1.39–1.27 [m, 2 H]. ¹³C NMR (100 MHz, CDCl₃): δ/ppm = 170.8 (C=O); 135.6; 135.5; 132.1; 126.9; 69.8; 66.5; 48.9; 45.7; 45.0; 41.8; 38.5; 21.1. HRMS (ESI-TOF) *m/z*: [M + Na]⁺ calcd for C₁₃H₁₆O₃Na⁺ 243.0992, found 243.0992. IR (KBr): $\tilde{\nu}/\text{cm}^{-1}$ = 3451; 2972; 1739; 1669; 1373; 1243; 1033.

1,4,4a,5,8,8a-Hexahydro-1,4-methanonaphthalene-5,8-diyl diacetate. Retention time: *t*_R = 22.4 min. *Preparation:* *meso*-Diol **34** (0.089 g, 0.5 mmol) was treated with acetic anhydride (66 μL, 0.7 mmol) in the presence of DMAP (0.012 g, 0.1 mmol) in 20 mL of Et₂O, and the resulting solution was stirred overnight at rt (25 °C). Et₂O was then removed in vacuo, and the diacetylated product was purified by silica flash gel chromatography (EtOAc/hexane 1:1, *R*_f = 0.49). Isolated diacetylated **34** (0.055 g, 0.21 mmol; 42%) was characterized and then subjected

to the GC assay described above to prove the origin of the GC signals. ^1H NMR (400 MHz, CDCl_3): δ/ppm = 5.86–5.82 [m, 2 H]; 5.44–5.34 [m, 4 H]; 3.11–3.02 [m, 2 H]; 2.88–2.82 [m, 2 H]; 2.14 [s, 6 H, CH_3]; 1.31 [q, 2 H, J = 8.7 Hz]. ^{13}C NMR (100 MHz, CDCl_3): δ/ppm = 170.6 ($\text{C}=\text{O}$); 135.5; 128.0; 69.4; 48.4; 45.8; 38.0; 21.1. HRMS (EI-sector field) m/z : $[\text{M}]^+$ calcd for $\text{C}_{15}\text{H}_{18}\text{O}_4^+$ 262.121, found 262.122. IR (KBr): $\tilde{\nu}/\text{cm}^{-1}$ = 2979; 2967; 2934; 2882; 1743; 1371; 1304; 1244; 1227; 1366; 1248; 1169.

Cyclopent-4-ene-1,3-diol (35). *meso*-Cyclopent-4-ene-1,3-diol **35** was purchased and used without further purification. Achiral diol **35** was separated from the other compounds of the reaction mixture using chiral GC employing a 30 m Chiraldex G-TA column (Astech). T (Injector + Detector) = 250 °C. Splitflow = 80 mL/min. Precolumn pressure = 0.8 bar. Conditions: 100–180 °C, 2 °C/min. Retention times: t_R = 13.0.

4-Hydroxycyclopent-2-en-1-yl acetate. Retention times: $t_{R,1}$ = 13.7 min; $t_{R,2}$ = 14.2 min. *Preparation:* *meso*-Cyclopent-4-ene-1,3-diol **35** (0.150 g, 1.5 mmol) was treated with acetic anhydride (186 μL , 2 mmol) in the presence of DMAP (0.018 g, 0.15 mmol) in 20 mL of dichloromethane, and the resulting solution was stirred overnight at rt (25 °C). Dichloromethane was then removed in vacuo, and the monoacetylated product was purified by silica flash gel chromatography (EtOAc, R_f = 0.47). Isolated racemic monoacetylated **35** (0.160 g, 1.1 mmol) was characterized and then subjected to the GC assay described above to prove the origin of the GC signals. ^1H NMR (400 MHz, CDCl_3): δ/ppm = 6.13–6.10 [m, 1 H]; 6.00–5.97 [m, 1 H]; 5.52–5.47 [m, 1 H]; 4.75–4.70 [m, 1 H]; 2.81 [td, 1 H, J_1 = 14.6 Hz, J_2 = 7.3 Hz]; 2.20 [bs, 1 H, OH]; 2.06 [s, 3 H, CH_3]; 1.66 [td, 1 H, J_1 = 14.6 Hz, J_2 = 3.9 Hz]. ^{13}C NMR (100 MHz, CDCl_3): δ/ppm = 170.8 ($\text{C}=\text{O}$); 138.5; 132.5; 77.1; 74.8; 40.5; 21.2. IR (KBr): $\tilde{\nu}/\text{cm}^{-1}$ = 3434; 3084; 2941; 1723; 1403; 1375; 1244; 1189; 1103; 1034. Analytical data of monoacetylated **35** differ slightly from those reported in the literature.^[119]

Cyclopent-4-ene-1,3-diyl diacetate. Retention time: t_R = 14.8. *Preparation:* *meso*-Cyclopent-4-ene-1,3-diol **35** (0.150 g, 1.5 mmol) was treated with acetic anhydride (186 μL , 2 mmol) in the presence of DMAP (0.018 g, 0.15 mmol) in 20 mL of dichloromethane, and the resulting solution was stirred overnight at rt (25 °C). DCM was then removed in vacuo, and the diacetylated product was purified by silica flash gel chromatography (EtOAc, R_f = 0.58). The isolated diacetate of **35** (0.063 g, 0.3 mmol; 20%) was characterized and then subjected to the

GC assay described above to prove the origin of the GC signals. ^1H NMR (400 MHz, CDCl_3): δ/ppm = 6.09 [d, 2 H, J = 0.5 Hz]; 5.55 [ddd, 2 H, J_1 = 7.4 Hz, J_2 = 3.9 Hz, J_3 = 0.7 Hz]; 2.88 [td, 1 H, J_1 = 15.0 Hz, J_2 = 7.5 Hz], 2.06 [s, 6 H, CH_3]; 1.74 [td, 1 H, J_1 = 15.0 Hz, J_2 = 3.8 Hz]. ^{13}C NMR (100 MHz, CDCl_3): δ/ppm = 170.6 (C=O); 134.6; 76.6; 37.1; 21.1. HRMS (ESI-TOF) m/z : $[\text{M} + \text{Na}]^+$ calcd for $\text{C}_9\text{H}_{12}\text{O}_4\text{Na}^+$ 207.0628, found 207.0624. IR (KBr): $\tilde{\nu}/\text{cm}^{-1}$ = 2951; 1737; 1435; 1366; 1329; 1233; 1194; 1076; 1020.

(Tetrahydrofuran-2,5-diyl)dimethanol (36).^[83] *meso*-**36** was prepared by the group of Christian Stark (University of Leipzig, now at the University of Hamburg, Germany) and used without further purification. Achiral diol **36** was separated from the other compounds of the reaction mixture using chiral GC employing a 30 m Chiraldex G-TA column (Astech). T (Injector + Detector) = 250 °C. Splitflow = 80 mL/min. Precolumn pressure = 0.8 bar. Conditions: 100–180 °C, 2 °C/min. Retention time: t_R = 23.9 min.

(5-(Hydroxymethyl)tetrahydrofuran-2-yl)methyl acetate. Retention times: $t_{R,1}$ = 22.3 min; $t_{R,2}$ = 23.0 min. *Preparation:* *meso*-Diol **36** (0.066 g, 0.5 mmol) was treated with acetic anhydride (71 μL , 0.75 mmol) in the presence of DMAP (0.005 g, 0.0375 mmol) in 5 mL of DCM, and the resulting solution was stirred overnight at rt (25 °C). DCM was then removed in vacuo, and the monoacetylated product was purified by silica flash gel chromatography (EtOAc, R_f = 0.26). Isolated racemic monoacetylated **36** (0.053 g, 0.31 mmol; 62%) was characterized and then subjected to the GC assay described above to prove the origin of the GC signals. ^1H NMR (400 MHz, CDCl_3): δ/ppm = 4.20–4.00 [m, 4 H]; 3.72–3.63 [m, 1 H]; 3.49–3.39 [m, 1 H]; 2.44 [bs, 1 H]; 2.04 [s, 3 H, CH_3]; 2.01–1.73 [m, 3 H]; 1.71–1.60 [m, 1 H]. ^{13}C NMR (100 MHz, CDCl_3): δ/ppm = 171.2 (C=O); 80.5; 77.3; 66.6; 64.5; 28.0; 26.7; 20.9. IR (KBr): $\tilde{\nu}/\text{cm}^{-1}$ = 3461; 2948; 1774; 1741; 1420; 1372; 1237; 1187; 1050. HRMS (ESI-TOF) m/z : $[\text{M} + \text{Na}]^+$ calcd for $\text{C}_8\text{H}_{14}\text{O}_4\text{Na}^+$ 197.0784, found 197.0784.

(Tetrahydrofuran-2,5-diyl)bis(methylene) diacetate. Retention time: t_R = 28.0 min. *Preparation:* *meso*-Diol **36** (0.066 g, 0.5 mmol) was treated with acetic anhydride (71 μL , 0.75 mmol) in the presence of DMAP (0.005 g, 0.0375 mmol) in 5 mL of DCM, and the resulting solution was stirred overnight at rt (25 °C). DCM was then removed in vacuo, and the diacetylated product was purified by silica flash gel chromatography (EtOAc, R_f = 0.51). Isolated diacetylated **36** (0.012 g, 0.06 mmol; 12%) was characterized and then subjected to the GC assay

described above to prove the origin of the GC signals. ^1H NMR (400 MHz, CDCl_3): δ/ppm = 4.18–4.07 [m, 4 H]; 3.98–3.90 [m, 2 H]; 2.03 [s, 6 H, CH_3]; 2.00–1.90 [m, 2 H]; 1.72–1.59 [m, 2 H]. ^{13}C NMR (100 MHz, CDCl_3): δ/ppm = 171.0 ($\text{C}=\text{O}$); 77.5; 66.5; 27.7; 20.9. HRMS (ESI-TOF) m/z : $[\text{M} + \text{Na}]^+$ calcd for $\text{C}_{10}\text{H}_{16}\text{O}_5\text{Na}^+$ 239.0890, found 239.0885. IR (KBr): $\tilde{\nu}/\text{cm}^{-1}$ = 2953; 2884; 1742; 1452; 1371; 1238; 1098; 1042.

Substrate (37). The diol **37** was synthesized by Y. Landais.^[84] Enantiomers of diol **37** were separated by HPLC employing a 25 cm, d = 0.46 cm Chiralpak IC column (Daicel). Eluent: Hexane/Isopropanol 93:7; flow = 1 mL/min; UV-detector λ = 254 nm. Retention times: $t_{\text{R},1}$ = 15.87 min; $t_{\text{R},2}$ = 17.48 min.

Substrate (38). Retention times: $t_{\text{R},1}$ = 12.72 min; $t_{\text{R},2}$ = 21.29 min.

Substrate (39). Retention times: $t_{\text{R},1}$ = 23.44 min; $t_{\text{R},2}$ = 37.84 min.

Substrate (40). Retention times: $t_{\text{R},1}$ = 19.43 min; $t_{\text{R},2}$ = 29.25 min.

The analytical data for **37** and **40** were in accordance with the literature.^[84] *Preparation:* Racemic diol **37** (0.043 g, 0.11 mmol) was treated with acetic anhydride (11.5 μL , 0.12 mmol) in the presence of DMAP (2.7 mg, 0.02 mmol) in 7 mL of DCM, and the resulting solution was stirred for 2 h at rt (25 °C). DCM was then removed in vacuo, and the monoacetylated products (\pm)-**38**, (\pm)-**39** and the diacylated product **40** were purified by silica flash gel chromatography (EtOAc/hexane (1:1), R_f (**38**) and (**39**) = 0.2; R_f (**40**) = 0.3. Isolated racemic (\pm)-**38** and (\pm)-**39** (0.026 mg, 0.06 mmol; 54%; colorless solid) and **40** (0.014 g, 0.03 mmol; 27%; colorless solid) were characterized and then subjected to the HPLC assay described above to prove the origin of the signals. NMR data for **38** and **39** are as follows. ^1H NMR (400 MHz, CDCl_3): δ/ppm = 7.56–7.50 [m, 2 H]; 7.33–7.26 [m, 3 H]; 6.38–6.25 [m, 2 H]; 5.50 [t, 1 H, J_3 = 4.0 Hz]; 4.88–4.82 [m, 1 H]; 4.64–4.56 [m, 1 H]; 4.23 [bs, 1 H]; 2.04 [s, 3 H]; 1.99 [s, 1 H]; 1.62 [q, 1 H, J_3 = 2.5 Hz]; 1.41 [s, 9 H]; 0.42 [s, 3 H]; 0.40 [s, 3 H]. ^{13}C NMR (50 MHz, CDCl_3): δ/ppm = 169.6 ($\text{C}=\text{O}$); 155.1 ($\text{C}=\text{O}$); 137.1; 134.2; 134.0; 129.3; 127.4; 82.1; 75.0; 73.6; 68.6; 54.8; 38.6; 28.2; 21.0; –2.9; –3.7.

4.3 Procedure for the Competitive Catalytic Run with Alcohols **1**, **41**, **42**, and **43**

The conditions for the kinetic resolutions for the competitive catalytic runs are given exemplary by the following experimental protocol. Catalyst **12b** (1.9 mg, 0.0025 mmol) was dissolved in 500 μL of dry toluene. 100 μL of this catalyst solution (0.0005 mmol, 2 mol%) were added to a clear solution of the alcohols **1**, **41**, **42**, and **43** (0.025 mmol of each alcohol) in 4.65 mL of dry toluene. The reaction mixture was cooled to 0 $^{\circ}\text{C}$, and 25 μL (0.1325 mmol, 5.3 equiv of acetic anhydride) of a solution of 100 μL of acetic anhydride in 100 μL of toluene (cooled to 0 $^{\circ}\text{C}$) were then added with an Eppendorf pipette and allowed to stir at 0 $^{\circ}\text{C}$. After the reaction, the reaction mixture was quenched with methanol and directly analyzed by GC and/or chiral GC analysis. The same conditions were used for the competitive catalytic run with DMAP (0.0025 mmol) as catalyst (for the chromatograms, see the Supporting Information). All signals were detected by GC-FID employing a 30 m 5890_V UP5 (Machery Nagel). T (Injector + Detector) = 250 $^{\circ}\text{C}$. Splitflow = 80 mL/min. Precolumn pressure = 0.8 bar. Conditions: 60 $^{\circ}\text{C}$ –250 $^{\circ}\text{C}$, 15 $^{\circ}\text{C}/\text{min}$. Retention times: **1** t_{R} = 6.69 min; **41** t_{R} = 6.33 min; **42** t_{R} = 1.44 min; **43** t_{R} = 4.09 min; **2** t_{R} = 8.57 min; **44** t_{R} = 8.02 min; **45** t_{R} = 2.21 min; **46** t_{R} = 2.37 (chromatograms for the **12b**-catalyzed run can be found in the Supporting Information).

(3a,7a)-Hexahydrobenzo-1,3-dioxo-2-one (47).^[108] Enantiomers of the cyclic carbonate **47** were separated by chiral GC employing a 30 m FS-Hydrodex β -6TBDM column (Macherey Nagel). T (Injector + Detector) = 250 $^{\circ}\text{C}$. Splitflow = 80 mL/min. Precolumn pressure = 0.8 bar. Conditions: 100–250 $^{\circ}\text{C}$, 2 $^{\circ}\text{C}/\text{min}$. Retention times: $t_{\text{R},1}$ = 29.5 min; $t_{\text{R},2}$ = 29.7 min. *Preparation:* *trans*-Diol **1** (0.50 g, 4.3 mmol) was treated with Boc_2O (2.94 mL, 12.9 mmol) in the presence of DMAP (0.52 g, 4.3 mmol) in 10 mL of dry acetonitrile, and the resulting solution was stirred overnight at rt (25 $^{\circ}\text{C}$). Acetonitrile was then removed in vacuo, and the *O,O*-di-*tert*-butoxylated product ((\pm)-**48**) and the cyclic carbonate ((\pm)-**47**) were purified by silica flash gel chromatography (hexane/EtOAc (3:1), R_{f} (**48**) = 0.52; R_{f} (**47**) = 0.26). Isolated racemic (\pm)-**47** (0.421 g, 3.0 mmol) and (\pm)-**48** (0.145 mg, 0.46 mmol) were characterized and then subjected to the GC assay to prove the origin of the GC signals. ^1H NMR (400 MHz, CDCl_3): δ/ppm = 3.96 [m, 2 H], 2.19 [m, 2 H], 1.92–1.80 [m, 2 H], 1.69–1.55 [m, 2 H], 1.42–1.29 [m, 2 H]. ^{13}C NMR (100 MHz, CDCl_3): δ/ppm = 155.1 (C=O), 83.5, 28.2, 23.2

***tert*-Butylcyclohexane-1,2-diyl dicarbonate (48).** Enantiomers of the di-*tert*-butoxycarbonylated product **48** were not separated by chiral GC employing a 30 m FS-Hydrodex β -6TBDM column (Macherey Nagel). T (Injector + Detector) = 250 $^{\circ}\text{C}$. Splitflow = 80 mL/min.

Precolumn pressure = 0.8 bar. Conditions: 100–250 °C, 2 °C/min. Retention time: $t_{R,1}$ = 39.6 min. *Preparation using DMAP as catalyst:* *trans*-Diol **1** (0.58 g, 5.0 mmol) was treated with Boc_2O (1.26 mL, 5.5 mmol) in the presence of DMAP (0.182 g, 1.5 mmol) in 100 mL of dry toluene, and the resulting solution was stirred overnight at rt (25 °C). Toluene was then removed *in vacuo*, and the *O*-*tert*-butoxylated product ((\pm)-**2e**), the *O,O*-di-*tert*-butoxylated product ((\pm)-**48**) and the cyclic carbonate ((\pm)-**47**) were purified by silica flash gel chromatography (DCM/MeOH (19:1), R_f (**48**) = 0.81; R_f (**47**) = 0.71; R_f (**2e**) = 0.62). Isolated racemic (\pm)-**2e** (0.842 g, 3.9 mmol, 78%) and (\pm)-**48** (0.126 mg, 0.4 mmol, 8%) were characterized and then subjected to the GC assay described to prove the origin of the GC signals. (\pm)-**87** could just be isolated in traces and was therefore synthesized using different reaction conditions. The NMR data for (\pm)-**2e** and (\pm)-**48** are in accordance with the literature.^[108] *Preparation using N-methylimidazole as catalyst:* *trans*-Diol **1** (0.58 g, 5.0 mmol) was treated with Boc_2O (1.26 mL, 5.5 mmol) in the presence of *N*-methylimidazole (123.2 μL , 1.5 mmol) in 100 mL of dry toluene, and the resulting solution was stirred overnight at rt (25 °C). Toluene was then removed *in vacuo*, and the *O*-*tert*-butoxylated product ((\pm)-**2e**), the *O,O*-di-*tert*-butoxylated product ((\pm)-**48**) and the cyclic carbonate ((\pm)-**3**) were purified by silica flash gel chromatography (DCM/MeOH (19:1), R_f (**48**) = 0.81; R_f (**47**) = 0.71; R_f (**2e**) = 0.62). Isolated racemic (\pm)-**2e** (0.821 g, 3.8 mmol, 76%) and (\pm)-**48** (0.94 g, 0.3 mmol, 6%) were characterized and then subjected to the GC assay described to prove the origin of the GC signals. (\pm)-**47** could just be isolated in traces and was therefore synthesized using different reaction conditions. The NMR data for (\pm)-**2e** and (\pm)-**48** are in accordance to the literature.^[108]

4.4 Description of the Preparative Kinetic Resolution Experiment of (\pm)-**1** with Boc_2O

Catalyst **12b** (38 mg, 0.05 mmol, 5 mol %) and diol (\pm)-**1** (116.2 mg, 1 mmol) were dissolved in 160 mL of dry toluene. 0.46 mL (2.0 mmol, 2.0 equiv) of Boc_2O was added and then allowed to stir for 48 h at rt. The reaction mixture was quenched with 10 mL of methanol and then filtered using 40 g silica gel suspended with DCM to remove the catalyst. The solvent was removed under reduced pressure. The crude product was directly purified via silica gel column chromatography (DCM/methanol (19:1)). 104.2 mg (0.48 mmol, 48.1%) of **2e** (R_f = 0.62) and 52.1 mg (0.45 mmol, 44%) of **1** (R_f = 0.71) were isolated and directly characterized by chiral GC and NMR.

General Procedure: Enantioselective Boc-Protection of *rac*-1. 2.9 mg (0.025 mmol) of *rac*-1 were dissolved in 4.45 mL of dry toluene. 1, 2, 5, or 10 mol % (0.38 mg, 0.76 mg, 1.9 mg or 3.8 mg) of **12b** and 5.74, 11.49, 28.88, or 54.7 μ L (0.025 mmol, 0.05 mmol, 0.1325 or 0.25 mmol) of Boc₂O were added, and the mixture was stirred at rt. The conversion and *ee* were determined by chiral GC. A stock solution was prepared: 4 mg **12b** in 800 μ L of dry toluene.

***trans*-2-Hydroxycyclohexyl-4-nitrobenzenesulfonate (53).** Enantiomers of the sulfonylated diol **53** were separated by using HPLC employing a 25 cm, *d* = 0.46 cm Chiralpak IB column (Daicel). Eluent: Hexane/Isopropanol 90:10; flow = 0.7 mL/min; UV-detector λ = 254 nm. Retention times: $t_{R,1}$ = 27.8 min; $t_{R,2}$ = 31.9 min.

4.5 Sulfonylation of *rac*-1 Using **12b** as Catalyst

116.2 mg (1.0 mmol) of *rac*-1, 2 mol % (15.2 mg) of **12b**, and 288 mg of 4-nitrobenzenesulfonyl chloride were dissolved in 5 mL of dry DCM, and 2 mL of a saturated NaHCO₃ solution was added. The two-phase system was stirred for 24 h. The products were purified via flash chromatography eluting with ethyl acetate/pentane (3: 1). 42 mg (0.13 mmol, 14%) of **53** (R_f = 0.52) and 39 mg (0.08 mmol, 8%) of disulfonylated diol (R_f = 0.61) were isolated as yellowish solids. The enantiomeric excess of **1** was determined by chiral GC. ¹H NMR (400 MHz, CDCl₃): δ /ppm = 8.33 [d, *J* = 12 Hz, 2 H], 8.08 [d, *J* = 12 Hz, 2 H], 4.36 [m, 1 H], 3.52 [m, 1 H], 1.99 [t, *J* = 12 Hz, 2 H], 1.85 [s, 2 H], 1.65 [m, 2 H], 1.43 [m, 1 H], 1.31–1.11 [m, 3 H]. ¹³C NMR (100 MHz, CDCl₃): δ /ppm = 150.3, 142.9, 129.1, 124.4, 87.9, 72.0, 32.6, 31.2, 24.0, 23.3. IR (KBr): ν /cm⁻¹ = 3538, 2939, 1609, 1534, 1351, 1185, 1095, 1076, 981, 926. HRMS (ESI-TOF) *m/z*: [M + Na]⁺ calcd for C₁₂H₁₅NO₆SN⁺ 324.0512, found 324.0513.

***trans*-Cyclohexane-1,2-diyl bis(4-nitrobenzenesulfonate).** ¹H NMR (400 MHz, CDCl₃): δ /ppm = 8.29 [d, *J* = 8 Hz, 4 H], 7.98 [d, *J* = 8 Hz, 4 H], 4.48 [m, 2 H], 2.04–1.94 [m, 2 H], 1.62–1.55 [m, 2 H], 1.52–1.38 [m, 2 H], 1.28–1.12 [m, 2 H]. ¹³C NMR (100 MHz, CDCl₃): δ /ppm = 150.8, 142.4, 129.1, 124.5, 81.3, 31.0, 22.6. IR (KBr): ν /cm⁻¹ = 2950, 1610, 1538, 1351, 1186, 1094, 977, 919. HRMS (ESI-TOF) *m/z*: [M + Na]⁺ calcd for C₁₈H₁₈N₂O₁₀S₂Na⁺ 509.0295, found 509.0300.

4.6 Sulfonation Test Reactions

11.6 mg (0.1 mmol) of *rac*-**1** was dissolved in 4.5 mL of dry toluene. 5 mol% (3.8 mg) of **12b**, 12.8 μ L (0.11 mmol) of 2,6-lutidine and 20.96 mg (0.11 mmol) of tosyl-chloride/21.1 mg (0.11 mmol) of 4-chlorobenzenesulfonyl chloride/18.2 μ L (0.11 mmol) of trifluoromethanesulfonic anhydride were added and allowed to stir for 24 h. The conversion was determined by TLC using EtOAc/hexane as eluent.

***trans*-2-Hydroxycyclohexyl diphenyl phosphate (54-Ph).** Enantiomers of **54-Ph** were separated by chiral GC employing a 30 m FS-Hydrodex β -6TBDM column (Macherey Nagel). *T* (Injector + Detector) = 250 °C. Splitflow = 80 mL/min. Precolumn pressure = 0.8 bar. Conditions: 140 °C isotherm 13 min; 140–250 °C, 2 °C/min; 250 °C isotherm 15 min. Retention times: $t_{R,1}$ = 37.5 min; $t_{R,2}$ = 37.9 min (**54-Ph**); $t_{R,1}$ = 10.4 min; $t_{R,2}$ = 10.9 min (**1**). *Preparation using DMAP as catalyst:* 580 mg (5 mmol) of *rac*-**1**, 0.826 mL (5 mmol) of Et₃N and 183 mg (1.5 mmol) of DMAP were dissolved in dry toluene. 1.035 mL (5 mmol) of diphenylchlorophosphate were added, and the mixture was stirred for 12 h at rt. The solvent was removed under reduced pressure, and the crude mixture was purified via silica gel chromatography utilizing ethylacetate/hexane (3:2) as eluent. 578 mg (1.6 mmol, 33.2%; R_f = 0.35) of a colorless solid were isolated. *Preparation using 12b as catalyst:* The same reaction was accomplished with 3 mmol of *rac*-**1** using 22 mg (0.03 mmol) of **12b** as catalyst. The reaction was stopped at a conversion of 50%. The crude product was purified by preparative HPLC (eluent: TBME/Hexane 60:40) UV-detector λ = 254 nm, E_{max} = 2.56; refractometer; column l = 250 mm, d = 8 mm, LiChrosorb Diol (7 μ m, Merck); 417 mg (1.2 mmol) of a colorless solid were isolated. The product seems to be sensitive toward acids. ¹H NMR (400 MHz, CDCl₃): δ /ppm = 7.41–7.31 [m, 4 H, H_{Ar} (Phe)], 7.29–7.17 [m, 6 H, H_{Ar} (Phe)], 4.34 [m, 1 H, H _{α} (OP(OPh)₂)], 3.61 [m, 1 H, H _{α} (OH)], 2.95 [s, 1 H, OH], 2.17–2.09 [m, 1 H], 2.08–2.00 [m, 1 H], 1.77–1.64 [s, 2 H], 1.49–1.40 [m, 1 H], 1.36–1.19 [m, 3 H]. ¹³C NMR (100 MHz, CDCl₃): δ /ppm = 150.6, 129.8, 125.5, 120.1, 85.3, 73.3, 32.4, 31.2, 23.9, 23.5. IR (KBr): ν /cm⁻¹ = 3471.6, 2936.6, 1589.0, 1489.5, 1265.4, 1186.9, 1086.4, 1018.2, 955.4, 774.0. HRMS (ESI-TOF) m/z : [M + Na]⁺ calcd for C₁₈H₂₁O₅PNa⁺ 371.1025, found 371.1019.

***trans*-2-Hydroxycyclohexyl diethyl phosphate (54-Et).** Enantiomers of **54-Et** were separated by chiral GC employing a 30 m FS-Hydrodex β -6TBDM column (Macherey Nagel). *T* (Injector + Detector) = 250 °C. Splitflow = 80 mL/min. Precolumn pressure = 0.8 bar. Conditions: 140 °C isotherm 13 min; 140–250 °C, 2 °C/min → 250 °C isotherm 15 min. Retention times: $t_{R,1}$ = 28.4 min; $t_{R,2}$ = 28.9 min (**54-Ph**); $t_{R,1}$ = 10.4 min; $t_{R,2}$ = 10.9 min (**1**). *Preparation using DMAP as catalyst:* 290 mg (2.5 mmol) of *rac*-**1**, 0.35 mL (2.5 mmol) of DIPEA and 91.6 mg

(0.75 mmol) of DMAP were dissolved in dry toluene. 0.36 mL (2.55 mmol) of diethylchlorophosphate were added, and the mixture was stirred for 12 h at rt. The solvent was removed under reduced pressure, and the crude mixture was purified via Al₂O₃ gel chromatography utilizing acetonitrile as eluent. 425 mg (1.6 mmol, 67%; *R_f* = 0.49) of a colorless liquid were isolated. ¹H NMR (400 MHz, CDCl₃): δ/ppm = 4.13–4.01 [q, 4 H, *J* = 6.8 Hz, O–CH₂–R], 4.00–3.96 [m, 1 H, H_α (OP(OEt)₂)], 3.63 [s, 1 H, OH], 3.53–3.47 [m, 1 H, H_α (OH)], 2.14–1.91 [m, 2 H], 1.70–1.58 [m, 2 H], 1.40–1.12 [m, 4 H], 1.32–1.27 [t, 6 H, *J* = 7.0 Hz, CH₃]. ¹³C NMR (100 MHz, CDCl₃): δ/ppm = 83.2, 73.5, 64.1, 32.9 31.7, 24.0, 23.6, 16.1. IR (Film): ν/cm^{–1} = 3404.3, 2938.6, 1453.1, 1258.4, 1028.0. HRMS (ESI-TOF) *m/z*: [M + Na]⁺ calcd for C₁₀H₂₁O₅PNa⁺ 275.1022, found 275.1019.

4.7 Competition Experiment with Different Electrophiles

2.9 mg (0.025 mmol) of *trans*-cyclohexane-1,2-diol **1**, 13.5 μL (0.1325 mmol) of Ac₂O, 27 mg (0.1325 mmol) of 4-nitrobenzenesulfonyl chloride, 19 μL (0.1325 mmol) of POCl(OEt)₂, and 80 mg (0.58 mmol) of K₂CO₃ were dissolved in 4.5 mL of abs. toluene, and the mixture was cooled to 0 °C. 2 mol % of peptide **1** was added, and the reaction was monitored via GC and TLC (the sulfonylated product cannot be detected via GC) and chiral GC. For reasons of comparability, the same reaction was performed with 2 mol% of DMAP as catalyst. All signals were detected by GC-FID employing a 30 m 5890_V UP5 (Machery Nagel). *T* (Injector + Detector) = 250 °C. Splitflow = 80 mL/min. Precolumn pressure = 0.8 bar. Conditions: 100 °C–250 °C, 15 °C/min. Retention times: **54-Ph** and **54-Et** were not detected; *trans*-cyclohexane-1,2-diol **1** *t_R* = 6.9 min; Acylated product **2** *t_R* = 8.8 min; POCl(OEt)₂ *t_R* = 6.7 min; POCl(OPh)₂ *t_R* = 15.2 min; DMAP *t_R* = 9.5 min. TLC: EtOAc = eluent (*Rac-1* *R_f* = 0.15 n.f.; **53** *R_f* = 0.6 f.; **54-Ph** *R_f* = 0.5 f.; **54-Et** *R_f* = 0.3 n.f.; **2** *R_f* = 0.6 n.f.; POCl(OPh)₂ *R_f* = 0.7 f.; SO₂ClPh-*p*-NO₂ *R_f* = 0.65 f.) f. = shows fluorescence; n.f. = shows no fluorescence. The spots were first detected under UV light and then by phosphomolybdic acid. The GC retention times and characterization of **1** can be found in the literature.^[60]

5. References

- [1] E. Schoffers, A. Golebiowski, C. R. Johnson, *Tetrahedron* **1996**, *52*, 3769–3826.
- [2] J. González-Sabín, R. Morán-Ramallal, F. Rebolledo, *Chem. Soc. Rev.* **2011**, *40*, 5321–5335.
- [3] J. M. J. Williams, R. J. Parker, C. Neri, Enzymatic Kinetic Resolution. In *Enzymes in Organic Synthesis*; K. Drauz, H. Waldmann, Eds.; Wiley-VCH: New York, **2002**; Vol. 1, pp 287–312.
- [4] U. Hanefeld, *Org. Biomol. Chem.* **2003**, *1*, 2405–2415.
- [5] A. Ghanem, H. Y. Aboul-Enein, *Tetrahedron: Asymmetry* **2004**, *15*, 3331–3351.
- [6] K. Naemura, R. Fukuda, M. Murata, M. Konishi, K. Hirose, Y. Tobe, *Tetrahedron: Asymmetry* **1995**, *6*, 2385–2394.
- [7] X. Li, H. Jiang, E. W. Uffman, L. Guo, Y. Zhang, X. Yang, V. B. Birman, *J. Org. Chem.* **2012**, *77*, 1722–1737.
- [8] T. Oriyama, K. Imai, T. Hosoya, T. Sano, *Tetrahedron Lett.* **1998**, *39*, 397–400.
- [9] E. P. Kündig, A. Enriquez Garcia, T. Lomberget, P. Perez Garcia, P. Romanens, *Chem. Commun.* **2008**, 3519–3521.
- [10] X. L. Geng, J. Wang, G. X. Li, P. Chen, S. F. Tian, J. Qu, *J. Org. Chem.* **2008**, *73*, 8558–8562.
- [11] J.-L. Cao, J. Qu, *J. Org. Chem.* **2010**, *75*, 3663–3670.
- [12] K. Ishihara, Y. Kosugi, M. Akakura, *J. Am. Chem. Soc.* **2004**, *126*, 12212–12213.
- [13] K. Ishihara, Y. Kosugi, S. Umemura, A. Sakakura, *Org. Lett.* **2008**, *10*, 3191–3194.
- [14] Y. Kosugi, M. Akakura, K. Ishihara, *Tetrahedron* **2007**, *63*, 6191–6203.
- [15] E. Vedejs, O. Daugulis, *J. Am. Chem. Soc.* **1999**, *121*, 5813–5814.
- [16] E. Vedejs, O. Daugulis, J. A. MacKay, E. Rozners, E. *Synlett* **2001**, 1499–1505.
- [17] S. Mizuta, Y. Ohtsubo, T. Tsuzuki, T. Fujimoto, I. Yamamoto, *Tetrahedron Lett.* **2006**, *47*, 8227–8229.
- [18] H. Aida, K. Mori, Y. Yamaguchi, S. Mizuta, T. Moriyama, I. Yamamoto, T. Fujimoto, *Org. Lett.* **2012**, *14*, 812–815.
- [19] Y. Matsumura, T. Maki, S. Murakami, O. Onomura, *J. Am. Chem. Soc.* **2003**, *125*, 2052–2053.
- [20] A. Gissibl, M. G. Finn, O. Reiser, *Org. Lett.* **2005**, *7*, 2325–2328.
- [21] C. Mazet, S. Roseblade, V. Köhler, A. Pfaltz, *Org. Lett.* **2006**, *8*, 1879–1882.
- [22] J. C. Ruble, G. C. Fu, *J. Org. Chem.* **1996**, *61*, 7230–7231.
- [23] J. C. Ruble, H. A. Latham, G. C. Fu, *J. Am. Chem. Soc.* **1997**, *119*, 1492–1493.
- [24] A. Spivey, S. Arseniyadis, *Top. Curr. Chem.* **2010**, *291*, 233–280.
- [25] C. E. Müller, P. R. Schreiner, *Angew. Chem. Int. Ed.* **2011**, *50*, 6012–6042.
- [26] J. M. Keith, J. F. Larrow, E. N. Jacobsen, *Adv. Synth. Catal.* **2001**, *343*, 5–26.
- [27] E. Vedejs, M. Jure, *Angew. Chem. Int. Ed.* **2005**, *44*, 3974–4001.
- [28] M. C. Willis, *J. Chem. Soc., Perkin Trans. 1* **1999**, 1765–1784.
- [29] H. Pellissier, *Tetrahedron* **2008**, *64*, 1563–1601.
- [30] H. Pellissier, *Adv. Synth. Catal.* **2011**, *353*, 659–676.
- [31] E. A. Davie, S. M. Mennen, Y. Xu, S. J. Miller, *Chem. Rev.* **2007**, *107*, 5759–5812.
- [32] H. Wennemers, *Chem. Commun.* **2011**, *47*, 12036–12041.
- [33] N. Sewald, H. Jakubke, *Peptides: Chemistry and Biology*, 2nd ed.; Wiley VCH: Weinheim, **2009**.
- [34] J. Oku, N. Ito, S. Inoue, *Makromol. Chem.* **1979**, *180*, 1089–1091.
- [35] J. Oku, S. Inoue, *J. Chem. Soc., Chem. Commun.* **1981**, 229–230.
- [36] J. Oku, N. Ito, S. Inoue, *Makromol. Chem.* **1982**, *183*, 579–586.
- [37] S. Asada, Y. Kobayashi, S. Inoue, *Makromol. Chem.* **1985**, *186*, 1755–1762.
- [38] Y. Kobayashi, S. Asada, I. Watanabe, H. Hayashi, Y. Motoo, S. Inoue, *Bull. Chem. Soc. Jpn.* **1986**, *59*, 893–895.
- [39] S. Juliá, J. Guixer, J. Masana, J. Rocas, S. Colonna, R. Annuziata, H. Molinari, *J. Chem. Soc., Perkin Trans. 1* **1982**, 1317–1324.
- [40] S. Colonna, H. Molinari, S. Banfi, S. Juliá, J. Masana, A. Alvarez, A. *Tetrahedron* **1983**, *39*, 1635–1641.
- [41] S. Banfi, S. Colonna, H. Molinari, S. Julia, J. Guixer, *Tetrahedron* **1984**, *40*, 5207–5211.
- [42] S. Juliá, J. Masana, J. C. Vega, *Angew. Chem. Int. Ed.* **1980**, *19*, 929–931.
- [43] P. Krattiger, R. Kovasy, J. D. Revell, S. Ivan, H. Wennemers, *Org. Lett.* **2005**, *7*, 1101–1103.

- [44] J. D. Revell, H. Wennemers, *Curr. Opin. Chem. Biol.* **2007**, *11*, 269–278.
- [45] J. D. Revell, H. Wennemers, *Adv. Synth. Catal.* **2008**, *350*, 1046–1052.
- [46] G. T. Copeland, E. R. Jarvo, S. J. Miller, *J. Org. Chem.* **1998**, *63*, 6784–6785.
- [47] S. J. Miller, G. T. Copeland, N. Papaioannou, T. E. Horstmann, E. M. Ruel, *J. Am. Chem. Soc.* **1998**, *120*, 1629–1630.
- [48] E. R. Jarvo, G. T. Copeland, N. Papaioannou, P. J. Bonitatebus Jr, S. J. Miller, *J. Am. Chem. Soc.* **1999**, *121*, 11638–11643.
- [49] M. M. Vasbinder, E. R. Jarvo, S. J. Miller, *Angew. Chem. Int. Ed.* **2001**, *113*, 2906–2909.
- [50] E. R. Jarvo, M. M. Vasbinder, S. J. Miller, *Tetrahedron* **2000**, *56*, 9773–9779.
- [51] G. T. Copeland, S. J. Miller, *J. Am. Chem. Soc.* **1999**, *121*, 4306–4307.
- [52] F. Formaggio, A. Barazza, A. Bertocco, C. Toniolo, Q. B. Broxterman, B. Kaptein, E. Brasola, P. Pengo, L. Pasquato, P. Scrimin, *J. Org. Chem.* **2004**, *69*, 3849–3856.
- [53] P. Chen, J. Qu, *J. Org. Chem.* **2011**, *76*, 2994–3004.
- [54] S. Bellemin-Laponnaz, J. Tweddell, J. C. Ruble, F. M. Breitling, G. C. Fu, *Chem. Commun.* **2000**, 1009–1010.
- [55] V. B. Birman, H. Jiang, X. Li, *Org. Lett.* **2007**, *9*, 3237–3240.
- [56] C. Choi, S. K. Tian, L. Deng, *Synthesis* **2001**, 1737–1741.
- [57] B. S. Fowler, K. M. Laemmerhold, S. J. Miller, *J. Am. Chem. Soc.* **2012**, *134*, 9755–9761.
- [58] C. A. Lewis, S. J. Miller, *Angew. Chem. Int. Ed.* **2006**, *45*, 5616–5619.
- [59] K. Griswold, S. J. Miller, *Tetrahedron* **2003**, *59*, 8869–8875.
- [60] C. E. Müller, L. Wanka, K. Jewell, P. R. Schreiner, *Angew. Chem. Int. Ed.* **2008**, *47*, 6180–6183.
- [61] M. M. Cruz Silva, S. Riva, M. L. Sá e Melo, *Tetrahedron* **2005**, *61*, 3065–3073.
- [62] C. Mazet, V. Köhler, A. Pfaltz, *Angew. Chem.* **2005**, *117*, 4966–4969.
- [63] R. C. Wende, P. R. Schreiner, *Green Chem.* **2012**, *14*, 1821–1849.
- [64] J. Zhou, *Chem. Asian J.* **2010**, *5*, 422–434.
- [65] C. E. Müller, D. Zell, P. R. Schreiner, *Chem.–Eur. J.* **2009**, *15*, 9647–9650.
- [66] R. Hrdina, C. E. Müller, P. R. Schreiner, *Chem. Commun.* **2010**, 2689–2690.
- [67] C. E. Müller, R. Hrdina, R. C. Wende, P. R. Schreiner, *Chem.–Eur. J.* **2011**, *17*, 6309–6314.
- [68] R. Hrdina, C. E. Müller, R. C. Wende, L. Wanka, P. R. Schreiner, *Chem. Commun.* **2012**, 2498–2500.
- [69] J. J. Klicic, R. A. Friesner, S.-Y. Liu, W. C. Guida, *J. Phys. Chem. A* **2002**, *106*, 1327–1335.
- [70] A. Sakakura, K. Kawajiri, T. Ohkubo, Y. Kosugi, K. Ishihara, *J. Am. Chem. Soc.* **2007**, *129*, 14775–14779.
- [71] Y. Zhao, J. Rodrigo, A. H. Hoveyda, M. L. Snapper, *Nature* **2006**, *443*, 67–70.
- [72] Immobilization of a catalyst simplifies the purification of the product as well as the recovery of the catalyst. Hence, we compared the selectivity of **12a** and the uncleaved peptide **12a-resin**, but **12a-resin** turned out to be less selective.
- [73] S. Yamada, J. S. Fossey, *Org. Biomol. Chem.* **2011**, *9*, 7275–7281.
- [74] Z. Zhang, K. M. Lippert, H. Hausmann, M. Kotke, P. R. Schreiner, *J. Org. Chem.* **2011**, *76*, 9764–9776.
- [75] D. Terakado, H. Koutaka, T. Oriyama, *Tetrahedron: Asymmetry* **2005**, *16*, 1157–1165.
- [76] C. A. Lewis, B. R. Sculimbrene, Y. Xu, S. J. Miller, *Org. Lett.* **2005**, *7*, 3021–3023.
- [77] H. B. Kagan, J. C. Fiaud, *Top. Stereochem.* **1988**, *18*, 249–330.
- [78] M. Juárez-Hernandez, D. V. Johnson, H. L. Holland, J. McNulty, A. Capretta, *Tetrahedron: Asymmetry* **2003**, *14*, 289–291.
- [79] Z. Li, X. Liang, F. Wu, B. Wan, *Tetrahedron: Asymmetry* **2004**, *15*, 665–669.
- [80] D. Cai, D. L. Hughes, T. R. Verhoeven, P. J. Reider, *Tetrahedron Lett.* **1995**, *36*, 7991–7994.
- [81] H. J. Schanz, M. A. Linseis, D. G. Gilheany, *Tetrahedron: Asymmetry* **2003**, *14*, 2763–2769.
- [82] Q. S. Hu, D. Vitharana, L. Pu, *Tetrahedron: Asymmetry* **1995**, *6*, 2123–2126.
- [83] H. Cheng, C. B. W. Stark, *Angew. Chem. Int. Ed.* **2010**, *49*, 1587–1590.
- [84] E. Girard, V. Desvergnès, C. Tarnus, Y. Landais, *Org. Biomol. Chem.* **2010**, *8*, 5628–5634.
- [85] D. Enders, C. Grondal, M. R. M. Hüttl, *Angew. Chem. Int. Ed.* **2007**, *46*, 1570–1581.
- [86] J. C. Wasilke, S. J. Obrey, R. T. Baker, G. C. Bazan, *Chem. Rev.* **2005**, *36*, 1001–1020.
- [87] D. E. Fogg, E. N. dos Santos, *Coord. Chem. Rev.* **2004**, *248*, 2365–2379.
- [88] L. M. Ambrosini, T. H. Lambert, *ChemCatChem* **2010**, *2*, 1373–1380.

- [89] Y. V. Venkatachalapathi, B. V. V. Prasad, P. Balaram, *Biochemistry* **1982**, *21*, 5502–5509.
- [90] S. H. Gellman, G. P. Dado, G. B. Liang, B. R. Adams, *J. Am. Chem. Soc.* **1991**, *113*, 1164–1173.
- [91] C. B. Shinisha, R. B. Sunoj, *Org. Lett.* **2009**, *11*, 3242–3245.
- [92] T. A. Halgren, *Encyclopedia of Computational Chemistry Vol. 2*; Eds.: P. von Schleyer, N. L. Allinger, T. Clark, J. Gasteiger, P. A. Kollman, H. F. Schaefer, P. R. Schreiner, Wiley: Chichester, **1998**.
- [93] Y. Zhao, D. G. Truhlar, *Acc. Chem. Res.* **2008**, *41*, 157–167.
- [94] Y. Zhao, D. G. Truhlar, *Theor. Chem. Account* **2008**, *120*, 215–241.
- [95] S. Grimme, P. R. Schreiner, *Angew. Chem. Int. Ed.* **2011**, *50*, 12639–12642.
- [96] P. R. Schreiner, L. V. Chernish, P. A. Gunchenko, E. Y. Tikhonchuk, H. Hausmann, M. Serafin, S. Schlecht, J. E. P. Dahl, R. M. K. Carlson, A. A. Fokin, *Nature* **2011**, *477*, 308–311.
- [97] C. Y. Legault, *CYLview, 1.0b*; Université de Sherbrooke, **2009**, (<http://www.cylview.org>).
- [98] E. Guibe-Jampel, G. Le Corre, M. Wakselman, *Tetrahedron Lett.* **1979**, *20*, 1157–1160.
- [99] A. C. Spivey, S. Arseniyadis, *Angew. Chem.* **2004**, *116*, 5552–5557.
- [100] G. Höfle, W. Steglich, H. Vorbrüggen, *Angew. Chem. Int. Ed.* **1978**, *17*, 569–583.
- [101] E. Kattnig, M. Albert, *Org. Lett.* **2004**, *6*, 945–948.
- [102] S. Xu, I. Held, B. Kempf, H. Mayr, W. Steglich, H. Zipse, *Chem.–Eur. J.* **2005**, *11*, 4751–4757.
- [103] E. Larionov, H. Zipse, *WIREs Comput. Mol. Sci.* **2011**, *1*, 601–619.
- [104] V. Lutz, J. Glatthaar, C. Würtele, M. Serafin, H. Hausmann, P. R. Schreiner, *Chem.–Eur. J.* **2009**, *15*, 8548–8557.
- [105] K. W. Fiori, A. L. A. Puchlopek, S. J. Miller, *Nat. Chem.* **2009**, *1*, 630–634.
- [106] B. R. Sculimbrene, S. J. Miller, *J. Am. Chem. Soc.* **2001**, *123*, 10125–10126.
- [107] B. R. Sculimbrene, A. J. Morgan, S. J. Miller, *J. Am. Chem. Soc.* **2002**, *124*, 11653–11656.
- [108] Y. Basel, A. Hassner, *J. Org. Chem.* **2000**, *65*, 6368–6380.
- [109] Y. Demizu, K. Matsumoto, O. Onomura, Y. Matsumura, *Tetrahedron Lett.* **2007**, *48*, 7605–7609.
- [110] L. Wanka, *γ -Aminoadamantane Carboxylic Acids: Orientating Building Blocks in Peptide Chemistry*. Ph. D. Thesis, Universität Gießen, **2007**.
- [111] L. Wanka, C. Cabrele, M. Vanejews, P. R. Schreiner, *Eur. J. Org. Chem.* **2007**, 1474–1490.
- [112] B. Das, V. S. Reddy, F. Tehseen, *Tetrahedron Lett.* **2006**, *47*, 6865–6868.
- [113] F. Xue, C. T. Seto, *Bioorg. Med. Chem.* **2006**, *14*, 8467–8487.
- [114] T. Yamaguchi, D. Heseck, M. Lee, A. G. Oliver, S. Mobashery, *J. Org. Chem.* **2010**, *75*, 3515–3517.
- [115] S. D. Stamatov, J. Stawinski, *Tetrahedron* **2005**, *61*, 3659–3669.
- [116] A. Nelson, S. Warren, *J. Chem. Soc., Perkin Trans. 1* **1999**, 3425–3433.
- [117] A. Lethbridge, R. O. C. Norman, C. B. Thomas, W. J. E. Parr, *J. Chem. Soc., Perkin Trans. 1* **1975**, 231–241.
- [118] A.-B. L. Fransson, Y. Xu, K. Leijondahl, J.-E. Bäckvall, *J. Org. Chem.* **2006**, *71*, 6309–6316.
- [119] W. Fröhner, B. Monse, T. M. Braxmeier, L. Casiraghi, H. Sahagún, P. Seneci, *Org. Lett.* **2005**, *7*, 4573–4576.

Associated Content

Supporting Information. NMR and IR spectra, as well as computational data and additional references. This material is available free of charge via the Internet at <http://pubs.acs.org>.

Author Information

Corresponding Author. *E-mail: prs@uni-giessen.de. Fax: (+49)-641-9934309.

Author Contributions.[#]C. E. Müller and D. Zell contributed equally.

Notes. The authors declare no competing financial interest.

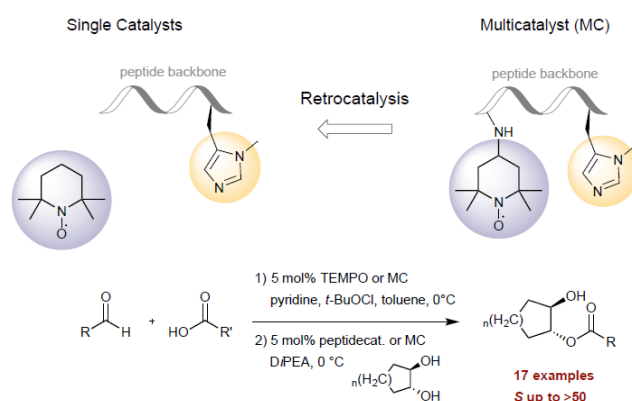
Acknowledgments

This work was supported by the Deutsche Forschungsgemeinschaft (SPP1179) and Alexander-von-Humboldt foundation (fellowship to R.H.). We thank Christian B. W. Stark (University of Hamburg) for supplying substrate **36** and Yannick Landais (ISM, Université Bordeaux-1) for providing **37**. Additionally we thank J. Romański for the synthesis of **32**, **33**, and **34**.

- Chapter III -

En Route to Multicatalysis: Kinetic Resolution of *trans*-Cycloalkane-1,2-diols *via* Oxidative Esterification

Christine Hofmann, Sören M. M. Schuler, Raffael C. Wende, and Peter R. Schreiner, *Chem. Commun.* **2014**, 50, 1221–1223

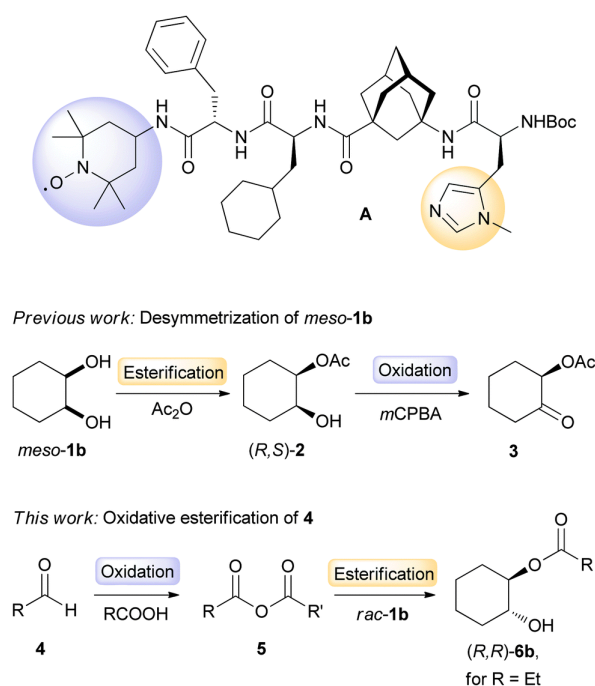


Abstract

We demonstrate the application of a multicatalyst to the oxidation of a broad variety of aldehydes and subsequent enantioselective esterification of the incipient acids with (\pm)-*trans*-cycloalkane-1,2-diols. This reaction operates well with a multicatalyst bearing two independent catalytic moieties that provide monoprotected 1,2-diols in one pot.

"Reproduced from *Chemical Communications* **2014**, 50, 1221–1223 with permission from The Royal Society of Chemistry."

Multicatalysts carry distinct catalytic moieties on a backbone that allows modular synthesis, for instance, an oligopeptide. The combination of several catalytic moieties provides reactivity and operational simplicity not attainable with multiple single catalysts, and complex molecules can be prepared from simple starting materials with high efficiency.^[1] The obvious challenges with this concept are the mutual compatibility of the catalytic moieties and the versatility as well as generality of a multicatalyst, for instance, in changing a particular reaction order. Based on the concept of retrocatalysis^[1] we designed peptide catalyst **A** (Scheme 1) as a multicatalyst, and it has previously been applied as an efficient multicatalyst for the one-pot desymmetrization of *cis*-cycloalkane-1,2-diols (e.g., *meso*-**1b**) and oxidation of the configurationally unstable monoacetate (*R,S*)-**2**.^[2] Therefore, we envisioned **A** also to be a promising catalyst for a reverse reaction sequence, for instance, the oxidation of aldehydes followed by an enantioselective esterification (Scheme 1).



Scheme 1. Versatility of multicatalyst **A**.

One-pot oxidative esterifications of aldehydes have become a conceptually and economically attractive alternative to traditional ester synthesis.^[3] Thus, there are several examples for oxidative esterifications of aldehydes activated by transition-metal catalysts^[4] or *N*-heterocyclic carbenes.^[5] Recently, Szpilman *et al.* reported an efficient TEMPO^[6] (**B**) catalyzed oxidation of aldehydes activated with carboxylic acid **7e** (Table 1) to yield mixed anhydrides that can be converted to esters in situ.^[7] We envisaged redesigning this oxidative esterification protocol as an application for multicatalyst **A**. Before using **A** we first elaborated the single-step reactions with **B** and oligopeptide **C**^[8] to determine the feasibility of the individual reactions and for optimization as well as comparison with existing procedures.

Recently, we have shown that oligopeptide catalysts^[9] bearing an *N*- π -methyl histidine moiety (e.g., **C**) very efficiently transfer acyl groups enantioselectively onto *trans*- and *cis*-cycloalkane-1,2-diols.^[10] Peptide catalyst **C** also led to the first realization of an enantioselective Steglich esterification.^[11] Using an aldehyde instead of the acid is advantageous because aldehydes are typically more soluble in organic solvents, easier to purify, more reactive and therefore a more practical intermediate in multistep syntheses.

We optimized the reaction conditions for the enantioselective oxidative esterification with propanal (**4a**) and tested various acids (**7a–f**) as activators for **4a** (Table 1). Toluene has proven to be the best solvent for the kinetic resolution of diols with **C** and therefore we also used it for the oxidation step.^[8] Complete conversion of **4** was achieved using a stoichiometric amount of pyridine, 1.1 equiv. of 4-nitrobenzoic acid **7a**, 5 mol% **B** and 1.05 equiv. of the oxidant, *t*-BuOCl, at a concentration of 1 M in toluene after 1 h. An excess of pyridine or catalytic

Table 1. Screening of various acids (**7a–f**) under optimized reaction conditions.

R		<i>C</i> ^a (%)	<i>ee</i> (%)		
			1	6	<i>S</i> ^b
7a	<i>p</i> -NO ₂ C ₆ H ₄	49	81	86	33
7b	2-CH ₃ -6-NO ₂ C ₆ H ₃	38	48	78	13
7c	2,4,6-(Cl) ₃ C ₆ H ₂	28	29	73	9
7d	2,4,6-(CH ₃) ₃ C ₆ H ₂	27	28	78	11
7e	C(CH ₃) ₃	23	27	90	25
7f	1-Adamantyl	12	12	92	27

^a Conversion of *rac*-**1b** determined by chiral GC after 24 h reaction time for esterification, 0.1 mmol **4a**. ^b *S* = selectivity factor.^[15]

amounts of the acid accelerated the background reaction and resulted in lower enantioselectivities. The esterification requires relatively high dilution^[8,12] (0.005 M) to achieve high enantioselectivities for **1b** and **6b**.

Under optimized reaction conditions **7a** and **7b** provided the highest conversions of *rac*-**1b** within 24 h. The best enantioselectivities were achieved with acid **7a**. Acids **7e** and **7f** with higher pK_a values^[13] showed lower conversion. To identify the ratios of the mixed and symmetric anhydrides of **4a** and **7a** formed during the reaction, NMR studies were undertaken.^[14] The anhydrides formed in a ratio of approximately 3 : 1 : 1 of mixed anhydride relative to the symmetric anhydrides of **4a** and **7a**. Further investigations are necessary to determine which of the formed anhydrides is transferred faster onto the acylation moiety.

Table 2. Kinetic resolution of *trans*-cycloalkane-1,2-diols **1a–1d**.

R	n	C ^a (yield 1 , 6) (%)	ee (%)		S ^b
			1	6	
1a	1	70 (n.d., n.d.)	76	31	4
1b	2	47 (46, 43)	81	88	39
1c	3	49 (48, 43)	86	88	43
1d	4	50 (39, 47)	94	93	>50

^a Conversion determined by chiral GC and HPLC, 1.0 mmol **4a**. ^b S = selectivity factors,^[15] n.d. = not determined.

To expand the substrate scope we tested various *trans*-cycloalkane-1,2-diols **1** in the kinetic resolution with 1 equiv. of acyl source affording the corresponding hydroxy ester with high enantioselectivities and good yields (Table 2). The selectivities depend on the ring size of the substrate, with *trans*-cyclooctane-1,2-diol (**1d**) showing the highest and *trans*-cyclopentane-1,2-diol (**1a**) the lowest selectivities.^[8]

Various aldehydes were employed to probe the generality and utility of this oxidative esterification protocol. To determine the time for full conversion of the aldehyde, we followed the conversion by NMR (see ESI† for details). Owing to the low solubility of **7a** in the reaction mixture, we used **7c** for the NMR investigations, assuming that the time for full conversion of **4** with **7c** and **7a** are similar (Table 1). Sterically hindered aldehydes require longer reaction times: for **4a** the oxidation was completed in 1 h, while isopentanal (**4c**) required 9 h and isobutanal (**4d**) 18 h. Aromatic aldehydes proved to be more reactive than aliphatic ones. However, benzaldehyde showed insufficient conversion under these conditions; this is due to the increased stability of the anhydride intermediate that we had prepared separately and which does not react under our standard conditions.

Table 3. Enantioselective oxidative esterification of *rac*-**1b** using various aldehydes **4b–i**.

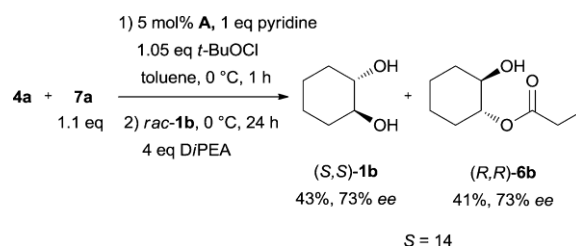
<p>Reaction scheme: Aldehyde 4 (R-CHO) reacts with 7a (1.1 eq) in the presence of 5 mol% B, 1 eq pyridine, 1.05 eq <i>t</i>-BuOCl, and toluene at 0 °C to form anhydride 8 (R-CO-O-CO-C₆H₄-NO₂). Anhydride 8 then reacts with <i>rac</i>-1b (5 mol%) and 1 eq DIPEA at 0 °C to yield the kinetic resolution products <i>(S,S)</i>-1b and <i>(R,R)</i>-9.</p>						
Aldehyde		<i>t</i> ^a (h)	<i>C</i> ^b (yield 1b , 9) (%)	<i>ee</i> (%)		<i>S</i> ^c
				1b	9	
4b	Decanal	1/24	47 (48, 42)	79	88	38
4c	Isopentanal	9/24	48 (43, 46)	76	82	24
4d	Isobutanal	18/6 ^d	44 (43, 40)	72	90	40
4e	Cyclohexanal	18/18 ^d	46 (37, 35)	52	62	7
4f	Pivaldehyde	24/48 ^d	4 (n.d., n.d.)	4	92	25
4g	Ph(CH ₂) ₂ CHO	0.5/6 ^{d,e}	50 (44, 44)	85	82	27
4h	PhCH ₂ CHO	0.5/6 ^{d,e}	35 (58, 27)	50	93	47
4i	PhCHO	18/48 ^{d,e}	7 (n.d., n.d.)	6	78	9

^a Reaction time for oxidation and esterification. ^b Conversion determined by chiral GC and HPLC, 1.0 mmol **4**. ^c *S* = selectivity factors.^[15] ^d 2 equiv. of generated anhydride. ^e Concentration for oxidation was 0.1 M. n.d. = not determined.

After having determined the time for full conversion, aromatic and aliphatic aldehydes were oxidized to their corresponding mixed anhydrides and tested in the kinetic resolution of *rac*-**1b**.

Aldehydes **4b–d**, **g**, and **h** afforded high enantioselectivities and good yields. Cyclohexanal **4e** gave lower selectivities while pivaldehyde (**4f**) showed insufficient conversion due to the increased steric hindrance (Table 3).

With these promising results in hand, our attention turned to the multicatalyst approach. We used 5 mol% of multicatalyst **A** instead of individual catalysts **B** and **C** and applied it to the enantioselective oxidative esterification of **4a** (Scheme 2). To keep the catalyst deprotonated at all times it is necessary to use an excess (4 equiv.) of DiPEA in the esterification step. We obtained 43% of **1b** and 41% of **6b** with good enantioselectivities (73% *ee*, for both **1b** and **6b**, respectively; *S* = 14) with **A**. Thus, the enantioselectivities as compared to the individual catalysts **B** and **C** are only slightly lower, and we consider this a proof-of-principle for our multicatalyst concept.



Scheme 2. Kinetic resolution of rac-**1b** with multicatalyst **A**.

We have shown that a variety of aldehydes can be activated by 4-nitrobenzoic acid and oxidized with TEMPO to furnish mixed anhydrides that can be enantioselectively transferred onto *trans*-cycloalkane-1,2-diols with good yields and enantioselectivities with catalyst **C**. The protocol with individual catalysts can be unified with multicatalyst **A**^[2] that was designed utilizing the retrocatalysis concept,^[1] with only slightly reduced enantioselectivities. A natural extension of this work would be the use of alcohols as the starting materials as this would constitute direct alcohol cross-coupling.

We thank Dr. H. Hausmann for NMR investigations, Dr. E. Röcker for competent analytical support and Dr. G. Jakab for helpful discussions.

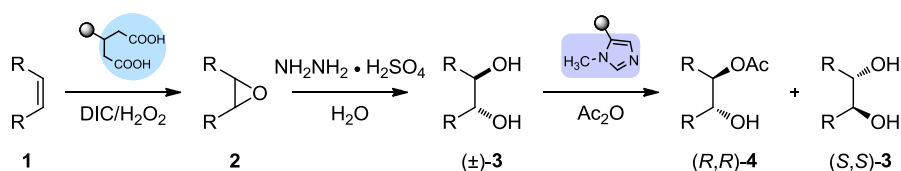
Notes and References

- [1] R. C. Wende, P. R. Schreiner, *Green Chem.* **2012**, *14*, 1821–1849.
- [2] C.E. Müller, R. Hrdina, R. C. Wende, P. R. Schreiner, *Chem.–Eur. J.* **2011**, *17*, 6309–6314.
- [3] K. Ekoue-Kovi, C. Wolf, *Chem.–Eur. J.* **2008**, *14*, 6302–6315.
- [4] a) K. Suzuki, T. Yamaguchi, K. Matsushita, C. Iitsuka, J. Miura, T. Akaogi, H. Ishida, *ACS Catal.* **2013**, *3*, 1845–1849; b) S. K. Rout, S. Guin, K. K. Ghara, A. Banerjee, B. K. Patel, *Org. Lett.* **2012**, *14*, 3982–3985; c) N. Yamamoto, Y. Obora, Y. Ishii, *J. Org. Chem.* **2011**, *76*, 2937–2941; d) N. A. Owston, T. D. Nixon, A. J. Parker, M. K. Whittlesey, J. M. J. Williams, *Synthesis* **2009**, 1578–1581; e) R. Lerebours, C. Wolf, *J. Am. Chem. Soc.* **2006**, *128*, 13052–13053; f) R. Gopinath, B. K. Patel, *Org. Lett.* **2000**, *2*, 577–579.
- [5] a) S. Kuwano, S. Harada, B. Kang, R. Oriez, Y. Yamaoka, K. Takasu, K.-i. Yamada, *J. Am. Chem. Soc.* **2013**, *135*, 11485–11488; b) S. De Sarkar, A. Biswas, C. H. Song, A. Studer, *Synthesis* **2011**, 1974–1983; c) S. Iwahana, H. Iida, E. Yashima, *Chem.–Eur. J.* **2011**, *17*, 8009–8013; d) B. E. Maki, A. Chan, E. M. Phillips, K. A. Scheidt, *Tetrahedron* **2009**, *65*, 3102–3109; e) C. Noonan, L. Baragwanath, S. J. Connon, *Tetrahedron Lett.* **2008**, *49*, 4003–4006; f) J. Guin, S. De Sarkar, S. Grimme, A. Studer, *Angew. Chem. Int. Ed.* **2008**, *47*, 8727–8730; g) B. E. Maki, K. A. Scheidt, *Org. Lett.* **2008**, *10*, 4331–4334; h) B. E. Maki, A. Chan, E. M. Phillips, K. A. Scheidt, *Org. Lett.* **2006**, *9*, 371–374.
- [6] a) L. Tebben, A. Studer, *Angew. Chem. Int. Ed.* **2011**, *50*, 5034–5068; b) J. M. Bobbit, C. Brückner, N. Merbouh, *Org. React.* **2010**, *74*, 103.
- [7] H. Toledo, E. Pisarevsky, A. Abramovich, A. M. Szpilman, *Chem. Commun.* **2013**, *49*, 4367–4369.
- [8] C. E. Müller, L. Wanka, K. Jewell, P. R. Schreiner, *Angew. Chem. Int. Ed.* **2008**, *47*, 6180–6185.
- [9] a) H. Wennemers, *Chem. Commun.* **2011**, *47*, 12036–12041; b) E. A. C. Davie, S. M. Mennen, Y. Xu, S. J. Miller, *Chem. Rev.* **2007**, *107*, 5759–5812.
- [10] a) C. E. Müller, D. Zell, R. Hrdina, R. C. Wende, L. Wanka, S. M. M. Schuler, P. R. Schreiner, *J. Org. Chem.* **2013**, *78*, 8465–8484; b) C. E. Müller, D. Zell, P. R. Schreiner, *Chem.–Eur. J.* **2009**, *15*, 9647–9650.
- [11] R. Hrdina, C. E. Müller, P. R. Schreiner, *Chem. Commun.* **2010**, *46*, 2689–2690.
- [12] E. R. Jarvo, G. T. Copeland, N. Papaioannou, P. J. Bonitatebus, S. J. Miller, *J. Am. Chem. Soc.* **1999**, *121*, 11638–11643.
- [13] F. G. Bordwell, *Acc. Chem. Res.* **1988**, *21*, 456–463.
- [14] a) I. Dhimitruka, J. SantaLucia, *Org. Lett.* **2005**, *8*, 47–50; b) I. Shiina, M. Kubota, H. Oshiumi, M. Hashizume, *J. Org. Chem.* **2004**, *69*, 1822–1830; c) J. Inanaga, K. Hirata, H. Saeki, T. Katsuki, M. Yamaguchi, *Bull. Chem. Soc. Jpn.* **1979**, *52*, 1989–1993.
- [15] H. B. Kagan, J. C. Fiaud, *Top. Stereochem.* **1988**, *18*, 249–330.

- Chapter IV -

Functionality, Effectiveness, and Mechanistic Evaluation of a Multicatalyst-Promoted Reaction Sequence by Electrospray Ionization Mass Spectrometry

M. Wasim Alachraf, Raffael C. Wende, Sören M. M. Schuler, Peter R. Schreiner, and Wolfgang Schrader, *Chem.–Eur. J.* **2015**, *21*, 16203–16208



Abstract

A multicatalytic three-step reaction consisting of epoxidation, hydrolysis, and enantioselective monoacylation of cyclohexene was studied by using mass spectrometry (MS). The reaction sequence was carried out in a one-pot reaction using a multicatalyst. All reaction steps were thoroughly analyzed by electrospray ionization (ESI) MS (and MS/MS), as well as high-resolution MS for structure elucidation. These studies allow us to shed light on the individual mode of action of each catalytic moiety. Thus, we find that under the epoxidation conditions, the catalytically active *N*-methyl imidazole for the terminal acylation step is partially deactivated through oxidation. This observation helps to explain the lower efficiency of the catalyst in the last step compared to the monoacylation performed separately. All reactive intermediates and products of the reaction sequence, as well as of the side-reactions, were monitored, and we present a working mechanism of the reaction.

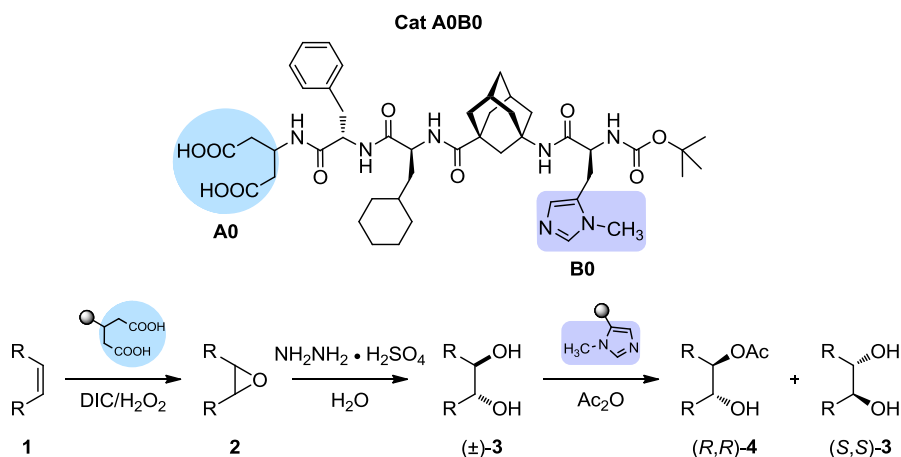
"Reproduced with permission from *Chemistry – A European Journal* **2015**, *21*, 16203–16208. Copyright 2015 Wiley-VCH Verlag GmbH & Co. KGaA, Weinheim."

1. Introduction

Various synthetic methods have been developed utilizing small organic molecules as organocatalysts.^[1] One especially intriguing development has been the use of cascade or tandem reactions,^[2] in which several reactions are subsequently carried out in one pot. These types of reactions promise higher efficiency while minimizing resource and energy requirements. Typical cascade or tandem reactions combine the reactants from the beginning,^[2] often giving rise to a broad variety of side-reactions. An alternative concept for cascade reactions is a catalyst bearing multiple catalytic moieties, separated by a spacer molecule, a so-called multicatalyst.^[2],3] This methodology is reminiscent of an assembly line, in which a complex molecule is consecutively assembled from simple starting materials in a manner that at the correct time each catalytic moiety is selectively activated.^[3]

The elucidation of reaction mechanisms of such complex reactions is rather challenging, because many intermediates are short-lived and occur often only in minor quantities. Indeed, one advantage of such reactions is that isolation of short-lived intermediates can be neglected, because they are generated in situ and consumed rapidly. Methods allowing the characterization of structural changes typically are NMR^[4] and, to a minor extent, IR spectroscopy.^[4e,5] A powerful tool for the investigation of complex organocatalytic reactions is mass spectrometry (MS) due to its advantages to detect components at low concentrations within short lifetimes. Even structural data can be derived with MS/MS experiments.^[6] The fragmentation of individual intermediates can be utilized for the characterization of catalytic reactions.^[7]

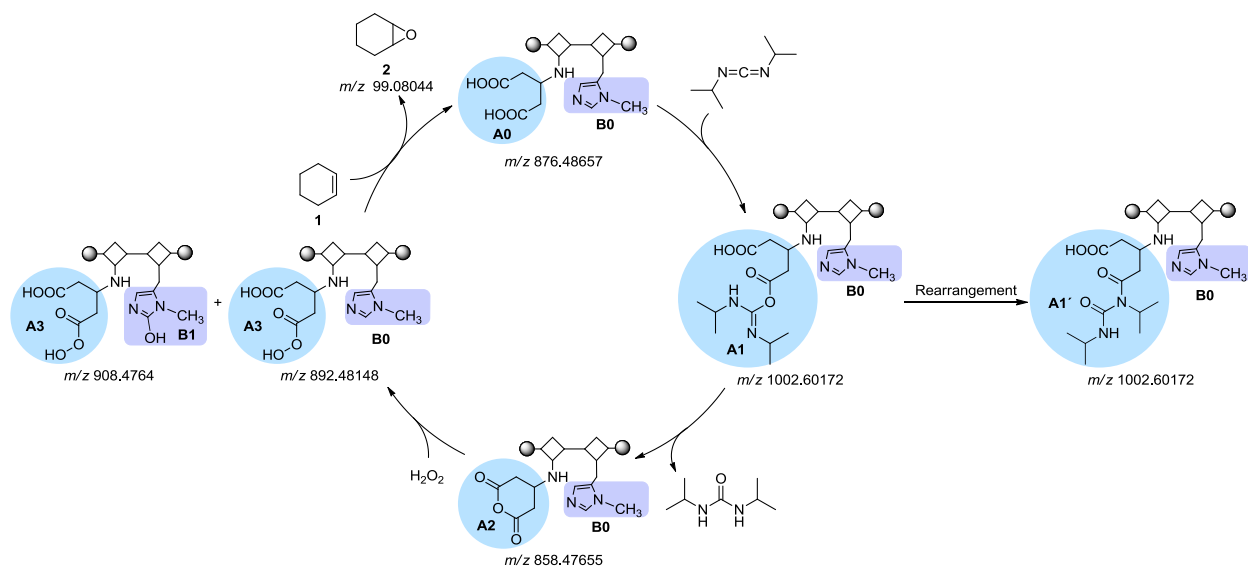
Due to the novelty of the multicatalyst approach, no mechanistic studies have been carried out yet. Herein, we report a detailed mechanistic investigation concerning the catalytic epoxidation of olefins followed by hydrolysis and enantioselective kinetic resolution through acylation.^[8] Each individual step can be defined by reaction intermediates as reaction markers that can be detected by ESI-MS. The multicatalyst **A0B0** used in this study consists of a chiral peptide backbone^[9] including an adamantane spacer^[3,10] separating two catalytic moieties. Dicarboxylic acid **A0** is responsible for the first reaction step, an epoxidation,^[11] and *N*-methyl imidazole moiety **B0** catalyzes the terminal acylation.^[3b] The individual catalytic moieties are activated by adding the corresponding reagent after a particular time interval, and this is the key difference to cascade reactions. Various catalysts have been developed, in which the catalytically active moieties were placed in different positions of the peptide backbone; herein, we employed the most effective catalyst **A0B0** (Scheme 1).^[3b]



Scheme 1. Reaction sequence using multicatalyst **A0B0**.

2. Results and Discussion

The first step in the mechanistic evaluation of a catalytic reaction with ESI-MS is the determination and characterization of reaction markers that allow an unequivocal assignment of the reaction intermediates. The first step of the reaction under consideration is the epoxidation of cyclohexene (**1**) to cyclohexene oxide (**2**). Although the reaction itself is straightforward, the identification of catalytically active moieties is more challenging. For the activation of catalytic moiety **A0**, diisopropylcarbodiimide (DIC) was added forming the *O*-acylisourea (**A1**), which, after cleavage, removes a molecule of water providing the corresponding anhydride **A2**. This further reacts with hydrogen peroxide to give the catalytically active peracid moiety **A3**. After formation of peracid **A3**, the catalyst reacts with **1** to give **2** (Scheme 2). The ESI MS/MS spectra of **2** and the appearing catalytic species are shown in Figures 1 and 2, respectively. One potential side reaction of *O*-acylisourea **A1** attached to the peptide is the formation of *N*-acylurea **A1'**, which was reported by Montalbetti and co-workers.^[12] We also observed this rearrangement, but the molecular ion is present in such low intensity that it is under standard conditions almost not detectable, implying that it is relatively unimportant for the catalytic step (Scheme 2; Figure 2). Due to the short lifetime of those and other intermediates, it was not possible to determine them from the reaction mixture alone. Therefore, some additional studies were carried out using an online microflow reactor as shown in Figure 6 in the Experimental Section. In these experiments, two different syringes were filled with different reaction solutions. The reaction takes place after



Scheme 2. Reaction cycle for the epoxidation reaction.

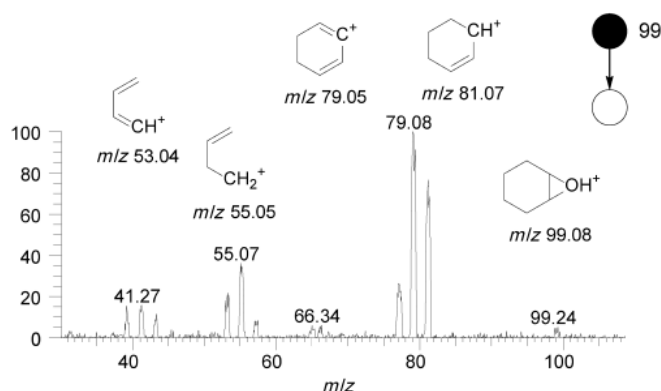


Figure 1. ESI MS/MS spectrum of epoxide intermediate **2** obtained with a triple quadrupole MS.

the two flows are combined in a mixing T-piece. The reaction time depends on the length of the capillary after the mixing T-piece and can be adjusted to the time frame of interest. This allows studying very reactive and short-lived intermediates. Due to the continuous formation of the same components, it is possible to study them in detail by MS and MS/MS methods.

Catalyst **A0B0** converts **57%** (± 3) into the final product **4** in the separately performed acylation reaction (2 mol% catalyst loading, 3 h). However, only 35% of the monoacetylated product **4** were obtained when the reaction was performed under multicatalysis conditions, even at 5 mol% catalyst loading and after longer reaction time (17 h), indicating a somewhat lower activity of the multicatalyst.^[3b] When studying the formation of the moiety **A3**, we found that another reaction occurs that could have a direct impact on the effectiveness of the methyl imidazole group **B0** that is responsible for the subsequent catalytic acylation. During formation of peracid **A3**, an

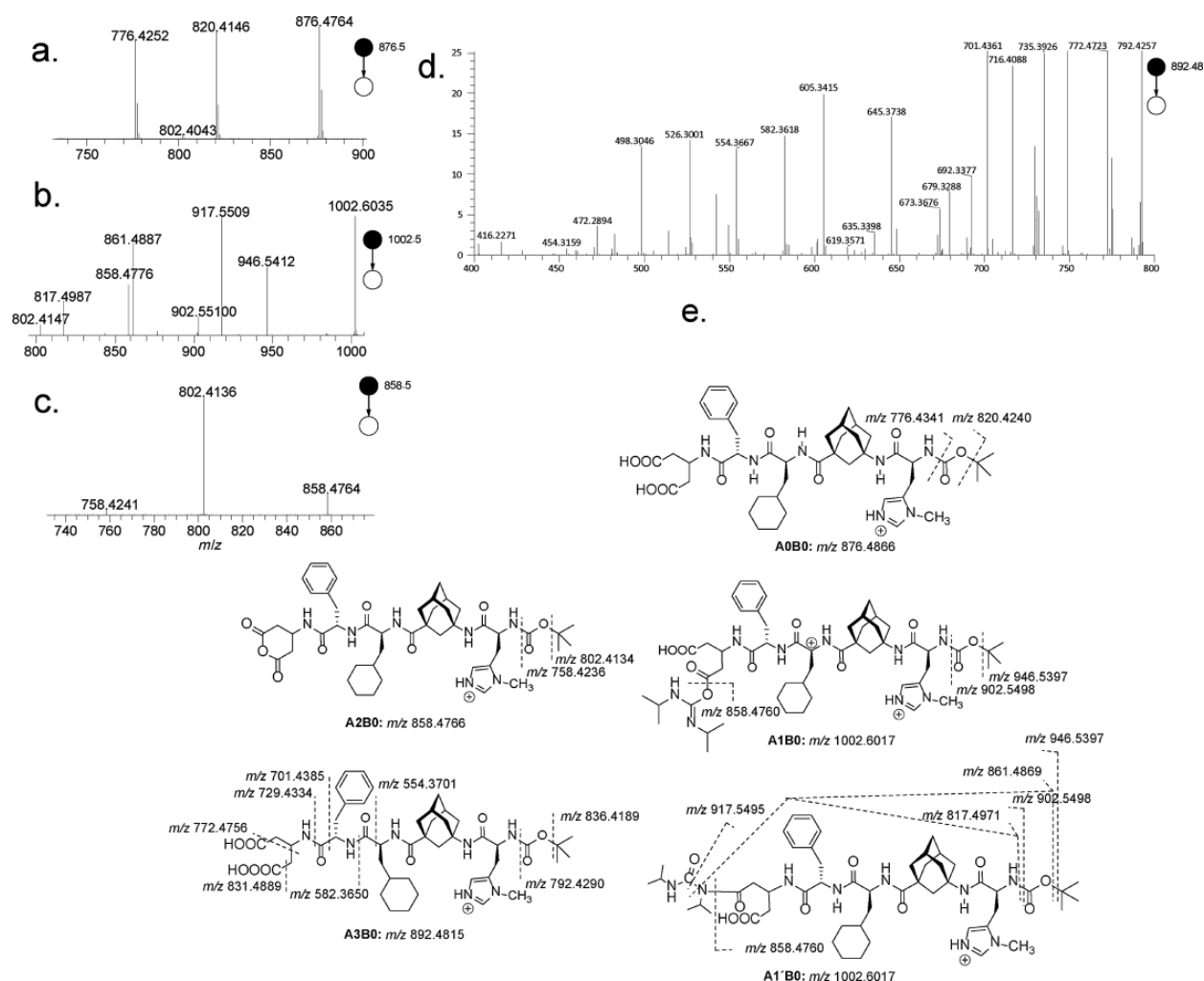


Figure 2. ESI MS/MS spectra of a) A0B0; b) A1B0 and A1'B0; c) A2B0; and d) A3B0; and the associated fragmentation. The spectrum of intermediate A1B0 was obtained by using a microflow reactor set-up by high-resolution MS.

additional signal was found at m/z 908 (Figure 3 a and b); the difference of 16 Da indicates oxidation of the catalyst. The position of the oxygenation was studied thoroughly with highly accurate MS/MS and MSⁿ experiments, in which the molecule was fragmented and the structural differences were analyzed (Figure 3 c, d). We determined the oxidation to occur at the imidazole group: activation of moiety A also leads to oxidation of moiety B, resulting in the formation of a hydantoin derivative B1 (Scheme 2 and Figure 3). The oxidation of the imidazole moiety leads to reduced effectiveness of the catalyst due to the resulting lower amount of active catalytic moiety utilizing the multicatalyst.

For the epoxide opening forming diol hydrazine bisulfate and water have to be added to the reaction mixture.^[7b] The hydrolysis of 2 was not investigated mechanistically, because the peptide catalyst is not involved in this step.

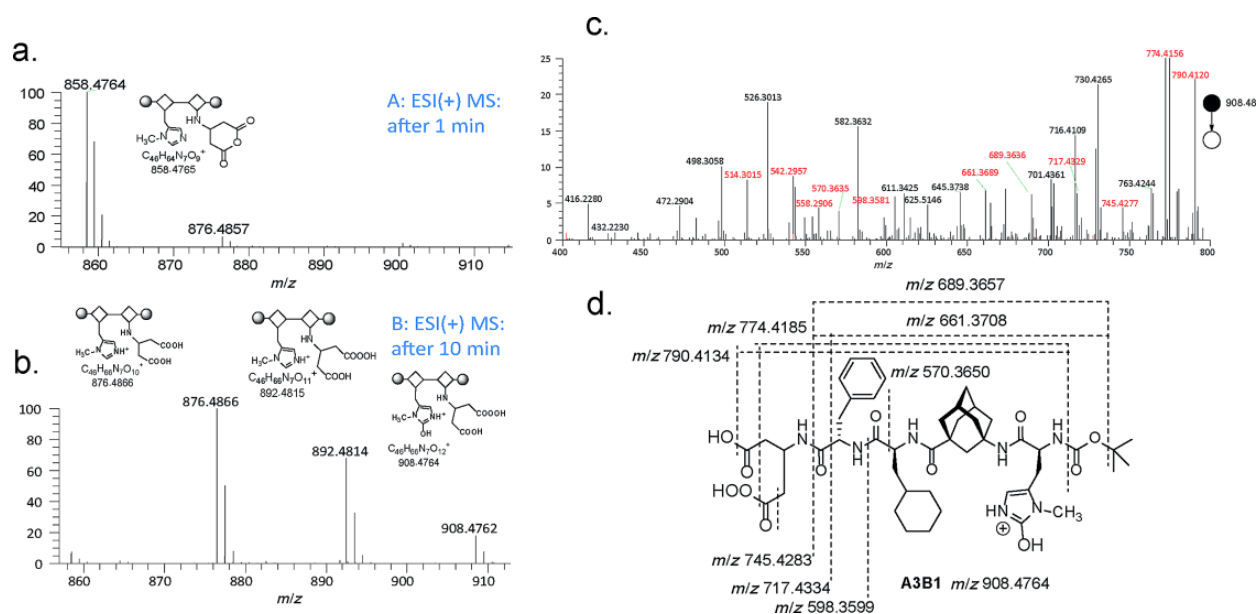


Figure 3. Characterization of completely oxidized catalyst **A3B1**: a) and b) MS spectra of the activation of catalytic moiety **A** [a] after adding DIC; b) after adding DIC and H_2O_2]; c) and d) ESI MS/MS spectra and the associated fragmentation⁽¹⁾ of **A3B1**.⁽¹⁾ Red numbers indicate the fragments of the oxidized imidazole functionality. Measuring was achieved by HRMS.

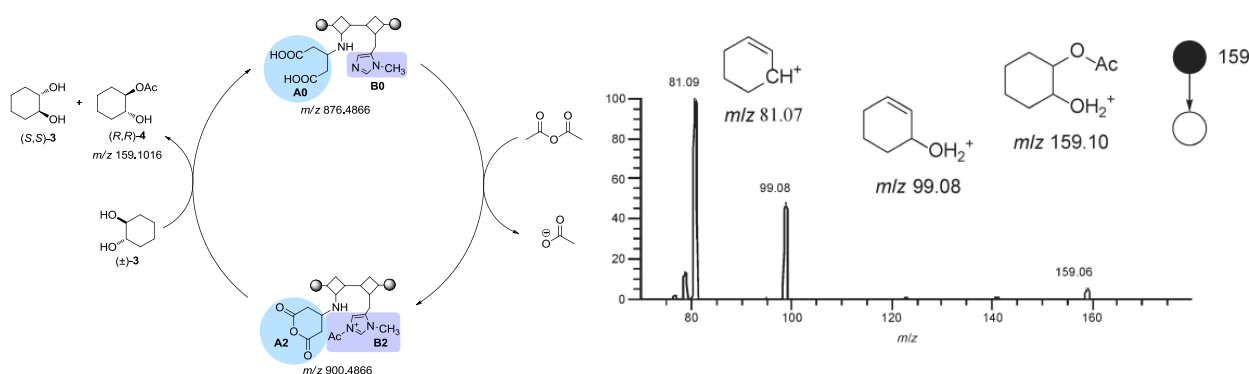


Figure 4. Activation of the catalytic moiety **B0** and MS/MS spectrum of the monoacetylated product by triple quadrupole MS/MS.

The second catalytic step investigated in this reaction sequence is the kinetic resolution of racemic diol. At the beginning, both catalytic sites of multicatalyst **A0B0** are inactive. After completion of the preceding reactions, the activation of catalytic moiety **B0** is accomplished by adding acetic anhydride to the reaction mixture providing acylium ion **B2** (Figure 4).

After activation of the catalyst, monoacylation of diol takes place. The corresponding MS/MS spectrum is depicted in Figure 4.

Our results also indicate that during the last step of the reaction, not only moiety **B** was activated by acetic anhydride, but also moiety **A** was directly converted to the intramolecular anhydride **A2** (Figure 4). In a subsequent step, **A2B2** was oxidized to **A3B2** by hydrogen peroxide, which is still present due to the one-pot conditions. Figure 5 shows the MS, the MS/MS, as well as the MS³ spectra of the detected catalytic species. The observed side-reactions may also have a direct influence on the enantioselectivity due to potential conformational changes in the peptide backbone. Indeed, the multicatalyst provides somewhat lower selectivities compared to the originally developed acylation catalyst.^[3b,10a]

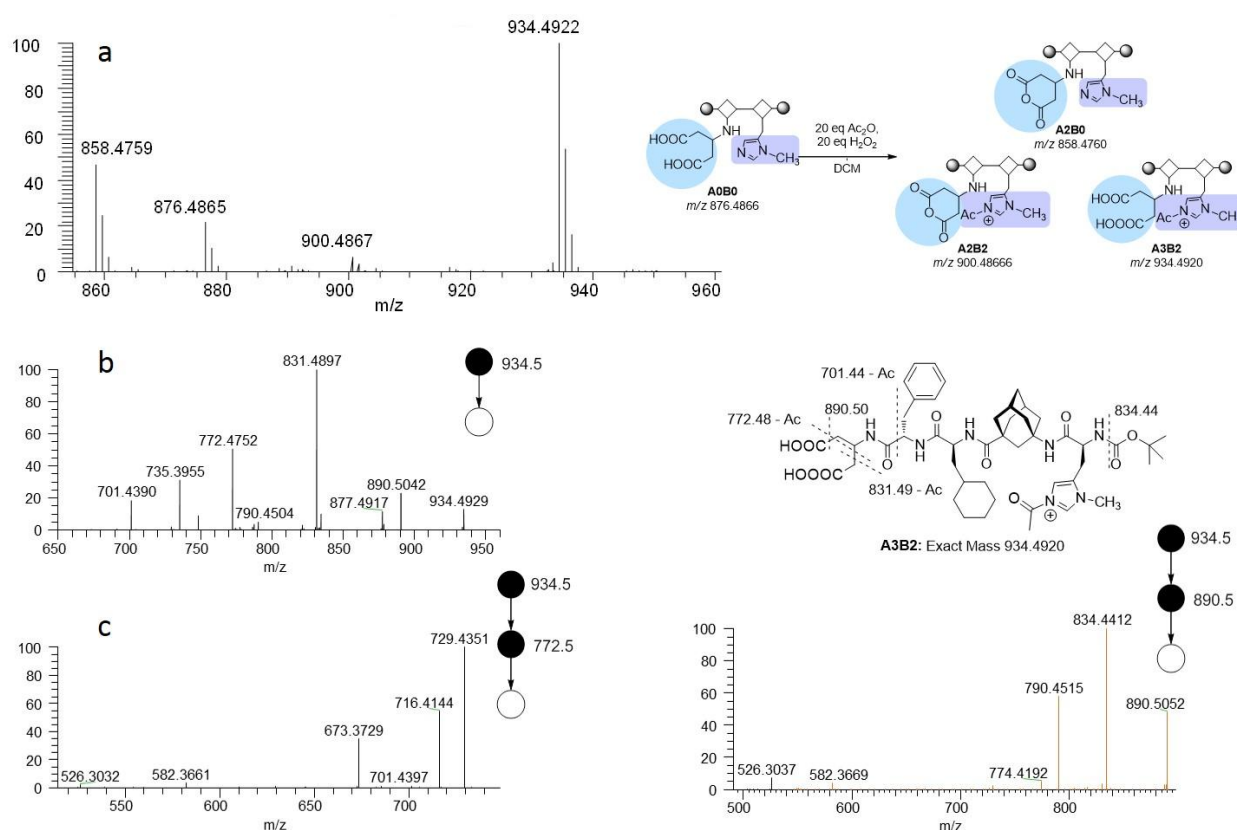


Figure 5. MSⁿ spectra of the catalytic species of the last reaction step by HRMS: a) MS spectrum of the activation sequence using acetic anhydride and hydrogen peroxide; b) MS/MS spectrum of catalyst **A3B2** after activation with acetic anhydride; c) MS³ spectra of catalyst **A3B2** detailing the structural characterization of both catalytic moieties.

3. Conclusion

A triple-cascade sequence consisting of an epoxidation, an epoxide opening, and an enantioselective acylation reaction catalyzed by an oligopeptide multicatalyst was studied thoroughly by using ESI-MS. The key reaction intermediates were successfully characterized. In addition to the activation of the catalytic moieties **A0** to **A3** in the first reaction step by reagents DIC and H₂O₂, a side-reaction takes place on the catalytic moiety for the second reaction step **B0** into **B1** leading to a partially oxidized methyl imidazole moiety that causes reduction of the activity of catalytic moiety **B0** for the acetylation in the terminal step.

Our detailed mass spectrometric study of the present multicatalyst allows the individual characterization of both catalytic reactions. This is a prime example how detailed mechanistic studies using highly accurate MS and MSⁿ data can help in understanding complex organocatalytic reactions.

4. Experimental Section

Reaction procedure. Catalyst (0.05 mmol, 21.9 mg, 5 mol%), cyclohexene (1 mmol, 101 μ L, 1 equiv), and DIC (1.2 mmol, 185 μ L, 1.2 equiv) were dissolved in dichloromethane (DCM; 2 mL). To this mixture, hydrogen peroxide (30%; 130 μ L, 1.2 equiv) was added, and the resulting reaction mixture was stirred at room temperature for 24 h. After this time, the addition of DIC (1.2 mmol, 185 μ L, 1.2 equiv) and 30% hydrogen peroxide (130 μ L, 1.2 equiv) was repeated, and the reaction mixture was stirred under the same conditions for additional 24 h. Then toluene (6 mL) was added, followed by the addition of H₂O (10 mmol, 180 μ L, 10 equiv) and hydrazine bisulfate (0.1 mmol, 13 mg, 0.1 equiv), and the mixture was stirred at room temperature for 18 h. In the next step, toluene (180 mL) and *i*Pr₂EtN (5.3 mmol, 901 μ L, 5.3 equiv) were added, and the reaction mixture was cooled to 0 °C. Finally, Ac₂O (5.3 mmol, 501 μ L, 5.3 equiv) was added, and the kinetic resolution was monitored by chiral GC. After 17 h, the reaction mixture was quenched by adding methanol (10 mL), the solvents were evaporated under reduced pressure, and the column chromatography on silica gel in hexane/EtOAc (1:1) gave 56 mg (35 %) of 1-acetoxy-2-cyclohexane alcohol (60% yield).

Microreactor procedure. One example that could only be investigated by the microreactor experiment is the intermediate **A2B0**. For this experiment, syringe I was filled with catalyst (0.005 mmol, 4.5 mg) in DCM (1 mL), syringe II with reagent diisopropyl carbodiimide (DIC; 0.12 mmol, 15 mg, 18.7 μL) in DCM (1 mL; Figure 6). The reaction took place in polyether ether ketone (PEEK) capillary after combining reactants from syringes I and II in the mixing chamber. Syringe pumps for I and II were adjusted to flow rates of 5 $\mu\text{L min}^{-1}$ and connected directly to the ion source. It was not just possible to determine the intermediate itself, but also the rearrangement product of this intermediate as fragments at m/z 917.54, 861.48, and 817.49, respectively, using tandem MS.

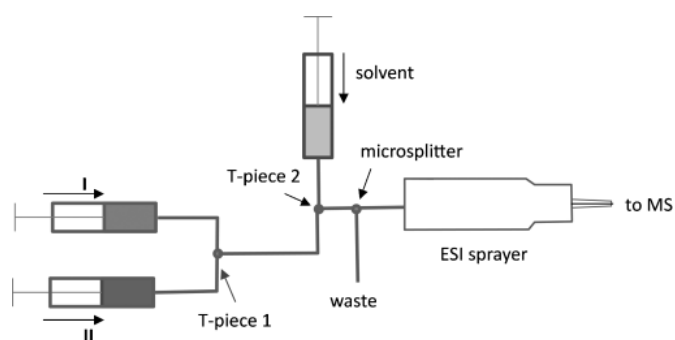


Figure 6. Experimental set-up of the microflow reactor.

Mass spectrometry. MS and MS/MS experiments were carried out using a Thermo TSQ Quantum Ultra AM triple quadrupole mass spectrometer (Thermo Scientific, Dreieich, Germany) equipped with an ESI source, which was controlled by Xcalibur software. The ESI spray voltages were set to 4000 and 3000 V for positive and negative ions, respectively. The heated capillary temperature was adjusted to 270 $^{\circ}\text{C}$. For MS/MS analysis, the collision energy was increased from 10 to 50 eV. The mass spectrometer was operated in the Q1 scan and product ion scan modes, with the mass width for Q1 set at 0.5 Da and for Q3 set at 0.7 Da. The collision cell, Q2, contained argon and was adjusted to a pressure of 1.5 mTorr to induce collision-induced dissociation (CID). Spectra were collected by averaging ten scans with a scan time of 1 s. The mass range was adjusted between 50 and 1500 Da. HRMS data were acquired by using an LTQ-Orbitrap Elite mass spectrometer (Thermo Scientific, Bremen, Germany). All experimental parameters were the same as for the triple quadrupole experiments, except that MS/MS measurements were carried out with an isolation window of 1 Da and different collision energies.

5. References

- [1] a) A. Berkessel, H. Gröger, *Asymmetric Organocatalysis: From Biomimetic Concepts to Applications in Asymmetric Synthesis*, Wiley-VCH, Weinheim, **2005**; b) P. I. Dalko, *Enantioselective Organocatalysis: Reactions and Experimental Procedures*, Wiley-VCH, Weinheim, **2007**; c) A. Dondoni, A. Massi, *Angew. Chem. Int. Ed.* **2008**, *47*, 4638–4660; *Angew. Chem.* **2008**, *120*, 4716–4739; d) D. W. C. MacMillan, *Nature* **2008**, *455*, 304–308; e) A. Moyano, R. Rios, *Chem. Rev.* **2011**, *111*, 4703–4832; f) F. Giacalone, M. Gruttadauria, P. Agrigento, R. Noto, *Chem. Soc. Rev.* **2012**, *41*, 2406–2447.
- [2] a) D. E. Fogg, E. N. dos Santos, *Coord. Chem. Rev.* **2004**, *248*, 2365–2379; b) J.-C. Wasilke, S. J. Obrey, R. T. Baker, G. C. Bazan, *Chem. Rev.* **2005**, *105*, 1001–1020; c) H. C. Guo, J. A. Ma, *Angew. Chem. Int. Ed.* **2006**, *45*, 354–366; *Angew. Chem.* **2006**, *118*, 362–375; d) C. J. Chapman, C. G. Frost, *Synthesis* **2007**, 1–21; e) D. Enders, C. Grondal, M. R. M. Hüttl, *Angew. Chem. Int. Ed.* **2007**, *46*, 1570–1581; *Angew. Chem.* **2007**, *119*, 1590–1601; f) A. M. Walji, D. W. C. MacMillan, *Synlett* **2007**, 1477–1489; g) X. Yu, W. Wang, *Org. Biomol. Chem.* **2008**, *6*, 2037–2046; h) A.-N. Alba, X. Companyó, M. Viciano, R. Rios, *Curr. Org. Chem.* **2009**, *13*, 1432–1474; i) C. Grondal, M. Jeanty, D. Enders, *Nat. Chem.* **2010**, *2*, 167–178; j) B. Westermann, M. Ayaz, S. S. van Berkel, *Angew. Chem. Int. Ed.* **2010**, *49*, 846–849; *Angew. Chem.* **2010**, *122*, 858–861; k) H. Pellissier, *Adv. Synth. Catal.* **2012**, *354*, 237–294; l) R. C. Wende, P. R. Schreiner, *Green Chem.* **2012**, *14*, 1821–1849.
- [3] a) C. E. Müller, R. Hrdina, R. C. Wende, P. R. Schreiner, *Chem.–Eur. J.* **2011**, *17*, 6309–6314; b) R. Hrdina, C. E. Müller, R. C. Wende, L. Wanka, P. R. Schreiner, *Chem. Commun.* **2012**, *48*, 2498–2500; c) C. Hofmann, S. M. M. Schuler, R. C. Wende, P. R. Schreiner, *Chem. Commun.* **2014**, *50*, 1221–1223.
- [4] a) M. B. Schmid, K. Zeitler, R. M. Gschwind, *Angew. Chem. Int. Ed.* **2010**, *49*, 4997–5003; *Angew. Chem.* **2010**, *122*, 5117–5123; b) M. B. Schmid, K. Zeitler, R. M. Gschwind, *J. Am. Chem. Soc.* **2011**, *133*, 7065–7074; c) M. B. Schmid, K. Zeitler, R. M. Gschwind, *J. Org. Chem.* **2011**, *76*, 3005–3015; d) Z. Zhang, K. M. Lippert, H. Hausmann, M. Kotke, P. R. Schreiner, *J. Org. Chem.* **2011**, *76*, 9764–9776; e) K. M. Lippert, K. Hof, D. Gerbig, D. Ley, H. Hausmann, S. Guenther, P. R. Schreiner, *Eur. J. Org. Chem.* **2012**, 5919–5927.
- [5] a) A. T. Messmer, K. M. Lippert, S. Steinwand, E.-B. W. Lerch, K. Hof, D. Ley, D. Gerbig, H. Hausmann, P. R. Schreiner, J. Bredenbeck, *Chem.–Eur. J.* **2012**, *18*, 14989–14995; b) A. T. Messmer, S. Steinwand, K. M. Lippert, P. R. Schreiner, J. Bredenbeck, *J. Org. Chem.* **2012**, *77*, 11091–11095; c) A. T. Messmer, K. M. Lippert, P. R. Schreiner, J. Bredenbeck, *Phys. Chem. Chem. Phys.* **2013**, *15*, 1509–1517.
- [6] a) J. Griep-Raming, S. Meyer, T. Bruhn, J. O. Metzger, *Angew. Chem. Int. Ed.* **2002**, *41*, 2738–2742; *Angew. Chem.* **2002**, *114*, 2863–2866; b) L. S. Santos, J. O. Metzger, *Angew. Chem. Int. Ed.* **2006**, *45*, 977–981; *Angew. Chem.* **2006**, *118*, 991–995; c) W. Schrader, P. P. Handayani, C. Burstein, F. Glorius, *Chem. Commun.* **2007**, 716–718.
- [7] a) J. B. Domingos, E. Longhinotti, T. A. S. Brandao, C. A. Bunton, L. S. Santos, M. N. Eberlin, F. Nome, *J. Org. Chem.* **2004**, *69*, 6024–6033; b) L. S. Santos, C. H. Pavam, W. P. Almeida, F. Coelho, M. N. Eberlin, *Angew. Chem. Int. Ed.* **2004**, *43*, 4330–4333; *Angew. Chem.* **2004**, *116*, 4430–4433; c) C. A. Marquez, F. Fabbretti, J. O. Metzger, *Angew. Chem. Int. Ed.* **2007**, *46*, 6915–6917; *Angew. Chem.* **2007**, *119*, 7040–7042; d) C. D. F. Milagre, H. M. S. Milagre, L. S. Santos, M. L. A. Lopes, P. J. S. Moran, M. N. Eberlin, J. A. R. Rodrigues, *J. Mass Spectrom.* **2007**, *42*, 1287–1293; e) W. Schrader, P. P. Handayani, J. Zhou, B. List, *Angew. Chem. Int. Ed.* **2009**, *48*, 1463–1466; *Angew. Chem.* **2009**, *121*, 1491–1494; f) G. W. Amarante, M. Benassi, H. M. S. Milagre, A. A. C. Braga, F. Maseras, M. N. Eberlin, F. Coelho, *Chem.–Eur. J.* **2009**, *15*, 12460–12469; g) M. W. Alachraf, P. P. Handayani, M. R. M. Hüttl, C. Grondal, D. Enders, W. Schrader, *Org. Biomol. Chem.* **2011**, *9*, 1047–1053.
- [8] a) C. E. Müller, P. R. Schreiner, *Angew. Chem. Int. Ed.* **2011**, *50*, 6012–6042; *Angew. Chem.* **2011**, *123*, 6136–6167; b) H. Pellissier, *Adv. Synth. Catal.* **2011**, *353*, 1613–1666; c) V. P. Krasnov, D. A. Gruzdev, G. L. Levit, *Eur. J. Org. Chem.* **2012**, 1471–1493.
- [9] a) E. A. C. Davie, S. M. Mennen, Y. Xu, S. J. Miller, *Chem. Rev.* **2007**, *107*, 5759–5812; b) H. Wennemers, *Chem. Commun.* **2011**, *47*, 12036–12041.

- [10] a) C. E. Müller, L. Wanka, K. Jewell, P. R. Schreiner, *Angew. Chem. Int. Ed.* **2008**, *47*, 6180–6183; *Angew. Chem.* **2008**, *120*, 6275–6278; b) C. E. Müller, D. Zell, P. R. Schreiner, *Chem.–Eur. J.* **2009**, *15*, 9647–9650; c) R. Hrdina, C. E. Müller, P. R. Schreiner, *Chem. Commun.* **2010**, *46*, 2689–2690; d) C. E. Müller, D. Zell, R. Hrdina, R. C. Wende, L. Wanka, S. M. M. Schuler, P. R. Schreiner, *J. Org. Chem.* **2013**, *78*, 8465–8484.
- [11] G. Peris, C. E. Jakobsche, S. J. Miller, *J. Am. Chem. Soc.* **2007**, *129*, 8710–8711.
- [12] C. Montalbetti, V. Falque, *Tetrahedron* **2005**, *61*, 10827–10852.

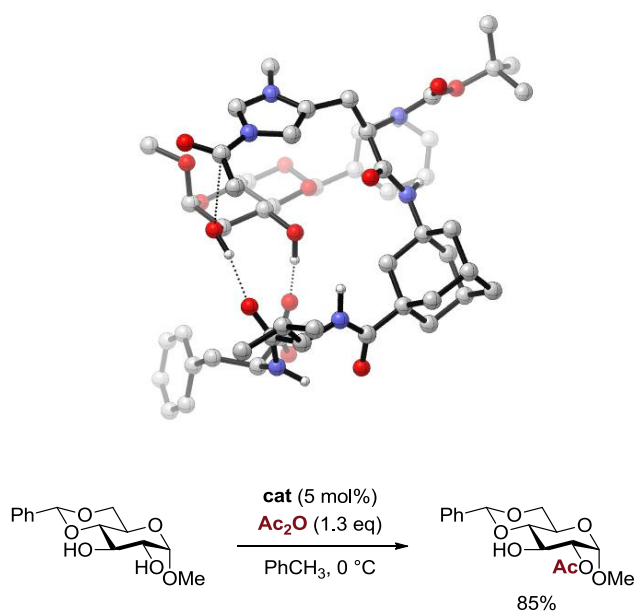
Acknowledgements

The authors acknowledge the generous funding from the Deutsche Forschungsgemeinschaft (DFG) under the Priority Program on Organocatalysis (SPP 1179).

– Chapter V –

Towards the Multicatalytic Synthesis of 2-Deoxygalactosides: Peptide-Catalyzed Regioselective Acetylation of Carbohydrates

Unpublished results

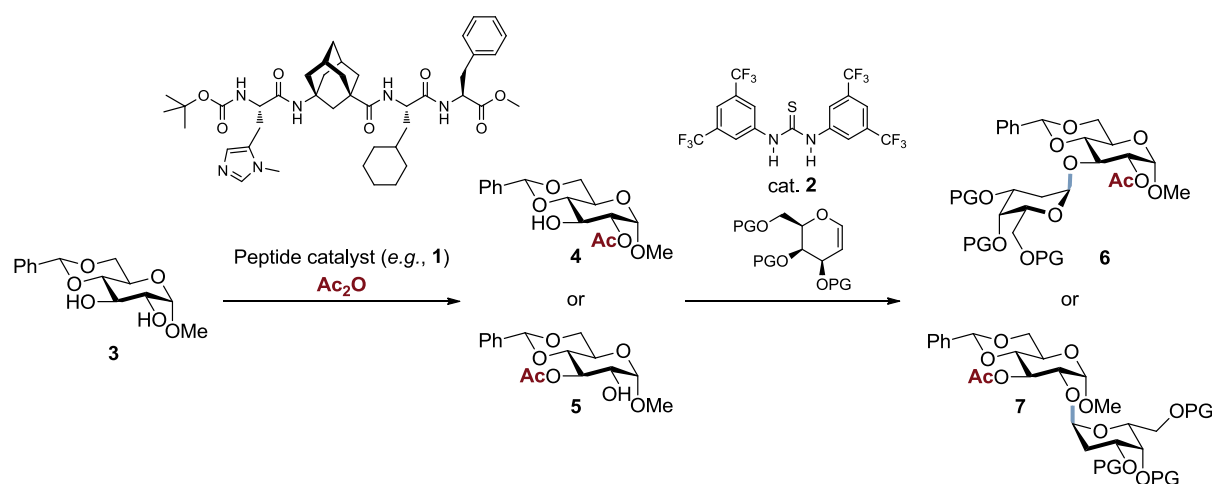


1. Introduction

Oligosaccharides and glycoconjugates play a crucial role in manifold biological processes.^[1] Consequently, a lot of effort has been devoted to the development of efficient strategies for the synthesis of these important biomolecules and their use, *e.g.*, as components of drugs or vaccines.^[2] Although numerous advances have been made in the field of carbohydrate chemistry over the last years, the preparation of well-defined oligosaccharides is still a formidable challenge that often requires demanding protecting group manipulations. An intriguing approach for the synthesis of carbohydrates relies on the catalytic, regioselective protection of particular hydroxyl groups on the monosaccharide building blocks whereas the others remain untouched.^[2m,q] The partially protected compounds are synthetically highly useful for subsequent steps, for example glycosidic bond formations.^[2]

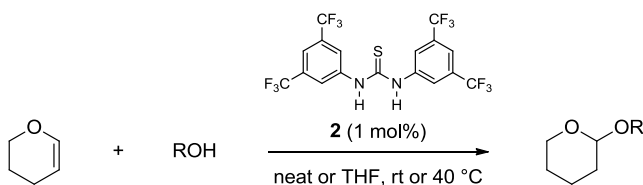
The reactivity trends observed for the different hydroxyl groups in monosaccharides generally result from electronic effects that are governed by intramolecular hydrogen bonding networks and sterics, also depending on the protecting groups present, as well as reactants and solvents used.^[3] Hence, various methods were developed to overcome the inherent reactivity and to address the desired hydroxyl groups.^[2m,q] Recently, organocatalytic variants were reported to provide superior regioselectivities in the acylation of carbohydrates and related polyols.^[4]

As part of our research on mult catalysis^[5] we envisioned to develop a synthetic strategy combining two of our privileged catalysts, an oligopeptide such as **1** and thiourea catalyst **2**, for the regioselective acetylation of carbohydrate derivatives and a concomitant glycosylation (Scheme 1). Indeed, both catalysts already showcased their extraordinary performance individually in similar reactions. Peptide catalyst **1** was previously used by our group in the

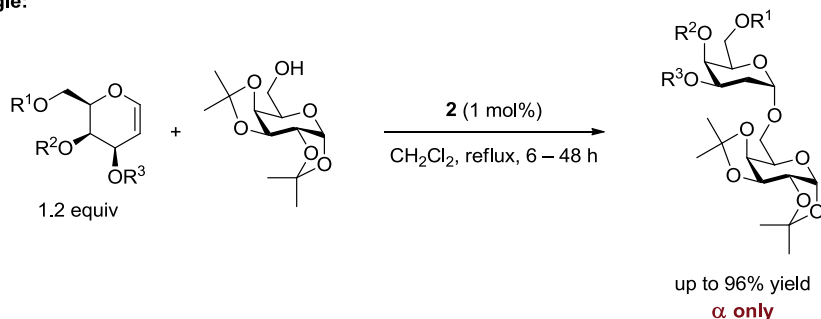


Scheme 1. Envisaged mult catalytic reaction sequence towards carbohydrate derivatives; PG = protecting group.

Schreiner:



McGarrigle:

**Scheme 2.** Previously reported reactions catalyzed by thiourea **2**.

kinetic resolution as well as the desymmetrization of, *e.g.*, *trans*- and *cis*-cycloalkane-1,2-diols, providing high enantioselectivities and exhibiting extraordinary chemoselectivities.^[6] Furthermore, the same catalyst and derivatives thereof were already successfully applied in multicatalytic reactions, *e.g.*, in combination with TEMPO as oxidation catalyst, and as multicatalysts, bearing two independent catalytic moieties (*cf.* previous chapters).^[7]

Since its development by Wittkopp and Schreiner,^[8] thiourea catalyst **2** has proven its efficiency in a plethora of reactions,^[9] one of the earliest examples being the tetrahydro-pyranlation of alcohols (Scheme 2).^[10] This concept was later extended by the McGarrigle group for the glycosylation of galactals with a variety of glycosyl acceptors with **2** as catalyst to afford the corresponding 2-deoxygalactosides in high yields exclusively as the α -epimer (Scheme 2).^[9d] Importantly, the reaction could be performed also with substrates comparable to **4** and **5** (benzyl instead of acetyl). More recently, the cooperative combination of **2** with Brønsted acids^[11] was reported by Schmidt *et al.* for glycosidation reactions of *O*-glycosyl trichloroacetimidates.^[9g] Furthermore, the same group applied **2** for the regioselective 4,6-*O*-arylideneation of methyl glucopyranosides,^[9f] highlighting the versatility of this organocatalyst in carbohydrate chemistry.

An extension of the aforementioned reactions, such as the addition of a regioselective acylation step, may meet the demands for an efficient multicatalytic synthesis of distinct carbohydrate derivatives (Scheme 1).

2. Results and Discussion

A publication by Miller *et al.* was of special interest in the context of peptide catalyzed regioselective acylation of carbohydrate diols (Figure 1).^[4a] The authors screened a library of 150 peptides for the acylation of aminosugar derivative **11** and compared the results to a reaction performed with *N*-methylimidazole (NMI). Importantly, most of the catalysts led to an amplification of the acetylation of the 3-hydroxyl group with the best working catalyst being **8**, affording 97% of **11** of total diacetylated products. However, only very few peptides were able to overcome the inherent reactivity of the substrate, thus to shift the product distribution towards **12**. Catalyst **9** provided a near 1:1 ratio of the monoacetylated products.

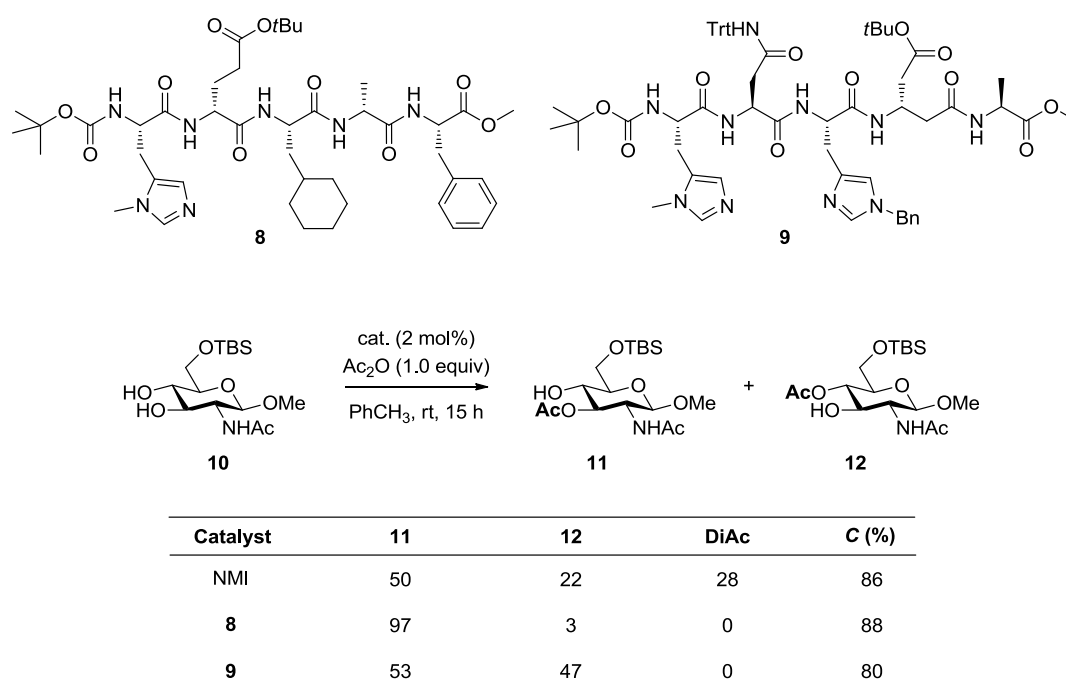


Figure 1. Peptide catalyzed regioselective acetylation of carbohydrate diols reported by Miller *et al.*; see: Ref. 4a. Trt = trityl; TBS = *tert*-butyldimethylsilyl; NMI = *N*-methylimidazole; DiAc = diacetylated product (not shown).

We started our own work on the acetylation of carbohydrates using methyl 4,6-*O*-benzylidene- α -D-glucopyranoside (**3**) (glucose is one of the most abundant mono-saccharides) as starting material, which was synthesized in the McGarrigle group. Thus, we first prepared the possible products to establish an appropriate analytical method for determining the outcome of the catalytic experiments. Using 4-dimethylaminopyridine (DMAP) as catalyst and acetic anhydride, the monoacetylated derivatives **4** and **5** (12% and 40%, respectively) as well as the diacetylate **13** (40%) were obtained (Figure 2). As the acetyl-CH₃ and benzylidene-*H* singlets separated well enough to allow an unambiguous determination we chose to perform ¹H NMR measurements on the crude reaction mixture to determine product ratios and conversion (Figure 2).

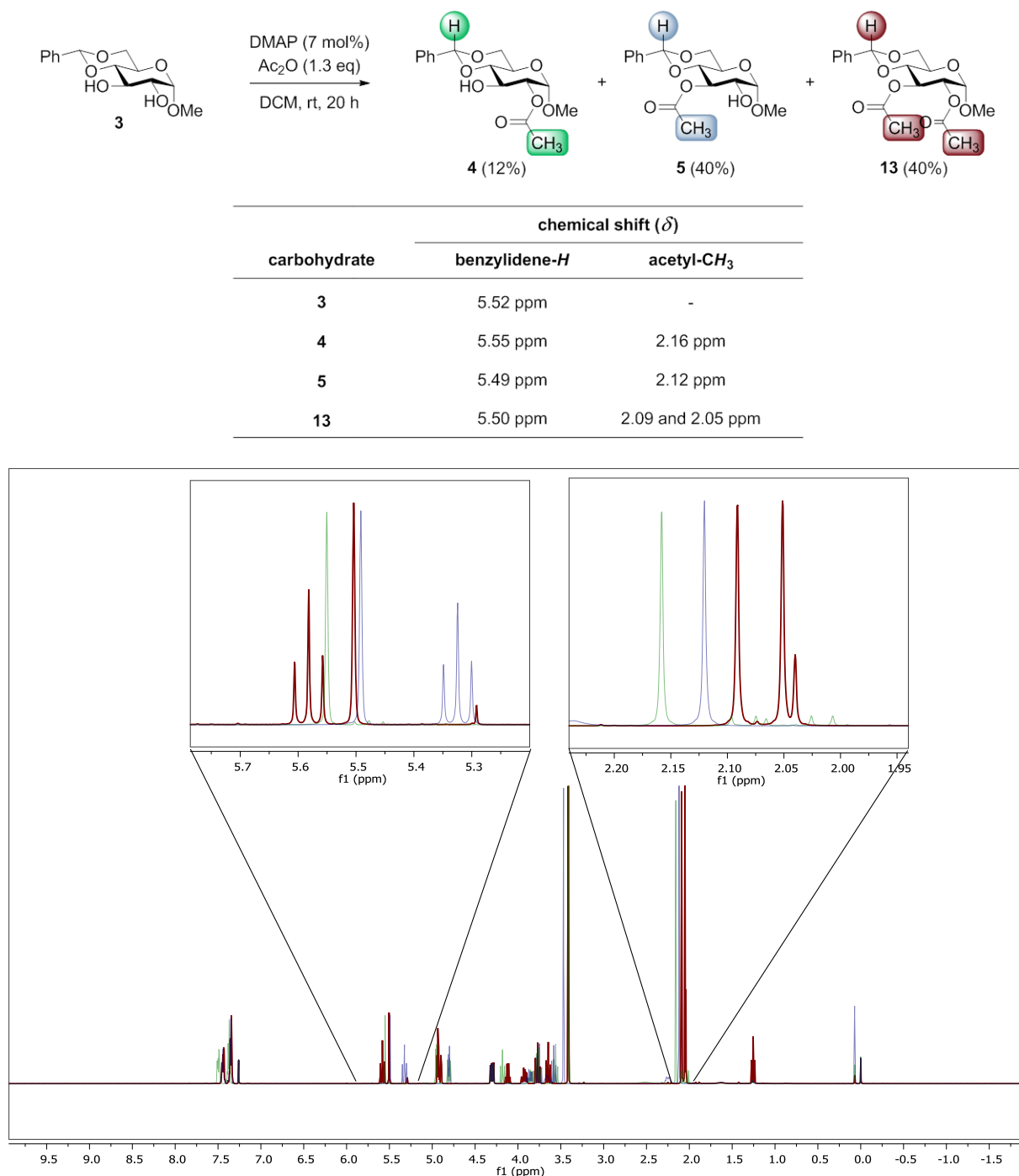


Figure 2. Top: DMAP catalyzed acetylation of **3** and selected ¹H NMR chemical shifts for the determination of conversion and selectivity. Yields are given for isolated products after column chromatography. Bottom: Superimposed ¹H NMR spectra of the isolated acetylated products **4** (green), **5** (blue), and **13** (dark red).

We then employed our peptide catalysts under reaction conditions comparable to those reported by Miller and coworkers.^[4a] According to the literature procedure NMI was used as reference catalyst to establish the intrinsic reactivity of the substrate under Lewis base catalysis. Thus, subjecting **3** to acetylation with NMI, the corresponding products were formed in a ratio of 23:71 (**4/5**) with good overall conversion (87%) and only a little diacetylation (Table 1, entry 1). Performing the reaction with peptide **1** (5 mol%; 1.3 equiv acetic anhydride), the ratio of the

products shifted to **4** being the major product although total conversion was low (64:36, 30% conversion; Table 1, entry 2). However, the low conversion is not surprising in this case as the configuration of the hydroxyl groups is that of the slow reacting enantiomer of the previously used cycloalkane-1,2-diols.^[6a,d] Thus, using the corresponding all-D-configured peptide **ent-1** led to overall good conversion with comparable selectivity (entry 3). Interestingly, catalysts **14** and **15** as well as **16–18** with the catalytically active π -methyl histidine (Pmh) located at the C-terminal end all showed a comparable preference to acetylate the 2-hydroxyl group and only differed in their reactivity (entries 4–8). This somehow indicates that the selectivities towards **4** may result from steric hindrance of the 3-hydroxyl group by the adjacent benzylidene protecting group. When **19**, bearing D-valine, was used as catalyst overall conversion increased to 82%, whereby regioselectivity was again comparable to the previous experiments (entry 9). Catalyst **20** bearing tryptophan that may allow for additional hydrogen bonding and CH- π interactions with the carbohydrate was studied next. Indeed, this amino acid is frequently used in highly selective carbohydrate acylation catalysts.^[4c,d,f] Moreover, two tryptophan units are part of the substrate-recognition site of a family of β -glucosidases.^[12] However, no beneficial effects were observed upon incorporation of tryptophan in our catalyst design (entry 10). With peptide-thiourea hybrid **21** conversion was high, but a 1:1 ratio of the monoacetylated products formed, indicating the possibility of the thiourea moiety to activate the anhydride and as a result to enhance 3-hydroxyl acetylation and consecutive diacetylation (entry 11). As the carbohydrate starting material already is a chiral substrate, we next investigated the possibility of stereochemical match-mismatch cases of catalyst and substrate. To study this effect, we used peptides **22** (all amino acids L-configured), **23** (D-valine), **24** (D-Pmh) and **25** (D-Pmh and D-valine). Although the first three catalysts only gave low conversion, the selectivity towards **4** could be significantly improved with peptide **24** (Table 1, entry 14), leading to high regioselectivity (**4/5** 86:14, 18% conversion). An extraordinary preference for the 2-hydroxyl group was also observed with catalyst **25** (73%) with full conversion of the starting material.

Remarkably, nearly all of our tested catalysts showed a significant deviation from the reaction with NMI, preferentially leading to acetylation of the 2-hydroxyl group in **3**. This is in sharp contrast to the results reported by Miller *et al.* (Scheme 2) where the best catalyst mutually enhanced the selectivity observed with NMI.^[4a] Additionally, this is a prime example wherein one of our hetero-configured catalysts performed better compared to the homo-configured analogue.

As a result of the low reactivity with most of the catalysts our attention then turned to an optimization of the reaction conditions with regard to increase conversion. Due to the small amounts of **24** available at that stage, **1** was mainly used as catalyst in the following experiments (Table 2). Increasing the amount of acetic anhydride (Table 2, entry 1) the conversion

Table 1. Preliminary catalyst screening experiments.

Entry	Catalyst	4 (%)	5 (%)	13 (%)	C (%)
1	NMI ^d	23	71	5	87
2		64	36	—	30
3	<i>ent</i> -1	61	35	4	95
4		61	35	4	72
5		65	32	3	54

Table 1. Preliminary catalyst screening experiments (continued).

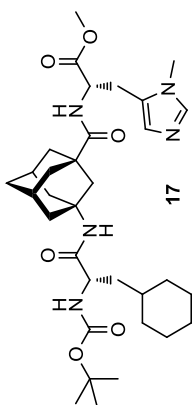
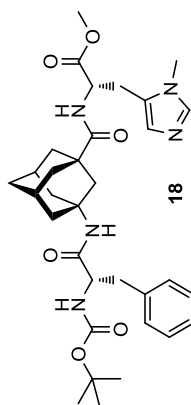
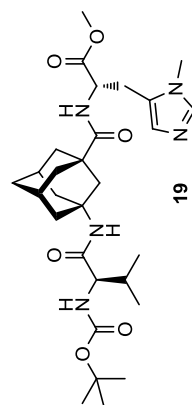
6		68	29	3	63
7		64	33	3	45
8		62	35	3	33
9		65	32	3	82

Table 1. Preliminary catalyst screening experiments (continued).

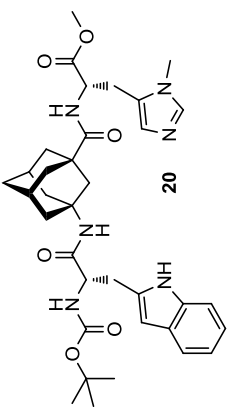
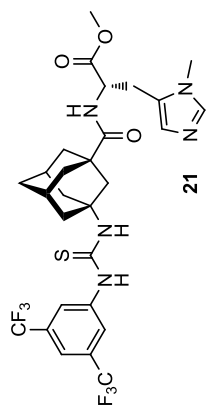
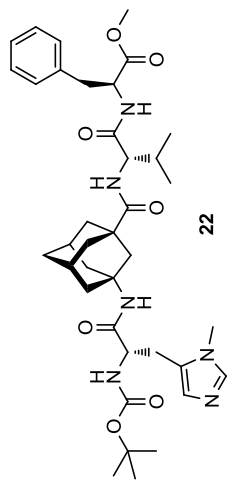
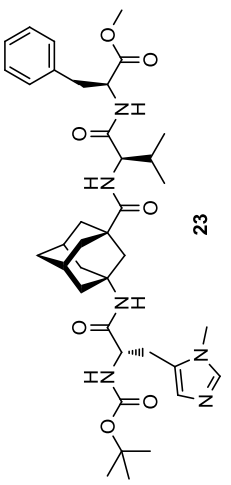
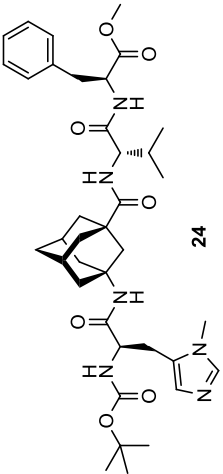
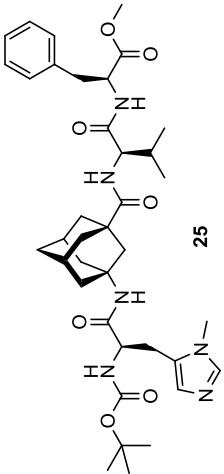
10		53	44	3	54
11		47	47	6	94
12		58	42	–	13
13		56	44	–	23

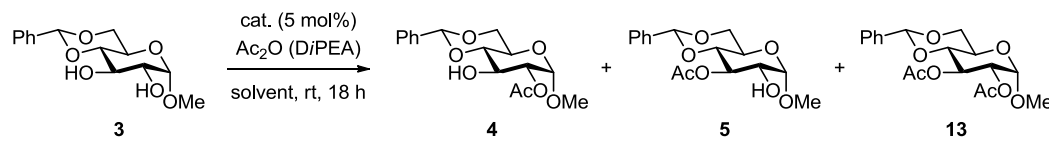
Table 1. Preliminary catalyst screening experiments (continued).

14		86	14	—	18
15 ^b		73	16	11	>95

Reactions were performed on 0.1 mmol scale with 5 mol% of catalyst and 1.3 equiv acetic anhydride in 10 mL of dry toluene at room temperature under N₂ for 18 h unless noted otherwise. Product distribution and conversion was determined by ¹H NMR after quenching the reaction with MeOH and evaporation of the solvent. ^a 10 mol% of catalyst were used; ^b Commercially available methyl 4,6-*O*-benzylidene- α -D-glucopyranoside (3) was used as starting material.

to 63% was improved thereby maintaining the previously observed regioselectivity (*cf.* Table 1, entry 2). The addition of a base (such as DiPEA) further enhanced reactivity and led to complete conversion, but had a deleterious effect on selectivity (entry 2). As a result of the low solubility of **3** in nonpolar solvents such as toluene, the substrate usually only completely dissolved upon acetylation. However, using a solution of substrate and catalyst in dichloromethane (entry 3) and dilution with toluene only slightly improved the previously observed conversion (30% *vs.* 38%; *cf.* Table 1, entry 2). As expected, more polar solvents, such as dichloromethane, acetonitrile (ACN), or tetrahydrofuran led to inferior selectivities, possibly due to perturbation of crucial hydrogen bonding-interactions of catalyst with substrate, and to variable conversions (entries 4–6). A similar effect on differing reactivity of carbohydrates in dichloromethane and tetrahydrofuran has also been observed previously.^[13] As the only encouraging modification of the standard conditions was the use of higher amounts of acetic anhydride, the same reaction was performed using the best working catalyst **24**. To our delight, under these conditions overall conversion increased to 88%, with a product ratio of 86:9:5 for **4/5/13** (entry 7).

Table 2. Screening experiments to improve conversion.

						
Entry	Catalyst	Variation	4 (%)	5 (%)	13 (%)	C (%)
1	1	5.3 equiv Ac ₂ O	60	37	3	63
2	1	5.3 equiv Ac ₂ O + 2.9 equiv DiPEA	49	37	14	>95
3 ^a	1	DCM/PhCH ₃ (9:1)	60	37	3	38
4 ^a	1	DCM	41	42	16	79
5 ^a	1	ACN	48	34	18	38
6 ^a	1	THF	54	46	–	10
7	24	5.3 equiv Ac ₂ O	86	9	5	88
8 ^b	24	5.3 equiv Ac ₂ O, 0 °C	32	9	59	>95
9 ^b	24	1.3 equiv Ac ₂ O, 0 °C	85	9	6	>95

Reactions were performed on a 0.1 mmol scale with 5 mol% of catalyst in 10 mL of dry solvent at room temperature under N₂ for 18 h. Product distribution and conversion was determined by ¹H NMR after quenching the reaction with MeOH and evaporation of the solvent. ^a Reaction was performed with 1.3 equiv acetic anhydride.

^b Commercially available methyl 4,6-*O*-benzylidene-α-D-glucopyranoside (**3**) was used as starting material.

In an attempt to further improve regioselectivity the reaction temperature was lowered to 0 °C. Unexpectedly, a reaction using commercially available **3** and 5.3 equivalents of anhydride led to excellent conversion, but diacetyl derivative **13** was the major product (entry 8). Lowering the amount of anhydride provided both complete conversion of the starting material and high regioselectivity (85:9:6 for **4/5/13**; entry 9 and Figure 3). This effect can be seen in Table 1 as well (entry 15) although a conclusive interpretation was not possible before. It appeared that the previously used starting material was contaminated with small amounts of benzaldehyde (or consequently benzoic acid) from the protection step that somehow hampered efficient catalysis. However, the selectivities observed with the different catalysts (Table 1) are indeed reliable and only the conversion was affected (*vide supra*).

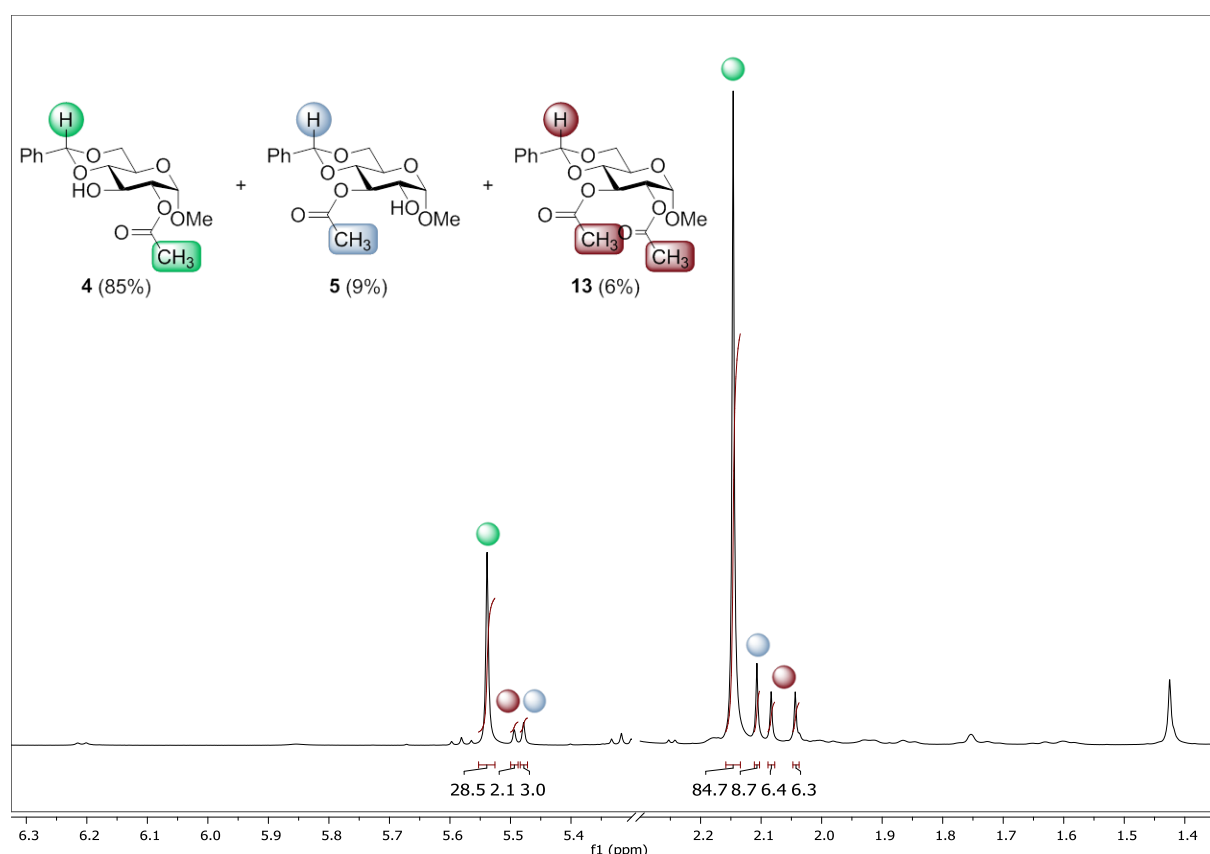
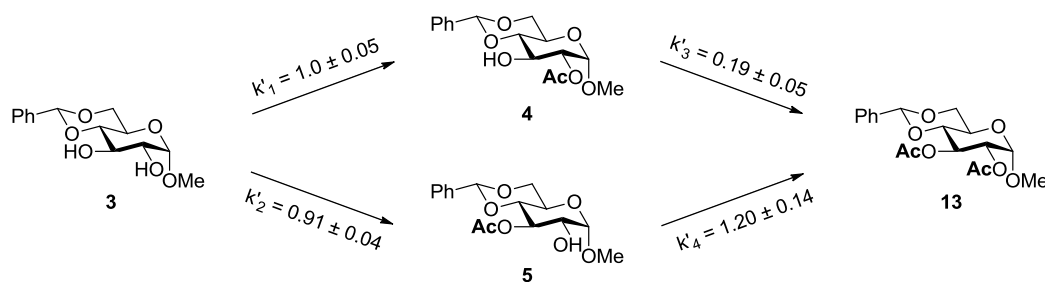


Figure 3. Selected sections of the ¹H NMR spectrum for the determination of the regioselectivity achieved with peptide **24**; cf. Table 2, entry 9. No starting material (δ (benzylidene-*H*) = 5.52 ppm) could be detected.

Another important feature becomes obvious from the aforementioned results. The major product **4** is consumed to form **13** whereas the amount of **5** stays constant, although kinetic studies previously revealed that over-acylation of **5** occurs approximately six times faster compared to **4** (Scheme 3).^[3b]



Scheme 3. Relative reaction rates for the acetylation of methyl 4,6-*O*-benzylidene- α -D-glucopyranoside (**3**) with pyridine and acetic anhydride.

We also envisioned using the corresponding glucopyranoside bearing a cyclohexylidene moiety for additional dispersion interactions that may further enhance selectivity. However, this protecting group was rather unstable (see the Experimental Part) and, therefore, this substrate was not investigated in catalytic experiments.

In comparison to other reported procedures for the regioselective acetylation of methyl 4,6-*O*-benzylidene- α -D-glucopyranoside (**3**) our catalyst performs remarkably well (Table 3). Thus, under typical acylation conditions with pyridine the ratio of the possible products significantly differs depending on the reaction conditions employed. Notably, no high regioselectivity was achieved and considerable quantities of **13** form (Table 3, entry 2)^[14] akin to the intrinsic reactivity of the substrate (*cf.* Scheme 3). The same holds true for the DMAP-catalyzed acetylation of **3** (entry 3).^[13] Another simple procedure for the acylation of various D-glucopyranosides was reported by Hung and co-workers.^[15] An excess of triethylamine and anhydride regioselectively provided the 2-acylated products, such as **4** (80%; entry 4), though the reaction conditions may not be negotiable to other monosaccharides. No regioselectivity (48:52, **4/5**) could be achieved using a trans-esterification protocol with sodium *tert*-butoxide and ethyl acetate as acyl-equivalent (entry 5), despite no diacetylated **13** did form.^[16]

The formation of metal-chelates with carbohydrates represents another common means for selective hydroxyl functionalization. Thus, zinc, mercury, and copper, as representative examples, were previously used to push the reaction towards a desired mono-acetylated product with divergent regioselectivities (entries 6–8).^[14b,17]

Recently, Allen and Miller reported a catalyst-controlled regioselective functionalization of carbohydrate derivatives (Table 3, entries 9–12).^[18] Employing copper-bis(oxazoline) catalysts afforded the products with moderate to good ratios. Importantly, the outcome of the reaction was highly dependent on the electrophile used (acetic anhydride *vs.* acetyl chloride).^[3e] A silver(I) oxide promoted acetylation of **3** gave mainly **5** (entry 13).^[19]

Table 3. Comparison of the performance of peptide **24** with selected literature procedures for the regioselective acetylation of **3**.

Entry	Reagents or Catalysts	4 (%)	5 (%)	13 (%)	C (%)
1	24	85	9	6	>95
2	pyridine ^[14]	3–29	32–42	6–26	77–93
3	cat. DMAP ^[13]	45–49	55–51	–	40–65
4	Et ₃ N ^[15]	80	5 ^b	15 ^b	–
5	NaOtBu, EtOAc ^[16]	48	52	–	76
6	ZnCl ₂ , pyridine ^[14b]	53	13	23	90
7	HgCl ₂ ^[17]	82	–	18	–
8	CuCl ₂ ^[17]	15	80	5	–
9	CuCl ₂ , (R)–PhBOX ^[18]	1.8 ^a	1.0 ^a	–	69
10	CuCl ₂ , (S)–PhBOX ^[18]	1.6 ^a	1.0 ^a	–	75
11	CuCl ₂ , (R)–PhBOX, AcCl ^[18]	74 (7.0)	(1.0) ^a	–	91
12	CuCl ₂ , (S)–PhBOX, AcCl ^[18]	(1.0) ^a	41 (4.5)	–	79
13	Ag ₂ O, KI, AcCl ^[19]	15	81	–	–
14	cat. TBAOAc, Me ₂ Si(OMe) ₂ ^[20]	65	–	–	–
15	cat. TBAOAc ^[21]	88	–	–	–
16	lipase, vinyl acetate ^[22]	up to 100	–	–	up to 94

Unless otherwise noted acetic anhydride was used as electrophile. BOX = bis(oxazoline); TBAOAc = tetrabutylammonium acetate. For entries with a dash either no compound formed or no data was available.

^a Only the ratio of the products was reported. ^b Values were obtained from reproducing the reaction under the conditions described in ref. 15.

An alternative procedure was described that proceeds through the formation of cyclic dioxasilolane intermediates and subsequent tetrabutylammonium acetate catalyzed acylation (Table 3, entry 14), but the observed regioselectivities were under substrate-control depending on the carbohydrate used.^[20] However, the same group later reported that tetrabutylammonium acetate alone may act as hydrogen-bonding catalyst to provide high regio-selectivities (88% for **4**; entry 15).^[21]

Unsurprisingly, enzymes, *e.g.*, various lipases, were used to catalyze the parent reaction affording **4** with perfect selectivity (entry 16).^[22] The choice of the enzyme also allowed to reverse the regioselectivity to give **5** (not shown). Careful investigation of the data in Table 3

reveals the astonishing performance of catalyst **24** (entry 1) that competes with the reported procedures to selectively obtain **4**. Although the aforementioned enzymes achieve higher selectivities the conversion is not complete in these cases (up to 85%),^[22] resulting in the same yield of desired product as with **24**. Furthermore, a judicious modification of the peptide-catalysts in principle may allow addressing every desired hydroxyl group in a given carbohydrate. Besides acetylation reactions, alternative procedures were reported that also afford **4**, such as the acetyl-migration employing **5**^[23] or the regioselective deacetylation of **13**,^[24] however, the selectivities do not compete with the values obtained with **24**.

To gain a deeper insight why the change in the configuration of the catalytically active Pmh has this significant influence on selectivity, we performed a molecular dynamics search for low-lying conformations for adducts of the acylium ions of **22–24** with **3** (Figure 4) utilizing the Merck Molecular Force Field (MMFF).^[25] Although this can be only considered as a first computational

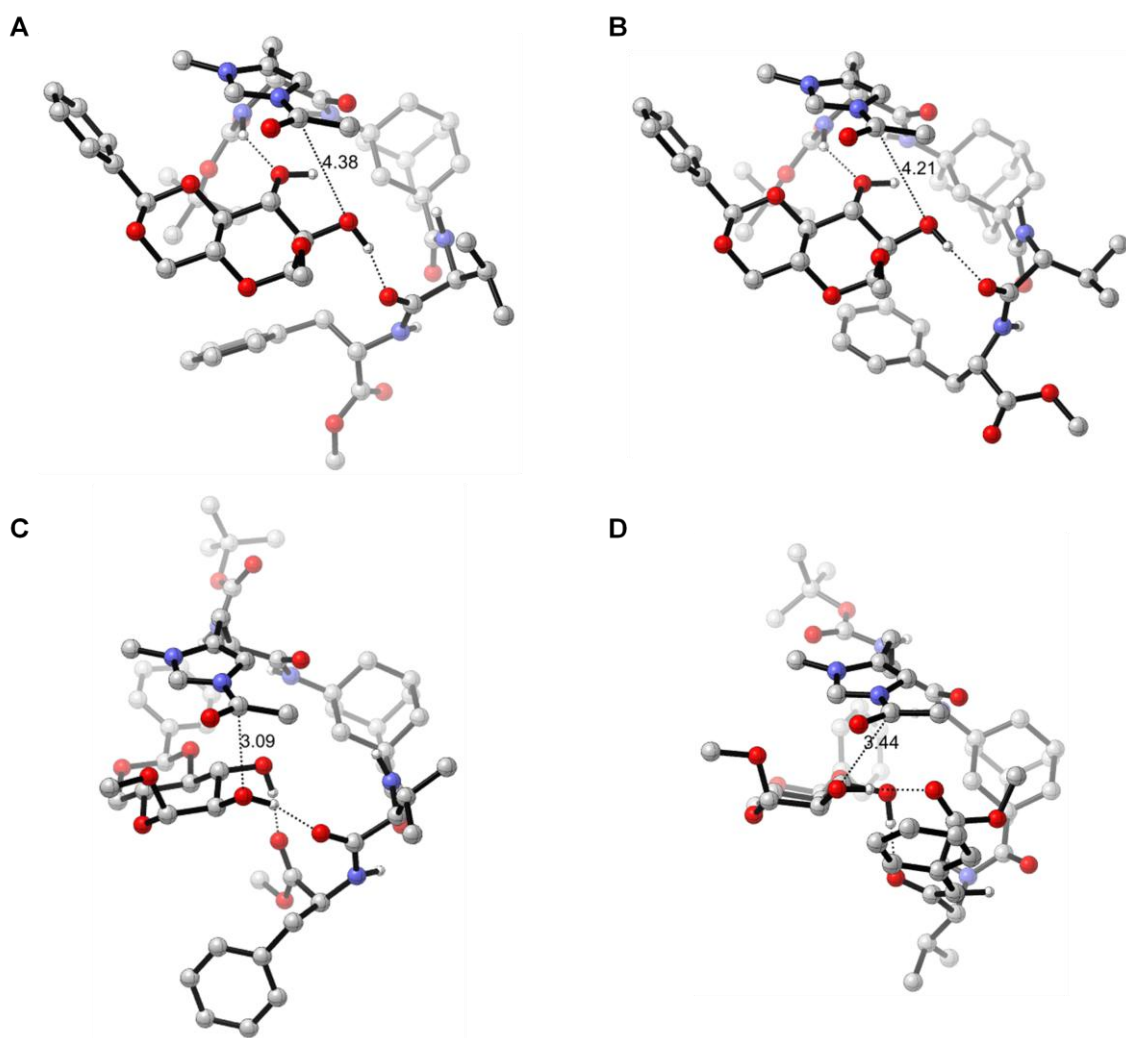
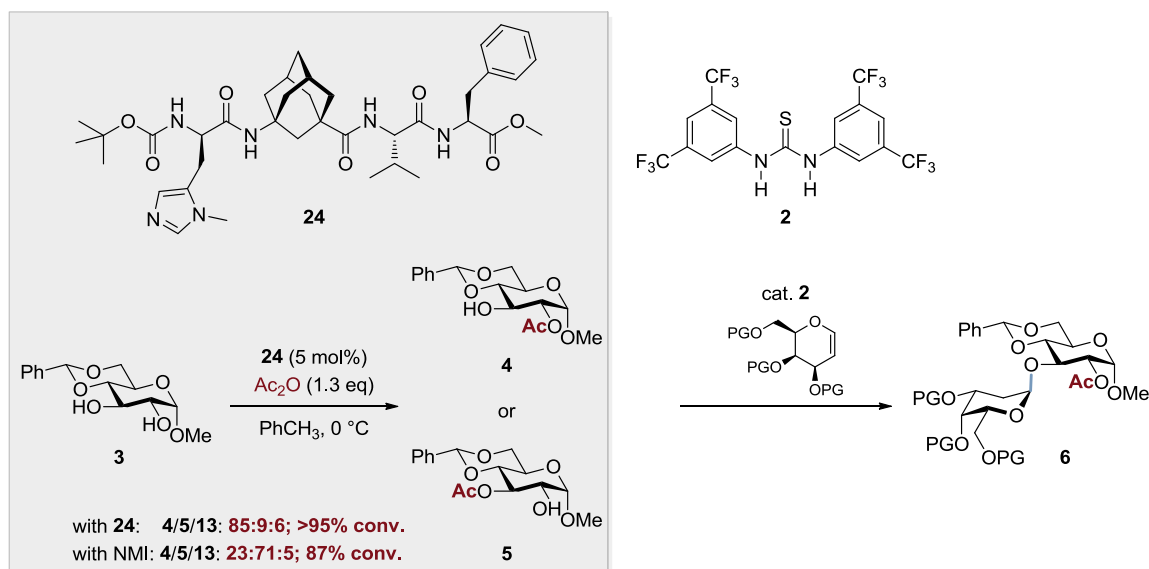


Figure 4. Lowest-lying conformations for hydrogen-bonded adducts of the acylium ions of oligopeptides **22** (A), **23** (B), **24** (C), and **25** (D) with carbohydrate **3**. All C–H have been omitted for clarity; C = gray, O = red, N = blue, H = white. Distances are given in Å.

approximation the results should be qualitatively valid as the reaction is performed in a nonpolar solvent. From the ensemble of obtained conformers the energetically lowest-lying adduct was chosen for each catalyst wherein **3** is suitably arranged for acetylation to take place. Apparently, some important features become obvious. Firstly, the rigid γ -amino adamantane carboxylic acid^[26] leads to a structurally less flexible oligopeptide and enables the formation of a catalytically active “dynamic pocket” for all four catalysts, as was already shown in our previous studies.^[6a,d] Secondly, hydrogen bonding (among other possible interactions) plays an important role for substrate recognition and fixation. Most importantly, the determined interatomic distances between the acylium ions and the distinct hydroxyl groups remarkably well correlate with the experimentally observed selectivities. Both the 2- and 3-hydroxyl groups in **3** show comparable distances, 4.4 vs. 4.3 Å and 4.2 vs. 4.3 Å, respectively, to the acylium ions of **22** and **23**, resulting in low selectivities (Figure 4, A and B). Contrary, the 2-hydroxyl group is in close proximity to the acylium ions of **24** (3.1 Å) and **25** (3.4 Å; Figure 4 C and D), whereas the 3-hydroxyl group is placed much further away (4.5 Å and 5.0 Å; also see Experimental Part). However, more accurate computations are still necessary to provide a more detailed picture of the substrate recognition process and enhanced selectivity of oligopeptide **24**.^[6d]

3. Conclusions and Outlook

In conclusion, we identified **24** as a potential catalyst for the first part of our proposed multicatalytic one-pot reaction (Scheme 5). In comparison to NMI, which preferentially leads to the acetylation of the 3-hydroxyl group on **3** (**4/5/13**: 23:71:5; 87% conversion), **24** mostly gives the 2-acetylated product (**4/5/13**: 85:9:6; >95% conversion), thus not only overcomes, but reverses the intrinsic reactivity of the substrate. These promising results will provide the basis for further developments.



Scheme 5. Proposed multicatalytic one-pot reaction sequence and results obtained so far.

Our future work aims at the application of other (partially protected) carbohydrate diols (*e.g.*, mannose and galactose derivatives or isosorbide) to develop a broadly applicable reaction. This will necessitate the synthesis of additional catalysts that may also provide information on the influence of the other amino acids, valine and phenylalanine, in **24**. As the factors determining the selectivity are yet not fully understood, these questions will be tackled by computational investigations of catalyst–substrate interactions and the corresponding transition states for the acylation process. The ultimate goal of our investigation is to merge the regioselective protection of the carbohydrate derivatives with a concurrent glycosylation step to give well-defined 2-deoxygalactosides **6**.

4. Experimental Part

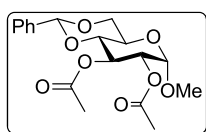
Materials and methods. Unless otherwise specified, reagents were purchased from commercial suppliers at the highest purity grade available and were used as received. All solvents were distilled prior to use. Dry and absolute solvents were prepared using standard laboratory procedures and were stored over appropriate drying agents under argon or nitrogen atmosphere. Acetic anhydride was distilled and stored under argon or nitrogen with 4 Å molecular sieves.

Flash column chromatography was performed using MN silica gel 60 M (Macherey-Nagel; 0.040 – 0.063 mm, 230 – 400 mesh ASTM). Analytical thin-layer chromatography (TLC) was performed using precoated polyester sheets Polygram[®] SIL G/UV₂₅₄ (Macherey-Nagel; 0.2 mm silica gel layer with fluorescent indicator). Visualization of the developed chromatograms was accomplished by irradiation with a UV lamp at 254 nm and/or phosphomolybdic acid solution, 2,4-dinitrophenylhydrazine solution or potassium permanganate solution, respectively. TLC R_f values are reported.

Instrumentation. NMR spectra were recorded on Bruker Avance II 200 MHz „Microbay“, Avance II 400 MHz, Varian 300 MHz and Varian 400 MHz, Avance III HD 400 MHz, or Avance III HD 600 MHz spectrometers, respectively, at 298 K. Chemical shifts (δ) are given in ppm relative to tetramethylsilane (TMS, δ = 0.00 ppm) as the internal standard or to the respective solvent residual peaks (CDCl₃: δ = 7.26 and 77.16 ppm; DMSO- d_6 : δ = 2.50 and 39.52 ppm; D₂O: δ = 4.79 ppm; MeOH- d_4 : δ = 3.31 and 49.00 ppm).^[27] Data are reported as follows: chemical shift, multiplicity (s = singlet, d = doublet, t = triplet, q = quartet, m = multiplet, br = broad, or combinations thereof), coupling constants (Hz), integration. Infrared spectra were acquired on a Bruker IFS25 spectrometer. ESI mass spectrometry was performed employing a Finnigan LCQDuo spectrometer using methanol solutions of the respective compounds. High resolution mass spectrometry (HRMS) was performed employing a Thermo Scientific LTQ FT Ultra spectrometer (ESI) using methanol solutions of the respective compounds or a Finnigan MAT95 sectorfield spectrometer (EI). Elemental analysis was performed on a Thermo Flash EA 1112.

4.1 Synthesis of Mono- and Diacetylated Carbohydrate Derivatives for Elucidation of Product Distribution and Conversion

The synthesis is exemplarily given by the following experimental protocol: To a solution of methyl 4,6-*O*-benzylidene- α -D-glucopyranoside (**3**; 298.2 mg, 1.06 mmol) in dry CH_2Cl_2 (10 mL) was added DMAP (8.5 mg, 7 mol%) and acetic anhydride (130.6 μL , 140.7 mg, 1.38 mmol) and the resulting solution was stirred at rt for 20 h. The reaction was quenched by addition of MeOH (2 mL) and stirring was continued for further 30 min. All volatiles were removed *in vacuo* and the reaction products were separated and purified by column chromatography eluting with EtOAc/cyclohexane (1:1).



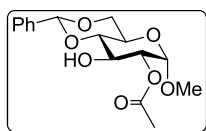
Methyl 2,3-di-*O*-acetyl-4,6-*O*-benzylidene- α -D-glucopyranoside (13**).**

Yield: 166.4 mg (0.45 mmol, 43%) as colorless solid. TLC (EtOAc/cyclohexane 1:1): R_f = 0.50.

^1H NMR (400 MHz, CDCl_3): δ = 7.46 – 7.42 (m, 2H), 7.37 – 7.32 (m, 3H), 5.58 (t, J = 9.7 Hz, 1H), 5.50 (s, 1H), 4.93 (t, J = 4.0 Hz, 1H), 4.91 (dd, J = 9.7, 3.8 Hz, 1H), 4.30 (dd, J = 10.2, 4.8 Hz, 1H), 3.93 (td, J = 9.9, 4.8 Hz, 1H), 3.77 (t, J = 10.3 Hz, 1H), 3.65 (t, J = 9.6 Hz, 1H), 3.41 (s, 3H), 2.09 (s, 3H), 2.05 (s, 3H) ppm.

^{13}C NMR (100 MHz, CDCl_3): δ = 170.5, 169.9, 137.1, 129.2, 128.4, 126.3, 101.7, 97.8, 79.4, 71.7, 69.1, 69.0, 62.5, 55.5, 21.0, 20.9 ppm.

The NMR data are in accordance with those reported previously.^[28]



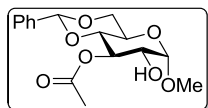
Methyl 2-*O*-acetyl-4,6-*O*-benzylidene- α -D-glucopyranoside (4**).**

Yield: 42.3 mg (0.13 mmol, 12%) as colorless solid. TLC (EtOAc/cyclohexane 1:1): R_f = 0.39.

^1H NMR (400 MHz, CDCl_3): δ = 7.52 – 7.47 (m, 2H), 7.40 – 7.35 (m, 3H), 5.55 (s, 1H), 4.95 (d, J = 3.8 Hz, 1H), 4.80 (dd, J = 9.7, 3.8 Hz, 1H), 4.30 (dd, J = 9.9, 4.5 Hz, 1H), 4.18 (t, J = 9.5 Hz, 1H), 3.85 (td, J = 9.6, 4.5 Hz, 1H), 3.76 (t, J = 10.2 Hz, 1H), 3.56 (t, J = 9.3 Hz, 1H), 3.40 (s, 3H), 2.52 (br s, 1H), 2.16 (s, 3H) ppm.

^{13}C NMR (100 MHz, CDCl_3): δ = 170.8, 137.1, 129.5, 128.5, 126.4, 102.2, 97.7, 81.5, 73.7, 69.0, 68.8, 62.1, 55.6, 21.1 ppm.

The NMR data are in accordance with those reported previously.^[18,20,29]



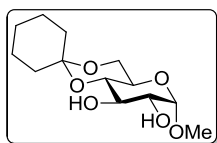
Methyl 3-*O*-acetyl-4,6-*O*-benzylidene- α -D-glucopyranoside (5**).**

Yield: 137.4 mg (0.42 mmol, 40%) as colorless solid. TLC (EtOAc/cyclohexane 1:1): R_f = 0.28.

^1H NMR (400 MHz, CDCl_3): δ = 7.47 – 7.42 (m, 2H), 7.38 – 7.33 (m, 3H), 5.49 (s, 1H), 5.32 (t, J = 9.7 Hz, 1H) 4.80 (d, J = 3.8 Hz, 1H), 4.30 (dd, J = 10.1, 4.7 Hz, 1H), 3.87 (td, J = 9.9, 4.7 Hz, 1H), 3.75 (t, J = 10.3 Hz, 1H), 3.70 – 3.63 (m, 1H), 3.58 (t, J = 9.6 Hz, 1H), 3.47 (s, 3H), 2.25 (br d, J = 11.1 Hz, 1H), 2.12 (s, 3H) ppm.

^{13}C NMR (100 MHz, CDCl_3): δ = 171.2, 137.2, 129.2, 128.4, 126.3, 101.7, 100.3, 78.8, 72.4, 72.0, 69.1, 62.9, 55.7, 21.2 ppm.

The NMR data are in accordance with those reported previously.^[18,29]



Methyl 4,6-*O*-cyclohexylidene- α -D-glucopyranoside (26**).** The substrate was provided by the group of E. M. McGarrigle and was used as received.

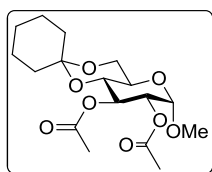
^1H NMR (400 MHz, CDCl_3): δ = 4.74 (d, J = 3.9 Hz, 1H), 3.84 (dd, J = 10.4, 5.2 Hz, 1H), 3.77 (t, J = 9.0 Hz, 1H), 3.73 (t, J = 10.3 Hz, 1H), 3.62 (dt, J = 10.2, 5.1 Hz, 1H), 3.59 – 3.50 (m, 2H), 3.41 (s, 3H), 2.55 (br s, 2H), 2.04 – 1.94 (m, 1H), 1.90 – 1.81 (m, 1H), 1.66 – 1.34 (m, 8H) ppm.

^{13}C NMR (100 MHz, CDCl_3): δ = 100.0, 99.9, 73.1, 72.7, 72.3, 63.5, 61.7, 55.5, 38.0, 27.9, 25.7, 22.9, 22.6 ppm.

The ^1H NMR data are in accordance with those reported previously.^[30]

The products obtained from acetylation of **26** were always contaminated with the corresponding 4,6-*O*-cyclohexylidene deprotected derivatives that formed upon removal of the solvent. Thus, an unequivocal assignment of NMR chemical shifts for the determination of conversion as well

as selectivity was not possible. As a consequence, this substrate was not used for catalytic experiments.



Methyl 2,3-di-O-acetyl-4,6-O-cyclohexylidene- α -D-glucopyranoside (27).

The compound was prepared using **26** on 1.0 mmol scale as described for **3**.

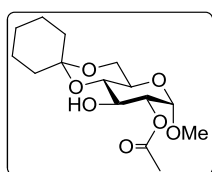
Yield: 116.1 mg (0.32 mmol, 32%) as colorless oil. TLC (EtOAc/hexanes 1:1): R_f = 0.63.

The obtained product was contaminated with the corresponding 4,6-O-cyclohexylidene deprotected derivative (~15% as judged by NMR). Multiplicities could not be assigned in some cases due to overlapping signals.

^1H NMR (400 MHz, CDCl_3): δ = 5.42 – 5.35 (m, 1H), 4.91 – 4.80 (m, 2H), 3.89 – 3.84 (m, 1H), 3.81 – 3.69 (m, 2H), 3.68 – 3.62 (m, 1H), 3.37 (s, 3H), 2.07 (s, 3H), 2.04 (s, 3H), 1.74 – 1.29 (m, 10H) ppm.

^{13}C NMR (100 MHz, CDCl_3): δ = 170.6, 170.0, 100.0, 97.8, 71.7, 71.5, 69.7, 63.5, 61.9, 55.4, 37.9, 27.7, 25.7, 22.9, 22.7, 20.9 ppm.

HRMS (ESI): m/z = 381.1522 $[\text{M}+\text{Na}]^+$ (calcd m/z = 381.1525)



Methyl 2-O-acetyl-4,6-O-cyclohexylidene- α -D-glucopyranoside (28).

The compound was prepared using **26** on 1.0 mmol scale as described for **3**.

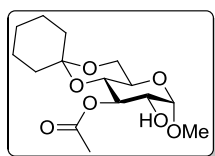
Yield: 63.2 mg (0.25 mmol, 25%) as colorless crystalline solid. TLC (EtOAc/hexanes 1:1): R_f = 0.39.

The obtained product was contaminated with the corresponding 4,6-O-cyclohexylidene deprotected derivative (~50% as judged by NMR). Multiplicities could not be assigned in some cases due to overlapping signals.

^1H NMR (400 MHz, CDCl_3): δ = 4.89 (d, J = 3.7 Hz, 1H), 4.76 (dd, J = 9.7, 3.8 Hz, 1H), 4.04 – 3.99 (m, 1H), 3.88 – 3.84 (m, 1H), 3.76 (t, J = 10.1 Hz, 1H), 3.66 – 3.57 (m, 3H), 3.36 (s, 3H), 2.64 (br s, 1H), 2.15 (s, 3H), 1.92 – 1.82 (m, 1H), 1.75 – 1.38 (m, 9H) ppm.

^{13}C NMR (100 MHz, CDCl_3): δ = 170.9, 100.2, 97.7, 73.8, 73.3, 69.3, 63.2, 61.7, 55.4, 38.1, 27.9, 25.7, 22.9, 22.7, 21.1 ppm.

HRMS (ESI): m/z = 339.1420 $[\text{M}+\text{Na}]^+$ (calcd m/z = 339.1420)



Methyl 3-*O*-acetyl-4,6-*O*-cyclohexylidene- α -D-glucopyranoside (29). The compound was prepared using **26** on 1.0 mmol scale as described for **3**. Yield: 79.1 mg (0.25 mmol, 25%) as colorless solid. TLC (EtOAc/hexanes 1:1): R_f = 0.31.

The obtained product was contaminated with the corresponding 4,6-*O*-cyclohexylidene deprotected derivative (~13% as judged by NMR). Multiplicities could not be assigned in some cases due to overlapping signals.

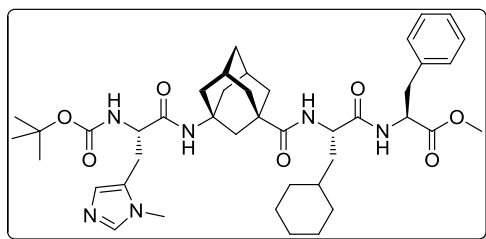
^1H NMR (400 MHz, CDCl_3): δ = 5.12 (t, J = 9.5 Hz, 1H), 4.75 (d, J = 3.8 Hz, 1H), 3.89 – 3.83 (m, 1H), 3.79 (t, J = 10.2 Hz, 1H), 3.71 – 3.63 (m, 1H), 3.62 – 3.57 (m, 2H), 3.42 (s, 3H), 2.35 (br s, 1H), 2.10 (s, 3H), 1.74 – 1.29 (m, 10H) ppm.

^{13}C NMR (100 MHz, CDCl_3): δ = 171.2, 100.2, 99.8, 73.0, 71.9, 70.8, 63.9, 61.9, 55.5, 38.0, 27.7, 25.7, 22.9, 22.6, 21.1 ppm.

HRMS (ESI): m/z = 339.1421 $[\text{M}+\text{Na}]^+$ (calcd m/z = 339.1420)

4.2 Availability of catalysts

Unless stated otherwise, the peptides were synthesized by standard HBTU/HOBt-mediated solid phase peptide synthesis (SPPS) employing fluorenylmethyloxycarbonyl (Fmoc) protected amino acids (see Chapter II for details) or by EDC/HOBt mediated peptide coupling in solution using the *N*-*tert*-butoxycarbonyl (Boc) protecting group strategy. A general procedure is given below for the synthesis of **1**. The partially protected aminoadamantanecarboxylic acid derivatives^[26] and the catalytically active Pmh^[31] were afforded by literature procedures.



Boc-L-Pmh-^AGly-L-Cha-L-Phe-OMe (1). *Coupling 1:* H-L-Phe-OMe • HCl (1.078 g, 5.00 mmol) and Boc-L-Cha-OH • DCHA (2.264 g, 5.00 mmol) were added to a round-bottom flask, along with 1-ethyl-3-(3-dimethylaminopropyl)carbodiimide hydrochloride (EDC • HCl; 1.054 g, 5.50 mmol) and 1-hydroxybenzotriazole

hydrate (HOBt • H₂O; 0.842 g, 5.5 mmol). CH₂Cl₂ (25 mL) was added, followed by Et₃N (0.77 mL, 0.559 g, 5.52 mmol), and the resulting suspension was stirred at rt for 24 h. The reaction mixture was diluted with EtOAc and subsequently washed with 0.5 M citric acid solution (3 × 50 mL), sat. aq. NaHCO₃ (3 × 50 mL) and brine (50 mL). The organic layer was dried over Na₂SO₄, filtered, and concentrated under reduced pressure to afford the crude peptide (2.124 g, 4.91 mmol, 98%) as colorless foam.

The peptides obtained using this procedure were usually sufficiently pure (as judged by NMR and/or ESI-MS) and were used for subsequent coupling steps without any purification.

Deprotection 1: The peptide fragment was treated with 4 M HCl in 1,4-dioxane (2 mL/mmol) and the resulting solution was stirred at rt for 45 min. The reaction flask was flushed with argon for 30 min to remove residual HCl and the solvent was removed under reduced pressure. After drying *in vacuo*, the resulting peptide hydrochloride was directly used for the next coupling step.

Coupling 2: The coupling of H-L-Cha-L-Phe-OMe • HCl and Boc-^AGly-OH was performed on 4.74 mmol scale according to the procedure described for coupling 1 (*vide supra*). Boc-^AGly-L-Cha-L-Phe-OMe was obtained as colorless foam (2.876 g, 4.72 mmol, 99%).

Deprotection 2: The deprotection was performed as described above for deprotection 1.

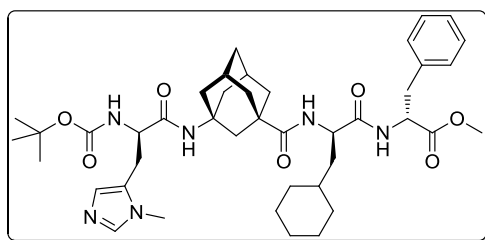
Coupling 3: The coupling of H-^AGly-L-Cha-L-Phe-OMe • HCl with Boc-L-Pmh-OH was performed on 2.10 mmol scale according to the previous couplings with the modification that 2.2 equiv of coupling reagents and base were used. The slightly yellow solution was diluted with EtOAc and washed with sat. aq. NaHCO₃ (3 × 50 mL) and brine (3 × 50 mL). The organic layer was dried over Na₂SO₄, filtered, and concentrated under reduced pressure to give a yellow foam. Purification by column chromatography eluting with CHCl₃/MeOH (10:1) afforded oligopeptide **1** (1.272 g, 1.67 mmol, 80%) as colorless foam. TLC (CHCl₃/MeOH 10:1): *R_f* = 0.41.

¹H NMR (400 MHz, CDCl₃): δ = 7.54 (s, 1H), 7.29 – 7.19 (m, 3H), 7.12 – 7.07 (m, 2H), 6.86 (s, 1H), 6.69 (d, *J* = 7.7 Hz, 1H), 6.16 (s, 1H), 6.09 (d, *J* = 7.9 Hz, 1H), 5.35 (br s, 1H), 4.82 – 4.75 (m, 1H), 4.48 – 4.40 (m, 1H), 4.28 – 4.16 (m, 1H), 3.68 (s, 3H), 3.61 (s, 3H), 3.11 (dd, *J* = 13.9, 5.9 Hz, 1H), 3.05 (dd, *J* = 13.9, 6.5 Hz, 1H), 2.98 (d, *J* = 6.9 Hz, 2H), 2.17 (m, 2H), 2.03 – 1.94

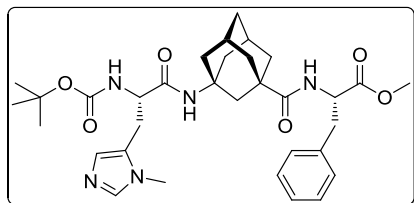
(m, 2H), 1.95 – 1.85 (m, 4H), 1.76 – 1.55 (m, 12H), 1.51 – 1.43 (m, 1H), 1.41 (s, 9H), 1.28 – 1.05 (m, 4H), 0.97 – 0.76 (m, 2H) ppm.

^{13}C NMR (100 MHz, CDCl_3): δ = 176.5, 172.1, 171.8, 169.8, 155.5, 138.0, 135.9, 129.3, 128.7, 127.8, 127.7, 80.5, 54.5, 53.4, 52.5, 52.4, 50.8, 42.6, 42.3, 40.4, 40.4, 39.6, 38.3, 38.1, 37.9, 35.3, 34.3, 33.6, 32.8, 31.8, 29.2, 29.2, 28.4, 27.1, 26.5, 26.3, 26.2 ppm.

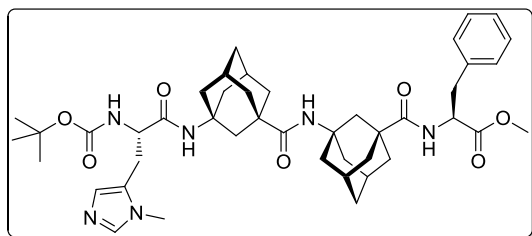
Spectroscopic data match those reported in the literature^[6a] and in Chapter II.



Boc-D-Pmh-^AGly-D-Cha-D-Phe-OMe (*ent*-1). For synthesis and complete characterization see Chapter II.

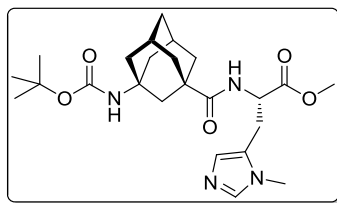


Boc-L-Pmh-^AGly-L-Phe-OMe (14). For synthesis and complete characterization see Chapter II.



Boc-L-Pmh-^AGly-^AGly-L-Phe-OMe (15).

For synthesis and complete characterization see Chapter II.



Boc-^AGly-L-Pmh-OMe (16). *H*-L-Pmh-OMe • 2 HCl: In accordance with a reported procedure,^[32] trimethylsilyl chloride (3.80 mL, 3.26 g, 30.0 mmol) was added dropwise to Boc-L-Pmh-OH (2.64 g, 9.8 mmol) with cooling. Dry MeOH (100 mL) was added slowly and the resulting solution was allowed to stir at rt for

24 h. All volatiles were removed *in vacuo* to afford H-L-Pmh-OMe • 2 HCl (quant.) as colorless solid.

¹H NMR (400 MHz, D₂O): δ = 8.75 (s, 1H), 7.48 (s, 1H), 4.55 (t, J = 7.3 Hz, 1H), 3.89 (s, 3H), 3.86 (s, 3H), 3.55 (dd, J = 16.3, 6.9 Hz, 1H), 3.42 (dd, J = 16.1, 7.3 Hz, 1H) ppm.

¹³C NMR (100 MHz, D₂O): δ = 168.8, 136.1, 128.1, 118.9, 54.0, 51.0, 33.4, 23.7 ppm.

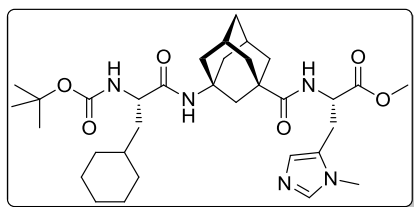
¹H NMR data are in accordance with those reported.^[33]

According to a literature procedure,^[34] Boc-^AGly-OH (886.1 mg, 3.0 mmol), H-L-Pmh-OMe • 2 HCl (768.4 mg, 3.0 mmol) and *O*-(benzotriazol-1-yl)-*N,N,N',N'*-tetramethyluronium hexafluorophosphate (HBTU; 1.138 g, 3.0 mmol) were dissolved in dry acetonitrile/methanol (10:1, 44 mL) and cooled to 0 °C with an ice bath. DiPEA (1.53 mL, 9.0 mmol) was added and the mixture was stirred for 3.5 h upon warming to rt. The reaction was quenched with brine (60 mL) and extracted with CHCl₃ (4 × 40 mL). The combined organic layers were successively washed with H₂O (2 × 50 mL), sat. aq. NaHCO₃ (2 × 50 mL) and brine (2 × 50 mL) and dried over Na₂SO₄. After filtration and removal of the solvent under reduced pressure the crude product was purified by column chromatography eluting with CHCl₃/MeOH (9:1) to yield **16** (952.2 mg, 2.07 mmol, 69%) as colorless solid. TLC (CHCl₃/MeOH 9:1): R_f = 0.33.

¹H NMR (600 MHz, CDCl₃): δ = 7.53 (s, 1H), 6.80 (s, 1H), 6.28 (d, J = 7.4 Hz, 1H), 4.79 – 4.75 (m, 1H), 4.43 (br s, 1H), 3.74 (s, 3H), 3.62 (s, 3H), 3.14 (dd, J = 15.4, 6.2 Hz, 1H), 3.06 (dd, J = 15.4, 6.4 Hz, 1H), 2.22 – 2.17 (m, 2H), 2.03 – 1.95 (m, 2H), 1.95 – 1.82 (m, 4H), 1.78 – 1.68 (m, 4H), 1.66 – 1.57 (m, 2H), 1.42 (s, 9H) ppm.

¹³C NMR (150 MHz, CDCl₃): δ = 176.7, 171.8, 154.2, 138.2, 127.5, 126.9, 79.1, 52.8, 51.4, 50.9, 43.0, 42.8, 41.1, 41.0, 38.3, 38.3, 35.4, 31.8, 29.3, 29.3, 28.6, 26.8 ppm.

For complete characterization see Chapter VI.



Boc-L-Cha-^AGly-L-Pmh-OMe (17). *Coupling 1:* The coupling of Boc-^AGly-OH (1.188 g, 4.0 mmol) and H-L-Pmh-OMe • 2 HCl (1.027 g, 4.0 mmol) was performed as described for catalyst **16**. The crude product obtained after work-up was used for the subsequent steps without further purification.

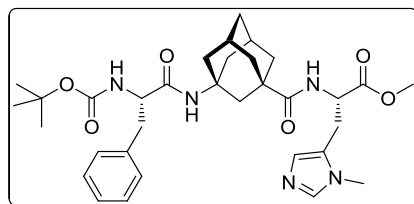
Deprotection: The deprotection was performed as described for the synthesis of peptide **1**.

Coupling 2: The coupling of H-^AGly-L-Pmh-OMe • 2 HCl and Boc-L-Cha-OH • DCHA was performed according to coupling 3 described for the synthesis of **1** with the modification that 3 equiv. of Et₃N were used. Column chromatography eluting with CH₂Cl₂/MeOH (95:5) gave Boc-L-Cha-^AGly-L-Pmh-OMe (**17**; 1.645 g, 2.68 mmol, 67% based on H-L-Pmh-OMe • 2 HCl) as colorless solid. TLC (CH₂Cl₂/MeOH, 95:5): *R_f* = 0.32.

¹H NMR (600 MHz, CDCl₃): δ = 7.44 (s, 1H), 6.76 (s, 1H), 6.27 (d, *J* = 7.5 Hz, 1H), 5.90 (br s, 1H), 4.89 (br s, 1H), 4.79 – 4.75 (m, 1H), 3.97 (br s, 1H), 3.74 (s, 3H), 3.60 (s, 3H), 3.13 (dd, *J* = 15.5, 6.1 Hz, 1H), 3.05 (dd, *J* = 15.4, 6.5 Hz, 1H), 2.07 (d, *J* = 11.8 Hz, 1H), 2.03 – 1.96 (m, 2H), 1.96 – 1.90 (m, 3H), 1.79 – 1.58 (m, 12H), 1.44 (s, 9H), 1.43 – 1.36 (m, 1H), 1.34 – 1.09 (m, 5H), 0.99 – 0.91 (m, 1H), 0.91 – 0.83 (m, 1H) ppm.

¹³C NMR (150 MHz, CDCl₃): δ = 176.5, 172.0, 171.8, 155.9, 138.4, 127.9, 126.7, 80.2, 53.1, 52.8, 52.2, 51.3, 42.7, 42.5, 40.7, 40.6, 40.0, 38.2, 38.2, 35.3, 34.3, 33.8, 32.8, 31.6, 29.2, 29.2, 28.5, 26.8, 26.6, 26.4, 26.2, 24.9, 23.1, 22.3 ppm.

For complete characterization see Chapter VI.



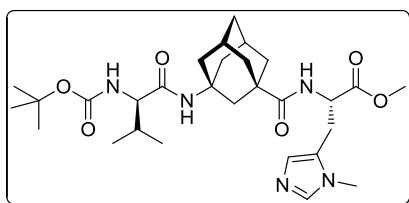
Boc-L-Phe-^AGly-L-Pmh-OMe (18). The deprotection of Boc-^AGly-L-Pmh-OMe (**16**; 230.5 mg, 0.50 mmol) was performed with 4 M HCl in 1,4-dioxane (2.0 mL) as described in the synthesis of **1**. Coupling of Boc-L-Phe-OH (132.8 mg, 0.50 mmol) with H-^AGly-L-Pmh-OMe • 2 HCl was performed

in the presence of HBTU (208.5 mg, 0.55 mmol), HOBT • H₂O (84.9 mg, 0.55 mmol), and Et₃N (0.23 mL, 167.0 mg, 1.65 mmol) in CH₂Cl₂ (5 mL) at rt for 24 h according to the procedure described for **16**. A sample of the crude peptide was purified by preparative HPLC for complete characterization and catalysis. LiChrosorb Diol column (Merck), 250 mm × 8 mm; eluent: 10% MeOH/TBME, 5.0 mL/min; UV-detector λ = 220 nm. Retention time: *t_R* = 7.5 min.

^1H NMR (600 MHz, CDCl_3): δ = 7.54 (s, 1H), 7.32 – 7.19 (m, 5H), 6.81 (s, 1H), 6.28 (d, J = 7.4 Hz), 5.42 (s, 1H), 5.14 (br s, 1H), 4.80 – 4.72 (m, 1H), 4.17 (br s, 1H), 3.75 (s, 3H), 3.61 (s, 3H), 3.14 (dd, J = 15.5, 6.1 Hz, 1H), 3.09 – 3.02 (m, 2H), 2.96 – 2.90 (m, 1H), 2.15 (s, 2H), 1.97 – 1.86 (m, 2H), 1.85 – 1.66 (m, 8H), 1.63 – 1.54 (m, 2H), 1.41 (s, 9H) ppm.

^{13}C NMR (150 MHz, CDCl_3): δ = 176.5, 171.8, 170.2, 155.5, 138.2, 137.2, 129.6, 128.8, 127.5, 127.1, 126.8, 80.2, 56.5, 52.8, 52.2, 51.3, 42.7, 42.4, 40.5, 40.4, 39.2, 38.2, 38.1, 35.2, 31.8, 29.2, 28.5, 26.8 ppm.

For complete characterization see Chapter VI.

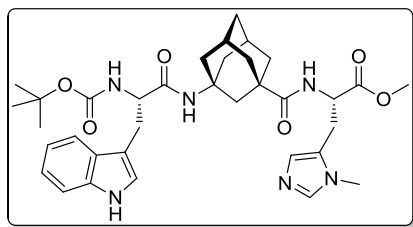


Boc-D-Val- Δ Gly-L-Pmh-OMe (19). The deprotection of Boc- Δ Gly-L-Pmh-OMe (**16**; 0.461 g, 1.00 mmol) was performed with 4 M HCl in 1,4-dioxane (2.0 mL) as described in the synthesis of **1**. Coupling of Boc-D-Val-OH (217.3 mg, 1.0 mmol) with H- Δ Gly-L-Pmh-OMe \cdot 2 HCl was performed in the presence of HBTU (379.3 mg, 1.0 mmol), HOBT \cdot 2 H_2O (153.1 mg, 1.0 mmol), and DiPEA (0.52 mL, 387.7 mg, 3.0 mmol) in CH_2Cl_2 (5 mL) at rt for 24 h according to the procedure described for **16**. Purification by column chromatography eluting with $\text{CHCl}_3/\text{MeOH}$ (9:1) afforded **19** (288.6 mg, 0.52 mmol, 52%) as colorless solid. TLC ($\text{CHCl}_3/\text{MeOH}$ 9:1): R_f = 0.39.

^1H NMR (600 MHz, CDCl_3): δ = 7.40 (s, 1H), 6.75 (s, 1H), 6.25 (d, J = 7.5 Hz, 1H), 5.69 (s, 1H), 5.06 (d, J = 8.3 Hz, 1H), 4.80 – 4.75 (m, 1H), 3.74 (s, 3H), 3.74 – 3.70 (m, 1H), 3.59 (s, 3H), 3.13 (dd, J = 15.4, 6.1 Hz, 1H), 3.04 (dd, J = 15.4, 6.5 Hz, 1H), 2.21 (m, 2H), 2.07 – 2.01 (m, 3H), 2.00 – 1.93 (m, 4H), 1.80 – 1.69 (m, 4H), 1.68 – 1.58 (m, 2H), 1.44 (s, 9H), 0.93 (d, J = 6.7 Hz, 3H), 0.89 (d, J = 6.8 Hz, 3H) ppm.

^{13}C NMR (150 MHz, CDCl_3): δ = 176.4, 171.9, 156.0, 138.5, 128.4, 126.5, 79.9, 60.5, 52.8, 52.4, 51.3, 42.7, 42.6, 40.6, 40.5, 38.2, 35.3, 31.6, 31.1, 29.2, 28.5, 26.8, 19.4, 18.0 ppm.

For complete characterization see Chapter VI.

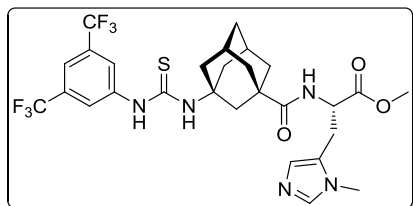


Boc-L-Trp-^AGly-L-Pmh-OMe (20). The tripeptide was synthesized on 0.3 mmol scale employing the procedure described for **17**. A sample of the crude peptide was purified by preparative HPLC for complete characterization and catalysis. LiChrosorb Diol column (Merck), 250 mm × 8 mm; eluent: 12% MeOH/TBME, 5.0 mL/min; UV-detector $\lambda = 220$ nm. Retention time: $t_R = 7.4$ min.

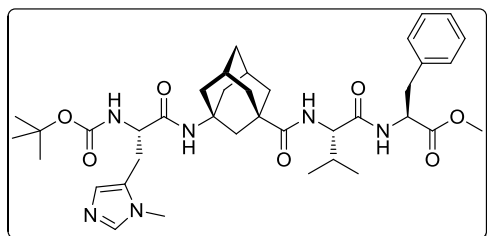
¹H NMR (600 MHz, CDCl₃): $\delta = 9.98$ (s, 1H), 7.67 (d, $J = 7.9$ Hz, 1H), 7.60 (s, 1H), 7.38 (d, $J = 8.1$ Hz, 1H), 7.18 – 7.14 (m, 1H), 7.12 – 7.08 (m, 1H), 7.02 (s, 1H), 6.85 (s, 1H), 6.33 (d, $J = 7.5$ Hz, 1H), 5.29 (br s, 1H), 5.25 (s, 1H), 4.81 – 4.76 (m, 1H), 4.36 (br s, 1H), 3.78 (s, 3H), 3.61 (s, 3H), 3.36 – 3.29 (m, 1H), 3.19 (dd, $J = 15.6, 5.3$ Hz, 1H), 3.06 – 2.97 (m, 2H), 2.08 (d, $J = 22.5$ Hz, 2H), 1.85 (d, $J = 12.1$ Hz, 1H), 1.76 (d, $J = 11.6$ Hz, 1H), 1.73 – 1.47 (m, 10H), 1.44 (s, 9H) ppm.

¹³C NMR (150 MHz, CDCl₃): $\delta = 176.5, 171.9, 170.7, 155.6, 138.0, 136.5, 127.6, 127.2, 126.8, 124.0, 122.0, 119.5, 118.8, 111.7, 110.3, 79.9, 55.6, 52.9, 52.0, 50.9, 42.6, 42.1, 40.5, 40.2, 38.0, 38.0, 35.2, 31.8, 29.1, 29.1, 29.0, 28.5, 26.6$ ppm.

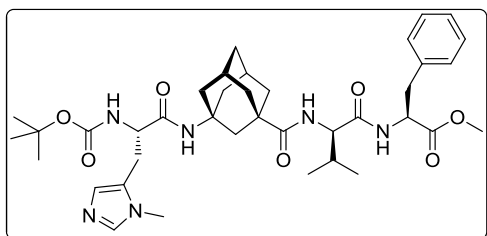
For complete characterization see Chapter VI.



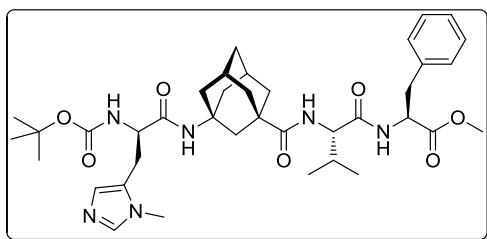
3,5-bis(trifluoromethyl)phenylthiourea-^AGly-L-Pmh-OMe (21). The synthesis and characterization data for **21** can be found in the literature.^[34]



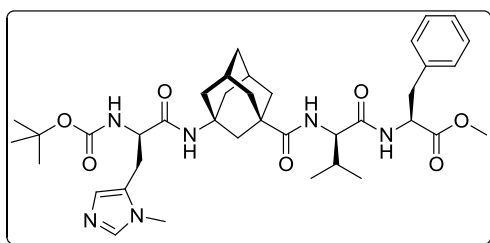
Boc-L-Pmh-^AGly-L-Val-L-Phe-OMe (22). For synthesis and complete characterization see Chapter II.



Boc-L-Pmh-^AGly-D-Val-L-Phe-OMe (23). For synthesis and complete characterization see Chapter II.



Boc-D-Pmh-^AGly-L-Val-L-Phe-OMe (24). For synthesis and complete characterization see Chapter II.



Boc-D-Pmh-^AGly-D-Val-L-Phe-OMe (25). For synthesis and complete characterization see Chapter II.

4.3 Description of Catalytic Experiments

General procedure for catalytic runs. Methyl 4,6-*O*-benzylidene- α -D-glucopyranoside (**3**; 28.2 mg, 0.1 mmol) and catalyst (5 mol%; 10 mol% for NMI) were suspended in dry toluene (10 mL) under nitrogen. Acetic anhydride (12 μ L, 13.0 mg, 1.3 mmol) was added and the mixture was stirred at rt for 18 h. The reaction was quenched by addition of MeOH (1 mL) and was allowed to stir for further 30 min. All volatiles were removed *in vacuo*, the obtained residue was redissolved in CDCl₃ and analyzed by ¹H NMR in order to determine conversion and product distribution.

The reactions described in Table 2 were performed with **3** (28 mg, 0.1 mmol) and peptide catalysts **1** (3.8 mg, 5 mol%) or **24** (3.1 mg, 5 mol%) according to the general procedure given above, with the exception that different solvents (10 mL), varying amounts of anhydride (1.3 equiv or 5.3 equiv) and different temperatures (rt or 0°C) were employed, or DiPEA (50 μ L, 37.1 mg, 0.29 mmol) was used as auxiliary base.

Acetylation of **3 in the presence of Et₃N.** The reaction was reproduced according the reaction conditions described in the literature^[15] with the purpose to determine the amounts of **5** and **13** formed upon acetylation. Methyl 4,6-*O*-benzylidene- α -D-glucopyranoside (**3**; 28.3 mg, 0.1 mmol) was dissolved in CH₂Cl₂ (0.7 mL), acetic anhydride (13.2 μ L, 14.3 mg, 0.14 mmol) was added and the solution was stirred at rt for 10 min. After addition of Et₃N (125 μ L, 91.3 mg,

0.9 mmol) the reaction mixture was allowed to stir at rt overnight, quenched with MeOH, and concentrated under reduced pressure. The obtained residue was redissolved in CDCl₃ and analyzed by ¹H NMR in order to determine conversion and product distribution. In accordance with the reported values, **4** was the major product (80%). The by-products **5** and **13** formed in 5% and 15%, respectively (Table 3).

4.4 Computational Details

The distance of the acylium ion C=O of peptides **22–25** to the 2-OH group of substrate **3** was initially set to 2.5 Å and a search for low-lying conformers was performed using the Merck Molecular Force Field without constraining the distance. From the obtained conformers of each catalyst some conformers were found where the carbohydrate was placed outside the catalytic pocket. However, for each catalyst the lowest-lying adduct was chosen that would allow acetylation of the substrate to take place.

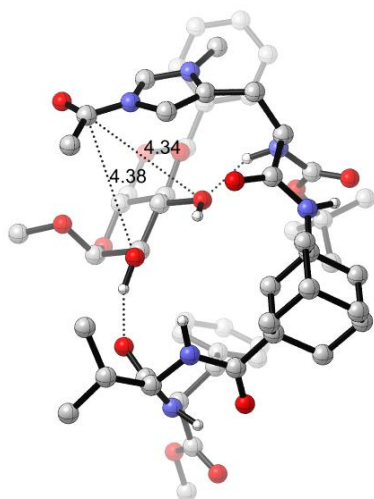


Table 4. Cartesian coordinates for complex **22Ac_3**.

Atom	X	Y	Z
C	-0.773772	1.171579	-4.028518
C	1.449341	2.390656	-3.768394
C	0.912386	1.172612	-5.929939
C	2.019559	1.548071	-4.937961
C	-0.156558	0.356051	-5.194137
C	0.362639	1.554375	-3.046302
H	2.493585	0.634981	-4.553424
H	0.285021	-0.574099	-4.811518

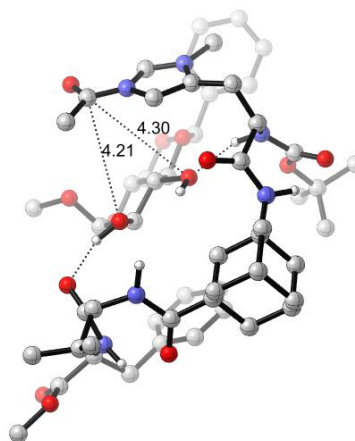


Table 5. Cartesian coordinates for complex **23Ac_3**.

Atom	X	Y	Z
C	-0.473383	1.429681	-3.536894
C	1.823566	2.355418	-2.911773
C	1.478776	1.209201	-5.148226
C	2.461552	1.450467	-3.993901
C	0.211300	0.535766	-4.602285
C	0.542819	1.656245	-2.388997
H	2.759847	0.488888	-3.557978
H	0.464851	-0.441260	-4.169269

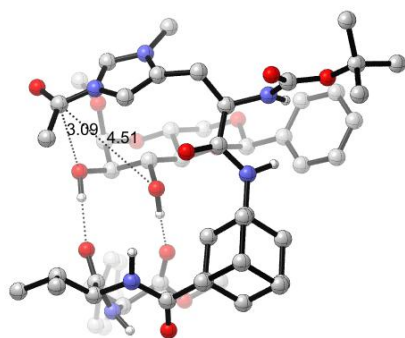
H	0.809644	0.648892	-2.612748	H	0.802041	0.698661	-1.916872
H	1.334621	0.577431	-6.747359	H	1.944899	0.562945	-5.900424
H	2.807267	2.107015	-5.460683	H	3.379971	1.909432	-4.383344
H	-0.941194	0.053257	-5.900628	H	-0.482815	0.332699	-5.428878
H	-0.045913	2.114973	-2.197232	H	0.082208	2.255651	-1.597357
C	0.796537	3.662627	-4.360641	C	1.431079	3.698767	-3.573297
H	0.371647	4.289806	-3.566739	H	0.970449	4.374839	-2.841954
H	1.555266	4.277222	-4.862752	H	2.328641	4.213469	-3.940859
C	-1.387427	2.463543	-4.623029	C	-0.817010	2.788298	-4.193501
H	-1.837140	3.080723	-3.836154	H	-1.303170	3.457265	-3.473041
H	-2.200258	2.210771	-5.316609	H	-1.537366	2.641270	-5.009078
C	-0.314943	3.287443	-5.354334	C	0.451576	3.465613	-4.734665
H	-0.766139	4.198620	-5.763047	H	0.189105	4.425728	-5.193074
C	0.279759	2.451069	-6.495307	C	1.106286	2.556011	-5.783725
H	-0.502911	2.193981	-7.219586	H	0.419375	2.397304	-6.624092
H	1.033920	3.036069	-7.035912	H	2.002380	3.039175	-6.192170
C	2.591858	2.766875	-2.814340	C	2.831985	2.611538	-1.778300
O	3.736515	2.336464	-2.941713	O	3.995692	2.217775	-1.816500
N	2.257865	3.607562	-1.775527	N	2.345159	3.339736	-0.718757
C	3.269970	4.030120	-0.802602	C	3.146329	3.771287	0.426517
C	3.496200	2.844423	0.166558	C	3.487747	2.545949	1.311248
O	2.782326	2.615619	1.142888	O	2.865277	2.311092	2.349986
H	1.282295	3.709058	-1.529346	H	1.376934	3.630848	-0.723151
H	4.205126	4.194324	-1.355411	N	4.452554	1.701638	0.827863
C	2.893998	5.367986	-0.126623	C	5.070007	0.644779	1.634229
H	2.750382	6.100730	-0.933317	C	6.337253	1.125176	2.358171
C	4.046582	5.878583	0.743968	O	6.910249	0.466794	3.219434
C	1.596244	5.361418	0.686281	H	4.842557	1.907327	-0.093354
H	0.754905	4.962880	0.113070	H	4.362240	0.358885	2.421041
H	1.331837	6.384847	0.976624	C	5.462898	-0.565244	0.775339
H	1.691456	4.785568	1.610871	C	4.280062	-1.403036	0.350000
H	4.232223	5.215711	1.595534	H	6.157012	-1.219336	1.320300
H	3.821654	6.875596	1.137891	H	6.019378	-0.236787	-0.113181
H	4.971628	5.953029	0.162575	C	2.140501	-3.016426	-0.463345
N	4.481818	1.975906	-0.248620	C	3.771458	-2.391738	1.203481
C	4.703154	0.670069	0.379206	C	3.692486	-1.220349	-0.907495
C	6.132173	0.224490	0.068417	C	2.627234	-2.024603	-1.312401
O	6.701113	0.428774	-0.997701	C	2.708574	-3.197772	0.795619
H	4.797659	2.063198	-1.220402	H	4.217931	-2.558849	2.182232
H	4.593639	0.810594	1.460350	H	4.078815	-0.464504	-1.588563
C	3.710442	-0.364365	-0.174567	H	2.193895	-1.890278	-2.299918
C	3.681881	-1.676359	0.574460	H	2.340220	-3.978893	1.455672
H	3.934048	-0.549360	-1.234460	H	1.331545	-3.660534	-0.791504
H	2.692354	0.043178	-0.167147	O	6.778074	2.325107	1.885109
C	3.629463	-4.126230	1.943487	C	7.978366	2.793610	2.502671
C	3.964475	-2.874173	-0.096259	H	8.802776	2.099719	2.311562
C	3.365857	-1.725092	1.939492	H	7.827243	2.932694	3.577664
C	3.342073	-2.943377	2.620020	H	8.229995	3.761540	2.060500
C	3.941133	-4.091542	0.586186	N	-1.689216	0.753200	-3.072256
H	4.217068	-2.870744	-1.155195	H	-2.036039	-0.010015	-3.655002
H	3.152016	-0.815285	2.494564	N	-3.464128	-0.988102	-1.507092
H	3.115438	-2.967798	3.683091	C	-3.828803	0.360907	-1.935767
H	4.174536	-5.013694	0.059116	C	-2.557876	1.225307	-2.107965
H	3.623188	-5.074494	2.475342	O	-2.360403	2.241197	-1.444956
O	6.668717	-0.439168	1.130020	H	-2.949778	-1.083298	-0.629020
C	7.993680	-0.922826	0.905731	C	-4.876819	1.025496	-1.032439
H	8.005793	-1.634427	0.074209	C	-4.559933	1.028800	0.421858
H	8.322268	-1.441914	1.810288	H	-5.036766	2.065386	-1.343967
H	8.678120	-0.090342	0.715241	H	-5.837234	0.515510	-1.169047

Peptide-Catalyzed Regioselective Acetylation of Carbohydrates

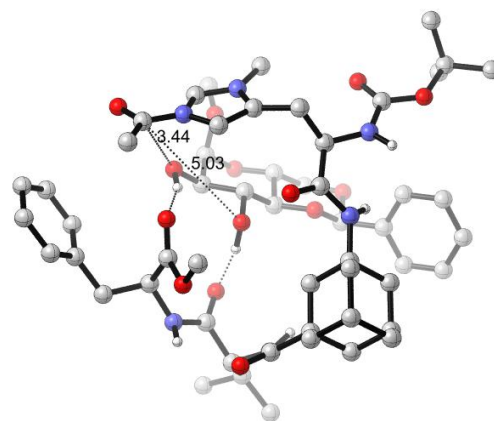
N	-1.799767	0.342374	-3.390106	C	-3.805607	1.905394	1.175919
H	-1.874474	-0.625550	-3.711348	H	-3.246602	2.788005	0.909931
N	-2.990648	-1.427492	-1.218382	C	-3.095568	-1.929549	-2.423143
C	-3.660356	-0.375371	-1.975532	O	-3.191661	-1.766808	-3.629917
C	-2.634257	0.717097	-2.359169	O	-2.565695	-3.000607	-1.793269
O	-2.560535	1.792694	-1.769922	C	-2.025296	-4.105011	-2.568876
H	-2.560787	-1.172101	-0.325760	C	-0.845827	-3.645552	-3.434829
C	-4.890745	0.210088	-1.269125	H	-0.137347	-3.056056	-2.843771
C	-4.696215	0.601158	0.153829	H	-1.168648	-3.006658	-4.262388
H	-5.251424	1.091741	-1.813844	H	-0.314187	-4.497946	-3.871148
H	-5.702721	-0.525065	-1.308246	C	-1.505918	-5.107834	-1.527569
C	-4.202787	1.764408	0.709835	H	-0.803465	-4.627890	-0.838395
H	-3.819642	2.669383	0.266541	H	-1.006274	-5.961179	-1.998039
C	-2.235601	-2.362629	-1.865440	H	-2.324855	-5.493039	-0.911111
O	-2.229579	-2.505568	-3.078654	C	-3.115773	-4.789180	-3.400799
O	-1.466122	-3.015157	-0.968921	H	-3.474500	-4.149296	-4.212486
C	-0.446409	-3.947510	-1.415801	H	-3.986993	-5.025820	-2.779544
C	0.622719	-3.228102	-2.247116	H	-2.748040	-5.716397	-3.853397
H	0.983266	-2.333722	-1.726085	N	-5.059844	0.091842	1.340880
H	0.231159	-2.890485	-3.211555	C	-5.943599	-1.034551	1.054949
H	1.477388	-3.882153	-2.450346	H	-6.882570	-0.655361	0.643166
C	0.204824	-4.468677	-0.126785	H	-6.160040	-1.576200	1.977598
H	0.609709	-3.641673	0.466655	H	-5.461922	-1.698546	0.336152
H	1.014556	-5.174827	-0.337643	C	-4.557695	0.335153	2.564520
H	-0.532629	-4.973098	0.507177	H	-4.728509	-0.271111	3.449610
C	-1.059815	-5.134180	-2.166269	N	-3.836693	1.453380	2.473108
H	-1.468140	-4.838931	-3.137286	C	-3.217306	1.969644	3.533301
H	-1.888210	-5.568460	-1.595268	O	-3.436526	1.388245	4.586959
H	-0.315409	-5.916371	-2.350372	C	-2.337612	3.178810	3.415730
N	-5.060956	-0.200896	1.247483	H	-1.895008	3.401139	4.390886
C	-5.652920	-1.535178	1.198040	H	-1.530086	2.987051	2.705805
H	-6.629187	-1.472653	0.710109	H	-2.930039	4.039152	3.095063
H	-5.791244	-1.914805	2.211970	H	2.065103	-0.203553	3.216272
H	-4.996835	-2.200690	0.635696	C	0.996275	-0.441161	3.179444
C	-4.728466	0.410268	2.398109	C	-0.995253	-0.517969	1.635852
H	-4.846073	-0.009106	3.393241	C	-0.527797	-2.250282	3.347563
N	-4.240670	1.608655	2.074704	C	-1.135855	-1.997581	1.967665
C	-3.814333	2.460663	3.005767	C	0.451757	-0.047648	1.787935
O	-3.999313	2.093778	4.157976	H	-1.643934	0.067382	2.289380
C	-3.165774	3.762526	2.638641	H	-1.108382	-1.707126	4.106540
H	-2.856538	4.282784	3.549683	H	-0.622234	-2.575863	1.187466
H	-2.278734	3.578512	2.027712	H	1.063966	-0.502078	1.003266
H	-3.876462	4.393236	2.099174	O	0.310451	0.330916	4.172802
H	1.685866	1.476000	3.493420	C	0.991630	0.297232	5.422700
C	0.697271	1.007347	3.424245	H	1.987835	0.739894	5.327691
C	-1.016763	0.141696	1.805817	H	1.066169	-0.727963	5.797169
C	-0.479239	-0.988830	3.949076	H	0.416210	0.888394	6.140124
C	-0.924387	-1.212141	2.500409	O	0.838662	-1.849349	3.406351
C	0.313256	0.877384	1.934635	C	-0.698861	-3.734633	3.645819
H	-1.821735	0.733588	2.240867	H	-0.343043	-3.962166	4.656239
H	-1.253143	-0.417614	4.480964	H	-0.114024	-4.358774	2.958944
H	-0.197177	-1.825116	1.950255	O	-2.519559	-2.377780	1.980051
H	1.078061	0.304616	1.401746	O	0.448571	1.372999	1.547043
O	-0.262933	1.841137	4.084458	H	1.235212	1.726638	2.023875
C	0.192486	2.249952	5.369953	O	-1.451595	-0.247679	0.299582
H	1.108179	2.842320	5.281434	H	-1.001694	0.591489	0.054954
H	0.362143	1.383776	6.016228	O	-2.081170	-4.080647	3.565418
H	-0.582469	2.874310	5.822706	C	-2.634615	-3.773917	2.284931
O	0.766888	-0.295415	4.025240	H	-2.123343	-4.374368	1.520798

C	-0.409358	-2.357678	4.618000
H	-0.184522	-2.247314	5.684121
H	0.388339	-2.978344	4.192161
O	-2.189271	-1.885692	2.488334
O	0.185304	2.137348	1.258064
H	1.082312	2.540806	1.322155
O	-1.348297	-0.003170	0.417231
H	-1.073044	0.847448	0.006567
O	-1.667157	-3.021859	4.488094
C	-2.042864	-3.166818	3.117485
H	-1.281329	-3.765494	2.599661
C	-3.374949	-3.876462	3.001690
C	-5.838312	-5.205495	2.725067
C	-4.314504	-3.870722	4.044805
C	-3.700124	-4.550366	1.811603
C	-4.921674	-5.213282	1.676142
C	-5.535924	-4.534474	3.908319
H	-4.088703	-3.366781	4.983151
H	-2.995314	-4.568419	0.982403
H	-5.151345	-5.749223	0.757932
H	-6.243432	-4.544281	4.734507
H	-6.781604	-5.738338	2.628268
H	-4.020486	-0.806792	-2.919878

C	-4.112869	-4.104550	2.271058
C	-6.857699	-4.720365	2.200803
C	-4.891543	-4.054229	3.438960
C	-4.742973	-4.449700	1.063772
C	-6.104185	-4.761228	1.029951
C	-6.252873	-4.364843	3.404518
H	-4.431793	-3.797204	4.392043
H	-4.173031	-4.485419	0.138537
H	-6.573329	-5.051235	0.092430
H	-6.836228	-4.349900	4.322523
H	-7.913088	-4.982637	2.179502
H	-4.279823	0.297045	-2.935706
C	4.363298	4.661001	0.077206
H	5.149125	4.065083	-0.400418
C	3.985977	5.792638	-0.886947
H	4.843433	6.450006	-1.067917
H	3.171899	6.403739	-0.482422
H	3.668682	5.402299	-1.858469
C	4.957996	5.280268	1.349204
H	5.849144	5.871078	1.111216
H	5.254046	4.514384	2.070816
H	4.237208	5.942454	1.841415
H	2.455422	4.380617	1.026289

Table 6. Cartesian coordinates for complex **24Ac_3**.

Atom	X	Y	Z
C	0.189277	0.710169	-3.162060
C	1.271493	-1.593240	-3.395719
C	-0.543636	-0.868027	-5.011729
C	0.064881	-2.056432	-4.246658
C	-1.003928	0.209866	-4.013580
C	0.764186	-0.514994	-2.415569
H	-0.700302	-2.513228	-3.604940
H	-1.788288	-0.200111	-3.364314
H	-0.002557	-0.944565	-1.756375
H	-1.399813	-1.210955	-5.603389
H	0.375242	-2.834070	-4.956925
H	-1.460980	1.048670	-4.555153
H	1.573678	-0.196852	-1.754766

Table 7. Cartesian coordinates for complex **25Ac_3**.

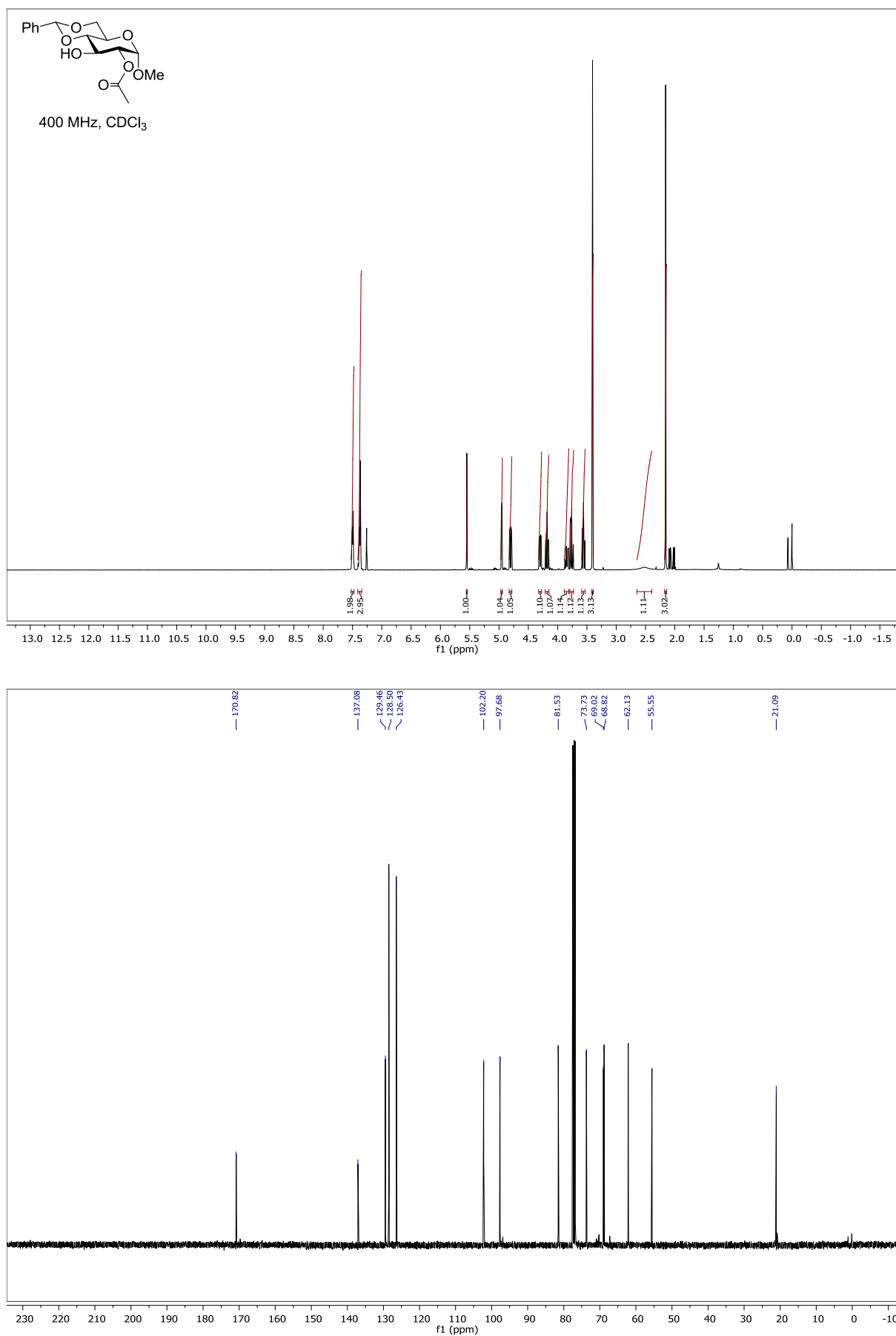
Atom	X	Y	Z
C	0.552750	0.956904	-3.201412
C	-1.759135	0.053752	-3.787335
C	-0.929741	2.187334	-4.868160
C	-2.162121	1.447708	-4.321304
C	0.107513	2.339267	-3.744448
C	-0.701549	0.227464	-2.671581
H	-2.620667	2.056742	-3.532467
H	-0.323229	2.935714	-2.932541
H	-1.116466	0.791102	-1.825310
H	-1.226753	3.177286	-5.232297
H	-2.920563	1.345603	-5.108368
H	0.977092	2.900346	-4.111579
H	-0.435666	-0.755669	-2.264817

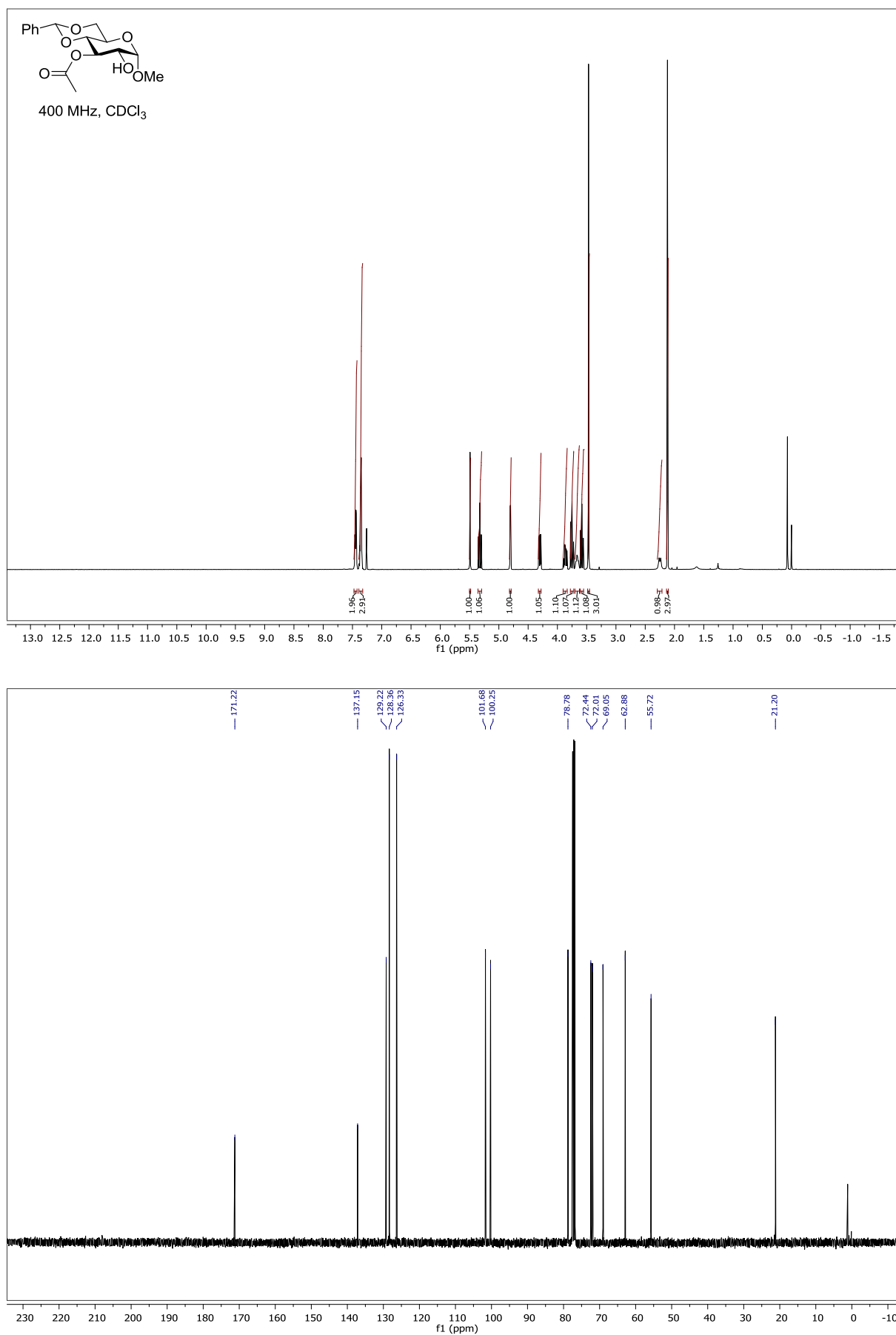
C	2.326624	-0.969642	-4.337703	C	-1.118102	-0.742558	-4.950641
H	3.199194	-0.622167	-3.769839	H	-0.820961	-1.742772	-4.612256
H	2.700268	-1.728178	-5.038016	H	-1.852197	-0.895931	-5.752736
C	1.257550	1.285262	-4.123278	C	1.150923	0.158152	-4.385216
H	2.127426	1.658015	-3.570211	H	1.479509	-0.837672	-4.068422
H	0.848995	2.147553	-4.666624	H	2.043119	0.667804	-4.771802
C	1.724419	0.211064	-5.118629	C	0.110952	-0.005078	-5.506552
H	2.482296	0.634123	-5.787590	H	0.546070	-0.582697	-6.329898
C	0.523219	-0.274000	-5.942664	C	-0.314595	1.377786	-6.016501
H	0.099222	0.560304	-6.514878	H	0.551978	1.909015	-6.428870
H	0.847764	-1.027090	-6.671185	H	-1.040330	1.270971	-6.832016
C	1.881201	-2.775600	-2.624535	C	-2.966477	-0.710595	-3.225033
O	1.480260	-3.933300	-2.736100	O	-3.237987	-1.868831	-3.532177
N	2.916946	-2.454232	-1.772847	N	-3.698341	-0.030734	-2.275474
C	3.556759	-3.456381	-0.919355	C	-4.727213	-0.719169	-1.497305
C	2.544242	-3.758739	0.216212	C	-3.927999	-1.432126	-0.386088
O	2.456539	-3.082248	1.239430	O	-3.388396	-0.820413	0.539021
H	3.040916	-1.486010	-1.506222	H	-3.286599	0.791366	-1.853263
H	3.720806	-4.365544	-1.511707	N	-3.742962	-2.783826	-0.588497
C	4.901279	-2.939164	-0.362475	C	-2.843124	-3.558227	0.280827
H	4.724583	-2.048193	0.254475	C	-1.419258	-3.602938	-0.294994
C	5.858898	-2.542284	-1.492725	O	-0.402772	-3.671171	0.391919
C	5.578788	-3.997223	0.516085	H	-3.771958	-3.073379	-1.568885
H	4.964526	-4.251084	1.385428	H	-2.785158	-3.050597	1.249715
H	6.539684	-3.630392	0.893004	C	-3.376195	-4.989700	0.448498
H	5.766551	-4.917948	-0.046873	C	-2.532576	-5.877764	1.334390
H	6.049595	-3.385963	-2.164789	H	-3.480214	-5.453400	-0.542033
H	6.820443	-2.208959	-1.087419	H	-4.390701	-4.957861	0.867636
H	5.454539	-1.717559	-2.088252	C	-0.958283	-7.543190	2.954929
N	1.687183	-4.794479	-0.104618	C	-2.032797	-7.091118	0.839254
C	0.513794	-5.190932	0.681501	C	-2.245373	-5.518855	2.658774
C	-0.632705	-4.201033	0.438030	C	-1.454824	-6.344004	3.460306
O	-0.533839	-2.977824	0.481722	C	-1.250690	-7.919012	1.646230
H	1.601967	-4.956365	-1.112567	H	-2.254788	-7.409198	-0.177590
H	0.220195	-6.153037	0.242024	H	-2.632899	-4.596863	3.086004
C	0.787995	-5.373651	2.180901	H	-1.230719	-6.054013	4.484138
C	-0.353373	-6.040420	2.913962	H	-0.876771	-8.862661	1.256402
H	0.998242	-4.414020	2.664371	H	-0.352640	-8.188905	3.585926
H	1.692894	-5.979214	2.323268	O	-1.450742	-3.666097	-1.655457
C	-2.496421	-7.273002	4.235850	C	-0.178595	-3.831724	-2.278995
C	-1.222856	-5.287111	3.715989	H	-0.316817	-3.762866	-3.360752
C	-0.569247	-7.419101	2.785502	H	0.226734	-4.820433	-2.044369
C	-1.636738	-8.031010	3.443574	H	0.514477	-3.048767	-1.964318
C	-2.289058	-5.902180	4.373418	N	1.523818	1.172961	-2.120987
H	-1.076620	-4.217650	3.842063	H	1.422086	2.040346	-1.598234
H	0.093417	-8.030112	2.175889	N	3.640653	1.922425	-0.534097
H	-1.796424	-9.101848	3.341514	C	2.998587	0.645983	-0.235248
H	-2.956835	-5.315204	4.998873	C	2.195119	0.162354	-1.457822
H	-3.324713	-7.753549	4.750813	O	2.110505	-1.029121	-1.744615
O	-1.786327	-4.871119	0.161102	H	3.792927	2.218030	-1.491780
C	-2.917297	-4.038487	-0.091566	H	2.279598	0.838496	0.568913
H	-3.155686	-3.440724	0.793796	C	4.016401	-0.421506	0.195823
H	-3.771279	-4.683322	-0.315756	C	3.410464	-1.475526	1.054851
H	-2.732463	-3.392537	-0.955688	H	4.475121	-0.901226	-0.678128
N	-0.273774	1.721574	-2.207928	H	4.847098	0.020784	0.756174
H	-1.201876	2.111461	-2.329003	C	2.953290	-2.738482	0.736947
N	-1.260821	4.018805	-1.003930	H	2.892515	-3.266575	-0.200431
C	-0.203133	3.290343	-0.310660	C	4.171189	2.706354	0.443693
C	0.540979	2.347510	-1.282039	O	4.130405	2.427748	1.631991

O	1.734629	2.085823	-1.140366	O	4.745085	3.788583	-0.117705
H	-2.227850	3.726745	-0.915417	C	5.454991	4.761058	0.695925
H	-0.725769	2.647162	0.404175	C	6.669962	4.121576	1.377694
C	0.777176	4.196609	0.451611	H	7.280600	3.574487	0.650598
C	1.439616	3.495479	1.590014	H	6.373761	3.399160	2.144464
H	1.565294	4.578848	-0.208347	H	7.298353	4.876408	1.862536
H	0.253026	5.072453	0.850627	C	5.949616	5.819202	-0.301406
C	2.550201	2.674097	1.612839	H	6.592647	5.365204	-1.064449
H	3.206699	2.324649	0.832581	H	6.512652	6.615782	0.196174
C	-1.013778	5.024015	-1.887112	H	5.107916	6.273128	-0.837365
O	0.097746	5.459544	-2.133625	C	4.526023	5.438255	1.709479
O	-2.180322	5.426376	-2.429790	H	4.176055	4.740615	2.475998
C	-2.208606	6.477425	-3.431153	H	3.633450	5.836464	1.216135
C	-1.436059	6.065297	-4.689214	H	5.032637	6.262384	2.223397
H	-1.749573	5.071947	-5.029776	N	3.224712	-1.352301	2.440896
H	-0.358623	6.008354	-4.507222	C	3.562291	-0.201901	3.277516
H	-1.593003	6.779311	-5.504865	H	4.579543	0.127658	3.054585
C	-3.692978	6.631124	-3.794917	H	3.518887	-0.490413	4.330785
H	-4.096762	5.691081	-4.188484	H	2.847284	0.601042	3.087952
H	-3.849419	7.413956	-4.544476	C	2.626715	-2.460431	2.920844
H	-4.288555	6.876255	-2.907745	H	2.303049	-2.612028	3.946648
C	-1.704005	7.805304	-2.856394	N	2.559118	-3.329256	1.911606
H	-0.632129	7.775597	-2.638703	C	2.134510	-4.578117	2.101563
H	-2.209751	8.037217	-1.912328	O	1.895166	-4.869199	3.266719
H	-1.873572	8.631876	-3.554810	C	2.102953	-5.576876	0.981060
N	1.009895	3.572865	2.927965	H	1.597838	-6.485037	1.319473
C	-0.154290	4.292018	3.431520	H	1.562046	-5.187131	0.118896
H	0.019562	5.366457	3.332518	H	3.126427	-5.829100	0.691867
H	-0.316282	4.046098	4.484514	H	-1.184278	-0.923968	5.193901
H	-1.037038	3.997314	2.857594	C	-0.678921	-0.319235	4.430945
C	1.840100	2.859305	3.713890	C	-0.399249	-0.101567	1.924847
H	1.757106	2.754926	4.790526	C	-0.698190	1.841085	3.437612
N	2.749715	2.302795	2.917995	C	-1.011529	1.293033	2.046451
C	3.675355	1.475109	3.400093	C	-0.909410	-0.996860	3.058367
O	3.758055	1.454634	4.621422	H	0.691905	-0.045965	1.946556
C	4.590119	0.709687	2.488643	H	0.390306	1.923047	3.564321
H	5.138811	-0.036736	3.069932	H	-2.096923	1.207600	1.897480
H	4.013144	0.187615	1.721264	H	-1.984894	-1.163935	2.923304
H	5.303081	1.394268	2.022875	O	0.724006	-0.277567	4.738520
H	0.370461	-1.597244	5.301383	C	0.934949	0.043843	6.112119
C	0.020744	-0.837301	4.591682	H	2.012281	0.063540	6.296295
C	0.052715	-0.222468	2.143453	H	0.487979	-0.718235	6.757661
C	-1.948581	0.040889	3.602769	H	0.526317	1.030578	6.348879
C	-1.476502	-0.265776	2.180610	O	-1.248005	0.999079	4.451768
C	0.612808	-1.175095	3.203576	C	-1.261453	3.257426	3.513012
H	0.397575	0.796791	2.325089	H	-0.969785	3.729724	4.457138
H	-1.644648	1.061568	3.874728	H	-2.358266	3.259120	3.488856
H	-1.803162	-1.267533	1.873644	O	-0.490344	2.160024	1.038258
H	0.317077	-2.199438	2.951176	O	-0.278197	-2.282974	2.976965
O	0.455060	0.457972	5.035347	H	-0.334565	-2.556921	2.034306
C	0.308705	0.581571	6.448695	O	-0.722698	-0.699098	0.661925
H	0.957258	-0.133279	6.964112	H	-1.697751	-0.630491	0.561464
H	-0.733782	0.433721	6.746050	O	-0.748368	4.044166	2.437342
H	0.610968	1.592056	6.736150	C	-1.065562	3.464989	1.173483
O	-1.416045	-0.891792	4.543152	H	-2.156233	3.399530	1.059541
C	-3.475063	0.029391	3.591293	C	-0.490325	4.326834	0.074201
H	-3.862628	0.340275	4.567289	C	0.586107	5.906723	-1.984355
H	-3.872368	-0.975545	3.402037	C	0.895570	4.527934	-0.026737
O	-2.036395	0.686961	1.276243	C	-1.329324	4.942350	-0.867515

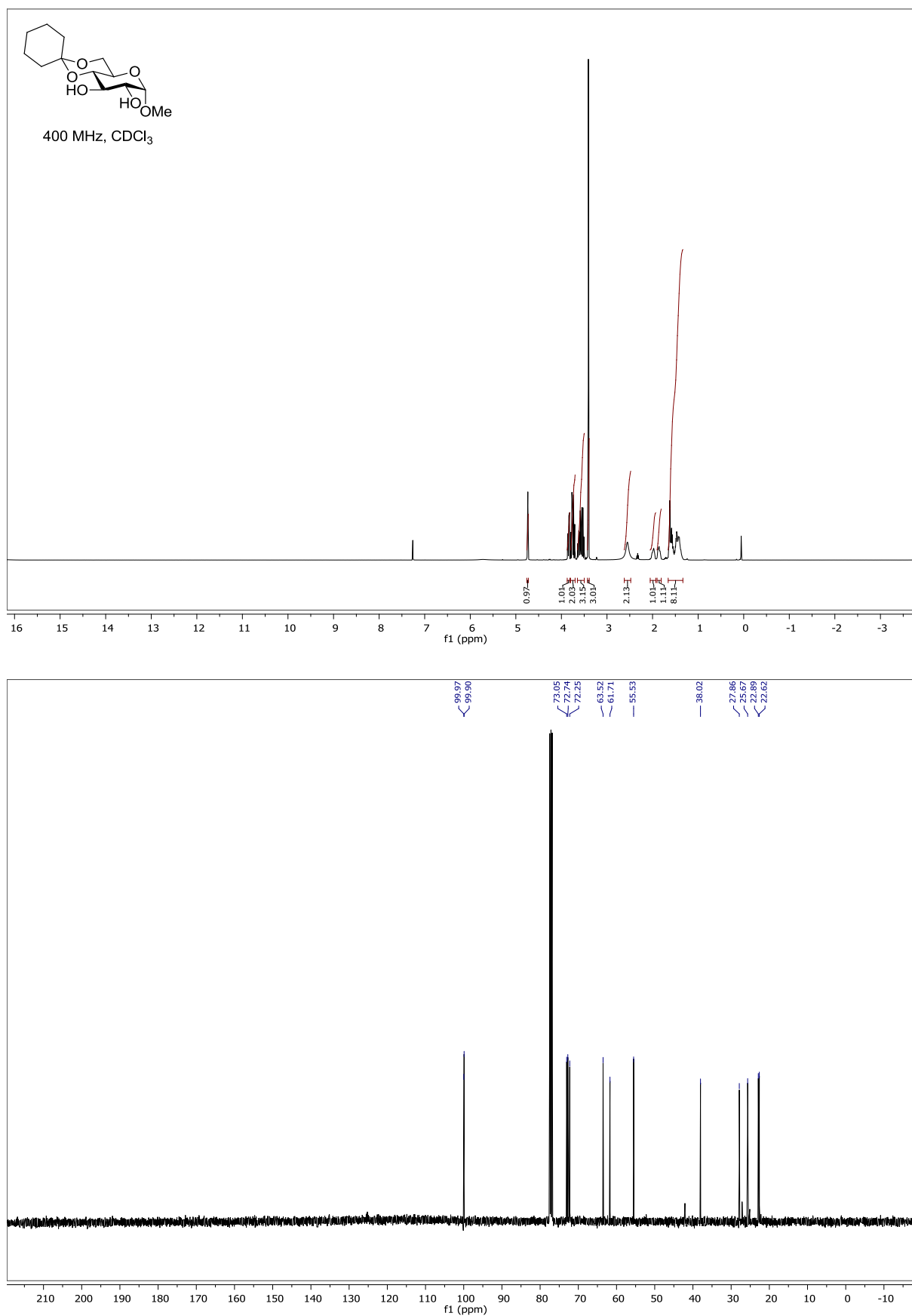
O	2.045377	-1.136611	3.188380	C	-0.792881	5.729107	-1.889346
H	2.300082	-1.712373	2.427854	C	1.430861	5.307271	-1.053146
O	0.560246	-0.561004	0.847269	H	1.556129	4.084447	0.715138
H	0.237501	-1.465767	0.633060	H	-2.408969	4.823953	-0.808629
O	-3.958827	0.941996	2.602572	H	-1.451429	6.210477	-2.608659
C	-3.463578	0.607640	1.305215	H	2.504421	5.463982	-1.116621
H	-3.800659	-0.404622	1.040407	H	1.000502	6.526465	-2.775975
C	-3.969555	1.566705	0.247846	C	-5.743370	0.279568	-0.907356
C	-4.885415	3.289356	-1.776561	H	-5.222369	0.996308	-0.258671
C	-4.564626	2.795625	0.569072	C	-6.445096	1.075072	-2.014027
C	-3.828672	1.224927	-1.109725	H	-7.184660	1.762115	-1.588740
C	-4.286283	2.078594	-2.114718	H	-6.964228	0.409516	-2.712154
C	-5.021703	3.649718	-0.437223	H	-5.731501	1.677523	-2.585325
H	-4.694960	3.088947	1.609102	C	-6.797033	-0.443229	-0.061184
H	-3.367007	0.278550	-1.386530	H	-7.527404	0.268084	0.339372
H	-4.190832	1.794476	-3.160222	H	-6.341068	-0.956852	0.791070
H	-5.498775	4.591752	-0.175612	H	-7.340200	-1.186563	-0.654740
H	-5.255449	3.951051	-2.556463	H	-5.236090	-1.456818	-2.129058

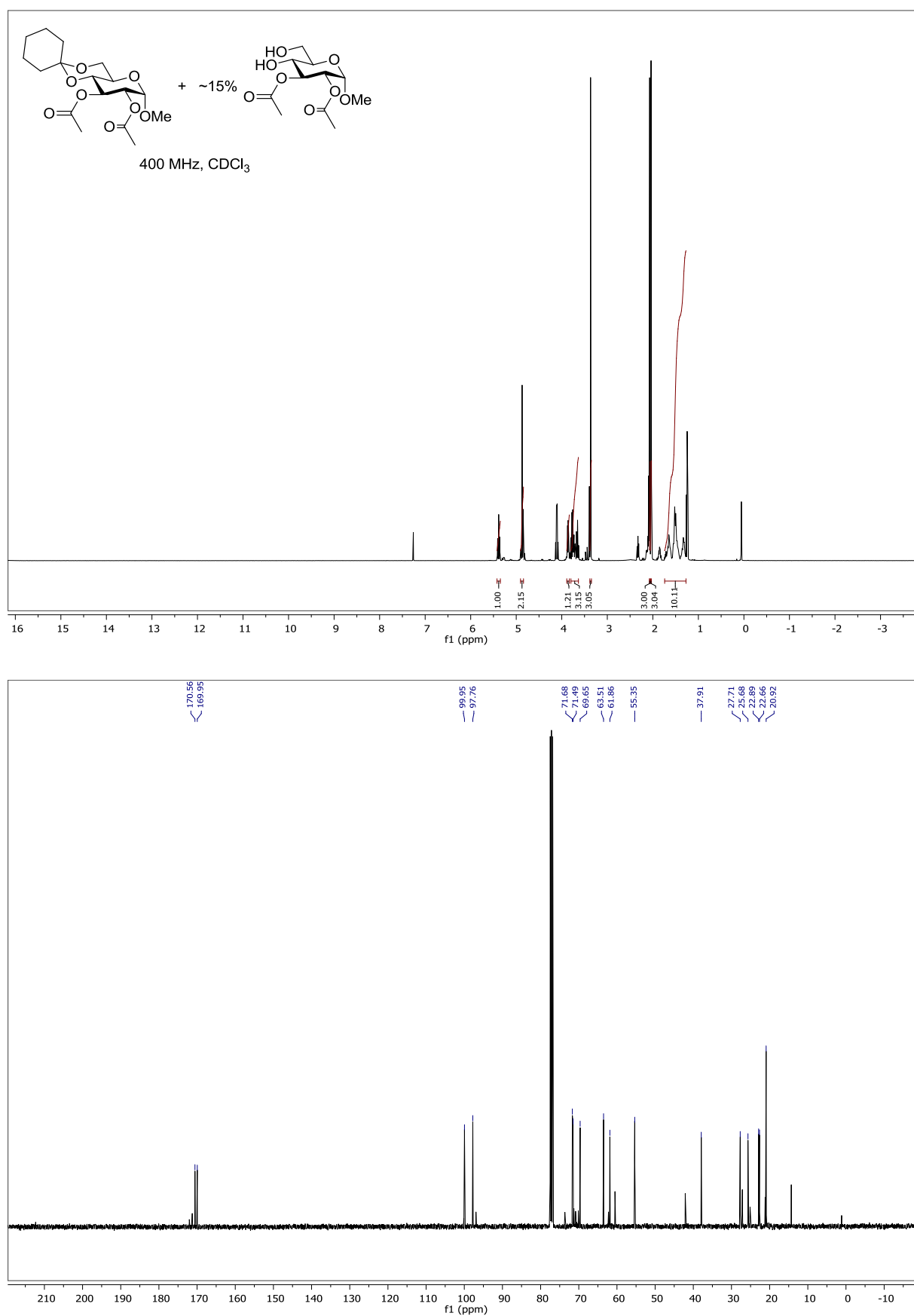
Methyl 2-*O*-acetyl-4,6-*O*-benzylidene- α -D-glucopyranoside (4)

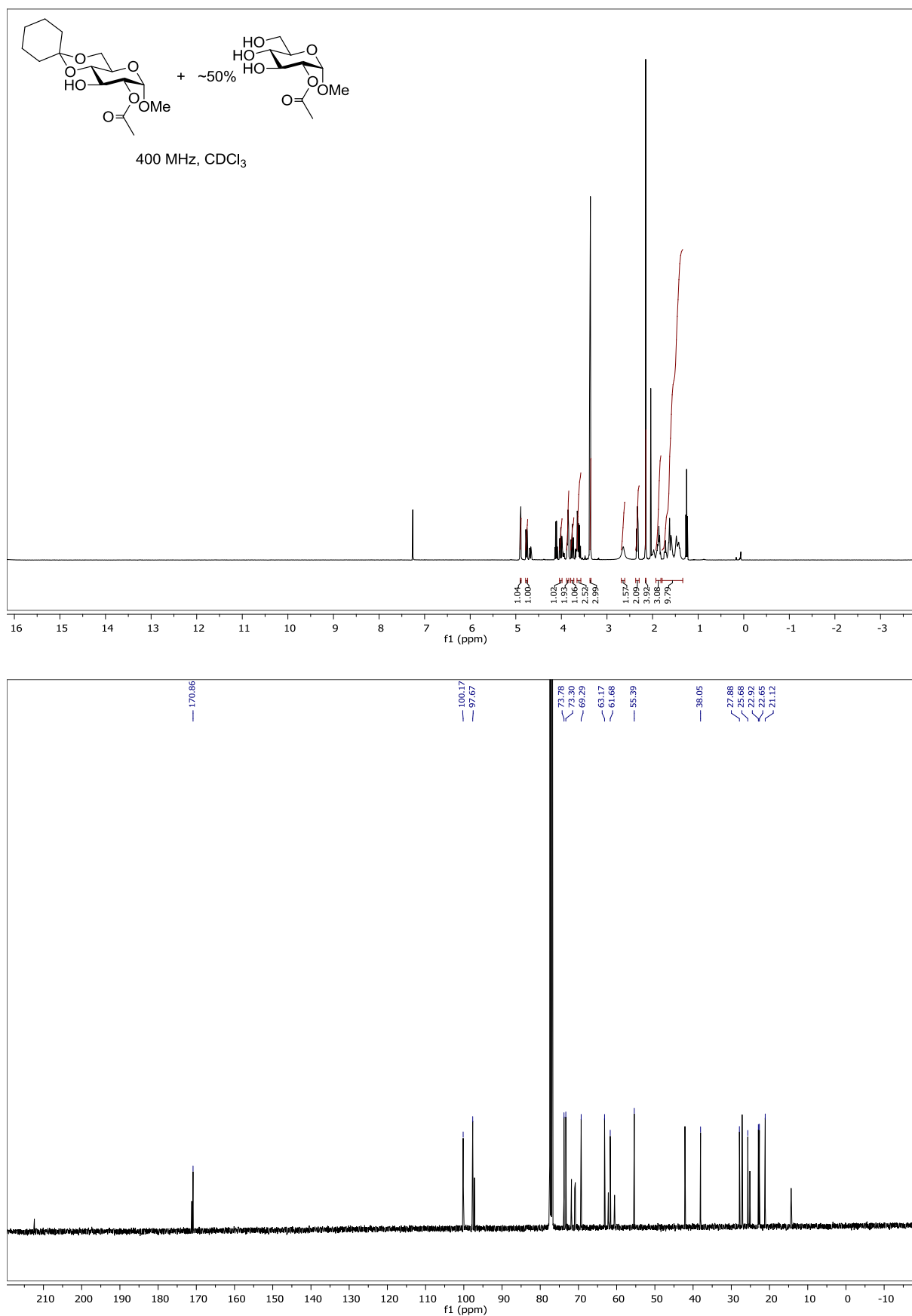


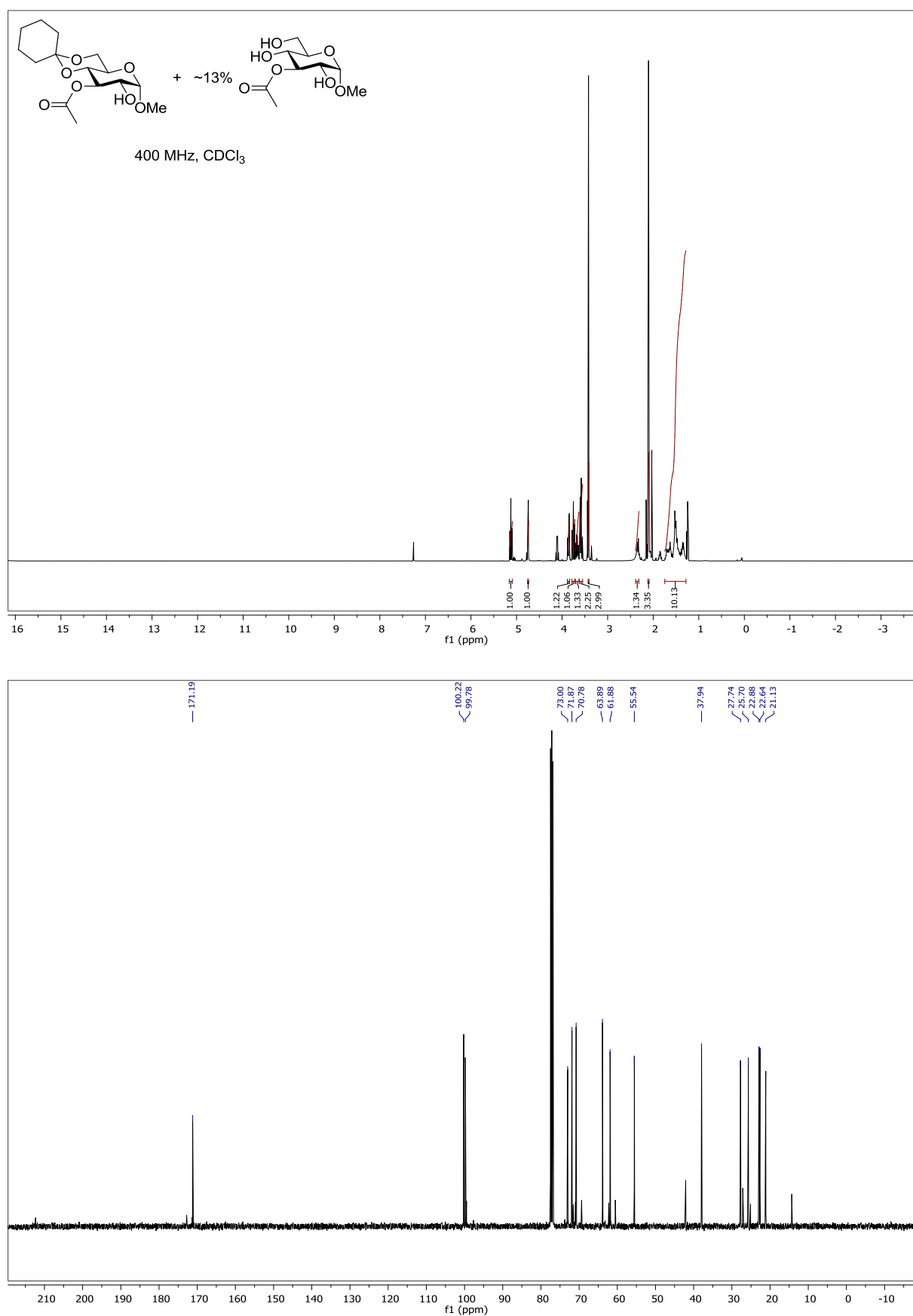
Methyl 3-*O*-acetyl-4,6-*O*-benzylidene- α -D-glucopyranoside (5)

Methyl 4,6-*O*-cyclohexylidene- α -D-glucopyranoside (26)



Methyl 2,3-di-*O*-acetyl-4,6-*O*-cyclohexylidene- α -D-glucopyranoside (27)

Methyl 2-*O*-acetyl-4,6-*O*-cyclohexylidene- α -D-glucopyranoside (28)


Methyl 3-*O*-acetyl-4,6-*O*-cyclohexylidene- α -D-glucopyranoside (29)

5. References

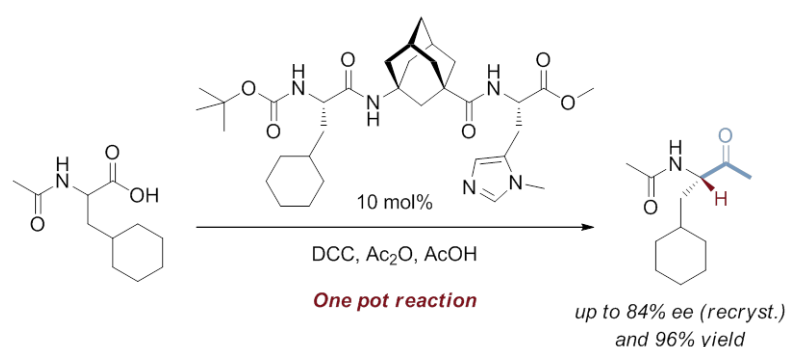
- [1] A. Varki, J. B. Lowe, *Essentials of Glycobiology*, 2nd ed., Cold Spring Harbor Laboratory Press, Cold Spring Harbor (NY), **2009**.
- [2] a) K. Toshima, K. Tatsuta, *Chem. Rev.* **1993**, *93*, 1503–1531; b) S. J. Danishefsky, M. T. Bilodeau, *Angew. Chem. Int. Ed.* **1996**, *35*, 1380–1419; c) S. Hanessian, B. Lou, *Chem. Rev.* **2000**, *100*, 4443–4464; d) K.-H. Jung, M. Müller, R. R. Schmidt, *Chem. Rev.* **2000**, *100*, 4423–4442; e) P. H. Seeberger, W.-C. Haase, *Chem. Rev.* **2000**, *100*, 4349–4394; f) P. Sears, C.-H. Wong, *Science* **2001**, *291*, 2344–2350; g) P. H. Seeberger, D. B. Werz, *Nat. Rev. Drug Discovery* **2005**, *4*, 751–763; h) T. J. Boltje, T. Buskas, G.-J. Boons, *Nat. Chem.* **2009**, *1*, 611–622; i) B. Ernst, J. L. Magnani, *Nat. Rev. Drug Discovery* **2009**, *8*, 661–677; j) X. Zhu, R. R. Schmidt, *Angew. Chem. Int. Ed.* **2009**, *48*, 1900–1934; k) M. C. Galan, D. Benito-Alifonso, G. M. Watt, *Org. Biomol. Chem.* **2011**, *9*, 3598–3610; l) C.-H. Hsu, S.-C. Hung, C.-Y. Wu, C.-H. Wong, *Angew. Chem. Int. Ed.* **2011**, *50*, 11872–11923; m) D. Lee, M. S. Taylor, *Synthesis* **2012**, *44*, 3421–3431; n) S. C. Ranade, A. V. Demchenko, *J. Carbohydr. Chem.* **2013**, *32*, 1–43; o) E. Lenci, G. Menchi, A. Trabocchi, *Org. Biomol. Chem.* **2016**, *14*, 808–825; p) S. V. Moradi, W. M. Hussein, P. Varamini, P. Simerska, I. Toth, *Chem. Sci.* **2016**, *7*, 2492–2500; q) M. Jäger, A. J. Minnaard, *Chem. Commun.* **2016**, *52*, 656–664.
- [3] a) K. W. Buck, A. B. Foster, A. R. Perry, J. M. Webber, *J. Chem. Soc.* **1963**, 4171–4177; b) J. Lehrfeld, *Carbohydr. Res.* **1975**, *39*, 364–367; c) T. Kurahashi, T. Mizutani, J.-i. Yoshida, *J. Chem. Soc., Perkin Trans. 1* **1999**, 465–474; d) T. Kurahashi, T. Mizutani, J.-i. Yoshida, *Tetrahedron* **2002**, *58*, 8669–8677; e) H. Dong, Z. Pei, S. Byström, O. Ramström, *J. Org. Chem.* **2007**, *72*, 1499–1502.
- [4] a) K. S. Griswold, S. J. Miller, *Tetrahedron* **2003**, *59*, 8869–8875; b) C. A. Lewis, S. J. Miller, *Angew. Chem. Int. Ed.* **2006**, *45*, 5616–5619; c) T. Kawabata, W. Muramatsu, T. Nishio, T. Shibata, H. Schedel, *J. Am. Chem. Soc.* **2007**, *129*, 12890–12895; d) Y. Ueda, W. Muramatsu, K. Mishiro, T. Furuta, T. Kawabata, *J. Org. Chem.* **2009**, *74*, 8802–8805; e) C. A. Lewis, K. E. Longcore, S. J. Miller, P. A. Wender, *J. Nat. Prod.* **2009**, *72*, 1864–1869; f) W. Muramatsu, K. Mishiro, Y. Ueda, T. Furuta, T. Kawabata, *Eur. J. Org. Chem.* **2010**, 827–831; g) X. Sun, H. Lee, S. Lee, K. L. Tan, *Nat. Chem.* **2013**, *5*, 790–795; h) S. Yoganathan, S. J. Miller, *J. Med. Chem.* **2015**, *58*, 2367–2377.
- [5] R. C. Wende, P. R. Schreiner, *Green Chem.* **2012**, *14*, 1821–1849.
- [6] a) C. E. Müller, L. Wanka, K. Jewell, P. R. Schreiner, *Angew. Chem. Int. Ed.* **2008**, *47*, 6180–6183; b) C. E. Müller, D. Zell, P. R. Schreiner, *Chem.–Eur. J.* **2009**, *15*, 9647–9650; c) R. Hrdina, C. E. Müller, P. R. Schreiner, *Chem. Commun.* **2010**, *46*, 2689–2690; d) C. E. Müller, D. Zell, R. Hrdina, R. C. Wende, L. Wanka, S. M. M. Schuler, P. R. Schreiner, *J. Org. Chem.* **2013**, *78*, 8465–8484.
- [7] a) C. E. Müller, R. Hrdina, R. C. Wende, P. R. Schreiner, *Chem.–Eur. J.* **2011**, *17*, 6309–6314; b) R. Hrdina, C. E. Müller, R. C. Wende, L. Wanka, P. R. Schreiner, *Chem. Commun.* **2012**, *48*, 2498–2500; c) C. Hofmann, S. M. M. Schuler, R. C. Wende, P. R. Schreiner, *Chem. Commun.* **2014**, *50*, 1221–1223; d) C. Hofmann, J. M. Schumann, P. R. Schreiner, *J. Org. Chem.* **2015**, *80*, 1972–1978.
- [8] P. R. Schreiner, A. Wittkopp, *Org. Lett.* **2002**, *4*, 217–220.
- [9] a) E. I. Balmond, M. C. Galan, E. M. McGarrigle, in *Encyclopedia of Reagents for Organic Synthesis*, John Wiley & Sons, Ltd, **2014**; b) Z. Zhang, Z. Bao, H. Xing, *Org. Biomol. Chem.* **2014**, *12*, 3151–3162; c) R. Hrdina, C. E. Müller, R. C. Wende, K. M. Lippert, M. Benassi, B. Spengler, P. R. Schreiner, *J. Am. Chem. Soc.* **2011**, *133*, 7624–7627; d) E. I. Balmond, D. M. Coe, M. C. Galan, E. M. McGarrigle, *Angew. Chem. Int. Ed.* **2012**, *51*, 9152–9155; e) G. Jakab, A. Hosseini, H. Hausmann, P. R. Schreiner, *Synthesis* **2013**, *45*, 1635–1640; f) Y. Geng, H. M. Faidallah, H. A. Albar, I. A. Mhkalid, R. R. Schmidt, *Eur. J. Org. Chem.* **2013**, 7035–7040; g) Y. Geng, A. Kumar, H. M. Faidallah, H. A. Albar, I. A. Mhkalid, R. R. Schmidt, *Angew. Chem. Int. Ed.* **2013**, *52*, 10089–10092; h) N. Mittal, K. M. Lippert, C. K. De, E. G. Klauber, T. J. Emge, P. R. Schreiner, D. Seidel, *J. Am. Chem. Soc.* **2015**, *137*, 5748–5758.
- [10] M. Kotke, P. R. Schreiner, *Synthesis* **2007**, 779–790.
- [11] T. Weil, M. Kotke, C. M. Kleiner, P. R. Schreiner, *Org. Lett.* **2008**, *10*, 1513–1516.
- [12] L. Verdoucq, J. Morinière, D. R. Bevan, A. Esen, A. Vasella, B. Henrissat, M. Czjze, *J. Biol. Chem.* **2004**, *279*, 31796–31803.
- [13] N. Moitessier, P. Englebienne, Y. Chapleur, *Tetrahedron* **2005**, *61*, 6839–6853.

- [14] a) R. W. Jeanloz, D. A. Jeanloz, *J. Am. Chem. Soc.* **1957**, 79, 2579–2583; b) S. Hanessian, M. Kagotani, *Carbohydr. Res.* **1990**, 202, 67–79.
- [15] X.-A. Lu, C.-H. Chou, C.-C. Wang, S.-C. Hung, *Synlett* **2003**, 1364–1366.
- [16] X. Liu, B. Becker, M. A. Cooper, *Aust. J. Chem.* **2014**, 67, 679–683.
- [17] R. Eby, K. T. Webster, C. Schuerch, *Carbohydr. Res.* **1984**, 129, 111–120.
- [18] C. L. Allen, S. J. Miller, *Org. Lett.* **2013**, 15, 6178–6181.
- [19] H. Wang, J. She, L.-H. Zhang, X.-S. Ye, *J. Org. Chem.* **2004**, 69, 5774–5777.
- [20] Y. Zhou, O. Ramström, H. Dong, *Chem. Commun.* **2012**, 48, 5370–5372.
- [21] Y. Zhou, M. Rahm, B. Wu, X. Zhang, B. Ren, H. Dong, *J. Org. Chem.* **2013**, 78, 11618–11622.
- [22] a) M. J. Chinn, G. Lacazio, D. G. Spackman, N. J. Turner, S. M. Roberts, *J. Chem. Soc., Perkin Trans. 1* **1992**, 661–662; b) L. Panza, M. Luisetti, E. Crociati, S. Riva, *J. Carbohydr. Chem.* **1993**, 12, 125–130.
- [23] B. Ren, M. Wang, J. Liu, J. Ge, H. Dong, *ChemCatChem* **2015**, 7, 761–765.
- [24] J. Li, Y. Wang, *Synth. Commun.* **2004**, 34, 211–217.
- [25] a) *Spartan '14*, 1.1.4, Wavefunction, Inc.; 18401 Von Karman Ave., Suite 370, Irvine, CA 92612; b) Visualization: C. Y. Legault, *CYLVview*, 1.0b; Université de Sherbrooke: Sherbrooke, QC, 2009; <http://www.cylvview.org>.
- [26] L. Wanka, C. Cabrele, M. Vanejews, P. R. Schreiner, *Eur. J. Org. Chem.* **2007**, 1474–1490.
- [27] a) H. E. Gottlieb, V. Kotlyar, A. Nudelman, *J. Org. Chem.* **1997**, 62, 7512–7515; b) G. R. Fulmer, A. J. M. Miller, N. H. Sherden, H. E. Gottlieb, A. Nudelman, B. M. Stoltz, J. E. Bercaw, K. I. Goldberg, *Organometallics* **2010**, 29, 2176–2179.
- [28] M. Adinolfi, L. De Napoli, G. Di Fabio, A. Iadonisi, D. Montesarchio, G. Piccialli, *Tetrahedron* **2002**, 58, 6697–6704.
- [29] M. Adinolfi, A. Iadonisi, A. Pastore, *Tetrahedron Lett.* **2009**, 50, 7051–7054.
- [30] P. A. Wallace, D. E. Minnikin, *Carbohydr. Res.* **1994**, 263, 43–59.
- [31] H. C. Beyerman, L. Maat, A. van Zon, *Recl. Trav. Chim. Pays-Bas* **1972**, 91, 246–250.
- [32] B.-C. Chen, A. P. Skoumbourdis, P. Guo, M. S. Bednarz, O. R. Kocy, J. E. Sundeen, G. D. Vite, *J. Org. Chem.* **1999**, 64, 9294–9296.
- [33] J. Rivier, W. Vale, M. Monahan, N. Ling, R. Burgus, *J. Med. Chem.* **1972**, 15, 479–482.
- [34] L. Wanka, PhD-Thesis, Justus-Liebig University (Gießen), **2007**.

- Chapter VI -

The Enantioselective Dakin–West Reaction

Raffael C. Wende, Alexander Seitz, Dominik Nidek, Sören M. M. Schuler, Christine Hofmann, Jonathan Becker, and Peter R. Schreiner, *Angew. Chem. Int. Ed.* **2016**, 55, 2719–2723



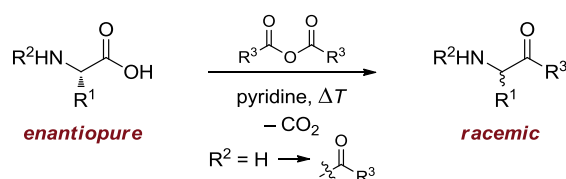
Abstract

Here we report the development of the first enantioselective Dakin–West reaction, yielding α -acetamido methylketones with up to 58 % *ee* with good yields. Two of the obtained products were recrystallized once to achieve up to 84 % *ee*. The employed methylimidazole-containing oligopeptides catalyze both the acetylation of the azlactone intermediate and the terminal enantioselective decarboxylative protonation. We propose a dispersion-controlled reaction path that determines the asymmetric reprotonation of the intermediate enolate after the decarboxylation.

"Reproduced with permission from *Angewandte Chemie International Edition* **2016**, 55, 2719–2723. Copyright 2016 Wiley-VCH Verlag GmbH & Co. KGaA, Weinheim."

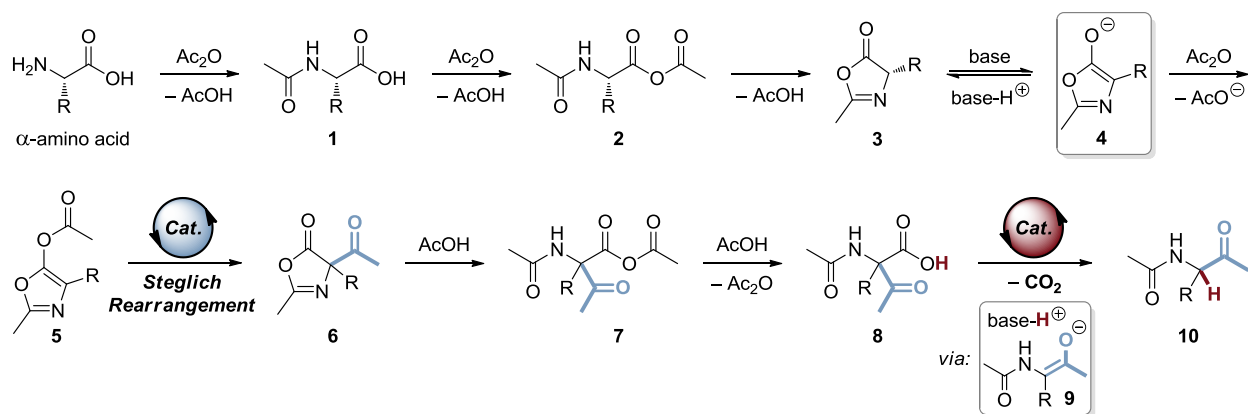
1. The Enantioselective Dakin–West Reaction

Even though the Dakin–West (DW) reaction dates back to 1928,^[1] it is still one of the most effective synthetic procedures to prepare α -acylamido ketones from primary α -amino acids.^[2] Generally, the treatment of an amino acid with an acid anhydride and base, typically pyridine, at elevated temperature provides the desired product upon liberation of CO_2 (Scheme 1). Numerous modifications of the original reaction conditions were developed,^[2] including catalytic variants,^[3] broadening its scope and applicability. Unsurprisingly, the DW reaction found application in the preparation of α -acylamido ketones as valuable precursors for various biologically active compounds,^[4] and even in Woodward's fundamental total synthesis of strychnine.^[5] Remarkably, no asymmetric variant has been developed to date, thus restricting the use of this important reaction in modern synthetic chemistry.



Scheme 1. The Dakin–West reaction of α -amino acids.

According to the currently accepted mechanism,^[6] the reaction of an amino acid with the anhydride leads to the *N*-acetyl derivative **1** and subsequently to the mixed anhydride **2** (Scheme 2). Cyclization of **2** provides the oxazol-5(4*H*)-one (azlactone) **3**. Such azlactones are acidic owing to the formation of resonance stabilized enolate **4** upon deprotonation. Subsequent acetylation may occur at the enolate oxygen atom (affording **5**) or directly at the carbon atom to give **6**.^[7] However, **6** is exclusively produced under the typical DW reaction conditions because



Scheme 2. Proposed mechanism for the Dakin–West reaction.

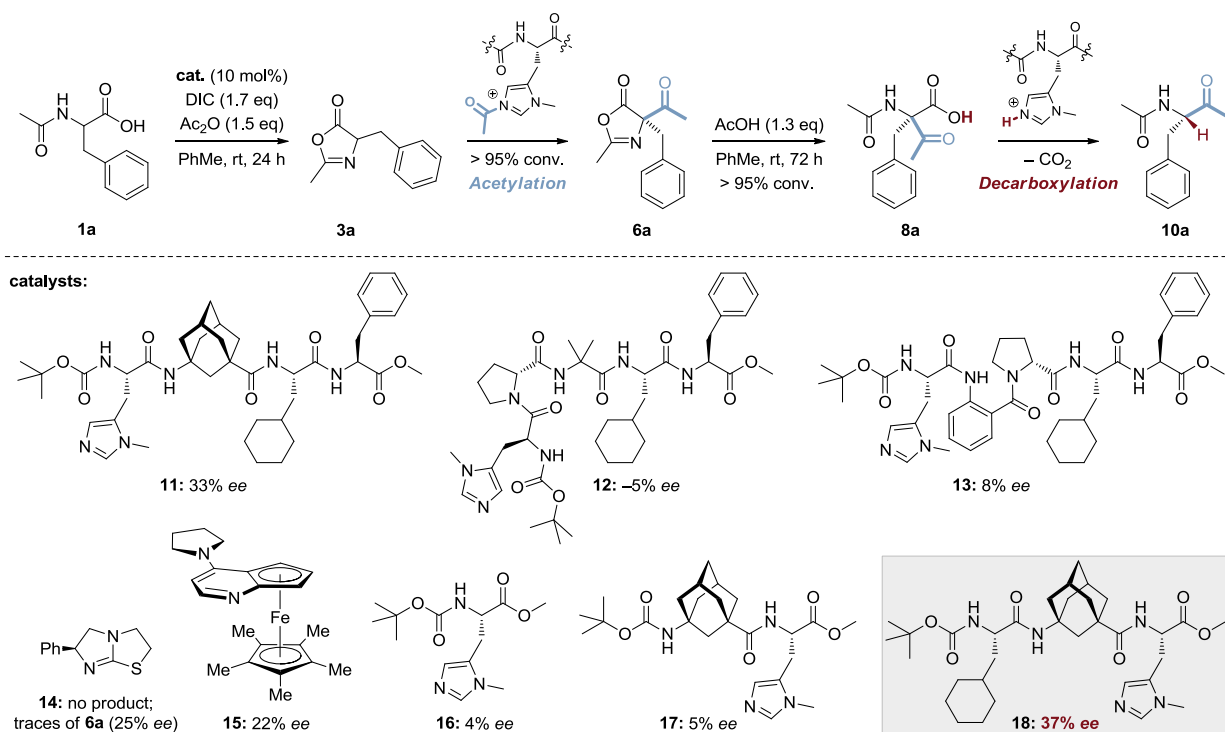
of concomitant O→C acyl transfer (Steglich rearrangement).^[8] Opening of **6** with acetic acid, formed in previous steps, to the mixed anhydride **7** and transacylation gives the β-keto acid **8**,^[6f] which is prone to decarboxylation upon deprotonation. This final reaction step affords the desired α-acetamido methylketone **10**, likely via enolate **9**. Other pathways, for example, the acylation of **2** to directly give **7**,^[9] were discussed as well but have been shown to be rather improbable. It is evident from this mechanistic picture that the intermediacy of **4** and **9** (Scheme 2) leads to the observed complete racemization, making an asymmetric reaction a difficult endeavor. We surmized, however, that an enantioselective decarboxylative protonation^[10] of **8** (via **9**) would afford enantioenriched products. Herein we show that this is indeed possible with a tailor-made catalytic system.

We chose synthetic oligopeptides as catalysts^[11] as these should be well-suited for binding the amino acid derived intermediates, as demonstrated for such platforms in acyl transfer reactions.^[12] Incorporation of catalytically active π-methylhistidine (Pmh) in a dual role as Lewis base for the acetyl transfer (Scheme 2) and as Brønsted base in the decarboxylative protonation (Scheme 2) may allow performing the entire reaction by employing a single catalyst.

Our investigation commenced with an evaluation of appropriate reaction conditions for the proposed reaction sequence starting from DL-phenylalanine and our previously successfully employed acylation catalyst **11**^[12] (Scheme 3; see the Supporting Information for details). We found that the methylimidazole moiety itself is not sufficiently basic to deprotonate the azlactone **3a** ($pK_a \approx 9$ ^[13] vs. $pK_a = 7.3$ for protonated *N*-methylimidazole)^[14] and acetic acid is continuously formed during the reaction. Addition of a base significantly increases the reaction rate but has a deleterious effect on enantioselectivity. Thus, we concluded that the mechanistic complexity of the reaction necessitates well-balanced reaction conditions to separate the acetylation of **3** and the decarboxylation. The use of a carbodiimide helps overcome these challenges: it enables fast cyclization of **1** to **3**, acts as auxiliary base in the deprotonation step, and converts the acetic acid produced back into the anhydride. Most importantly, the only side-product formed is the corresponding urea derivative, which cannot participate as a base in the final decarboxylation step and therefore does not erode enantioselectivity. Indeed, **3a** immediately forms when *N,N'*-diisopropylcarbodiimide (DIC) is used as an additive. Addition of acetic anhydride then furnishes the key intermediate **6a** with full conversion of **3a**. Further addition of acetic acid initiates the decarboxylation step, thus leading to the formation of the α-acetamido methylketone **10a** with 33% *ee*, enriched in the *S*-configured enantiomer (Scheme 3). We were able to monitor the reaction by GC-MS and observed some of the intermediates (see the Supporting Information, Figure S2).

The feasibility of our catalyst design concept was next evaluated using different turns instead of the adamantane amino acid (Scheme 3).^[15] Incorporation of a d-Pro-Aib-turn (**12**), frequently

used by Miller *et al.*,^[11a,16] or an 2-Abz-D-Pro pseudo- β -hairpin (**13**),^[17] resulted in 5% and 8% *ee*, respectively. We also studied (*S*)-tetramisol (**14**) and the chiral (*S*)-PPY* **15**,^[18] reported by Fu and co-workers, as both catalysts were previously employed in an asymmetric Steglich rearrangement.^[8,19] With **14** only traces of enantioenriched **6a** (25% *ee*) formed, and **10a** could not be detected. Remarkably, **15** gave 22% *ee* for the desired product and may be considered a potential catalyst for further optimization. To gain further insight into the factors determining enantioselectivity and to improve catalyst performance, we modularly built the catalyst from the C-terminal Pmh. Thus, Boc-L-Pmh-OMe (**16**) and dipeptide **17** did not provide enantioenriched product as neither catalyst is able to form a dynamic binding pocket^[12] for the enolate **9a**, and they also lack the necessary hydrogen bonding contacts. However, when tripeptides were used the selectivities substantially increased (see the Supporting Information for complete catalyst library), with **18**, bearing cyclohexylalanine, being the best catalyst. The strikingly better performance of the shorter tripeptide **18** compared to that of the tetrapeptide **11** is probably a result of the C-terminal Pmh (interchange of the amide NH and C=O groups), which leads to more efficient substrate binding.

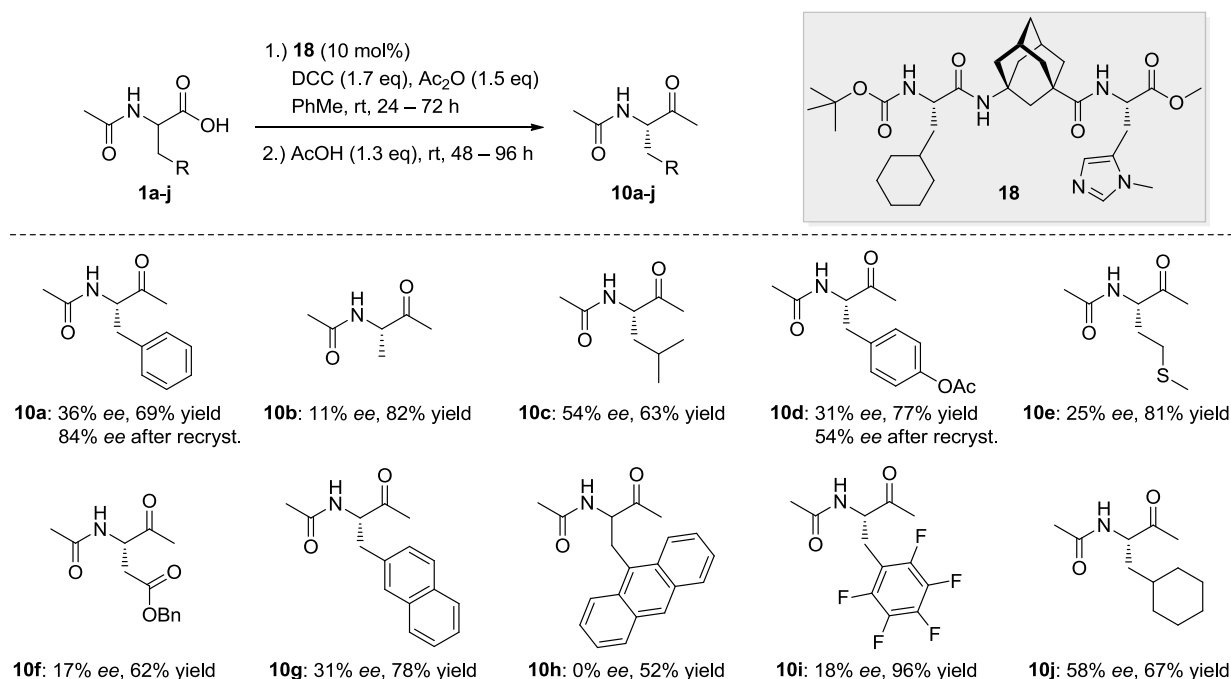


Scheme 3. Testing and optimizing reaction conditions for selected catalysts. Reactions were performed on an analytical scale (0.1 mmol). The absolute configuration of **10a** was determined to be *S* by comparison of the retention times of an authentic sample on chiral-phase HPLC. Enantiomeric excesses (a negative sign indicates the formation of the opposite enantiomer) for **6a** and **10a** were determined by chiral-phase GC. Conversion was >95% for the individual reaction steps as judged by GC-MS unless noted otherwise. For complete catalyst library see the Supporting Information.

Note that most of the catalysts employed were also able to enantioselectively acetylate the azlactone intermediate. However, no correlation is apparent from the selectivity obtained for **6a** and the final product **10a**, and no amplification of stereoselectivity was observed. That is, the enantioenrichment of **10a** does not ensue from kinetic resolution of **6a**. As we anticipated by the proposed mechanism, the selectivity for **6a** is not preserved in the product and only results from the final decarboxylation and enantioselective enolate reprotonation. To further prove this observation, DMAP was used as an achiral catalyst for the in situ formation of **6a**, and **18** was only added for the decarboxylation step. However, the selectivities differed only marginally (see the Supporting Information, Table S5).

From this point on, we used **18** for substrate screening and *N,N'*-dicyclohexylcarbodiimide (DCC) instead of DIC because it is easier to remove the corresponding urea derivative in the purification of the final products (Scheme 4). Thus, **10a** was isolated in 69% yield with 36% *ee*. Substrates with sterically less demanding side chains, such as alanine and methionine derivatives, afforded the desired products with low selectivities but with high yields (**10b** and **10e**). The product **10c**, derived from leucine, was isolated with appreciable higher enantioselectivity (54%) and 63% yield. The tyrosine-derived **1d** gave 31% *ee* with 77% yield, whereas polar functional groups led to low selectivities (**10f**: 17%). We next employed sterically more demanding amino acids bearing aromatic side chains, namely, naphthyl- and anthranylalanine derivatives, **1g** and **1h**, respectively. Lower enantioselectivity (31% *ee*, 78% yield) resulted for **10g**, whereas **10h** was obtained in racemic form in a moderate 52% yield. Strongly electron-withdrawing side-chains, such as that in **1i**, afforded the product with excellent yield but lower selectivity (**10i**: 18% *ee*, 96% yield), and probably resulting from racemization (see the Supporting Information). To our delight, as seen for **1c**, the selectivity was further enhanced to 58% *ee* (67% yield) when the aliphatic cyclohexylalanine **1j** was used as a substrate. Importantly, **10a** and **10d** could be obtained, with up to 84% *ee* (for **10a**), after one recrystallization.

The observed selectivities can effectively compete with previously reported organocatalytic enantioselective decarboxylative protonation reactions which are typically in the range of 30–60% *ee*.^[10a,c,d] Organocatalytic variants that achieve higher enantioselectivities (above 70% *ee*) are rare.^[20] Higher selectivities (>90% *ee*) have, so far, only been achieved either in the presence of stoichiometric amounts of base^[21] or by employing transition metals, for example, palladium complexes^[22] or enzymes.^[10a,23] Unlike the former examples, as well as decarboxylative addition reactions,^[10c,d,24] the DW reaction described herein is particularly challenging as it presupposes the stereoselective transfer of the smallest electrophile, a proton, in the presence of significant amounts of acid in a complex multistep reaction (Scheme 2).



Scheme 4. Substrate scope and limitations. Stereochemistry for the products was assigned as *S* by analogy to **10a**. Enantiomeric excesses were determined by chiral-phase GC or HPLC. Yields refer to those of isolated products. Values within parentheses correspond to recrystallized products.

Although the exact nature of the decarboxylation step is not yet clear, the stereoinduction probably arises from the deprotonation of β -keto acid **8** (Scheme 2) by the catalyst, release of CO₂, and subsequent enantioselective reprotonation as reported for related organocatalytic decarboxylative protonation reactions.^[10a,c,d,25] Thus, we computationally identified possible adducts of the protonated catalyst **18** and enolate **9j** as minima wherein the transferred proton is in close proximity to the α -carbon atom of the intermediate (1.94 Å for both structures), thus supporting our mechanistic proposal (Figure 1). These data also emphasized the importance of the amino acid at the *i*–2 position for binding. Indeed, the computed structure that would afford the observed *S* selectivity (Figure 1 A) is favored by 2.1 kcal mol^{–1} compared to the complex leading to (*R*)-**10j** (Figure 1 B). The observed selectivities mainly result from shielding of one face of the enolate by its side-chain and by the catalysts cyclohexyl residue, thus precluding unselective reprotonation, for example, by acetic acid. However, the higher selectivities observed with **1c** and **1j** are likely to originate from attractive dispersion interactions between the catalysts cyclohexyl moiety and the isopropyl and cyclohexyl residue, respectively. Whereas the competing structure does not allow efficient stacking of the cyclohexyl rings, this interaction is enhanced for the favorably bound enolate (see noncovalent interactions (NCI)^[26] plot in Figure 1, C), leading to a more compact transition-state structure. Remarkably, the same effects were recently confirmed experimentally by NMR studies for the performance of **11** in enantioselective acylation reactions.^[12,27] The present example provides further evidence for the importance of attractive dispersion interactions in catalysis, even in the presence of hydrogen bonds or ion pairs.^[28]

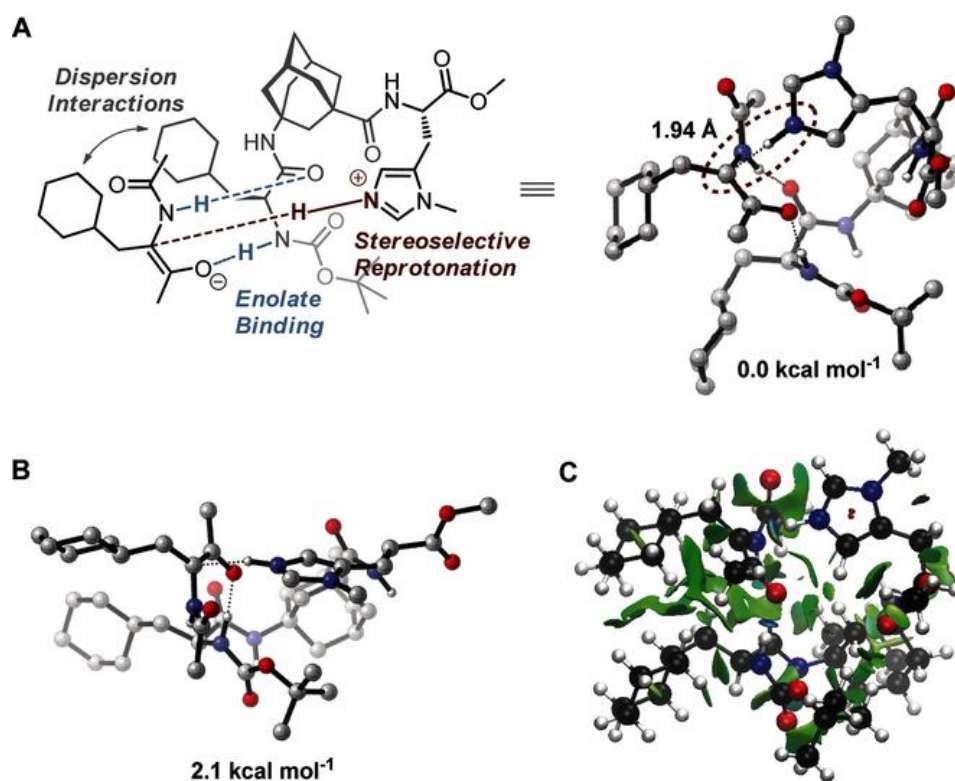


Figure 1. B3LYP-D3(BJ)/6-31+G(d,p) optimized structures representing the association of the protonated **18** with enolate **9j** and key catalyst–substrate interactions. A) Adduct leading to (*S*)-**10j**. B) Adduct leading to (*R*)-**10j**. All C–H bonds were omitted for clarity. C) NCI plot; green isosurfaces indicate attractive interactions.

The development of the first enantioselective Dakin–West reaction opens a new avenue to further develop related reactions. We now focus on the detailed investigation and elucidation of the decarboxylation step with the goal to rationally design novel and highly selective catalysts. Moreover, we will investigate the applicability of functionalized anhydrides, for example, towards the synthesis of enantiomerically enriched halo- and acyloxymethyl ketones that are frequently found chemical warheads in serine, cysteine, and threonine protease inhibitors.^[29]

Acknowledgments

We gratefully acknowledge financial support by the Deutsche Forschungsgemeinschaft (SPP1807 Dispersion, Schr 597/27-1).

1.1 References

- [1] a) H. D. Dakin, R. West, *J. Biol. Chem.* **1928**, 78, 91–104; b) H. D. Dakin, R. West, *J. Biol. Chem.* **1928**, 78, 745–756.
- [2] a) G. L. Buchanan, *Chem. Soc. Rev.* **1988**, 17, 91–109; b) F. K. Behbahani, T. S. Dalooee, *Monatsh. Chem.* **2014**, 145, 683–709.
- [3] a) W. Steglich, G. Höfle, *Angew. Chem. Int. Ed. Engl.* **1969**, 8, 981; *Angew. Chem.* **1969**, 81, 1001; b) G. Höfle, W. Steglich, H. Vorbrüggen, *Angew. Chem. Int. Ed. Engl.* **1978**, 17, 569–583; *Angew. Chem.* **1978**, 90, 602–615.
- [4] a) T. T. Curran, *J. Fluorine Chem.* **1995**, 74, 107–112; b) A. G. Godfrey, D. A. Brooks, L. A. Hay, M. Peters, J. R. McCarthy, D. Mitchell, *J. Org. Chem.* **2003**, 68, 2623–2632; c) C.-M. Kam, M. G. Götz, G. Koot, M. McGuire, D. Thiele, D. Hudig, J. C. Powers, *Arch. Biochem. Biophys.* **2004**, 427, 123–134; d) J. Yu, L. Tang, Y. Yang, R. Ji, *Eur. J. Med. Chem.* **2008**, 43, 2428–2435; e) K. Otake, S. Azukizawa, M. Fukui, K. Kunishiro, H. Kamemoto, M. Kanda, T. Miike, M. Kasai, H. Shirahase, *Bioorg. Med. Chem.* **2012**, 20, 1060–1075; f) B. Dulla, K. T. Kirla, V. Rathore, G. S. Deora, S. Kavela, S. Maddika, K. Chatti, O. Reiser, J. Iqbal, M. Pal, *Org. Biomol. Chem.* **2013**, 11, 3103–3107.
- [5] R. B. Woodward, M. P. Cava, W. D. Ollis, A. Hunger, H. U. Daeniker, K. Schenker, *Tetrahedron* **1963**, 19, 247–288.
- [6] a) G. H. Cleland, C. Niemann, *J. Am. Chem. Soc.* **1949**, 71, 841–843; b) J. W. Cornforth, D. F. Elliott, *Science* **1950**, 112, 534–535; c) C. S. Rondestvedt, B. Manning, S. Tabibian, *J. Am. Chem. Soc.* **1950**, 72, 3183–3184; d) W. Steglich, G. Höfle, *Tetrahedron Lett.* **1968**, 9, 1619–1624; e) W. Steglich, G. Höfle, *Chem. Ber.* **1971**, 104, 3644–3652; f) G. Höfle, A. Prox, W. Steglich, *Chem. Ber.* **1972**, 105, 1718–1725; g) N. L. Allinger, G. L. Wang, B. B. Dewhurst, *J. Org. Chem.* **1974**, 39, 1730–1735; h) L. Dalla-Vechia, V. G. Santos, M. N. Godoi, D. Cantillo, C. O. Kappe, M. N. Eberlin, R. O. M. A. de Souza, L. S. M. Miranda, *Org. Biomol. Chem.* **2012**, 10, 9013–9020.
- [7] T. H. Black, *Org. Prep. Proced.* **1989**, 21, 179–217.
- [8] a) W. Steglich, G. Höfle, *Angew. Chem. Int. Ed. Engl.* **1968**, 7, 61; *Angew. Chem.* **1968**, 80, 44; b) W. Steglich, G. Höfle, *Chem. Ber.* **1969**, 102, 883–898; c) W. Steglich, G. Höfle, *Tetrahedron Lett.* **1970**, 11, 4727–4730.
- [9] P. A. Levene, R. E. Steiger, *J. Biol. Chem.* **1928**, 79, 95–103.
- [10] a) J. Blanchet, J. Baudoux, M. Amere, M.-C. Lasne, J. Rouden, *Eur. J. Org. Chem.* **2008**, 5493–5506; b) J. T. Mohr, A. Y. Hong, B. M. Stoltz, *Nat. Chem.* **2009**, 1, 359–369; c) Y. Pan, C.-H. Tan, *Synthesis* **2011**, 2044–2053; d) S. Nakamura, *Org. Biomol. Chem.* **2014**, 12, 394–405.
- [11] a) E. A. C. Davie, S. M. Mennen, Y. Xu, S. J. Miller, *Chem. Rev.* **2007**, 107, 5759–5812; b) H. Wennemers, *Chem. Commun.* **2011**, 47, 12036–12041; c) B. Lewandowski, H. Wennemers, *Curr. Opin. Chem. Biol.* **2014**, 22, 40–46.
- [12] C. E. Müller, D. Zell, R. Hrdina, R. C. Wende, L. Wanka, S. M. M. Schuler, P. R. Schreiner, *J. Org. Chem.* **2013**, 78, 8465–8484.
- [13] J. De Jersey, B. Zerner, *Biochemistry* **1969**, 8, 1967–1974.
- [14] J. J. Kličić, R. A. Friesner, S.-Y. Liu, W. C. Guida, *J. Phys. Chem. A* **2002**, 106, 1327–1335.
- [15] L. Wanka, C. Cabrele, M. Vanejews, P. R. Schreiner, *Eur. J. Org. Chem.* **2007**, 1474–1490.
- [16] a) E. R. Jarvo, S. J. Miller, *Tetrahedron* **2002**, 58, 2481–2495; b) J. T. Blank, S. J. Miller, *Biopolymers* **2006**, 84, 38–47.
- [17] R. V. Nair, A. S. Kotmale, S. A. Dhokale, R. L. Gawade, V. G. Puranik, P. R. Rajamohanam, G. J. Sanjayan, *Org. Biomol. Chem.* **2014**, 12, 774–782.
- [18] J. C. Ruble, G. C. Fu, *J. Am. Chem. Soc.* **1998**, 120, 11532–11533.
- [19] F. R. Dietz, H. Gröger, *Synthesis* **2009**, 4208–4218.
- [20] a) H. Brunner, P. Schmidt, *Eur. J. Org. Chem.* **2000**, 2119–2133; b) H. Brunner, M. A. Baur, *Eur. J. Org. Chem.* **2003**, 2854–2862; c) T. Seitz, J. Baudoux, H. Bekolo, D. Cahard, J.-C. Plaquevent, M.-C. Lasne, J. Rouden, *Tetrahedron* **2006**, 62, 6155–6165; d) T. Tite, M. Sabbah, V. Levacher, J.-F. Briere, *Chem. Commun.* **2013**, 49, 11569–11571.
- [21] M. Amere, M.-C. Lasne, J. Rouden, *Org. Lett.* **2007**, 9, 2621–2624.

- [22] a) J. T. Mohr, T. Nishimata, D. C. Behenna, B. M. Stoltz, *J. Am. Chem. Soc.* **2006**, *128*, 11348–11349; b) S. C. Marinescu, T. Nishimata, J. T. Mohr, B. M. Stoltz, *Org. Lett.* **2008**, *10*, 1039–1042; c) R. Doran, P. J. Guiry, *J. Org. Chem.* **2014**, *79*, 9112–9124; d) R. Zhao, Z. Sun, M. Mo, F. Peng, Z. Shao, *Org. Lett.* **2014**, *16*, 4178–4181.
- [23] a) K. Okrasa, C. Levy, M. Wilding, M. Goodall, N. Baudendistel, B. Hauer, D. Leys, J. Micklefield, *Angew. Chem. Int. Ed.* **2009**, *48*, 7691–7694; *Angew. Chem.* **2009**, *121*, 7827–7830; b) R. Lewin, M. Goodall, M. L. Thompson, J. Leigh, M. Breuer, K. Baldenius, J. Micklefield, *Chem.–Eur. J.* **2015**, *21*, 6557–6563.
- [24] Z.-L. Wang, *Adv. Synth. Catal.* **2013**, *355*, 2745–2755.
- [25] A. Sengupta, R. B. Sunoj, *J. Org. Chem.* **2012**, *77*, 10525–10536.
- [26] E. R. Johnson, S. Keinan, P. Mori-Sánchez, J. Contreras-García, A. J. Cohen, W. Yang, *J. Am. Chem. Soc.* **2010**, *132*, 6498–6506.
- [27] A. Kolmer, PhD thesis, Technical University Darmstadt, **2015**.
- [28] J. P. Wagner, P. R. Schreiner, *Angew. Chem. Int. Ed.* **2015**, *54*, 12274–12296; *Angew. Chem.* **2015**, *127*, 12446–12471.
- [29] J. C. Powers, J. L. Asgian, Ö. D. Ekici, K. E. James, *Chem. Rev.* **2002**, *102*, 4639–4750.

2. Supporting Information

2.1 General remarks

Materials and methods. Unless otherwise specified, reagents were purchased from commercial suppliers at the highest purity grade available and were used as received. All solvents were distilled prior to use. Dry and absolute solvents were prepared using standard laboratory procedures and were stored over appropriate drying agents under argon atmosphere. Acetic anhydride was distilled and stored under argon with 4 Å molecular sieves.

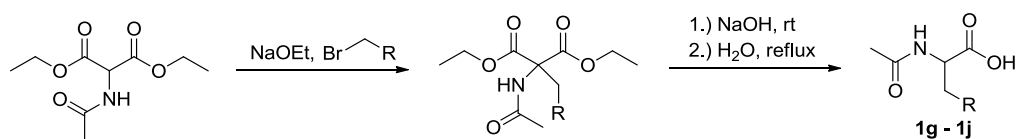
Flash column chromatography was performed using MN silica gel 60 M (Macherey-Nagel; 0.040 – 0.063 mm, 230 – 400 mesh ASTM). Analytical thin-layer chromatography (TLC) was performed using precoated polyester sheets Polygram[®] SIL G/UV₂₅₄ (Macherey-Nagel; 0.2 mm silica gel layer with fluorescent indicator). Visualization of the developed chromatograms was accomplished by irradiation with a UV lamp at 254 nm and/or phosphomolybdic acid solution, 2,4-dinitrophenylhydrazine solution or potassium permanganate solution, respectively. TLC R_f values are reported.

Instrumentation. NMR spectra were recorded on Bruker AV600, AV400 or AV200 spectrometers, respectively, at 298 K. Chemical shifts (δ) are given in ppm relative to tetramethylsilane (TMS, δ = 0.00 ppm) as the internal standard or to the respective solvent residual peaks (CDCl₃: δ = 7.26 and 77.16 ppm; DMSO- d_6 : δ = 2.50 and 39.52 ppm; D₂O: δ = 4.79 ppm; MeOH- d_4 : δ = 3.31 and 49.00 ppm).^[1] Data are reported as follows: chemical shift, multiplicity (s = singlet, d = doublet, t = triplet, q = quartet, m = multiplet, br = broad, or combinations thereof), coupling constants (Hz), integration. Infrared spectra were acquired on a Bruker IFS25 spectrometer. ESI mass spectrometry was performed employing a Finnigan LCQDuo spectrometer using methanol solutions of the respective compounds. High resolution mass spectrometry (HRMS) was performed employing a Thermo Scientific LTQ FT Ultra spectrometer (ESI) using methanol solutions of the respective compounds or a Finnigan MAT95 sectorfield spectrometer (EI). Elemental analysis was performed on a Thermo Flash EA 1112. Melting points were measured using a Krüss KSP1N capillary melting point apparatus and are uncorrected. GC-MS was carried out on a Hewlett Packard 5890 gas chromatograph with flame-ionization detector (FID) and Hewlett Packard 5971 mass selective detector (EI, 70 eV) equipped with J & W Scientific fused silica DB-5MS column (30 m \times 0.25 mm). Enantioselectivities were determined by chiral stationary phase GC analyses on Hewlett Packard 5890 or 6890 gas chromatographs, respectively, or by chiral stationary phase HPLC with a Dionex P680 pump in conjunction with a Shodex RI-101 detector. Preparative HPLC was performed employing a Gynkotec M480 pump with Knauer WellChrom K-2501 spectro-

photometer and a Dionex UltiMate 3000 equipped with a Shodex RI-101 detector for analytical runs.

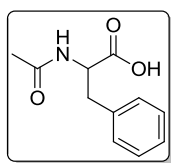
2.2 Starting Materials and Reaction Intermediates

N-acetyl derivatives of DL-leucine and DL-methionine were purchased from commercial suppliers and were used as received. *N*-acetyl-DL-phenylalanine (**1a**), *N*-acetyl DL-alanine (**1b**), *O,N*-diacetyl-L-tyrosine (**1d**) and *N*-acetyl-L-aspartic acid 4-benzyl ester (**1f**) were obtained through acetylation of the corresponding amino acids.



Starting materials **1g** – **1j** were synthesized from commercially available diethyl acetamidomalonate employing the procedure reported by Snyder *et al.*^[2] through the alkylation–saponification–decarboxylation^[3] reaction sequence shown above.

2.2.1 Synthesis of starting materials



***N*-acetyl-DL-phenylalanine (1a).** A suspension of DL-phenylalanine (3.35 g, 20.3 mmol) and acetic anhydride (5.0 mL, 5.40 g, 52.9 mmol) in methanol (9.0 mL) was stirred under reflux for 6 h. After cooling to rt all volatiles were removed under reduced pressure and the residue was triturated with ethyl acetate.

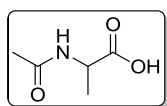
The resulting colorless solid was collected by filtration and dried *in vacuo*. Yield: 3.03 g (14.6 mmol, 72%), colorless solid. Mp 143 – 144 °C (lit.^[4] mp 142 °C).

¹H NMR (400 MHz, DMSO-*d*₆): δ = 12.57 (br s, 1H), 8.19 (d, *J* = 8.1 Hz, 1H), 7.31 – 7.17 (m, 5H), 4.40 (ddd, *J* = 9.5, 8.0, 4.9 Hz, 1H), 3.04 (dd, *J* = 13.8, 4.9 Hz, 1H), 2.83 (dd, *J* = 13.8, 9.6 Hz, 1H), 1.78 (s, 3H) ppm.

^{13}C NMR (100 MHz, DMSO- d_6): δ = 173.2, 169.2, 137.8, 129.1, 128.2, 126.4, 53.5, 36.8, 22.4 ppm.

IR (KBr): $\tilde{\nu}$ = 3359, 3031, 2933, 2737, 2500, 1711, 1618, 1548, 1495, 1445, 1428, 1343, 1253, 1220, 1199, 1188, 1120, 802, 739, 702, 671, 623, 606 cm^{-1} .

The spectroscopic data are in accordance with those reported.^[5]



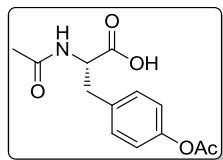
***N*-acetyl-DL-alanine (1b).** The title compound was synthesized following the procedure described for **1a** using DL-alanine (1.81 g, 20.3 mmol), acetic anhydride (5.0 mL, 5.40 g, 52.9 mmol) and methanol (9.0 mL). Yield: 1.69 g (12.9 mmol, 64%), colorless solid. Mp 136–136.5 °C (lit.^[6] mp 136 – 137 °C).

^1H NMR (400 MHz, D_2O): δ = 4.29 (q, J = 7.3 Hz, 1H), 1.98 (s, 3H), 1.37 (d, J = 7.3 Hz, 3H) ppm.

^{13}C NMR (100 MHz, D_2O): δ = 176.7, 173.9, 48.6, 21.4, 16.0 ppm.

IR (KBr): $\tilde{\nu}$ = 3346, 3265, 2986, 2943, 1937, 1720, 1593, 1550, 1447, 1379, 1346, 1300, 1272, 1225, 1152, 1091, 1045, 1016, 978, 914, 847, 750, 704, 609, 557, 536 cm^{-1} .

The NMR data are in accordance with those reported.^[5b]

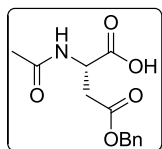


***O,N*-diacetyl-L-tyrosine (1d).** According to a reported procedure,^[7] a suspension of L-tyrosine (3.70 g, 20.4 mmol) in H_2O (30 mL) was cooled with an ice-bath and 1 N NaOH (21 mL) was slowly added. Acetic anhydride (4.3 mL, 4.64 g, 45.5 mmol) and 1 N NaOH (~ 40 mL) were slowly added simultaneously to maintain the pH at 6 – 8. The ice-bath was removed and the clear solution stirred at rt for 45 min. The reaction mixture was acidified with conc. HCl to pH ~ 2 upon cooling with an ice-bath and the resulting solid was filtered off, washed with H_2O , and dried in a vacuum desiccator over CaCl_2 and paraffin to afford **1d** (2.61 g, 9.8 mmol, 48%) as a colorless solid. Mp 174 °C (lit.^[8] mp 168.5 – 171 °C).

^1H NMR (400 MHz, DMSO- d_6): δ = 12.70 (br s, 1H), 8.22 (d, J = 8.0 Hz, 1H), 7.28 – 7.22 (m, 2H), 7.06 – 7.00 (m, 2H), 4.40 (ddd, J = 9.5, 8.0, 4.8 Hz, 1H), 3.04 (dd, J = 13.9, 4.9 Hz, 1H), 2.84 (dd, J = 13.9, 9.6 Hz, 1H), 2.24 (s, 3H), 1.79 (s, 3H) ppm.

^{13}C NMR (100 MHz, DMSO-d_6): δ = 173.1, 169.3, 169.2, 149.1, 135.2, 130.0, 121.5, 53.5, 36.1, 22.4, 20.9 ppm.

IR (KBr): $\tilde{\nu}$ = 3338, 2893, 2613, 2468, 1769, 1702, 1624, 1556, 1508, 1444, 1369, 1270, 1240, 1215, 1195, 1172, 1117, 910, 851, 835, 680, 598, 560, 524 cm^{-1} .



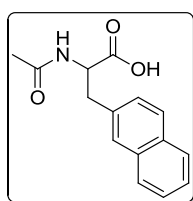
***N*-acetyl-L-aspartic acid 4-benzyl ester (1f).** Boc-L-aspartic acid 4-benzyl ester (3.23 g, 10.0 mmol) was treated with 4 M HCl in 1,4-dioxane (20.0 mL, 80.0 mmol) and the resulting solution was stirred at rt for 45 min. The reaction flask was flushed with argon for 30 min to remove residual HCl. After removal of the solvent under reduced pressure, the obtained hydrochloride was suspended in H_2O /1,4-dioxane (1:1; 100 mL). Et_3N (4.2 mL, 3.07 g, 30.3 mmol) and acetic anhydride (0.95 mL, 1.03 g, 10.0 mmol) were subsequently added and the reaction mixture was allowed to stir at rt for 18 h. Dioxane was removed under reduced pressure, the remaining solution acidified with 1 N HCl to pH \sim 1, and extracted with EtOAc (3 x 50 mL). The combined organic layers were dried over Na_2SO_4 , filtered, and concentrated *in vacuo* to afford **1f** (1.77 g, 6.67 mmol, 67%) as a colorless waxy solid.

^1H NMR (400 MHz, DMSO-d_6): δ = 12.81 (s, 1H), 8.28 (d, J = 8.1 Hz, 1H), 7.39 – 7.30 (m, 5H), 5.11 (s, 2H), 4.64 – 4.57 (m, 1H), 2.84 (dd, J = 16.2, 5.8 Hz, 1H), 2.71 (dd, J = 16.3, 7.5 Hz, 1H), 1.83 (s, 3H) ppm.

^{13}C NMR (100 MHz, DMSO-d_6): δ = 172.3, 170.1, 169.2, 136.0, 128.4, 128.0, 127.9, 65.8, 48.6, 36.1, 22.4 ppm.

IR (KBr): $\tilde{\nu}$ = 3347, 3063, 3033, 2988, 2958, 2888, 2737, 2528, 1716, 1613, 1535, 1457, 1428, 1376, 1351, 1297, 1265, 1232, 1206, 1141, 1040, 1026, 989, 968, 908, 804, 755, 696, 671, 625, 596, 535, 490 cm^{-1} .

The ^1H NMR data are in accordance with those reported.^[9]



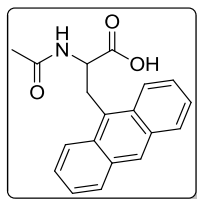
***N*-acetyl-DL-2-naphthylalanine (1g).**^[10] A solution of NaOEt (1.64 g, 24.0 mmol) and diethyl acetamidomalonate (4.35 g, 20.0 mmol) in abs. EtOH (20 mL) was stirred at reflux for 30 min under argon. 2-(bromo-methyl)naphthalene (4.43 g, 20.0 mmol) was added and the solution was refluxed for additional 20 h. The reaction mixture was concentrated under

reduced pressure and extracted with Et₂O (3 × 50 mL). The combined organic layers were successively washed with H₂O (3 × 50 mL), sat. aq. NaHCO₃ (3 × 50 mL), and brine (50 mL). Drying over Na₂SO₄, filtration, and removal of the solvent gave a yellow solid. The crude alkylation product was treated with 10% NaOH (15 mL) and the resulting suspension was stirred at rt for 24 h. The mixture was carefully acidified to pH ~ 4 with conc. HCl. The obtained solid was filtered off, resuspended in H₂O (100 mL) and refluxed for 5 h. Filtration, washing with hexane (to remove traces of 2-(ethoxymethyl)naphthalene), and drying in a vacuum desiccator over CaCl₂ and paraffin afforded **1g** (2.15 g, 8.36 mmol, 42% over three steps) as light yellow solid. Mp 171 – 172 °C.

¹H NMR (400 MHz, DMSO-*d*₆): δ = 12.72 (br s, 1H), 8.26 (d, *J* = 8.0 Hz, 1H), 7.89 – 7.81 (m, 3H), 7.73 (br s, 1H), 7.52 – 7.43 (m, 2H), 7.41 (dd, *J* = 8.4, 1.7 Hz, 1H), 4.53 (ddd, *J* = 9.3, 8.0, 5.1 Hz, 1H), 3.22 (dd, *J* = 13.8, 5.1 Hz, 1H), 3.02 (dd, *J* = 13.8, 9.4 Hz, 1H), 1.78 (s, 3H) ppm.

¹³C NMR (100 MHz, DMSO-*d*₆): δ = 173.2, 169.3, 135.4, 133.0, 131.9, 127.6, 127.6, 127.5, 127.5, 127.4, 126.0, 125.5, 53.5, 37.0, 22.4 ppm.

IR (KBr): $\tilde{\nu}$ = 3338, 3053, 2932, 2623, 2571, 2487, 1709, 1626, 1554, 1416, 1385, 1370, 1329, 1252, 1172, 1120, 1048, 979, 898, 864, 820, 735 cm⁻¹.



***N*-acetyl-DL-9-anthranylalanine (1h).** 9-(bromomethyl)anthracene: According to a reported procedure,^[11] a suspension of anthracen-9-ylmethanol (1.50 g, 7.20 mmol) in abs. toluene (40 mL) was cooled to 0 °C with an ice-bath under argon. PBr₃ (0.80 mL, 2.30 g, 8.51 mmol) was added dropwise and the reaction mixture was stirred at 0 °C for 1 h. The resulting solution was

allowed to warm to rt and sat. aq. Na₂CO₃ (15 mL) was slowly added. The phases were separated and the organic layer was successively washed with H₂O (10 mL) and brine (10 mL), dried over MgSO₄, filtered, and the solvent was removed under reduced pressure yielding 9-(bromomethyl)anthracene (1.797 g, 6.63 mmol, 92%) as yellow solid.

¹H NMR (400 MHz, CDCl₃): δ = 8.48 (s, 1H), 8.30 (dd, *J* = 8.9, 1.0 Hz, 2H), 8.05 – 8.02 (m, 2H), 7.65 (ddd, *J* = 8.9, 6.5, 1.3 Hz, 2H), 7.51 (ddd, *J* = 7.8, 6.6, 1.0 Hz, 2H), 5.53 (s, 2H) ppm.

¹³C NMR (100 MHz, CDCl₃): δ = 131.7, 129.8, 129.4, 129.3, 128.0, 126.9, 125.5, 123.6, 27.1 ppm.

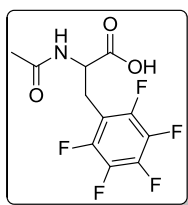
The NMR data are in accordance with those reported.^[12]

A solution of NaOEt (0.408 g, 6.00 mmol) and diethyl acetamidomalonate (1.09 g, 5.02 mmol) in abs. EtOH (10 mL) was stirred at reflux for 30 min under argon. 9-(bromomethyl)-anthracene (1.36 g, 5.0 mmol) in abs. toluene (5 mL) was added dropwise with stirring and the solution was refluxed for additional 21 h. The reaction mixture was concentrated under reduced pressure, H₂O (50 mL) was added, and extracted with CHCl₃ (3 × 20 mL). The combined organic layers were washed with H₂O (2 × 30 mL) and brine (30 mL), dried over Na₂SO₄ and filtered. The solvent was removed under reduced pressure yielding a yellow solid. The crude alkylation product was dissolved in EtOH (10 mL), treated with 10% NaOH (15 mL) and the resulting suspension was stirred at rt for 24 h. The mixture was carefully acidified to pH ~ 4 with conc. HCl. The obtained solid was filtered off, resuspended in H₂O (50 mL) and refluxed for 4 h. Filtration, washing with H₂O and EtOAc and drying *in vacuo* afforded **1h** (505.7 mg, 1.65 mmol, 33%) as yellow solid. Mp 262 – 263 °C (lit.^[13] mp 265 – 267 °C).

¹H NMR (400 MHz, DMSO-d₆): δ = 12.77 (br s, 1H), 8.52 (br s, 1H), 8.46 (d, *J* = 8.4 Hz, 1H), 8.40 (d, *J* = 8.7 Hz, 2H), 8.08 (d, *J* = 8.1 Hz, 2H), 7.60 – 7.48 (m, 4H), 4.65 – 4.57 (m, 1H), 4.07 (dd, *J* = 14.4, 5.9 Hz, 1H), 3.93 (dd, *J* = 14.4, 8.6 Hz, 1H), 1.68 (s, 3H) ppm.

¹³C NMR (100 MHz, DMSO-d₆): δ = 173.1, 169.2, 131.1, 130.3, 130.0, 129.0, 126.5, 125.9, 125.0, 124.4, 53.7, 29.6, 22.4 ppm.

IR (KBr): $\tilde{\nu}$ = 3318, 3054, 2892, 2465, 1713, 1620, 1551, 1446, 1323, 1269, 1251, 1160, 1119, 986, 954, 895, 849, 790, 734 cm⁻¹.



***N*-acetyl-DL-pentafluorophenylalanine (1i).** According to a reported procedure,^[14] NaOEt (0.944 g, 13.87 mmol) and diethyl acetamidomalonate (2.26 g, 10.40 mmol) were dissolved in abs. DMF (20 mL) under argon. Pentafluorobenzyl bromide (1.72 mL, 2.97 g, 11.38 mmol) was added and the resulting solution was heated to 55 °C for 24 h. The reaction mixture was poured into iced water (200 mL), the resulting cream colored solid was filtered off, washed with H₂O and dried *in vacuo*. The crude alkylation product was treated with 10% NaOH (7.5 mL) and the resulting suspension was stirred at rt for 24 h. The mixture was carefully acidified to pH ~ 4 with conc. HCl, the obtained solid was filtered off, resuspended in H₂O (50 mL) and refluxed for 4 h. Filtration, washing with H₂O and drying *in vacuo* afforded **1i** (1.264 g, 4.25 mmol, 41% over three steps) as colorless solid. Mp 169 – 170 °C (lit.^[15] mp 171 – 173 °C).

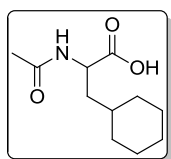
¹H NMR (400 MHz, DMSO-d₆): δ = 12.99 (s, 1H), 8.30 (d, *J* = 8.5 Hz, 1H), 4.53 – 4.46 (m, 1H), 3.16 (dd, *J* = 14.1, 6.2 Hz, 1H), 3.02 (dd, *J* = 14.1, 8.3 Hz, 1H), 1.78 (s, 3H) ppm.

^{13}C NMR (100 MHz, DMSO-d_6): δ = 171.9, 169.3, 146.3 (m), 143.9 (m), 137.9 (m), 111.6 (m), 50.7, 24.8, 22.2 ppm.

^{19}F NMR (376 MHz, DMSO-d_6): δ = -142.4 (m), -157.2 (t, J = 22.1 Hz), -163.6 (m) ppm.

IR (KBr): $\tilde{\nu}$ = 3258, 3080, 1719, 1648, 1566, 1523, 1503, 1420, 1378, 1338, 1309, 1282, 1246, 1199, 1124, 1062, 968, 736, 686, 651, 625, 572, 528, 458 cm^{-1} .

The ^1H NMR data are in accordance with those reported.^[16]



***N*-acetyl-DL-cyclohexylalanine (1j).** Diethyl 2-acetamido-2-(cyclohexylmethyl)-malonate: A solution of NaOEt (0.750 g, 11.02 mmol) and diethyl acetamidomalonate (2.00g, 9.21 mmol) in 10 mL abs. EtOH was stirred at reflux for 30 min under argon. Bromomethylcyclohexane (1.30 mL, 1.65 g, 9.32 mmol)

was added dropwise and the resulting solution was refluxed for additional 24 h. The reaction mixture was concentrated under reduced pressure and extracted with Et_2O ($5 \times 25\text{ mL}$). The combined organic extracts were successively washed with H_2O ($2 \times 20\text{ mL}$), sat. aq. NaHCO_3 ($2 \times 20\text{ mL}$), and H_2O (20 mL), dried over Na_2SO_4 , filtered, and the solvent was removed under reduced pressure. The residual oil was triturated with hexane and left standing at $-20\text{ }^\circ\text{C}$ overnight to afford the desired alkylation product (1.343 g, 4.28 mmol, 46%) as colorless crystals.

^1H NMR (400 MHz, CDCl_3): δ = 6.83 (br s, 1H), 4.21 (q, J = 7.1 Hz, 4H), 2.27 (d, J = 6.0 Hz, 2H), 2.02 (s, 3H), 1.65 – 1.50 (m, 5H), 1.23 (t, J = 7.1 Hz, 6H), 1.20 – 1.06 (m, 4H), 0.98 – 0.88 (m, 2H) ppm.

^{13}C NMR (100 MHz, CDCl_3): δ = 169.0, 168.8, 66.0, 62.6, 38.9, 33.9, 33.5, 26.3, 26.2, 23.2, 14.1 ppm.

IR (KBr): $\tilde{\nu}$ = 3281, 2976, 2921, 2851, 1747, 1647, 1510, 1445, 1373, 1298, 1274, 1231, 1190, 1136, 1098, 1052, 1019, 953, 900, 862, 841, 805, 769, 693, 608 cm^{-1} .

The spectroscopic data are in accordance with those reported.^[17]

The malonate (1.167 g, 3.72 mmol) was suspended in 10% NaOH (5.8 mL) and stirred at rt for 42 h. The resulting solution was acidified (pH ~ 2) with conc. HCl and the colorless solid thus obtained was extracted with EtOAc (3 × 20 mL). The combined organic extracts were concentrated under reduced pressure and the resulting solid was refluxed in H₂O (30 mL) for 5 h. Filtration and washing with H₂O afforded **1j** (0.643 g, 3.01 mmol, 81%) as silky flakes. Mp 175 – 176 °C.

¹H NMR (400 MHz, MeOH-d₄): δ = 4.43 (dd, J = 10.3, 4.8 Hz, 1H), 1.98 (s, 3H), 1.84 – 1.52 (m, 7H), 1.45 – 1.12 (m, 4H), 1.05 – 0.84 (m, 2H) ppm.

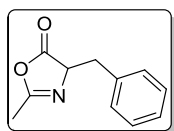
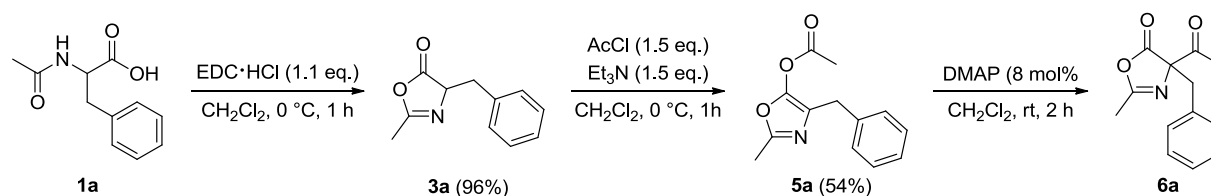
¹³C NMR (100 MHz, MeOH-d₄): δ = 176.3, 173.4, 51.4, 40.2, 35.5, 34.8, 33.2, 27.6, 27.4, 27.2, 22.3 ppm.

IR (KBr): $\tilde{\nu}$ = 3334, 2924, 2850, 2500, 1700, 1626, 1557, 1448, 1254, 1154, 964, 678, 599 cm⁻¹.

The spectroscopic data are in accordance with those reported.^[18]

2.2.2 Synthesis of possible reaction intermediates

The following stepwise reactions were performed for the synthesis of probably occurring intermediates of the Dakin-West reaction with **1a**. The products obtained were purified if possible, characterized and subjected to GC-MS and chiral GC analyses for the elucidation of retention times.



4-benzyl-2-methyloxazol-5(4H)-one (3a). According to a literature procedure,^[19] *N*-acetyl-DL-phenylalanine (**1a**; 414.5 mg, 2.0 mmol) was suspended in dry CH₂Cl₂ (20 mL) under argon. After cooling to 0 °C, EDC · HCl (421.7 mg, 2.2 mmol) was added and the reaction mixture was stirred for 1 h at 0 °C. The

solution was diluted with CH_2Cl_2 (20 mL) and washed with H_2O (20 mL), sat. aq. NaHCO_3 (2×20 mL), and H_2O (20 mL). The organic layer was dried over MgSO_4 , filtered, and the solvent was removed under reduced pressure to afford azlactone **3a** (365.3 mg, 1.87 mmol, 96%) as colorless oil.

^1H NMR (400 MHz, CDCl_3): δ = 7.32 – 7.24 (m, 3H), 7.23 – 7.19 (m, 2H), 4.46 – 4.41 (m, 1H), 3.25 (dd, J = 14.0, 4.8 Hz, 1H), 3.06 (dd, J = 14.0, 6.8 Hz, 1H), 2.08 (d, J = 2.0 Hz, 3H) ppm.

^{13}C NMR (100 MHz, CDCl_3): δ = 178.0, 163.0, 135.3, 129.6, 128.5, 127.3, 66.1, 37.0, 15.1 ppm.

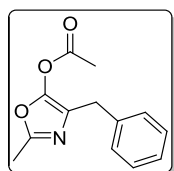
IR (film): $\tilde{\nu}$ = 3063, 3031, 2931, 1821, 1730, 1684, 1497, 1455, 1434, 1385, 1285, 1242, 1134, 1084, 1062, 1011, 901, 742, 701, 628, 528 cm^{-1} .

NMR data are in accordance with those reported.^[20]

GC-MS: Conditions: 60 °C isothermal, 5 min; 60 – 250 °C, 10 °C/min; 250 °C isothermal, 10 min. Retention time: t_R = 17.9 min; m/z (%) = 189 (16), 103 (1), 91 (100), 77 (2), 65 (3), 51 (2).

Chiral stationary phase GC: FS-Hydrodex γ -TBDAc column (Macherey-Nagel), l = 30 m; splitflow: 80 mL/min; precolumn pressure: 0.8 bar; T (injector + detector) = 250 °C; conditions: 100 – 220 °C, 2 °C/min. Retention time: t_R = 25.8 min.

The enantiomers of **3a** could not be separated under the conditions applied and only a single broad peak was observed.



4-benzyl-2-methyloxazol-5-yl acetate (5a). 4-benzyl-2-methyloxazol-5(4*H*)-one (**3a**; 105.3 mg, 0.56 mmol) was dissolved in dry CH_2Cl_2 (3 mL) under argon and Et_3N (116.0 μL , 85.0 mg, 0.84 mmol) was added upon cooling to 0 °C with an ice-bath. Acetyl chloride (60.0 μL , 65.9 mg, 0.84 mmol) was slowly added and the reaction mixture was stirred at 0 °C for 1 h. The precipitated ammonium salt was filtered off, washed with CH_2Cl_2 and the solvent was removed under reduced pressure. The residue was redissolved in Et_2O (20 mL) and washed with H_2O (2×20 mL). The organic layer was dried over Na_2SO_4 , filtered and the solvent was removed under reduced pressure without heating. The crude product was purified by column chromatography eluting with TBME to afford **5a** (69.7 mg, 0.30 mmol, 54%) as colorless oil. TLC (TBME): R_f = 0.49.

^1H NMR (600 MHz, CDCl_3): δ = 7.29 – 7.25 (m, 2H), 7.22 – 7.18 (m, 3H), 3.71 (s, 2H), 2.36 (s, 3H), 2.08 (s, 3H) ppm.

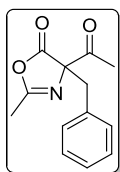
^{13}C NMR (150 MHz, CDCl_3): δ = 167.5, 155.5, 145.7, 137.7, 129.1, 128.6, 126.6, 121.7, 31.6, 20.0, 14.3 ppm.

IR (film): $\tilde{\nu}$ = 3063, 3030, 2930, 1797, 1757, 1725, 1669, 1584, 1496, 1454, 1433, 1371, 1266, 1161, 1104, 1044, 1009, 952, 908, 875, 826, 729, 702, 581, 504 cm^{-1} .

HRMS (ESI): m/z = 254.0790 $[\text{M}+\text{Na}]^+$ (calcd m/z = 254.0793).

GC-MS: Conditions: 60 °C isothermal, 5 min; 60 – 250 °C, 10 °C/min; 250 °C isothermal, 10 min. Retention time: t_R = 20.5 min; m/z (%) = 231 (1), 189 (100), 147 (22), 130 (4), 118 (44), 103 (6), 91 (50), 78 (18), 65 (7), 51 (5).

Chiral stationary phase GC: FS-Hydrodex γ -TBDAc column (Macherey-Nagel), l = 30 m; splitflow: 80 mL/min; precolumn pressure: 0.8 bar; T (injector + detector) = 250 °C; conditions: 100 – 220 °C, 2 °C/min. Retention time: t_R = 34.8 min.



4-acetyl-4-benzyl-2-methyloxazol-5(4H)-one (6a). DMAP (2.0 mg, 7.9 mol%) was added to a solution of **5a** (48.1 mg, 0.21 mmol) in dry CH_2Cl_2 (1 mL) under argon and the solution was stirred at rt for 2 h. The reaction mixture was concentrated under reduced pressure and the crude rearrangement product was directly analyzed by NMR.

The obtained product was contaminated with **3a**, **5a**, and **10a**. It was, however, not possible to purify **6a**, *e.g.*, by column chromatography because of decomposition.

^1H NMR (400 MHz, CDCl_3): δ = 7.28 – 7.22 (m, 3H), 7.16 – 7.11 (m, 2H), 3.35 (d, J = 13.5 Hz, 1H), 3.29 (d, J = 13.5 Hz, 1H), 2.26 (s, 3H), 2.05 (s, 3H) ppm.

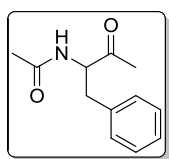
^{13}C NMR (150 MHz, CDCl_3): δ = 198.4, 173.4, 164.0, 132.9, 130.3, 128.4, 127.8, 82.4, 40.8, 26.9, 15.0 ppm.

GC-MS: Conditions: 60 °C isothermal, 5 min; 60 – 250 °C, 10 °C/min; 250 °C isothermal, 10 min. Retention time: t_R = 19.9 min; m/z (%) = 231 (1), 189 (100), 147 (23), 130 (5), 118 (43), 103 (6), 91 (93), 78 (14), 65 (13), 51 (7).

Chiral stationary phase GC: FS-Hydrodex γ -TBDAc column (Macherey-Nagel), $l = 30$ m; splitflow: 80 mL/min; precolumn pressure: 0.8 bar; T (injector + detector) = 250 °C; conditions: 100 – 220 °C, 2 °C/min. Retention time: $t_R(R)$ = 35.8 min, $t_R(S)$ = 36.1 min.

2.3 Synthesis of Racemic Products

The *N*-protected amino acids were converted to the corresponding racemic α -acetamido methylketones employing the DMAP-catalyzed procedure reported by Steglich and Höfle.^[21]



***N*-(3-oxo-1-phenylbutan-2-yl)acetamide (10a).** A mixture of **1a** (414.5 mg, 2.0 mmol), DMAP (12.2 mg, 0.1 mmol, 5 mol%), Et₃N (0.4 mL, 292.0 mg, 2.9 mmol), and acetic anhydride (0.4 mL, 432.0 mg, 4.2 mmol) was stirred at rt for 30 min. Glacial acetic acid (3 mL) was then added and stirring was continued for further 30 min. After concentration of the solution under reduced pressure, the residual yellow oil was treated with sat. aq. NaHCO₃ (50 mL), followed by extraction with CHCl₃ (4 \times 10 mL). The combined organic layers were washed with 1 N HCl (3 \times 10 mL) and brine (10 mL), dried over Na₂SO₄, filtered, and the solvent was removed *in vacuo*. Recrystallization from hexane/EtOAc (4:1) afforded **10a** (279.7 mg, 1.36 mmol, 68%) as colorless crystalline solid. TLC (EtOAc): R_f = 0.34. Mp 94.5 – 95 °C (lit.^[22] 95 – 95.5 °C).

¹H NMR (400 MHz, CDCl₃): δ = 7.29 – 7.18 (m, 3H), 7.11 – 7.06 (m, 2H), 6.10 (d, J = 6.6 Hz, 1H), 4.87 – 4.80 (m, 1H), 3.10 (dd, J = 14.0, 6.7 Hz, 1H), 3.02 (dd, J = 14.1, 5.6 Hz, 1H), 2.12 (s, 3H), 1.95 (s, 3H) ppm.

¹³C NMR (100 MHz, CDCl₃): δ = 206.4, 169.8, 135.9, 129.3, 128.8, 127.3, 59.6, 37.3, 28.2, 23.3 ppm.

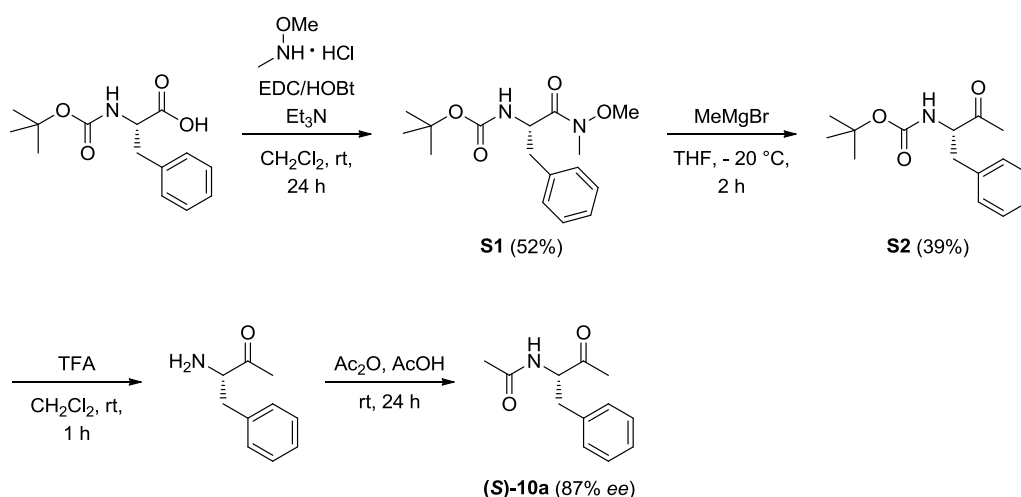
IR (KBr): $\tilde{\nu}$ = 3331, 3030, 2921, 1711, 1634, 1536, 1495, 1439, 1354, 1327, 1270, 1203, 1166, 1121, 1032, 955, 740, 698, 615, 600 cm⁻¹.

The spectroscopic data are in accordance with those reported.^[23]

GC-MS: Conditions: 60 °C isothermal, 5 min; 60 – 250 °C, 10 °C/min; 250 °C isothermal, 10 min. Retention time: t_R = 20.7 min; m/z (%) = 205 (3), 162 (38), 146 (7), 131 (4), 120 (100), 103 (7), 91 (18), 77 (4), 72 (16), 65 (4).

Chiral stationary phase GC: FS-Hydrodex γ -TBDAC column (Macherey-Nagel), $l = 30$ m; splitflow: 80 mL/min; precolumn pressure: 0.8 bar; T (injector + detector) = 250 °C; conditions: 100 – 220 °C, 1 °C/min. Retention times: t_R (R) = 44.7 min, t_R (S) = 44.9 min.

Chiral stationary phase HPLC: Chiralpak IC column (Daicel), 250 mm \times 4.6 mm; eluent: 15% *i*-PrOH/hexanes, 1.0 mL/min; UV-detector $\lambda = 254$ nm. Retention times: t_R (S) = 15.4 min, t_R (R) = 18.6 min.



(*S*)-*N*-(3-oxo-1-phenylbutan-2-yl)acetamide ((*S*)-10a). The title compound was synthesized from Boc-L-Phe-OH through the multistep reaction sequence shown above in order to determine the absolute configuration of the products obtained from the enantioselective Dakin–West reaction.

(*S*)-tert-butyl (1-(methoxy(methyl)amino)-1-oxo-3-phenylpropan-2-yl)carbamate (S1**):** Boc-L-Phe-OH (1.329 g, 5.00 mmol), *N,O*-dimethylhydroxylamine hydrochloride (0.490 g, 5.02 mmol), 1-ethyl-3-(3-dimethylaminopropyl)carbodiimide hydrochloride (EDC \cdot HCl; 1.056 g, 5.50 mmol) and 1-hydroxybenzotriazole hydrate (HOBt \cdot H₂O; 0.842 g, 5.50 mmol) were suspended in CH₂Cl₂ (50 mL). Et₃N (0.76 mL, 0.555 g, 5.50 mmol) was added and the resulting suspension was stirred at rt for 24 h. The reaction mixture was diluted with EtOAc and subsequently washed with sat. aq. NaHCO₃ (3 \times 20 mL), 0.5 M citric acid solution (3 \times 20 mL), and brine (3 \times 20 mL). The organic layer was dried over Na₂SO₄, filtered, and concentrated under reduced pressure to afford a yellow oil. The crude product was purified by column chromatography eluting with hexane/EtOAc (1:1) to obtain the desired intermediate **S1** (0.798 g, 2.59 mmol, 52%) as colorless oil. TLC (hexane/EtOAc 1:1): $R_f = 0.46$.

¹H NMR (600 MHz, CDCl₃): δ = 7.30 – 7.25 (m, 2H), 7.23 – 7.19 (m, 1H), 7.18 – 7.15 (m, 2H), 5.15 (br s, 1H), 4.95 (br s, 1H), 3.65 (s, 3H), 3.16 (s, 3H), 3.05 (dd, J = 13.6, 6.1 Hz, 1H), 2.91 – 2.84 (m, 1H), 1.39 (s, 9H) ppm.

¹³C NMR (150 MHz, CDCl₃): δ = 172.5, 155.3, 136.8, 129.6, 128.5, 126.9, 79.7, 61.7, 51.7, 39.0, 32.2, 28.5 ppm.

The NMR data are in accordance with those reported.^[24]

(S)-*tert*-butyl (3-oxo-1-phenylbutan-2-yl)carbamate (**S2**): Following a reported procedure,^[25] **S1** (0.280 g, 0.92 mmol) was suspended in abs. THF (2 mL) and cooled to –20 °C under argon. Methylmagnesium bromide (3 M in Et₂O; 1.0 mL, 3.0 mmol) was added slowly and the resulting solution was stirred at –20 °C for 2 h. The reaction mixture was quenched with sat. aq. NH₄Cl and extracted with EtOAc (3 × 2 mL). The combined organic layers were washed with brine, dried over Na₂SO₄, filtered, and the solvent was removed under reduced pressure. Column chromatography eluting with hexane/EtOAc (2:1) afforded methyl ketone **S2** (94.7 mg, 0.36 mmol, 39%) as colorless solid. TLC (hexane/EtOAc 2:1): R_f = 0.49.

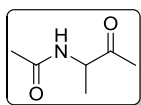
¹H NMR (600 MHz, CDCl₃): δ = 7.31 – 7.27 (m, 2H), 7.26 – 7.22 (m, 1H), 7.17 – 7.14 (m, 2H), 5.12 (m, 1H), 4.53 (m, 1H), 3.09 (dd, J = 14.0, 6.5 Hz, 1H), 2.98 (dd, J = 13.9, 6.5 Hz, 1H), 2.12 (s, 3H), 1.41 (s, 9H) ppm.

¹³C NMR (150 MHz, CDCl₃): δ = 207.0, 155.3, 136.3, 129.4, 128.8, 127.2, 80.0, 60.9, 37.7, 28.5, 28.1 ppm.

The NMR data are in accordance with those reported.^[26]

(S)-*N*-(3-oxo-1-phenylbutan-2-yl)acetamide (**(S)**-**10a**): A solution of **S2** (94.7 mg, 0.36 mmol) in CH₂Cl₂ (1.5 mL) was cooled to 0 °C with an ice-bath. Upon addition of TFA (0.36 mL) the reaction mixture was allowed to warm to rt and stirred for 1 h. After removal of the solvent, residual TFA was co-evaporated with CH₂Cl₂ *in vacuo*. Acetic acid (0.5 mL) and acetic anhydride (40.8 μ L, 44.1 mg, 0.43 mmol) were added and the resulting solution was stirred at rt for 24 h. All volatiles were then removed under reduced and the residue was purified by column chromatography eluting with EtOAc to afford **(S)**-**10a** (87% *ee* determined by chiral stationary phase HPLC).

The NMR data were identical with those obtained from the Dakin-West reaction of **1a** (*vide supra*).



N-(3-oxobutan-2-yl)acetamide (10b). The title compound was synthesized on 10.0 mmol scale employing the reaction conditions and work-up procedure described for **10a**. Fractional distillation *in vacuo* afforded **10b** (250.8 mg, 1.94 mmol, 19%) as colorless oil. TLC (EtOAc): R_f = 0.15.

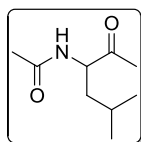
^1H NMR (200 MHz, CDCl_3): δ = 6.43 (br s, 1H), 4.57 (m, 1H), 2.19 (s, 3H), 1.98 (s, 3H), 1.34 (d, J = 7.2 Hz, 3H) ppm.

^{13}C NMR (50 MHz, CDCl_3): δ = 207.1, 169.7, 54.7, 26.7, 23.2, 17.6 ppm.

IR (KBr): $\tilde{\nu}$ = 3288, 3067, 2985, 2938, 1720, 1657, 1543, 1454, 1375, 1303, 1234, 1201, 1146, 1109, 1064, 1043, 1016, 986, 954, 727, 610, 544, 515 cm^{-1} .

The spectroscopic data are in accordance with those reported.^[23]

Chiral stationary phase GC: FS-Hydrodex β -TBDAC column (Macherey-Nagel), l = 30 m; splitflow: 80 mL/min; precolumn pressure: 0.8 bar; T (injector + detector) = 250 $^{\circ}\text{C}$; conditions: 100 – 180 $^{\circ}\text{C}$, 2 $^{\circ}\text{C}/\text{min}$. Retention times: t_R (R) = 27.0 min, t_R (S) = 27.9 min.



N-(5-methyl-2-oxohexan-3-yl)acetamide (10c). The title compound was synthesized on 3.0 mmol scale employing the reaction conditions and work-up procedure described for **10a** with the exception that the reaction time was 1 h. Fractional distillation *in vacuo* afforded **10c** (246.7 mg, 1.44 mmol, 48%) as colorless oil. TLC (EtOAc): R_f = 0.29.

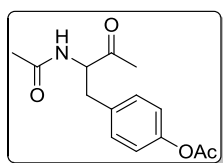
^1H NMR (400 MHz, CDCl_3): δ = 6.12 (d, J = 7.5 Hz, 1H), 4.66 (ddd, J = 9.5, 7.9, 3.8 Hz, 1H), 2.21 (s, 3H), 2.01 (s, 3H), 1.71 – 1.55 (m, 2H), 1.42 – 1.33 (m, 1H), 0.96 (d, J = 6.3 Hz, 3H), 0.91 (d, J = 6.5 Hz, 3H) ppm.

^{13}C NMR (100 MHz, CDCl_3): δ = 207.6, 170.2, 57.4, 40.6, 27.5, 25.1, 23.4, 23.2, 22.0 ppm.

IR (film): $\tilde{\nu}$ = 3291, 3064, 2959, 2872, 1720, 1657, 1543, 1437, 1372, 1293, 1228, 1146, 1031, 610 cm^{-1} .

Spectroscopic data are in accordance with those reported.^[27]

Chiral stationary phase GC: FS-Hydrodex β -TBDAC column (Macherey-Nagel), l = 30 m; splitflow: 80 mL/min; precolumn pressure: 0.8 bar; T (injector + detector) = 250 °C; conditions: 100 – 180 °C, 2 °C/min. Retention times: t_R (*R*) = 25.8 min, t_R (*S*) = 26.6 min.



4-(2-acetamido-3-oxobutyl)phenyl acetate (10d). The title compound was synthesized on 2.0 mmol scale employing the reaction conditions and work-up procedure described for **10a**. The crude yellow solid obtained after removal of the solvent was digested with Et₂O, filtered off, and washed with

Et₂O yielding **10d** (387.1 mg, 1.47 mmol, 74%) as colorless solid. TLC (EtOAc): R_f = 0.25. Mp 123 – 123.5 °C (lit.^[22] 121 – 122.5 °C).

¹H NMR (400 MHz, CDCl₃): δ = 7.14 – 7.09 (m, 2H), 7.03 – 6.99 (m, 2H), 6.14 (d, J = 7.3 Hz, 1H), 4.87 – 4.80 (m, 1H), 3.13 (dd, J = 14.2, 6.7 Hz, 1H), 3.02 (dd, J = 14.2, 5.7 Hz, 1H), 2.28 (s, 3H), 2.16 (s, 3H), 1.97 (s, 3H) ppm.

¹³C NMR (100 MHz, CDCl₃): δ = 206.2, 169.8, 169.5, 149.9, 133.5, 130.3, 121.9, 59.5, 36.5, 28.2, 23.2, 21.3 ppm.

IR (KBr): $\tilde{\nu}$ = 3312, 3072, 2961, 2924, 1746, 1721, 1649, 1547, 1511, 1436, 1367, 1238, 1204, 1165, 1122, 1045, 1023, 920, 850, 695 cm^{-1} .

HRMS (ESI): m/z = 264.1229 [$\text{M}+\text{H}$]⁺ (calcd m/z = 264.1236); m/z = 286.1054 [$\text{M}+\text{Na}$]⁺ (calcd m/z = 286.1055).

Elem. Anal.: calcd for C₁₄H₁₇NO₄: C 63.87, H 6.51, N 5.32; found: C 63.72, H 6.45, N 5.13.

Chiral stationary phase HPLC: Chiralpak IC column (Daicel), 250 mm \times 4.6 mm; eluent: 25% *i*-PrOH/hexanes, 1.0 mL/min; UV-detector λ = 254 nm. Retention times: t_R (*S*) = 17.1 min, t_R (*R*) = 24.4 min.

Crystals of **10d** suitable for X-ray diffraction (Figure S1) were grown from *i*-PrOH/hexane (1:1).

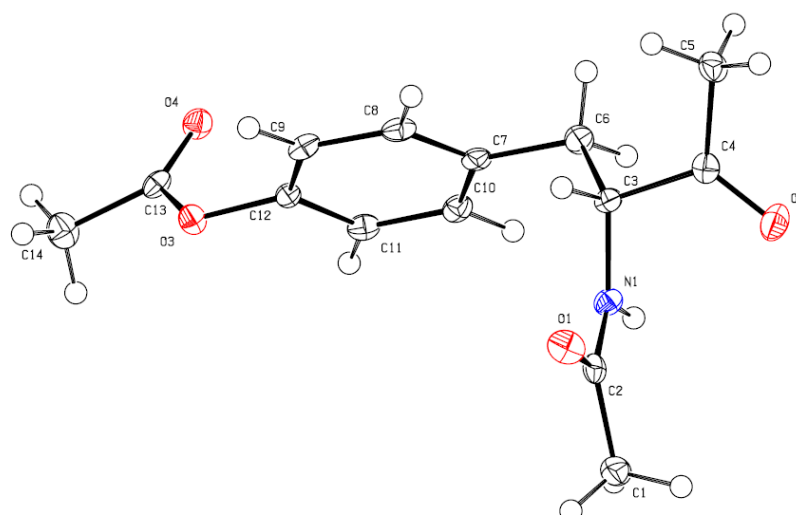


Figure S1. ORTEP plot of **10d**. Ellipsoids are drawn at the 50% probability level.

The data for **10d** were obtained using a BRUKER D8 Venture system with dual I μ S microfocus sources, a PHOTON100 detector and an OXFORD CRYOSYSTEMS 700 low temperature system. Data collection was performed using Mo α radiation with wavelength 0.71073 Å and a collimating Quazar multilayer mirror. Semi-empirical absorption correction from equivalents was applied using SADABS-2014/4 and the structure was solved by intrinsic phasing using SHELXT2014.^[28] Refinement was performed against F² using SHELXL-2014/7.^[29] All non-hydrogen atoms were refined anisotropically, all hydrogen atoms were located in difference map and refined isotropically. Crystallographic data for the structure have been deposited within the Cambridge Crystallographic Data Centre as CCDC No. 1429040.

Table S1. Crystal data and structure refinement for **10d**.

Identification code	CCDC No. 1429040	
Empirical formula	C ₁₄ H ₁₇ N O ₄	
Formula weight	263.28	
Temperature	100(2) K	
Wavelength	0.71073 Å	
Crystal system	Triclinic	
Space group	P-1	
Unit cell dimensions	a = 6.9769(3) Å	$\alpha = 79.182(2)^\circ$.
	b = 7.3634(4) Å	$\beta = 82.684(2)^\circ$.
	c = 13.9340(7) Å	$\gamma = 70.563(2)^\circ$.

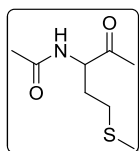
Volume	661.42(6) Å ³
Z	2
Density (calculated)	1.322 Mg/m ³
Absorption coefficient	0.097 mm ⁻¹
F(000)	280
Crystal size	0.332 × 0.284 × 0.149 mm ³
Theta range for data collection	2.970 to 25.050°.
Index ranges	-7 ≤ h ≤ 8, -8 ≤ k ≤ 8, -16 ≤ l ≤ 16
Reflections collected	20268
Independent reflections	2341 [R(int) = 0.0473]
Completeness to theta = 25.050°	99.9 %
Absorption correction	Semi-empirical from equivalents
Max. and min. transmission	0.7452 and 0.6764
Refinement method	Full-matrix least-squares on F ²
Data / restraints / parameters	2341 / 0 / 240
Goodness-of-fit on F ²	1.142
Final R indices [I > 2σ(I)]	R1 = 0.0412, wR2 = 0.0904
R indices (all data)	R1 = 0.0492, wR2 = 0.0944
Extinction coefficient	n/a
Largest diff. peak and hole	0.225 and -0.234 e.Å ³

Table S2. Bond lengths [Å] and angles [°] for **10d**.

O(1)-C(2)	1.229(2)
N(1)-C(2)	1.347(2)
N(1)-C(3)	1.443(2)
N(1)-H(1)	0.86(2)
C(1)-C(2)	1.500(2)
C(1)-H(1C)	0.92(3)
C(1)-H(1B)	0.98(2)
C(1)-H(1A)	0.98(3)
O(2)-C(4)	1.217(2)
C(3)-C(4)	1.529(2)
C(3)-C(6)	1.535(2)
C(3)-H(3)	0.976(18)
O(3)-C(13)	1.365(2)

O(3)-C(12)	1.4110(19)
C(4)-C(5)	1.499(2)
O(4)-C(13)	1.200(2)
C(5)-H(5C)	0.92(2)
C(5)-H(5B)	1.00(2)
C(5)-H(5A)	0.95(2)
C(6)-C(7)	1.510(2)
C(6)-H(6B)	1.00(2)
C(6)-H(6A)	0.98(2)
C(7)-C(10)	1.392(2)
C(7)-C(8)	1.393(2)
C(8)-C(9)	1.390(2)
C(8)-H(8)	0.972(19)
C(9)-C(12)	1.384(2)
C(9)-H(9)	0.98(2)
C(10)-C(11)	1.386(2)
C(10)-H(10)	0.99(2)
C(11)-C(12)	1.378(2)
C(11)-H(11)	0.967(19)
C(13)-C(14)	1.490(2)
C(14)-H(14C)	0.96(2)
C(14)-H(14B)	0.93(3)
C(14)-H(14A)	0.94(3)
C(2)-N(1)-C(3)	120.75(14)
C(2)-N(1)-H(1)	120.6(13)
C(3)-N(1)-H(1)	116.2(13)
C(2)-C(1)-H(1C)	108.9(15)
C(2)-C(1)-H(1B)	112.9(13)
H(1C)-C(1)-H(1B)	108(2)
C(2)-C(1)-H(1A)	107.8(14)
H(1C)-C(1)-H(1A)	110(2)
H(1B)-C(1)-H(1A)	108.5(19)
O(1)-C(2)-N(1)	122.13(15)
O(1)-C(2)-C(1)	121.78(16)
N(1)-C(2)-C(1)	116.09(15)
N(1)-C(3)-C(4)	111.48(13)
N(1)-C(3)-C(6)	111.10(14)
C(4)-C(3)-C(6)	110.87(14)
N(1)-C(3)-H(3)	109.8(10)
C(4)-C(3)-H(3)	105.6(10)
C(6)-C(3)-H(3)	107.8(10)
C(13)-O(3)-C(12)	117.89(12)
O(2)-C(4)-C(5)	121.71(15)
O(2)-C(4)-C(3)	120.84(15)
C(5)-C(4)-C(3)	117.45(14)
C(4)-C(5)-H(5C)	110.3(12)
C(4)-C(5)-H(5B)	107.9(13)
H(5C)-C(5)-H(5B)	107.5(18)
C(4)-C(5)-H(5A)	111.3(12)
H(5C)-C(5)-H(5A)	113.0(17)
H(5B)-C(5)-H(5A)	106.5(18)
C(7)-C(6)-C(3)	112.04(14)

C(7)-C(6)-H(6B)	111.4(12)
C(3)-C(6)-H(6B)	106.3(12)
C(7)-C(6)-H(6A)	109.8(11)
C(3)-C(6)-H(6A)	107.8(11)
H(6B)-C(6)-H(6A)	109.3(16)
C(10)-C(7)-C(8)	118.34(15)
C(10)-C(7)-C(6)	120.69(15)
C(8)-C(7)-C(6)	120.97(15)
C(9)-C(8)-C(7)	121.38(16)
C(9)-C(8)-H(8)	119.3(11)
C(7)-C(8)-H(8)	119.3(11)
C(12)-C(9)-C(8)	118.49(16)
C(12)-C(9)-H(9)	118.9(11)
C(8)-C(9)-H(9)	122.6(11)
C(11)-C(10)-C(7)	121.09(16)
C(11)-C(10)-H(10)	120.8(12)
C(7)-C(10)-H(10)	118.1(12)
C(12)-C(11)-C(10)	119.13(16)
C(12)-C(11)-H(11)	118.9(11)
C(10)-C(11)-H(11)	121.9(11)
C(11)-C(12)-C(9)	121.55(15)
C(11)-C(12)-O(3)	119.86(14)
C(9)-C(12)-O(3)	118.35(14)
O(4)-C(13)-O(3)	123.03(15)
O(4)-C(13)-C(14)	126.23(16)
O(3)-C(13)-C(14)	110.74(14)
C(13)-C(14)-H(14C)	110.1(14)
C(13)-C(14)-H(14B)	107.5(17)
H(14C)-C(14)-H(14B)	109(2)
C(13)-C(14)-H(14A)	111.3(15)
H(14C)-C(14)-H(14A)	110(2)
H(14B)-C(14)-H(14A)	109(2)



***N*-(1-(methylthio)-4-oxopentan-3-yl)acetamide (10e).**^[30] The title compound was synthesized on 2.0 mmol scale employing the reaction conditions and work-up procedure described for **10a**. Purification by column chromatography eluting with EtOAc afforded **10e** (269.9 mg, 1.43 mmol, 71%) as colorless oil. TLC (EtOAc):

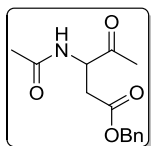
$R_f = 0.22$.

^1H NMR (400 MHz, CDCl_3): $\delta = 6.53 - 6.38$ (br s, 1H), 4.74 – 4.66 (m, 1H), 2.54 – 2.36 (m, 2H), 2.22 (s, 3H), 2.22 – 2.13 (m, 1H), 2.06 (s, 3H), 2.00 (s, 3H), 1.87 – 1.75 (m, 1H) ppm.

^{13}C NMR (100 MHz, CDCl_3): $\delta = 206.3, 170.1, 58.2, 30.9, 30.0, 27.4, 23.3, 15.7$ ppm.

IR (KBr): $\tilde{\nu} = 3289, 3061, 2918, 1720, 1655, 1542, 1438, 1373, 1299, 1159, 1121, 1040, 608$ cm^{-1} .

Chiral stationary phase GC: FS-Hydrodex β -6-TBDM column (Macherey-Nagel), $l = 30$ m; splitflow: 80 mL/min; precolumn pressure: 0.8 bar; T (injector + detector) = 250 °C; conditions: 100 – 210 °C, 2 °C/min. Retention times: t_R (R) = 40.7 min, t_R (S) = 41.8 min.



Benzyl 3-acetamido-4-oxopentanoate (10f). The title compound was synthesized on 2.0 mmol scale employing the reaction conditions and work-up procedure described for **10a**. Purification by column chromatography eluting with EtOAc afforded **10f** (220.5 mg, 0.84 mmol, 42%) as a colorless oil which solidified upon standing at rt overnight. TLC (EtOAc): $R_f = 0.32$. Mp 71 °C.

^1H NMR (400 MHz, CDCl_3): $\delta = 7.39 - 7.29$ (m, 5H), 6.67 (d, $J = 8.0$ Hz, 1H), 5.10 (s, 2H), 4.78 – 4.72 (m, 1H), 3.01 (dd, $J = 17.0, 4.5$ Hz, 1H), 2.85 (dd, $J = 17.0, 4.9$ Hz, 1H), 2.21 (s, 3H), 2.00 (s, 3H) ppm.

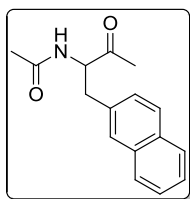
^{13}C NMR (100 MHz, CDCl_3): $\delta = 205.3, 171.3, 170.0, 135.4, 128.7, 128.6, 128.4, 67.0, 55.2, 35.4, 26.8, 23.2$ ppm.

IR (KBr): $\tilde{\nu} = 3357, 3040, 2947, 1719, 1644, 1512, 1459, 1430, 1352, 1249, 1197, 1165, 1129, 1025, 939, 914, 841, 752, 700, 668, 604$ cm^{-1} .

HRMS (ESI): $m/z = 286.1057$ [$\text{M}+\text{Na}$] $^+$ (calcd $m/z = 286.1055$); $m/z = 549.2222$ [$2\text{M}+\text{Na}$] $^+$ (calcd $m/z = 549.2213$)

Elem. Anal.: calcd for $\text{C}_{14}\text{H}_{17}\text{NO}_4$: C 63.87, H 6.51, N 5.32; found: C 63.98, H 6.51, N 5.38.

Chiral stationary phase HPLC: Chiralpak IC column (Daicel), 250 mm \times 4.6 mm; eluent: 25% *i*-PrOH/hexanes, 1.0 mL/min; UV-detector $\lambda = 220$ nm. Retention times: t_R (R) = 16.8 min, t_R (S) = 22.4 min.



***N*-(1-(naphthalen-2-yl)-3-oxobutan-2-yl)acetamide (10g).** The title compound was synthesized on 2.0 mmol scale employing the reaction conditions and work-up procedure described for **10a** with the exception that the reaction time was 45 min. Purification by column chromatography eluting with EtOAc afforded **10g** (366.8 mg, 1.44 mmol, 72%) as colorless solid. TLC (EtOAc): $R_f = 0.32$. Mp 110 – 112 °C.

^1H NMR (400 MHz, CDCl_3): δ = 7.84 – 7.75 (m, 3H), 7.57 (s, 1H), 7.50 – 7.43 (m, 2H), 7.29 – 7.25 (m, 1H), 6.19 (d, J = 7.1 Hz, 1H), 4.98 – 4.91 (m, 1H), 3.29 (dd, J = 14.1, 6.9 Hz, 1H), 3.20 (dd, J = 14.1, 5.8 Hz, 1H), 2.16 (s, 3H), 1.97 (s, 3H) ppm.

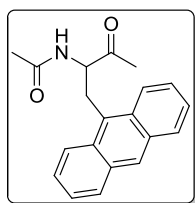
^{13}C NMR (100 MHz, CDCl_3): δ = 206.5, 169.8, 133.5, 133.5, 132.6, 128.5, 128.0, 127.8, 127.7, 127.2, 126.4, 126.0, 59.6, 37.5, 28.3, 23.2 ppm.

IR (KBr): $\tilde{\nu}$ = 3315, 3057, 2971, 2923, 2829, 1914, 1715, 1638, 1544, 1437, 1372, 1354, 1329, 1293, 1275, 1265, 1202, 1166, 1153, 1126, 1031, 946, 890, 855, 827, 799, 739, 611, 529, 478 cm^{-1} .

HRMS (EI): m/z = 255.1266 $[\text{M}]^{*+}$ (calcd m/z = 255.1259).

Elem. Anal.: calcd for $\text{C}_{16}\text{H}_{17}\text{NO}_2$: C 75.27, H 6.71, N 5.49; found: C 75.24, H 6.73, N 5.26.

Chiral stationary phase HPLC: Chiralpak IC column (Daicel), 250 mm \times 4.6 mm; eluent: 15% *i*-PrOH/hexanes, 1.0 mL/min; UV-detector λ = 254 nm. Retention times: t_{R} (*S*) = 21.4 min, t_{R} (*R*) = 23.9 min.



***N*-(1-(anthracen-9-yl)-3-oxobutan-2-yl)acetamide (10h)**. The title compound was synthesized on 0.5 mmol scale as described for **10a** with the exception that 200 μL (216 mg, 2.10 mmol) Ac_2O and 200 μL (146 mg, 1.44 mmol) Et_3N were used. After removal of all volatiles *in vacuo* the crude product was directly subjected to column chromatography eluting with TBME to afford **10h** (87.8 mg, 0.29 mmol, 58%) as yellow solid. TLC (TBME): R_f = 0.22. Mp 187 $^\circ\text{C}$.

^1H NMR (400 MHz, CDCl_3): δ = 8.40 (s, 1H), 8.37 (d, J = 9.1 Hz, 2H), 8.01 (d, J = 8.4 Hz, 2H), 7.57 (ddd, J = 8.9, 6.5, 1.4 Hz, 2H), 7.48 (ddd, J = 7.9, 6.6, 1.1 Hz, 2H), 6.47 (d, J = 6.9 Hz, 1H), 5.09 – 5.02 (m, 1H), 4.17 (dd, J = 14.3, 6.7 Hz, 1H), 3.88 (dd, J = 14.3, 9.2 Hz, 1H), 1.96 (s, 3H), 1.48 (s, 3H) ppm.

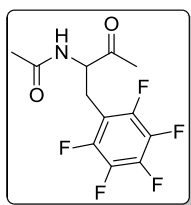
^{13}C NMR (100 MHz, CDCl_3): δ = 207.9, 170.0, 131.5, 130.5, 129.5, 128.2, 127.5, 126.7, 125.3, 124.1, 59.8, 30.8, 29.4, 23.2 ppm.

IR (KBr): $\tilde{\nu}$ = 3318, 3052, 2919, 1713, 1640, 1542, 1445, 1369, 1353, 1325, 1288, 1255, 1213, 1186, 1167, 1120, 1027, 954, 884, 843, 774, 731, 607, 562, 525, 481 cm^{-1} .

HRMS (EI): $m/z = 305.1418$ $[M]^{++}$ (calcd $m/z = 305.1416$).

Elem. Anal.: calcd for $C_{20}H_{19}NO_2$: C 78.66, H 6.27, N 4.59; found: C 77.80, H 6.18, N 4.01.

Chiral stationary phase HPLC: Chiralpak IC column (Daicel), 250 mm \times 4.6 mm; eluent: 25% *i*-PrOH/hexanes, 1.0 mL/min; UV-detector $\lambda = 254$ nm. Retention times: $t_R(S) = 14.2$ min, $t_R(R) = 22.3$ min.



***N*-(3-oxo-1-(perfluorophenyl)butan-2-yl)acetamide (10i).** The title compound was synthesized on 0.5 mmol scale employing the reaction conditions and work-up procedure described for **10a** with the exception that DCM (100 μ L) was used as solvent. Purification by column chromatography eluting with EtOAc/hexanes (1:1) afforded **10i** (134.6 mg, 0.46 mmol, 91%) as colorless solid. TLC (EtOAc/hexanes 1:1): $R_f = 0.26$. Mp 155 – 156 $^{\circ}C$.

1H NMR (400 MHz, $CDCl_3$): $\delta = 6.13$ (d, $J = 7.7$ Hz, 1H), 4.98 – 4.91 (m, 1H), 3.45 – 3.38 (m, 1H), 3.00 – 2.92 (m, 1H), 2.34 (s, 3H), 1.96 (s, 3H) ppm.

^{13}C NMR (100 MHz, $CDCl_3$): $\delta = 204.6, 170.0, 109.8$ (m), 57.7, 27.4, 24.7, 23.1 ppm.

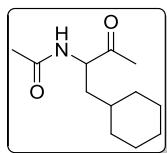
^{19}F NMR (376 MHz, $CDCl_3$): $\delta = -142.2$ (m), -154.6 (t, $J = 20.8$ Hz), -161.7 (m) ppm.

IR (KBr): $\tilde{\nu} = 3307, 3065, 2931, 1722, 1644, 1544, 1524, 1504, 1441, 1426, 1375, 1335, 1294, 1268, 1220, 1176, 1167, 1122, 1167, 1033, 974, 921, 893, 716, 680, 610, 563, 532, 498, 466, 432$ cm^{-1} .

HRMS (ESI): $m/z = 296.0728$ $[M+H]^+$ (calcd $m/z = 296.0710$); $m/z = 318.0529$ $[M+Na]^+$ (calcd $m/z = 318.0529$); $m/z = 613.1180$ $[2M+Na]^+$ (calcd $m/z = 613.1161$).

Elem. Anal.: calcd for $C_{12}H_{10}F_5NO_2$: C 48.82, H 3.41, N 4.74; found: C 48.62, H 3.32, N 4.67.

Chiral stationary phase GC: FS-Hydrodex β -6-TBDM column (Macherey-Nagel), $l = 30$ m; splitflow: 80 mL/min; precolumn pressure: 0.8 bar; T (injector + detector) = 250 $^{\circ}C$; conditions: 100 – 210 $^{\circ}C$, 2 $^{\circ}C/min$. Retention times: $t_R(S) = 38.3$ min, $t_R(R) = 38.7$ min.



***N*-(1-cyclohexyl-3-oxobutan-2-yl)acetamide (10j).** The title compound was synthesized on 1.0 mmol scale employing the reaction conditions and work-up procedure described for **10a** with the exception that the reaction time was 2 h.

Purification by column chromatography eluting with EtOAc afforded **10j** (132.4 mg, 0.63 mmol, 63%) as colorless oil which crystallized upon standing at rt over night. TLC (EtOAc): $R_f = 0.32$.

^1H NMR (400 MHz, CDCl_3): $\delta = 6.12$ (d, $J = 7.9$ Hz, 1H), 4.66 (ddd, $J = 9.2, 7.9, 4.1$ Hz, 1H), 2.19 (s, 3H), 2.00 (s, 3H), 1.89 – 1.81 (m, 1H), 1.72 – 1.54 (m, 5H), 1.38 – 1.04 (m, 5H), 0.98 – 0.80 (m, 2H) ppm.

^{13}C NMR (100 MHz, CDCl_3): $\delta = 207.9, 170.1, 56.7, 39.0, 34.3, 34.1, 32.7, 27.4, 26.4, 26.3, 26.1, 23.3$ ppm.

IR (KBr): $\tilde{\nu} = 3319, 3043, 2922, 2850, 2666, 1714, 1645, 1538, 1447, 1379, 1360, 1304, 1264, 1236, 1195, 1131, 1110, 1046, 1012, 937, 922, 890, 674, 595, 531, 512\text{ cm}^{-1}$.

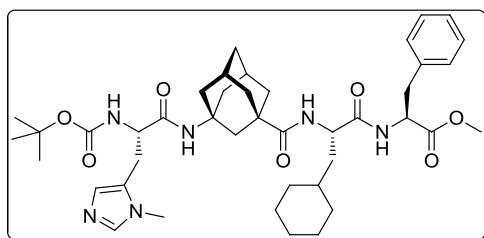
HRMS (EI): $m/z = 211.1564$ $[\text{M}]^{*+}$ (calcd $m/z = 211.1572$).

Elem. Anal.: calcd for $\text{C}_{12}\text{H}_{21}\text{NO}_2$: C 68.21, H 10.02, N 6.63; found: C 68.21, H 10.03, N 6.68.

Chiral stationary phase HPLC: Chiralpak IC column (Daicel), 250 mm \times 4.6 mm; eluent: 15% *i*-PrOH/hexanes, 1.0 mL/min; UV-detector $\lambda = 220$ nm. Retention times: t_R (*S*) = 16.0 min, t_R (*R*) = 22.4 min.

2.4 Availability of Catalysts

Unless otherwise noted, peptides were synthesized by EDC/HOBt mediated peptide coupling in solution using the *N*-*tert*-butoxycarbonyl (Boc) protecting group strategy. Boc-4-aminoadamantanecarboxylic acid (Boc-^AGly-OH),^[31] Boc-anthranilic acid (Boc-2-Abz-OH),^[32] Boc-D-Pro-OH,^[33] and Boc-L-Pmh-OH,^[34] were prepared according to literature procedures. H-L-Pmh-OMe \cdot 2 HCl and Boc-L-Pmh-OMe were synthesized as described below. All other amino acids and coupling reagents were purchased from commercial suppliers and were used as received.



Boc-L-Pmh-^AGly-L-Cha-L-Phe-OMe (11). *Coupling 1:* H-L-Phe-OMe • HCl (1.078 g, 5.00 mmol) and Boc-L-Cha-OH • DCHA (2.264 g, 5.00 mmol) were added to a round-bottom flask, along with 1-Ethyl-3-(3-dimethylaminopropyl)carbodiimide hydrochloride (EDC • HCl; 1.054 g, 5.50 mmol) and 1-hydroxybenzotriazole

hydrate (HOBt • H₂O; 0.842 g, 5.5 mmol). CH₂Cl₂ (25 mL) was added, followed by Et₃N (0.77 mL, 0.559 g, 5.52 mmol), and the resulting suspension was stirred at rt for 24 h. The reaction mixture was diluted with EtOAc and subsequently washed with 0.5 M citric acid solution (3 × 50 mL), sat. aq. NaHCO₃ (3 × 50 mL) and brine (50 mL). The organic layer was dried over Na₂SO₄, filtered, and concentrated under reduced pressure to afford the crude peptide (2.124 g, 4.91 mmol, 98%) as colorless foam.

The peptides obtained using this procedure were usually sufficiently pure (as judged by NMR and/or ESI-MS) and were used for subsequent coupling steps without any purification.

Deprotection 1: The peptide fragment was treated with 4 M HCl in 1,4-dioxane (2 mL/mmol) and the resulting solution was stirred at rt for 45 min. The reaction flask was flushed with argon for 30 min to remove residual HCl and the solvent was removed under reduced pressure. After drying *in vacuo*, the resulting peptide hydrochloride was directly used for the next coupling step.

Coupling 2: The coupling of H-L-Cha-L-Phe-OMe • HCl and Boc-^AGly-OH was performed on 4.74 mmol scale according to the procedure described for coupling 1 (*vide supra*). Boc-^AGly-L-Cha-L-Phe-OMe was obtained as colorless foam (2.876 g, 4.72 mmol, 99%).

Deprotection 2: The deprotection was performed as described above for deprotection 1.

Coupling 3: The coupling of H-^AGly-L-Cha-L-Phe-OMe • HCl with Boc-L-Pmh-OH was performed on 2.10 mmol scale according to the previous couplings with the modification that 2.2 equiv of coupling reagents and base were used. The slightly yellow solution was diluted with EtOAc and washed with sat. aq. NaHCO₃ (3 × 50 mL) and brine (3 × 50 mL). The organic layer was dried over Na₂SO₄, filtered, and concentrated under reduced pressure to give a yellow foam. Purification by column chromatography eluting with CHCl₃/MeOH (10:1) afforded oligopeptide **11** (1.272 g, 1.67 mmol, 80%) as colorless foam. TLC: *R*_f = 0.41 (CHCl₃/MeOH 10:1)

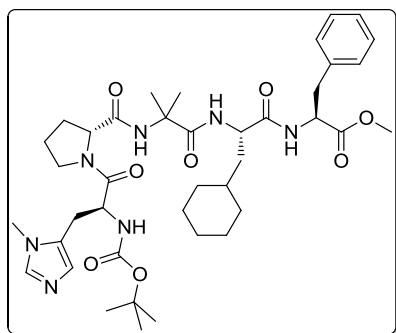
¹H NMR (400 MHz, CDCl₃): δ = 7.54 (s, 1H), 7.29 – 7.19 (m, 3H), 7.12 – 7.07 (m, 2H), 6.86 (s, 1H), 6.69 (d, *J* = 7.7 Hz, 1H), 6.16 (s, 1H), 6.09 (d, *J* = 7.9 Hz, 1H), 5.35 (br s, 1H), 4.82 – 4.75 (m, 1H), 4.48 – 4.40 (m, 1H), 4.28 – 4.16 (m, 1H), 3.68 (s, 3H), 3.61 (s, 3H), 3.11 (dd, *J* = 13.9, 5.9 Hz, 1H), 3.05 (dd, *J* = 13.9, 6.5 Hz, 1H), 2.98 (d, *J* = 6.9 Hz, 2H), 2.17 (m, 2H), 2.03 – 1.94

(m, 2H), 1.95 – 1.85 (m, 4H), 1.76 – 1.55 (m, 12H), 1.51 – 1.43 (m, 1H), 1.41 (s, 9H), 1.28 – 1.05 (m, 4H), 0.97 – 0.76 (m, 2H) ppm.

^{13}C NMR (100 MHz, CDCl_3): δ = 176.5, 172.1, 171.8, 169.8, 155.5, 138.0, 135.9, 129.3, 128.7, 127.8, 127.7, 80.5, 54.5, 53.4, 52.5, 52.4, 50.8, 42.6, 42.3, 40.4, 40.4, 39.6, 38.3, 38.1, 37.9, 35.3, 34.3, 33.6, 32.8, 31.8, 29.2, 29.2, 28.4, 27.1, 26.5, 26.3, 26.2 ppm.

IR (KBr): $\tilde{\nu}$ = 3308, 3062, 3030, 2922, 2853, 1748, 1664, 1509, 1450, 1391, 1366, 1279, 1248, 1215, 1169, 1110, 1052, 1022, 929, 889, 816, 747, 701, 662, 616 cm^{-1} .

Spectroscopic data match those reported in the literature.^[35]



Boc-L-Pmh-D-Pro-Aib-L-Cha-L-Phe-OMe (12). The pentapeptide was synthesized employing the procedure described for **11**. Purification by column chromatography eluting with $\text{CH}_2\text{Cl}_2/\text{MeOH}$ (9:1) afforded **12** in 42% overall yield as colorless solid. TLC ($\text{CHCl}_3/\text{MeOH}$ 9:1): R_f = 0.44.

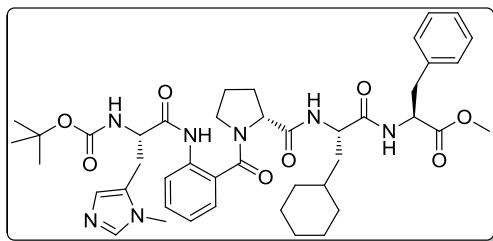
^1H NMR (600 MHz, CDCl_3): δ = 7.37 (s, 1H), 7.28 – 7.24 (m, 3H), 7.22 – 7.18 (m, 3H), 6.92 (d, J = 8.3 Hz, 1H), 6.81 (s, 1H), 6.54 (s, 1H), 6.47 (d, J = 9.2 Hz, 1H), 4.81 – 4.75 (m, 1H), 4.65 – 4.58 (m, 1H), 4.48 – 4.42 (m, 1H), 4.07 (m, 1H), 3.64 (s, 3H), 3.61 (s, 3H), 3.60 – 3.55 (m, 1H), 3.35 (ddd, J = 10.3, 7.1, 5.3 Hz, 1H), 3.21 – 3.14 (m, 2H), 3.07 (dd, J = 13.7, 6.7 Hz, 1H), 2.92 (dd, J = 15.0, 5.7 Hz, 1H), 2.12 – 2.06 (m, 1H), 2.06 – 1.96 (m, 2H), 1.84 – 1.74 (m, 2H), 1.73 – 1.64 (m, 5H), 1.59 (s, 3H), 1.46 (s, 3H), 1.42 (s, 9H), 1.37 – 1.31 (m, 1H), 1.27 – 1.08 (m, 4H), 1.00 – 0.92 (m, 1H), 0.90 – 0.82 (m, 1H) ppm.

^{13}C NMR (150 MHz, CDCl_3): δ = 174.4, 171.9, 171.8, 171.7, 170.2, 155.9, 137.9, 136.4, 129.7, 128.6, 128.0, 127.0, 80.1, 61.4, 57.4, 53.6, 52.0, 51.9, 50.7, 47.7, 37.8, 37.8, 34.4, 33.9, 32.6, 31.6, 28.9, 28.5, 27.8, 26.9, 26.6, 26.4, 26.3, 25.4, 23.9 ppm.

IR (KBr): $\tilde{\nu}$ = 3317, 2978, 2926, 2852, 1747, 1710, 1673, 1637, 1509, 1448, 1366, 1322, 1246, 1168, 1111, 1049, 1027, 933, 816, 746, 702, 665 cm^{-1} .

HRMS (ESI): m/z = 766.4506 $[\text{M}+\text{H}]^+$ (calcd m/z = 766.4503).

Elem. Anal.: calcd for $\text{C}_{40}\text{H}_{59}\text{N}_7\text{O}_8$: C 62.72, H 7.76, N 12.80; found: C 61.65, H 7.84, N 12.11.

**Boc-L-Pmh-2-Abz-D-Pro-L-Cha-L-Phe-OMe (13).**

The pentapeptide was synthesized employing the procedure described for **11**. A sample of the peptide was purified by preparative HPLC for complete characterization and catalysis. LiChrosorb Si-100-phase column (Merck), 250 mm × 8 mm; eluent: 55% *i*-PrOH/hexanes, 4.0 mL/min; UV-detector λ = 210 nm. Retention time: t_R = 5.4 min.

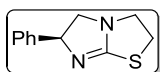
^1H NMR (600 MHz, CDCl_3): δ = 9.07 (s, 1H), 8.18 (d, J = 6.2 Hz, 1H), 7.88 (d, J = 6.8 Hz, 1H), 7.44 – 7.38 (m, 2H), 7.30 (d, J = 7.7 Hz, 1H), 7.24 – 7.20 (m, 2H), 7.18 – 7.12 (m, 4H), 6.90 (s, 1H), 6.83 (br s, 1H), 5.99 (d, J = 8.8 Hz, 1H), 4.82 – 4.71 (m, 2H), 4.52 – 4.44 (m, 2H), 3.66 – 3.58 (m, 4H), 3.55 (s, 3H), 3.37 – 3.29 (m, 2H), 3.26 – 3.20 (m, 1H), 3.15 – 3.00 (m, 4H), 2.30 – 2.23 (m, 1H), 2.11 – 1.96 (m, 2H), 1.88 – 1.81 (m, 1H), 1.73 – 1.59 (m, 6H), 1.38 (s, 9H), 1.37 – 1.31 (m, 1H), 1.22 – 1.08 (m, 4H), 0.97 – 0.84 (m, 2H) ppm.

^{13}C NMR (150 MHz, CDCl_3): δ = 174.4, 171.9, 171.8, 171.7, 170.2, 155.9, 138.0, 136.8, 134.4, 130.6, 129.4, 128.6, 127.6, 127.1, 126.9, 126.8, 124.7, 123.3, 80.0, 60.5, 54.2, 53.8, 52.4, 51.8, 49.7, 39.8, 37.5, 34.4, 33.5, 32.8, 31.9, 29.6, 28.5, 27.4, 26.5, 26.3, 26.2, 25.5 ppm.

IR (KBr): $\tilde{\nu}$ = 3341, 2977, 2925, 2851, 1746, 1658, 1588, 1512, 1453, 1422, 1392, 1367, 1276, 1248, 1212, 1166, 1110, 1050, 1027, 930, 758, 701, 662 cm^{-1} .

HRMS (ESI): m/z = 800.4347 $[\text{M}+\text{H}]^+$ (calcd m/z = 800.4346); m/z = 822.4160 $[\text{M}+\text{H}]^+$ (calcd m/z = 822.4166).

Elem. Anal.: calcd for $\text{C}_{43}\text{H}_{57}\text{N}_7\text{O}_8$: C 64.56, H 7.18, N 12.26; found: C 63.06, H 7.32, N 11.22.



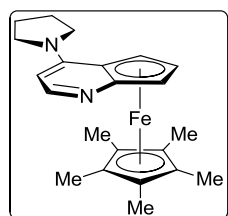
(S)-Tetramisol (14). Levamisol hydrochloride (240.8 mg, 1.0 mmol) was dissolved in H_2O (10 mL) and 33% NaOH (20 mL) was added. The reaction mixture was stirred for at rt for 1 h and extracted with CH_2Cl_2 (4×15 mL). The combined organic layers were dried over Na_2SO_4 , filtered and the solvent was removed *in vacuo* yielding **14** (204.0 mg, 1.0 mmol, quant.) as colorless solid.

^1H NMR (400 MHz, CDCl_3): δ = 7.37 – 7.31 (m, 4H), 7.28 – 7.22 (m, 1H), 5.45 (t, J = 8.9 Hz, 1H), 3.70 – 3.60 (m, 2H), 3.52 (ddd, J = 10.8, 6.4, 4.4 Hz, 1H), 3.36 (ddd, J = 8.6, 6.5, 4.4 Hz, 1H), 3.12 (dt, J = 8.6, 6.4 Hz, 1H), 2.98 (dd, J = 9.2, 8.3 Hz, 1H) ppm.

^{13}C NMR (100 MHz, CDCl_3): δ = 174.4, 142.9, 128.5, 127.3, 126.6, 77.0, 58.5, 49.2, 34.2 ppm.

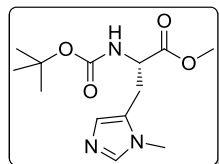
IR (KBr): $\tilde{\nu}$ = 3054, 3030, 2988, 2964, 2943, 2919, 2881, 2838, 1944, 1870, 1805, 1746, 1594, 1580, 1494, 1471, 1452, 1368, 1349, 1326, 1299, 1289, 1276, 1258, 1202, 1159, 1079, 1052, 1037, 1012, 976, 956, 925, 905, 873, 836, 757, 698, 672, 639, 620, 587, 544, 530, 493 cm^{-1} .

The NMR data are in accordance with those reported.^[36]



(S)-(-)-4-Pyrrolidinopyrindinyl(pentamethylcyclopentadienyl)iron (15).

Catalyst was purchased from ABCR and was used without further purification.



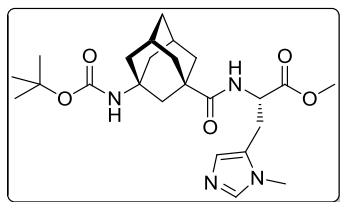
Boc-L-Pmh-OMe (16). The title compound was synthesized from Boc-L-Pmh-OH (0.673 g, 2.50 mmol) and MeOH (0.41 mL, 0.321 g, 10.00 mmol) employing the procedure described for coupling **3** in the synthesis of **11**. Yield: 0.691 g (2.44 mmol, 98%). TLC ($\text{CHCl}_3/\text{MeOH}$ 9:1): R_f = 0.38.

^1H NMR (400 MHz, CDCl_3): δ = 7.37 (s, 1H), 6.76 (s, 1H), 5.21 (d, J = 7.8 Hz, 1H), 4.56 – 4.48 (m, 1H), 3.73 (s, 3H), 3.56 (s, 3H), 3.11 (dd, J = 15.4, 5.8 Hz, 1H), 3.04 (dd, J = 15.4, 6.0 Hz, 1H), 1.40 (s, 9H) ppm.

^{13}C NMR (100 MHz, CDCl_3): δ = 171.8, 155.2, 138.5, 128.4, 126.6, 80.3, 53.1, 52.7, 31.4, 28.4, 27.0 ppm.

IR (KBr): $\tilde{\nu}$ = 2980, 1736, 1697, 1537, 1510, 1437, 1367, 1324, 1291, 1245, 1219, 1201, 1166, 1110, 1054, 1039, 991, 935, 854, 815, 786, 753, 699, 664 cm^{-1} .

The spectroscopic data are in accordance with those reported.^[37]



Boc-^AGly-L-Pmh-OMe (17). *H-L-Pmh-OMe • 2 HCl: Method A:* Dry MeOH (45 mL) was cooled to 0 °C with an ice-bath and freshly distilled SOCl₂ (3.9 mL, 6.40 g, 53.8 mmol) was added dropwise. After stirring for 30 min at 0 °C, H-L-Pmh-OH • 2 HCl (3.64 g, 15.0 mmol) was added and the reaction mixture was stirred

at 0 °C for 1 h, and additional 24 h at rt. All volatiles were removed *in vacuo* to afford H-L-Pmh-OMe • 2 HCl (quant.) as colorless to brownish solid.

H-L-Pmh-OMe • 2 HCl: Method B: In accordance with a reported procedure,^[38] trimethylsilyl chloride (3.80 mL, 3.26 g, 30.0 mmol) was added dropwise to Boc-L-Pmh-OH (2.64 g, 9.8 mmol) with cooling. Dry MeOH (100 mL) was added slowly and the resulting solution was allowed to stir at rt for 24 h. All volatiles were removed *in vacuo* to afford H-L-Pmh-OMe • 2 HCl (quant.) as colorless solid.

¹H NMR (400 MHz, D₂O): δ = 8.75 (s, 1H), 7.48 (s, 1H), 4.55 (t, J = 7.3 Hz, 1H), 3.89 (s, 3H), 3.86 (s, 3H), 3.55 (dd, J = 16.3, 6.9 Hz, 1H), 3.42 (dd, J = 16.1, 7.3 Hz, 1H) ppm.

¹³C NMR (100 MHz, D₂O): δ = 168.8, 136.1, 128.1, 118.9, 54.0, 51.0, 33.4, 23.7 ppm.

¹H NMR data are in accordance with those reported.^[39]

According to a literature procedure,^[40] Boc-^AGly-OH (886.1 mg, 3.0 mmol), H-L-Pmh-OMe • 2 HCl (768.4 mg, 3.0 mmol) and *O*-(benzotriazol-1-yl)-*N,N,N',N'*-tetramethyluronium hexafluorophosphate (HBTU; 1.138 g, 3.0 mmol) were dissolved in dry acetonitrile/methanol (10:1, 44 mL) and cooled to 0 °C with an ice bath. DiPEA (1.53 mL, 1.163 g, 9.0 mmol) was added and the mixture was stirred for 3.5 h upon warming to rt. The reaction was quenched with brine (60 mL) and extracted with CHCl₃ (4 × 40 mL). The combined organic layers were successively washed with H₂O (2 × 50 mL), sat. aq. NaHCO₃ (2 × 50 mL) and brine (2 × 50 mL) and dried over Na₂SO₄. After filtration and removal of the solvent under reduced pressure the crude product was purified by column chromatography eluting with CHCl₃/MeOH (9:1) to yield **17** (952.2 mg, 2.07 mmol, 69%) as colorless solid. TLC (CHCl₃/MeOH 9:1): R_f = 0.33.

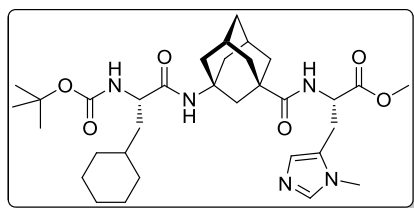
¹H NMR (600 MHz, CDCl₃): δ = 7.53 (s, 1H), 6.80 (s, 1H), 6.28 (d, J = 7.4 Hz, 1H), 4.79 – 4.75 (m, 1H), 4.43 (br s, 1H), 3.74 (s, 3H), 3.62 (s, 3H), 3.14 (dd, J = 15.4, 6.2 Hz, 1H), 3.06 (dd, J = 15.4, 6.4 Hz, 1H), 2.22 – 2.17 (m, 2H), 2.03 – 1.95 (m, 2H), 1.95 – 1.82 (m, 4H), 1.78 – 1.68 (m, 4H), 1.66 – 1.57 (m, 2H), 1.42 (s, 9H) ppm.

^{13}C NMR (150 MHz, CDCl_3): δ = 176.7, 171.8, 154.2, 138.2, 127.5, 126.9, 79.1, 52.8, 51.4, 50.9, 43.0, 42.8, 41.1, 41.0, 38.3, 38.3, 35.4, 31.8, 29.3, 29.3, 28.6, 26.8 ppm.

IR (KBr): $\tilde{\nu}$ = 3332, 2977, 2931, 2909, 2855, 1750, 1710, 1686, 1637, 1529, 1453, 1364, 1341, 1303, 1277, 1247, 1220, 1175, 1072, 1021, 938, 878, 665 cm^{-1} .

HRMS (EI): m/z = 460.2681 $[\text{M}]^{*+}$ (calcd m/z = 460. 2680).

Elem. Anal.: calcd for $\text{C}_{24}\text{H}_{36}\text{N}_4\text{O}_5$: C 62.59, H 7.88, N 12.16; found: C 60.98, H 7.86, N 10.90.



Boc-L-Cha-^AGly-L-Pmh-OMe (18). *Coupling 1:* The coupling of Boc-^AGly-OH (1.188 g, 4.0 mmol) and H-L-Pmh-OMe • 2 HCl (1.027 g, 4.0 mmol) was performed as described for catalyst **17**. The crude product obtained after work-up was used for the subsequent steps without further purification.

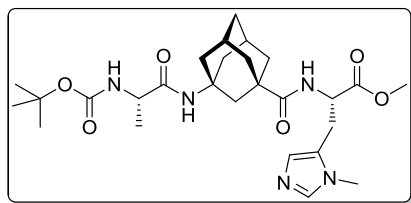
Deprotection: The deprotection was performed as described for the synthesis of **11**.

Coupling 2: The coupling of H-^AGly-L-Pmh-OMe • 2 HCl and Boc-L-Cha-OH • DCHA was performed according to coupling 3 described for the synthesis of **11** with the modification that 3 equiv of Et_3N were used. Column chromatography eluting with $\text{CH}_2\text{Cl}_2/\text{MeOH}$ (95:5) gave Boc-L-Cha-^AGly-L-Pmh-OMe (**18**; 1.645 g, 2.68 mmol, 67% based on H-L-Pmh-OMe • 2 HCl) as colorless solid. TLC ($\text{CH}_2\text{Cl}_2/\text{MeOH}$, 95:5): R_f = 0.32.

^1H NMR (600 MHz, CDCl_3): δ = 7.44 (s, 1H), 6.76 (s, 1H), 6.27 (d, J = 7.5 Hz, 1H), 5.90 (br s, 1H), 4.89 (br s, 1H), 4.79 – 4.75 (m, 1H), 3.97 (br s, 1H), 3.74 (s, 3H), 3.60 (s, 3H), 3.13 (dd, J = 15.5, 6.1 Hz, 1H), 3.05 (dd, J = 15.4, 6.5 Hz, 1H), 2.07 (d, J = 11.8 Hz, 1H), 2.03 – 1.96 (m, 2H), 1.96 – 1.90 (m, 3H), 1.79 – 1.58 (m, 12H), 1.44 (s, 9H), 1.43 – 1.36 (m, 1H), 1.34 – 1.09 (m, 5H), 0.99 – 0.91 (m, 1H), 0.91 – 0.83 (m, 1H) ppm.

^{13}C NMR (150 MHz, CDCl_3): δ = 176.5, 172.0, 171.8, 155.9, 138.4, 127.9, 126.7, 80.2, 53.1, 52.8, 52.2, 51.3, 42.7, 42.5, 40.7, 40.6, 40.0, 38.2, 38.2, 35.3, 34.3, 33.8, 32.8, 31.6, 29.2, 29.2, 28.5, 26.8, 26.6, 26.4, 26.2, 24.9, 23.1, 22.3 ppm.

IR (KBr): $\tilde{\nu}$ = 3337, 2923, 2854, 1745, 1701, 1660, 1509, 1450, 1366, 1281, 1246, 1170, 1110, 1046, 1022, 926, 847, 754, 664 cm^{-1} .



Boc-L-Ala-^AGly-L-Pmh-OMe (S7). The tripeptide was prepared on 0.3 mmol scale employing the procedure described for **18**. Purification by column chromatography eluting with CH₂Cl₂/MeOH (10:1) afforded **S7** (90.0 mg, 0.17 mmol, 61%) as colorless solid. TLC (CH₂Cl₂/MeOH,

10:1): R_f = 0.43.

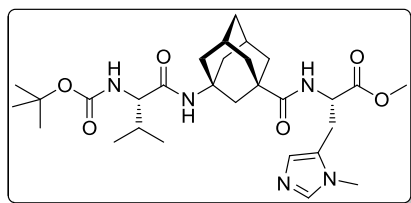
¹H NMR (600 MHz, CDCl₃): δ = 7.40 (s, 1H), 6.75 (s, 1H), 6.24 (d, J = 7.5 Hz, 1H), 5.96 (br s, 1H), 5.01 (br s, 1H), 4.80 – 4.75 (m, 1H), 4.02 (br s, 1H), 3.74 (s, 3H), 3.59 (s, 3H), 3.13 (dd, J = 15.4, 6.2 Hz, 1H), 3.04 (dd, J = 15.4, 6.4 Hz, 1H), 2.03 (m, 2H), 2.09 – 2.05 (m, 1H), 2.03 – 1.89 (m, 5H), 1.78 – 1.70 (m, 4H), 1.68 – 1.58 (m, 2H), 1.44 (s, 9H), 1.29 (d, J = 7.0 Hz, 3H) ppm.

¹³C NMR (150 MHz, CDCl₃): δ = 176.5, 171.9, 155.8, 138.6, 128.4, 126.4, 80.2, 52.8, 52.1, 51.3, 42.7, 42.5, 40.7, 40.6, 38.2, 38.2, 35.3, 31.6, 29.2, 29.2, 28.5, 26.8 ppm.

IR (KBr): $\tilde{\nu}$ = 3340, 2913, 2857, 1744, 1660, 1510, 1452, 1366, 1249, 1168, 1108, 1069, 1052, 1022, 926, 803, 754, 664 cm⁻¹.

HRMS (ESI): m/z = 532.3130 [M+H]⁺ (calcd m/z = 532.3135).

Elem. Anal.: calcd for C₂₇H₄₁N₅O₆: C 61.00, H 7.77, N 13.17; found: C 57.03, H 7.68, N 11.54.

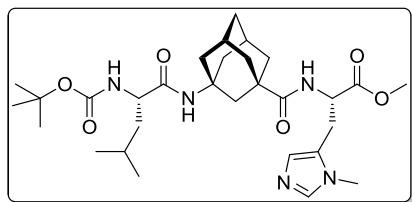


Boc-L-Val-^AGly-L-Pmh-OMe (S8). The tripeptide was prepared from purified dipeptide **17** (139.4 mg, 0.30 mmol) and Boc-L-Val-OH (56.8 mg, 0.31 mmol) according to the procedure described for **18**. Purification by column chromatography eluting with CH₂Cl₂/MeOH (10:1) afforded

S7 (71.0 mg, 0.13 mmol, 43%) as colorless solid. TLC (CH₂Cl₂/MeOH, 10:1): R_f = 0.45.

¹H NMR (600 MHz, CDCl₃): δ = 7.39 (s, 1H), 6.74 (s, 1H), 6.28 (d, J = 7.5 Hz, 1H), 5.76 (s, 1H), 5.08 (d, J = 8.9 Hz, 1H), 4.78 – 4.73 (m, 1H), 3.75 – 3.70 (m, 1H), 3.73 (s, 3H), 3.58 (s, 3H), 3.11 (dd, J = 15.4, 6.1 Hz, 1H), 3.04 (dd, J = 15.4, 6.5 Hz, 1H), 2.19 (m, 2H), 2.08 – 2.00 (m, 3H), 1.98 – 1.92 (m, 4H), 1.78 – 1.68 (m, 4H), 1.67 – 1.56 (m, 2H), 1.42 (s, 9H), 0.92 (d, J = 6.7 Hz, 3H), 0.88 (d, J = 6.8 Hz, 3H) ppm.

¹³C NMR (150 MHz, CDCl₃): δ = 176.4, 171.9, 156.0, 138.5, 128.3, 126.5, 79.9, 60.5, 52.8, 52.3, 51.3, 42.7, 42.5, 40.6, 40.5, 38.2, 38.1, 35.2, 31.6, 31.2, 29.2, 28.4, 26.8, 19.4, 18.0 ppm.



Boc-L-Leu-^AGly-L-Pmh-OMe (S10). The tripeptide was prepared from purified dipeptide **17** (461.3 mg, 1.00 mmol) and Boc-L-Leu-OH • H₂O (250.7 mg, 1.00 mmol) according to the procedure described for **18**. Purification by column chromatography eluting with CH₂Cl₂/MeOH (10:1) afforded **S10** (316.0 mg, 0.55 mmol, 55%) as colorless solid.

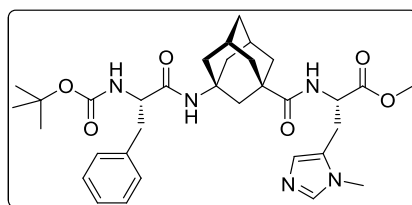
¹H NMR (600 MHz, CDCl₃): δ = 7.38 (s, 1H), 6.74 (s, 1H), 6.25 (d, J = 7.5 Hz, 1H), 5.91 (br s, 1H), 4.91 (m, 1H), 4.79 – 4.74 (m, 1H), 3.99 – 3.90 (m, 1H), 3.73 (s, 3H), 3.58 (s, 3H), 3.12 (dd, J = 15.4, 6.2 Hz, 1H), 3.04 (dd, J = 15.4, 6.4 Hz, 1H), 2.20 (m, 2H), 2.09 – 1.91 (m, 6H), 1.78 – 1.69 (m, 4H), 1.67 – 1.57 (m, 4H), 1.43 (s, 9H), 1.43 – 1.38 (m, 1H), 0.92 (t, J = 5.9 Hz, 6H) ppm.

¹³C NMR (150 MHz, CDCl₃): δ = 176.5, 171.9, 171.8, 155.9, 138.6, 128.5, 126.4, 80.1, 53.6, 52.8, 52.2, 51.4, 42.7, 42.4, 41.4, 40.6, 40.5, 38.2, 38.2, 35.3, 31.5, 29.2, 29.2, 28.5, 26.8, 24.9, 23.1, 22.3 ppm.

IR (KBr): $\tilde{\nu}$ = 3346, 2913, 2860, 1745, 1660, 1508, 1453, 1366, 1248, 1168, 1110, 1046, 1022, 926, 663 cm⁻¹.

HRMS (ESI): m/z = 574.3603 [M+H]⁺ (calcd m/z = 574.3605).

Elem. Anal.: calcd for C₃₀H₄₇N₅O₆: C 62.80, H 8.26, N 12.21; found: C 62.46, H 8.54, N 12.04.



Boc-L-Phe-^AGly-L-Pmh-OMe (S11). The deprotection of Boc-^AGly-L-Pmh-OMe (**17**; 230.5 mg, 0.50 mmol) was performed with 4 M HCl in 1,4-dioxane (2.0 mL) as described in the synthesis of **11**. Coupling of Boc-L-Phe-OH (132.8 mg, 0.50 mmol) with H-^AGly-L-Pmh-OMe • 2 HCl was performed

in the presence of HBTU (208.5 mg, 0.55 mmol), HOBT • H₂O (84.9 mg, 0.55 mmol), and Et₃N (0.23 mL, 167.0 mg, 1.65 mmol) in CH₂Cl₂ (5 mL) at rt for 24 h according to the procedure described for **17**. A sample of the crude peptide was purified by preparative HPLC for complete characterization and catalysis. LiChrosorb Diol column (Merck), 250 mm × 8 mm; eluent: 10% MeOH/TBME, 5.0 mL/min; UV-detector λ = 220 nm. Retention time: t_R = 7.5 min.

¹H NMR (600 MHz, CDCl₃): δ = 7.54 (s, 1H), 7.32 – 7.19 (m, 5H), 6.81 (s, 1H), 6.28 (d, J = 7.4 Hz), 5.42 (s, 1H), 5.14 (br s, 1H), 4.80 – 4.72 (m, 1H), 4.17 (br s, 1H), 3.75 (s, 3H), 3.61 (s, 3H),

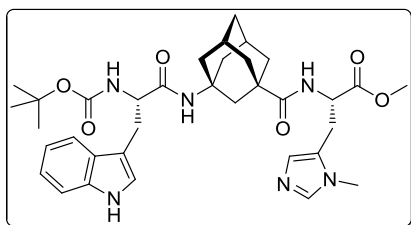
3.14 (dd, $J = 15.5, 6.1$ Hz, 1H), 3.09 – 3.02 (m, 2H), 2.96 – 2.90 (m, 1H), 2.15 (s, 2H), 1.97 – 1.86 (m, 2H), 1.85 – 1.66 (m, 8H), 1.63 – 1.54 (m, 2H), 1.41 (s, 9H) ppm.

^{13}C NMR (150 MHz, CDCl_3): $\delta = 176.5, 171.8, 170.2, 155.5, 138.2, 137.2, 129.6, 128.8, 127.5, 127.1, 126.8, 80.2, 56.5, 52.8, 52.2, 51.3, 42.7, 42.4, 40.5, 40.4, 39.2, 38.2, 38.1, 35.2, 31.8, 29.2, 28.5, 26.8$ ppm.

IR (KBr): $\tilde{\nu} = 3331, 2913, 2856, 1743, 1662, 1508, 1454, 1391, 1365, 1287, 1248, 1218, 1169, 1110, 753$ cm^{-1} .

HRMS (ESI): $m/z = 608.3446$ $[\text{M}+\text{H}]^+$ (calcd $m/z = 608.3448$).

Elem. Anal.: calcd for $\text{C}_{33}\text{H}_{45}\text{N}_5\text{O}_6$: C 65.22, H 7.46, N 11.52; found: C 63.91, H 7.30, N 10.49.



Boc-L-Trp-A-Gly-L-Pmh-OMe (S12). The tripeptide was synthesized on 0.3 mmol scale employing the procedure described for **18**. A sample of the crude peptide was purified by preparative HPLC for complete characterization and catalysis. LiChrosorb Diol column (Merck), 250 mm \times 8 mm; eluent: 12% MeOH/TBME, 5.0 mL/min; UV-detector $\lambda =$

220 nm. Retention time: $t_R = 7.4$ min.

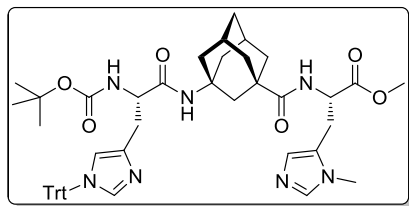
^1H NMR (600 MHz, CDCl_3): $\delta = 9.98$ (s, 1H), 7.67 (d, $J = 7.9$ Hz, 1H), 7.60 (s, 1H), 7.38 (d, $J = 8.1$ Hz, 1H), 7.18 – 7.14 (m, 1H), 7.12 – 7.08 (m, 1H), 7.02 (s, 1H), 6.85 (s, 1H), 6.33 (d, $J = 7.5$ Hz, 1H), 5.29 (br s, 1H), 5.25 (s, 1H), 4.81 – 4.76 (m, 1H), 4.36 (br s, 1H), 3.78 (s, 3H), 3.61 (s, 3H), 3.36 – 3.29 (m, 1H), 3.19 (dd, $J = 15.6, 5.3$ Hz, 1H), 3.06 – 2.97 (m, 2H), 2.08 (d, $J = 22.5$ Hz, 2H), 1.85 (d, $J = 12.1$ Hz, 1H), 1.76 (d, $J = 11.6$ Hz, 1H), 1.73 – 1.47 (m, 10H), 1.44 (s, 9H) ppm.

^{13}C NMR (150 MHz, CDCl_3): $\delta = 176.5, 171.9, 170.7, 155.6, 138.0, 136.5, 127.6, 127.2, 126.8, 124.0, 122.0, 119.5, 118.8, 111.7, 110.3, 79.9, 55.6, 52.9, 52.0, 50.9, 42.6, 42.1, 40.5, 40.2, 38.0, 38.0, 35.2, 31.8, 29.1, 29.1, 29.0, 28.5, 26.6$ ppm.

IR (KBr): $\tilde{\nu} = 3418, 2914, 2856, 1660, 1509, 1456, 1365, 1248, 1168, 744, 663$ cm^{-1} .

HRMS (ESI): $m/z = 647.3555$ $[\text{M}+\text{H}]^+$ (calcd $m/z = 647.3557$).

Elem. Anal.: calcd for C₃₅H₄₆N₆O₆: C 65.00, H 7.17, N 12.99; found: C 62.57, H 7.07, N 12.30.



Boc-(Trt)-L-His-^AGly-L-Pmh-OMe (S13). The tripeptide was synthesized on 0.3 mmol scale employing the procedure described for **18**. A sample of the crude peptide was purified by preparative HPLC for complete characterization and catalysis. LiChrosorb Diol column (Merck), 250 mm × 8 mm;

eluent: 10% MeOH/TBME, 5.0 mL/min; UV-detector λ = 220 nm. Retention time: t_R = 13.5 min.

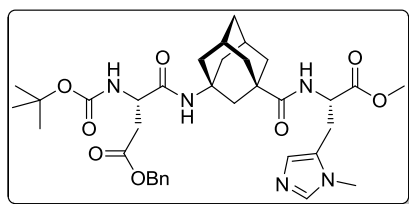
¹H NMR (600 MHz, CDCl₃): δ = 7.45 (s, 1H), 7.39 (s, 1H), 7.34 – 7.29 (m, 9H), 7.11 – 7.07 (m, 6H), 6.78 (s, 1H), 6.70 (br s, 1H), 6.66 (s, 1H), 6.29 (d, J = 7.4 Hz, 1H), 6.17 (br s, 1H), 4.78 – 4.73 (m, 1H), 4.29 (br s, 1H), 3.72 (s, 3H), 3.59 (s, 3H), 3.11 (dd, J = 15.4, 6.3 Hz, 1H), 3.05 (dd, J = 15.4, 6.4 Hz, 1H), 3.01 – 2.94 (m, 1H), 3.89 (dd, J = 14.7, 6.1 Hz, 1H), 2.18 – 2.13 (m, 2H), 2.06 (d, J = 11.8 Hz, 1H), 2.00 – 1.78 (m, 5H), 1.77 – 1.68 (m, 4H), 1.64 – 1.55 (m, 2H), 1.42 (s, 9H) ppm.

¹³C NMR (150 MHz, CDCl₃): δ = 176.6, 171.8, 170.9, 155.8, 142.4, 138.5, 136.8, 129.9, 128.4, 128.3, 128.2, 128.0, 126.7, 119.6, 79.8, 75.7, 54.9, 52.8, 52.0, 51.4, 42.7, 42.5, 40.6, 40.3, 38.3, 38.2, 35.3, 31.7, 30.8, 29.2, 29.2, 28.5, 26.8 ppm.

IR (KBr): $\tilde{\nu}$ = 3423, 2912, 2855, 1663, 1498, 1448, 1365, 1244, 1168, 750, 703, 661 cm⁻¹.

HRMS (ESI): m/z = 840.4448 [M+H]⁺ (calcd m/z = 840.4449), m/z = 862.4266 [M+Na]⁺ (calcd m/z = 862.4268).

Elem. Anal.: calcd for C₄₉H₅₇N₇O₆: C 70.06, H 6.84, N 11.67; found: C 67.22, H 6.70, N 10.22.



Boc-L-(OBn)-Asp-^AGly-L-Pmh-OMe (S14). The tripeptide was synthesized on 0.3 mmol scale employing the procedure described for **18**. A sample of the crude peptide was purified by preparative HPLC for complete characterization and catalysis. LiChrosorb Diol column (Merck), 250 mm × 8 mm;

eluent: 10% MeOH/TBME, 5.0 mL/min; UV-detector λ = 220 nm. Retention time: t_R = 17.7 min.

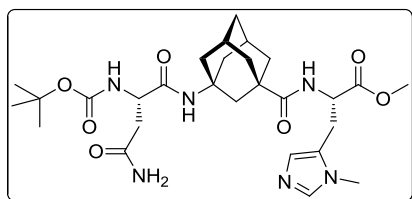
^1H NMR (600 MHz, CDCl_3): δ = 7.47 (s, 1H), 7.36 – 7.29 (m, 5H), 6.78 (s, 1H), 6.31 – 6.24 (m, 2H), 5.66 (br s, 1H), 5.17 – 5.08 (m, 2H), 4.79 – 4.73 (m, 1H), 4.39 (br s, 1H), 3.73 (s, 3H), 3.59 (s, 3H), 3.12 (dd, J = 15.4, 6.3 Hz, 1H), 3.05 (dd, J = 15.4, 6.3 Hz, 1H), 2.95 (dd, J = 17.0, 4.5 Hz, 1H), 2.67 (dd, J = 17.1, 6.6 Hz, 1H), 2.18 (br s, 2H), 2.06 – 1.98 (m, 2H), 1.95 – 1.83 (m, 4H), 1.78 – 1.68 (m, 4H), 1.65 – 1.56 (m, 2H), 1.44 (s, 9H) ppm.

^{13}C NMR (150 MHz, CDCl_3): δ = 176.5, 171.9, 171.8, 169.8, 155.7, 138.4, 135.6, 128.7, 128.5, 128.4, 127.8, 126.7, 80.6, 66.9, 52.8, 52.2, 51.4, 51.2, 42.7, 42.3, 40.5, 40.4, 38.2, 38.1, 36.6, 35.3, 31.7, 29.2, 29.2, 28.4, 26.8 ppm.

IR (KBr): $\tilde{\nu}$ = 3409, 2913, 2856, 1739, 1664, 1508, 1455, 1365, 1248, 1167, 1050, 750, 699, 663 cm^{-1} .

HRMS (ESI): m/z = 666.3501 $[\text{M}+\text{H}]^+$ (calcd m/z = 666.3503), m/z = 688.3322 $[\text{M}+\text{Na}]^+$ (calcd m/z = 688.3322).

Elem. Anal.: calcd for $\text{C}_{35}\text{H}_{47}\text{N}_5\text{O}_8$: C 63.14, H 7.12, N 10.52; found: C 62.12, H 6.87, N 8.90.



Boc-L-Asn-A-Gly-L-Pmh-OMe (S15). The tripeptide was synthesized on 0.3 mmol scale employing the procedure described for **18**. A sample of the crude peptide was purified by preparative HPLC for complete characterization and catalysis. LiChrosorb Diol column (Merck), 250 mm \times 8 mm;

eluent: 75% *i*-PrOH/hexanes, 3.0 mL/min; UV-detector λ = 230 nm. Retention time: t_R = 5.0 min.

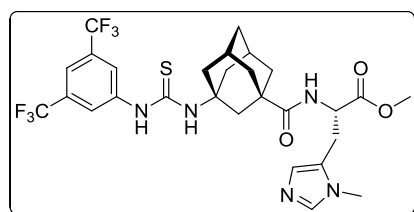
^1H NMR (600 MHz, CDCl_3): δ = 7.68 (s, 1H), 6.87 (s, 1H), 6.56 – 6.35 (m, 2H), 6.31 – 6.24 (m, 2H), 5.74 (br s, 1H), 4.82 – 4.75 (m, 1H), 4.39 (br s, 1H), 3.76 (s, 3H), 3.65 (s, 3H), 3.17 (dd, J = 15.5, 5.6 Hz, 1H), 3.05 (dd, J = 15.2, 7.5 Hz, 1H), 2.91 – 2.77 (m, 2H), 2.21 (m, 2H), 2.07 – 1.96 (m, 4H), 1.93 – 1.84 (m, 2H), 1.80 – 1.57 (m, 6H), 1.46 (s, 9H) ppm.

^{13}C NMR (150 MHz, CDCl_3): δ = 176.6, 176.6, 171.7, 167.9, 155.5, 138.0, 127.2, 126.6, 81.1, 52.9, 52.8, 52.8, 51.3, 50.9, 50.8, 42.7, 40.5, 40.2, 38.1, 38.0, 37.9, 35.2, 32.0, 29.3, 29.2, 29.2, 28.4, 26.7 ppm.

IR (KBr): $\tilde{\nu}$ = 3420, 2922, 2857, 1669, 1525, 1454, 1367, 1279, 1249, 1165, 1109, 1064, 663, 625 cm^{-1} .

HRMS (ESI): m/z = 557.3092 $[M-H_2O+H]^+$ (calcd m/z = 557.3088), m/z = 579.2912 $[M-H_2O+Na]^+$ (calcd m/z = 579.2907).

Elem. Anal.: calcd for $C_{28}H_{42}N_6O_7$: C 58.52, H 7.37, N 14.62; found: C 56.69, H 7.42, N 13.16.



3,5-bis(trifluoromethyl)phenylthiourea-^AGly-L-Pmh-OMe (S16). The synthesis and characterization data for **S16** can be found in the literature.^[40]

2.5 Catalytic Experiments

2.5.1 Reaction optimization

General procedure for preliminary reaction investigation. Phenylalanine (0.1 mmol) or *N*-acetyl phenylalanine (to prevent peptide coupling of starting material for reactions performed at higher concentration or with DIC) and **11** (10 mol%) were suspended in dry toluene. Acetic anhydride was added followed by base and the reaction mixture was allowed to stir at rt for 72 h. The reaction progress was monitored by GC-MS and chiral stationary phase GC. The corresponding results are summarized in Table S3. Except the entries 8, 9 and 10 in Table 3 only traces of **10a** (< 10%) formed after 72 h as judged by GC-MS.

We started our investigation using peptide catalyst **11** and DL-phenylalanine as starting material. Upon treatment of the amino acid with 10 eq acetic anhydride in the presence of catalyst **11** azlactone **3a** was the main product and only traces of desired product **10a** formed, although with 31% *ee* (Table S3, entry 1). The conversion could not be considerably enhanced when higher amounts of anhydride or higher concentrations were used (entries 2 – 6) and little lower selectivities were observed for **10a**. However, the reaction could be greatly accelerated by the addition of base (entries 7 – 9) even in the presence of lower amounts of anhydride. Although conversion significantly improved, diminished selectivities were determined with increasing base strength. When DIC was used as an additive (entry 10) the azlactone intermediate **3a** was fully converted to enantiomerically enriched acetyl derivative **6a** overnight. The decarboxylation step was then initiated by addition of acetic acid, affording desired product **10a**.

Table S3. Preliminary evaluation of concentration, amount of acetic anhydride and base.

<p>DL-Phe or 1a $\xrightarrow[\text{PhMe, rt, 72 h}]{\text{11 (10 mol\%), Ac}_2\text{O (X eq), base}}$ 10a</p>						
Entry	R	Ac ₂ O	Base	Concentration	Major product ^a	ee 10a (%) ^b
1	H	10 eq	—	0.04 M	3a	31
2	H	20 eq	—	0.04 M	3a	30
3	H	50 eq	—	0.04 M	3a	30
4	H	50 eq	—	0.02 M	3a	27
5	H	10 eq	—	0.1 M	3a	29
6	H	10 eq	—	0.2 M	3a	24
7	Ac	2.2 eq	2,6-lutidine (2.2 eq)	0.2 M	3a	31
8	Ac	2.2 eq	Et ₃ N (2.2 eq)	0.2 M	10a	11
9	Ac	2.2 eq	DBU (2.2 eq)	0.2 M	10a	9
10 ^c	Ac	1.1 eq	DIC (2.2 eq)	0.2 M	<p>6a</p>	23 ^d

^a Major product was determined by GC-MS; ^b Enantiomeric excess for **10a** was determined by chiral stationary phase GC; ^c Conversion of **3a** was complete after 22 h; ^d Complete conversion of **6a** to **10a** after addition of AcOH (10 eq) after 24 h. Stereochemistry for **10a** was determined as (*S*) by comparison of the retention times of an authentic sample ((*S*)-**10a**; *vide supra*) on chiral stationary phase HPLC.

General procedure for reaction optimization. DIC (or DCC in Table S4, entry 5) was added to **3a** (0.1 mmol) and **11** (10 mol%) in the solvent given in Table S4 (0.5 mL) and the resulting suspension was stirred at rt for 30 min. After addition of acetic anhydride the reaction mixture was stirred at rt for 24 h. Acetic acid was added to initiate decarboxylation and stirring was continued for further 72 h. The results are summarized in Table S4. Except entries 3, 8 and 9 the conversion was > 95% for each individual step.

We found that a ~ 0.2 M concentration of acetic acid in general afforded the best enantioselectivities. H₂O could be applied to promote the decarboxylation step as well (entry 3), however, the reaction was slow and sometimes accompanied by the formation of by-products. Although other common solvents gave somehow lower enantioselectivities compared to toluene,

the effect was not as pronounced as in our previous investigations.^[35,37] By monitoring the reaction progress with GC-MS as well as chiral stationary phase GC we observed that the reaction indeed follows the currently accept mechanism (Figure S2).^[41]

Table S4. Reaction optimization.

Entry	DIC	Ac ₂ O	AcOH	Solvent	ee 10a (%) ^a
1	2.2 eq	1.1 eq	10 eq	PhMe	23
2	1.7 eq	1.5 eq	10 eq	PhMe	19
3	1.7 eq	1.5 eq	H ₂ O; 10 eq	PhMe	29 ^b
4	1.7 eq	1.5 eq	1.3 eq	PhMe	33
5	DCC, 1.7 eq	1.5 eq	1.3 eq	PhMe	31
6	1.7 eq	1.5 eq	1.3 eq	acetonitril	11
7	1.7 eq	1.5 eq	1.3 eq	CHCl ₃	22
8	1.7 eq	1.5 eq	1.3 eq	1,4-dioxane	26 ^b
9	1.7 eq	1.5 eq	1.3 eq	EtOAc	26 ^b
10	1.7 eq	1.5 eq	1.3 eq	THF	26

^a Enantiomeric excess for **10a** was determined by chiral stationary phase GC; ^b Conversion was not complete.

Other transient intermediates, e.g., the mixed anhydride or the β -keto acid formed before decarboxylation could not be detected by GC-MS. The *O*-acetyl derivative **5a** ($t_R = 20.5$ min) was not observed as well, thus *C*-acetylation to **6a** is preferred under the reaction conditions and/or **5a** is immediately rearranged to **6a** by the catalyst after formation.

Importantly, there was no change of selectivity over time. Thus, there is no higher selectivity for the asymmetric protonation followed by gradual racemization.

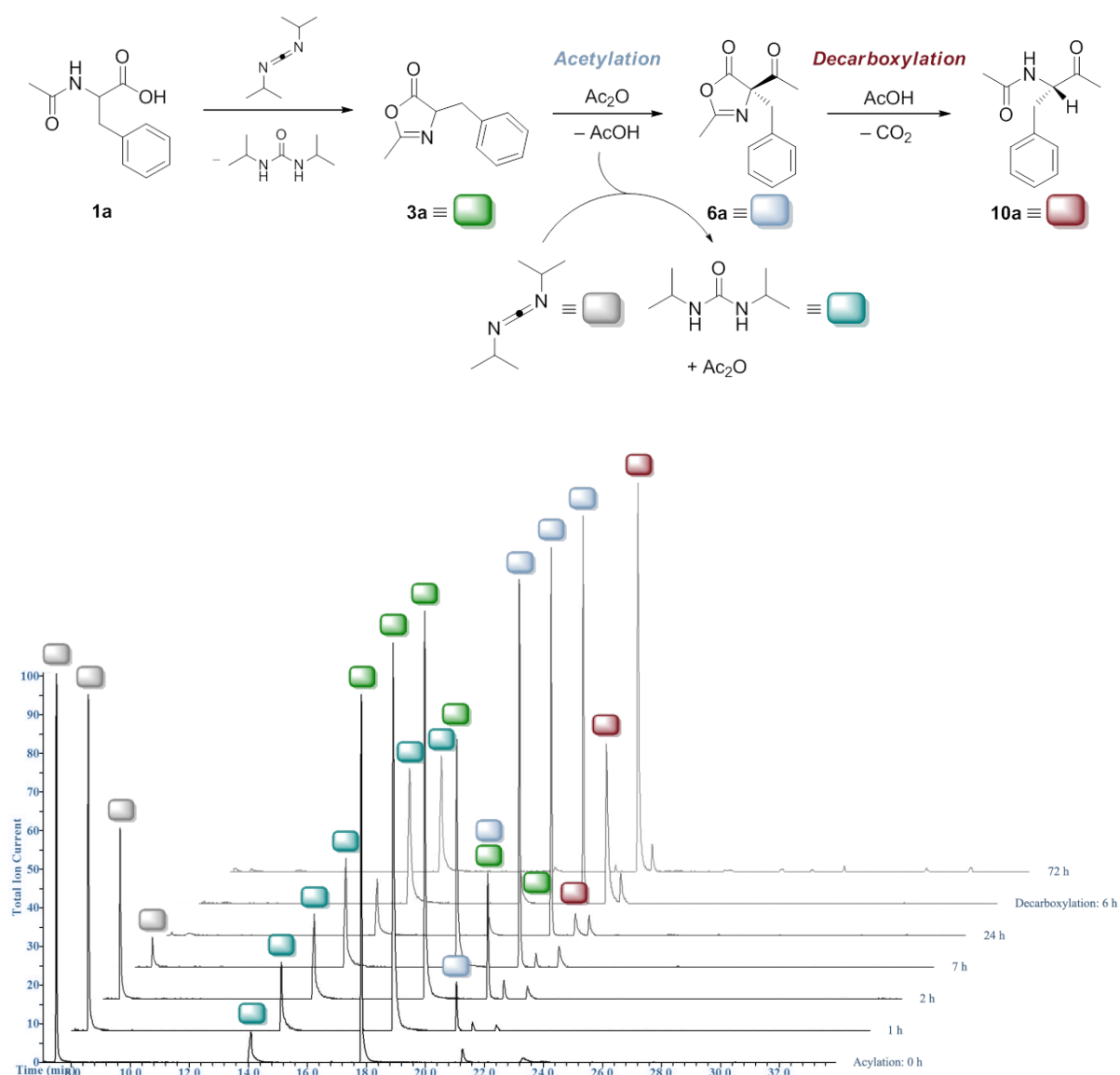


Figure S2. Reaction progress of the Dakin-West reaction under optimized reaction conditions. with catalyst **11**; highest peak has been set to 100%.

2.5.2 Catalyst screening

General procedure. DIC (26.5 μ L, 21.5 mg, 0.17 mmol) was added to **1a** (20.7 mg, 0.1 mmol) and catalyst (10 mol%) in dry toluene (0.5 mL) and the resulting suspension was stirred for 30 min at rt. After addition of acetic anhydride (14.2 μ L, 15.3 mg, 0.15 mmol) the reaction mixture was stirred for 24 h (unless indicated otherwise). An aliquot was injected on chiral stationary GC to determine the enantioselectivity for **6a**. Acetic acid (7.44 μ L, 7.81 mg, 0.13 mmol) was added to initiate decarboxylation and stirring was continued for further 72 h. The reaction progress was monitored by GC-MS and chiral stationary phase GC. The corresponding results are summarized in Table S5.

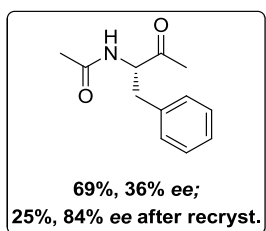
Table S5. Catalyst screening under optimized reaction conditions.

Entry	Cat.	<i>ee</i> 6a (%) ^a	<i>ee</i> 10a (%) ^a	
1	Boc-L-Pmh- ^A Gly-L-Cha-L-Phe-OMe (11)	–22	33	
2	Boc-L-Pmh- ^A Gly-L-Val-L-Phe-OMe (S3)	–13 (48 h)	29	
3	Boc-D-Pmh- ^A Gly-L-Val-L-Phe-OMe (S4)	10 (48 h)	7	
4	Boc-L-Pmh- ^A Gly-D-Val-L-Phe-OMe (S5)	0 (48 h)	0	
5	Boc-D-Pmh- ^A Gly-D-Val-L-Phe-OMe (S6)	18 (48 h)	–18	
6	Boc-L-Pmh-D-Pro-Aib-L-Cha-L-Phe-OMe (12)	20 (48 h)	–5	
7	Boc-L-Pmh-2-Abz-D-Pro-L-Cha-L-Phe-OMe (13)	16	8	
8	(<i>S</i>)-Tetramisol (14)	25 (traces)	not detected	
9	(<i>S</i>)-PPY* (15)	16	22 (24 h)	
10	Boc-L-Pmh-OMe (16)	8 (conv. not complete)	4	
11	Boc- ^A Gly-L-Pmh-OMe (17)	16	5	
12	Boc-L-Ala- ^A Gly-L-Pmh-OMe (S7)	25	27	
13	Boc-L-Val- ^A Gly-L-Pmh-OMe (S8)	17	22	
14	Boc-D-Val- ^A Gly-L-Pmh-OMe (S9)	not determined	27	
15	Boc-L-Leu- ^A Gly-L-Pmh-OMe (S10)	24	29	
16	Boc-L-Cha- ^A Gly-L-Pmh-OMe (18)	25	37	
17 ^b	DMAP + Boc-L-Cha- ^A Gly-L-Pmh-OMe (18)	–	33 (24 h)	
18	Boc-L-Phe- ^A Gly-L-Pmh-OMe (S11)	25	31	
19	Boc-L-Trp- ^A Gly-L-Pmh-OMe (S12)	14	20	
20	Boc-L-(Trt)-His- ^A Gly-L-Pmh-OMe (S13)	23 (46 h)	5	
21	Boc-L-(OBn)-Asp- ^A Gly-L-Pmh-OMe (S14)	22 (46 h)	20	
22	Boc-L-Asn- ^A Gly-L-Pmh-OMe (S15)	18 (42 h)	17	
23	TU- ^A Gly-L-Pmh-OMe (S16)	23 (42 h)	0	

^a Selectivity was determined by chiral stationary phase GC; absolute configuration for **6a** was determined by comparison of retention times of the corresponding product obtained with catalyst **14**.^[42] ^b First part of the reaction was performed with DMAP (5 mol%) in the absence of **18**. Negative values indicate formation of the (*R*)-enantiomer. Unless otherwise noted, conversion was > 95% for the individual steps.

2.5.3 Preparative enantioselective Dakin-West Reaction

The reactions were usually performed with racemic amino acids, except with **1d** and **1f** where the L-amino acids were applied. However, we found that this has no effect on the selectivity of the reaction; L-, D- and DL-phenylalanine derivatives provided the same stereoselectivities. This outcome is in accordance with the accepted reaction mechanism.

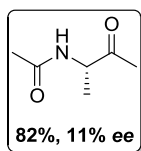


***N*-(3-oxo-1-phenylbutan-2-yl)acetamide (10a).** To a suspension of *N*-acetyl-DL-phenyl-alanine (**1a**; 207.2 mg, 1.0 mmol) and catalyst **18** (61.4 mg, 10 mol%) in dry toluene (5.0 mL) was added DCC (60 wt% in xylenes; 651 μ L, 1.7 mmol) and the reaction mixture was stirred at rt for 30 min. After addition of acetic anhydride (142 μ L, 153.4 mg, 1.5 mmol) stirring was continued for 44 h. Acetic acid (74.4 μ L, 78.1 mg, 1.3 mmol)

was then added to initiate decarboxylation and stirring was continued for additional 72 h. The formed *N,N'*-dicyclohexyl urea was filtered off, washed with CH_2Cl_2 and the obtained clear solution was directly subjected to column chromatography to afford **10a** (141.3 mg, 0.69 mmol, 69%) as colorless solid with 36% *ee*. The NMR data were identical with those reported for the racemic samples.

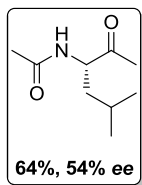
The eluent for column chromatography and the corresponding R_f value as well as the conditions for determination of the enantioselectivity are provided in chapter 5.3.

Upon recrystallization of the obtained enantiomerically enriched **10a** from xylenes crystals with 84% *ee* (25% yield) were collected.



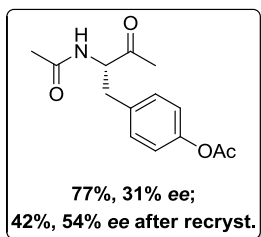
***N*-(3-oxobutan-2-yl)acetamide (10b).** The reaction was performed following the general procedure described above with **1b** (131.2 mg, 1.0 mmol) affording **10b** (105.7 mg, 0.82 mmol, 82%) as colorless oil with 11% *ee*. Reaction time for acetylation was 24 h and for decarboxylation 72 h.

The eluent for column chromatography and the corresponding R_f value as well as the conditions for determination of the enantioselectivity are provided in chapter 5.3.



***N*-(5-methyl-2-oxohexan-3-yl)acetamide (10c).** The reaction was performed following the general procedure described above with **1c** (173.2 mg, 1.0 mmol) affording **10c** (110.2 mg, 0.64 mmol, 64%) as colorless oil with 54% *ee*. Reaction time for acetylation was 64 h and for decarboxylation 92 h.

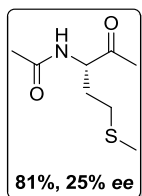
The eluent for column chromatography and the corresponding R_f value as well as the conditions for determination of the enantioselectivity are provided in chapter 5.3.



4-(2-acetamido-3-oxobutyl)phenyl acetate (10d). The reaction was performed following the general procedure described above with **1d** (265.3 mg, 1.0 mmol) affording **10d** (202.7 mg, 0.77 mmol, 77%) as colorless solid with 31% *ee*. The product was contaminated with traces of *N,N'*-di-cyclohexyl urea that could not be sufficiently removed by column chromatography. Reaction time for acetylation was 24 h and for decarboxylation 84 h.

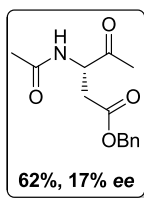
The eluent for column chromatography and the corresponding R_f value as well as the conditions for determination of the enantioselectivity are provided in chapter 5.3.

Upon recrystallization of the obtained enantiomerically enriched **10d** from Et₂O crystals with 54% *ee* (42% yield) were collected.



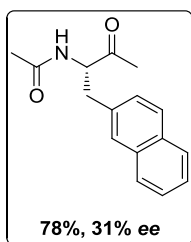
***N*-(1-(methylthio)-4-oxopentan-3-yl)acetamide (10e).** The reaction was performed following the general procedure described above with **1e** (191.3 mg, 1.0 mmol) affording **10e** (153.2 mg, 0.81 mmol, 81%) as colorless oil with 25% *ee*. Reaction time for acetylation was 24 h and for decarboxylation 72 h.

The eluent for column chromatography and the corresponding R_f value as well as the conditions for determination of the enantioselectivity are provided in chapter 5.3.



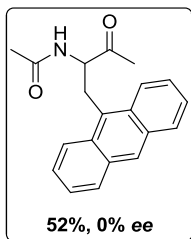
***N*-(1-(methylthio)-4-oxopentan-3-yl)acetamide (10f).** The reaction was performed following the general procedure described above with **1f** (265.4 mg, 1.0 mmol) affording **10f** (162.4 mg, 0.62 mmol, 62%) as colorless solid with 17% *ee*. Reaction time for acetylation was 48 h and for decarboxylation 74 h.

The eluent for column chromatography and the corresponding R_f value as well as the conditions for determination of the enantioselectivity are provided in chapter 5.3.



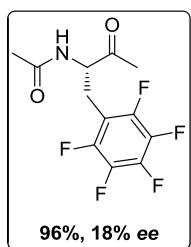
***N*-(1-(naphthalen-2-yl)-3-oxobutan-2-yl)acetamide (10g).** The reaction was performed following the general procedure described above with **1g** (128.6 mg, 0.5 mmol) affording **10g** (99.5 mg, 0.39 mmol, 78%) as colorless solid with 31% *ee*. Reaction time for acetylation was 48 h and for decarboxylation 72 h.

The eluent for column chromatography and the corresponding R_f value as well as the conditions for determination of the enantioselectivity are provided in chapter 5.3.



***N*-(1-(anthracen-9-yl)-3-oxobutan-2-yl)acetamide (10h).** The reaction was performed following the general procedure described above with **1h** (153.7 mg, 0.5 mmol) affording racemic **10h** (78.4 mg, 0.26 mmol, 52%) as yellow solid. Reaction time for acetylation was 24 h and for decarboxylation 84 h.

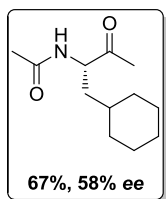
The eluent for column chromatography and the corresponding R_f value as well as the conditions for determination of the enantioselectivity are provided in chapter 5.3.



***N*-(3-oxo-1-(perfluorophenyl)butan-2-yl)acetamide (10i).** The reaction was performed following the general procedure described above with **1i** (148.6 mg, 0.5 mmol) affording **10i** (141.7 mg, 0.48 mmol, 96%) as colorless solid with 18% *ee*. The product was contaminated with traces of *N,N'*-dicyclohexyl urea that could not be sufficiently removed by column chromatography. Reaction time for acetylation was 24 h and for decarboxylation 48 h.

The eluent for column chromatography and the corresponding R_f value as well as the conditions for determination of the enantioselectivity are provided in chapter 5.3.

We observed significant racemization of **10i** during column chromatography. A sample that was injected on chiral stationary phase GC prior to work-up showed 31% *ee*.



***N*-(1-(anthracen-9-yl)-3-oxobutan-2-yl)acetamide (**10j**)**. The reaction was performed following the general procedure described above with **1j** (106.7 mg, 0.5 mmol) affording **10j** (70.9 mg, 0.34 mmol, 67%) as colorless solid with 58% *ee*. Reaction time for acetylation was 72 h and for decarboxylation 96 h.

The eluent for column chromatography and the corresponding R_f value as well as the conditions for determination of the enantioselectivity are provided in chapter 5.3.

2.6 Mechanistic Investigations

2.6.1 Computational details

We performed a molecular dynamics search for low-lying conformations of the adduct of protonated peptide **18** and enolate **9j** employing the Merck molecular force field (MMFF).^[43] For preliminary energy minimization **9j** was arranged in the ‘binding-pocket’ of the peptide in a way to give the stereoselectively preferred product (*S*)-**10j** (**18-9j-S**) or the potential enantiomer (*R*)-**10j** (**18-9j-R**), respectively. The lowest-lying conformations found were reoptimized at the B3LYP level of theory with the D3(BJ) correction,^[44] accounting for dispersion interactions, in conjunction with a 6-31+G(d,p) basis set. The self-consistent reaction field (SCRF)^[45] with the polarizable continuum model (PCM) was employed to incorporate toluene as solvent and the United Atom topological model applied on radii optimized for the HF/6-31G(d) level of theory (UAHF)^[46] was used to describe the bulk solvent. The Gaussian09 program package^[47] was used to compute the complexes. The found minimum displayed only real frequencies. Visualization of the computed structures was performed with CYLview^[48] and with ‘Visual Molecular Dynamics’ (VMD)^[49] for non-covalent interaction surfaces.

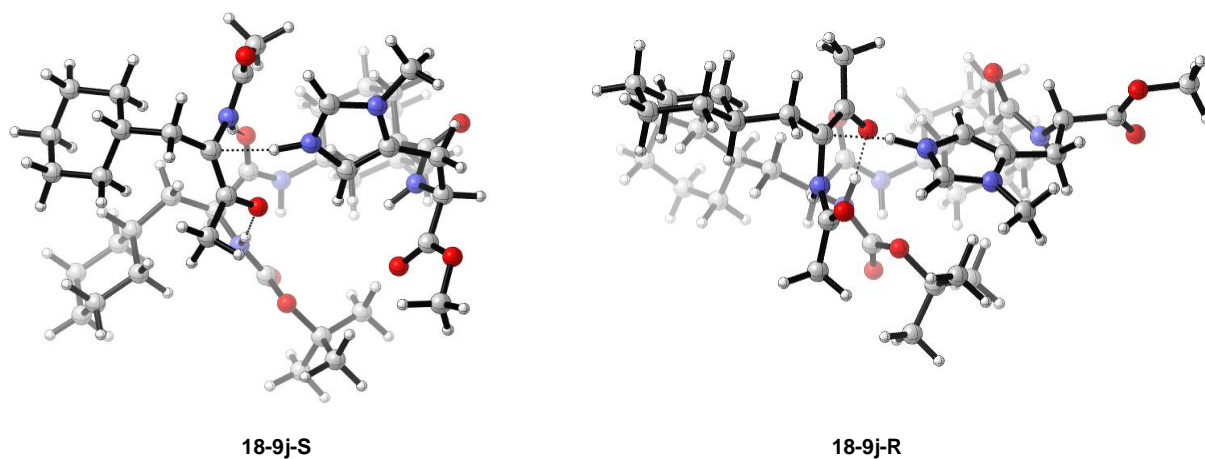


Figure S3. B3LYP-D3(BJ)/6-31+G(d,p) optimized structures of enolate **9j** in the binding pocket of protonated peptide catalyst **18**. Left: Complex leading to (*S*)-**10j**; Right: Complex leading to (*R*)-**10j**.

Table S6.

Complex	Energy (–au)	ZPVE (au)	E+ZPVE (–au)	G ₂₉₈ (–au)	ΔG ₂₉₈ (kcal mol ^{–1})
18-9j-S	2689.0993488	1.1524363	2687.9469125	2688,0441180	0.0
18-9j-R	2689.0898497	1.1504966	2686,8936214	2688,0407120	2.1

Table S7. xyz-coordinates for **18-9j-S**.

Atom	X	Y	Z
1	-1.630991000	-0.048619000	1.380730000
6	-2.191786000	-0.970854000	1.559820000
6	-2.257285000	-3.115364000	2.856693000
6	-4.404553000	-2.001747000	2.165287000
6	-3.711931000	-2.825594000	3.264880000
6	-3.649637000	-0.659910000	1.959675000
6	-1.490894000	-1.792958000	2.666830000
1	-2.232815000	-3.690222000	1.921868000
1	-5.443549000	-1.794037000	2.443038000
1	-2.148289000	-1.571911000	0.643172000
1	-1.756137000	-3.716345000	3.624949000
1	-4.419059000	-2.563426000	1.222710000
1	-4.246473000	-3.774332000	3.391542000
6	-3.728810000	-2.033438000	4.584498000
1	-3.265598000	-2.624946000	5.383937000
1	-4.763813000	-1.829939000	4.886296000
6	-3.640274000	0.122124000	3.293296000
1	-4.668403000	0.366710000	3.573312000
1	-3.104955000	1.069747000	3.154785000

Table S8. xyz-coordinates for **18-9j-R**.

Atom	X	Y	Z
1	1.024273000	-1.668868000	-1.177765000
6	1.706872000	-2.113504000	-0.450135000
6	2.171514000	-4.106332000	1.008484000
6	4.079077000	-2.790311000	0.031912000
6	3.593975000	-4.198181000	0.430044000
6	3.138798000	-2.192109000	-1.037815000
6	1.212171000	-3.521489000	-0.044084000
1	2.168117000	-3.470661000	1.902976000
1	4.088892000	-2.161790000	0.931873000
1	1.702912000	-1.463575000	0.431908000
1	1.817385000	-5.099285000	1.310386000
1	5.105994000	-2.847045000	-0.350912000
1	4.268771000	-4.602835000	1.193452000
6	3.588823000	-5.114450000	-0.805299000
1	3.269593000	-6.124569000	-0.520139000
1	4.602794000	-5.196804000	-1.217393000
6	3.113231000	-3.128601000	-2.269954000
1	4.118816000	-3.188787000	-2.705908000
1	2.452364000	-2.699693000	-3.027479000

6	-1.505018000	-1.010679000	3.992832000	6	1.205683000	-4.441096000	-1.278114000
1	-1.006310000	-1.609694000	4.764348000	1	0.847600000	-5.434697000	-0.981659000
1	-0.939112000	-0.084823000	3.876070000	1	0.509164000	-4.046486000	-2.019369000
6	-2.961324000	-0.713701000	4.392472000	6	2.630847000	-4.530662000	-1.857350000
1	-2.967016000	-0.142876000	5.328404000	1	2.616431000	-5.175506000	-2.743873000
6	-4.418694000	0.143401000	0.908182000	6	3.512976000	-0.782091000	-1.496456000
8	-5.434953000	0.791053000	1.187537000	8	3.021311000	-0.278674000	-2.508667000
7	-0.128725000	-2.131434000	2.228075000	7	-0.114647000	-3.398920000	0.586877000
1	-0.038451000	-3.024834000	1.745226000	1	-0.066330000	-3.203588000	1.584097000
7	1.286040000	-1.896435000	-0.384173000	7	-1.252538000	-0.812137000	1.343385000
6	1.896031000	-1.783765000	0.939924000	6	-2.058521000	-1.969044000	0.934206000
6	0.818056000	-1.220578000	1.886675000	6	-1.184916000	-2.803519000	-0.032211000
8	0.795797000	-0.034704000	2.237767000	8	-1.397087000	-2.848355000	-1.240366000
1	1.096835000	-1.000149000	-0.881451000	1	-0.945870000	-0.188704000	0.542206000
1	2.144968000	-2.795203000	1.270167000	1	-2.267380000	-2.555838000	1.832366000
6	3.147974000	-0.908126000	0.914381000	6	-3.350148000	-1.483519000	0.279459000
1	3.394031000	-0.662666000	1.953918000	1	-3.080478000	-0.943207000	-0.633342000
1	2.902665000	0.041089000	0.429768000	1	-3.818896000	-0.761809000	0.961822000
7	-3.960407000	0.076544000	-0.368555000	7	4.362081000	-0.063490000	-0.692733000
6	-4.632371000	0.737539000	-1.465355000	6	4.921428000	1.197799000	-1.129505000
6	-4.060420000	0.184947000	-2.765622000	6	6.438055000	1.056765000	-1.261134000
8	-3.186432000	-0.658715000	-2.818559000	8	7.087701000	0.163193000	-0.753707000
1	-3.142661000	-0.470886000	-0.598839000	1	4.900624000	-0.566131000	-0.000714000
1	-5.699281000	0.484807000	-1.443400000	1	4.502793000	1.416829000	-2.115090000
6	-4.552305000	2.277582000	-1.384720000	6	4.614089000	2.367703000	-0.169513000
6	-3.157448000	2.807398000	-1.304893000	6	3.170647000	2.753581000	-0.132788000
1	-5.106876000	2.566867000	-0.487923000	1	5.212355000	3.230083000	-0.483652000
1	-5.078956000	2.697326000	-2.248641000	1	4.954872000	2.096789000	0.839252000
6	-1.929103000	2.233785000	-1.509188000	6	2.045932000	2.217155000	-0.703251000
1	-1.615622000	1.235717000	-1.768177000	1	1.909538000	1.357607000	-1.340008000
6	-1.576478000	4.328026000	-0.882619000	6	1.405684000	3.973645000	0.485626000
1	-1.066452000	5.217543000	-0.550770000	1	0.759443000	4.691937000	0.967482000
7	-2.904203000	4.126737000	-0.914712000	7	2.738889000	3.859084000	0.608894000
6	-3.915025000	5.120689000	-0.561092000	6	3.585496000	4.728883000	1.419255000
1	-4.583973000	5.289679000	-1.407105000	1	2.960509000	5.494790000	1.876883000
1	-4.491426000	4.775198000	0.299369000	1	4.340569000	5.207530000	0.792289000
1	-3.411653000	6.052504000	-0.306320000	1	4.074798000	4.147448000	2.203621000
8	-4.638449000	0.741433000	-3.833825000	8	6.959268000	2.060579000	-1.977027000
6	-4.154952000	0.291749000	-5.123038000	6	8.396906000	2.051006000	-2.146144000
1	-4.726316000	0.858083000	-5.855755000	1	8.888781000	2.109403000	-1.173348000
1	-3.087479000	0.500384000	-5.212566000	1	8.620038000	2.929506000	-2.748468000
1	-4.332025000	-0.779367000	-5.233888000	1	8.704507000	1.139022000	-2.660525000
6	0.579371000	-2.995642000	-0.721230000	6	-0.430748000	-0.894988000	2.416209000
8	0.427348000	-3.987312000	0.007550000	8	-0.362198000	-1.849703000	3.197724000
8	0.074539000	-2.873743000	-1.968814000	8	0.311435000	0.236461000	2.522684000
6	-0.846295000	-3.875105000	-2.526545000	6	1.328952000	0.390800000	3.567517000
6	-2.116823000	-3.943080000	-1.674469000	6	1.901985000	1.774368000	3.260052000
1	-1.900813000	-4.327132000	-0.676528000	1	1.120195000	2.536530000	3.312527000
1	-2.566823000	-2.949467000	-1.597122000	1	2.328266000	1.781793000	2.254357000
1	-2.841706000	-4.608106000	-2.155363000	1	2.685738000	2.024462000	3.981538000
6	-1.157511000	-3.304124000	-3.910523000	6	0.682880000	0.365843000	4.954144000
1	-0.240759000	-3.220607000	-4.501987000	1	-0.118396000	1.108262000	5.011363000

1	-1.851118000	-3.968632000	-4.435581000	1	1.434885000	0.614779000	5.710049000
6	-0.149896000	-5.232656000	-2.648544000	1	0.270151000	-0.618367000	5.175815000
1	0.067033000	-5.656320000	-1.668094000	6	2.415699000	-0.676050000	3.412464000
1	-0.797350000	-5.921785000	-3.201031000	1	2.824796000	-0.649265000	2.397972000
1	0.787098000	-5.125476000	-3.204256000	1	2.020960000	-1.672509000	3.611106000
7	1.258995000	2.477474000	0.708240000	1	3.229077000	-0.473205000	4.116763000
1	1.163931000	1.539757000	1.100654000	6	-4.363844000	-2.582744000	-0.063393000
6	2.880203000	3.657907000	-0.807503000	6	-5.979006000	-4.343912000	0.821751000
1	2.992966000	3.851540000	-1.879191000	6	-6.564375000	-3.045379000	-1.269186000
1	2.509470000	4.589305000	-0.367058000	6	-7.114450000	-3.745028000	-0.019075000
6	4.288669000	3.384465000	-0.221061000	6	-5.510682000	-1.993645000	-0.901419000
6	5.707524000	3.055394000	1.861214000	6	-4.927565000	-3.285347000	1.184217000
6	6.399226000	1.955828000	-0.315772000	1	-5.494151000	-5.148284000	0.250175000
6	6.403262000	1.849670000	1.215987000	1	-6.107705000	-3.795517000	-1.930471000
6	4.986571000	2.182416000	-0.873434000	1	-7.665497000	-3.013283000	0.589795000
6	4.286666000	3.227991000	1.309103000	1	-5.989770000	-1.185344000	-0.329435000
1	6.291754000	3.964577000	1.656312000	1	-5.385137000	-2.528610000	1.840107000
1	7.042884000	2.795722000	-0.615226000	1	-3.853812000	-3.334601000	-0.679730000
1	5.875031000	0.934966000	1.518377000	1	-6.380391000	-4.803925000	1.733114000
1	4.376969000	1.288591000	-0.702153000	1	-7.379923000	-2.580372000	-1.836734000
1	3.687624000	2.350613000	1.580389000	1	-7.832306000	-4.525010000	-0.301240000
1	4.890004000	4.279862000	-0.452205000	1	-5.101327000	-1.532087000	-1.807824000
1	5.679978000	2.937872000	2.951709000	1	-4.121262000	-3.752906000	1.761584000
1	6.837311000	1.052542000	-0.759115000	7	0.980318000	2.993341000	-0.301422000
1	7.431876000	1.754223000	1.585692000	1	-0.028377000	2.848777000	-0.567289000
1	5.033886000	2.321012000	-1.960951000	6	-1.753363000	3.157700000	1.687125000
1	3.797228000	4.095135000	1.769901000	8	-1.353952000	4.312375000	1.434406000
6	2.139802000	1.450515000	-2.861508000	7	-1.989765000	2.229056000	0.738539000
1	1.331462000	1.424812000	-3.601615000	1	-2.175925000	1.289461000	1.068980000
1	2.679192000	0.501456000	-2.951422000	6	-1.921109000	2.432831000	-0.685437000
1	2.826981000	2.259546000	-3.111387000	6	-1.292635000	1.427561000	-1.411499000
6	0.729835000	3.493994000	1.418832000	6	-2.849851000	3.499592000	-1.212177000
8	0.615561000	4.659429000	0.979384000	1	-2.644875000	4.443942000	-0.692475000
6	0.286269000	3.157121000	2.828911000	1	-2.648523000	3.680989000	-2.272617000
1	0.269261000	2.084094000	3.022744000	6	-2.046216000	2.729071000	3.111700000
1	0.975573000	3.634469000	3.534441000	1	-2.996576000	3.172850000	3.427523000
1	-1.614043000	-2.316153000	-3.821546000	1	-1.265170000	3.115985000	3.769599000
1	-0.704978000	3.586603000	3.000581000	1	-2.110633000	1.644427000	3.222572000
7	-0.980659000	3.198500000	-1.245640000	6	-1.322200000	1.400751000	-2.928683000
1	0.057775000	3.043811000	-1.234284000	1	-1.739033000	2.296552000	-3.391245000
6	1.528305000	1.542401000	-1.473896000	1	-1.916962000	0.537543000	-3.248999000
6	1.835904000	2.582316000	-0.605389000	1	-0.304742000	1.239359000	-3.298817000
8	0.659906000	0.623322000	-1.181124000	8	-0.598842000	0.484550000	-0.861054000
6	4.395693000	-1.517387000	0.250946000	6	-4.349088000	3.173039000	-1.040613000
6	4.284046000	-1.711246000	-1.270811000	6	-6.722222000	4.073700000	-1.275938000
6	5.621356000	-2.168307000	-1.868253000	6	-6.264230000	1.611620000	-1.651529000
6	6.118812000	-3.456319000	-1.197040000	6	-7.132461000	2.812851000	-2.049471000
6	6.206080000	-3.293238000	0.327015000	6	-4.770370000	1.917689000	-1.819163000
6	4.868719000	-2.821853000	0.915971000	6	-5.225187000	4.369387000	-1.442584000
1	5.195837000	-0.780054000	0.409883000	1	-6.942134000	3.927329000	-0.208346000
1	3.958465000	-0.776516000	-1.739413000	1	-6.462467000	1.356568000	-0.600348000
1	3.509976000	-2.454150000	-1.492953000	1	-7.015393000	2.998664000	-3.127192000

1	5.520878000	-2.318006000	-2.950249000	1	-4.549413000	2.073047000	-2.886099000
1	6.370030000	-1.374923000	-1.727713000	1	-5.021695000	4.619085000	-2.495490000
1	7.094336000	-3.748926000	-1.604486000	1	-4.525393000	2.976587000	0.028742000
1	5.420363000	-4.273155000	-1.429654000	1	-7.318853000	4.933976000	-1.604204000
1	6.514039000	-4.236839000	0.793660000	1	-6.538866000	0.729261000	-2.241456000
1	6.983599000	-2.553583000	0.566611000	1	-8.193630000	2.590431000	-1.881761000
1	4.960797000	-2.677785000	2.000635000	1	-4.168340000	1.061112000	-1.499175000
1	4.118103000	-3.609589000	0.762727000	1	-4.943011000	5.250493000	-0.851882000

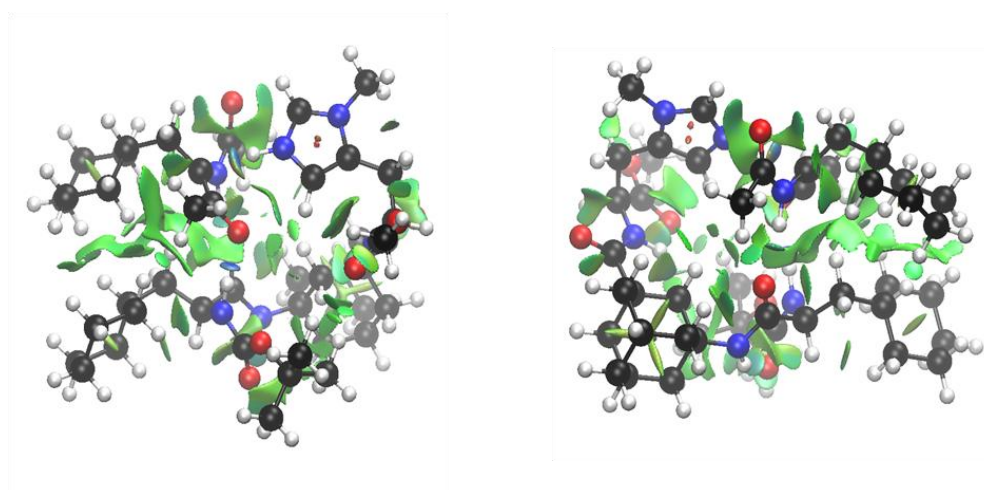
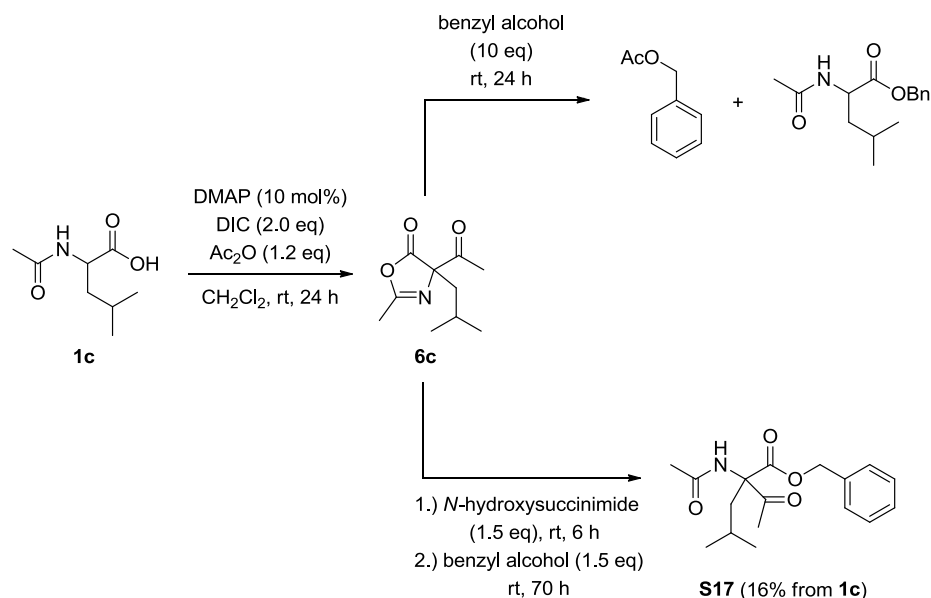


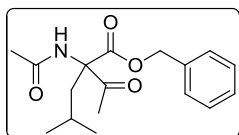
Figure S4. Non-covalent interaction (NCI) plots for **18-9j-S** in the binding pocket of protonated peptide catalyst **18**. Green isosurfaces provide evidence for attractive interactions. Blue spots indicate stronger interactions, *e.g.*, hydrogen bonds, and small red spots indicate steric repulsion. Left: front view on protonated imidazole; Right: side view on enolate **9j**.

2.6.2 Additionally performed reactions towards the investigation of the enantio-selective decarboxylative protonation

To gain more insight into the factors determining the asymmetric induction we envisaged to study the decarboxylation step independently. As *N*-acetyl leucine (**1c**) afforded high selectivities when employed in the DWR (see preparative experiments above) we accordingly chose this derivative for the synthesis of its corresponding β -ketoacid (**8c**) and for further studies.



Although nucleophilic opening of acetylated azlactone intermediates, *e.g.*, by alcohols, was described previously^[42,50] this strategy leads to the esters that are probably decarboxylated upon saponification. Therefore, we chose the benzyl protecting group, because it can be easily removed by hydrogenation under neutral conditions. However, when benzylalcohol was added to *in situ* formed **6c** this intermediate readily underwent deacetylation affording benzyl acetate and the benzylester of **1c** and no product could be isolated. A similar observation was earlier made also by Steglich and Höfle.^[50] The authors reported that the use of *N*-hydroxysuccinimide as nucleophile affords the corresponding hydroxysuccinimide ester, which can indeed be converted to the desired product **S17**.



Benzyl 2-acetamido-2-acetyl-4-methylpentanoate (S17). *N*-acetyl leucine (346.4 mg, 2.0 mmol) and DMAP (24.4 mg, 10 mol%) were suspended in dry CH₂Cl₂ (5 mL) and DIC (631 μL, 504.8 mg, 4.0 mmol) followed by Ac₂O (227 μL, 245.0 mg, 2.4 mmol) and the reaction mixture was stirred at

rt for 24 h. *N*-hydroxysuccinimide (345.3 mg, 3.0 mmol) was then added and stirring was continued for 6 h. After subsequent addition of benzyl alcohol (310 μL, 324.4 mg, 3.0 mmol) the reaction was allowed to stir for further 70 h. The formed diisopropyl urea was filtered off, the obtained solution diluted with EtOAc (50 mL), and subsequently washed with 0.5 M citric acid solution (3 × 20 mL) and brine (3 × 20 mL). The organic layer was dried over Na₂SO₄, filtered, and concentrated under reduced pressure. The crude product was purified by column chromatography eluting with hexane/EtOAc (1:1) to obtain the desired intermediate **S17** (95.0 mg, 0.31 mmol, 16%) as colorless oil. TLC (hexane/EtOAc 1:1): *R_f* = 0.51.

^1H NMR (400 MHz, CDCl_3): δ = 7.31 – 7.21 (m, 5H), 6.94 (br s, 1H), 5.11 (m, 2H), 2.36 (dd, J = 14.9, 6.9 Hz, 1H), 2.19 (dd, J = 14.9, 6.2 Hz, 1H), 1.98 (s, 3H), 1.96 (s, 3H), 1.35 (m, 1H), 0.76 (d, J = 6.8 Hz, 3H), 0.74 (d, J = 6.7 Hz, 3H) ppm.

^{13}C NMR (100 MHz, CDCl_3): δ = 200.4, 169.2, 169.0, 134.8, 128.8, 128.7, 128.6, 127.1, 72.2, 68.3, 39.5, 24.5, 24.3, 23.7, 23.4, 23.1 ppm.

IR (film): $\tilde{\nu}$ = 3388, 2960, 2873, 1723, 1661, 1498, 1455, 1369, 1299, 1223, 1173, 1025, 959, 752, 699 cm^{-1} .

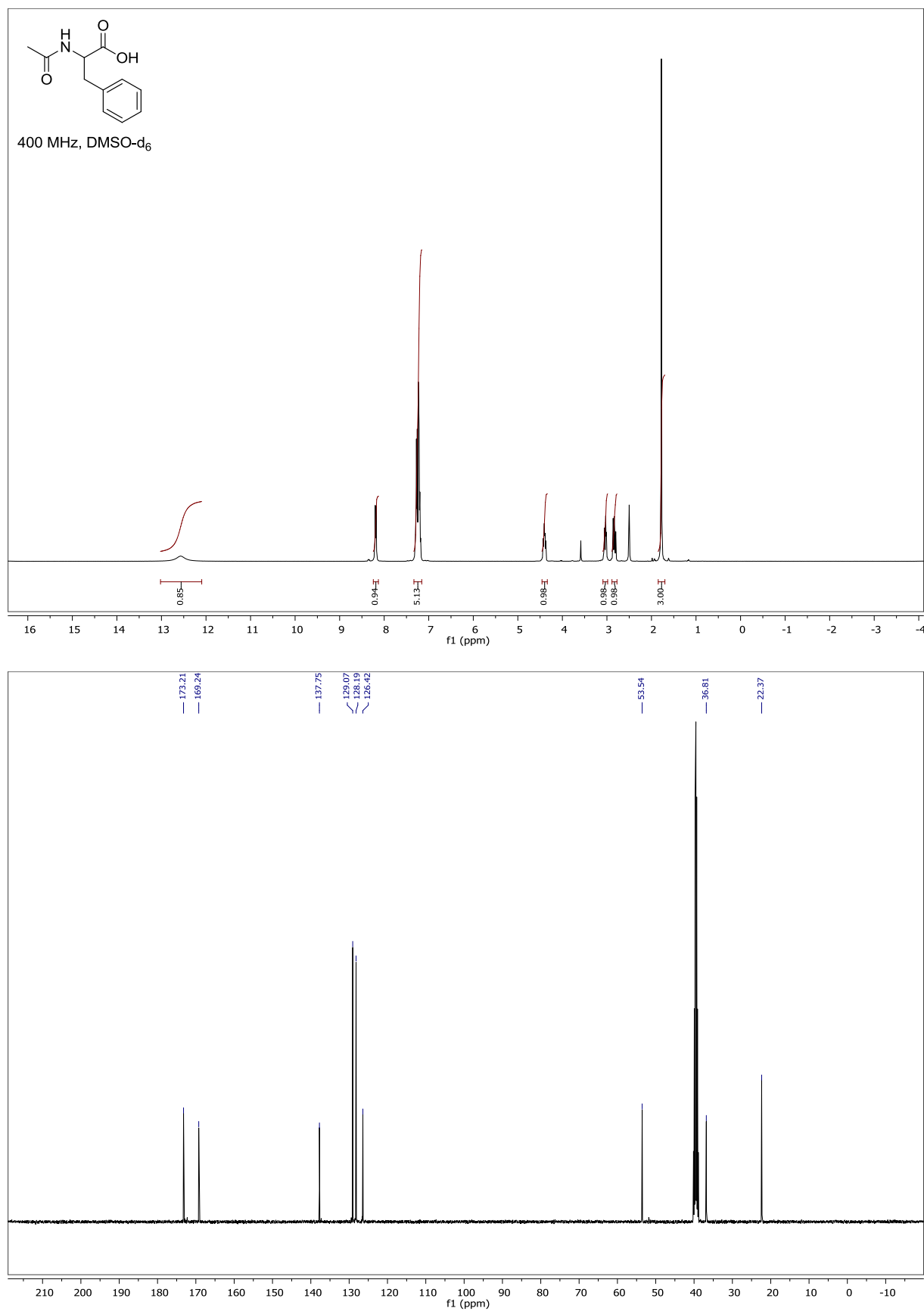
HRMS (ESI): m/z = 328.1525 $[\text{M}+\text{Na}]^+$ (calcd m/z = 328.1525), m/z = 633.3127 $[2\text{M}+\text{Na}]^+$ (calcd m/z = 633.3152).

We subjected **S17** to hydrogenation with Pd/C in order to obtain β -keto acid **8c**. Unfortunately, this attempt also led to decarboxylation and we only isolated the DW reaction product **10c**.

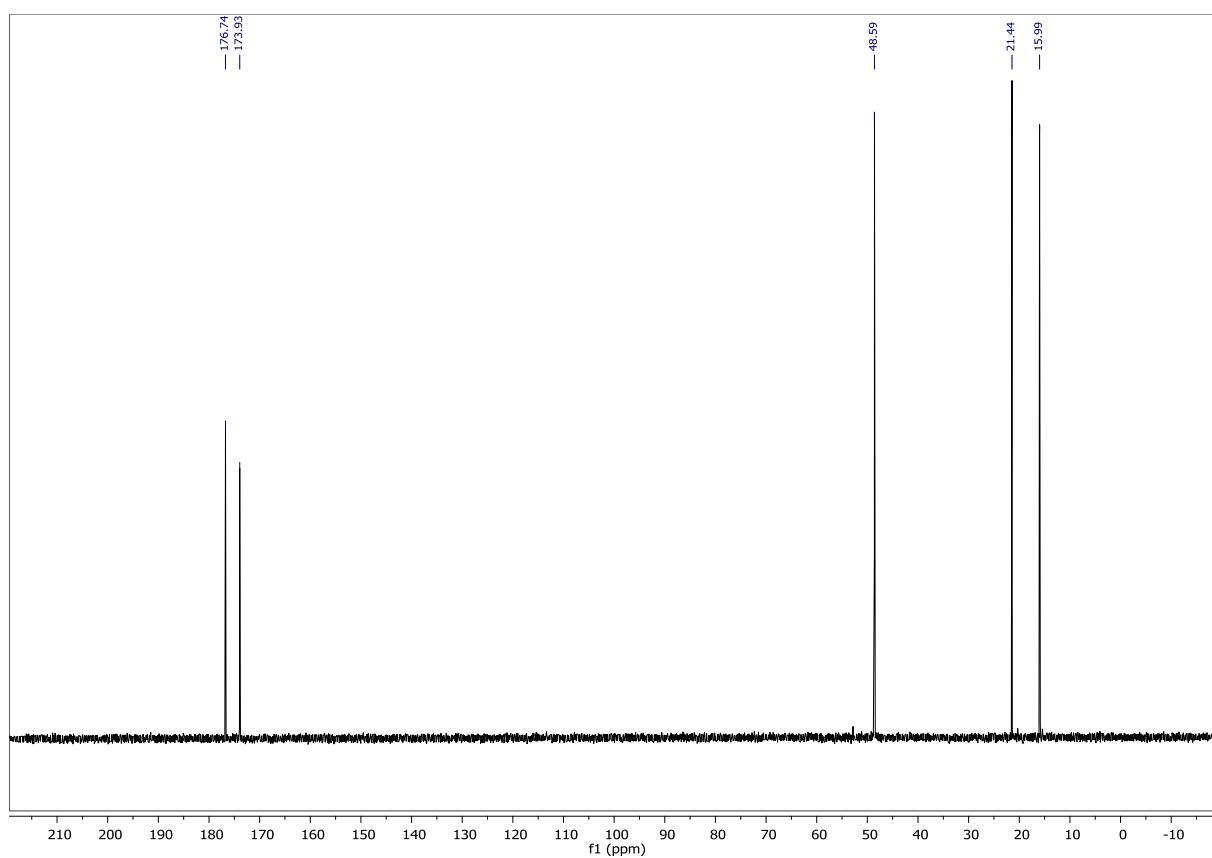
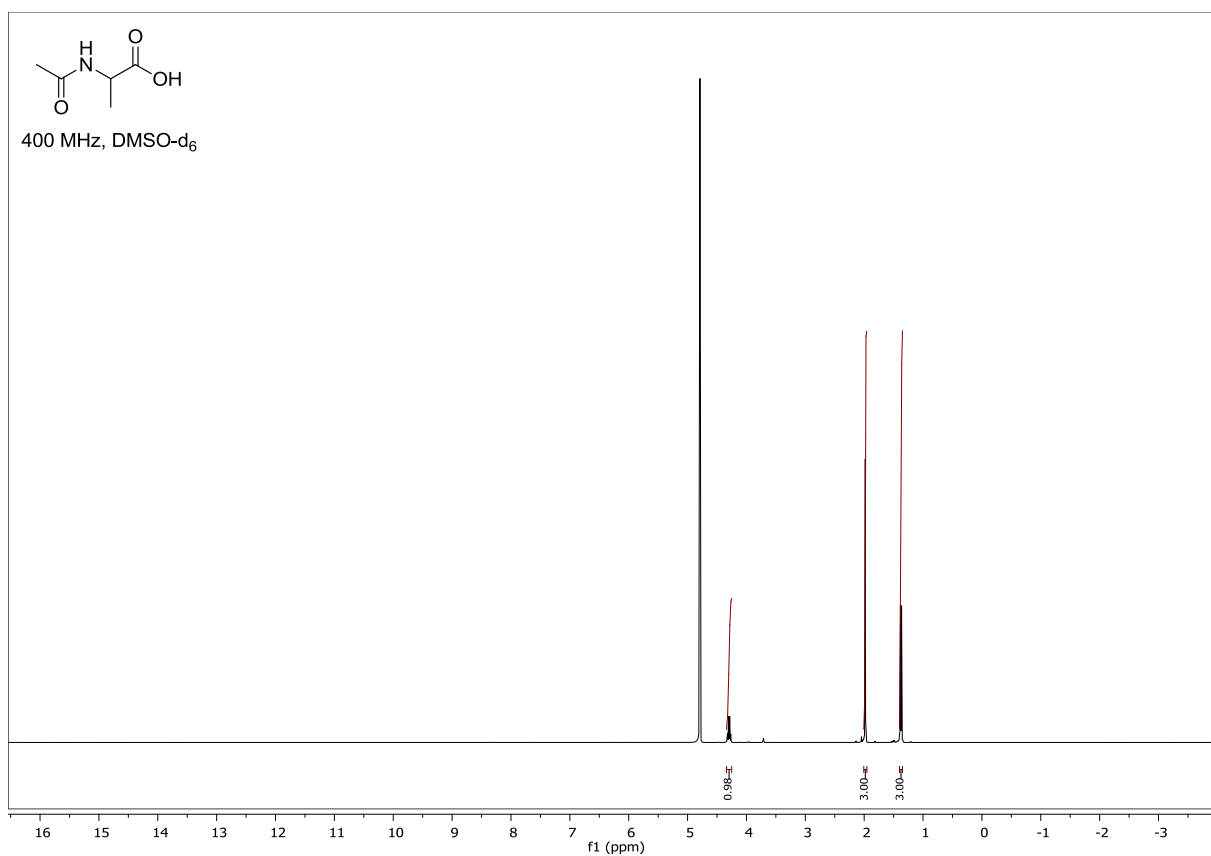
Two additional experiments were performed using **1c** (0.1 mmol) and either 20 mol% **18** or AcOH-d_4 (1.3 eq) under otherwise identical reaction (see 2.5.2 for reaction conditions). In both cases, no significant change in enantioselectivity was observed (56% and 57% *ee* vs. 54% *ee* under the standard conditions). Therefore, we can exclude a significant background reaction but it is not possible to discuss kinetic isotope effects on the basis of this experiment.

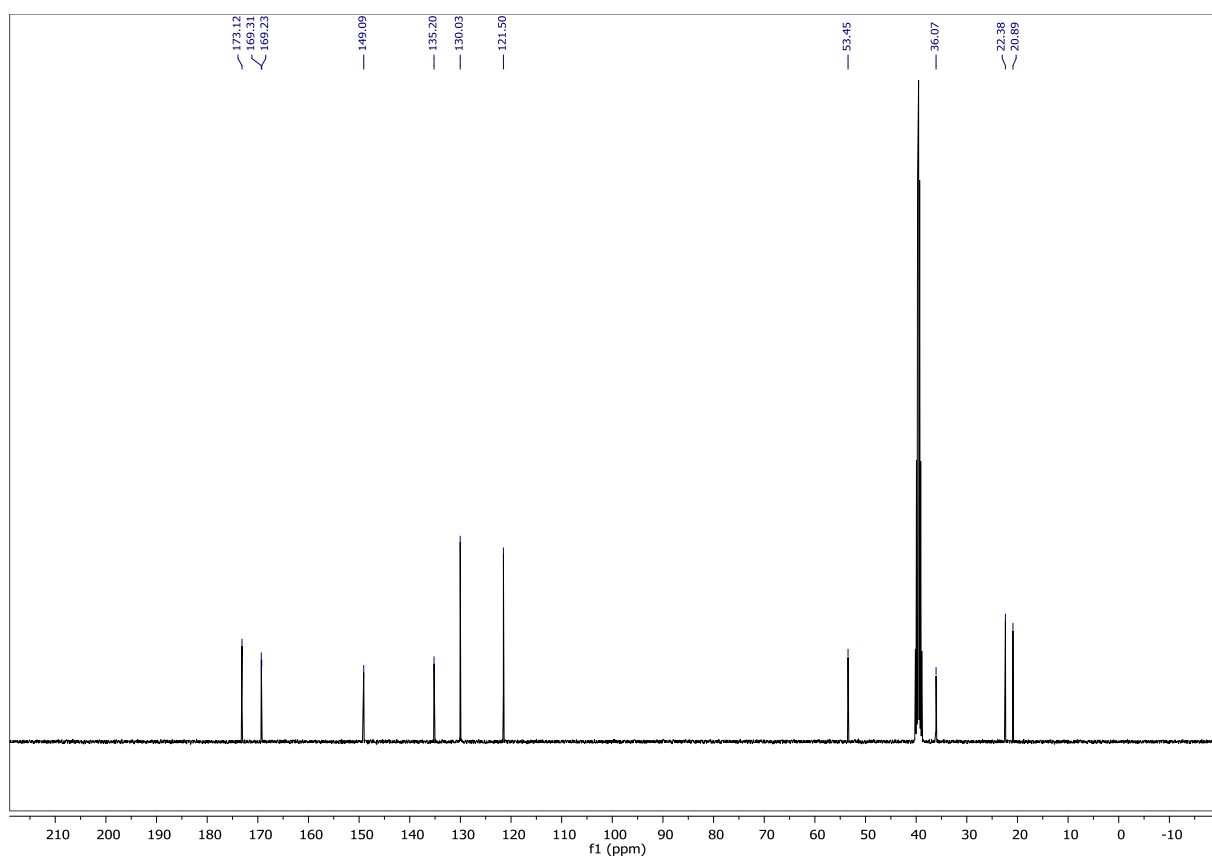
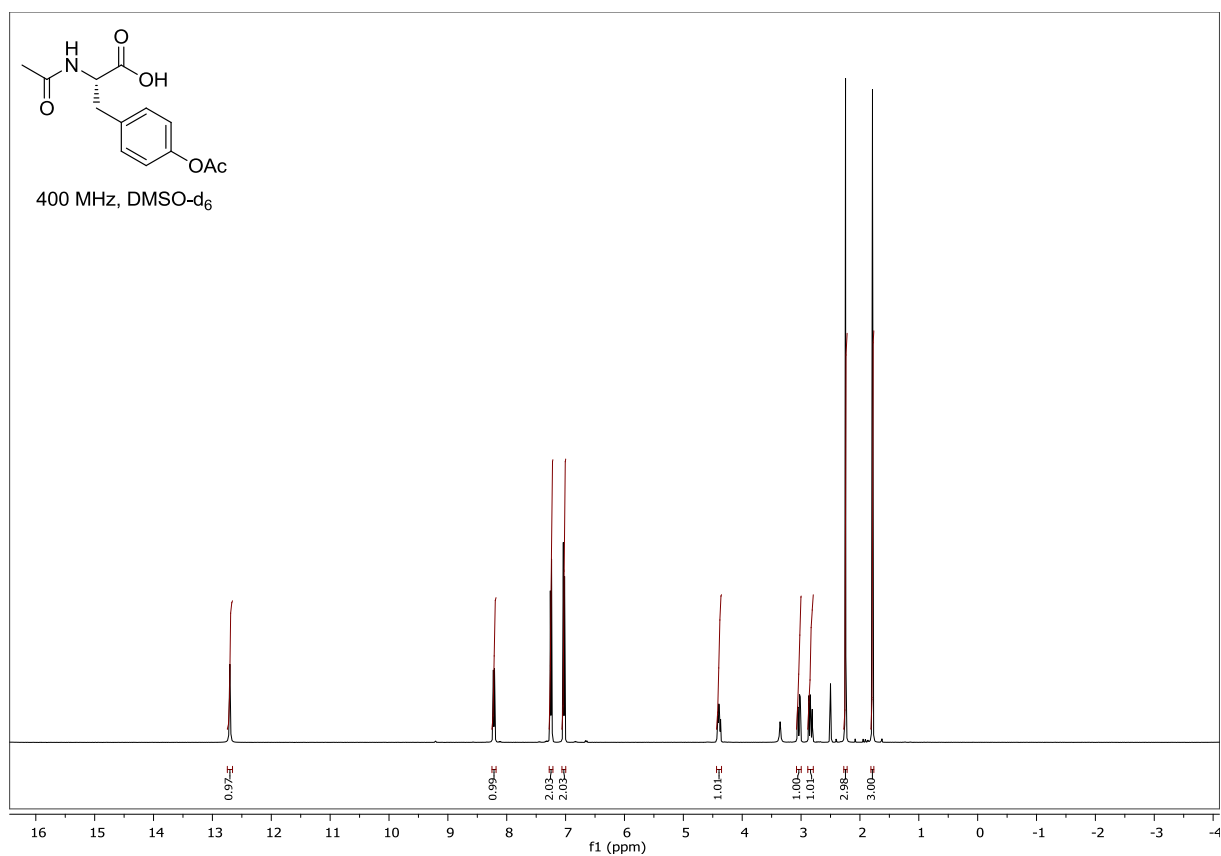
2.7 NMR Spectra

N-acetyl-DL-phenylalanine (1a)

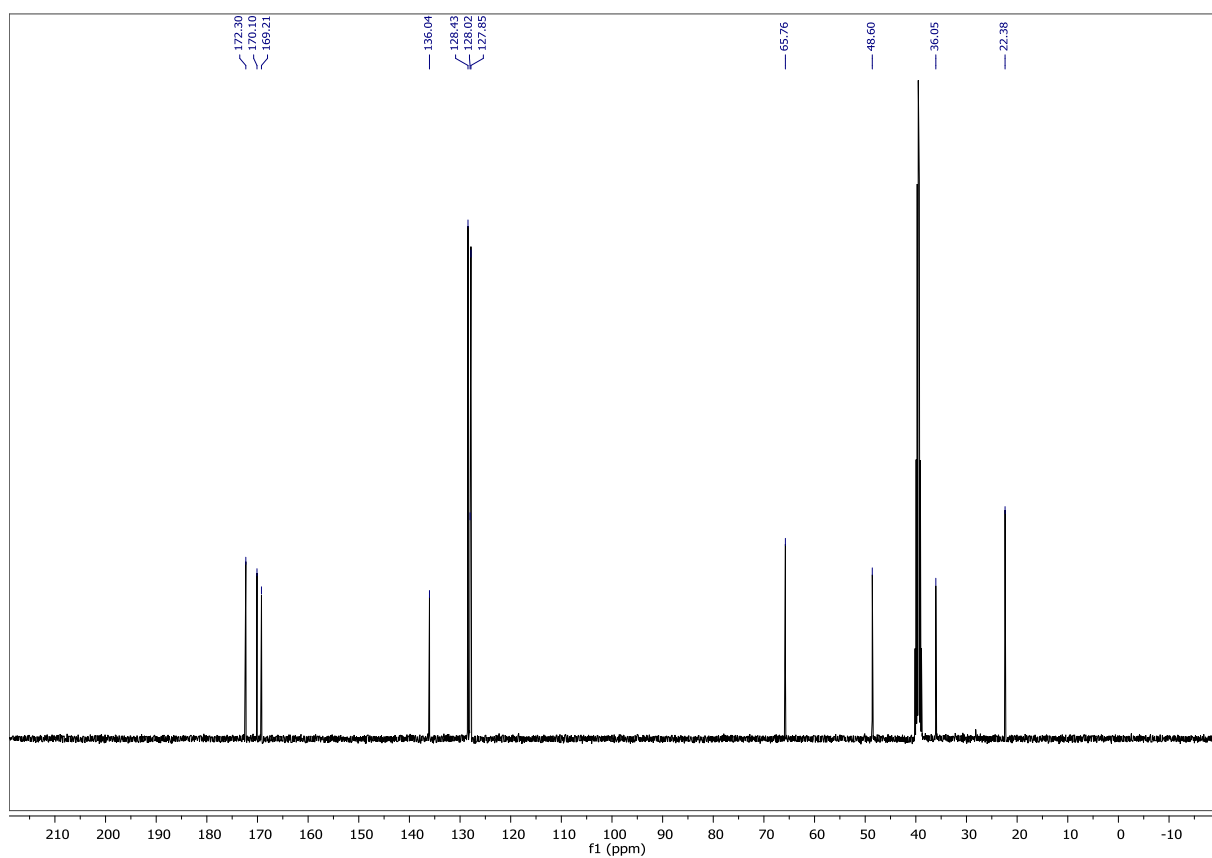
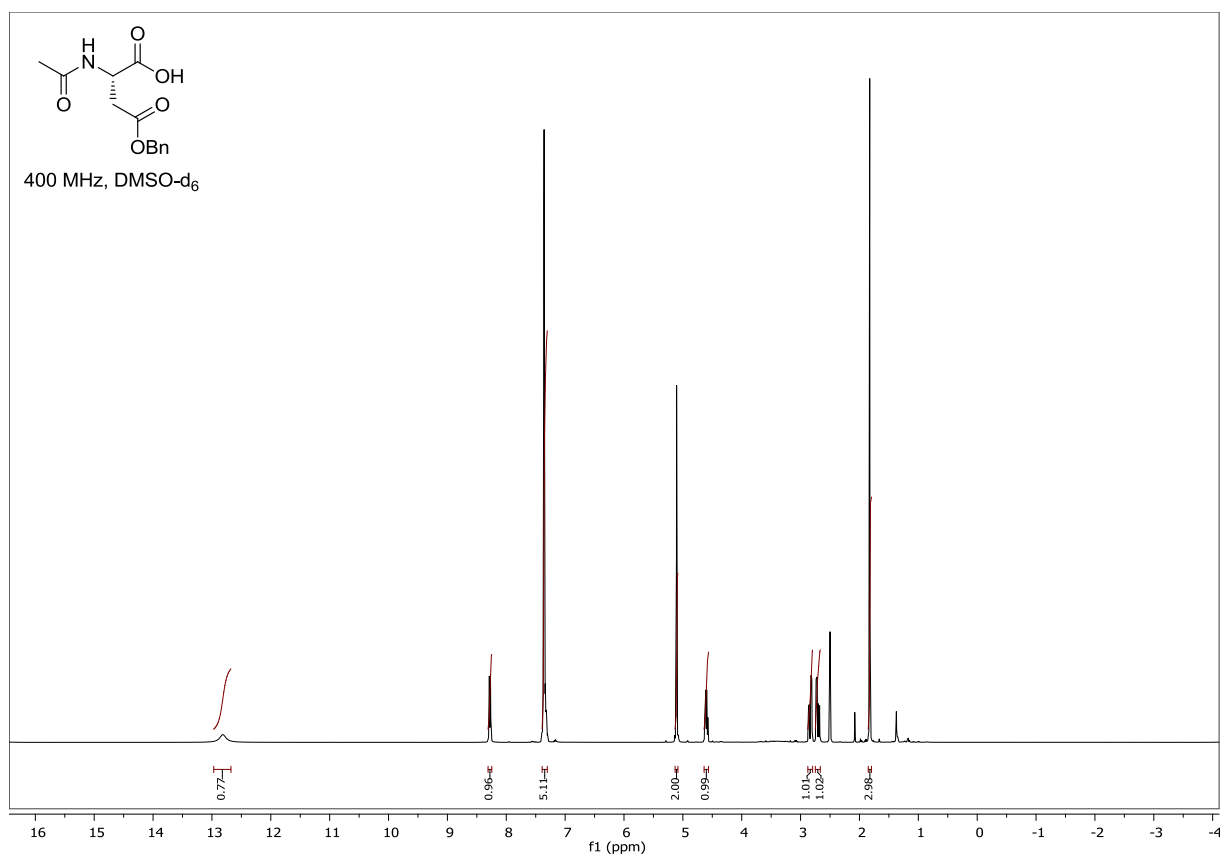


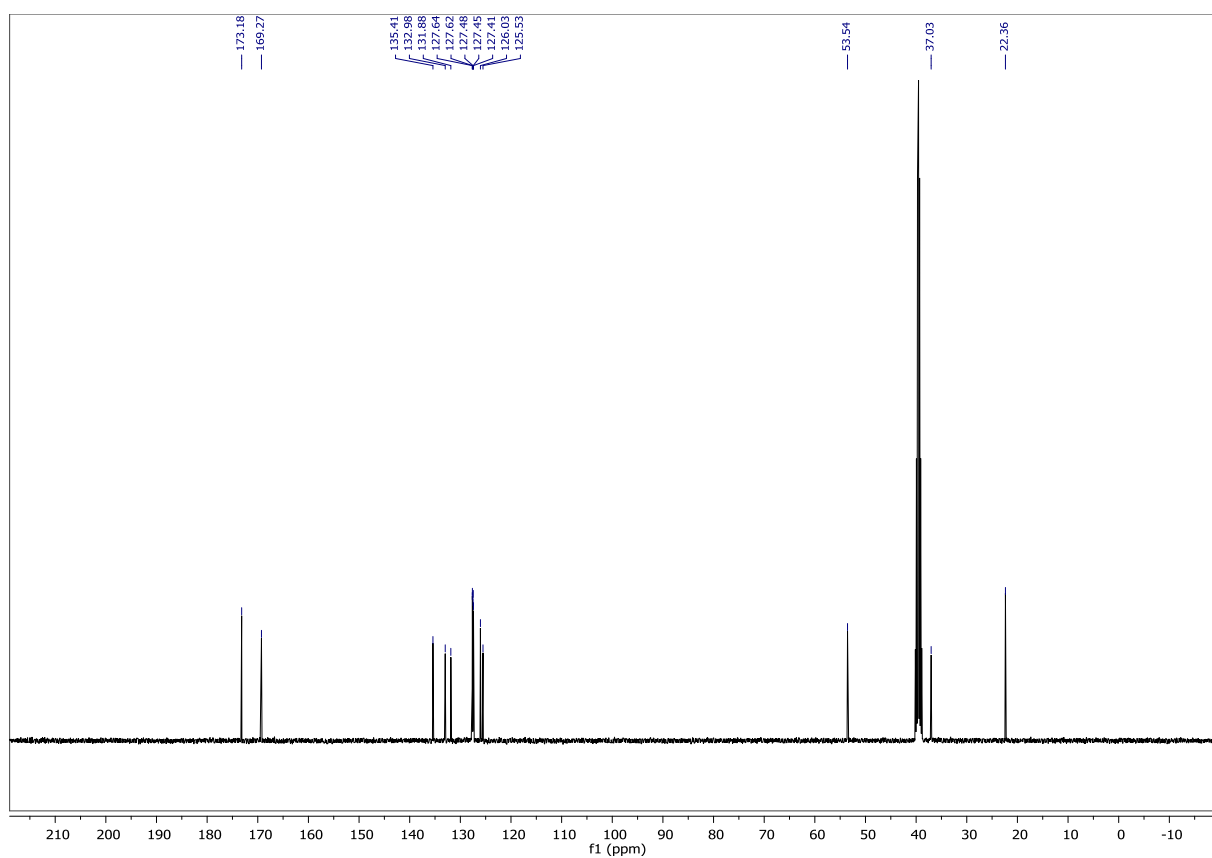
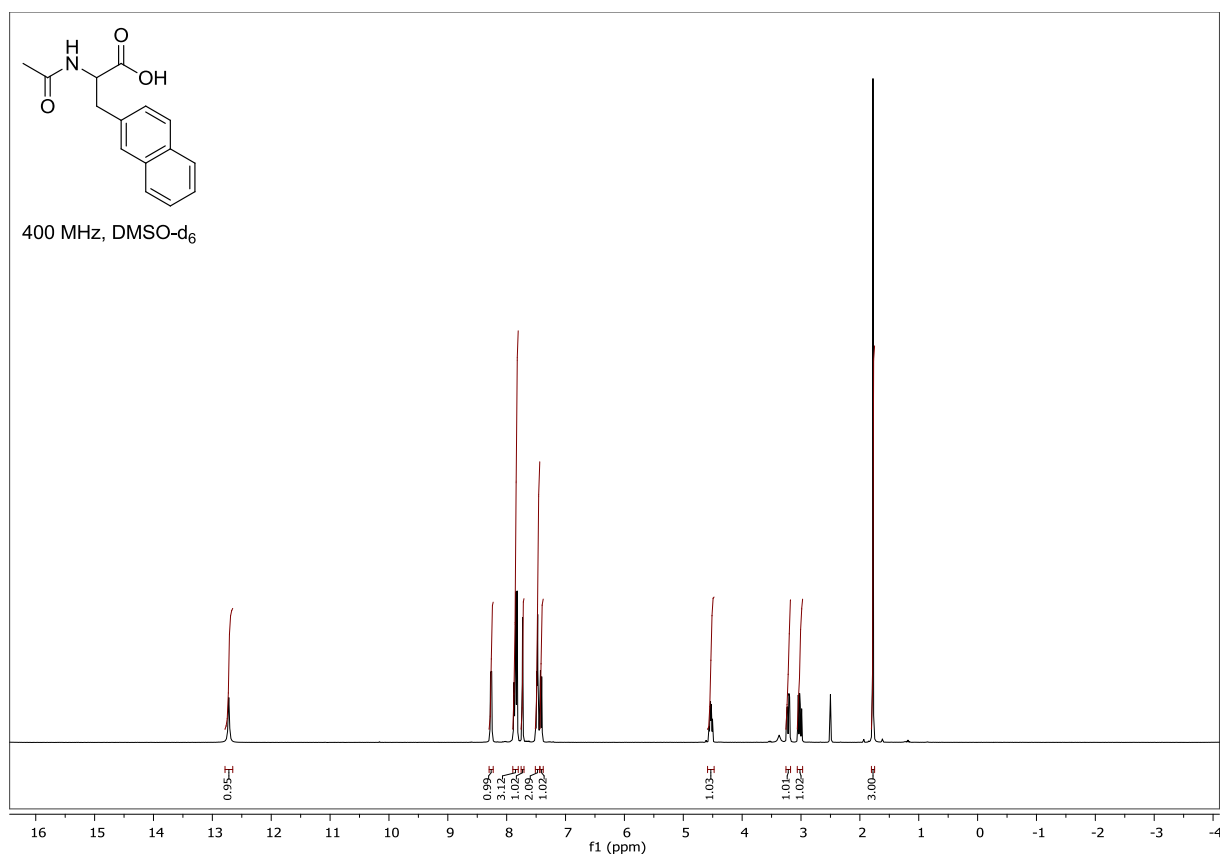
***N*-acetyl-DL-alanine (1b)**



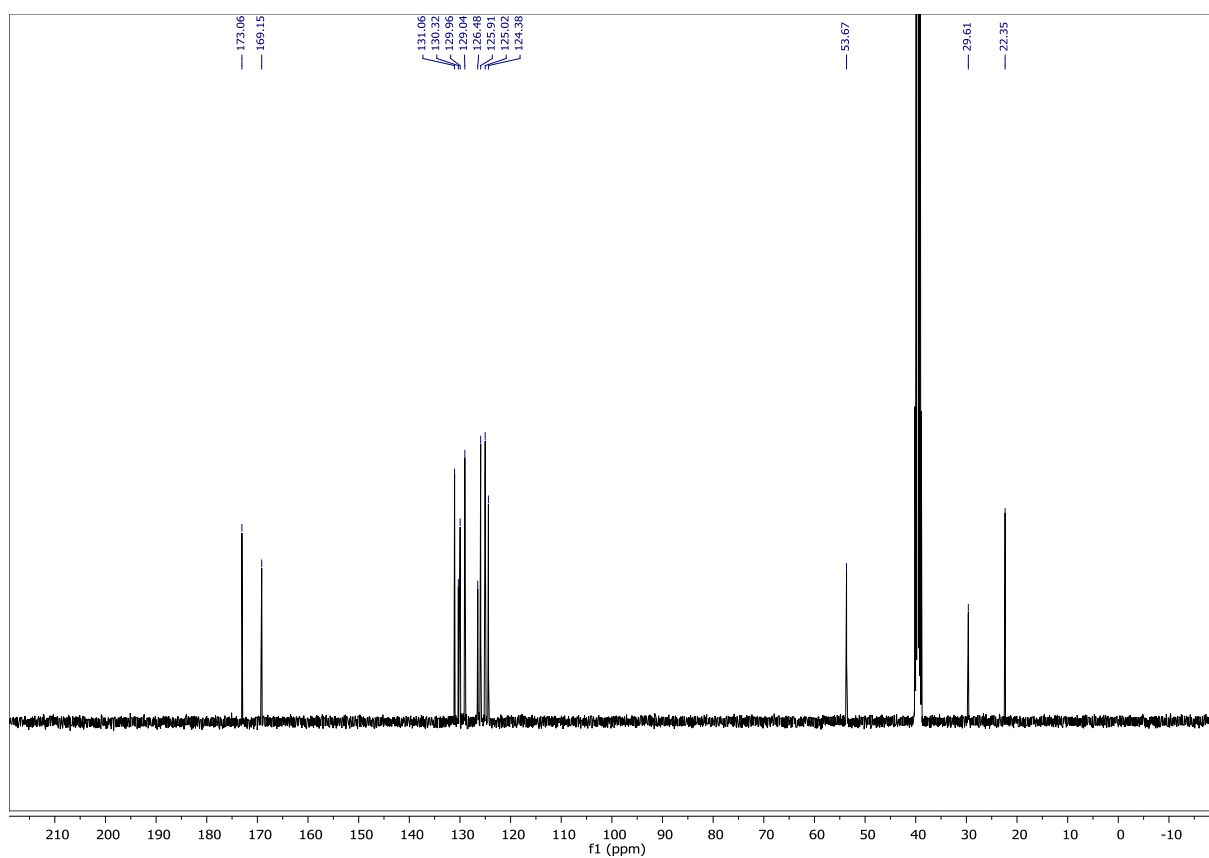
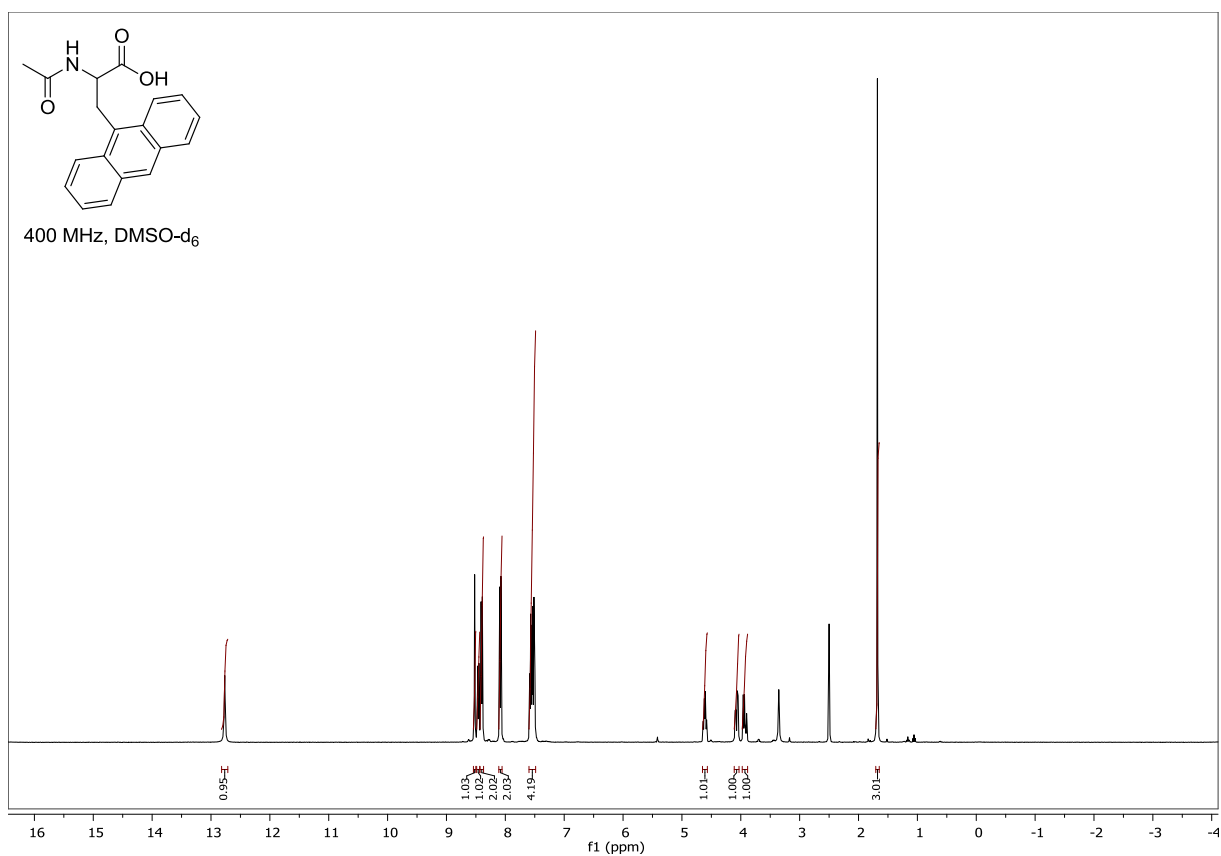
***O,N*-diacetyl-L-tyrosine (1d)**

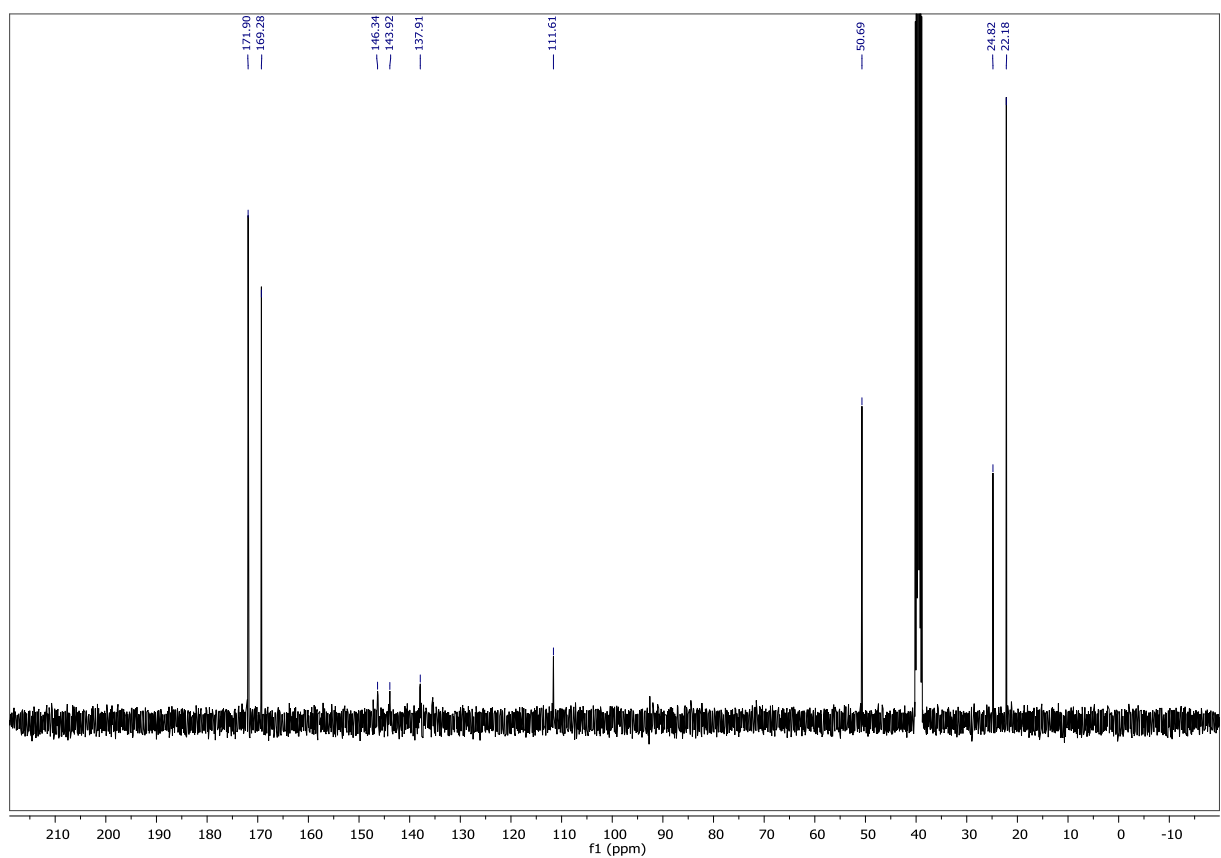
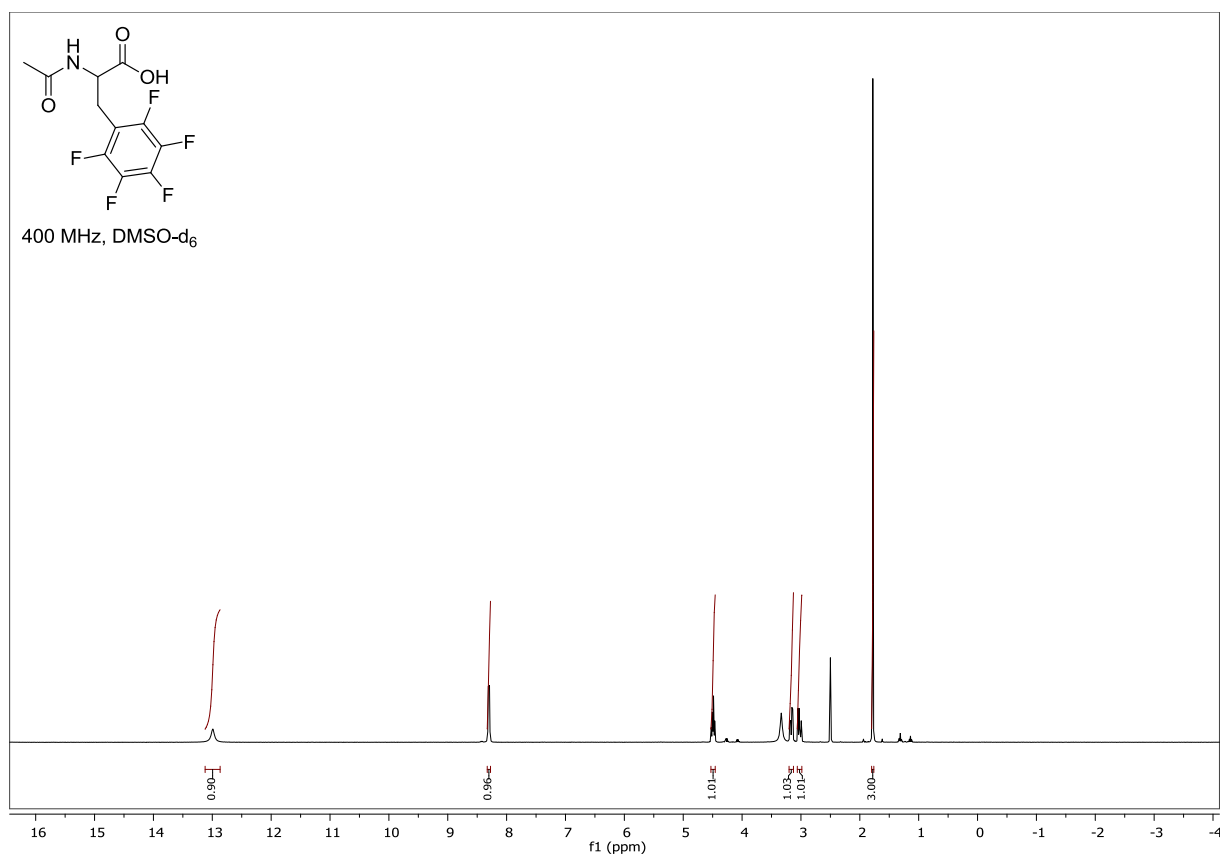
N-acetyl-L-aspartic acid 4-benzyl ester (1f)



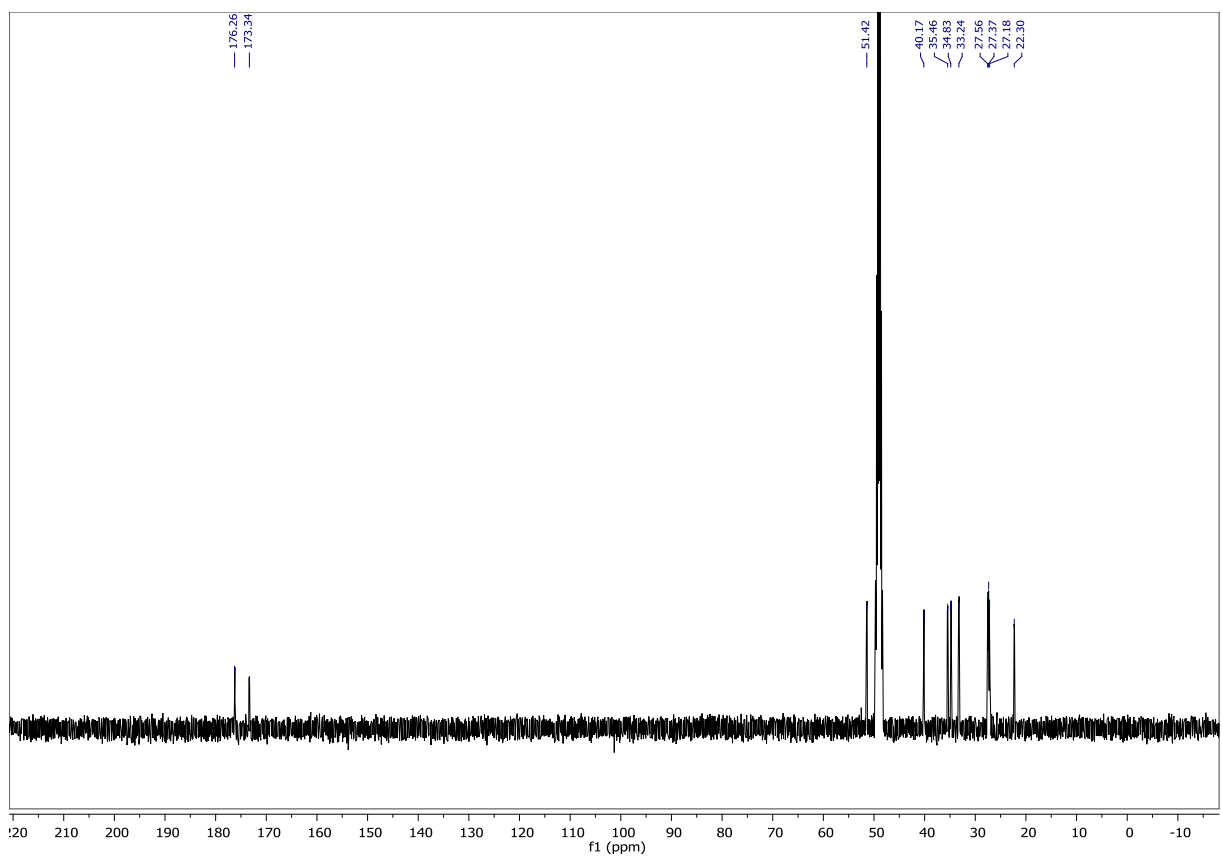
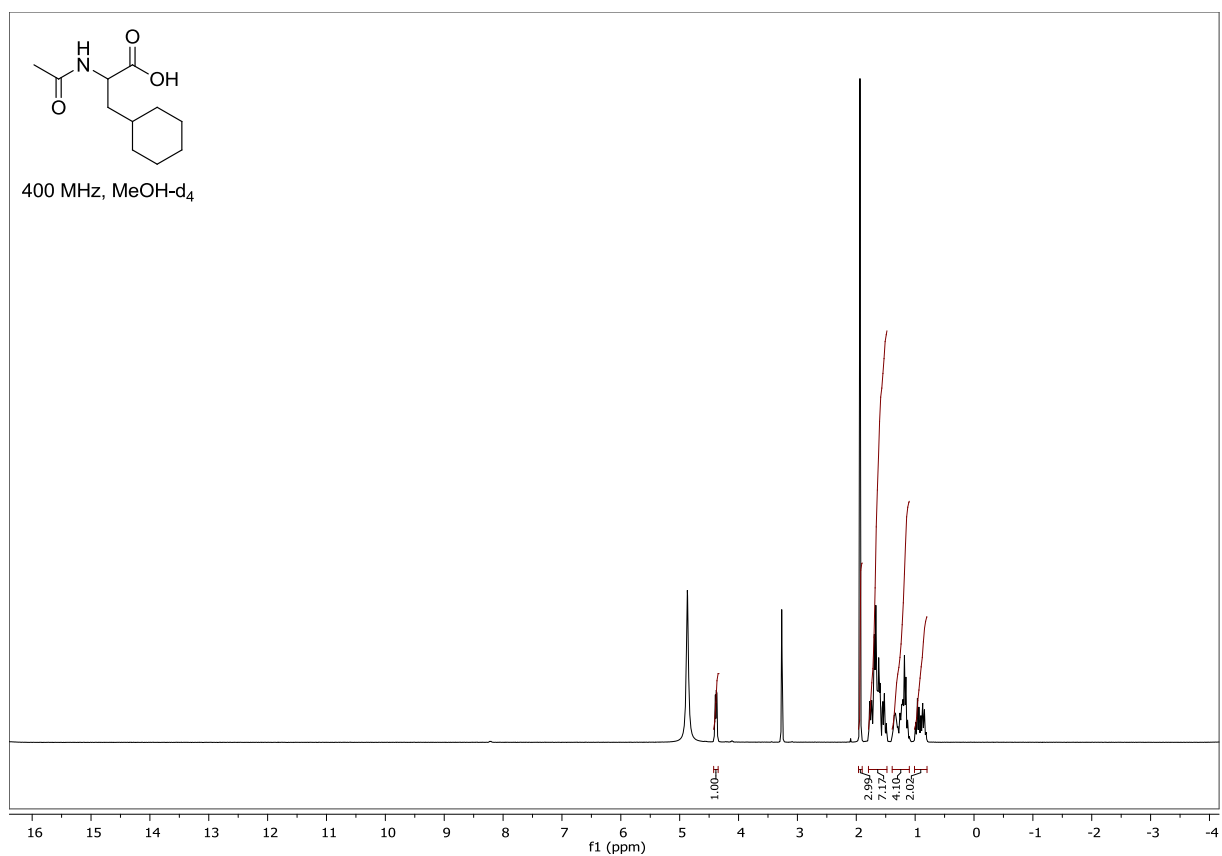
***N*-acetyl-DL-2-naphthylalanine (1g)**

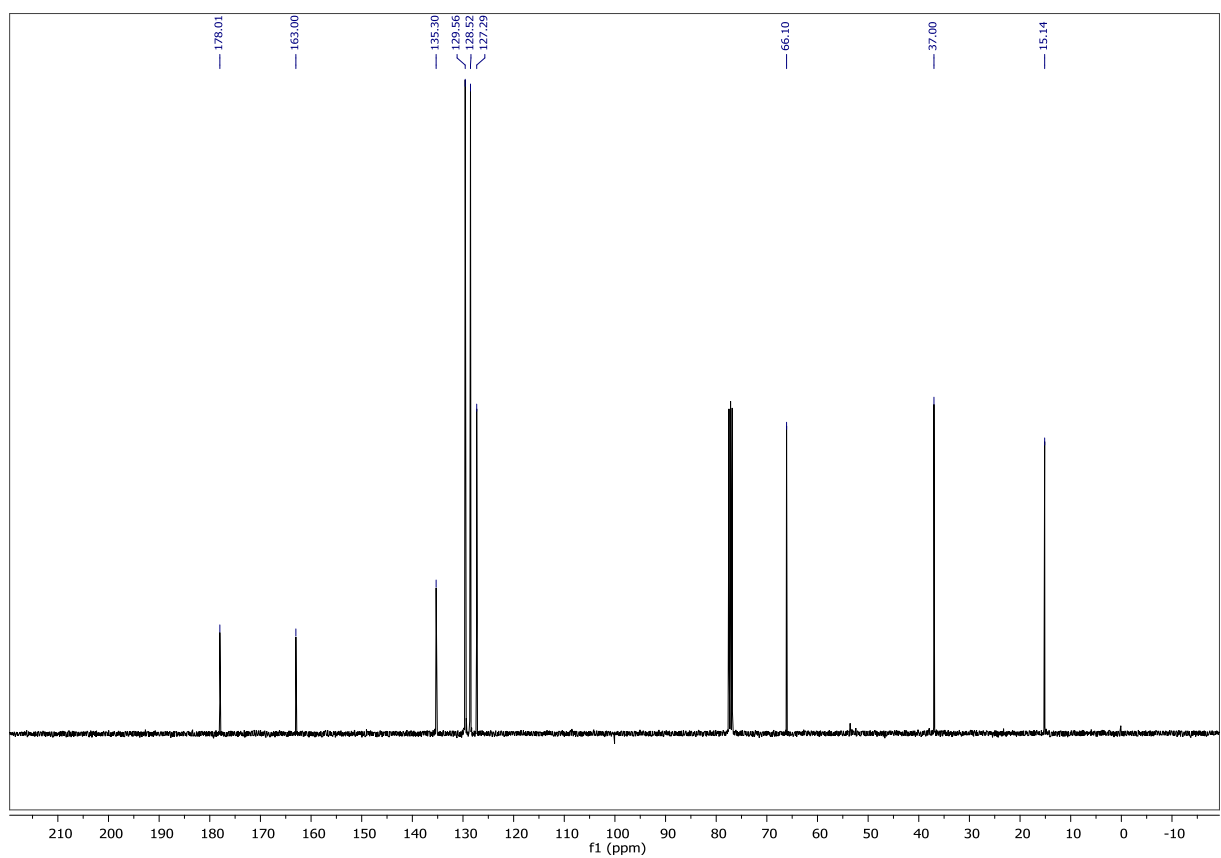
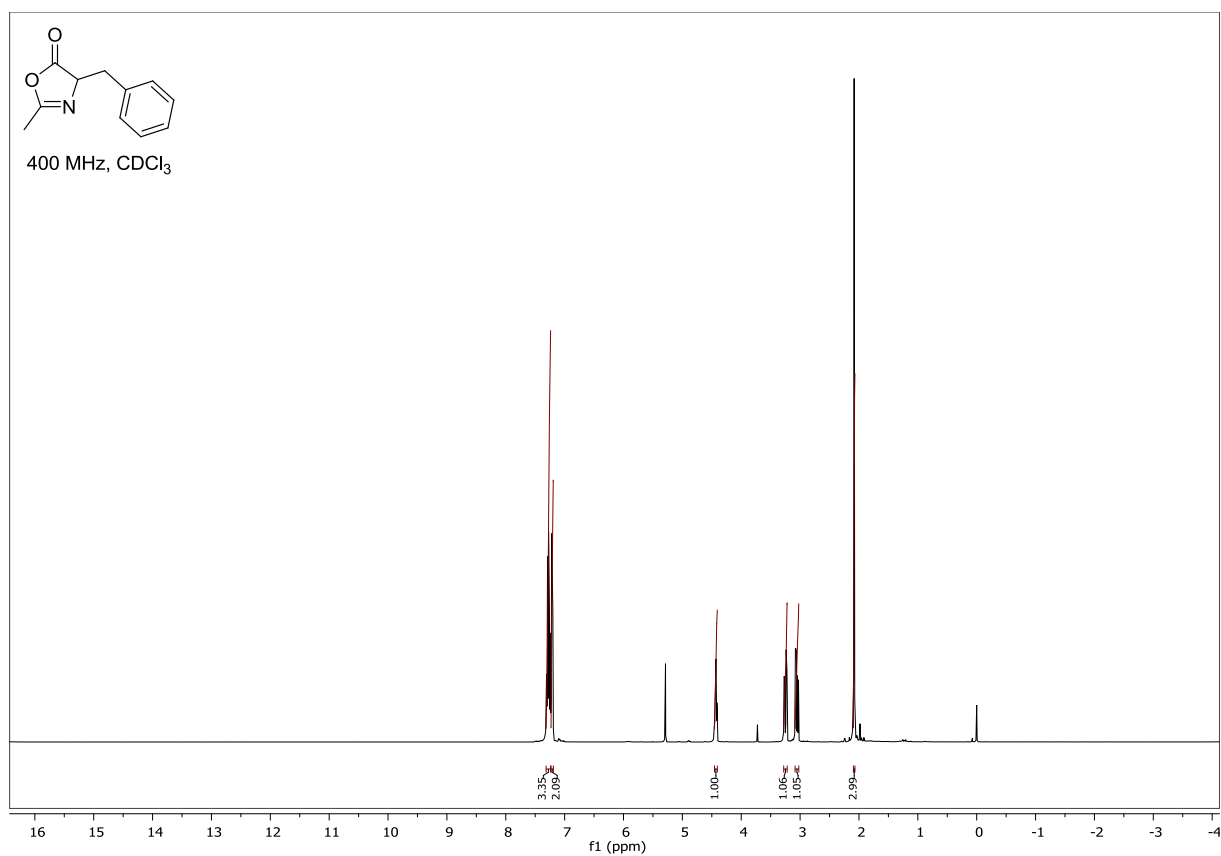
N-acetyl-DL-9-anthranylalanine (**1h**)



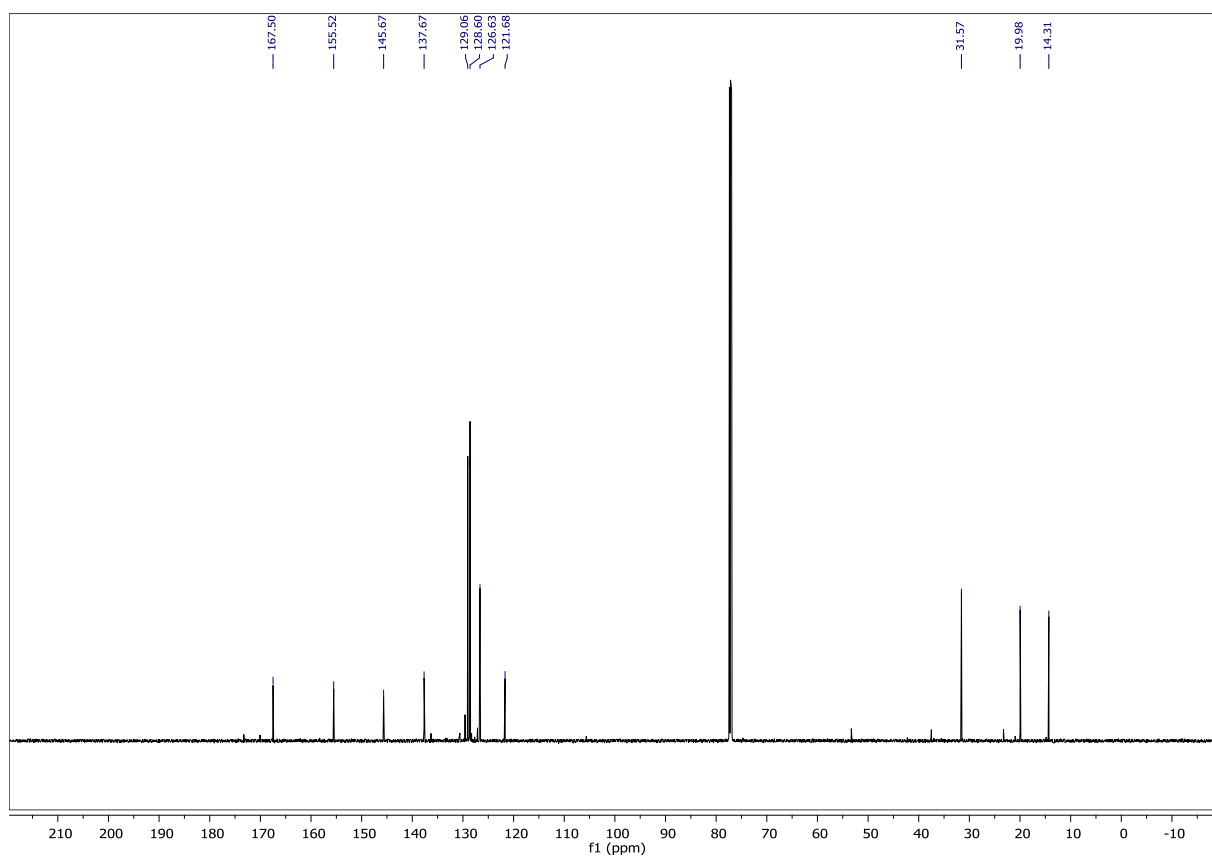
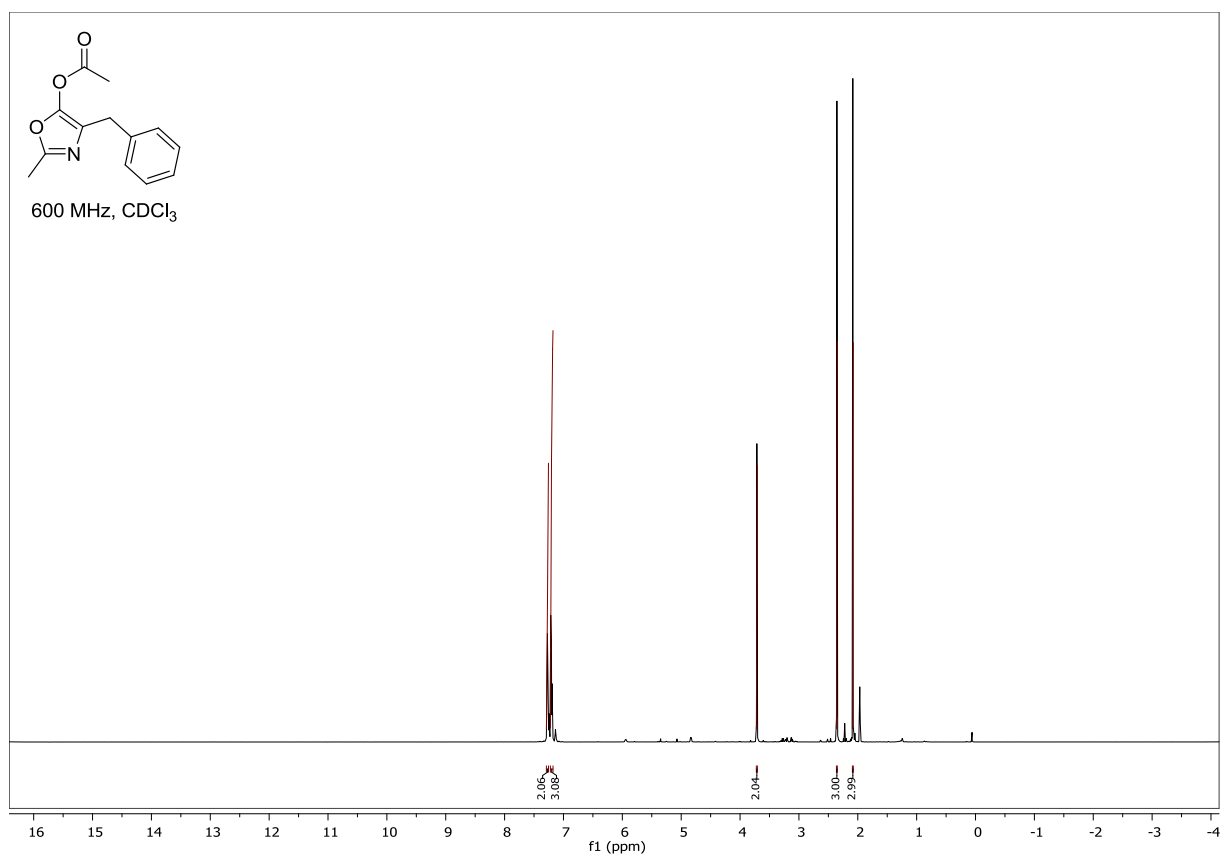
***N*-acetyl-DL-pentafluorophenylalanine (1i)**

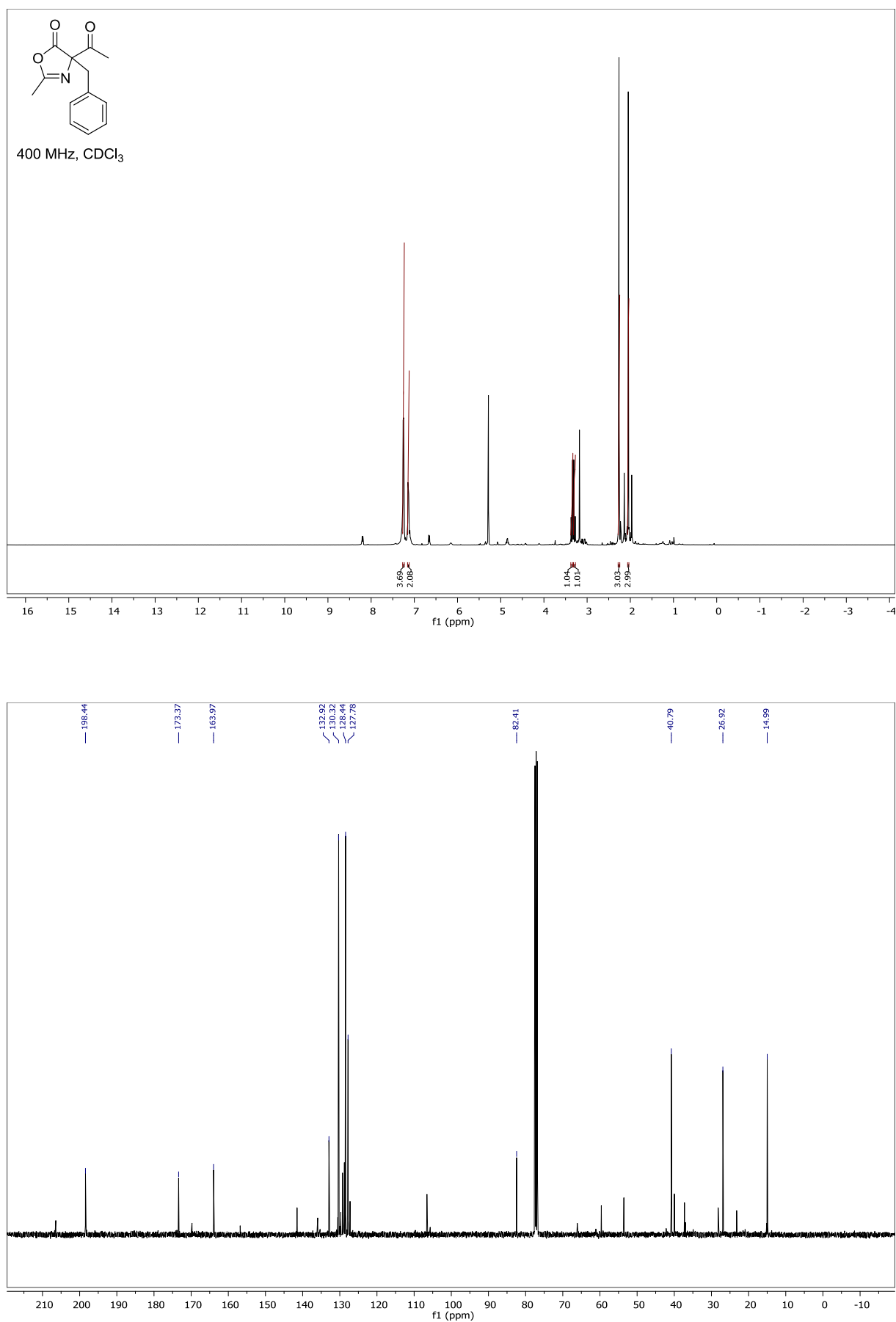
***N*-acetyl-DL-cyclohexylalanine (1j)**



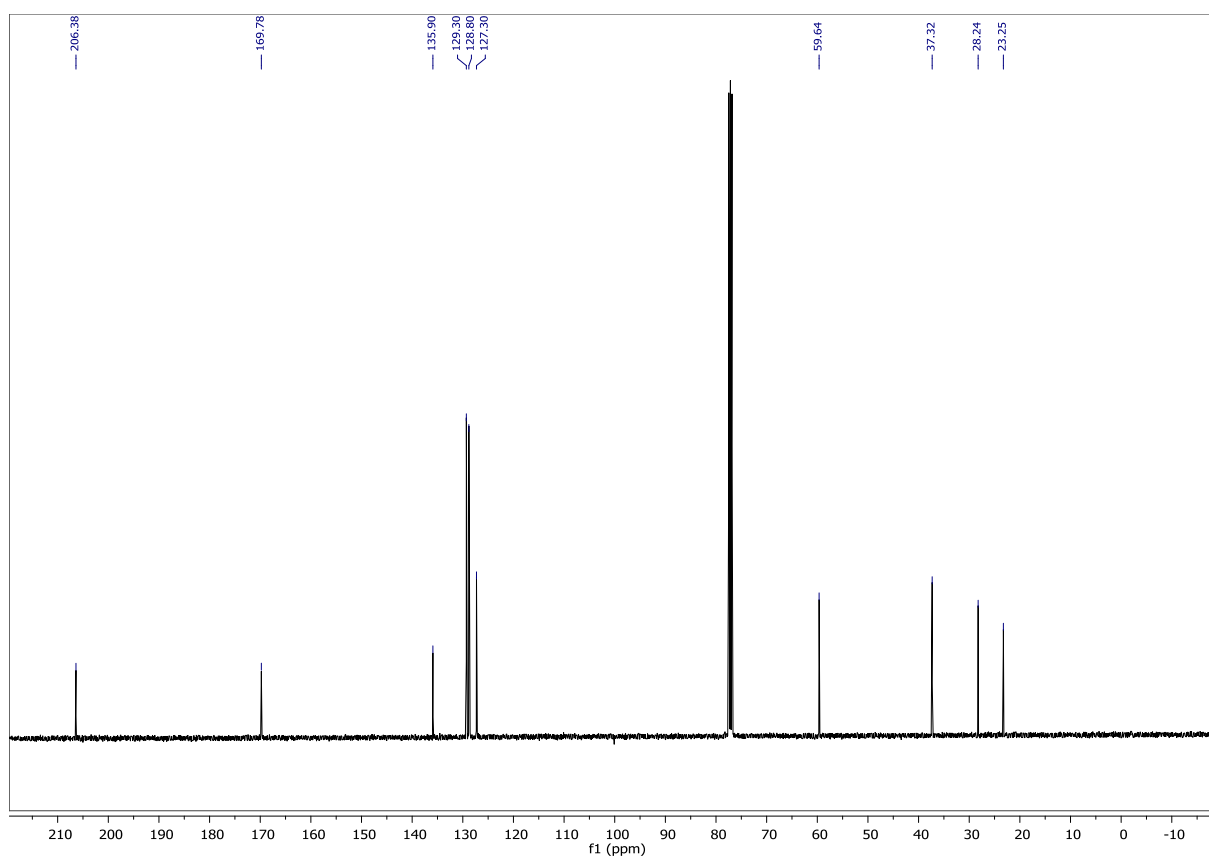
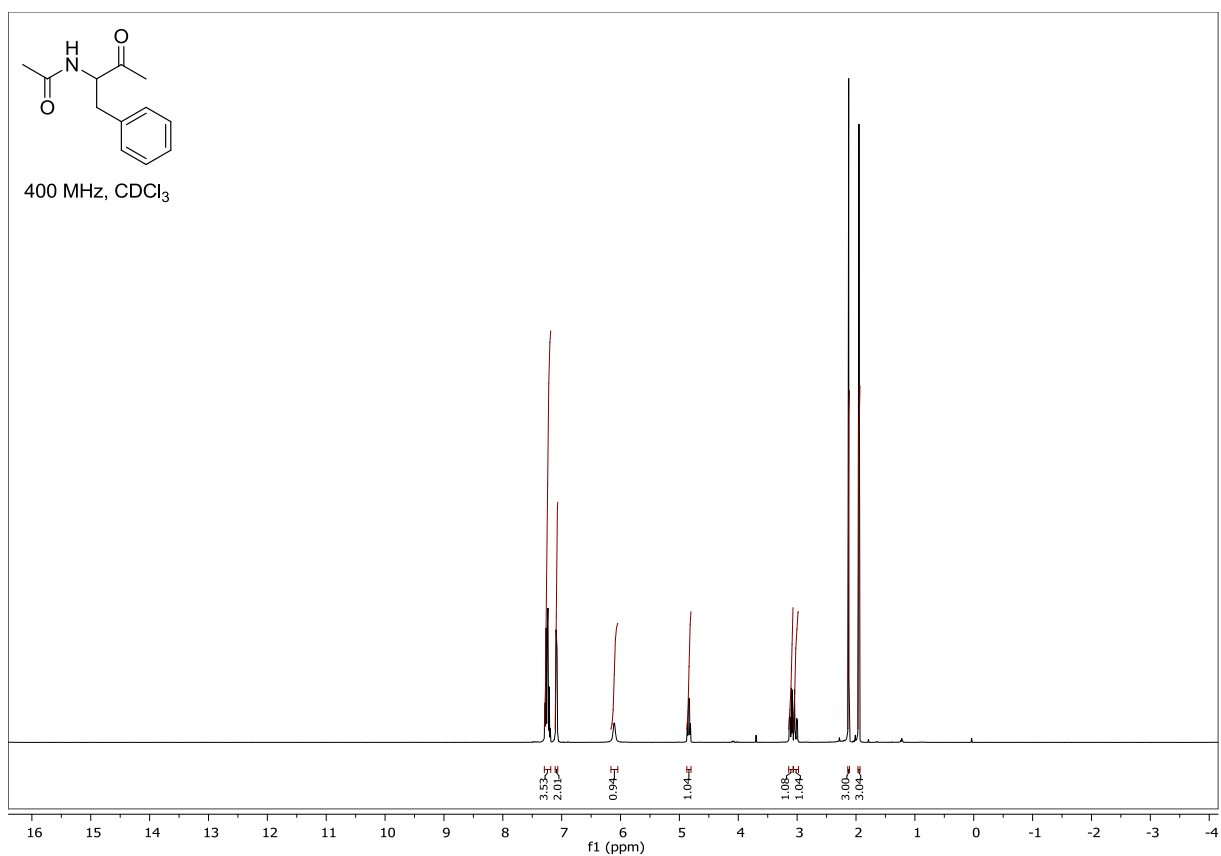
4-benzyl-2-methyloxazol-5(4H)-one (3a)

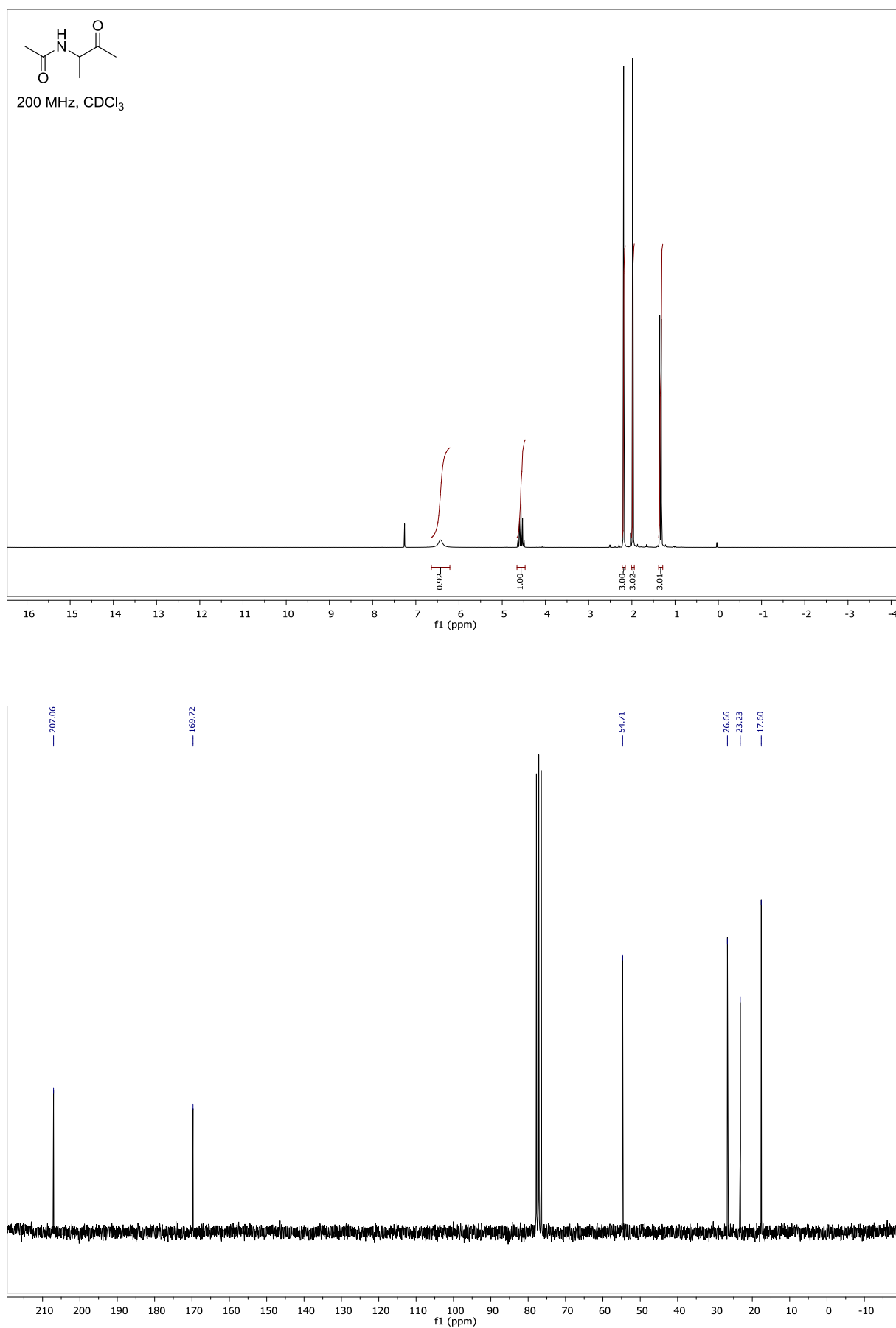
4-benzyl-2-methyloxazol-5-yl acetate (5a)



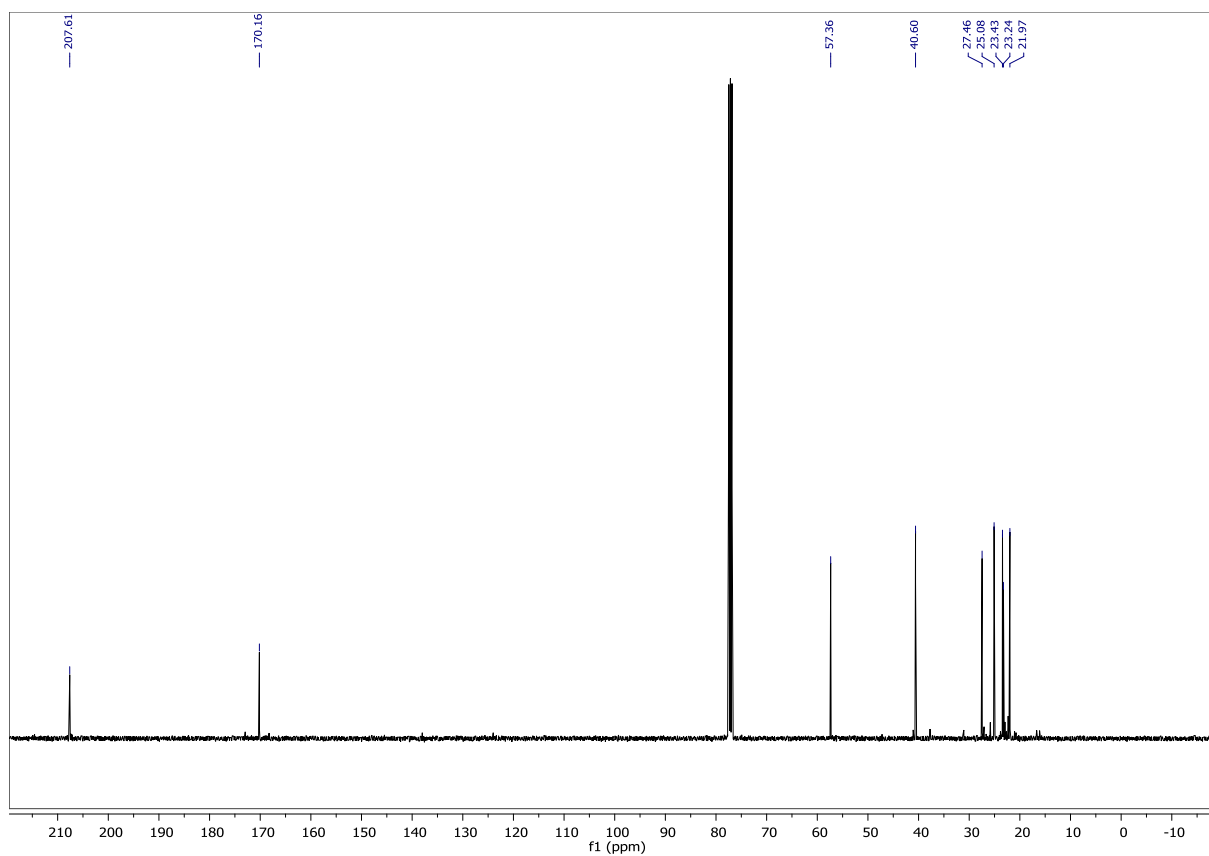
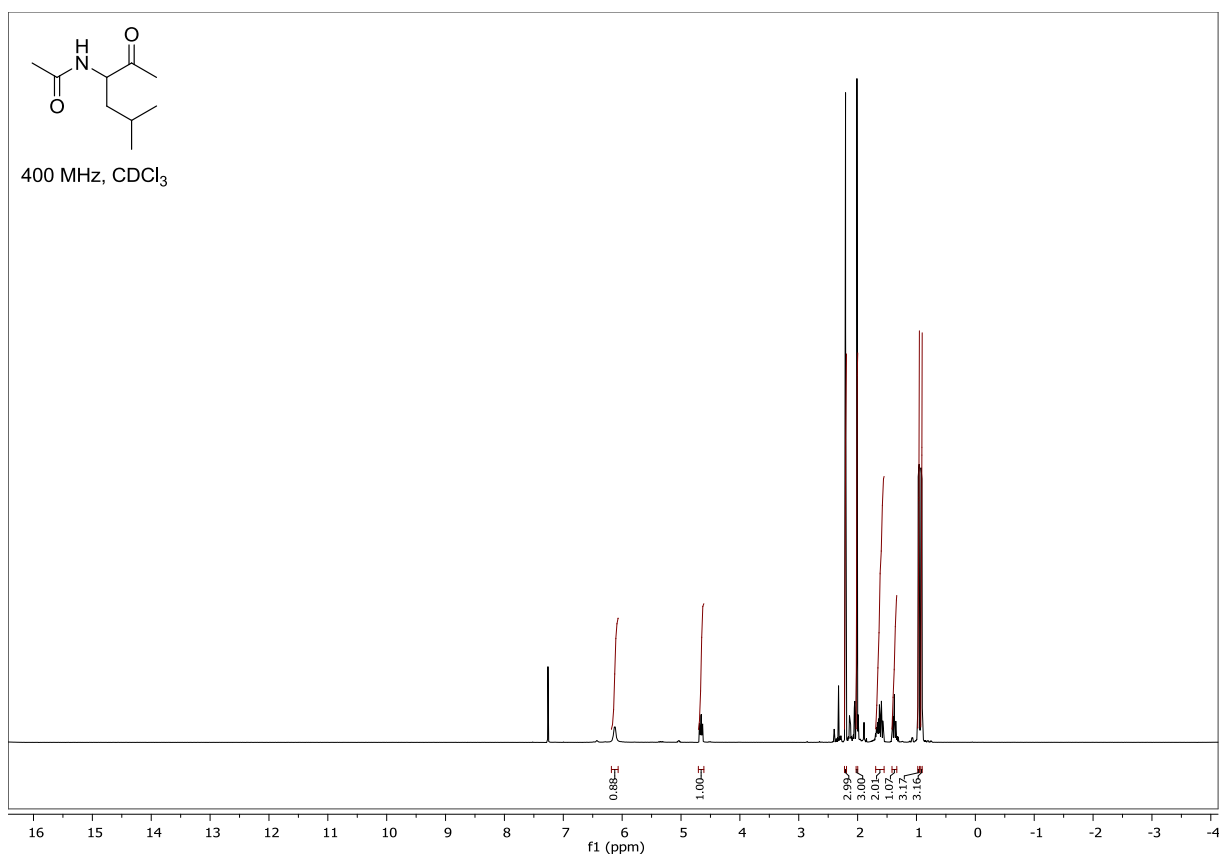
4-acetyl-4-benzyl-2-methyloxazol-5(4*H*)-one (6a)

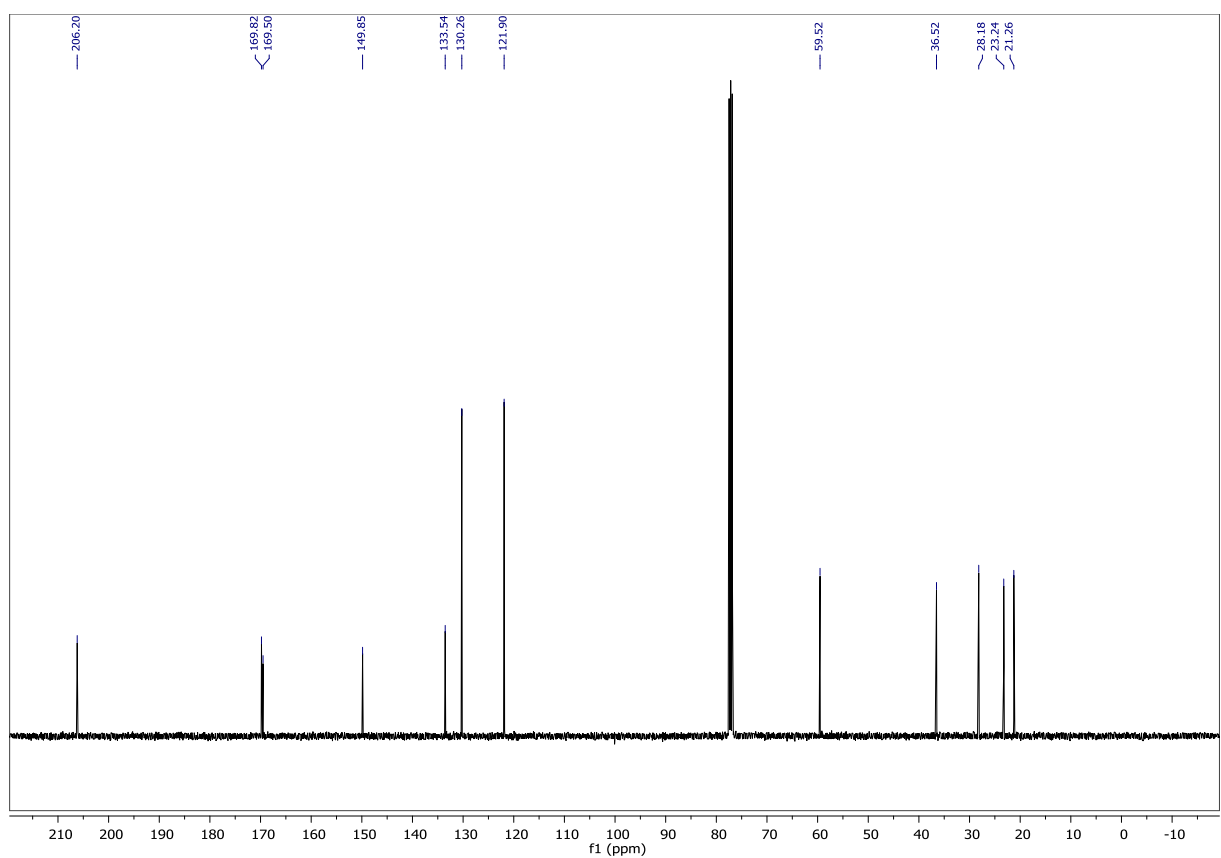
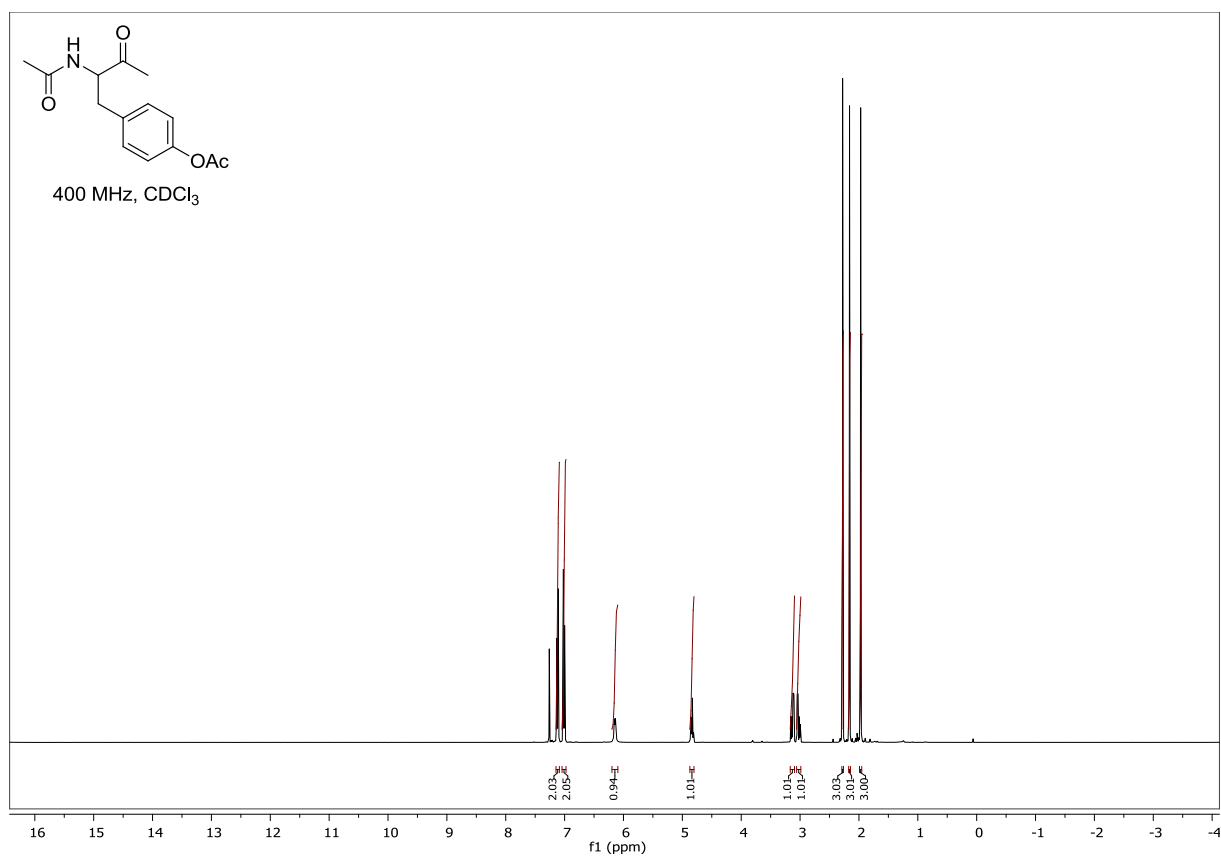
***N*-(3-oxo-1-phenylbutan-2-yl)acetamide (10a)**



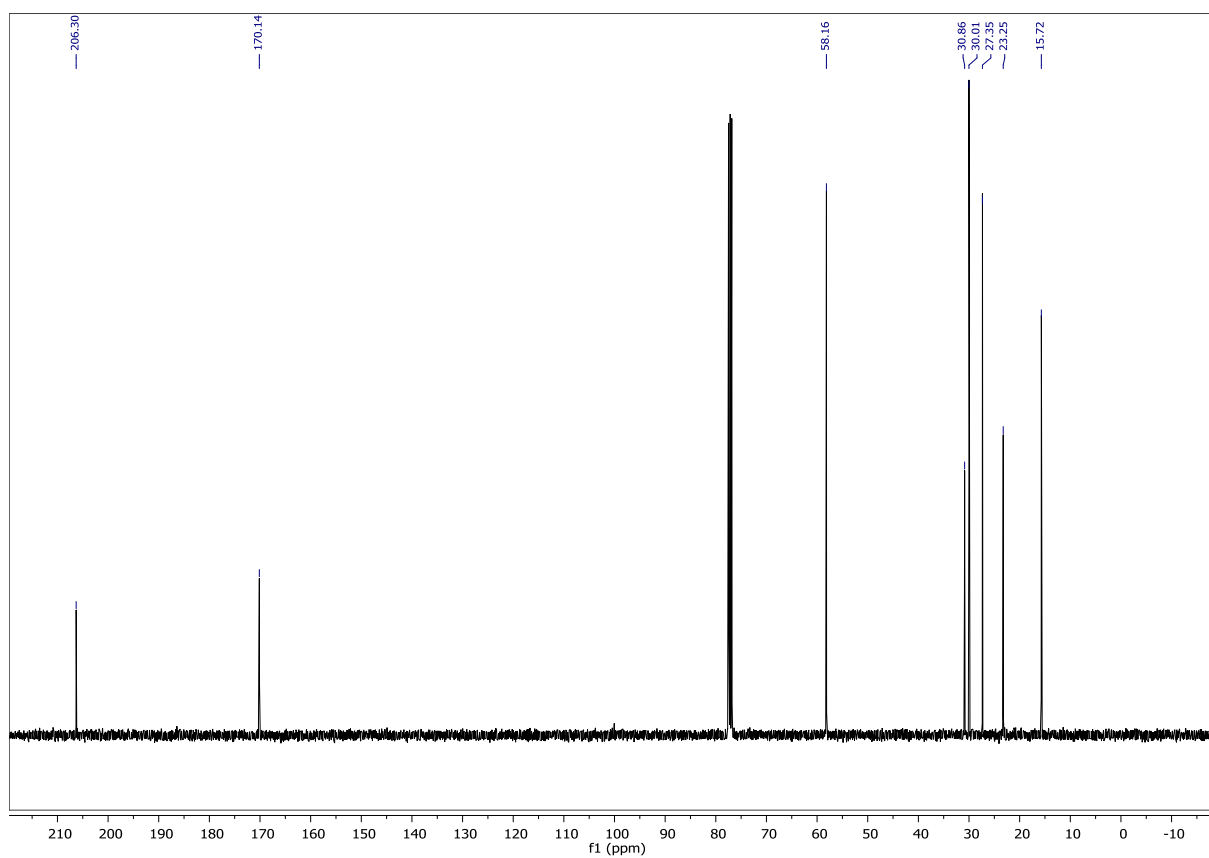
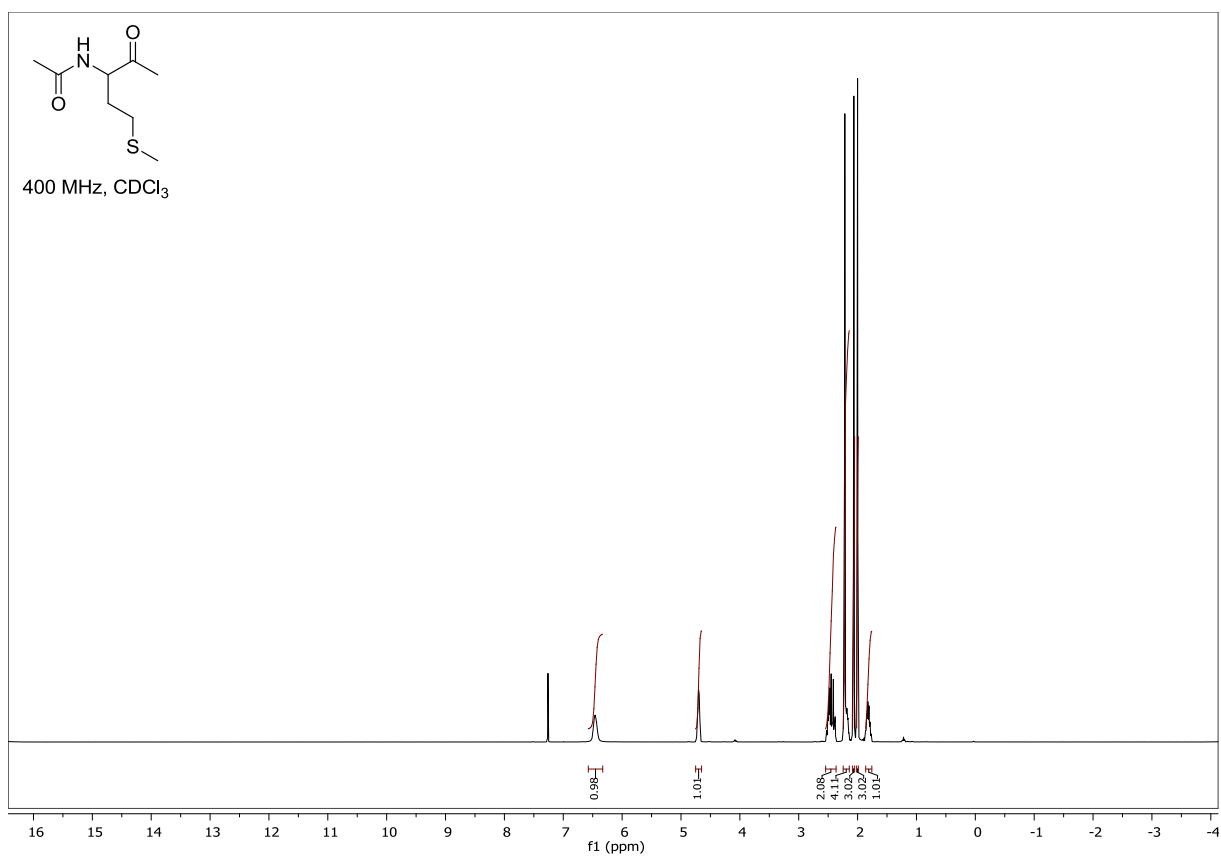
***N*-(3-oxobutan-2-yl)acetamide (10b)**

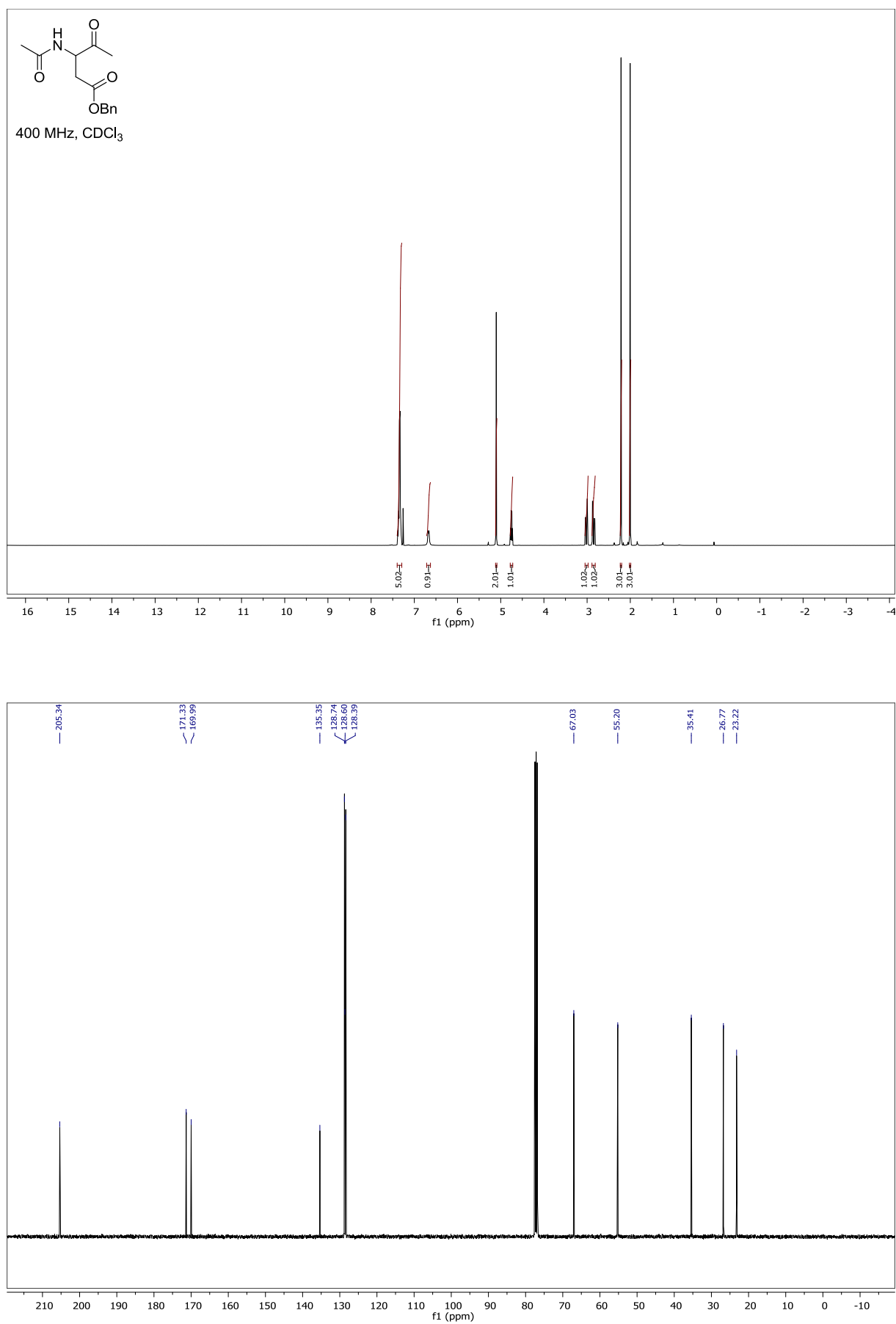
***N*-(5-methyl-2-oxohexan-3-yl)acetamide (10c)**



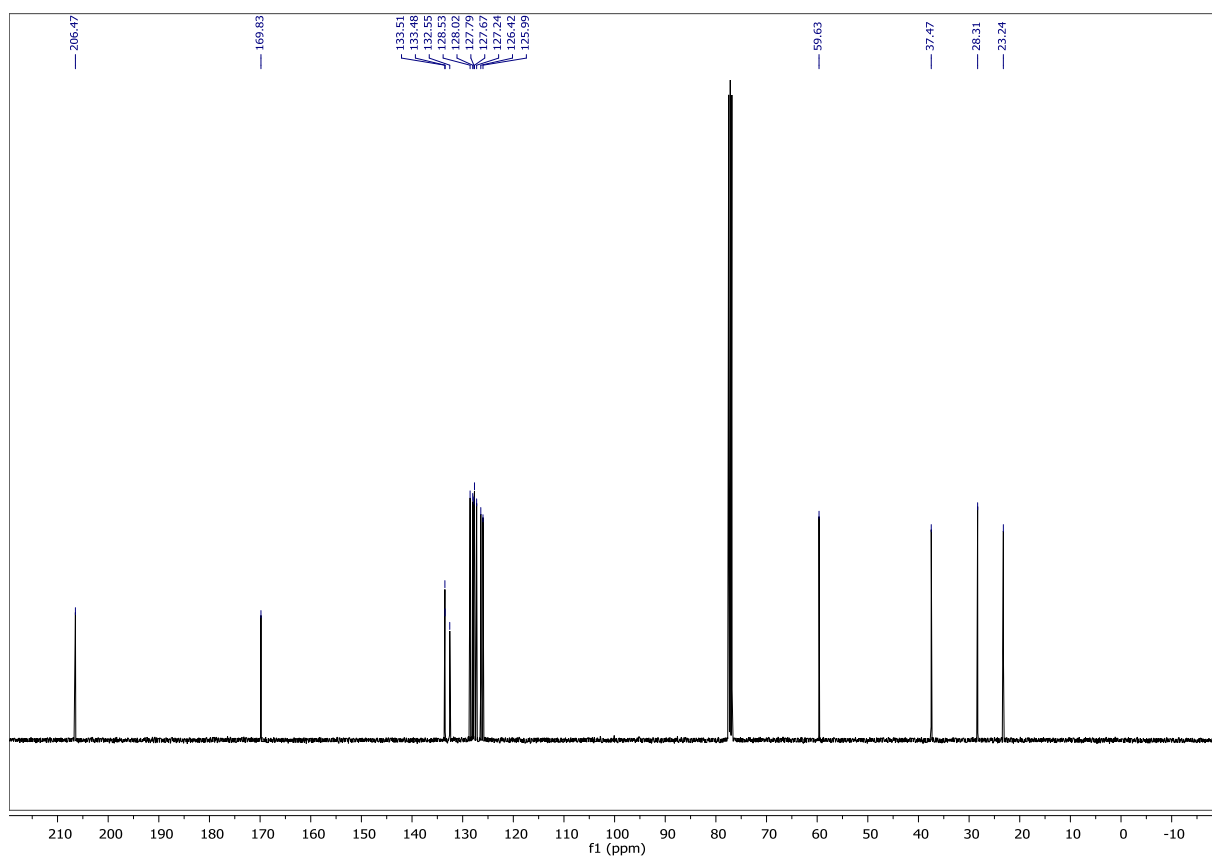
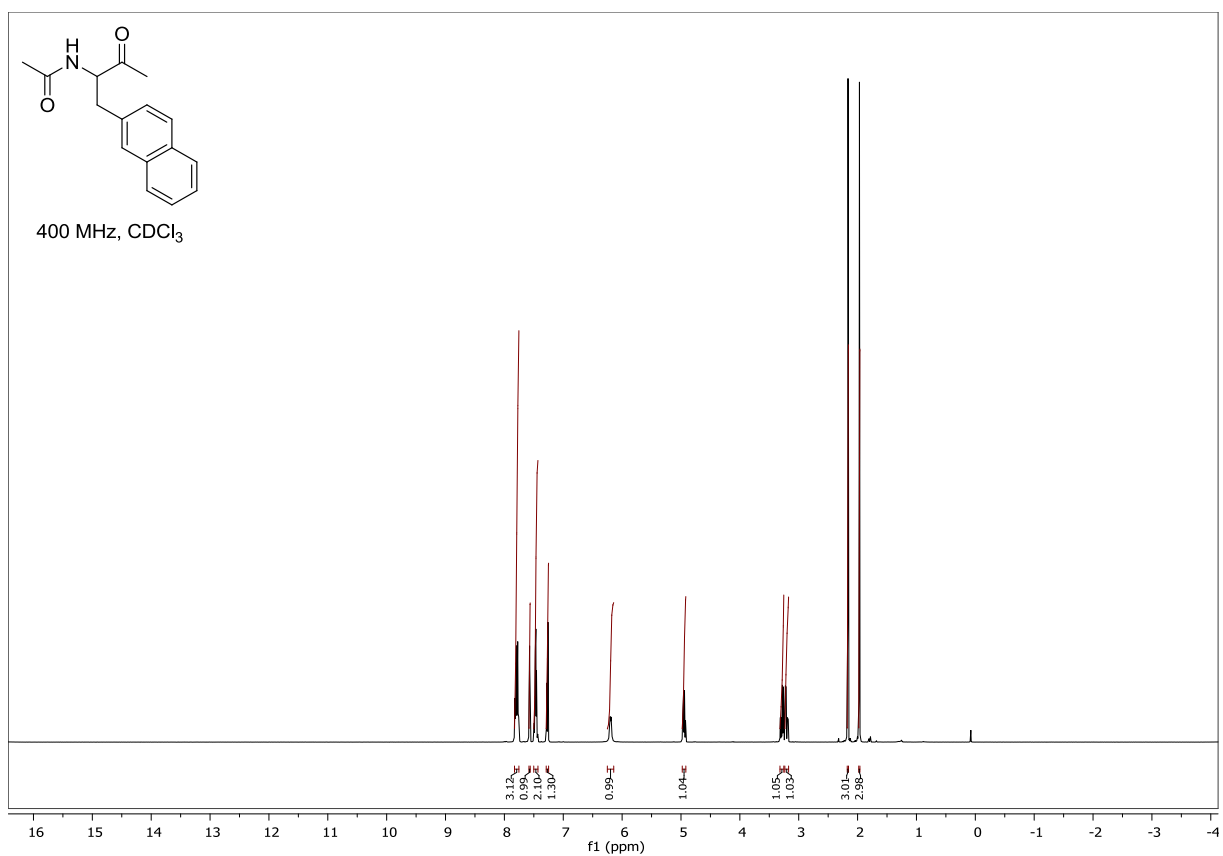
4-(2-acetamido-3-oxobutyl)phenyl acetate (10d)

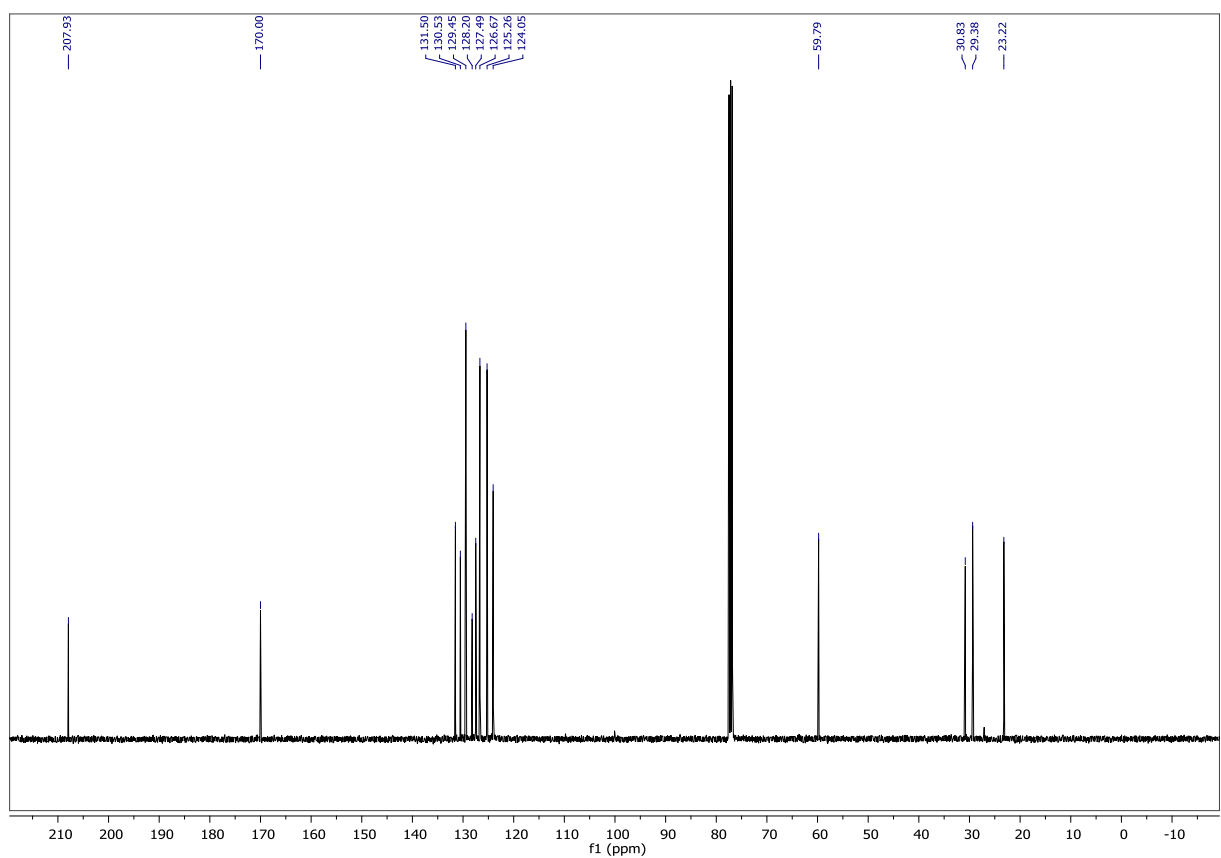
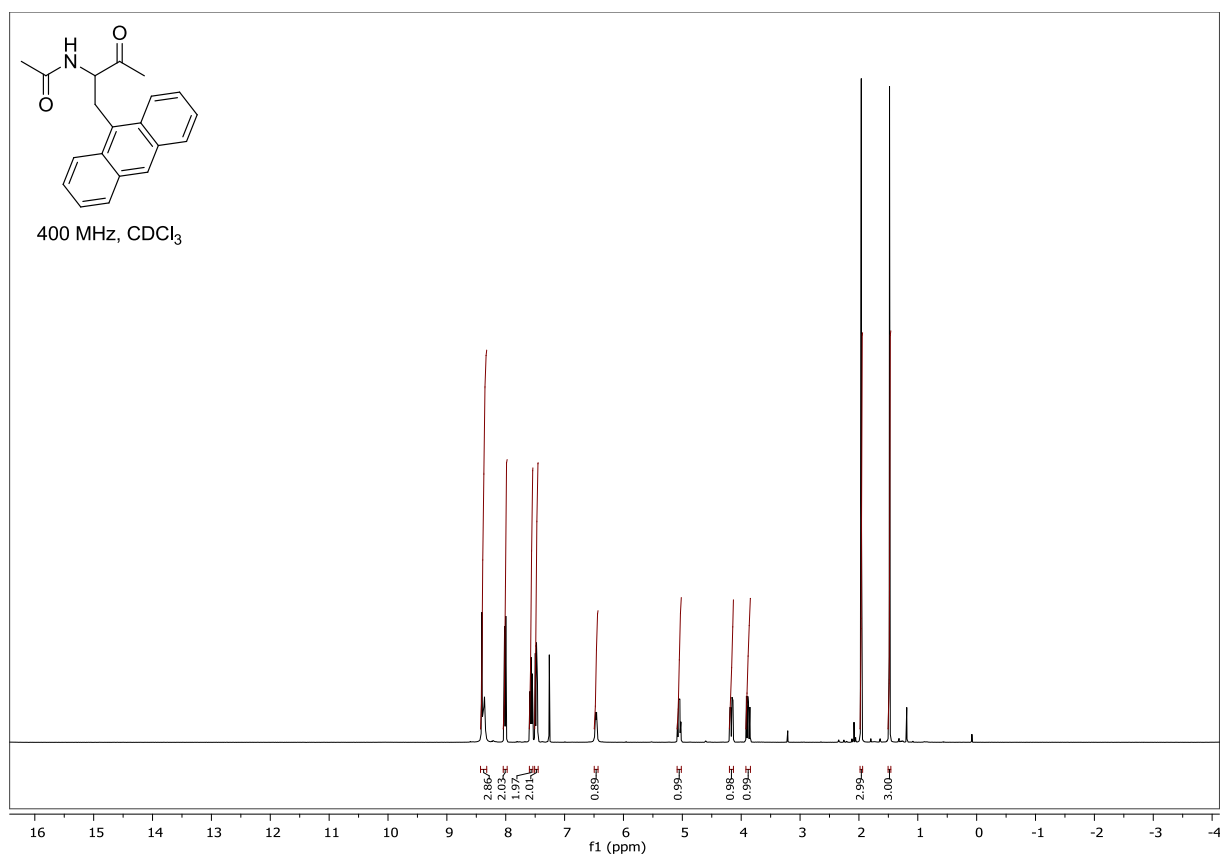
***N*-(1-(methylthio)-4-oxopentan-3-yl)acetamide (10e)**



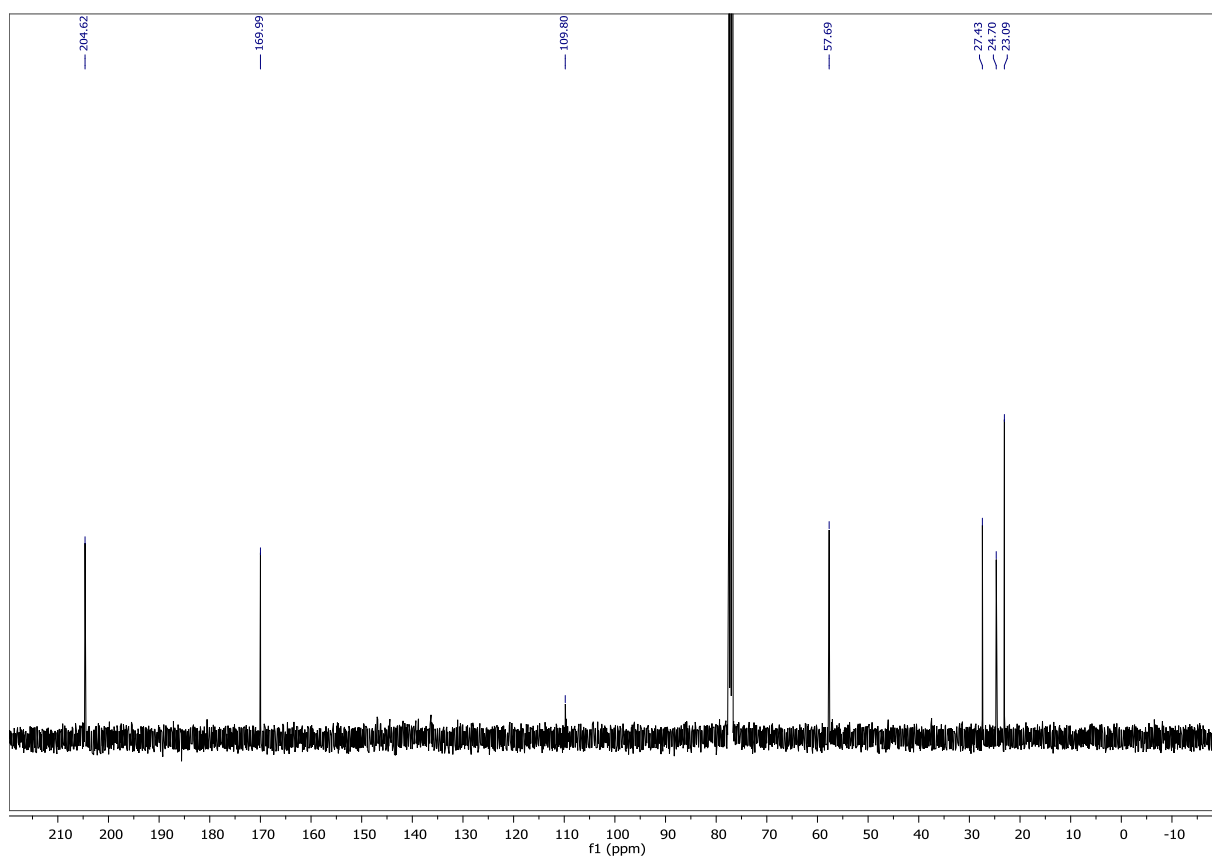
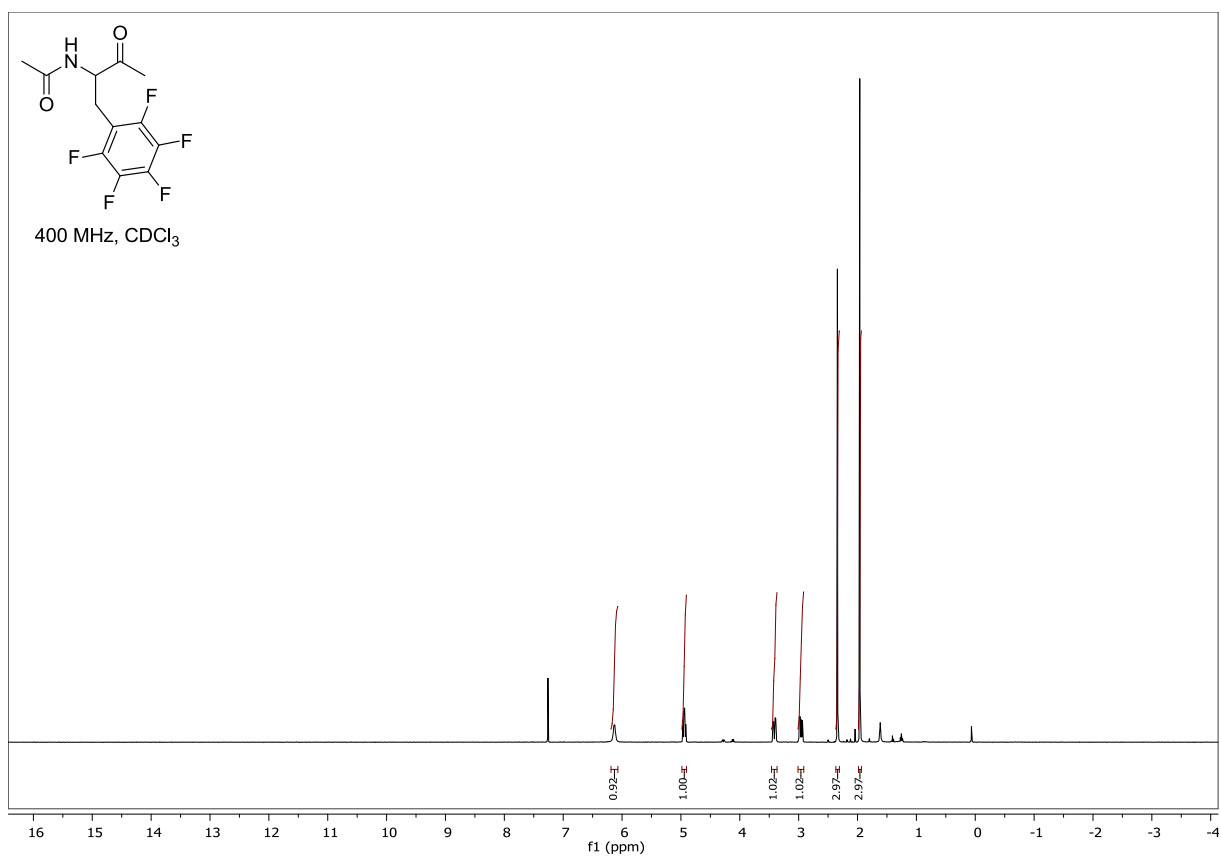
Benzyl 3-acetamido-4-oxopentanoate (10f)

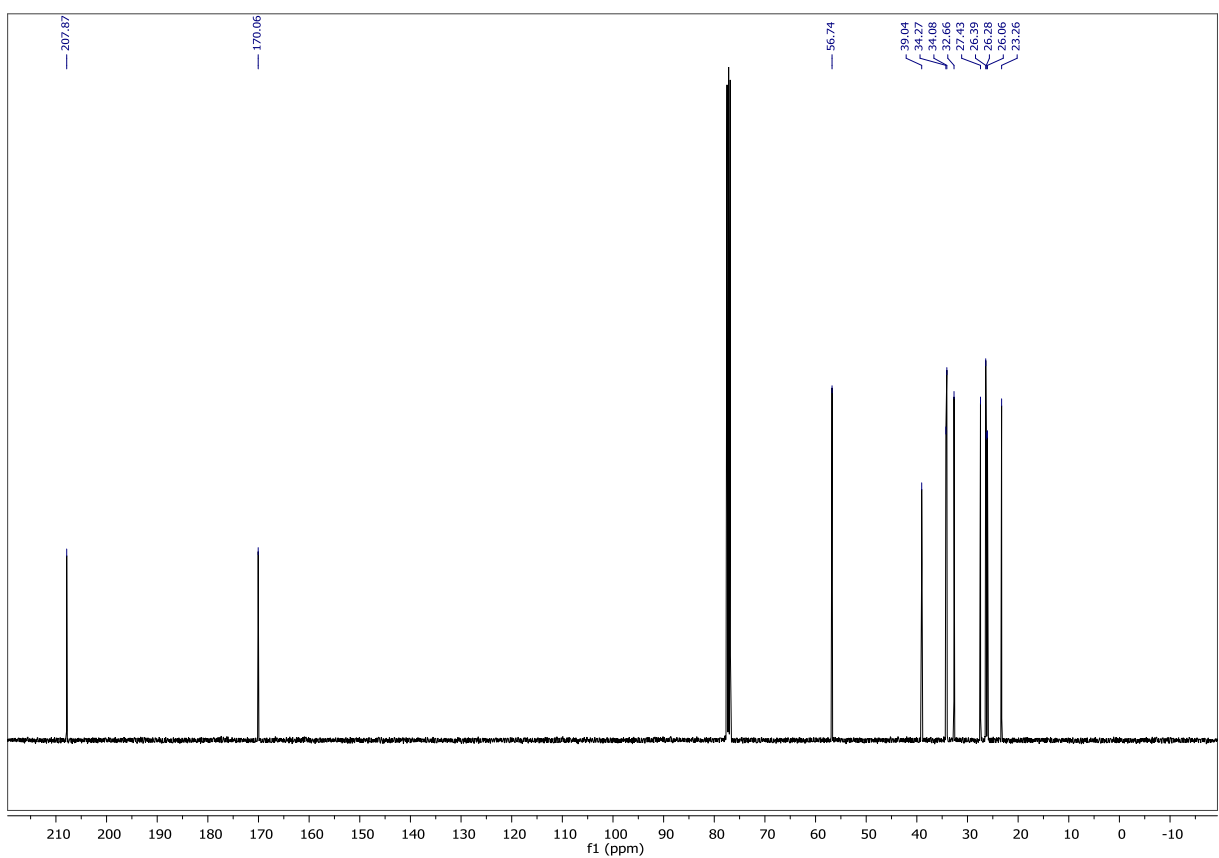
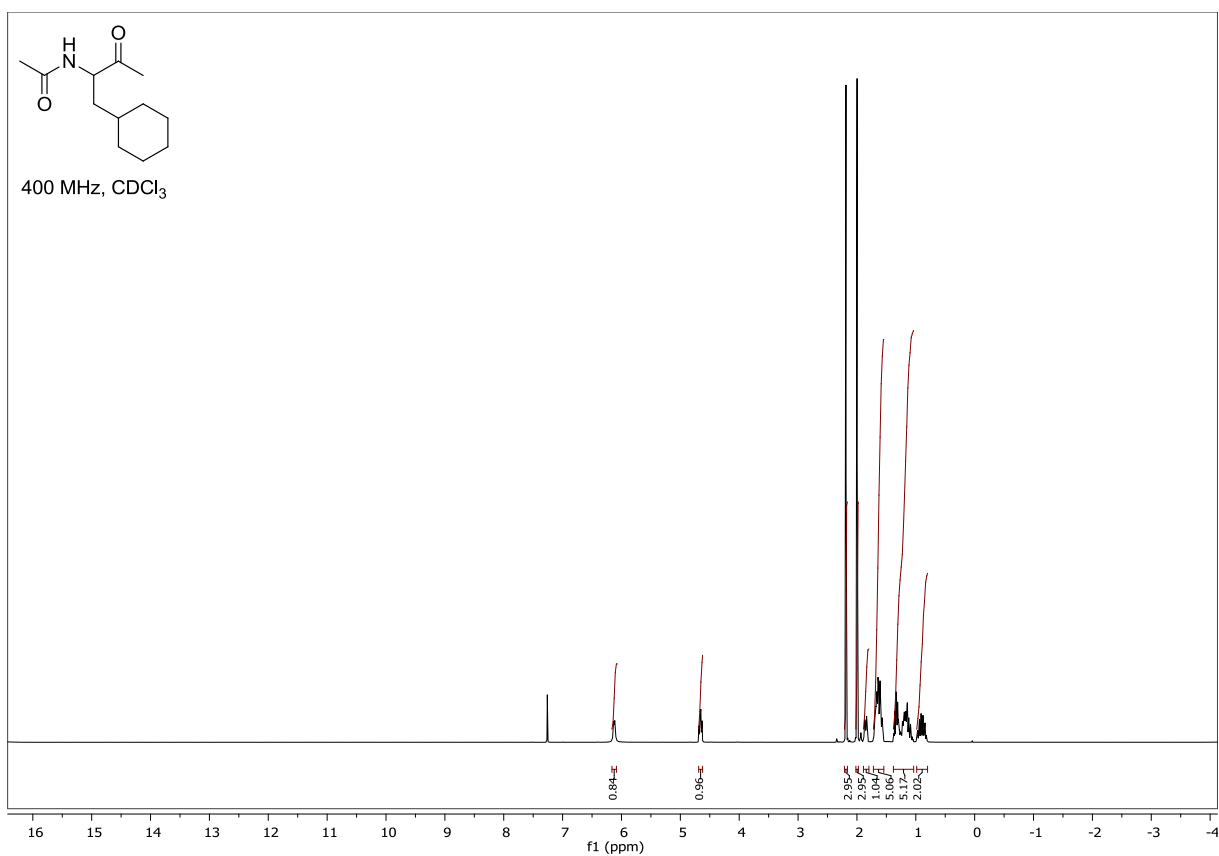
***N*-(1-(naphthalen-2-yl)-3-oxobutan-2-yl)acetamide (10g)**



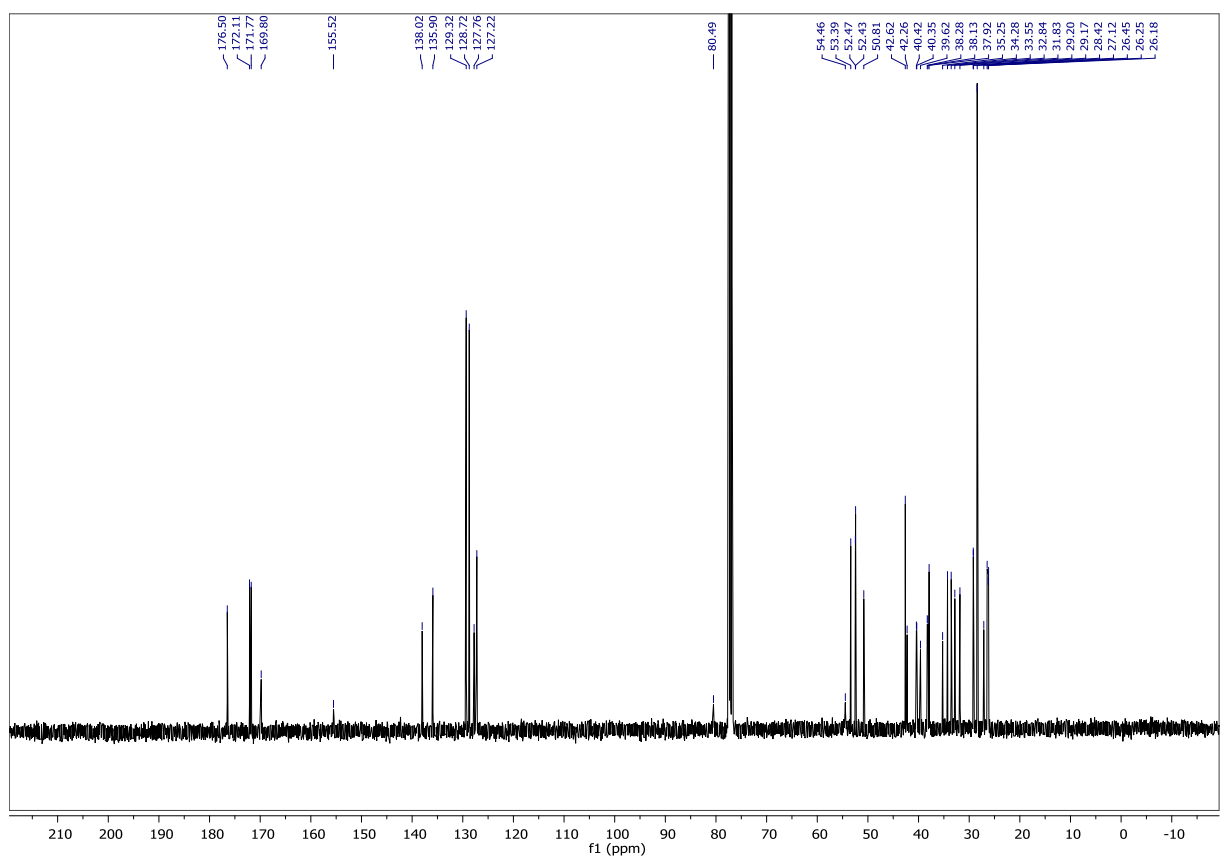
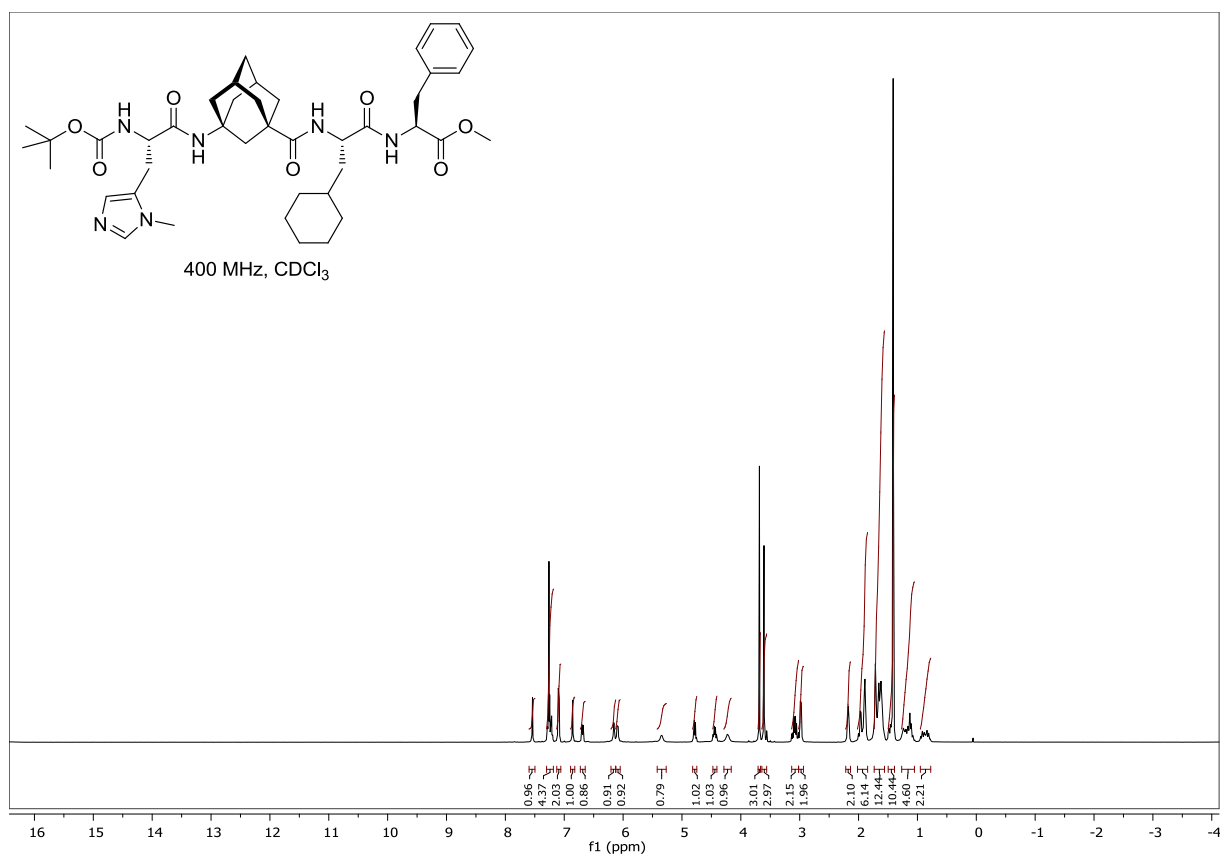
***N*-(1-(anthracen-9-yl)-3-oxobutan-2-yl)acetamide (10h)**

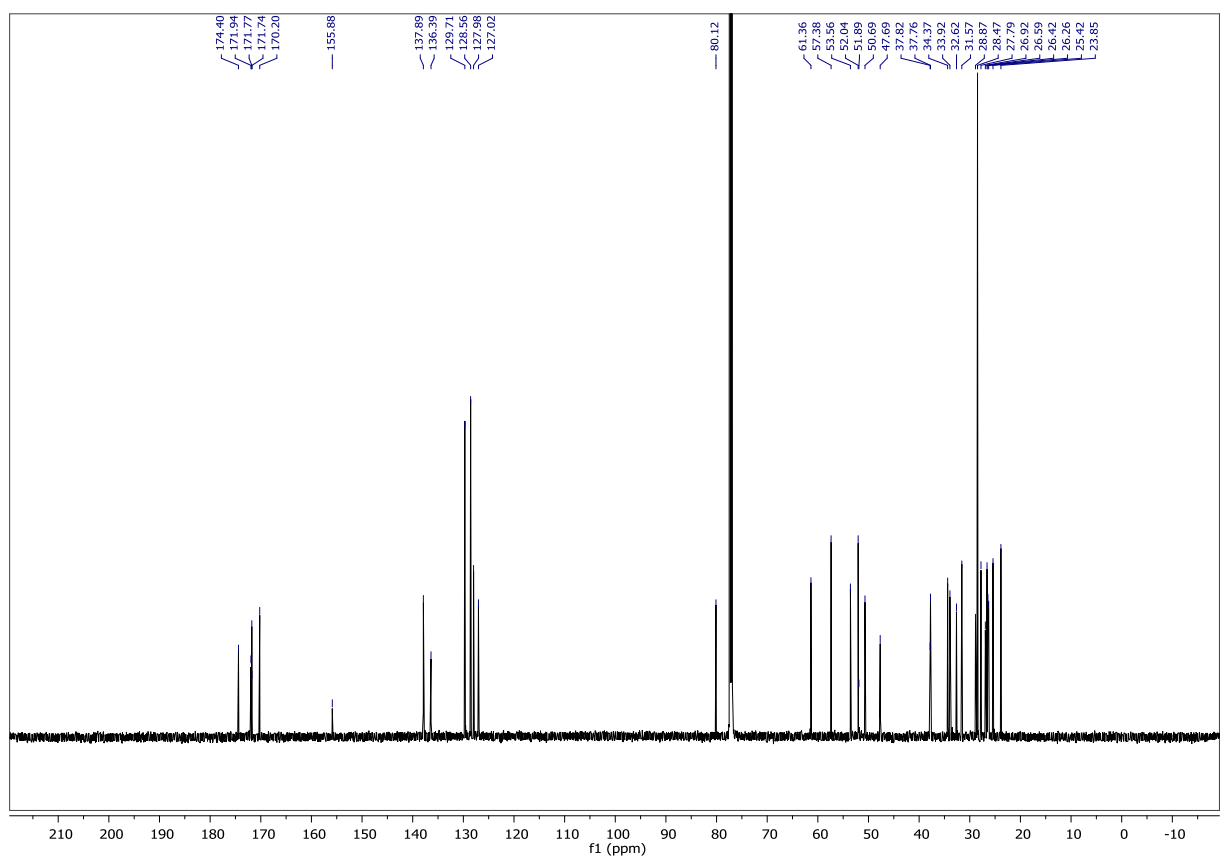
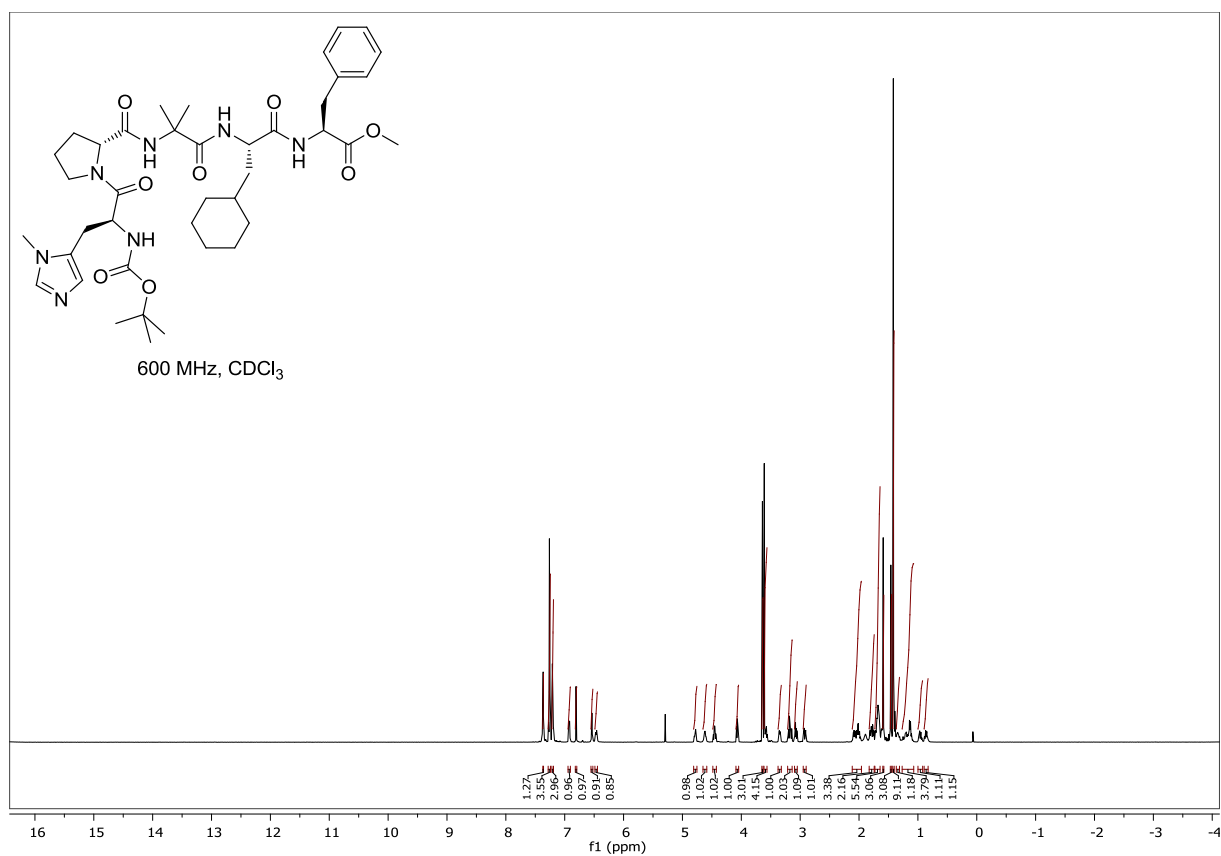
***N*-(3-oxo-1-(perfluorophenyl)butan-2-yl)acetamide (10i)**



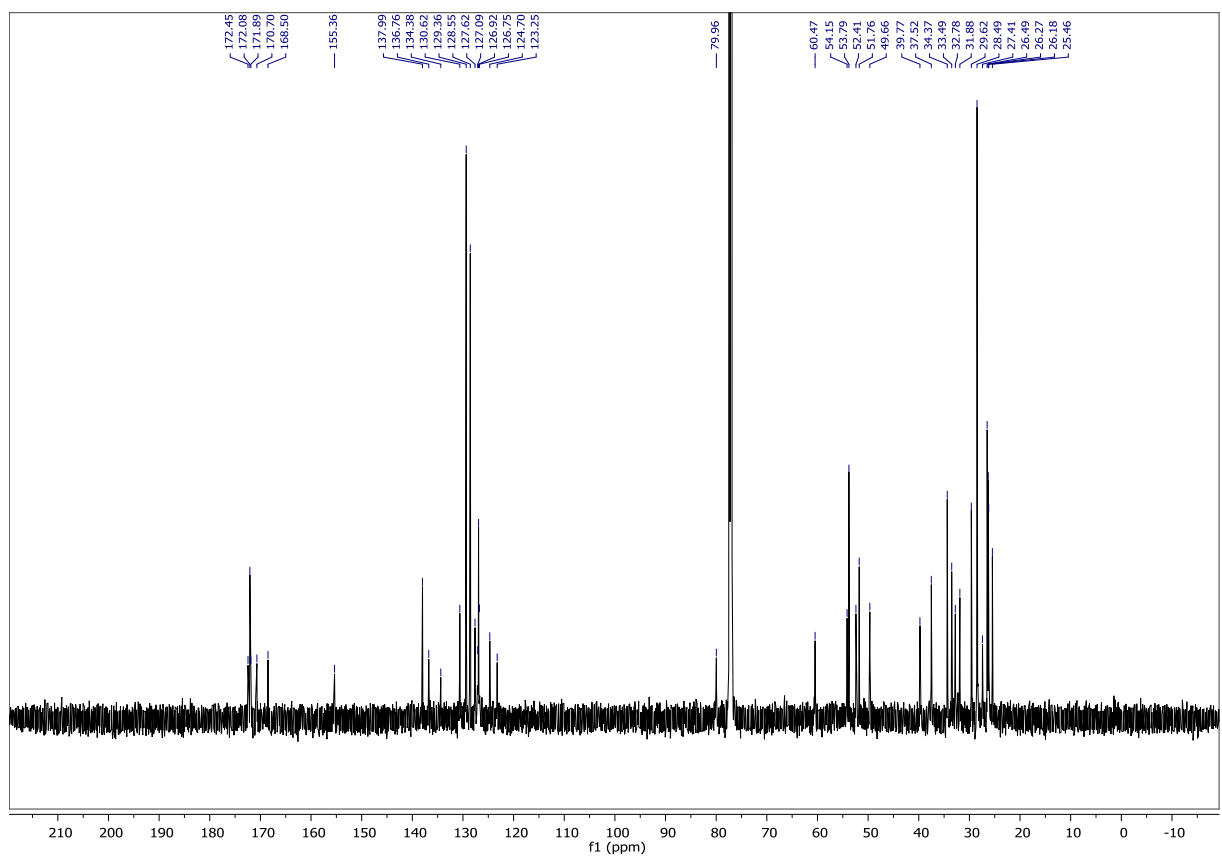
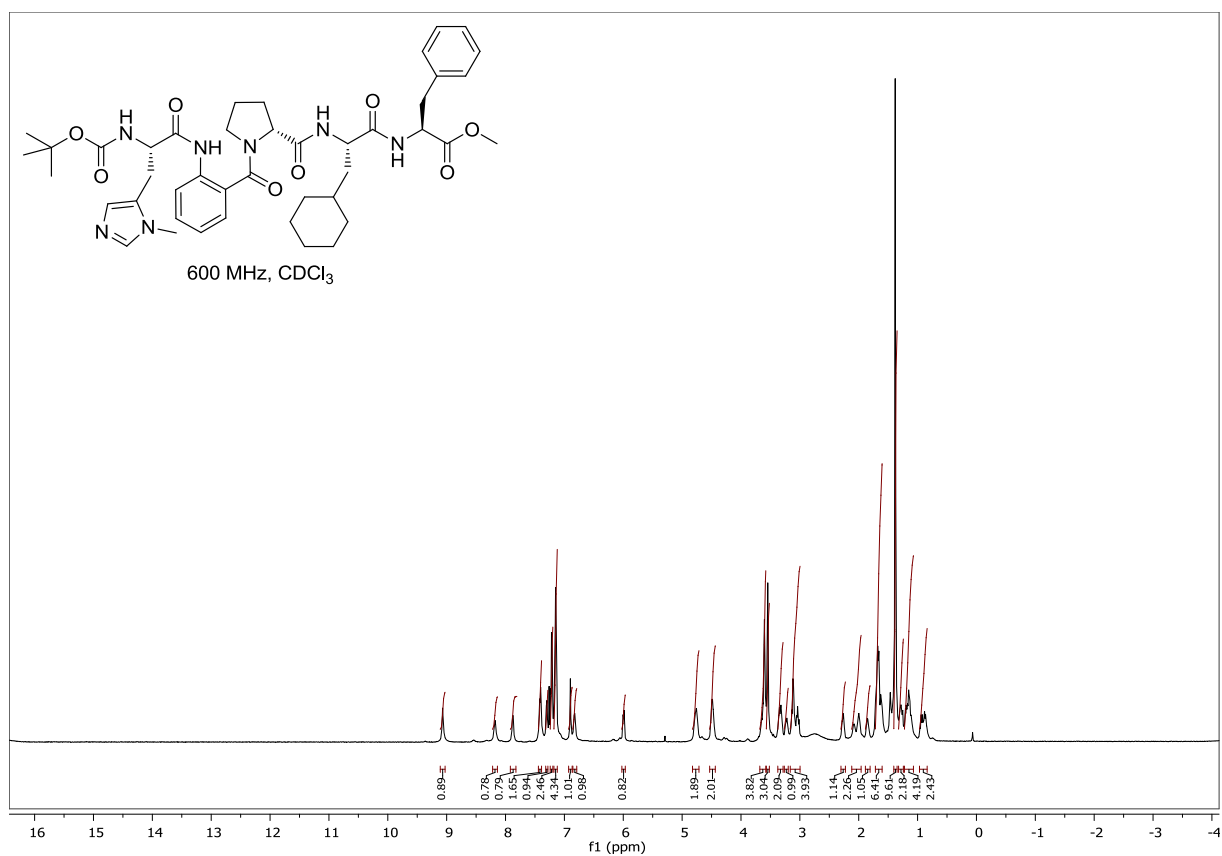
***N*-(1-cyclohexyl-3-oxobutan-2-yl)acetamide (10j)**

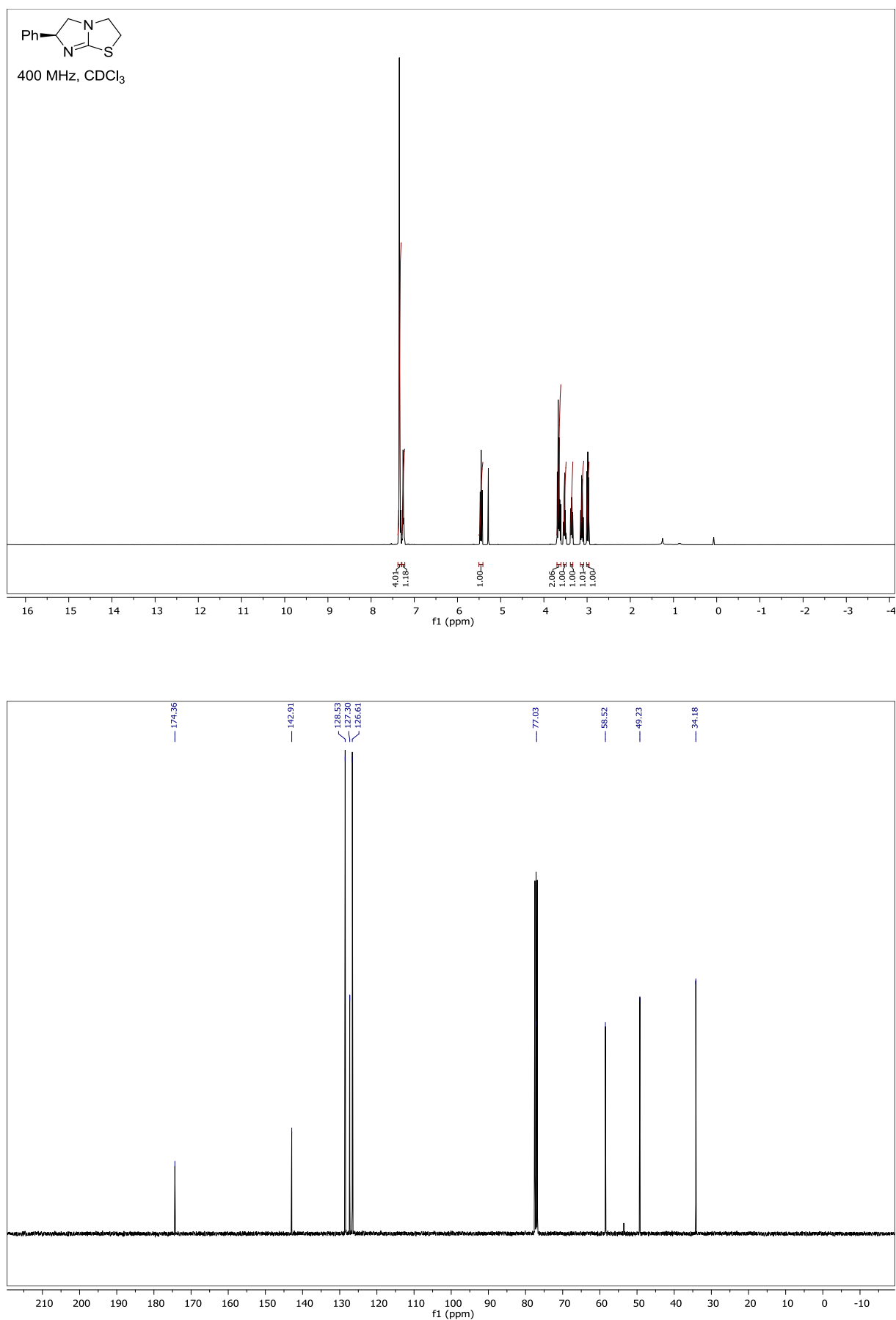
Boc-L-Pmh-^AGly-L-Cha-L-Phe-OMe (11)



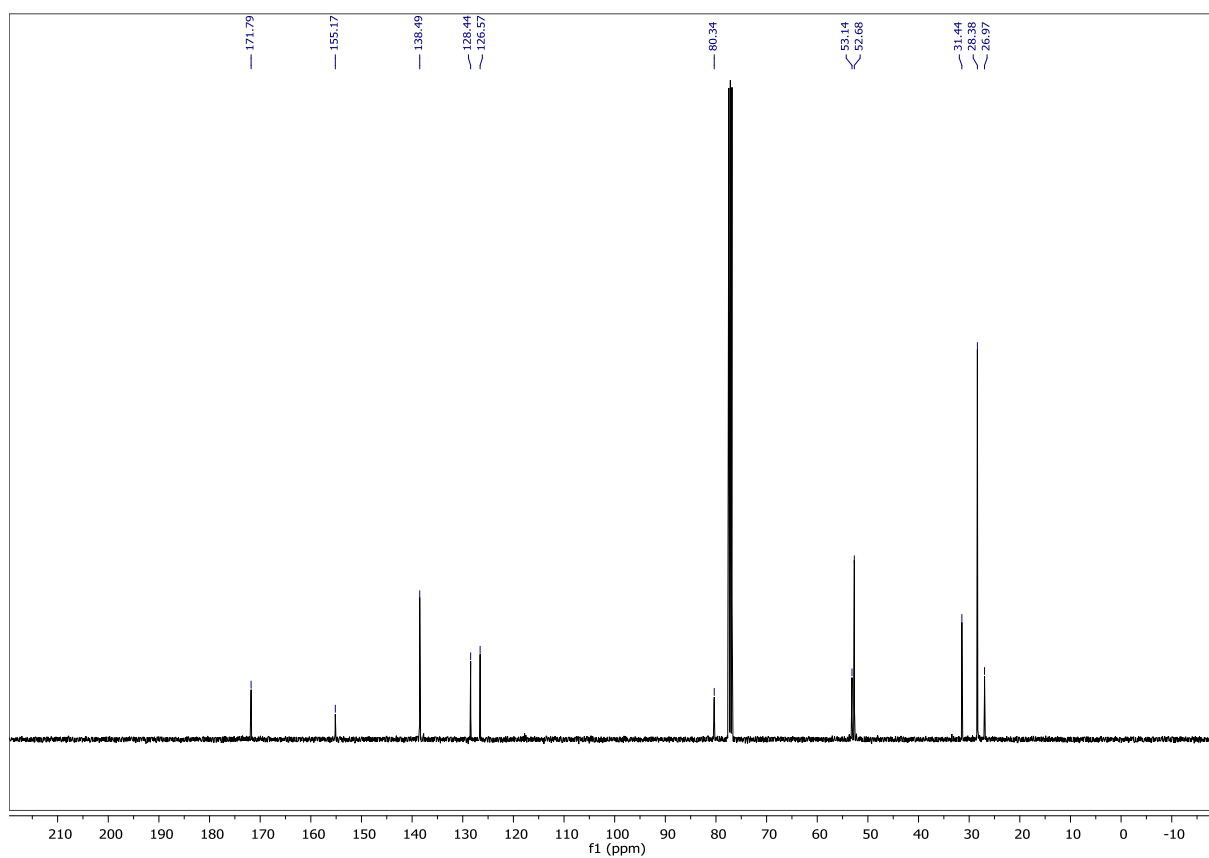
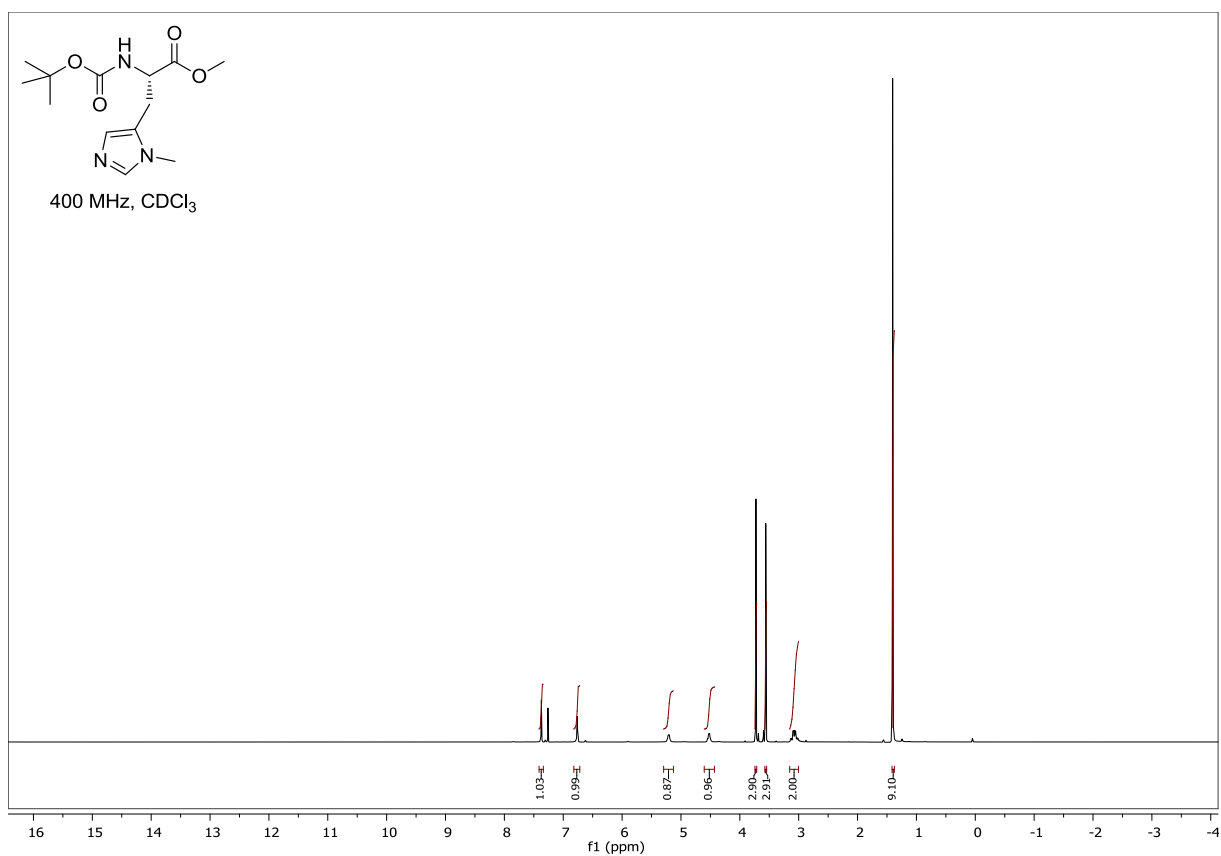
Boc-L-Pmh-D-Pro-Aib-L-Cha-L-Phe-OMe (12)

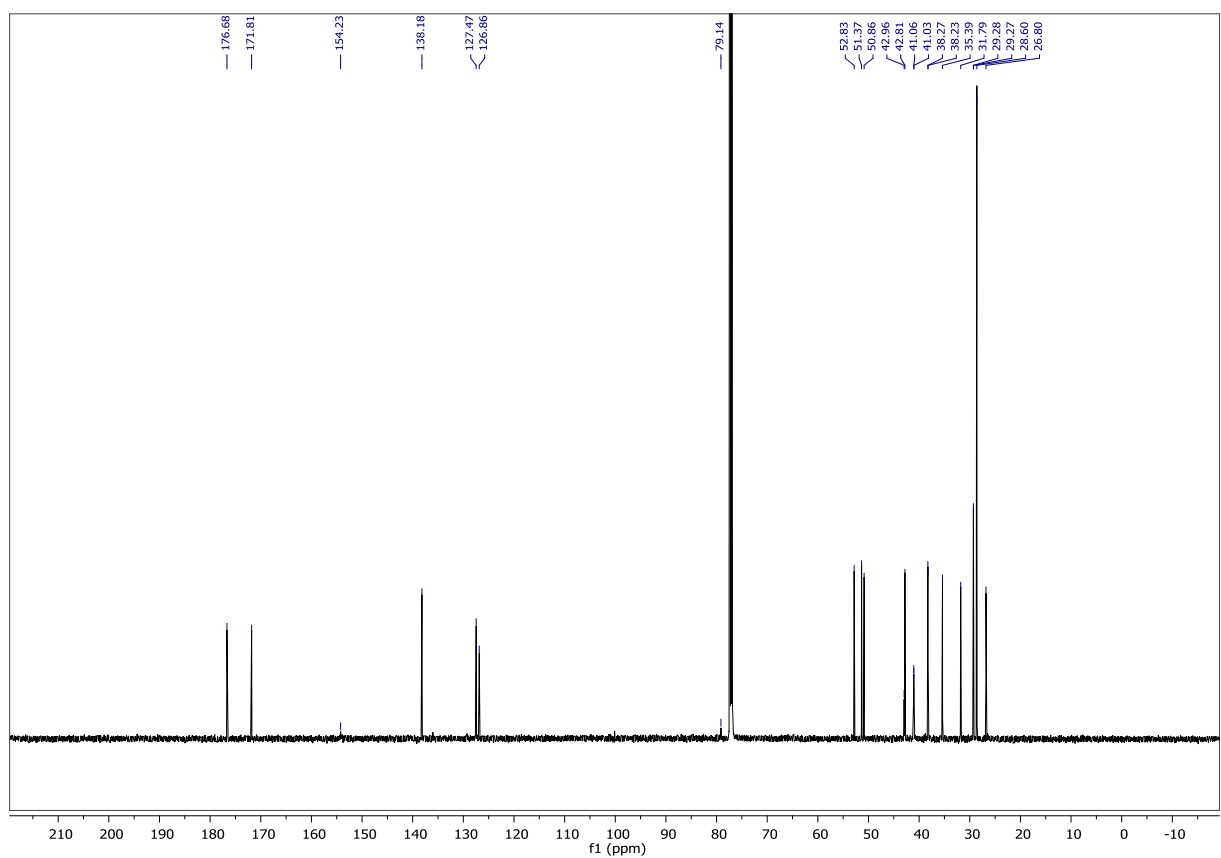
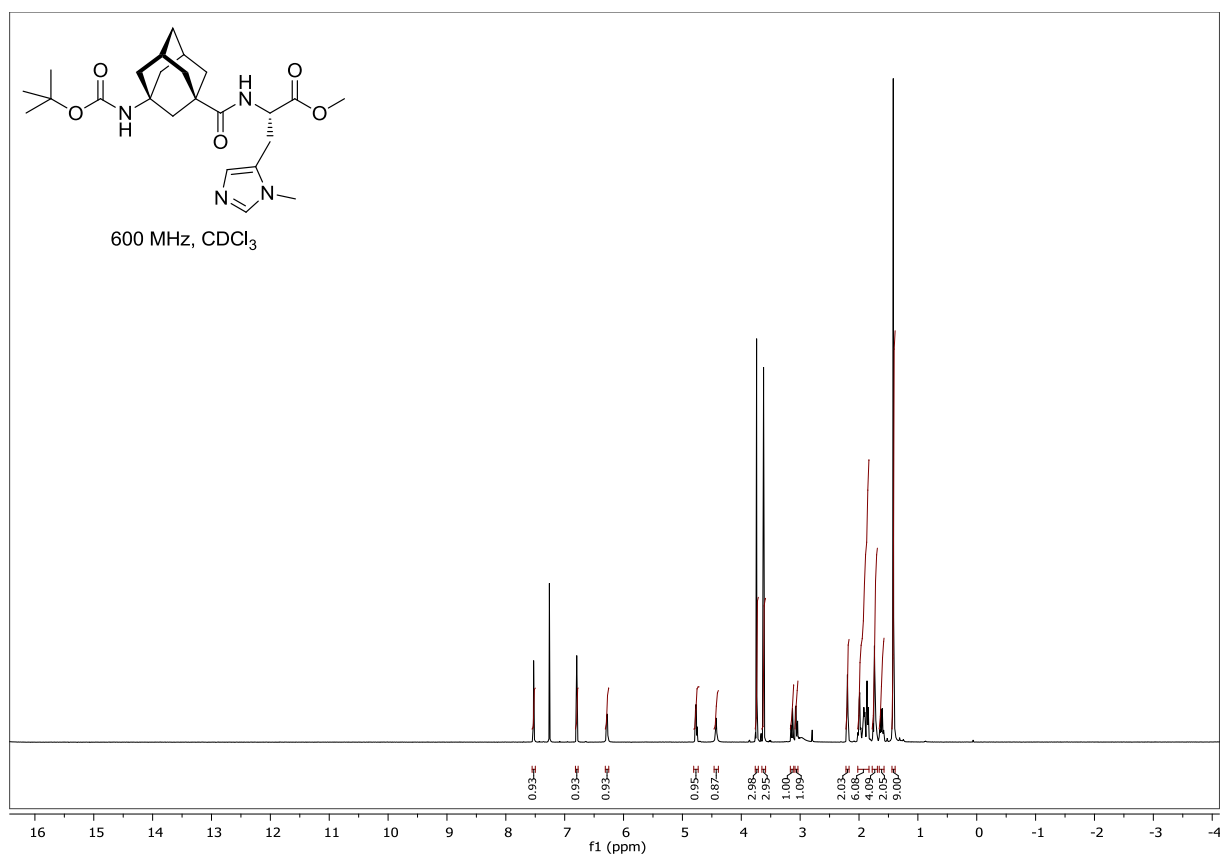
Boc-L-Pmh-2-Abz-D-Pro-L-Cha-L-Phe-OMe (13)



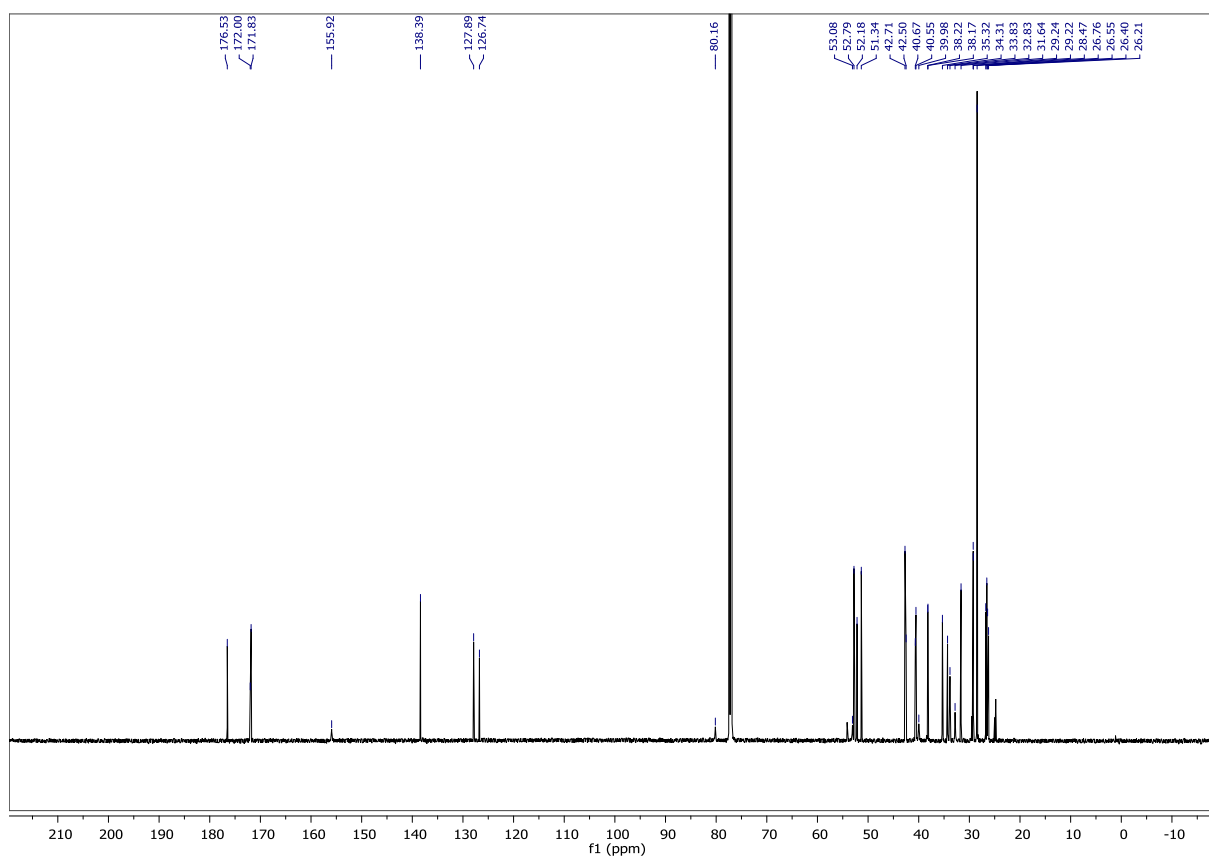
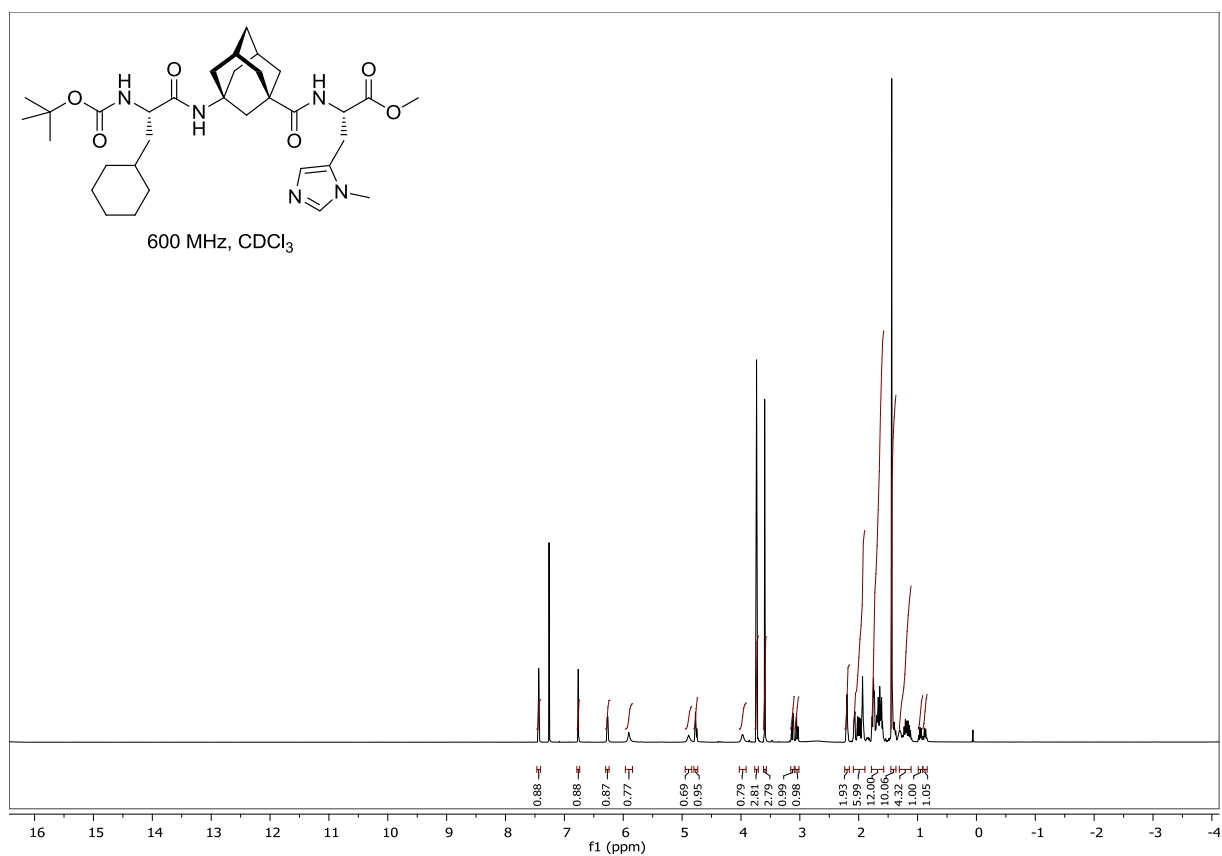
(S)-Tetramisol (14)

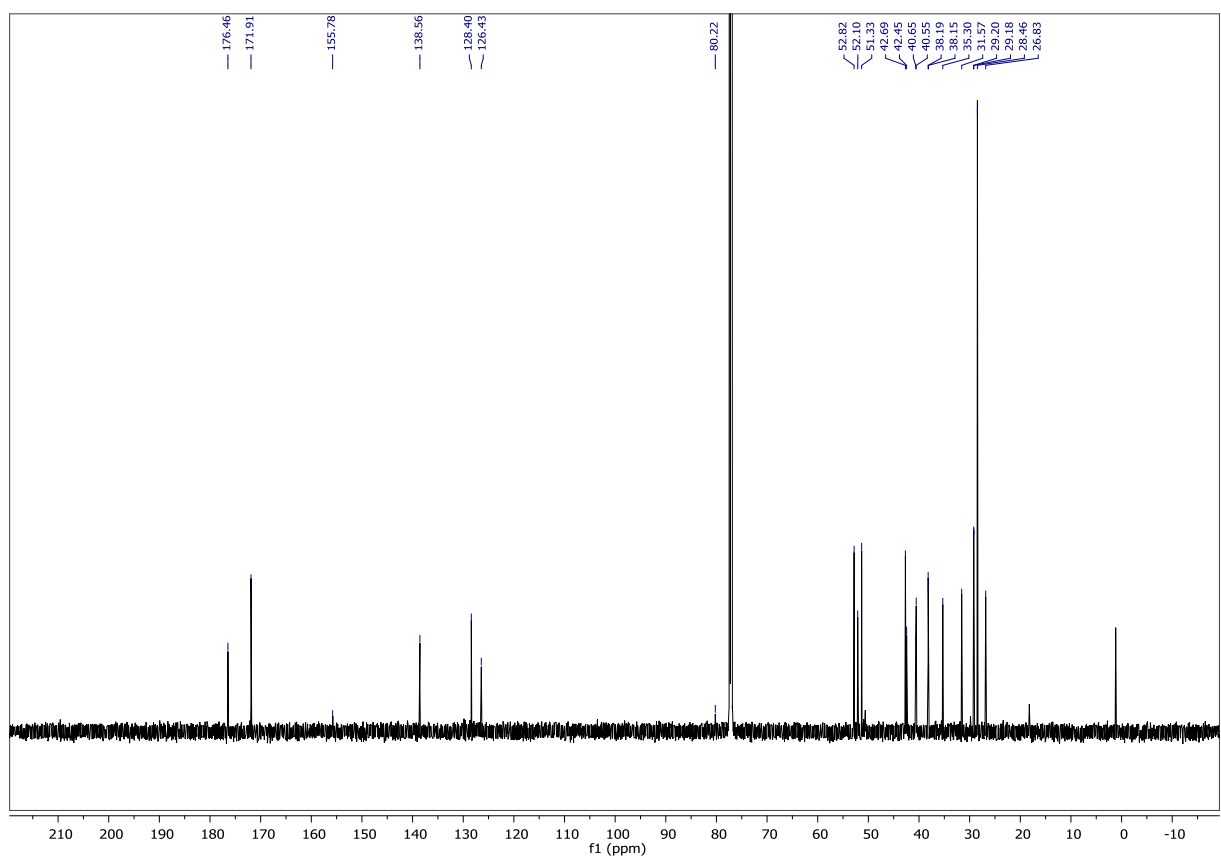
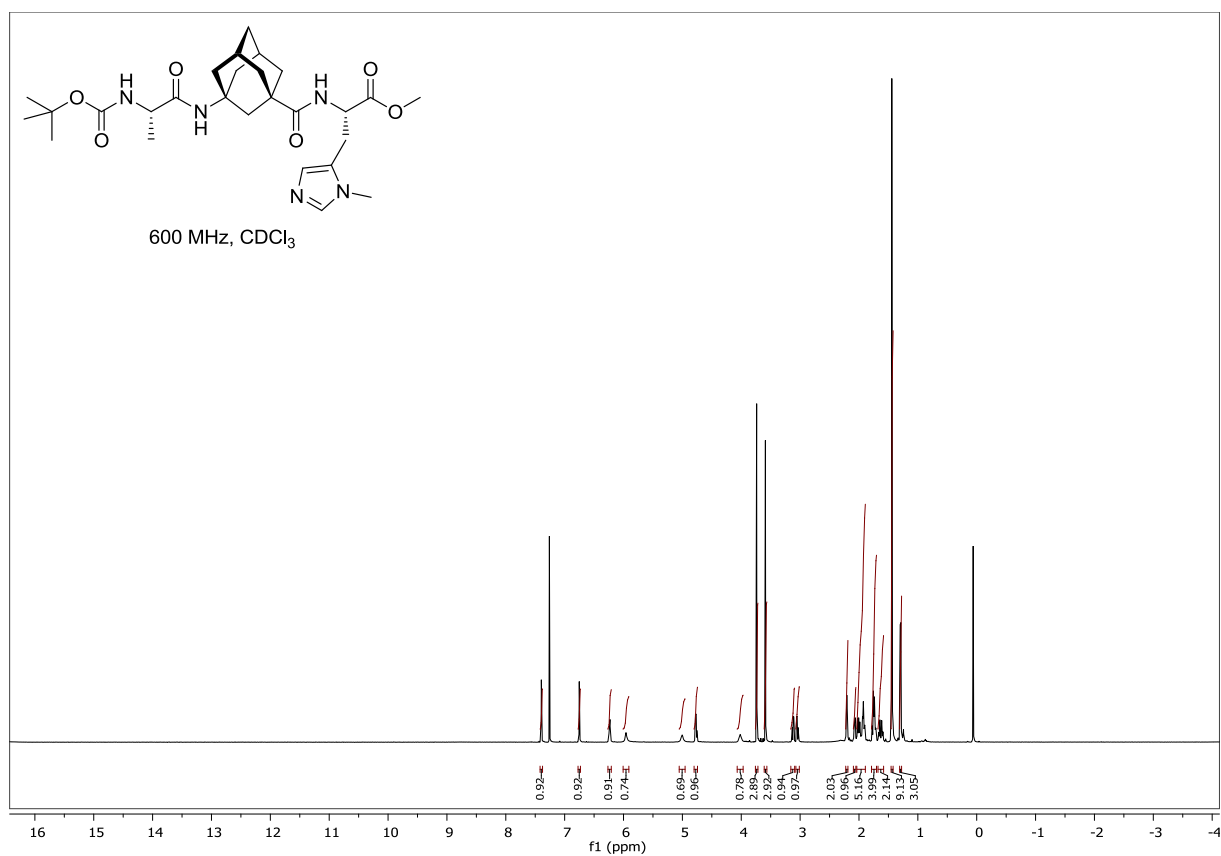
Boc-L-Pmh-OMe (16)



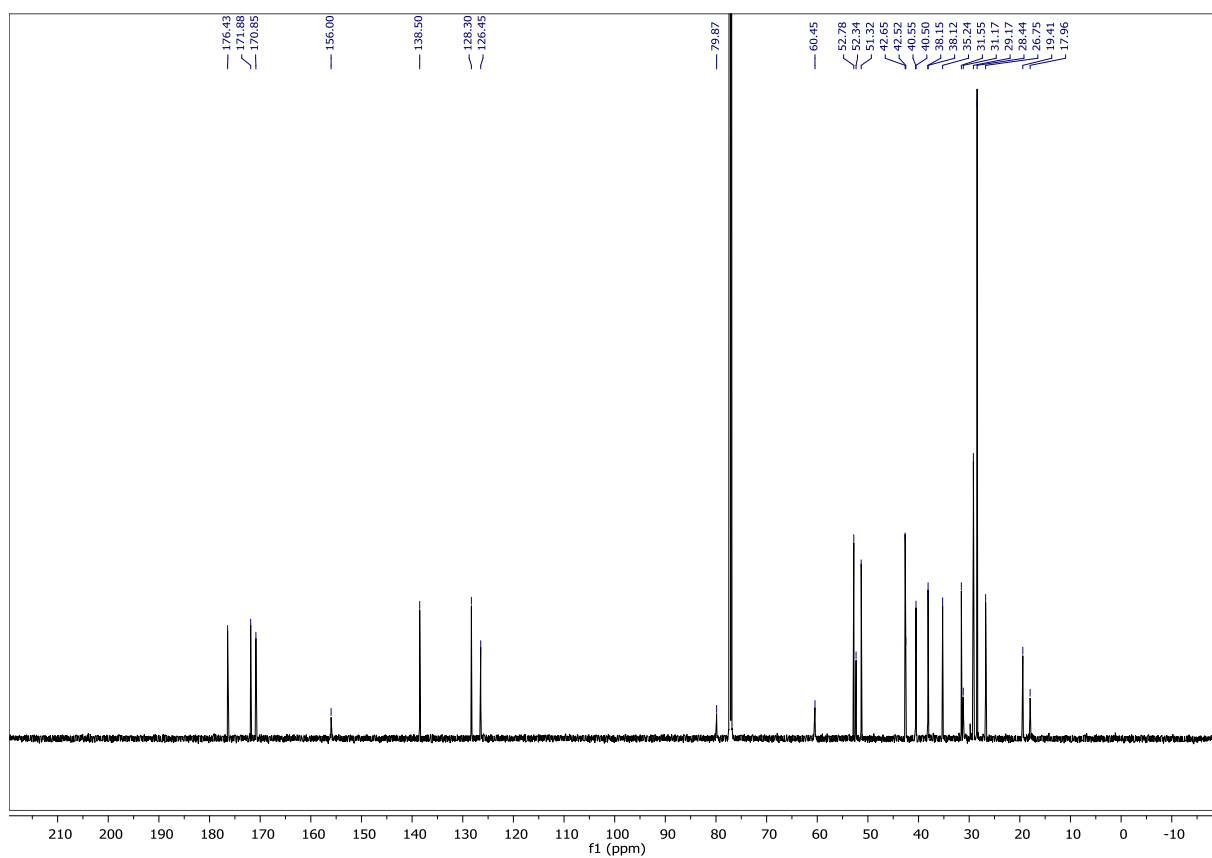
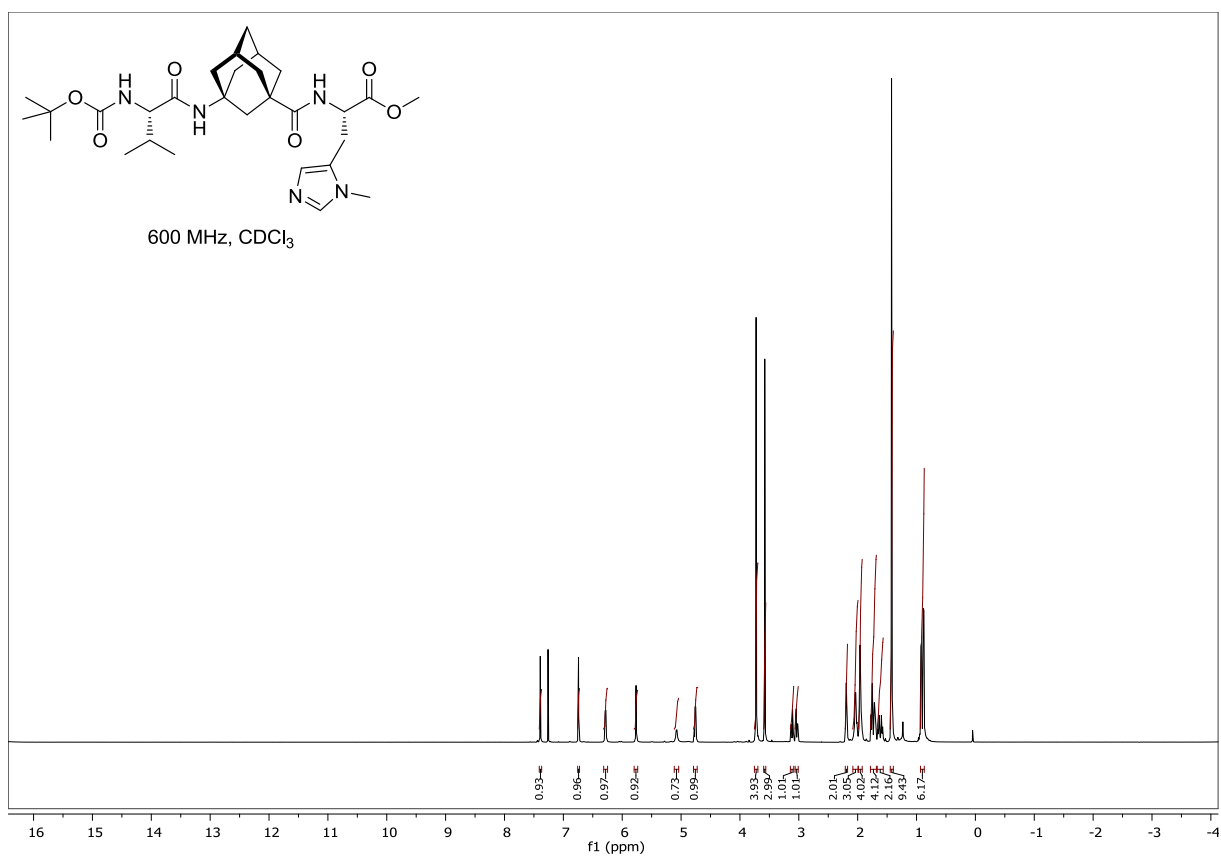
Boc-^AGly-L-Pmh-OMe (17)

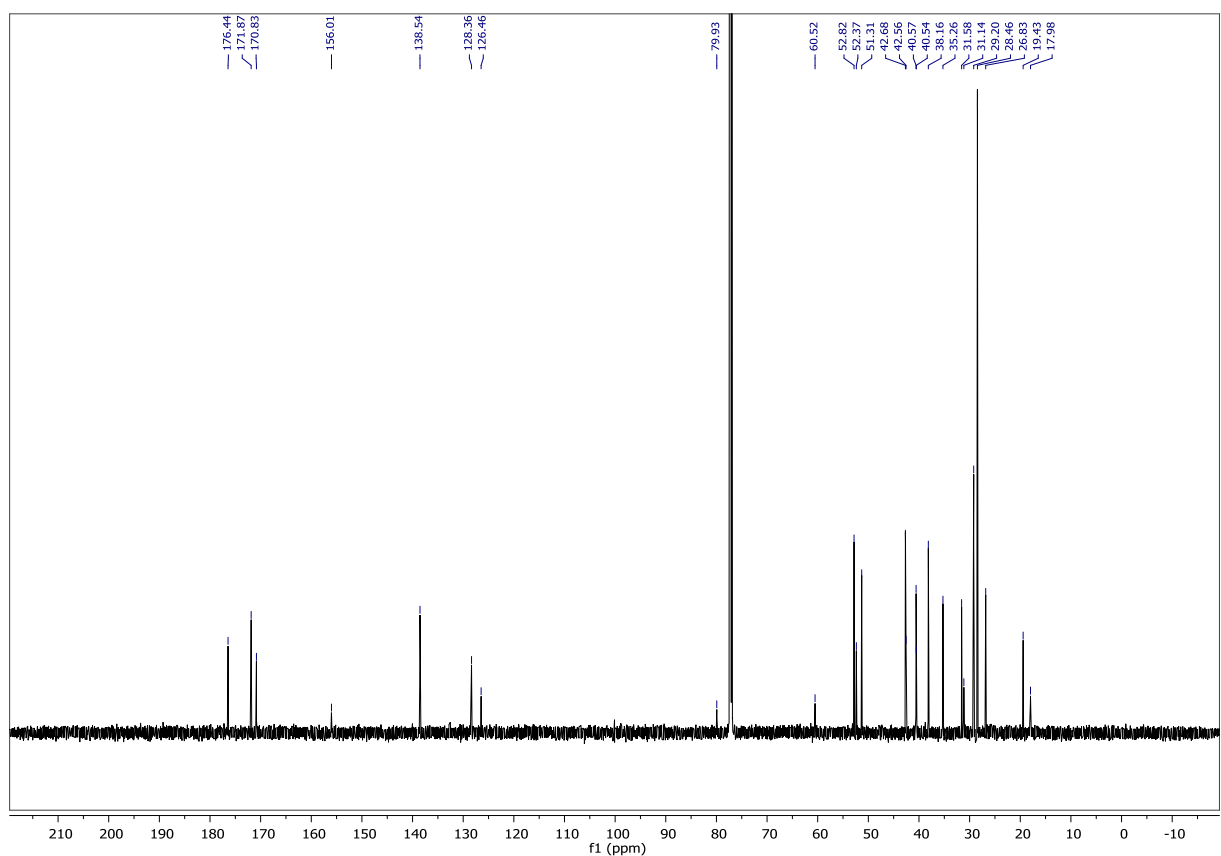
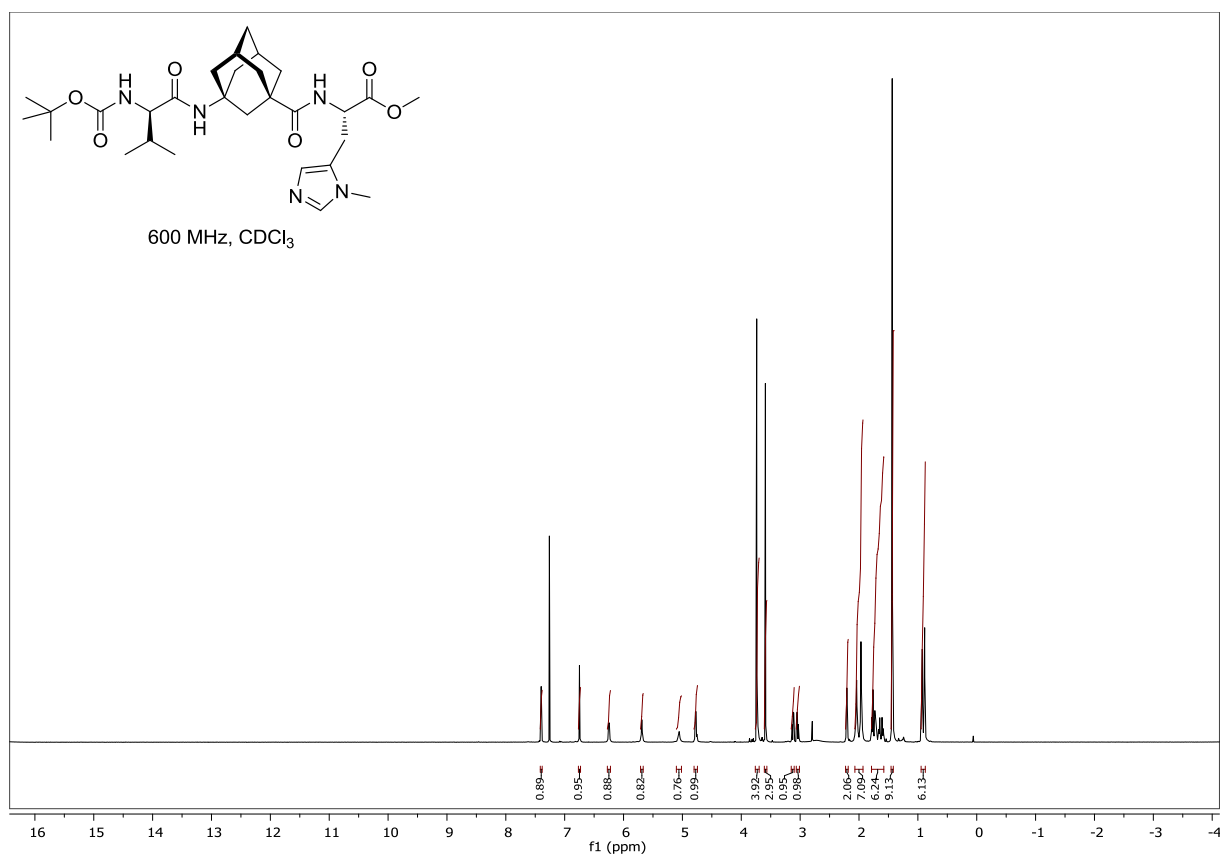
Boc-L-Cha-^AGly-L-Pmh-OMe (18)



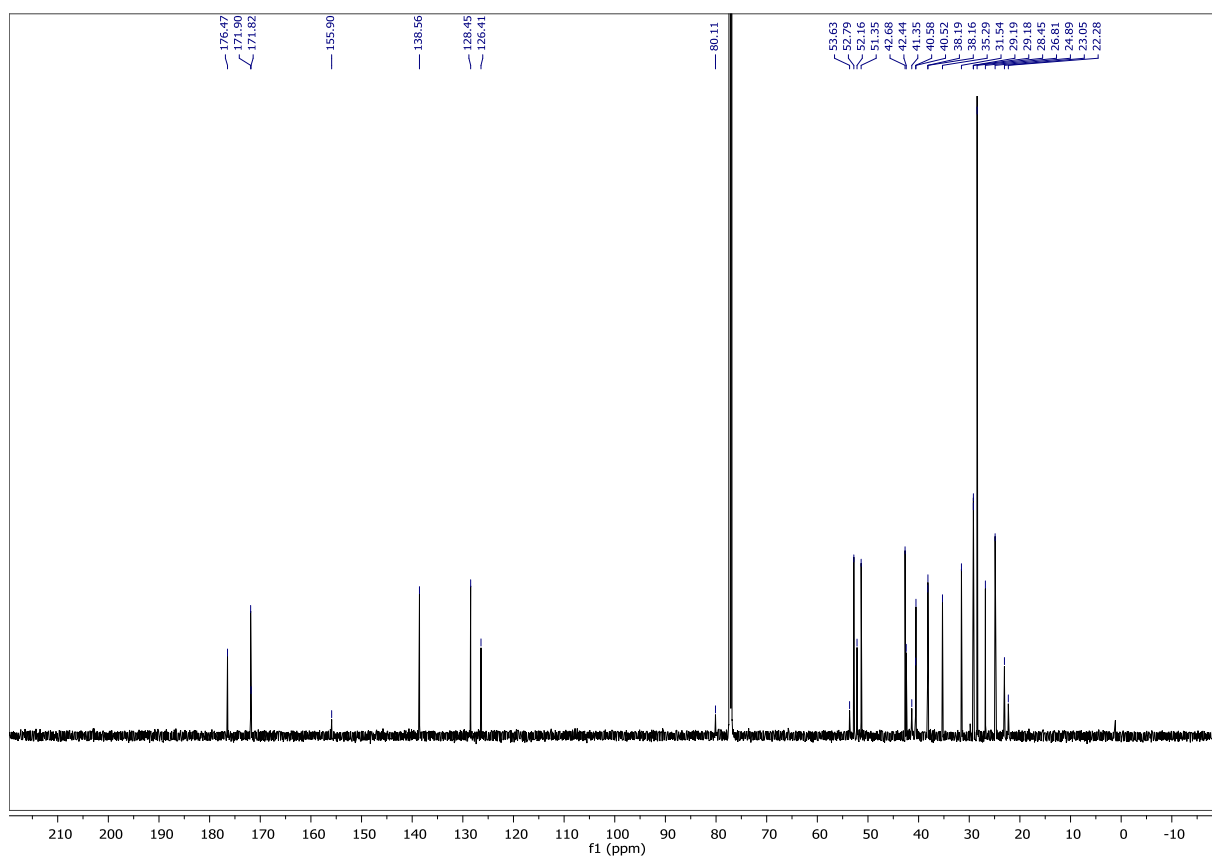
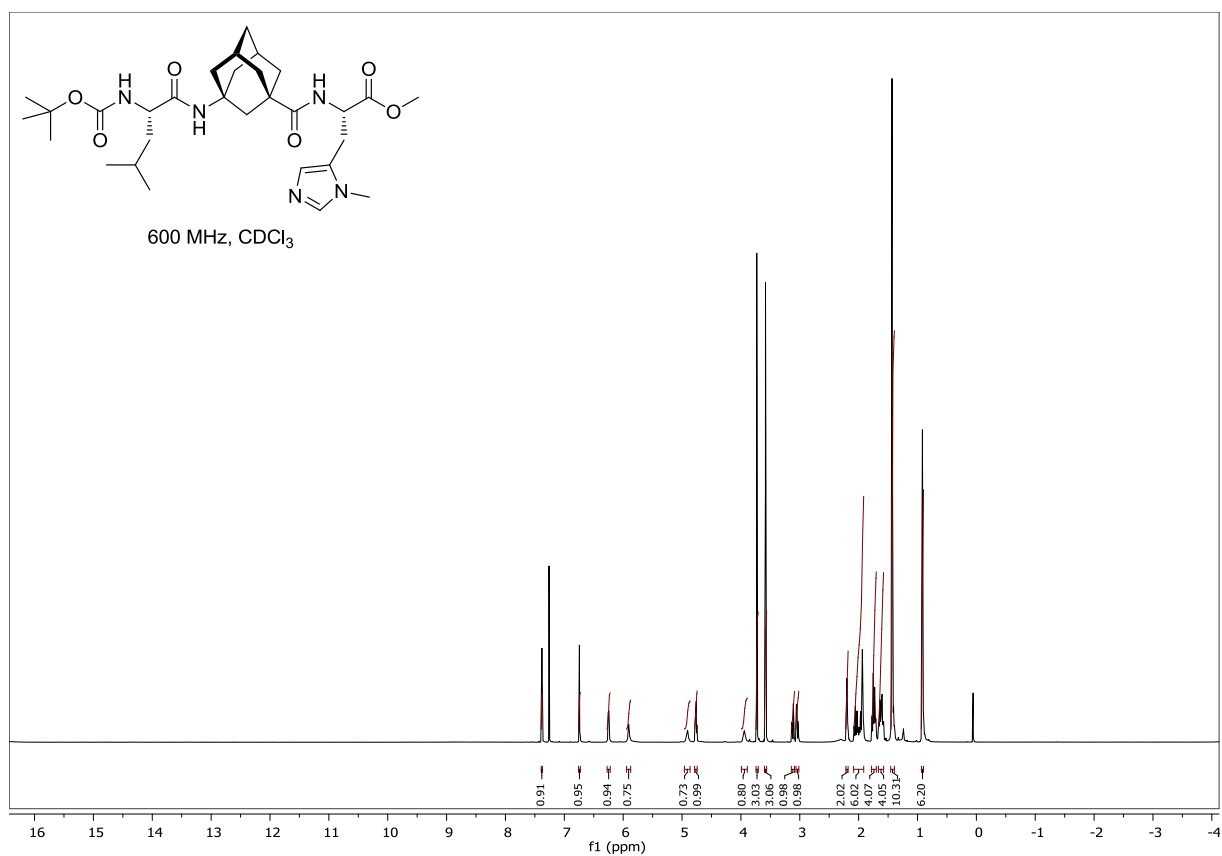
Boc-L-Ala-^AGly-Pmh-OMe (S7)

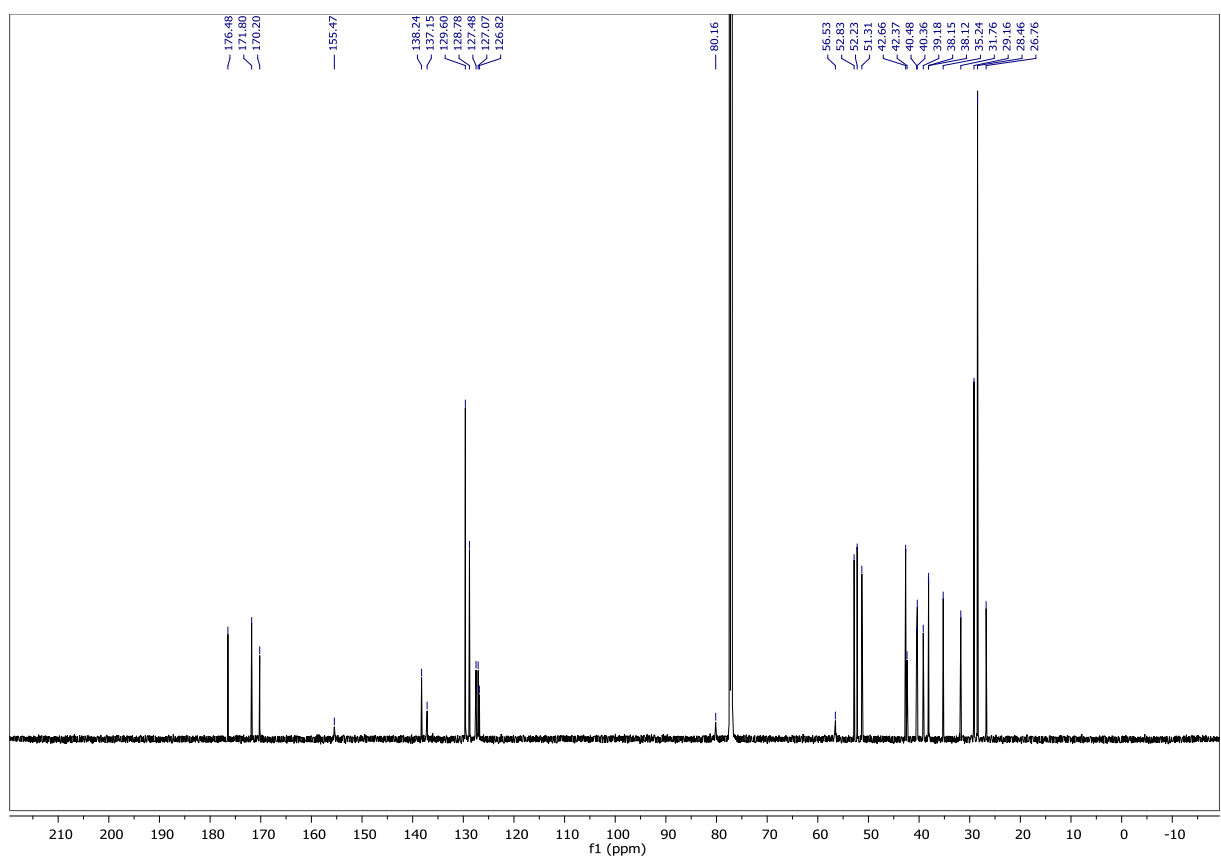
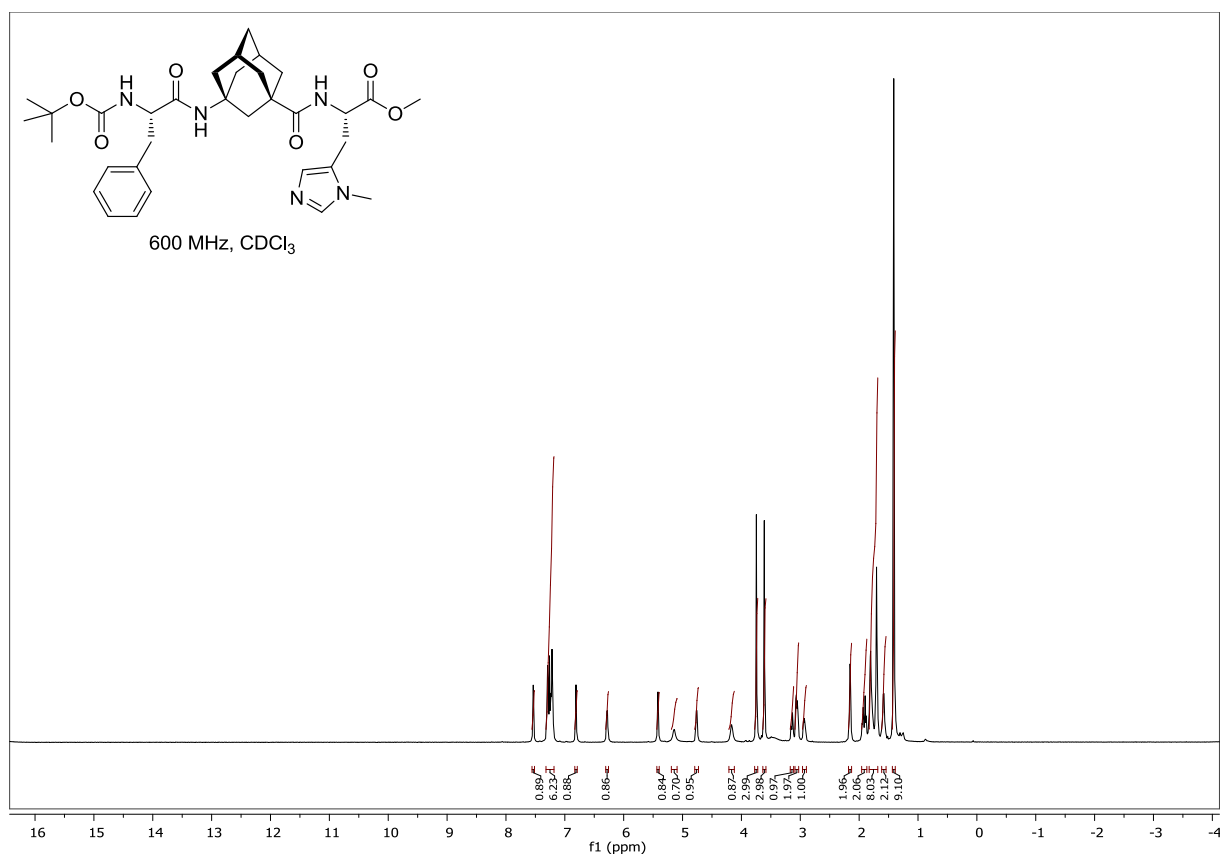
Boc-L-Val-^AGly-L-Pmh-OMe (S8)



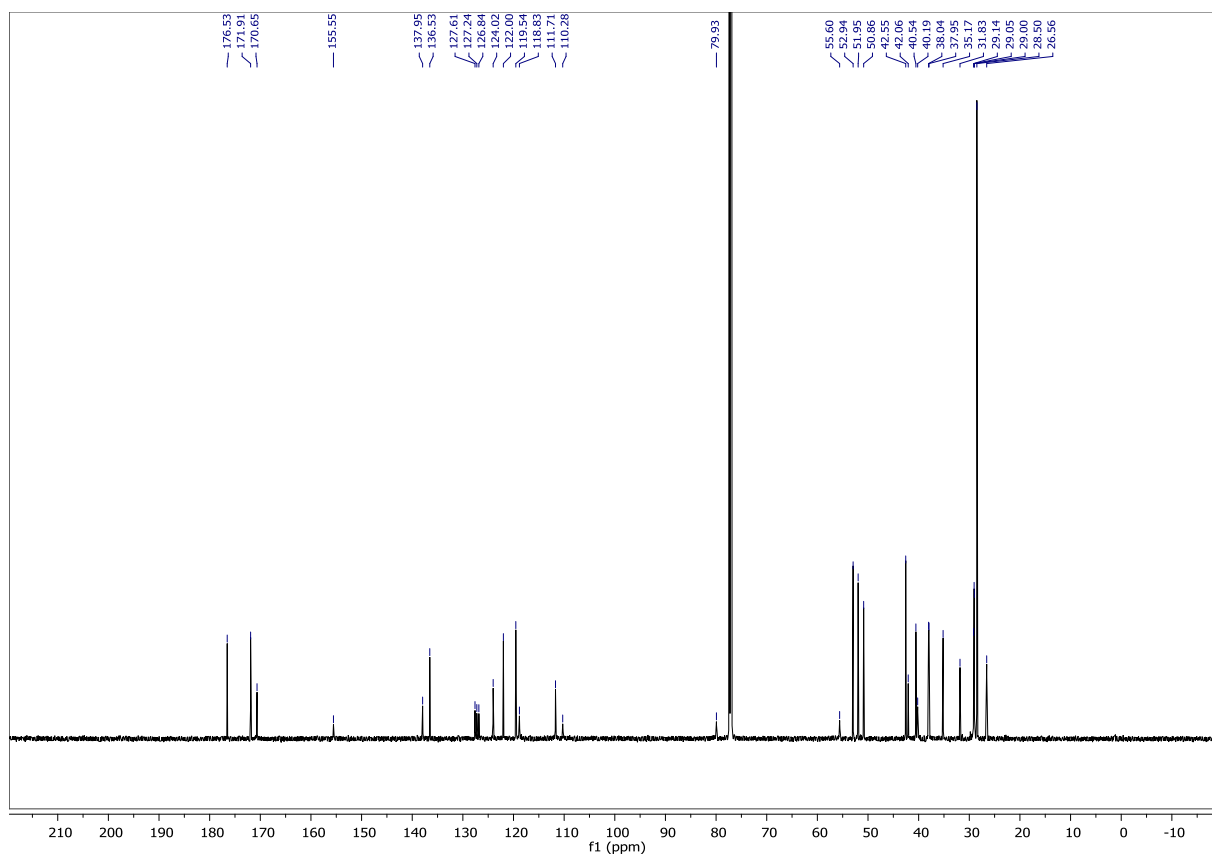
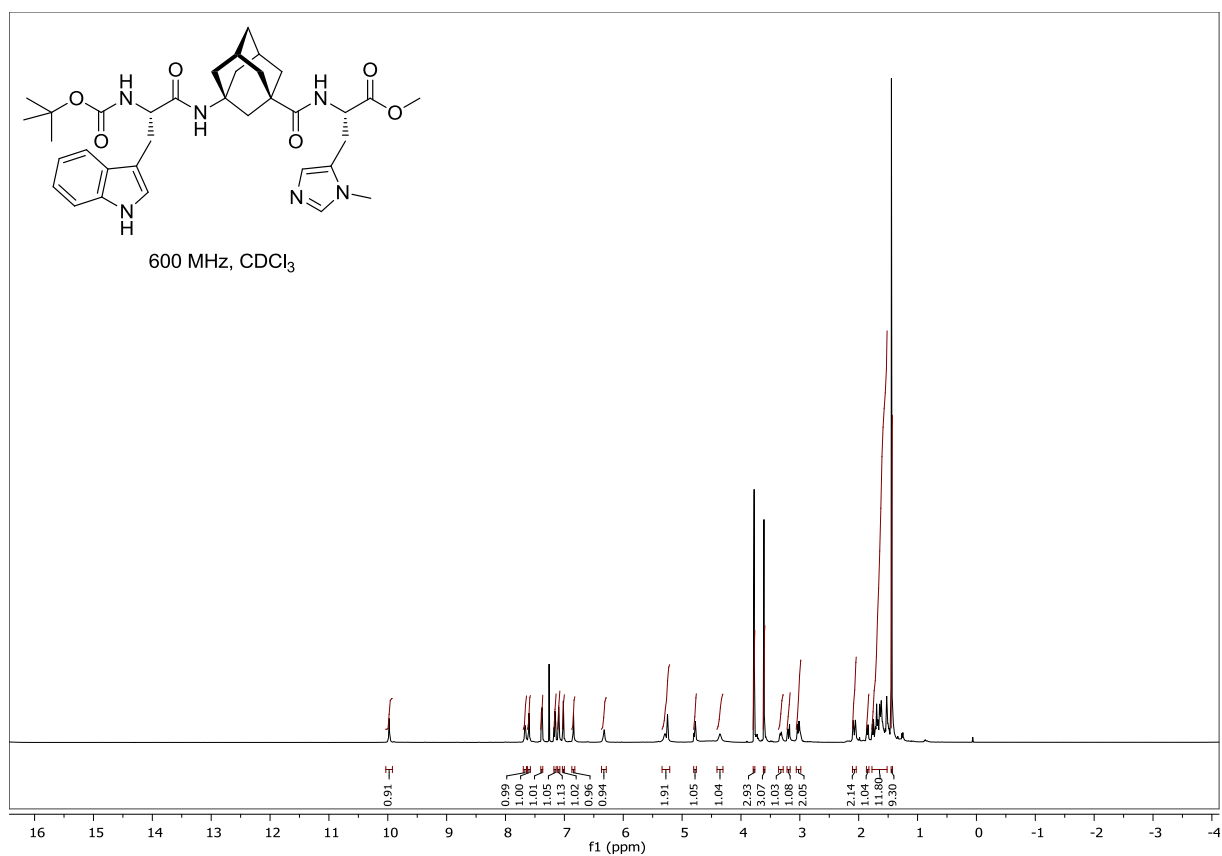
Boc-D-Val-^AGly-L-Pmh-OMe (S9)

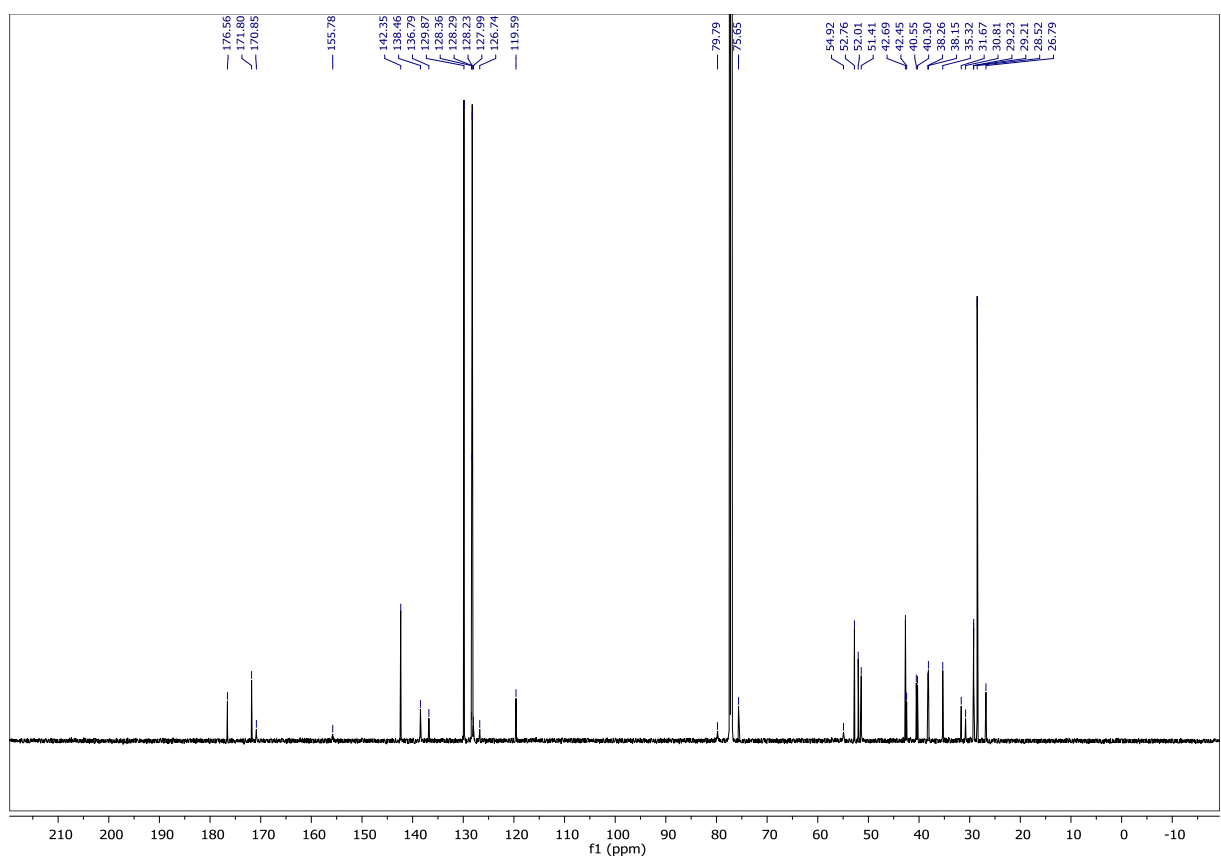
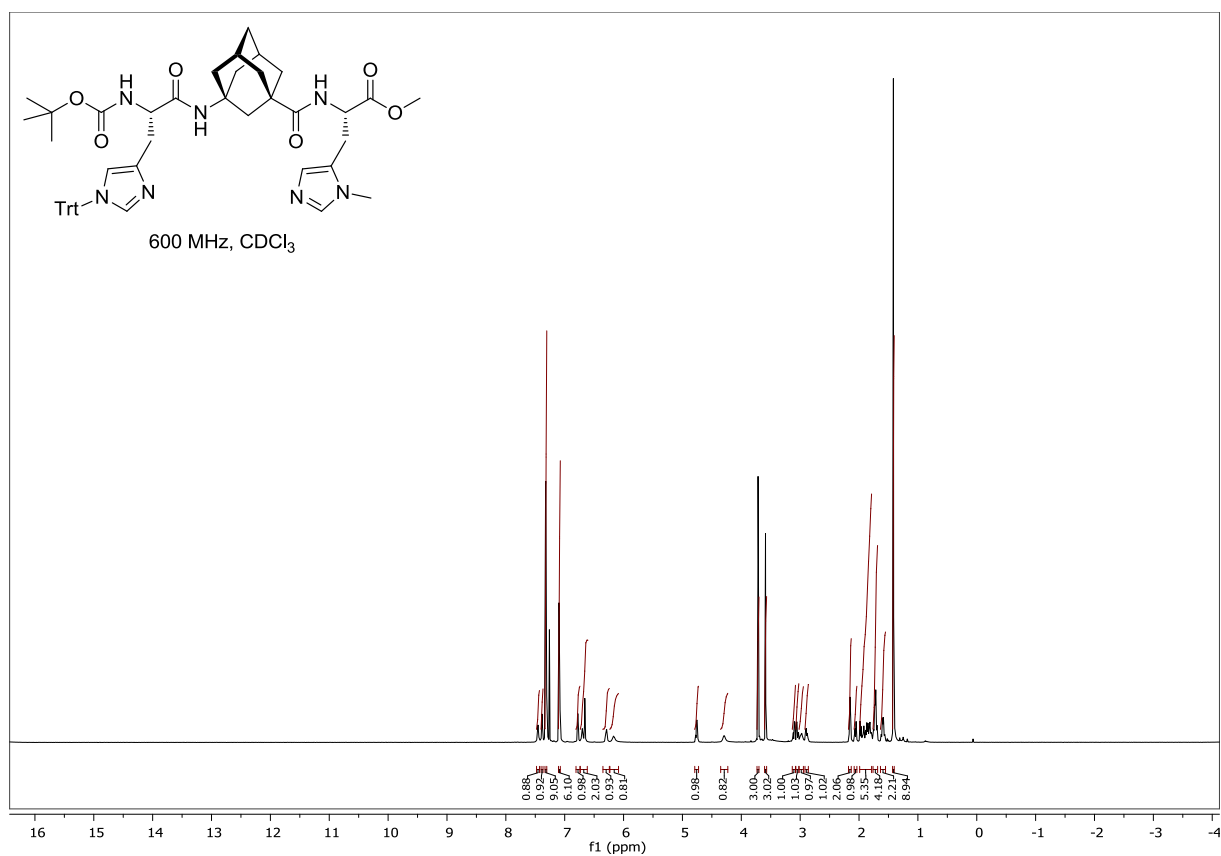
Boc-L-Leu-^AGly-L-Pmh-OMe (S10)

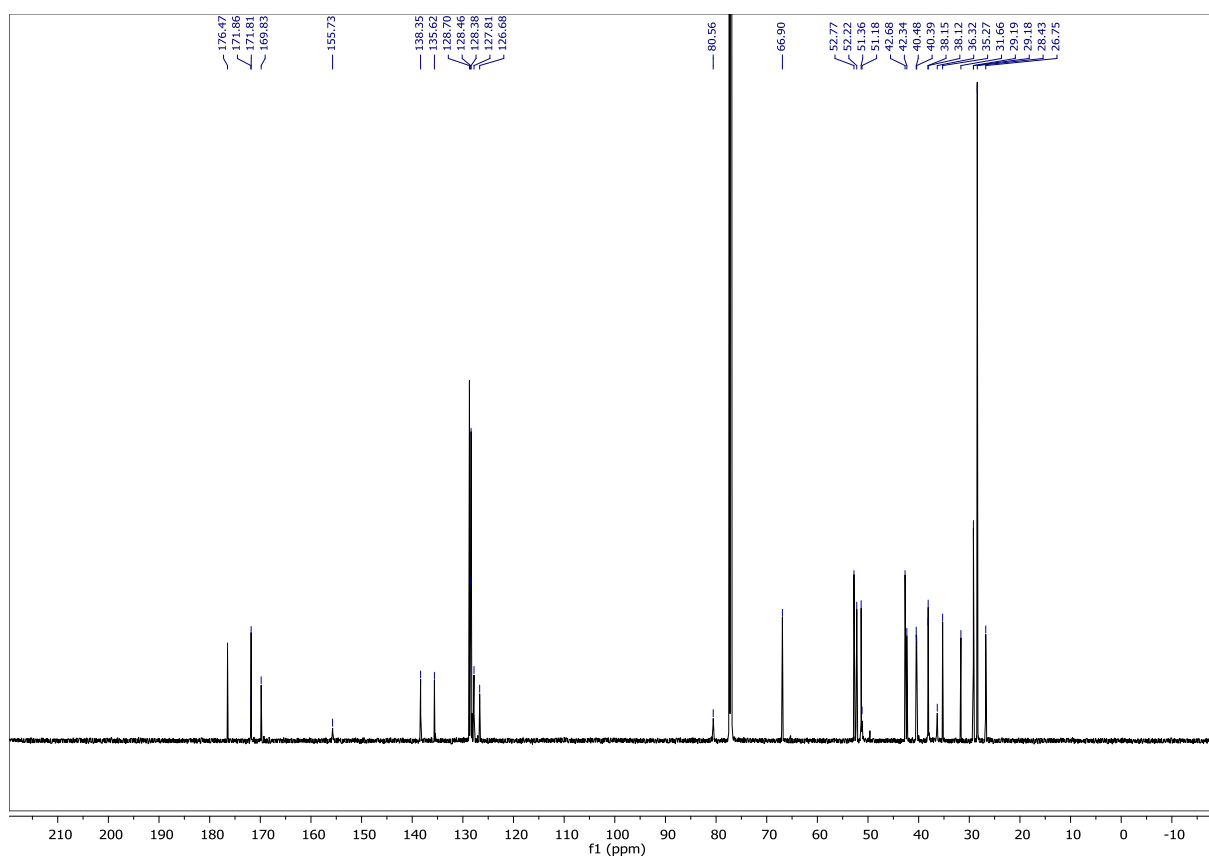
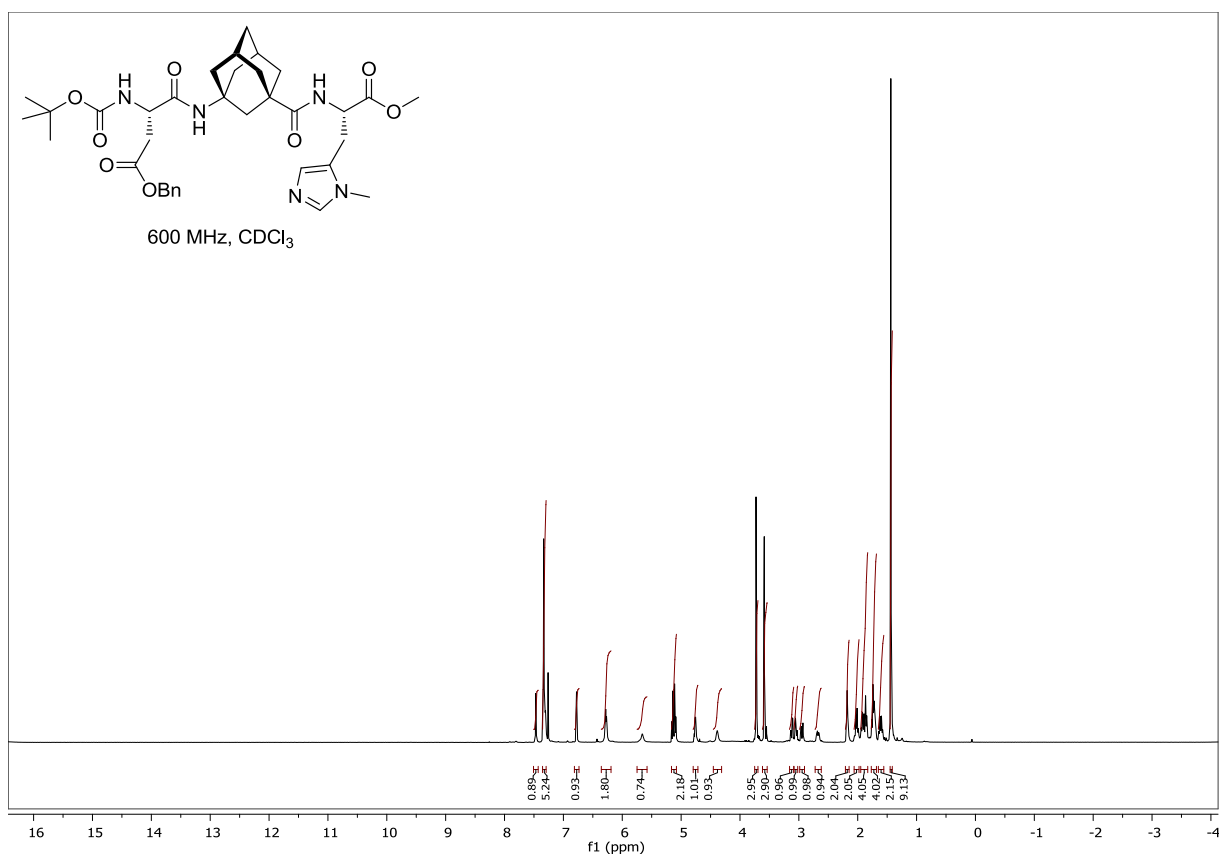


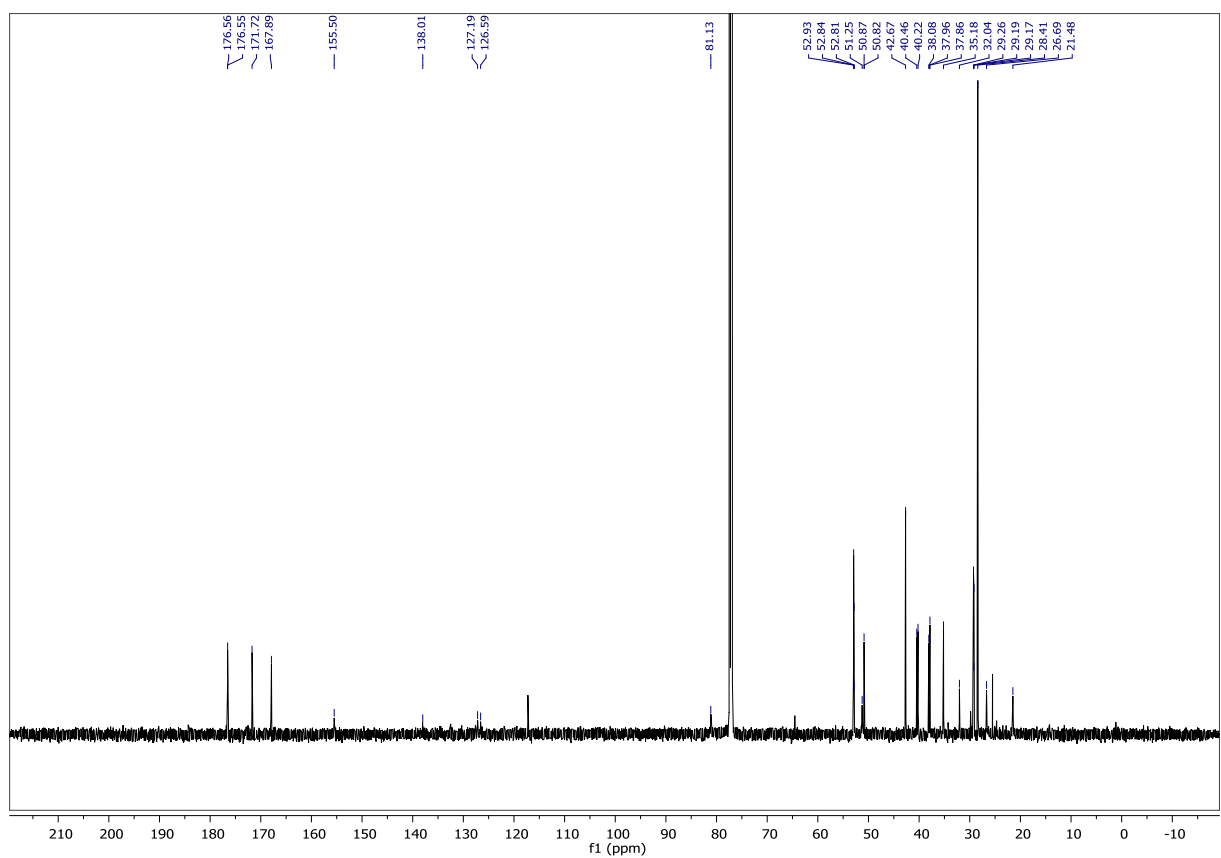
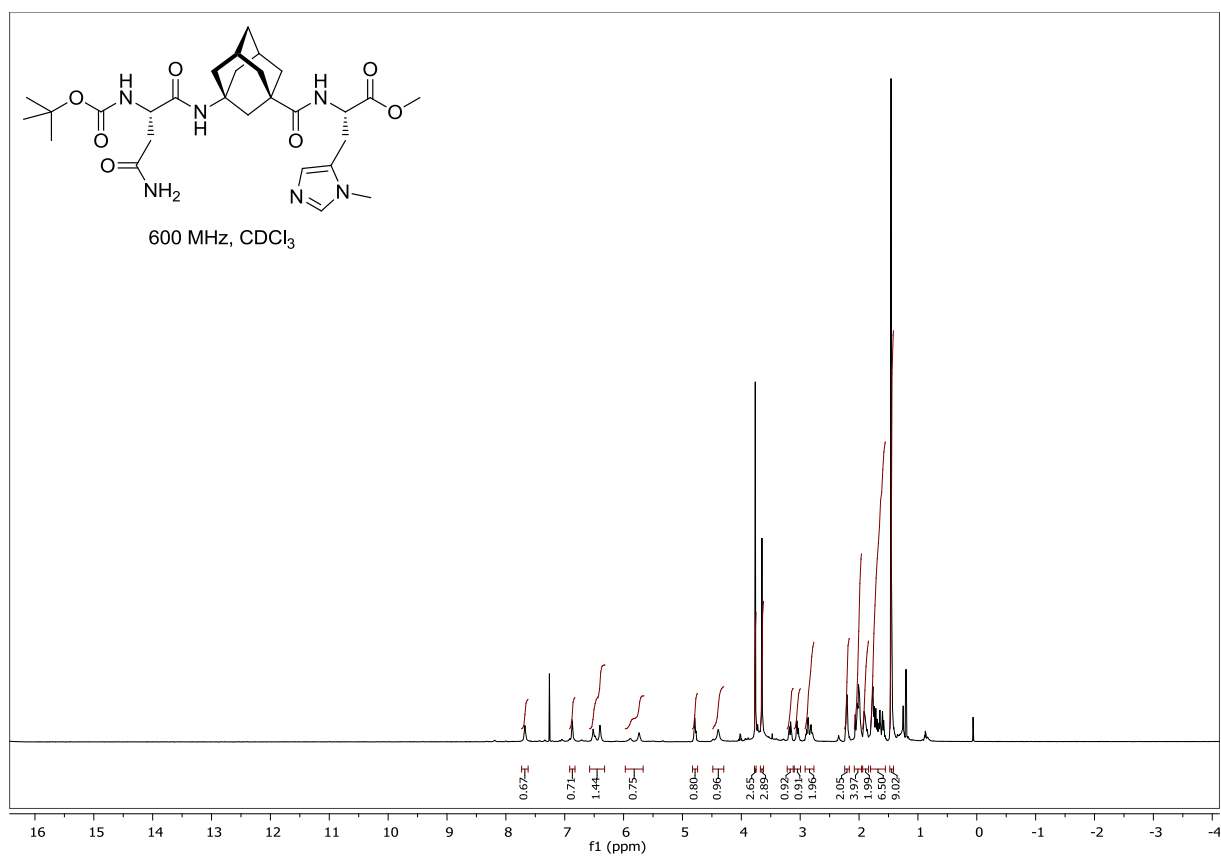
Boc-L-Phe-^AGly-L-Pmh-OMe (S11)

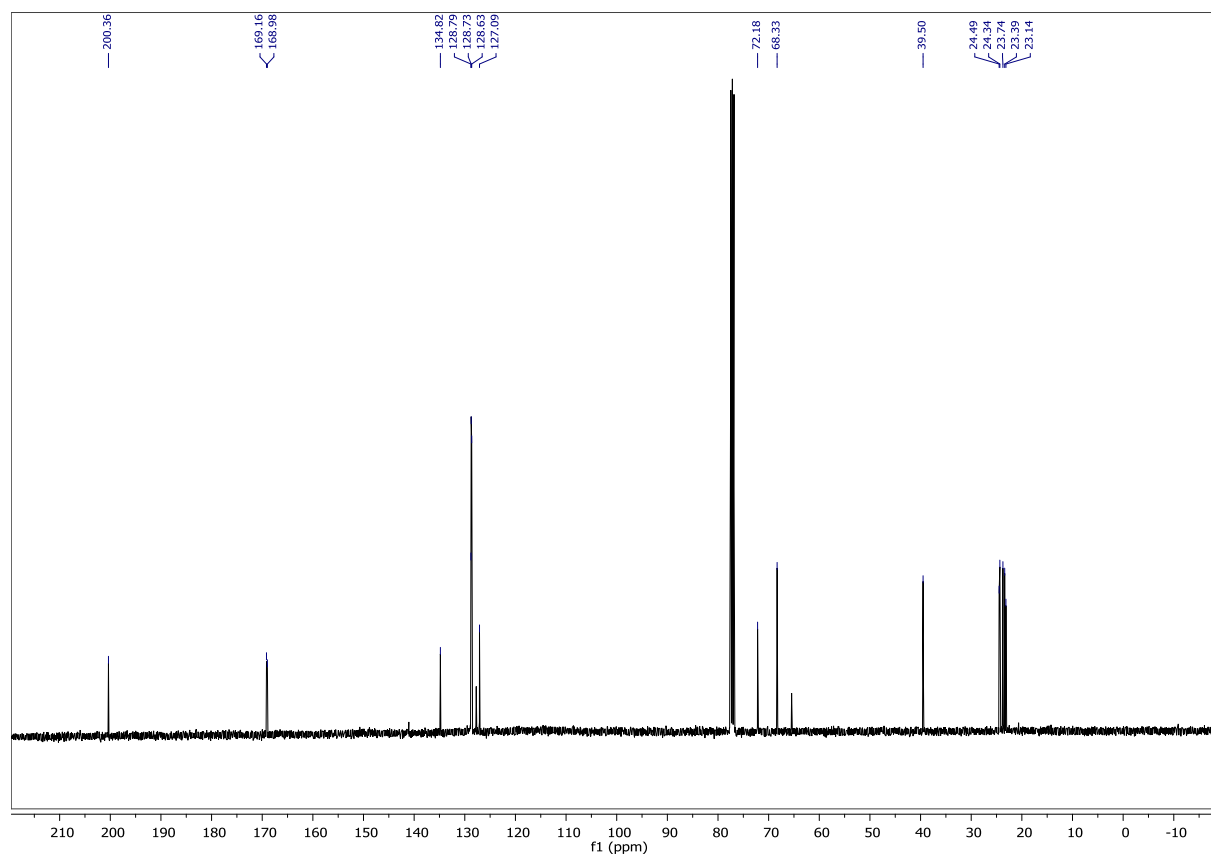
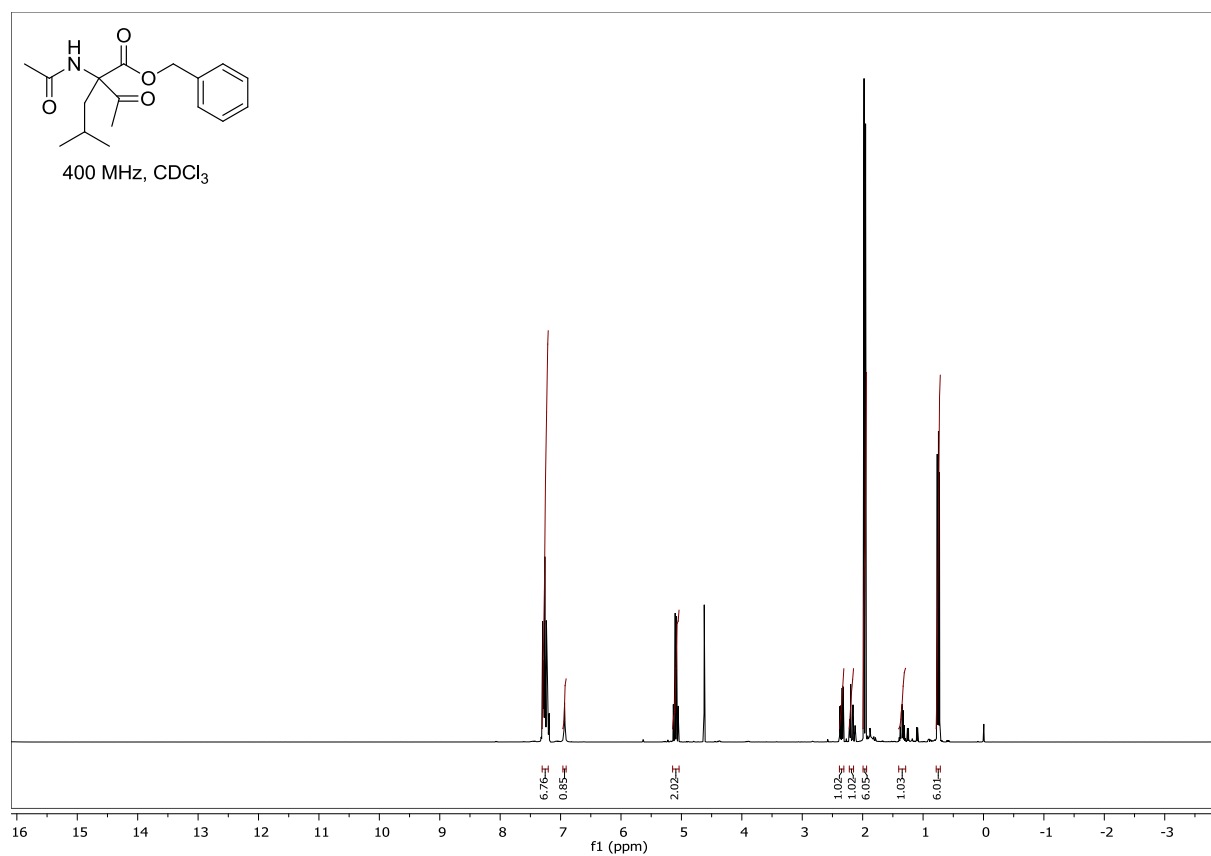
Boc-L-Trp-^AGly-L-Pmh-OMe (S12)



Boc-L-(Trt)-His-^AGly-L-Pmh-OMe (S13)

Boc-L-(OBn)-Asp-^AGly-L-Pmh-OMe (S14)


Boc-L-Asn-^AGly-L-Pmh-OMe (S15)

Benzyl 2-acetamido-2-acetyl-4-methylpentanoate (S17)


2.8 References

- [1] a) H. E. Gottlieb, V. Kotlyar, A. Nudelman, *J. Org. Chem.* **1997**, *62*, 7512–7515; b) G. R. Fulmer, A. J. M. Miller, N. H. Sherden, H. E. Gottlieb, A. Nudelman, B. M. Stoltz, J. E. Bercaw, K. I. Goldberg, *Organometallics* **2010**, *29*, 2176–2179.
- [2] H. R. Snyder, J. F. Shekleton, C. D. Lewis, *J. Am. Chem. Soc.* **1945**, *67*, 310–312.
- [3] a) H. Watanabe, S. Kuwata, S. Nakajima, K. Koshida, M. Hayashi, *Bull. Chem. Soc. Japan* **1965**, *38*, 1461–1464; b) A. W. Coulter, P. Talalay, *J. Biol. Chem.* **1968**, *243*, 3238–3247.
- [4] X.-J. Wang, Q. Yang, F. Liu, Q.-D. You, *Synth. Commun.* **2008**, *38*, 1028–1035.
- [5] a) B. Zhu, X. Jiang, *Synlett* **2006**, 2795–2798; b) G. Naturale, M. Lamblin, C. Commandeur, F.-X. Felpin, J. Dessolin, *Eur. J. Org. Chem.* **2012**, 5774–5788.
- [6] B. Gillis, *J. Org. Chem.* **1959**, *24*, 1027–1029.
- [7] J. B. Rothbard, P. A. Wender, K. Pattabiraman, E. T. Pelkey, T. C. Jessop, Guanidinium transport reagents and conjugates. WO2003049772A2, **2003**.
- [8] J. Protiva, V. Krecek, B. Maca, J. Urban, M. Budesinsky, M. Prochazka, *Collect. Czech. Chem. Commun.* **1989**, *54*, 1012–1018.
- [9] C. A. Kettner, S. Jagannathan, T. P. Forsyth, Preparation of peptide boronic acid inhibitors of hepatitis C virus protease. WO2001002424A2, **2001**.
- [10] J. Porter, J. Dykert, J. Rivier, *Int. J. Pept. Prot. Res.* **1987**, *30*, 13–21.
- [11] P. Lan, D. Berta, J. A. Porco, M. S. South, J. J. Parlow, *J. Org. Chem.* **2003**, *68*, 9678–9686.
- [12] C. Shu, C.-B. Chen, W.-X. Chen, L.-W. Ye, *Org. Lett.* **2013**, *15*, 5542–5545.
- [13] S. Egusa, M. Sisido, Y. Imanishi, *Bull. Chem. Soc. Japan* **1986**, *59*, 3175–3178.
- [14] J. E. Redman, M. R. Ghadiri, *Org. Lett.* **2002**, *4*, 4467–4469.
- [15] G. V. Shishkin, V. P. Mamaev, *Zh. Obshch. Khim.* **1966**, *36*, 660–664.
- [16] J.-L. Fauchère, R. Schwyzler, *Helv. Chim. Acta* **1971**, *54*, 2078–2080.
- [17] A. Varnavas, L. Lassiani, V. Valenta, L. Mennuni, F. Makovec, D. Hadjipavlou-Litina, *Eur. J. Med. Chem.* **2005**, *40*, 563–581.
- [18] a) M. Nishiki, H. Miyataka, Y. Niino, N. Mitsuo, T. Satoh, *Tetrahedron Lett.* **1982**, *23*, 193–196; b) T. Maegawa, A. Akashi, K. Yaguchi, Y. Iwasaki, M. Shigetsura, Y. Monguchi, H. Sajiki, *Chem.–Eur. J.* **2009**, *15*, 6953–6963.
- [19] F. M. F. Chen, K. Kuroda, N. L. Benoiton, *Synthesis* **1979**, 230–232.
- [20] V. P. Krasnov, E. A. Zhdanova, N. Z. Solieva, L. S. Sadretdinova, I. M. Bukrina, A. M. Demin, G. L. Levit, M. A. Ezhikova, M. I. Kodess, *Russ. Chem. Bull.* **2004**, *53*, 1331–1334.
- [21] W. Steglich, G. Höfle, *Angew. Chem. Int. Ed.* **1969**, *8*, 981.
- [22] P. A. Levene, R. E. Steiger, *J. Biol. Chem.* **1928**, *79*, 95–103.
- [23] C. Yuan, D. Chen, *Synthesis* **1992**, 531–532.
- [24] T. Niu, K.-H. Wang, D. Huang, C. Xu, Y. Su, Y. Hu, Y. Fu, *Synthesis* **2014**, *46*, 320–330.
- [25] Z. Su, L. Peng, C. Melander, *Tetrahedron Lett.* **2012**, *53*, 1204–1206.
- [26] T. K. Pradhan, K. S. Krishnan, J.-L. Vasse, J. Szymoniak, *Org. Lett.* **2011**, *13*, 1793–1795.
- [27] S. Bondock, A. G. Griesbeck, *Monatsh. Chem.* **2006**, *137*, 765–777.
- [28] G. M. Sheldrick, *Acta Cryst., Sect. A* **2015**, *71*, 3–8.
- [29] G. M. Sheldrick, *Acta Cryst., Sect. A* **2008**, *64*, 112–122.
- [30] F. E. Lehmann, A. Bretscher, H. Kühne, E. Sorkin, M. Erne, H. Erlenmeyer, *Helv. Chim. Acta* **1950**, *33*, 1217–1226.
- [31] L. Wanka, C. Cabrele, M. Vanejews, P. R. Schreiner, *Eur. J. Org. Chem.* **2007**, 1474–1490.
- [32] K. N. Vijayadas, R. V. Nair, R. L. Gawade, A. S. Kotmale, P. Prabhakaran, R. G. Gonnade, V. G. Puranik, P. R. Rajamohanan, G. J. Sanjayan, *Org. Biomol. Chem.* **2013**, *11*, 8348–8356.
- [33] M. Sharma, M. Gupta, D. Singh, M. Kumar, P. Kaur, *Chem. Biol. Drug Des.* **2013**, *82*, 156–166.
- [34] H. C. Beyerman, L. Maat, A. van Zon, *Recl. Trav. Chim. Pays-Bas* **1972**, *91*, 246–250.
- [35] C. E. Müller, L. Wanka, K. Jewell, P. R. Schreiner, *Angew. Chem. Int. Ed.* **2008**, *47*, 6180–6183.
- [36] J. A. Cabeza, I. del Río, M. G. Sánchez-Vega, M. Suárez, *Organometallics* **2006**, *25*, 1831–1834.

- [37] C. E. Müller, D. Zell, R. Hrdina, R. C. Wende, L. Wanka, S. M. M. Schuler, P. R. Schreiner, *J. Org. Chem.* **2013**, 78, 8465–8484.
- [38] B.-C. Chen, A. P. Skoumbourdis, P. Guo, M. S. Bednarz, O. R. Kocy, J. E. Sundeen, G. D. Vite, *J. Org. Chem.* **1999**, 64, 9294–9296.
- [39] J. Rivier, W. Vale, M. Monahan, N. Ling, R. Burgus, *J. Med. Chem.* **1972**, 15, 479–482.
- [40] L. Wanka, PhD-Thesis, Justus-Liebig University (Gießen), **2007**.
- [41] a) G. H. Cleland, C. Niemann, *J. Am. Chem. Soc.* **1949**, 71, 841–843; b) J. W. Cornforth, D. F. Elliott, *Science* **1950**, 112, 534–535; c) C. S. Rondestvedt, B. Manning, S. Tabibian, *J. Am. Chem. Soc.* **1950**, 72, 3183–3184; d) W. Steglich, G. Höfle, *Tetrahedron Lett.* **1968**, 9, 1619–1624; e) W. Steglich, G. Höfle, *Chem. Ber.* **1971**, 104, 3644–3652; f) G. Höfle, A. Prox, W. Steglich, *Chem. Ber.* **1972**, 105, 1718–1725; g) N. L. Allinger, G. L. Wang, B. B. Dewhurst, *J. Org. Chem.* **1974**, 39, 1730–1735; h) L. Dalla-Vechia, V. G. Santos, M. N. Godoi, D. Cantillo, C. O. Kappe, M. N. Eberlin, R. O. M. A. de Souza, L. S. M. Miranda, *Org. Biomol. Chem.* **2012**, 10, 9013–9020.
- [42] a) F. R. Dietz, H. Gröger, *Synlett* **2008**, 663–666; b) F. R. Dietz, H. Gröger, *Synthesis* **2009**, 4208–4218.
- [43] T. A. Halgren, *Encyclopedia of Computational Chemistry*, Vol. 2, Wiley, Chichester, **1998**.
- [44] S. Grimme, S. Ehrlich, L. Goerigk, *J. Comput. Chem.* **2011**, 32, 1456–1465.
- [45] J. Tomasi, B. Mennucci, R. Cammi, *Chem. Rev.* **2005**, 105, 2999–3094.
- [46] V. Barone, M. Cossi, J. Tomasi, *J. Chem. Phys.* **1997**, 107, 3210–3221.
- [47] Gaussian 09, Revision D.01, M. J. Frisch, G. W. Trucks, H. B. Schlegel, G. E. Scuseria, M. A. Robb, J. R. Cheeseman, G. Scalmani, V. Barone, B. Mennucci, G. A. Petersson, H. Nakatsuji, M. Caricato, X. Li, H. P. Hratchian, A. F. Izmaylov, J. Bloino, G. Zheng, J. L. Sonnenberg, M. Hada, M. Ehara, K. Toyota, R. Fukuda, J. Hasegawa, M. Ishida, T. Nakajima, Y. Honda, O. Kitao, H. Nakai, T. Vreven, J. A. Montgomery, Jr., J. E. Peralta, F. Ogliaro, M. Bearpark, J. J. Heyd, E. Brothers, K. N. Kudin, V. N. Staroverov, T. Keith, R. Kobayashi, J. Normand, K. Raghavachari, A. Rendell, J. C. Burant, S. S. Iyengar, J. Tomasi, M. Cossi, N. Rega, J. M. Millam, M. Klene, J. E. Knox, J. B. Cross, V. Bakken, C. Adamo, J. Jaramillo, R. Gomperts, R. E. Stratmann, O. Yazyev, A. J. Austin, R. Cammi, C. Pomelli, J. W. Ochterski, R. L. Martin, K. Morokuma, V. G. Zakrzewski, G. A. Voth, P. Salvador, J. J. Dannenberg, S. Dapprich, A. D. Daniels, O. Farkas, J. B. Foresman, J. V. Ortiz, J. Cioslowski, D. J. Fox, Gaussian, Inc., Wallingford CT, **2013**.
- [48] C. Y. Legault, CYLview 1.0b, Université de Sherbrooke; <http://www.cylview.org>, **2009**.
- [49] W. Humphrey, A. Dalke, K. Schulten, *J. Molec. Graphics* **1996**, 14, 33–38.
- [50] W. Steglich, G. Höfle, *Chem. Ber.* **1969**, 102, 883–898.

– Chapter VII –

Unpublished Results

After our development of the first asymmetric Dakin–West reaction^[1] the main focus was to mutually increase the previously achieved enantioselectivities. As we were able to show that binding of the intermittently formed enolates through hydrogen bonding *and* attractive interactions with the catalysts side-chain play a crucial role (*cf.* Chapter VI),^[1] these effects were studied in more detail. Both computational and experimental investigations were performed and are discussed in this chapter. Moreover, additional reactions were envisioned that are directly based on our previous investigations and findings, such as an enantioselective decarboxylative protonation of malonic acid half esters or an asymmetric Steglich rearrangement of acetyl groups.

1. The Importance of Side-Chain Interactions

First, complexes of the formerly identified best-working protonated catalyst **1** with enolates of methyl ketones of alanine (**2b**), phenylalanine (**2c**), leucine (**2d**) and cyclohexylalanine (**2e**) were computed to determine the strength of (dispersion) interactions of both side-chains. Unfortunately, the protonated peptide catalyst **1** did not completely converge to a minimum. Therefore, we determined the interaction energy of enolates **2b–2e** side-chains with the cyclohexyl residue of **1** with respect to the glycine-derived intermediate **2a** using the following equations. Subtraction of the energy of the enolate (E_{2a}) from the energy of the corresponding complex with the catalyst ($E_{(1_2a)}$) affords the energy of the catalyst itself and also takes into account charge separation as well as the hydrogen bonding ($\Delta E_{(1_HB)}$; Eq 1).

Accordingly, subtracting the energy of an arbitrary enolate (E_{Enol} , **2b–2e** in this case; see Figure 1) from the catalyst complex ($E_{(1_Enol)}$) will give the energy of the catalyst, the hydrogen bonding energy *and* the contribution of the side-chain (Eq 2; $\Delta E_{(1_HB_SI)}$). Assuming that the hydrogen bonding interactions are comparably strong for all investigated complexes the difference of both energies (Eq 3) will deliver only the side-chain interaction energies ($\Delta\Delta E_{SI}$) resulting from, *e.g.*, dispersion interactions.^[2]

$$E_{(1_2a)} - E_{2a} = \Delta E_{(1_HB)} \quad (\text{Eq 1})$$

$$E_{(1_Enol)} - E_{Enol} = \Delta E_{(1_HB_SI)} \quad (\text{Eq 2})$$

$$\Delta E_{(1_HB_SI)} - \Delta E_{(1_HB)} = \Delta \Delta E_{SI} \quad (\text{Eq 3})$$

Previously computed **1_2e** (see Chapter VI) was used as starting geometry and the side-chains were replaced by the desired residue. The structures were then reoptimized using the popular hybrid density functional B3LYP^[3] using Grimme's D3-dispersion correction^[4] with the Becke–Johnson damping function^[5] in conjunction with a 6-31+G(d,p) double- ζ basis set. The self-consistent reaction field (SCRF)^[6] with the polarizable continuum model (PCM) was employed to incorporate toluene as solvent and the United Atom topological model applied on radii optimized for the HF/6-31G(d) level of theory (UAHF)^[7] was used to describe the bulk solvent. All computations were performed with the *Gaussian 09* program package.^[8] The corresponding $\Delta\Delta G$ and $\Delta\Delta H$ values (Figure 1) were then calculated using the above given equations.

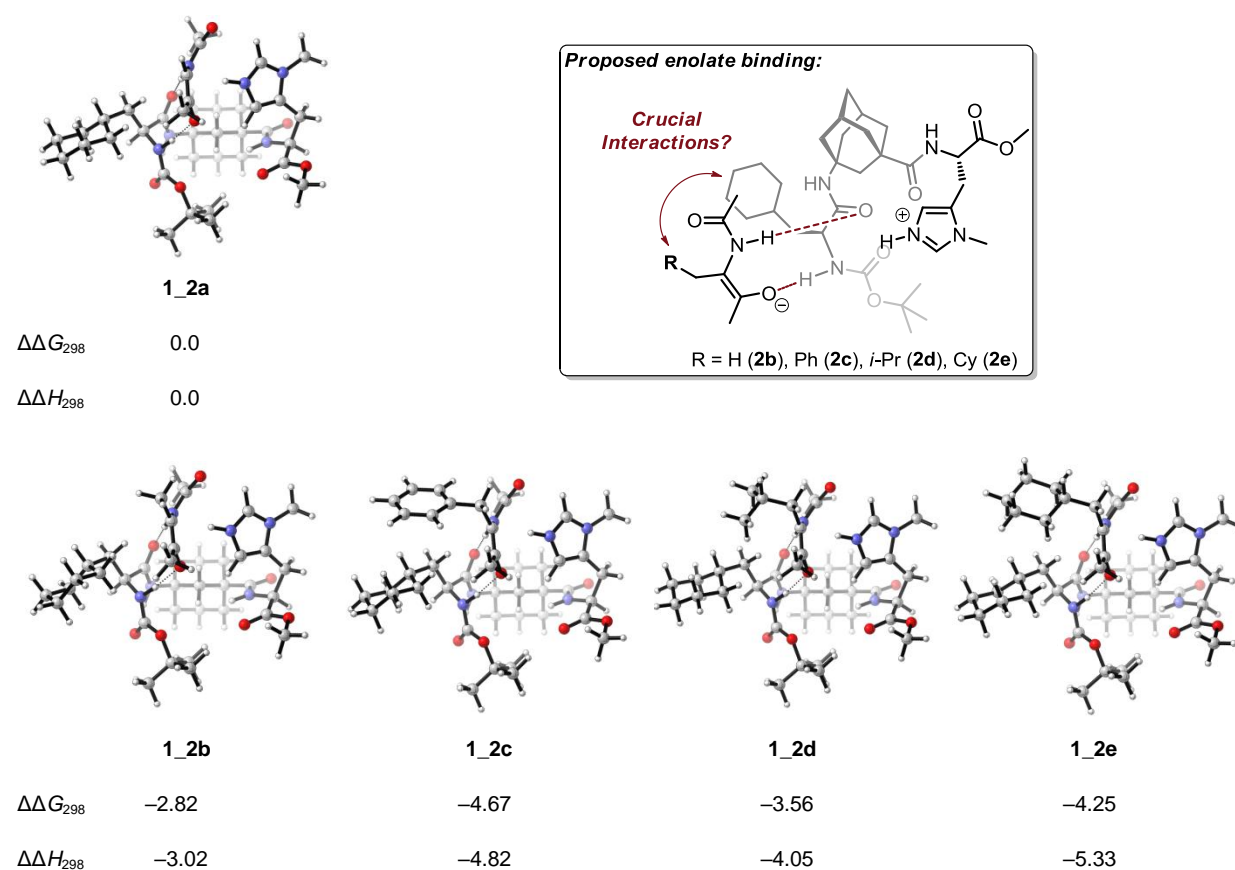


Figure 1. Interaction energies between the catalysts and substrates side-chains. B3LYP-D3(BJ)/6-31+G(d,p) optimized structures. Visualization was performed using CYLview.^[9] Values are in kcal mol⁻¹. C = gray, N = blue, O = red.

Compared to **1_2a** the other structures are lower in energy. Interestingly, a single methyl group already contributes around 3 kcal mol⁻¹ (**1_2b**). The trends that were observed for the asymmetric induction are generally reproduced by the determined side-chain interaction energies. Surprisingly, the determined values for **1_2c** did not correlate with the previously observed enantioselectivities and shows a stronger interaction than **1_2d** ($\Delta\Delta H_{298} = -4.82$ vs -4.05 kcal mol⁻¹). This may be due to efficient *CH*- π -interactions whereas the attractive dispersion in **1_2d** is comparably weak.

To further study the importance of side-chain interactions, peptide **3** was employed for the Dakin–West reaction of pentafluorophenylalanine **4** under the previously optimized conditions (Figure 2). Of special note, the Dakin–West reaction of *N*-acetyl phenylalanine with **3** did provide lower selectivities compared to catalyst **1** in our previous experiments (Chapter VI, Supporting Information), although π - π -interactions may operate in this case. However, the inverse electronic structure of the perfluorated aromatic ring in **4** should lead to stronger interactions with the phenylalanine of **3**. As for the above examples, a complex of the methylketone enolate of **4** with protonated **3** was computed. Indeed, the aromatic rings adapt a favorable “slipped parallel” orientation that was previously reported for benzene-hexafluorobenzene dimers (Figure 2).^[10]

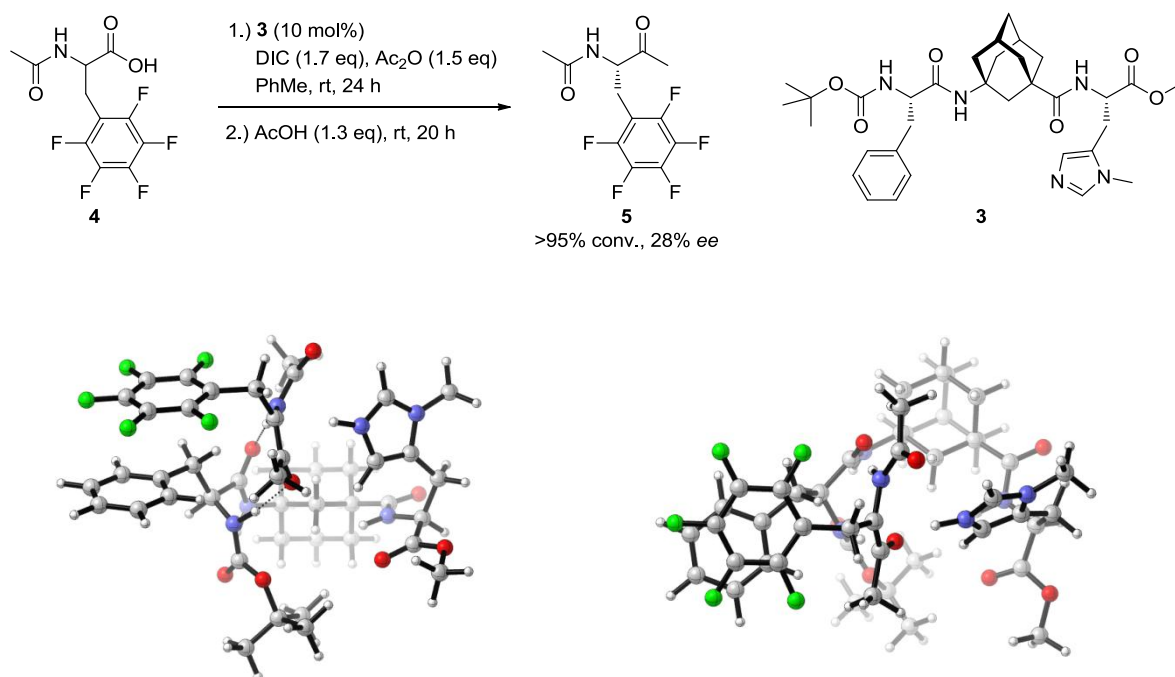


Figure 2. Top: Enantioselective Dakin–West reaction of *N*-acetyl pentafluorophenylalanine (**4**) with catalyst **3**. Reaction was performed on an analytical scale (0.1 mmol). Bottom: B3LYP-D3(BJ)/6-31+G(d,p) optimized structure of an adduct of protonated **3** with methylketone enolate of **4**. Left: side-view; right: top-view. Visualization was performed using CYLview.^[9] C = gray, N = blue, O = red, F = green.

Although this catalyst-substrate combination seemed to be well-suited for enhancing the previously determined enantioselectivity using **1** (up to 31% *ee*; Chapter VI, Supporting Information) the desired product formed with comparable selectivity 28% *ee* (Figure 2).

Apparently, the described results indicate that other aspects are decisive to achieve high asymmetric induction and that transition state stabilization is probably the most important factor. Thus, the protonation of the enolate in the former two examples may necessitate a reorientation of the perfectly aligned side-chains and would therefore weaken the interactions. This might then allow reprotonation, *e.g.*, by acetic acid, to occur from the otherwise unfavored side. On the other hand, dispersion interactions are directionally less dependent and consequently will still play operate. This may explain the significantly higher enantio-selectivities for the reaction with **1** and *N*-acetyl cyclohexylalanine as well as *N*-acetyl leucine (58% *ee* and 54% *ee*, respectively; *cf.* Chapter VI).^[1] A computational investigation of the corresponding transition states is necessary to confirm these assumptions. However, this is highly demanding and could yet not be performed.

2. Binding of the Transient Enolate

The binding of the enolate is another important aspect for further improvements of the enantioselective Dakin–West reaction. Therefore, we also studied various leucine derivatives (leucine previously gave high enantioselectivities) with different *N*-protecting groups and a sterically demanding anhydride (Table 1).

Compared to *N*-acetyl leucine (**6a**) that afforded desired methylketone **7a** with 54% *ee* in 64% yield (Table 1, entry 1 and Chapter VI) the other derivatives gave lower conversion and/or selectivity, whereby formyl-protected **6b** was the only exception. Thus, desired product **7b** formed with comparable enantioselectivity (52% *ee*). Furthermore, essentially complete conversion was observed after much shorter reaction times (Table 1, entry 2). Contrary, isobutyryl-protected leucine **6c** gave 44% *ee* and low conversion (entry 3). Little conversion to the methyl ketone was also observed with **6d** although the selectivity was not affected (entry 4). The deacetylation to form the azlactone was a pronounced side reaction in this case.

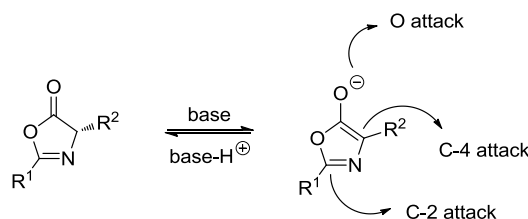
Note that some of the starting materials were not used as the racemate. However, according to the proposed mechanism and our previous studies this does not affect the stereochemical outcome of the reaction (*cf.* Chapter VI).

Table 1. Variation of protecting group and anhydride.

<div style="display: flex; align-items: center; justify-content: space-around;"> <div style="text-align: center;"> <p>6</p> </div> <div style="text-align: center;"> <p>1.) 1 (10 mol%) DIC (1.7 eq) anhydride (1.5 eq) PhMe, rt, t_1</p> <p>2.) AcOH (1.3 eq), rt, t_2</p> </div> <div style="text-align: center;"> <p>1</p> </div> </div>					
Entry	Starting material	Product	t_1 / t_2 (h)	C^a (%)	ee^b (%)
1			64 / 92	64 ^c	54
2			18 / 48	>95	52
3			72 / 72	<30	44
4			72 / 72	<20	52
5 ^d			— / —	n.d.	—
6			72 / 72	traces	22

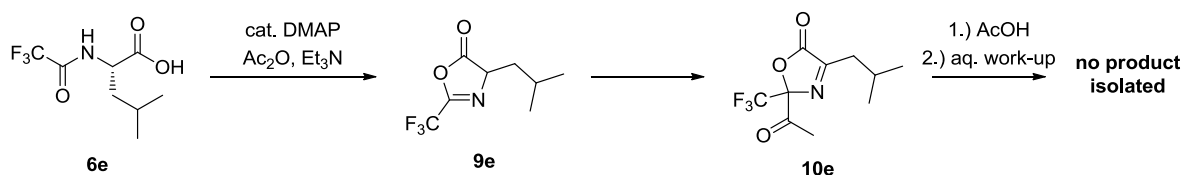
Reactions were performed on analytical scale (0.1 mmol). The absolute configuration of the products was determined as (*S*) according to the previous results (Chapter VI). ^a Conversion to product was estimated by GC-MS based on the possible intermediates. ^b Enantiomeric excesses were determined by chiral stationary phase GC. ^c Yield of isolated product. ^d Reaction was performed with DMAP as catalyst under the conditions reported by Steglich and Höfle (see Scheme 2 and Experimental Section).^[11]

Attempts to prepare racemic trifluoroacetyl-protected methyl ketones always failed using the DMAP-catalyzed standard procedure (Table 1, entry 5).^[11] Importantly, depending on the reagents used and the substitution on the azlactones, these compounds can react either at the C-2, C-4, or at the exocyclic oxygen after deprotonation (Scheme 1).^[12] Strongly electron-withdrawing groups, such as trifluoromethyl, predominantly give the C-2 addition product with activated electrophiles.^[13]



Scheme 1. Diverse reaction paths of azlactones.

In the present case, **6e** would first cyclize to azlactone **9e** under the reaction conditions applied (cat. DMAP, Ac₂O, Et₃N)^[11] and subsequently may be acetylated affording **10e** (Scheme 2). As a consequence, work-up would lead to the opening of the oxazolone ring of **10e** liberating the acid that will be removed during aqueous work-up. We followed the reaction with GC-MS and chiral GC applying *N*-acetyl phenylalanine as starting material and DMAP as catalyst in DCM under otherwise identical reaction conditions. Two major products with $m/z = 285$ (one probably being **10e**) formed upon acetylation that corresponds to acetylated azlactone intermediates. Interestingly, no significant change was observed upon addition of acetic acid after three days.



Scheme 2. Proposed formation of C-2 acetylated azlactone intermediates during the Dakin–West reaction of *N*-trifluoroacetyl amino acids.

The influence of the anhydride was studied next (Table 1, entry 6). Using *N*-acetyl leucine (**6a**) and isobutyric anhydride only traces of **7f** formed with considerably decreased enantioselectivity (22% *ee*).

The results summarized above provide evidence that the transient enolate will bind as previously proposed. For simplicity this is further exemplified with complex **1_2b** (Figure 3). Owing to the relatively ‘open’ side, variation of the protecting group is indeed possible, whereas appropriate binding of enolates derived from hindered anhydrides is prevented due to steric reasons. Hence, this explains the high enantioselectivities that are preserved for **7a** – **7d** while the asymmetric reprotonation to afford **7f** shows diminished selectivity. However, the protecting group has a significant influence on the conversion to the desired product (Table 1; compare, *e.g.*, entry 2 and entry 4) that may result from stereoelectronic effects.

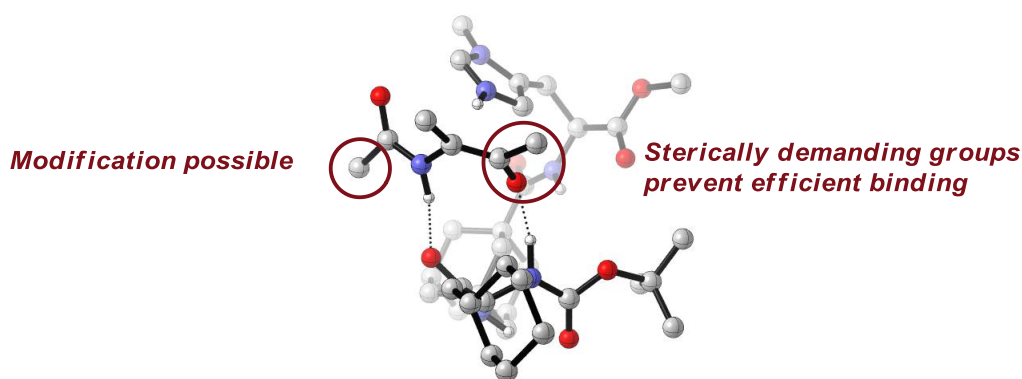
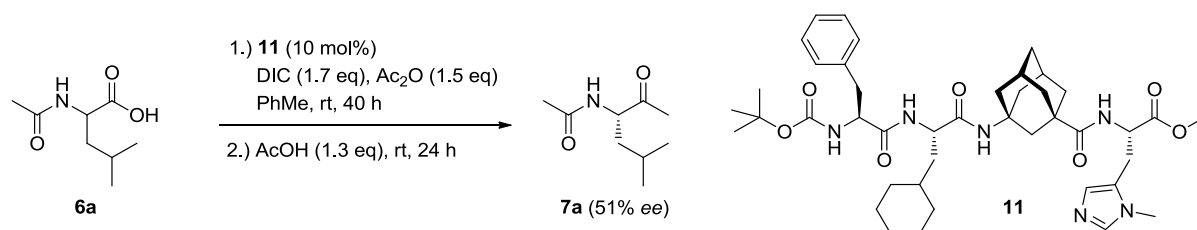


Figure 3. Binding of the enolate intermediate taking **1_2a** as representative example and explanation for the observed influence of protecting groups and anhydride used. B3LYP-D3(BJ)/6-31+G(d,p) optimized structure (*vide supra*). Visualization was performed using CYLview.^[9] All C–H hydrogens were omitted for clarity. C = gray, N = blue, O = red.

Finally, tripeptide **1** was modified with phenylalanine at its *C*-terminus affording Boc-L-Phe-L-Cha-^AGly-L-Pmh-OMe (**11**), the retropeptide of our highly efficient acylation catalyst. Performing the Dakin–West reaction of **6a** with **11** as catalyst again did not lead to a significant change in selectivity (51% *ee*, Scheme 3). It appears that the additional amino acid plays a minor role in enolate binding.

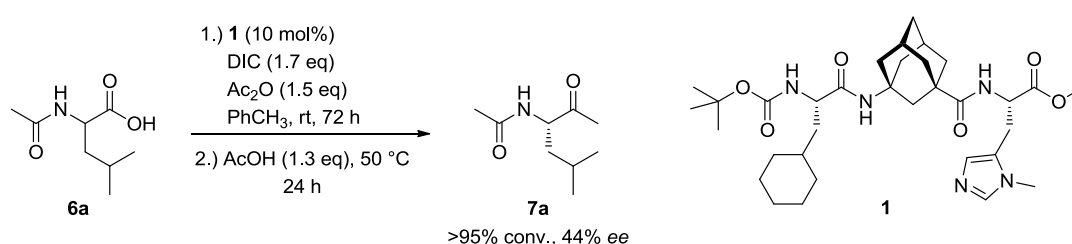


Scheme 3. Dakin–West reaction of *N*-acetyl leucine (**6a**) with oligopeptide **11**.

In 2003, Brunner *et al.* reported an enantioselective decarboxylative protonation^[14] of 2-aminomalonic acid derivatives mediated by cinchona alkaloid derived catalysts affording the

corresponding α -amino acid derivatives with up to 70% *ee*.^[15] Importantly, slightly higher enantioselectivities were obtained at elevated temperature (70 °C).^[15]

Intrigued by these results, the enantioselective decarboxylation step was performed at 50 °C (Scheme 4). Reasonably, the enolate can adapt either a *Z* or *E* configuration. The higher temperature may influence the *E/Z*-ratio on the enolate and consequently binding to the catalyst. Moreover, dispersion interactions are temperature independent and will still play a decisive role.^[2] Although the reaction time for the decarboxylation could be reduced to 24 h, the selectivity dropped to 44% *ee* (Scheme 4).

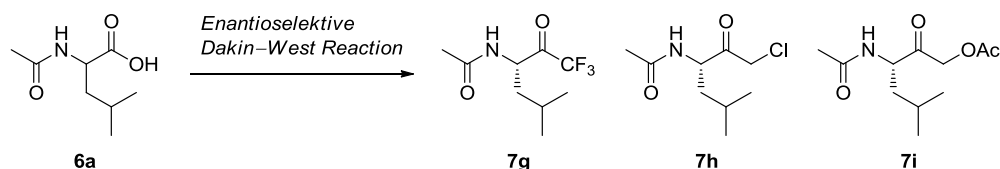


Scheme 4. Dakin–West reaction of *N*-acetyl leucine (**6a**) with oligopeptide **1** at elevated temperature.

3. Synthesis of Protease Inhibitor Warheads

Peptidyl halomethyl and acyloxymethyl ketones have been reported to be potent inhibitors of serine, cysteine and threonine proteases.^[16] Consequently, the enantioselective Dakin–West reaction was envisaged to provide an entry towards the synthesis of amino acid derived, enantioenriched trifluoromethyl, chloromethyl, and acetyloxymethyl ketones (**7g–7i**) as chemical warheads (Scheme 5). Again, **6a** was used as starting material.

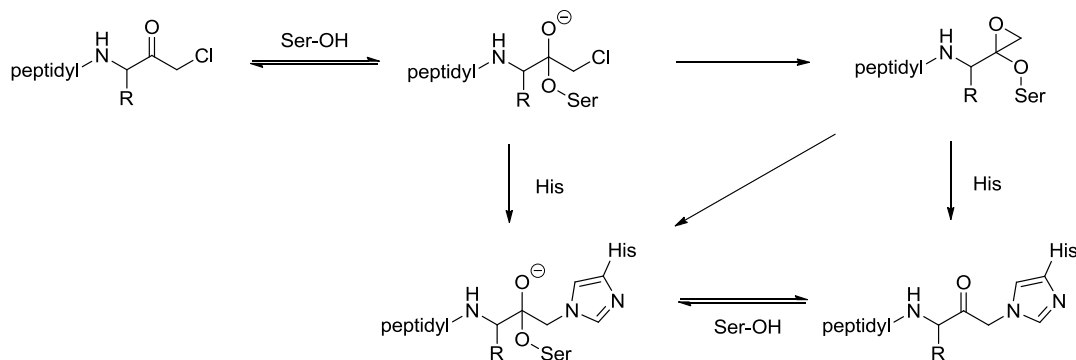
The preparation of racemic **7g** did not yield the desired product under standard conditions. As a result, our previously developed Dakin–West reaction conditions were applied using DMAP as catalyst and trifluoroacetic anhydride and the reaction progress was followed *via* GC-MS. Although clean formation of two intermediates was observed during the acylation step, the reaction did not progress further after addition of acetic acid. The structures of the two products



Scheme 5. Application of the enantioselective Dakin–West reaction for the synthesis of protease inhibitor warheads **7g–7i**.

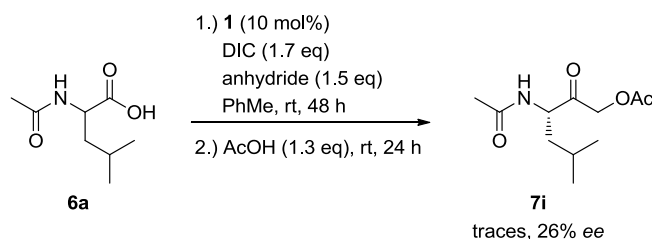
could not be unambiguously determined based on the GC-MS measurements. However, the fragmentation patterns suggest that both derive from the reaction of the *in situ* formed azlactone with the anhydride. Of special note, the general Dakin–West reaction has been shown to be unsuitable for the synthesis of trifluoromethyl ketones of amino acids. Typically the corresponding azlactones are first reacted with, *e.g.*, trifluoroacetic anhydride and decarboxylation is initiated by addition of anhydrous oxalic acid.^[17]

Next, **6a** was reacted with chloroacetic anhydride in the presence of peptide **1**. Again the desired product **7a** could not be obtained. Apparently, the nucleophilic peptide is not compatible with the highly reactive chloromethyl ketone and catalyst inhibition by the product might be the major problem. This is also in agreement with the proposed inhibition mechanism, for instance, of serine proteases by these compounds whereby a histidine residue is irreversibly binding to the inhibitor (Scheme 6).^[16]



Scheme 6. Proposed mechanism for the inhibition of serine proteases.

As a last attempt, **6a** was treated with 2-acetoxyacetic anhydride under standard conditions using oligopeptide **1** as catalyst to afford acetoxymethyl ketone **7i** (Scheme 7). Indeed, in this case traces of the desired product formed, albeit with lower selectivity and conversion. The decrease of selectivity may be explained by the sterically more demanding anhydride used (*vide supra*).

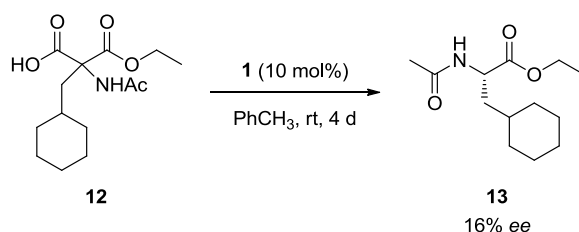


Scheme 7. Synthesis of acetoxymethyl ketone **7i**.

4. Enantioselective Decarboxylative Protonation and the Acetylation of *In Situ* Formed Azlactones

The development of the enantioselective Dakin–West reaction led to interesting findings that may be further pursued. Firstly, the Pmh-containing oligopeptides were capable of stereoselectively acetylating the *in situ* formed azlactone, a reaction that is closely related to the Steglich rearrangement. Secondly, the same peptides also efficiently catalyzed the enantioselective decarboxylative protonation for which only few organocatalytic variants exist.^[18,14b,c]

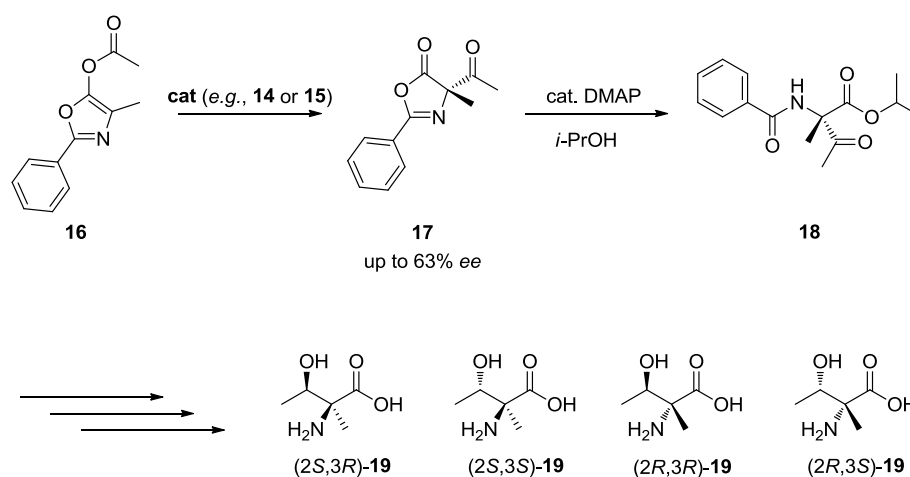
Cyclohexylalanine afforded the highest selectivities in the Dakin–West reaction. As a consequence malonic acid half ester **12**, a precursor for the synthesis of cyclohexylalanine, was envisioned as the substrate of choice for an enantioselective decarboxylative protonation with peptide **1** (Scheme 8). Although some selectivity was observed for the formed cyclohexylalanine derivative **13** (16% *ee*), the conversion was unexpectedly low. Reasonably, a more basic catalyst is necessary to achieve high conversion for this transformation. Moreover, the comparably low enantiomeric induction may be a result of a somehow different binding of the ester enolate to the catalyst.



Scheme 8. Enantioselective decarboxylative protonation of malonic acid half ester.

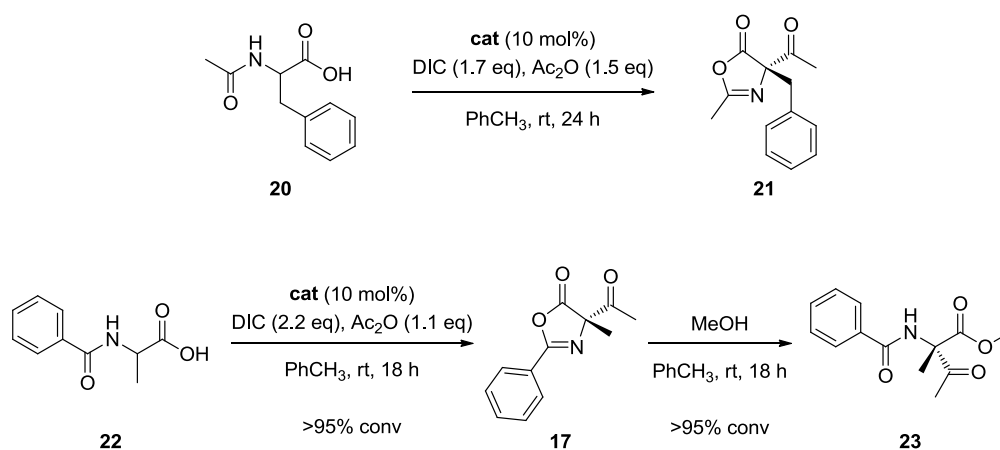
The Steglich rearrangement^[13a,19] represents a viable reaction for the preparation of synthetically useful compounds, such as quaternary amino acid derivatives. Although a variety of organocatalytic enantioselective versions exist, the carbonates are mainly used as starting materials^[20] (rearrangement of alkoxycarbonyl or benzyloxycarbonyl groups) and only few examples for the asymmetric rearrangement of acetyl groups have been reported to date.^[21] However, *C*-acetylated azlactones may give rise to α -amino β -hydroxy acid derivatives (threonine and serine, for instance) and to structural motifs that are preserved in complex natural products, such as the antibiotics vancomycin and chloramphenicol.^[22]

In 2008, Dietz and Gröger reported the organocatalytic enantioselective Steglich rearrangement of acetyl groups making use of, *e.g.*, (*S*)-tetramisole (**14**) or Fu's chiral (*S*)-PPY* (**15**)^[20a] as catalysts as a key step towards the synthesis of all stereoisomers of α -methylthreonine **19** (Scheme 9).^[21]



Scheme 9. Enantioselective Steglich rearrangement for the synthesis of α -methylthreonine derivatives reported by Dietz and Gröger.

During the development and optimization of the Dakin–West reaction we found that the *in situ* formed *C*-acetylated azlactone **21** was enantioenriched. Intrigued by this observation selected catalysts were also applied for the enantioselective Steglich rearrangement-type reaction using *N*-benzoyl alanine (**22**) as starting material under similar conditions as before (Table 2). After complete consumption of the intermediate azlactone methanol was added (instead of acetic acid) to afford desired product **23**. Compared to the enantioselectivities previously determined for the reaction with *N*-acetyl phenylalanine (**20**) most catalysts provided appreciably higher *ee* values for **23**. This profound effect is a consequence of the *N*-protecting group and has been also observed previously.^[20a,k]

Table 2. Catalyst screening for the enantioselective acetylation of azlactones.

Entry	Catalyst	<i>ee</i> 21 (%) ^a	<i>ee</i> 23 (%) ^a
1	(<i>S</i>)-Tetramisol (14)	25 (traces)	63 ^b
2	(<i>S</i>)-PPY* (15)	16	37
3	Boc-L-Pmh- ^A Gly-L-Cha-L-Phe-OMe (24)	–22	–9
4	Boc-L-Pmh- ^A Gly-L-Val-L-Phe-OMe (25)	–13	–14
5	Boc-L-Pmh- ^A Gly-L-Phe-OMe (26)	n.d.	–12
6	Boc-L-Pmh- ^A Gly- ^A Gly-L-Phe-OMe (27)	n.d.	–11
7	Boc- ^A Gly-L-Pmh-OMe (29)	16	28
8	Boc-L-Val- ^A Gly-L-Pmh-OMe (30)	17	39
9	Boc-L-Cha- ^A Gly-L-Pmh-OMe (1)	25	40
10	Boc-L-Phe- ^A Gly-L-Pmh-OMe (3)	25	43
11	Boc-L-Trp- ^A Gly-L-Pmh-OMe (31)	14	29
12	Boc-L-Asn- ^A Gly-L-Pmh-OMe (33)	18	44
13	TU- ^A Gly-L-Pmh-OMe (34)	23	29

Reactions were performed on analytical scale (0.1 mmol). For the reaction **20**→**21**, see Chapter VI. The absolute configuration of the products was determined as (*S*) by comparison of the retention times with the reaction using **14**; negative values indicate formation of the opposite enantiomer. ^a Enantiomeric excesses were determined by chiral stationary phase GC. ^b Reported value; reaction was performed in CDCl₃ with 32 mol% **14** and *i*-PrOH was used as nucleophile (cf Scheme 9).^[21] n.d. = not determined.

In comparison to **14** that was reported to afford the highest selectivity (63% *ee*; Table 2, entry 1 and Scheme 9) and **15** (entry 2) some of the tested peptide catalysts perform considerably well with enantioselectivities ranging from 39–44% (entries 8–10 and entry 12). Thus, peptides **1**, **3**, **30** and **33** may be considered as appropriate candidates for further modification and optimization. Moreover, our approach allows the direct use of the amino acid derivatives instead

of the *O*-acetylated azlactones (such as **16**) making this reaction particular attractive. Importantly, catalyst **14** usually gave only traces of **17** under these reaction conditions.

Of special note, *N*-benzoylalanine methylester always formed as a major side-product along with the azlactone upon opening with methanol, although **17** was the only product after the acetylation step. Reasonably, **17** is prone to deacetylation affording the azlactone and subsequently the methylester, a side-reaction that was also described by Steglich and Höfle.^[13a] Therefore, the influence of the nucleophile was investigated using DMAP as catalyst and different alcohols, amines and thiols (Table 3).

Table 3. Influence of the nucleophile on the yield of isolated **23**.

Entry	Nucleophile	Product	Yield (%)
1	MeOH (1.0 equiv)	23a	12
2	MeOH (2.5 equiv)	23a	30
3	MeOH (10 equiv)	23a	31
4	MeOH/DCM 1:1	23a	31
5	EtOH (10 equiv)	23b	16
6	<i>i</i> -PrOH (10 equiv)	23c	10
7	<i>i</i> -PrOH ^b	23c	44
8	BnNH ₂	23d	14
9	<i>n</i> -PrNH ₂	23e	25
10	<i>i</i> -PrNH ₂	23f	13
11	EtSH	23g	62
12	<i>i</i> -PrSH	23h	45

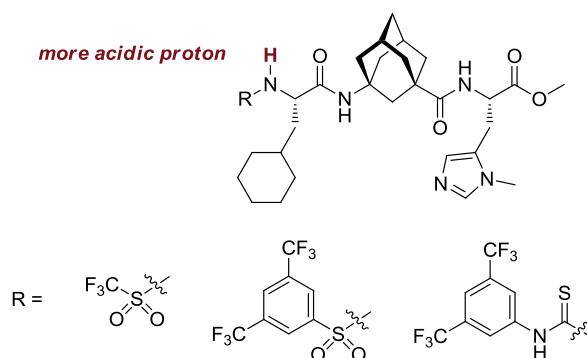
^a *O*-acetylated azlactone **16** was used as starting material employing a literature procedure.^[21]

First, the appropriate amount of the nucleophile was determined using methanol (Table 3, entries 1–4). We found that 2.5 equiv afford 30% of desired product **23a** and the yield did not increase with higher amounts of methanol. Consequently, the products **23a–23h** were prepared employing 2.5 equiv or 10 equiv of the nucleophile. The yield decreased when ethanol or isopropanol were

used for the opening of **17** (entries 5 and 6). This is in contrast to the results reported by Dietz and Gröger where isopropanol afforded significantly higher yields.^[21] Indeed, when the reaction was performed with **16** as starting material without addition of acetic anhydride or carbodiimide product **23c** was isolated with 44% yield (entry 7). Although the difference in yield is not yet understood it probably results from the addition of the carbodiimide or its corresponding urea that is formed. Note that benzylalcohol was previously tested as well for the opening of a related derivative, but no product could be isolated (see Chapter VI, Supporting Information). Next, different amines were investigated, but also afforded low yields (entries 8–10). However, according to a reported procedure the corresponding amides are accessible through the opening of **17** with *N*-hydroxysuccinimide and subsequent treatment with, *e.g.*, benzylamine.^[13a] An important observation was made with thiols that gave the thioesters **23g** and **23h** with 62% and 45% yield, respectively. According to Pearson's concept of hard and soft acids and bases (HSAB),^[23] thiols are softer nucleophiles compared to alcohols and amines. Obviously, former preferentially react with the C-5 carbonyl on **17**. This result may not only lead to a high yielding enantioselective Steglich rearrangement-type reaction, but also allows the preparation of synthetically useful thioester derivatives.

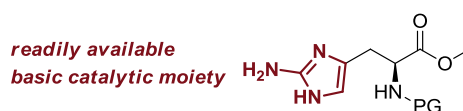
5. Conclusions and Outlook

The results described herein build the basis for future investigations. The additionally performed computational and experimental investigations reveal the importance of proper enolate-binding that also derives from attractive side-chain interactions for the enantioselective Dakin–West reaction. It was found that the anhydride has a major influence on selectivity and conversion, whereas the *N*-protecting group may be modified. As discussed above, computing the transition states is indispensable to draw a complete picture. Although the previously reported enantioselectivities could not be enhanced so far, this may be possible by a judicious modification of the peptide catalyst. Apparently, the Boc-protecting group could be exchanged by phenylalanine without significant influence on conversion and selectivity. Thus, replacing the Boc-group by, *e.g.*, electron-deficient CF₃SO₂–, 3,5-(CF₃)PhSO₂–, or the corresponding thiourea would lead to the acidification of the amine and presumably to stronger enolate binding (Scheme 10). The enhanced binding may also allow the use of different (sterically demanding) anhydrides.



Scheme 10. Possible modification of oligopeptide **1** to achieve stronger enolate binding.

The development of a peptide that is capable of catalyzing the demanding enantioselective decarboxylative protonation of malonic acid derivatives or related substrates with high selectivities is another important issue. So far, only one experiment has been performed that afforded the product with low conversion and selectivity (16% *ee*). Obviously, the synthesis and screening of novel peptides is inevitable to increase the observed enantioselectivity. On the other hand, catalytic moieties with increased basicity are required and may be potentially used for further Brønsted base mediated reactions. An example for such a basic site is offered by 2-aminoimidazole that can be readily synthesized and introduced into peptide catalysts (Scheme 11).



Scheme 11. Example for a novel catalytic moiety.

The possibility to obtain enantiomerically enriched *C*-acetylated azlactones directly from the corresponding amino acid derivatives is another important finding. As the selectivities are yet moderate (up to 44% *ee*), extensive catalyst screening and modification is also necessary in this case. Moreover, the previously reported and reproduced finding that deacetylation occurs as a major side-reaction during opening of the intermediate products can be largely avoided by using soft nucleophiles, such as thiols. Other nucleophiles, *e.g.*, hydride, or a direct reduction after azlactone opening can also be envisaged and may allow the one-pot synthesis of synthetically useful α -amino β -hydroxy acid derivatives (*vide supra*). This is now a part of our ongoing research.

6. Experimental Section

6.1 General Remarks

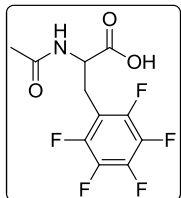
Materials and methods. Unless otherwise specified, reagents were purchased from commercial suppliers at the highest purity grade available and were used as received. All solvents were distilled prior to use. Dry and absolute solvents were prepared using standard laboratory procedures and were stored over appropriate drying agents under argon or nitrogen atmosphere. Acetic anhydride was distilled and stored under nitrogen.

Flash column chromatography was performed using MN silica gel 60 M (Macherey-Nagel; 0.040 – 0.063 mm, 230 – 400 mesh ASTM). Analytical thin-layer chromatography (TLC) was performed using precoated polyester sheets Polygram[®] SIL G/UV₂₅₄ (Macherey-Nagel; 0.2 mm silica gel layer with fluorescent indicator). Visualization of the developed chromatograms was accomplished by irradiation with a UV lamp at 254 nm and/or phosphomolybdic acid solution or potassium permanganate solution, respectively. TLC R_f values are reported.

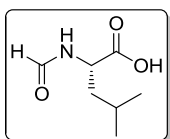
Instrumentation. NMR spectra were recorded on Bruker AV600, AV400 or AV200 spectrometers, respectively, at 298 K. Chemical shifts (δ) are given in ppm relative to tetramethylsilane (TMS, δ = 0.00 ppm) as the internal standard or to the respective solvent residual peaks (CDCl₃: δ = 7.26 and 77.16 ppm; DMSO-d₆: δ = 2.50 and 39.52 ppm; D₂O: δ = 4.79 ppm; MeOH-d₄: δ = 3.31 and 49.00 ppm).^[24] Data are reported as follows: chemical shift, multiplicity (s = singlet, d = doublet, t = triplet, q = quartet, p = pentet, hept = heptet, m = multiplet, br = broad, or combinations thereof), coupling constants (Hz), integration. Infrared spectra were acquired on Bruker IFS25 or ALPHA spectrometers. ESI mass spectrometry was performed employing a Finnigan LCQDuo spectrometer using methanol solutions of the respective compounds. High resolution mass spectrometry (HRMS) was performed employing a Thermo Scientific LTQ FT Ultra spectrometer (ESI) using methanol solutions of the respective compounds or a Finnigan MAT95 sectorfield spectrometer (EI). Elemental analysis was performed on a Thermo Flash EA 1112. Melting points were measured using a Krüss KSP1N capillary melting point apparatus and are uncorrected. GC-MS was carried out on a Hewlett Packard 5890 gas chromatograph with flame-ionization detector (FID) and Hewlett Packard 5971 mass selective detector (EI, 70 eV) equipped with J & W Scientific fused silica DB-5MS column (30 m \times 0.25 mm). Enantioselectivities were determined by chiral stationary phase GC analyses on Hewlett Packard 5890 or 6890 gas chromatographs, respectively, or by chiral stationary phase HPLC with a Dionex P680 pump in conjunction with a Shodex RI-101 detector. Preparative HPLC was performed employing a Gynkotek M480 pump with Knauer WellChrom K-2501 spectrophotometer and a Dionex UltiMate 3000 equipped with a Shodex RI-101 detector for analytical runs.

6.2 Availability of Starting Materials

N-acetyl DL-leucine (**6a**) and *N*-benzoyl DL-leucine (**6d**) were purchased from commercial suppliers and were used as received.



2-Acetamido-3-(perfluorophenyl)propanoic acid (4). For the synthesis and characterization see Chapter VI, Supporting Information.



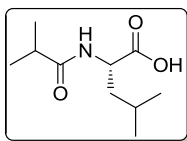
(S)-2-formamido-4-methylpentanoic acid (6b). According to a literature procedure,^[25] L-leucine (1.313 g, 10.0 mmol) was dissolved in formic acid (50 mL). After cooling to 0 °C with an ice-bath acetic anhydride (28 mL) was

slowly added with stirring. The reaction mixture was allowed to warm to ambient temperature and stirred over night. H₂O (50 mL) was then added and all volatiles were removed under reduced pressure. After addition of acetone, flash evaporation, and drying *in vacuo* the desired product (1.425 g, 8.95 mmol, 90%) was obtained as a colorless solid.

¹H NMR (400 MHz, DMSO-*d*₆): δ = 12.54 (br s, 1H), 8.33 (d, *J* = 8.0 Hz, 1H), 4.32 – 4.25 (m, 1H), 1.67 – 1.56 (m, 1H), 1.53 – 1.49 (m, 2H), 0.89 (d, *J* = 6.5 Hz, 3H), 0.85 (d, *J* = 6.5 Hz, 3H) ppm.

¹³C NMR (100 MHz, DMSO-*d*₆): δ = 173.7, 160.9, 48.8, 24.3, 22.8, 21.3 ppm.

The NMR spectra are in accordance with those reported in the literature.^[25]



(S)-2-isobutyramido-4-methylpentanoic acid (6c). To a suspension of L-leucine (393.5 mg, 3.0 mmol) in EtOAc (3 mL) were added Et₃N (1.25 mL, 912.5 mg, 9.0 mmol) and isobutyric anhydride (1.0 mL, 954.0 mg, 6.0 mmol).

After stirring at rt over night 1 N HCl (20 mL) was added, the phases were separated, and the aqueous phase was extracted with EtOAc (3 × 20 mL). The combined organic phases were subsequently washed with 1 N HCl (2 × 20 mL) and brine (20 mL), and dried (Na₂SO₄). After

filtration the solvent was removed under reduced pressure. The obtained colorless oil was lyophilized to remove residual isobutyric acid. Crystallization from H₂O, filtration, and drying *in vacuo* afforded **6c** (459.2 mg, 2.3 mmol, 76%) as a colorless waxy solid.

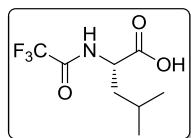
¹H NMR (400 MHz, MeOH-d₄): δ = 4.42 (dd, J = 8.0, 6.9 Hz, 1H), 2.52 (hept, J = 6.5 Hz, 1H), 1.76 – 1.66 (m, 1H), 1.66 – 1.60 (m, 2H), 1.12 (d, J = 2.2 Hz, 3H), 1.11 (d, J = 2.2 Hz, 3H), 0.97 (d, J = 6.4 Hz, 3H), 0.93 (d, J = 6.3 Hz, 3H) ppm.

¹³C NMR (100 MHz, MeOH-d₄): δ = 180.2, 176.2, 51.8, 41.6, 35.9, 26.1, 23.4, 21.8, 19.9, 19.7 ppm.

IR (ATR): $\tilde{\nu}$ = 3336, 2963, 2934, 2875, 1711, 1628, 1544, 1469, 1388, 1370, 1328, 1266, 1229, 1210, 1154, 1098, 975, 940, 860, 688, 581 cm⁻¹.

HRMS (ESI): m/z = 224.1268 [M+Na]⁺ (calcd m/z = 224.1263); m/z = 425.2634 [2M+Na]⁺ (calcd m/z = 425.2628).

Elem. Anal.: calcd for C₁₀H₁₉NO₃: C 59.68, H 9.52, N 6.96; found: C 59.43, H 9.73, N 7.08.



(S)-4-methyl-2-(2,2,2-trifluoroacetamido)pentanoic acid (6e). According to a literature procedure,^[26] Et₃N (750 μ L, 514.6 mg, 5.1 mmol) was added to a stirred solution of L-leucine (708.0 mg, 5.4 mmol) in methanol (2.5 mL). After 5 min ethyl trifluoroacetate (805 μ L, 958 mg, 6.74 mmol) was added and the reaction mixture was stirred over-night. All volatiles were removed under reduced pressure, the residue was dissolved with H₂O (15 mL), acidified with conc. HCl (2.3 mL), and extracted with EtOAc (3 \times 15 mL). The combined organic extracts were washed with brine (20 mL) and dried (MgSO₄). The drying agent was filtered-off and the solvent was removed *in vacuo* affording **6e** (224.5 mg, 0.99 mmol, 18%) as a colorless crystalline solid.

¹H NMR (400 MHz, CDCl₃): δ = 9.60 (br s, 1H), 6.72 (d, J = 8.3 Hz, 1H), 4.73 – 4.65 (m, 1H), 1.86 – 1.77 (m, 1H), 1.76 – 1.65 (m, 2H), 0.99 (d, J = 6.4 Hz, 3H), 0.98 (d, J = 6.4 Hz, 3H) ppm.

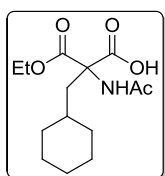
¹³C NMR (100 MHz, CDCl₃): δ = 176.7, 157.2 (q, J = 37.9 Hz), 115.7 (q, J = 287.6 Hz) 51.2, 41.1, 25.0, 22.8, 21.9 ppm.

^{19}F NMR (376 MHz, CDCl_3): $\delta = -75.9$ ppm.

IR (KBr): $\tilde{\nu} = 3295, 3109, 2964, 2875, 2742, 1709, 1560, 1469, 1427, 1391, 1373, 1322, 1276, 1188, 1161, 966, 934, 873, 776, 731, 699, 606, 547, 520, 467, 430\text{ cm}^{-1}$.

HRMS (ESI): $m/z = 250.0669$ $[\text{M}+\text{Na}]^+$ (calcd $m/z = 250.0667$).

Elem. Anal.: calcd for $\text{C}_8\text{H}_{12}\text{F}_3\text{NO}_3$: C 42.29, H 5.32, N 6.17; found: C 42.00, H 5.14, N 5.68.



2-Acetamido-2-(cyclohexylmethyl)-3-ethoxy-3-oxopropanoic acid (12). *Di-*

ethyl 2-acetamido-2-(cyclohexylmethyl)malonate: A solution of NaOEt (0.750 g, 11.02 mmol) and diethyl acetamidomalonate (2.00g, 9.21 mmol) in 10 mL abs.

EtOH was stirred at reflux for 30 min under argon. Bromomethylcyclohexane (1.30 mL, 1.65 g, 9.32 mmol) was added dropwise and the resulting solution was refluxed for additional 24 h. The reaction mixture was concentrated under reduced pressure and extracted with Et_2O ($5 \times 25\text{ mL}$). The combined organic extracts were successively washed with H_2O ($2 \times 20\text{ mL}$), sat. aq. NaHCO_3 ($2 \times 20\text{ mL}$), and H_2O (20 mL), dried over Na_2SO_4 , filtered, and the solvent was removed under reduced pressure. The residual oil was triturated with hexane and left standing at $-20\text{ }^\circ\text{C}$ overnight to afford the desired alkylation product (1.343 g, 4.28 mmol, 46%) as colorless crystals.

^1H NMR (400 MHz, CDCl_3): $\delta = 6.83$ (br s, 1H), 4.21 (q, $J = 7.1\text{ Hz}$, 4H), 2.27 (d, $J = 6.0\text{ Hz}$, 2H), 2.02 (s, 3H), 1.65 – 1.50 (m, 5H), 1.23 (t, $J = 7.1\text{ Hz}$, 6H), 1.20 – 1.06 (m, 4H), 0.98 – 0.88 (m, 2H) ppm.

^{13}C NMR (100 MHz, CDCl_3): $\delta = 169.0, 168.8, 66.0, 62.6, 38.9, 33.9, 33.5, 26.3, 26.2, 23.2, 14.1$ ppm.

IR (KBr): $\tilde{\nu} = 3281, 2976, 2921, 2851, 1747, 1647, 1510, 1445, 1373, 1298, 1274, 1231, 1190, 1136, 1098, 1052, 1019, 953, 900, 862, 841, 805, 769, 693, 608\text{ cm}^{-1}$.

The spectroscopic data are in accordance with those reported.^[27]

The malonate (51.5 mg, 0.16 mmol) was dissolved in 1,4-dioxane (1.6 mL). LiOH (4.8 mg, 0.20 mmol) and H_2O (0.8 mL) were added and the reaction mixture was stirred at rt for 42 h. After

dilution with H₂O (15 mL) the solution was acidified with 1 N HCl. Extraction with EtOAc (3 × 10 mL), drying over Na₂SO₄, and removal of the solvent under reduced pressure without warming afforded **12** (46.6 mg, 0.16 mmol, quant.) as a colorless solid. The obtained product was contaminated with the corresponding decarboxylation product.

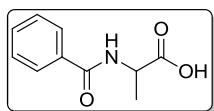
¹H NMR (400 MHz, DMSO-d₆): δ = 13.44 (br s, 1H), 8.11 (s, 1H), 4.07 (q, J = 7.1 Hz, 2H), 2.14 – 1.98 (m, 2H), 1.89 (s, 3H), 1.63 – 1.50 (m, 5H), 1.20 – 1.08 (m, 4H), 1.13 (t, J = 7.0 Hz, 3H), 0.94 – 0.82 (m, 2H) ppm.

¹³C NMR (100 MHz, DMSO-d₆): δ = 169.6, 168.7, 168.3, 65.4, 61.1, 38.8, 33.6, 33.3, 32.8, 25.7, 25.7, 25.7, 22.2, 13.8 ppm.

IR (KBr): $\tilde{\nu}$ = 3321, 2923, 2852, 1724, 1656, 1605, 1523, 1446, 1370, 1301, 1268, 1253, 1203, 1171, 1098, 1046, 1017, 953, 894, 867, 752, 705, 651, 619, 539, 466, 434 cm⁻¹.

HRMS (ESI): m/z = 308.1470 [M+Na]⁺ (calcd m/z = 308.1474).

Elem. Anal.: calcd for C₁₄H₂₃NO₅: C 58.93, H 8.12, N 4.91; found: C 59.16, H 8.17, N 4.85.



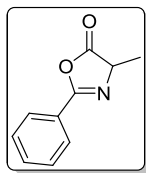
***N*-Benzoyl D,L-alanine (22).** Following a literature procedure,^[28] D,L-alanine (3.56 g, 40.0 mmol) and NaOH (6.40 g, 160.0 mmol) were dissolved in H₂O/acetonitrile (3:1, 130 mL). After cooling to 0 °C with an ice-bath,

benzoyl chloride (4.84 mL, 5.90 g, 42.0 mmol) was added dropwise. The reaction mixture was stirred at 0 °C for 2 h and for 1 h at rt. All volatiles were removed under reduced pressure and the residue was acidified with conc. HCl (60 mL) to precipitate the desired product. The obtained colorless solid was filtered off, washed with cold Et₂O, and dried over paraffin wax and CaCl₂ in a vacuum desiccator over night. Yield: 5.58 g (28.9 mmol, 72%) as colorless solid.

¹H NMR (400 MHz, DMSO-d₆): δ = 12.57 (br s, 1H), 8.69 (d, J = 7.3 Hz, 1H), 7.91 – 7.87 (m, 2H), 7.56 – 7.51 (m, 1H), 7.50 – 7.44 (m, 2H), 4.42 (p, J = 7.3 Hz, 1H), 1.40 (d, J = 7.3 Hz, 3H) ppm.

¹³C NMR (100 MHz, DMSO-d₆): δ = 174.2, 166.2, 133.9, 131.4, 128.3, 127.5, 48.2, 16.9 ppm.

The NMR data are in accordance with the literature.^[29]

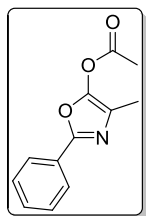


4-Methyl-2-phenyloxazol-5(4H)-one (24). Following a literature procedure,^[30] *N*-Benzoyl D,L-alanine (**22**; 1.937 g, 10.0 mmol) was suspended in dry CH₂Cl₂ (80 mL). After cooling to 0 °C with an ice-bath, 1-ethyl-3-(3-dimethylamino-propyl)carbodiimide hydrochloride (EDC • HCl; 2.182 g, 11.4 mmol) was added and the reaction mixture was stirred at this temperature for 2 h. The resulting clear solution was diluted with CH₂Cl₂ (80 mL) and successively washed with ice-cold H₂O (30 mL), cold sat. aq. NaHCO₃ (2 × 30 mL), and ice-cold H₂O (30 mL). After drying of the organic phase over Na₂SO₄, filtration and removal of the solvent *in vacuo* azlactone **24** (1.554, 8.87 mmol, 89%) was obtained as colorless solid.

¹H NMR (400 MHz, CDCl₃): δ = 8.01 – 7.97 (m, 2H), 7.60 – 7.54 (m, 1H), 7.52 – 7.44 (m, 2H), 4.45 (q, *J* = 7.6 Hz, 1H), 1.59 (d, *J* = 7.6 Hz, 3H) ppm.

¹³C NMR (100 MHz, CDCl₃): δ = 179.0, 161.8, 132.9, 128.9, 128.0, 125.9, 61.1, 17.0 ppm.

The NMR data are in accordance with the literature.^[30]



4-Methyl-2-phenyloxazol-5-yl acetate (16). According to a reported procedure,^[21b] 4-Methyl-2-phenyloxazol-5(4H)-one (**24**; 174.5 mg, 1.0 mmol) and acetyl chloride (106 μ L, 116.6 mg, 1.49 mmol) were dissolved in abs. THF. After cooling to 0 °C with an ice-bath, Et₃N (207 μ L, 151.1 mg, 1.49 mmol) was added dropwise and the reaction mixture was stirred at 0 °C for 1 h. The precipitated colorless solid was filtered off. The solvent was removed under reduced pressure, the residue redissolved in TBME and washed with 1 N HCl (2 × 5 mL). The organic layer was dried over Na₂SO₄ and the solvent was removed *in vacuo* yielding **16** (185.5 mg, 0.85 mmol, 85%) as colorless solid.

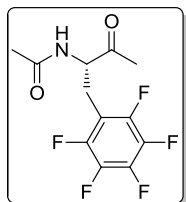
¹H NMR (400 MHz, CDCl₃): δ = 7.96 – 7.91 (m, 2H), 7.45 – 7.39 (m, 3H), 2.36 (s, 3H), 2.11 (s, 3H) ppm.

¹³C NMR (100 MHz, CDCl₃): δ = 167.3, 155.1, 145.8, 130.4, 128.8, 127.2, 125.9, 120.6, 20.3, 10.4 ppm.

The NMR data are in accordance with the literature.^[13a]

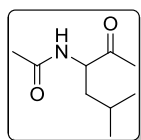
6.3 Synthesis of Racemic Products

The *N*-protected amino acids were converted to the corresponding racemic methylketones employing the DMAP-catalyzed procedure reported by Steglich and Höfle.^[11] Yields are not optimized for the individual substrates.



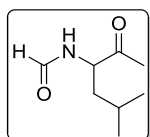
***N*-(3-oxo-1-(perfluorophenyl)butan-2-yl)acetamide (5).** For the synthesis and characterization see Chapter VI, Supporting Information.

Chiral stationary phase GC: FS-Hydrodex β -TBDAC column (Macherey-Nagel), $l = 30$ m; splitflow: 80 mL/min; precolumn pressure: 0.8 bar; T (injector + detector) = 250 °C; conditions: 100 – 180 °C, 2 °C/min. Retention times: t_R (*R*) = 25.8 min, t_R (*S*) = 26.6 min.



***N*-(5-methyl-2-oxohexan-3-yl)acetamide (7a).** For the synthesis and characterization see Chapter VI, Supporting Information.

Chiral stationary phase GC: FS-Hydrodex β -TBDAC column (Macherey-Nagel), $l = 30$ m; splitflow: 80 mL/min; precolumn pressure: 0.8 bar; T (injector + detector) = 250 °C; conditions: 100 – 180 °C, 2 °C/min. Retention times: t_R (*R*) = 25.8 min, t_R (*S*) = 26.6 min.



***N*-(5-methyl-2-oxohexan-3-yl)formamide (7b).** *General procedure:* A mixture of **6b** (159.2 mg, 1.0 mmol), DMAP (6.1 mg, 0.05 mmol, 5 mol%), Et₃N (0.2 mL, 146.0 mg, 1.4 mmol), and acetic anhydride (0.2 mL, 216.0 mg, 2.1 mmol) was stirred at rt for 1 h. Glacial acetic acid (1.5 mL) was then added and stirring was continued for 1 h. After concentration of the solution under reduced pressure, the residual yellow oil was treated with sat. aq. NaHCO₃ (25 mL), followed by extraction with CHCl₃ (3 \times 10 mL). The combined organic layers were washed with 1 N HCl (2 \times 5 mL) and brine (10 mL), dried over Na₂SO₄, filtered, and the solvent was removed *in vacuo*. The crude product was purified by column chromatography eluting with EtOAc to obtain **7b** (47.2 mg, 0.3 mmol, 30%) as a colorless oil. TLC (EtOAc): $R_f = 0.50$.

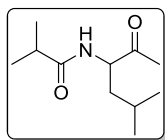
^1H NMR (400 MHz, CDCl_3): δ = 8.22 (s, 1H), 6.17 (br s, 1H), 4.80 – 4.74 (m, 1H), 2.24 (s, 3H), 1.72 – 1.61 (m, 2H), 1.46 – 1.38 (m, 1H), 0.99 (d, J = 6.2 Hz, 3H), 0.94 (d, J = 6.4 Hz, 3H) ppm.

^{13}C NMR (100 MHz, CDCl_3): δ = 206.7, 160.9, 56.0, 40.7, 27.4, 25.1, 23.4, 21.9 ppm.

IR (film): $\tilde{\nu}$ = 2959, 1722, 1665, 1530, 1384, 1262, 1022, 573, 517, 462, 426, 412 cm^{-1} .

HRMS (ESI): m/z = 180.1000 $[\text{M}+\text{Na}]^+$ (calcd m/z = 180.1001).

Chiral stationary phase GC: FS-Hydrodex β -TBDAC column (Macherey-Nagel), l = 30 m; splitflow: 80 mL/min; precolumn pressure: 0.8 bar; T (injector + detector) = 250 $^{\circ}\text{C}$; conditions: 100 – 180 $^{\circ}\text{C}$, 2 $^{\circ}\text{C}/\text{min}$. Retention times: t_{R} (R) = 30.5 min, t_{R} (S) = 32.0 min.



***N*-(5-methyl-2-oxohexan-3-yl)isobutyramide (7c)**. The title compound was synthesized on 0.854 mmol scale employing the reaction conditions and work-up procedure described for **7b**. Reaction time was 2 h for each step. Purification by column chromatography eluting with EtOAc afforded **7c** (114.5 mg, 0.575 mmol, 67%) as colorless oil. TLC (EtOAc): R_f = 0.73.

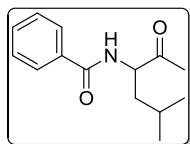
^1H NMR (400 MHz, CDCl_3): δ = 6.02 (d, J = 7.7 Hz, 1H), 4.65 (ddd, J = 9.1, 7.8, 3.5 Hz, 1H), 2.40 (hept, J = 6.9 Hz, 1H), 2.20 (s, 3H), 1.68 – 1.57 (m, 2H), 1.43 – 1.34 (m, 1H), 1.15 (d, J = 6.9 Hz, 3H), 1.14 (d, J = 6.9 Hz, 3H), 0.96 (d, J = 6.1 Hz, 3H), 0.92 (d, J = 6.4 Hz, 3H) ppm.

^{13}C NMR (100 MHz, CDCl_3): δ = 213.9, 170.0, 54.9, 41.1, 38.3, 25.2, 23.6, 23.3, 22.0, 19.9, 19.1, 17.8 ppm.

IR (ATR): $\tilde{\nu}$ = 3293, 2960, 2873, 1716, 1646, 1530, 1469, 1385, 1368, 1209, 1176, 1132, 1097, 1019, 928, 599, 549 cm^{-1} .

HRMS (ESI): m/z = 222.1472 $[\text{M}+\text{Na}]^+$ (calcd m/z = 222.1470).

Chiral stationary phase GC: FS-Hydrodex β -TBDAC column (Macherey-Nagel), l = 30 m; splitflow: 80 mL/min; precolumn pressure: 0.8 bar; T (injector + detector) = 250 $^{\circ}\text{C}$; conditions: 100 – 180 $^{\circ}\text{C}$, 2 $^{\circ}\text{C}/\text{min}$. Retention times: t_{R} (R) = 26.9 min, t_{R} (S) = 27.3 min.



***N*-(5-methyl-2-oxohexan-3-yl)benzamide (7d).** The title compound was synthesized on 2.0 mmol scale employing the reaction conditions and work-up procedure described for **7b**. Reaction time was 2 h for each step. Purification by column chromatography eluting with EtOAc afforded **7d** (391.6 mg, 1.68 mmol, 84%) as colorless oil. TLC (EtOAc): R_f = 0.81.

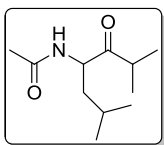
^1H NMR (400 MHz, CDCl_3): δ = 7.82 – 7.78 (m, 2H), 7.53 – 7.48 (m, 1H), 7.46 – 7.41 (m, 2H), 6.76 (d, J = 7.7 Hz, 1H), 4.89 (ddd, J = 9.1, 7.7, 3.5 Hz, 1H), 2.28 (s, 3H), 1.79 – 1.70 (m, 2H), 1.58 – 1.49 (m, 1H), 1.03 (d, J = 6.1 Hz, 3H), 0.95 (d, J = 6.3 Hz, 3H) ppm.

^{13}C NMR (100 MHz, CDCl_3): δ = 207.5, 167.3, 134.1, 131.9, 128.7, 127.2, 57.8, 40.9, 27.5, 25.3, 23.5, 22.1 ppm.

IR (ATR): $\tilde{\nu}$ = 3307, 3064, 2957, 2871, 1716, 1637, 1603, 1580, 1525, 1488, 1469, 1367, 1292, 1210, 1178, 1156, 1133, 1074, 1027, 927, 801, 711, 693 cm^{-1} .

HRMS (ESI): m/z = 256.1304 $[\text{M}+\text{Na}]^+$ (calcd m/z = 256.1314).

Chiral stationary phase GC: FS-Hydrodex β -6-TBDM column (Macherey-Nagel), l = 30 m; splitflow: 80 mL/min; precolumn pressure: 0.8 bar; T (injector + detector) = 250 $^{\circ}\text{C}$; conditions: 100 – 160 $^{\circ}\text{C}$, 1 $^{\circ}\text{C}/\text{min}$; 160 – 220 $^{\circ}\text{C}$, 1.5 $^{\circ}\text{C}/\text{min}$. Retention times: t_R (R) = 80.6 min, t_R (S) = 80.9 min (no complete baseline separation).



***N*-(2,6-dimethyl-3-oxoheptan-4-yl)acetamide (7f).** The title compound was prepared on 1.0 mmol scale employing the reaction conditions for the synthesis of **7b**. After stirring for 24 h the reaction mixture was diluted with Et_2O and successively washed with sat. aq. NaHCO_3 (3×10 mL), 1 N HCl (3×10 mL), and brine (10 mL). The organic phase was dried over Na_2SO_4 , filtered, and the solvent was removed under reduced pressure. Purification by column chromatography eluting with EtOAc afforded **7f** (17.2 mg, 0.086 mmol, 9%) as a slightly yellow oil. TLC (EtOAc): R_f = 0.63.

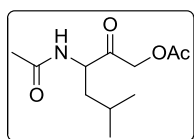
^1H NMR (400 MHz, CDCl_3): δ = 6.10 (d, J = 8.4 Hz, 1H), 4.85 (ddd, J = 9.8, 8.4, 3.7 Hz, 1H), 2.80 (hept, J = 6.8 Hz, 1H), 2.00 (s, 3H), 1.73 – 1.60 (m, 2H), 1.55 – 1.47 (m, 1H), 1.13 (d, J = 7.0 Hz, 3H), 1.10 (d, J = 6.9 Hz, 3H), 0.97 (d, J = 6.5 Hz, 3H), 0.91 (d, J = 6.6 Hz, 3H) ppm.

^{13}C NMR (100 MHz, CDCl_3): δ = 213.9, 170.0, 54.9, 41.1, 38.3, 25.2, 23.6, 23.3, 22.0, 19.9, 19.1, 17.8 ppm.

IR (ATR): $\tilde{\nu}$ = 3272, 2960, 2935, 2873, 1783, 1715, 1650, 1535, 1468, 1370, 1265, 1137, 1097, 1041, 991, 923, 658, 595, 467 cm^{-1} .

HRMS (ESI): m/z = 222.1477 $[\text{M}+\text{Na}]^+$ (calcd m/z = 222.1470).

Chiral stationary phase GC: FS-Hydrodex β -TBDAC column (Macherey-Nagel), l = 30 m; splitflow: 80 mL/min; precolumn pressure: 0.8 bar; T (injector + detector) = 250 $^{\circ}\text{C}$; conditions: 100 – 180 $^{\circ}\text{C}$, 2 $^{\circ}\text{C}/\text{min}$. Retention times: t_R (R) = 26.9 min, t_R (S) = 27.6 min.



3-Acetamido-5-methyl-2-oxohexyl acetate (7i). *2-acetoxyacetic anhydride:*

To 2-acetoxyacetic acid (1.049 g, 8.88 mmol) in dry CH_2Cl_2 (50 mL) was added 1-ethyl-3-(3-dimethylaminopropyl)carbodiimide hydrochloride (EDC • HCl; 0.955 g, 4.98 mmol) and the reaction mixture was stirred at rt for 1 h. The resulting solution was washed with cold H_2O (2×10 mL), cold sat. aq. NaHCO_3 (10 mL), and cold H_2O (20 mL). The organic phase was dried over Na_2SO_4 , filtered, and the solvent was removed under reduced pressure affording the anhydride as a colorless liquid that was used without further purification.

^1H NMR (400 MHz, CDCl_3): δ = 4.73 (s, 4H), 2.18 (s, 6H) ppm.

^{13}C NMR (100 MHz, CDCl_3): δ = 170.1, 162.8, 60.7, 20.4 ppm.

DMAP (6.11 mg, 0.05 mmol, 5 mol%) and **6a** (173.2 mg, 1.0 mmol) were suspended in CH_2Cl_2 (0.2 mL). 2-Acetoxyacetic anhydride (0.35 mL, 457.6 mg, 2.1 mmol) and Et_3N (0.2 mL, 146.0 mg, 1.44 mmol) were added and the reaction mixture was allowed to stir at rt for 2.5 h. Glacial acetic acid (1.5 mL) was then added and stirring was continued for 1 h. The work-up was performed as described for **7b**. The crude product was purified by column chromatography eluting with EtOAc to obtain **7i** (57.1 mg, 0.25 mmol, 25%) as a colorless oil. TLC (EtOAc): R_f = 0.54.

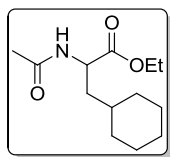
^1H NMR (400 MHz, CDCl_3): δ = 6.42 (d, J = 7.9 Hz, 1H), 4.78 (d, J = 2.9 Hz, 2H), 4.67 (ddd, J = 9.8, 7.9, 4.2 Hz, 1H), 2.12 (s, 3H), 1.98 (s, 3H), 1.69 – 1.52 (m, 2H), 1.44 – 1.35 (m, 1H), 0.91 (d, J = 6.4 Hz, 3H), 0.90 (d, J = 6.5 Hz, 3H) ppm.

^{13}C NMR (100 MHz, CDCl_3): δ = 203.5, 170.7, 170.3, 66.7, 53.8, 40.0, 24.9, 23.2, 22.9, 21.7, 20.5 ppm.

IR (ATR): $\tilde{\nu}$ = 3272, 2959, 2873, 1734, 1651, 1535, 1469, 1417, 1371, 1227, 1145, 1042, 921, 842, 732, 599, 438 cm^{-1} .

HRMS (ESI): m/z = 252.1215 $[\text{M}+\text{Na}]^+$ (calcd m/z = 252.1212); m/z = 481.2536 $[2\text{M}+\text{Na}]^+$ (calcd m/z = 481.2526).

Chiral stationary phase GC: FS-Hydrodex β -TBDAC column (Macherey-Nagel), l = 30 m; splitflow: 80 mL/min; precolumn pressure: 0.8 bar; T (injector + detector) = 250 $^{\circ}\text{C}$; conditions: 100 – 200 $^{\circ}\text{C}$, 2 $^{\circ}\text{C}/\text{min}$. Retention times: $t_{\text{R}}(R)$ = 44.7 min, $t_{\text{R}}(S)$ = 45.2 min.



Ethyl 2-acetamido-3-cyclohexylpropanoate (13). *Cyclohexylalanine hydrochloride*: diethyl 2-acetamido-2-(cyclohexylmethyl)malonate (626.8 mg, 2.0 mmol; *vide supra*) was heated to reflux with 6 N HCl (15 mL) overnight. After cooling to rt and filtration the desired product (282.5 mg, 1.36 mmol, 68%) was obtained as a colorless solid.

^1H NMR (600 MHz, $\text{DMSO}-d_6$): δ = 13.67 (br s, 1H), 8.45 (s, 3H), 3.83 – 3.79 (m, 1H), 1.74 – 1.57 (m, 7H), 1.53 – 1.45 (m, 1H), 1.26 – 1.08 (m, 3H), 0.93 – 0.81 (m, 2H) ppm.

^{13}C NMR (150 MHz, $\text{DMSO}-d_6$): δ = 171.4, 49.8, 37.6, 32.6, 32.4, 32.1, 25.8, 25.5, 25.4 ppm.

The NMR data are in accordance with those reported in the literature.^[27]

Ethyl 2-amino-3-cyclohexylpropanoate hydrochloride: Following a literature procedure,^[31] trimethylsilyl chloride (134 μL , 115.2 mg, 1.06 mmol) was added dropwise to cyclohexylalanine hydrochloride (110.0 mg, 0.53 mmol). EtOH (1.5 mL) was then slowly added and the resulting suspension was stirred at rt for 49 h. After removal of all volatiles *in vacuo* the desired product was obtained as a colorless solid.

The ethylester (117.8 mg, 0.50 mmol) was suspended in CH_2Cl_2 (5 mL). After cooling to 0 $^{\circ}\text{C}$ with an ice-bath, Et_3N (155 μL , 113.2 mg, 1.12 mmol) was added and stirred for 15 min. Acetic anhydride (150 μL , 162.0 mg, 1.59 mmol) was added, the reaction mixture was allowed to warm to rt and stirred for 24 h. The resulting solution was diluted with EtOAc (25 mL), washed with 1 N HCl (3×10 mL), sat. aq. NaHCO_3 (3×10 mL) and brine (10 mL), and dried over Na_2SO_4 . After removal of the solvent *in vacuo* ethyl 2-acetamido-3-cyclohexylpropanoate **13** (106.3 mg, 0.44 mmol, 88%) was obtained as colorless oil.

^1H NMR (400 MHz, CDCl_3): δ = 5.91 (d, J = 8.4 Hz, 1H), 4.66 – 4.59 (m, 1H), 4.17 (dq, J = 7.1, 1.0 Hz, 2H), 2.02 (s, 3H), 1.82 – 1.75 (m, 1H), 1.72 – 1.60 (m, 5H), 1.50 (ddd, J = 14.1, 8.8, 5.9 Hz, 1H), 1.32 – 1.12 (m, 4H), 1.27 (t, J = 7.1 Hz, 3H), 1.00 – 0.83 (m, 2H) ppm.

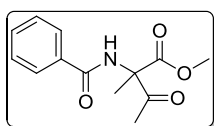
^{13}C NMR (100 MHz, CDCl_3): δ = 173.5, 170.0, 61.4, 50.4, 40.5, 34.3, 33.6, 32.8, 26.5, 26.3, 26.2, 23.3, 14.3 ppm.

IR (film): $\tilde{\nu}$ = 3283, 3069, 2981, 2925, 2852, 1745, 1656, 1547, 1449, 1374, 1229, 1278, 1255, 1195, 1154, 1116, 1097, 1030, 957, 889, 863, 596, 523, 462 cm^{-1} .

HRMS (ESI): m/z = 264.1576 $[\text{M}+\text{Na}]^+$ (calcd m/z = 264.1576); m/z = 505.3259 $[2\text{M}+\text{Na}]^+$ (calcd m/z = 505.3254).

Chiral stationary phase HPLC: Chiralpak IC column (Daicel), 250 mm \times 4.6 mm; eluent: 15% *i*-PrOH/hexanes, 1.0 mL/min; UV-detector λ = 220 nm. Retention times: t_R (S) = 10.4 min, t_R (R) = 14.7 min.

6.4 Opening of C-Acetylated Azlactones with Different Nucleophiles



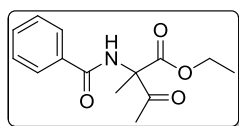
Methyl 2-benzamido-2-methyl-3-oxobutanoate (23a). *N*-benzoyl D,L-alanine (**22**; 0.975 g, 5.0 mmol) was suspended in CH_2Cl_2 (40 mL). EDC \cdot HCl (2.109 g, 11.0 mmol) was added and the reaction mixture was stirred at rt for 1 h. Acetic anhydride (0.57 mL, 0.613 g, 6.0 mmol) and DMAP (61.1 mg, 0.5 mmol) were subsequently added and the solution was stirred for 24 h. Then methanol (0.51 mL, 0.401 g, 12.5 mmol) was added and stirring was continued for further 24 h (the reaction progress was monitored by TLC and/or GC-MS). Upon complete consumption of the *in situ* formed C-acetylated azlactone the reaction mixture was diluted with EtOAc (150 mL) and successively washed with sat. aq. NaHCO_3 (2×50 mL), 2 N HCl (2×50 mL) and brine (2×50 mL). The organic layer was dried over Na_2SO_4 , filtered, and the solvent was removed under reduced pressure yielding the crude product. Purification by column chromatography eluting with hexanes/EtOAc (2:1) afforded **23a** (0.358 g, 1.44 mmol, 29%) as colorless oil. TLC (hexanes/EtOAc, 2:1): R_f = 0.26.

^1H NMR (400 MHz, CDCl_3): δ = 7.85 – 7.82 (m, 2H), 7.76 (br s, 1H), 7.55 – 7.50 (m, 1H), 7.47 – 7.43 (m, 2H), 3.79 (s, 3H), 2.25 (s, 3H), 1.84 (s, 3H) ppm.

^{13}C NMR (100 MHz, CDCl_3): δ = 200.3, 169.7, 165.9, 133.3, 132.0, 128.7, 127.2, 68.6, 53.6, 24.1, 20.3 ppm.

The NMR data are in accordance with those reported in the literature.^[32]

Chiral stationary phase GC: FS-Hydrodex β -TBDAC column (Macherey-Nagel), l = 30 m; splitflow: 80 mL/min; precolumn pressure: 0.8 bar; T (injector + detector) = 250 °C; conditions: 100 – 220 °C, 2 °C/min. Retention times: $t_{\text{R},1}$ = 52.7 min, $t_{\text{R},2}$ = 53.0 min.



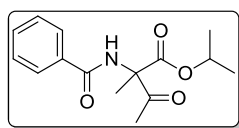
Ethyl 2-benzamido-2-methyl-3-oxobutanoate (23b). The title compound was synthesized on 0.5 mmol scale employing the reaction conditions and work-up procedure described for **23a** using EtOH (296 μL , 233.8 mg, 5.07 mmol) as nucleophile. Yield: 20.5 mg (0.08 mmol, 16%) as colorless oil. TLC (hexanes/EtOAc, 2:1): R_f = 0.48.

^1H NMR (400 MHz, CDCl_3): δ = 7.85 – 7.81 (m, 2H), 7.75 (br s, 1H), 7.55 – 7.50 (m, 1H), 7.48 – 7.42 (m, 2H), 4.33 – 4.19 (m, 2H), 2.25 (s, 3H), 1.83 (s, 3H), 1.25 (t, J = 7.2 Hz, 3H) ppm.

^{13}C NMR (100 MHz, CDCl_3): δ = 200.4, 169.2, 166.0, 133.5, 132.1, 128.8, 127.2, 68.7, 62.8, 24.2, 20.3, 14.1 ppm.

IR (ATR): $\tilde{\nu}$ = 3405, 2984, 2940, 1721, 1661, 1602, 1581, 1508, 1478, 1440, 1371, 1289, 1260, 1190, 1118, 1099, 1074, 1018, 917, 858, 803, 713, 692, 630, 606, 535 cm^{-1} .

HRMS (ESI): m/z = 286.1058 $[\text{M}+\text{Na}]^+$ (calcd m/z = 286.1055); m/z = 549.2206 $[2\text{M}+\text{Na}]^+$ (calcd m/z = 549.2213).

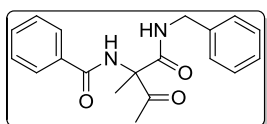


Isopropyl 2-benzamido-2-methyl-3-oxobutanoate (23c). The title compound was synthesized on 0.5 mmol scale employing the reaction conditions and work-up procedure described for **23a** using *i*-PrOH (385 μL , 300.3 mg, 5.0 mmol) as nucleophile. Yield: 14.1 mg (0.05 mmol, 10%) as colorless oil. TLC (hexanes/EtOAc, 2:1): R_f = 0.54.

¹H NMR (400 MHz, CDCl₃): δ = 7.85 – 7.80 (m, 2H), 7.74 (br s, 1H), 7.55 – 7.50 (m, 1H), 7.48 – 7.43 (m, 2H), 5.12 (hept, J = 6.3 Hz, 1H), 2.24 (s, 3H), 1.82 (s, 3H), 1.25 (d, J = 6.3 Hz, 3H), 1.21 (d, J = 6.3 Hz, 3H) ppm.

¹³C NMR (100 MHz, CDCl₃): δ = 200.4, 168.8, 166.0, 133.7, 132.0, 128.8, 127.2, 70.7, 68.8, 24.2, 21.6, 21.6, 20.2 ppm.

The NMR data are in accordance with those reported in the literature.^[21]



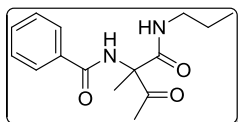
***N*-(1-(benzylamino)-2-methyl-1,3-dioxobutan-2-yl)benzamide (23d).**

The title compound was synthesized on 0.5 mmol scale employing the reaction conditions described for **23a** using BnNH₂ (136 μ L, 133.2 mg, 1.24 mmol) as nucleophile. Washing was performed with 0.5 M citric acid solution and brine. Yield: 23.0 mg (0.07 mmol, 14%) as colorless oil. TLC (hexanes/EtOAc, 1:1): R_f = 0.48.

¹H NMR (400 MHz, CDCl₃): δ = 8.10 (br s, 1H), 7.80 (d, J = 7.3 Hz, 2H), 7.48 (t, J = 7.3 Hz, 1H), 7.40 (t, J = 7.5 Hz, 2H), 7.28 – 7.18 (m, 3H), 7.14 (d, J = 7.3 Hz, 2H), 6.51 (m, 1H), 4.45 – 4.33 (m, 2H), 2.16 (s, 3H), 1.77 (s, 3H) ppm.

¹³C NMR (100 MHz, CDCl₃): δ = 205.6, 167.9, 166.3, 137.4, 133.4, 132.3, 129.0, 128.9, 127.9, 127.5, 127.3, 69.1, 44.3, 25.0, 20.9 ppm.

The NMR data are in accordance with those reported in the literature.^[13a]



***N*-(2-methyl-1,3-dioxo-1-(propylamino)butan-2-yl)benzamide (23e).**

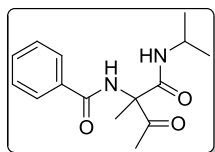
The title compound was synthesized on 0.5 mmol scale employing the reaction conditions described for **23a** using PrNH₂ (105 μ L, 75.6 mg, 1.28 mmol) as nucleophile. Washing was performed with 0.5 M citric acid solution and brine. Yield: 34.6 mg (0.13 mmol, 25%) as colorless oil. TLC (hexanes/EtOAc, 1:1): R_f = 0.43.

¹H NMR (400 MHz, CDCl₃): δ = 8.21 (br s, 1H), 7.89 – 7.85 (m, 2H), 7.56 – 7.51 (m, 1H), 7.49 – 7.43 (m, 2H), 6.25 (m, 1H), 3.28 – 3.20 (m, 2H), 2.21 (s, 3H), 1.80 (s, 3H), 1.51 (h, J = 7.3 Hz, 2H), 0.88 (t, J = 7.4 Hz, 3H) ppm.

^{13}C NMR (100 MHz, CDCl_3): δ = 205.9, 167.8, 166.2, 133.5, 132.2, 128.8, 127.3, 69.0, 42.1, 24.9, 22.7, 21.0, 11.3 ppm.

IR (ATR): $\tilde{\nu}$ = 3368, 3066, 2965, 2936, 2876, 1721, 1648, 1603, 1580, 1506, 1474, 1437, 1374, 1355, 1286, 1215, 1194, 1147, 1099, 1074, 909, 912, 804, 714, 691, 646, 629, 603, 539, 507 cm^{-1} .

HRMS (ESI): m/z = 299.1370 $[\text{M}+\text{Na}]^+$ (calcd m/z = 299.1372); m/z = 575.2844 $[2\text{M}+\text{Na}]^+$ (calcd m/z = 575.2846).



***N*-(1-(isopropylamino)-2-methyl-1,3-dioxobutan-2-yl)benzamide (23f).**

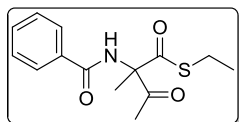
The title compound was synthesized on 0.5 mmol scale employing the reaction conditions described for **23a** using *i*-PrNH₂ (107 μL , 77.0 mg, 1.30 mmol) as nucleophile. Washing was performed with 0.5 M citric acid solution and brine. Yield: 18.3 mg (0.07 mmol, 13%) as colorless oil. TLC (hexanes/EtOAc, 1:1): R_f = 0.48.

^1H NMR (400 MHz, CDCl_3): δ = 8.20 (br s, 1H), 7.87 (d, J = 7.2 Hz, 2H), 7.57 – 7.51 (m, 1H), 7.50 – 7.43 (m, 2H), 5.87 (d, J = 7.9 Hz, 1H), 4.12 – 3.99 (m, 1H), 2.21 (s, 3H), 1.78 (s, 3H), 1.16 (d, J = 6.6 Hz, 3H), 1.13 (d, J = 6.6 Hz, 3H) ppm.

^{13}C NMR (100 MHz, CDCl_3): δ = 205.9, 166.9, 166.1, 133.5, 132.2, 128.8, 127.2, 69.0, 42.7, 24.9, 22.4, 22.4, 20.9 ppm.

IR (ATR): $\tilde{\nu}$ = 3359, 3064, 2975, 2937, 1724, 1672, 1653, 1602, 1580, 1538, 1504, 1471, 1435, 1368, 1355, 1323, 1277, 1216, 1171, 1154, 1130, 1096, 1074, 1024, 960, 915, 842, 804, 715, 691, 627, 604, 569, 526, 506, 431 cm^{-1} .

HRMS (ESI): m/z = 299.1363 $[\text{M}+\text{Na}]^+$ (calcd m/z = 299.1372); m/z = 575.2825 $[2\text{M}+\text{Na}]^+$ (calcd m/z = 575.2846).



***S*-Ethyl 2-benzamido-2-methyl-3-oxobutanethioate (23g).** The title compound was synthesized on 0.5 mmol scale employing the reaction conditions described for **23a** using EtSH (96.1 μL , 80.7 mg, 1.30 mmol) as

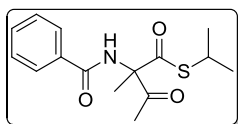
nucleophile with the exception that washing was performed solely with brine. Yield: 87.1 mg (0.31 mmol, 62%) as colorless oil. TLC (hexanes/EtOAc, 2:1): R_f = 0.53.

^1H NMR (400 MHz, CDCl_3): δ = 8.00 (br s, 1H), 7.87 – 7.84 (m, 2H), 7.56 – 7.52 (m, 1H), 7.50 – 7.44 (m, 2H), 3.00 – 2.81 (m, 2H), 2.24 (s, 3H), 1.90 (s, 3H), 1.22 (t, J = 7.4 Hz, 3H) ppm.

^{13}C NMR (100 MHz, CDCl_3): δ = 200.5, 197.0, 166.1, 133.8, 132.2, 128.8, 127.3, 75.6, 24.1, 23.4, 19.7, 14.3 ppm.

IR (ATR): $\tilde{\nu}$ = 3395, 2972, 2933, 1723, 1665, 1602, 1581, 1504, 1473, 1436, 1367, 1279, 1232, 1185, 1143, 1099, 1074, 1001, 963, 912, 885, 802, 784, 710, 691, 660, 639, 540 cm^{-1} .

HRMS (ESI): m/z = 302.0826 $[\text{M}+\text{Na}]^+$ (calcd m/z = 302.0827); m/z = 581.1752 $[2\text{M}+\text{Na}]^+$ (calcd m/z = 581.1756).



***S*-Isopropyl 2-benzamido-2-methyl-3-oxobutanethioate (23h).** The title compound was synthesized on 0.5 mmol scale employing the reaction conditions described for **23a** using *i*-PrSH (119 μL , 97.6 mg, 1.28 mmol) as nucleophile with the exception that washing was performed solely with brine. Yield: 65.8 mg (0.22 mmol, 45%) as colorless oil. TLC (hexanes/EtOAc, 2:1): R_f = 0.56.

^1H NMR (400 MHz, CDCl_3): δ = 7.97 (br s, 1H), 7.87 – 7.83 (m, 2H), 7.56 – 7.51 (m, 1H), 7.49 – 7.44 (m, 2H), 3.65 (hept, J = 6.9 Hz, 1H), 2.24 (s, 3H), 1.88 (s, 3H), 1.28 (d, J = 6.9 Hz, 3H), 1.27 (d, J = 6.9 Hz, 3H) ppm.

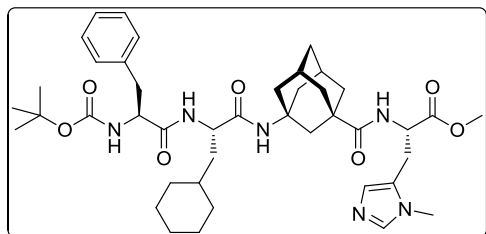
^{13}C NMR (100 MHz, CDCl_3): δ = 200.6, 196.9, 166.0, 133.9, 132.1, 128.8, 127.3, 75.6, 35.7, 23.5, 22.8, 22.6, 19.7 ppm.

IR (ATR): $\tilde{\nu}$ = 3396, 2967, 2930, 2869, 1723, 1667, 1602, 1581, 1504, 1473, 1437, 1367, 1280, 1246, 1185, 1142, 1099, 1073, 1059, 1001, 963, 912, 881, 802, 785, 711, 691, 661, 637, 527 cm^{-1} .

HRMS (ESI): m/z = 316.0988 $[\text{M}+\text{Na}]^+$ (calcd m/z = 316.0983); m/z = 609.2064 $[2\text{M}+\text{Na}]^+$ (calcd m/z = 609.2069).

6.5 Availability of Catalysts

For the synthesis and availability as well as characterization data for the employed catalysts, see Chapter VI. The preparation and characterization data for peptide **11** are provided below.



Boc-L-Phe-L-Cha-^AGly-L-Pmh-OMe (11). Peptide **1** (306.9 mg, 0.5 mmol) was treated with 4 M HCl in 1,4-dioxane (1 mL) and the resulting solution was stirred at rt for 30 min. The reaction flask was flushed with argon for 30 min to remove residual HCl and the solvent was removed under reduced pressure. After drying *in vacuo*, the resulting H-L-Cha-^AGly-L-Pmh-OMe • 2 HCl was directly used for the next coupling step.

Boc-L-Phe-OH (132.7 mg, 0.5 mmol), H-L-Cha-^AGly-L-Pmh-OMe • 2 HCl, 1-hydroxy-benzotriazole (HOBt; 84.2 mg, 0.55 mmol) and *O*-(benzotriazol-1-yl)-*N,N,N',N'*-tetramethyluronium hexafluorophosphate (HBTU; 208.6 mg, 0.55 mmol) were dissolved in dry CH₂Cl₂ (5 mL). Et₃N (229 μL, 167.0 mg, 1.65 mmol) was added and the resulting solution was stirred at rt for 24 h. The reaction mixture was diluted with EtOAc (30 mL) and successively washed with sat. aq. NaHCO₃ (4 × 10 mL) and brine (4 × 10 mL) and dried over Na₂SO₄. After filtration and removal of the solvent under reduced pressure the crude product was purified by column chromatography eluting with CHCl₃/MeOH (9:1) to yield **11** (282.1 mg, 0.37 mmol, 74%) as colorless solid. TLC (CHCl₃/MeOH 9:1): *R_f* = 0.46.

¹H NMR (400 MHz, CDCl₃): δ = 7.37 (s, 1H), 7.31 – 7.20 (m, 3H), 7.19 – 7.15 (m, 2H), 6.74 (s, 1H), 6.45 (d, *J* = 8.0 Hz, 1H), 6.25 (d, *J* = 7.5 Hz, 1H), 5.99 (br s, 1H), 5.08 (d, *J* = 6.8 Hz, 1H), 4.80 – 4.72 (m, 1H), 4.38 – 4.42 (m, 2H), 3.71 (s, 3H), 3.57 (s, 3H), 3.15 – 2.97 (m, 4H), 2.18 (m, 2H), 2.07 – 1.97 (m, 2H), 1.96 – 1.85 (m, 4H), 1.79 – 1.54 (m, 12H), 1.43 – 1.34 (m, 1H), 1.39 (s, 9H), 1.26 – 1.07 (m, 4H), 0.96 – 0.78 (m, 2H) ppm.

¹³C NMR (100 MHz, CDCl₃): δ = 176.4, 171.9, 171.3, 170.8, 155.6, 138.6, 136.5, 129.4, 128.8, 128.5, 127.1, 126.4, 80.5, 55.9, 52.7, 52.2, 51.8, 51.4, 42.7, 42.4, 40.4, 39.5, 38.1, 38.1, 37.8, 35.3, 34.1, 33.7, 32.7, 31.5, 29.2, 28.4, 26.8, 26.5, 26.2, 26.1 ppm.

IR (KBr): $\tilde{\nu}$ = 3317, 3063, 3030, 2922, 2853, 1743, 1652, 1509, 1451, 1390, 1366, 1343, 1275, 1248, 1169, 1110, 1081, 1048, 1021, 925, 891, 817, 750, 700, 663 cm⁻¹.

HRMS (ESI): *m/z* = 761.4602 [M+H]⁺ (calcd *m/z* = 761.4602).

6.6 Procedures for Catalytic Experiments

Enantioselective Dakin–West reaction. To a suspension of *N*-protected amino acid (1.0 equiv) and catalyst (10 mol%) in dry toluene (5 mL/mmol) was added carbodiimide (1.7 equiv) and the mixture was stirred at rt for 30 min. Anhydride (1.5 equiv) was added and the reaction progress was monitored by GC-MS and chiral stationary phase GC. After consumption of the azlactone acetic acid (1.3 equiv) was added and stirring was continued. Conversion and enantioselectivity were determined by GC-MS and chiral stationary phase GC.

Enantioselective decarboxylative protonation. Malonic acid half ester **12** (14.3 mg, 0.05 mmol) and catalyst **1** (3.07 mg, 10 mol%) were suspended in dry toluene (250 μ L) and stirred at rt for 4 d. After quenching with 0.1 N HCl the desired product was extracted with EtOAc. The solvent was removed under reduced pressure and the enantioselectivity was determined by chiral stationary phase HPLC.

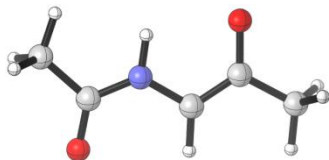
Enantioselective acetylation of azlactones. To a suspension of *N*-benzoyl-D,L-alanine (**22**; 19.3 mg, 0.1 mmol) and catalyst (10 mol%) in dry toluene (1 mL) was added DIC (34.7 μ L, 27.8 mg, 0.22 mmol) and the mixture was stirred at rt for 1 h. Acetic anhydride (10.4 μ L, 11.2 mg, 0.11 mmol) was subsequently added and stirring was continued for 18 h. Then MeOH (1 mL) was added and stirring was continued for additional 18 h. The reaction progress was followed by GC-MS and the enantioselectivity for **23a** was determined by chiral stationary phase GC. The formation of the *N*-benzoyl alanine methylester was unambiguously assigned by comparison of the retention times with an authentic sample.

Preparation of 23c by Steglich rearrangement (Table 3, entry 6). According to a literature procedure,^[21] *C*-acetylated azlactone **16** (269.3 mg, 1.24 mmol) and DMAP (12.2 mg, 8 mol%) were dissolved in CH₂Cl₂ (7 mL). After stirring at rt for 3 h the solvent was removed *in vacuo* to afford **17** as yellow oil. To 1.01 mmol of the crude product was added DMAP (10.1 mg, 7.5 mol%) and *i*-PrOH (7 mL) and the reaction mixture was stirred for 3 d. The excess of *i*-PrOH was removed under reduced pressure and the obtained crude product was purified by column chromatography. Yield: 133.0 mg, 0.48 mmol, 44%. Analytical data for **23c** are provided above.

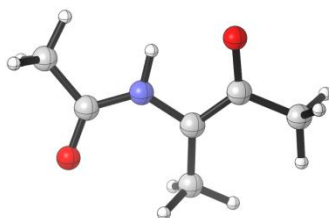
6.7 Energies and Cartesian Coordinates for Computed Structures

Table 4. Computed energies for enolates 2a – 2e and complexes with protonated peptide 1.

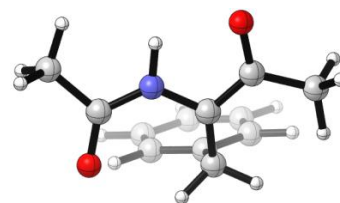
Structure	Energy (–au)	ZPVE (au)	E+ZPVE (–au)	G ₂₉₈ (–au)	H ₂₉₈ (–au)	ΔG ₂₉₈ (–au)	ΔH ₂₉₈ (–au)	ΔΔG ₂₉₈ (kcal mol ^{–1})	ΔΔH ₂₉₈ (kcal mol ^{–1})
1_2a	2415,0436909	0,9726331	2414,0710578	2414,1604140	2414,0167530	2013,5482740	2013,4487460	0.00	0.00
2a	400,7044640	0,1264679	400,5779961	400,6121400	400,5680070				
1_2b	2454,3646412	1,0000042	2453,3646370	2453,4556630	2453,3085680	2013,5527670	2013,4535560	–2.82	–3.02
2b	440,0208215	0,1542449	439,8665766	439,9028960	439,8550120				
1_2c	2685,4641897	1,0822771	2684,3819126	2684,4801570	2684,3216240	2013,5557210	2013,4564320	–4.67	–4.82
2c	671,1172293	0,2363189	670,8809104	670,9244360	670,8651920				
1_2d	2572,3365663	1,0860835	2571,2504828	2571,3462790	2571,1908690	2013,5539440	2013,4551990	–3.56	–4.05
2d	557,9905222	0,2396299	557,7508923	557,7923350	557,7356700				
1_2e	2689,0993488	1,1524363	2687,9469125	2688,0441180	2687,8856460	2013,5550530	2013,4572460	–4.25	–5.33
2e	674,7510504	0,3057456	674,4453048	674,4890650	674,4284000				

**Table 5.** Cartesian coordinates for enolate **2a**.

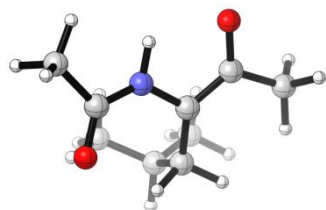
Atom	X	Y	Z
7	-0.557173000	0.232584000	0.000013000
1	-0.352559000	1.227373000	0.000084000
6	3.112149000	-0.653982000	0.000030000
1	3.711037000	-0.392944000	0.881803000
1	3.711194000	-0.392720000	-0.881567000
1	2.939059000	-1.736565000	-0.000113000
6	-1.826917000	-0.200664000	0.000008000
8	-2.145082000	-1.412361000	-0.000053000
6	-2.898337000	0.878496000	0.000032000
1	-2.488359000	1.893212000	0.000279000
1	-3.534894000	0.754375000	-0.882742000
1	-3.535186000	0.754043000	0.882547000
6	1.815508000	0.142753000	-0.000015000
6	0.620454000	-0.547511000	0.000009000
8	1.896447000	1.433673000	-0.000052000
1	0.501858000	-1.619913000	0.000074000

**Table 6.** Cartesian coordinates for enolate **2b**.

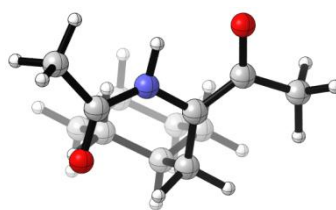
Atom	X	Y	Z
7	0.605945000	-0.344158000	-0.118353000
1	0.384456000	-1.335943000	-0.202771000
6	-0.568140000	1.879725000	-0.210654000
1	-1.578966000	2.294152000	-0.228602000
1	-0.001981000	2.391489000	0.575461000
1	-0.082855000	2.157398000	-1.159702000
6	-3.134898000	0.094756000	0.089669000
1	-3.631544000	-0.290511000	0.989468000
1	-3.702742000	-0.284244000	-0.770529000
1	-3.205855000	1.185924000	0.099215000
6	1.887663000	0.019296000	0.054867000
8	2.287935000	1.175555000	0.320632000
6	2.900764000	-1.107824000	-0.114313000
1	2.440103000	-2.085238000	-0.286670000
1	3.559171000	-0.875696000	-0.958798000
1	3.526323000	-1.160187000	0.782878000
6	-1.714195000	-0.448174000	0.037880000
6	-0.613571000	0.390448000	-0.027508000
8	-1.599617000	-1.745229000	0.055477000

**Table 7.** Cartesian coordinates for enolate **2c**.

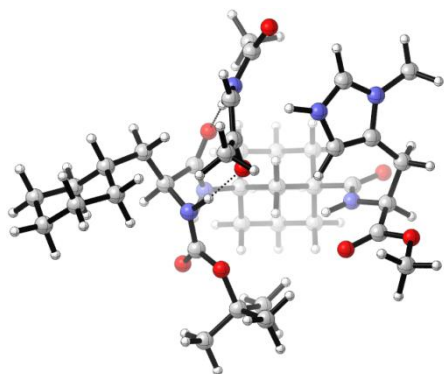
Atom	X	Y	Z
7	-1.694346000	-0.385450000	-0.286131000
1	-2.131272000	-0.077463000	-1.153296000
6	0.008771000	0.481041000	1.351165000
1	0.198932000	1.388552000	1.929647000
1	-0.267351000	-0.310147000	2.053539000
6	-0.861635000	3.257634000	0.236939000
1	-1.672509000	3.983847000	0.368733000
1	-0.198973000	3.654982000	-0.543468000
1	-0.293995000	3.195695000	1.169484000
6	-1.903686000	-1.648636000	0.121798000
8	-1.574162000	-2.108188000	1.239216000
6	-2.564456000	-2.557035000	-0.905748000
1	-2.879460000	-2.029846000	-1.811122000
1	-1.862818000	-3.349675000	-1.188756000
1	-3.434966000	-3.037456000	-0.447950000
6	-1.458627000	1.935821000	-0.225743000
6	-1.122445000	0.733474000	0.384786000
8	-2.280870000	1.996516000	-1.223356000
6	1.287853000	0.074098000	0.637046000
6	1.546060000	-1.273291000	0.341753000
6	2.214985000	1.036877000	0.210250000
1	0.832985000	-2.023665000	0.671914000
1	2.022822000	2.085625000	0.422260000
6	2.694830000	-1.644707000	-0.363518000
6	3.367891000	0.670220000	-0.487359000
1	2.874419000	-2.693866000	-0.585635000
1	4.074389000	1.433507000	-0.803864000
6	3.612499000	-0.676150000	-0.781007000
1	4.506239000	-0.964647000	-1.327639000

**Table 8.** Cartesian coordinates for enolate **2d**.

Atom	X	Y	Z
7	1.050610000	-0.671467000	-0.130210000
1	1.077081000	-1.465154000	-0.769749000
6	-0.691796000	0.730797000	1.065238000
1	-1.533708000	0.525433000	1.737268000
1	0.131846000	1.090766000	1.688731000
6	-1.114967000	1.900946000	0.129248000
6	-2.412569000	1.593915000	-0.627031000
6	-0.000542000	2.291685000	-0.850159000
1	-2.284115000	0.702533000	-1.250895000
1	0.178976000	1.481899000	-1.565993000
1	-1.303401000	2.767254000	0.785034000
1	-3.242304000	1.400702000	0.063214000
1	0.938946000	2.480344000	-0.321612000
6	-2.533231000	-1.709161000	0.416628000
1	-2.704314000	-2.676258000	0.905618000
1	-3.169742000	-1.686636000	-0.478040000
1	-2.861999000	-0.912779000	1.089052000
6	2.214475000	-0.098900000	0.217916000
8	2.363266000	0.764108000	1.113627000
6	3.417773000	-0.540987000	-0.606731000
1	3.195882000	-1.363189000	-1.293710000
1	3.786133000	0.311490000	-1.188996000
1	4.221718000	-0.846386000	0.070438000
6	-1.069635000	-1.620630000	0.009983000
6	-0.274858000	-0.547080000	0.388784000
8	-0.615713000	-2.605814000	-0.704493000
1	-2.699560000	2.429599000	-1.277837000
1	-0.274039000	3.190780000	-1.417385000

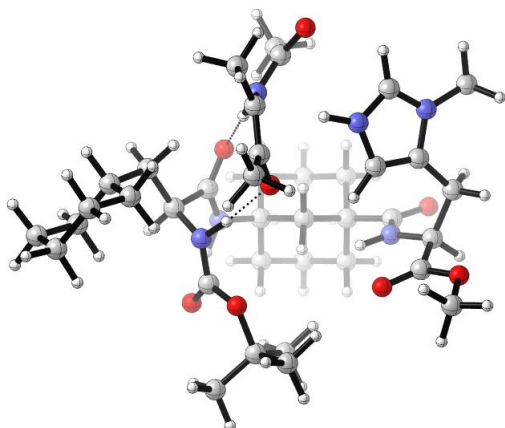
**Table 9.** Cartesian coordinates for enolate **2e**.

Atom	X	Y	Z
7	-1.889779000	-0.194521000	-0.266081000
1	-2.303262000	0.199954000	-1.110902000
6	-0.112759000	0.425698000	1.436158000
1	0.086826000	1.295723000	2.073335000
1	-0.560463000	-0.339885000	2.076469000
6	1.259346000	-0.117517000	0.950616000
6	2.492104000	-1.921763000	-0.356045000
6	3.465534000	0.410329000	-0.215698000
6	3.323593000	-0.851928000	-1.077859000
6	2.096486000	0.947390000	0.225759000
6	1.124873000	-1.370103000	0.070005000
1	3.041808000	-2.262403000	0.534608000
1	4.063732000	0.167505000	0.675695000
1	2.822210000	-0.586471000	-2.019956000
1	1.535131000	1.292827000	-0.652122000
1	0.548664000	-1.105540000	-0.826150000
1	1.817127000	-0.412635000	1.857551000
1	2.364346000	-2.801654000	-1.000494000
1	4.019689000	1.184117000	-0.763512000
1	4.313023000	-1.246173000	-1.345667000
1	2.229065000	1.822690000	0.875173000
1	0.541202000	-2.130933000	0.599478000
6	-0.482609000	3.270267000	0.210144000
1	-1.190931000	4.095135000	0.351396000
1	0.222722000	3.584955000	-0.570394000
1	0.079134000	3.125091000	1.136373000
6	-2.299161000	-1.409512000	0.133816000
8	-2.008543000	-1.955031000	1.223443000
6	-3.154905000	-2.161438000	-0.878947000
1	-3.419318000	-1.561699000	-1.755178000
1	-2.611708000	-3.052346000	-1.214895000
1	-4.071491000	-2.503557000	-0.387903000
6	-1.252512000	2.043680000	-0.254900000
6	-1.099367000	0.812470000	0.367460000
8	-2.049306000	2.221469000	-1.265116000

**Table 10.** Cartesian coordinates for complex **1_2a**.

Atom	X	Y	Z
1	-1.110687000	0.628210000	-1.300593000
6	-1.188958000	1.680560000	-1.014836000
6	-0.303065000	3.989866000	-1.418432000
6	-2.700564000	3.670375000	-0.729338000
6	-1.738396000	4.514357000	-1.584372000
6	-2.638101000	2.185949000	-1.181658000
6	-0.220774000	2.522091000	-1.877638000
1	0.008256000	4.061718000	-0.368854000
1	-3.726596000	4.039772000	-0.833829000
1	-0.849371000	1.771616000	0.023825000
1	0.395813000	4.593432000	-2.010142000
1	-2.427731000	3.743847000	0.330977000
1	-1.782555000	5.556899000	-1.248244000
6	-2.148382000	4.422588000	-3.064797000
1	-1.484552000	5.045790000	-3.676792000
1	-3.168557000	4.803785000	-3.197421000
6	-3.024608000	2.099347000	-2.675761000
1	-4.057166000	2.436649000	-2.799134000
1	-2.983362000	1.052532000	-3.001392000
6	-0.626944000	2.434181000	-3.359759000
1	0.071358000	3.032911000	-3.956676000
1	-0.547737000	1.397770000	-3.696346000
6	-2.066810000	2.955061000	-3.522637000
1	-2.359150000	2.879687000	-4.576530000
6	-3.655193000	1.397870000	-0.352681000
8	-4.854759000	1.349450000	-0.650588000
7	1.160945000	2.076064000	-1.645428000
1	1.684267000	2.624317000	-0.963635000
7	2.455195000	0.382079000	0.438120000
6	2.869789000	0.505837000	-0.958533000
6	1.598828000	0.800297000	-1.781617000
8	1.008976000	-0.065034000	-2.442450000
1	1.943434000	-0.488035000	0.695387000
1	3.521042000	1.380470000	-1.026394000
6	3.607615000	-0.739273000	-1.453173000
1	3.647208000	-0.674281000	-2.546635000
1	3.013557000	-1.628178000	-1.220876000
7	-3.186717000	0.778695000	0.762021000
6	-4.053389000	0.041309000	1.653719000
6	-3.294606000	-0.199482000	2.953526000
8	-2.149774000	0.161104000	3.148683000
1	-2.210895000	0.835448000	1.018452000
1	-4.931097000	0.652594000	1.894432000
6	-4.596155000	-1.261702000	1.025208000
6	-3.531848000	-2.192910000	0.541540000
1	-5.227218000	-0.956451000	0.186235000
1	-5.241366000	-1.758176000	1.758277000
6	-2.184107000	-2.273391000	0.782468000
1	-1.506839000	-1.673134000	1.367633000
6	-2.690129000	-3.888157000	-0.645512000
1	-2.568279000	-4.690215000	-1.357486000
7	-3.821449000	-3.221267000	-0.361265000
6	-5.133363000	-3.507327000	-0.938319000
1	-5.850190000	-3.727248000	-0.145108000
1	-5.478816000	-2.649231000	-1.518229000
1	-5.042748000	-4.372388000	-1.594240000
8	-4.043863000	-0.853652000	3.845177000
6	-3.411841000	-1.144514000	5.115841000
1	-4.165364000	-1.675044000	5.694453000
1	-2.529427000	-1.766933000	4.958041000
1	-3.124034000	-0.214754000	5.609329000
6	2.299360000	1.478697000	1.209577000
8	2.566155000	2.636555000	0.854133000
8	1.823306000	1.139602000	2.427905000
6	1.411202000	2.157842000	3.404863000
6	0.279426000	3.008819000	2.821961000
1	0.631352000	3.610802000	1.983346000
1	-0.540058000	2.364256000	2.491201000
1	-0.107645000	3.679111000	3.596321000
6	0.898745000	1.309996000	4.569655000
1	1.697468000	0.666707000	4.950623000
1	0.560141000	1.962635000	5.380596000
6	2.613287000	3.000874000	3.835364000
1	2.988557000	3.602805000	3.007826000
1	2.315380000	3.664223000	4.654275000
1	3.417489000	2.352051000	4.196575000
7	0.603491000	-2.923327000	-1.886113000
1	0.848776000	-1.934235000	-1.965085000
6	1.930315000	-3.840018000	1.571999000
1	1.262813000	-3.855980000	2.441733000
1	2.854459000	-3.343607000	1.889089000
1	2.166134000	-4.868085000	1.279984000
6	-0.226742000	-3.445858000	-2.811762000
8	-0.680923000	-4.607989000	-2.734002000
6	-0.593396000	-2.541852000	-3.971512000
1	-0.194540000	-1.532253000	-3.863463000
1	-0.214281000	-2.984134000	-4.898709000
1	0.063265000	0.684343000	4.248114000
1	-1.684200000	-2.501467000	-4.054745000
7	-1.701044000	-3.329461000	0.041765000
1	-0.691974000	-3.605694000	-0.047604000
6	1.288440000	-3.040675000	0.451127000
6	1.091318000	-3.658008000	-0.769621000
8	0.910735000	-1.832697000	0.717463000
6	5.041228000	-0.935917000	-0.925150000
6	5.121431000	-1.314802000	0.564380000
6	6.566153000	-1.617503000	0.984997000
6	7.497530000	-0.436936000	0.674506000
6	7.414629000	-0.036199000	-0.805288000
6	5.966056000	0.257849000	-1.219626000
1	5.441870000	-1.793816000	-1.488255000
1	4.476876000	-2.179794000	0.758742000
1	4.728689000	-0.492737000	1.173311000

1	6.604912000	-1.860460000	2.053996000
1	6.922055000	-2.507931000	0.446319000
1	8.531662000	-0.684029000	0.944458000
1	7.205307000	0.422682000	1.294774000
1	8.048624000	0.837561000	-0.999448000
1	7.807964000	-0.855717000	-1.424014000
1	5.918346000	0.515236000	-2.286121000
1	5.617092000	1.139614000	-0.664926000
1	1.392601000	-4.679103000	-0.963916000

Table 11. Cartesian coordinates for complex **1_2b**.

Atom	X	Y	Z
1	1.198472000	-0.624217000	-1.215301000
6	1.383079000	-1.684962000	-1.022006000
6	0.768688000	-4.026782000	-1.668812000
6	3.087355000	-3.522855000	-0.828345000
6	2.259748000	-4.382266000	-1.800424000
6	2.884312000	-2.017764000	-1.154152000
6	0.550649000	-2.539755000	-2.006174000
1	0.420308000	-4.225316000	-0.646935000
1	4.150800000	-3.771872000	-0.911105000
1	1.013951000	-1.911514000	-0.014160000
1	0.166720000	-4.643857000	-2.346688000
1	2.780186000	-3.718900000	0.206771000
1	2.400935000	-5.440433000	-1.550977000
6	2.726535000	-4.116096000	-3.242828000
1	2.164552000	-4.747452000	-3.942300000
1	3.787229000	-4.376155000	-3.347992000
6	3.324684000	-1.755840000	-2.613173000
1	4.392964000	-1.967982000	-2.708927000
1	3.179467000	-0.694685000	-2.851520000
6	1.012976000	-2.281623000	-3.452186000
1	0.412038000	-2.897496000	-4.132136000
1	0.836440000	-1.235517000	-3.709090000
6	2.506248000	-2.630594000	-3.578804000
1	2.835466000	-2.430976000	-4.605335000
6	3.778083000	-1.213003000	-0.207931000
8	4.991405000	-1.075302000	-0.406822000
7	-0.877679000	-2.247387000	-1.816781000
1	-1.367229000	-2.860887000	-1.166581000
7	-2.434579000	-0.721576000	0.233538000

6	-2.765701000	-0.864645000	-1.183557000
6	-1.436671000	-1.017513000	-1.948521000
8	-0.910659000	-0.082239000	-2.564526000
1	-1.931725000	0.152936000	0.505932000
1	-3.323900000	-1.797631000	-1.287863000
6	-3.600655000	0.298283000	-1.719635000
1	-3.727221000	0.115493000	-2.793483000
1	-3.031468000	1.228086000	-1.634100000
7	3.186146000	-0.684458000	0.894128000
6	3.931679000	0.057190000	1.886432000
6	3.061478000	0.181095000	3.131826000
8	1.937044000	-0.272437000	3.223243000
1	2.198507000	-0.812084000	1.065976000
1	4.825868000	-0.511716000	2.167307000
6	4.434509000	1.422527000	1.366119000
6	3.349265000	2.299557000	0.831245000
1	5.153840000	1.201510000	0.573034000
1	4.978264000	1.924146000	2.174177000
6	1.983584000	2.259236000	0.942339000
1	1.301600000	1.574721000	1.419857000
6	2.482849000	3.980703000	-0.358261000
1	2.363266000	4.807507000	-1.040203000
7	3.634856000	3.393577000	0.007608000
6	4.966111000	3.806435000	-0.431005000
1	5.594176000	4.021518000	0.435236000
1	5.423014000	3.014493000	-1.027942000
1	4.868232000	4.704602000	-1.039448000
8	3.689084000	0.846630000	4.105715000
6	2.942750000	1.028014000	5.333722000
1	3.603447000	1.592482000	5.988651000
1	2.024390000	1.582020000	5.131993000
1	2.699683000	0.056877000	5.768173000
6	-2.247074000	-1.821889000	0.996653000
8	-2.400011000	-2.988340000	0.606589000
8	-1.886277000	-1.472736000	2.251271000
6	-1.446399000	-2.476102000	3.231638000
6	-0.200635000	-3.197879000	2.710430000
1	-0.430685000	-3.788160000	1.822238000
1	0.581019000	-2.469714000	2.476769000
1	0.181605000	-3.869314000	3.486305000
6	-1.099416000	-1.619059000	4.449585000
1	-1.982232000	-1.070856000	4.792030000
1	-0.750309000	-2.260981000	5.264638000
6	-2.588766000	-3.440990000	3.557498000
1	-2.835481000	-4.065522000	2.699061000
1	-2.292609000	-4.082341000	4.394294000
1	-3.480112000	-2.879960000	3.855893000
7	-0.755482000	2.803854000	-1.849665000
1	-0.912692000	1.801478000	-1.967312000
6	-2.049032000	4.745448000	-0.982545000
1	-2.381341000	5.230258000	-0.063203000
1	-1.389675000	5.440561000	-1.510289000
1	-2.935119000	4.591974000	-1.617859000
6	-2.142479000	3.164487000	1.695041000
1	-1.401484000	3.264687000	2.497876000
1	-2.861508000	2.407606000	2.023174000
1	-2.665031000	4.115668000	1.580954000
6	0.136561000	3.384415000	-2.680838000
8	0.587120000	4.537778000	-2.508965000
6	0.578777000	2.554038000	-3.870054000

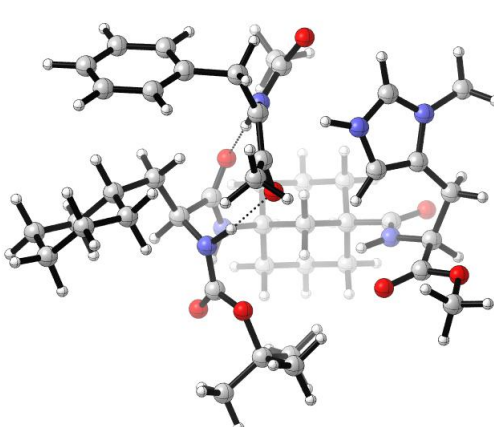
1	0.202695000	1.530970000	-3.836863000	1	4.058606000	-4.038158000	-3.223263000
1	0.227062000	3.039114000	-4.786801000	6	3.656738000	-2.295965000	-4.459076000
1	-0.311562000	-0.904667000	4.201131000	1	3.175423000	-2.877504000	-5.255182000
1	1.672578000	2.546329000	-3.906367000	1	4.706267000	-2.155123000	-4.746086000
7	1.484101000	3.309111000	0.202856000	6	3.662660000	-0.113011000	-3.211268000
1	0.466724000	3.505159000	0.042204000	1	4.706282000	0.072758000	-3.479037000
6	-1.447412000	2.663374000	0.439870000	1	3.174190000	0.863233000	-3.099495000
6	-1.346397000	3.440530000	-0.703941000	6	1.482758000	-1.145721000	-3.924487000
8	-0.898511000	1.489151000	0.534827000	1	0.965736000	-1.735425000	-4.691182000
6	-4.989205000	0.497998000	-1.078514000	1	0.965000000	-0.189250000	-3.838070000
6	-4.943460000	1.288179000	0.241288000	6	2.957947000	-0.934246000	-4.305082000
6	-6.352373000	1.559605000	0.784170000	1	3.008670000	-0.383441000	-5.251655000
6	-7.145180000	0.256294000	0.955957000	6	4.404557000	-0.080918000	-0.817338000
6	-7.191104000	-0.542349000	-0.354552000	8	5.476647000	0.474419000	-1.087601000
6	-5.778259000	-0.808899000	-0.892719000	7	0.016771000	-2.142064000	-2.161973000
1	-5.558383000	1.116950000	-1.790133000	1	-0.146112000	-3.019237000	-1.668891000
1	-4.407534000	2.230764000	0.081595000	7	-1.483989000	-1.745856000	0.393898000
1	-4.369436000	0.721210000	0.982536000	6	-2.028105000	-1.620807000	-0.958003000
1	-6.291725000	2.096985000	1.738669000	6	-0.875954000	-1.162216000	-1.871032000
1	-6.890348000	2.217910000	0.086077000	8	-0.753648000	0.010794000	-2.246436000
1	-8.162202000	0.469836000	1.307395000	1	-1.220339000	-0.859553000	0.870657000
1	-6.663847000	-0.356561000	1.731744000	1	-2.331198000	-2.620849000	-1.275818000
1	-7.722679000	-1.489985000	-0.204521000	6	-3.220025000	-0.664455000	-1.018050000
1	-7.762782000	0.025493000	-1.102960000	1	-3.409619000	-0.459819000	-2.077819000
1	-5.830581000	-1.357185000	-1.842857000	1	-2.944195000	0.294794000	-0.571879000
1	-5.247893000	-1.456543000	-0.181907000	7	3.899543000	-0.049323000	0.442885000
				6	4.583092000	0.619947000	1.527254000
				6	3.956004000	0.155414000	2.836706000
				8	3.037095000	-0.637642000	2.907012000
				1	3.034812000	-0.520764000	0.669758000
				1	5.633920000	0.307284000	1.539654000
				6	4.594450000	2.158128000	1.377094000
				6	3.235258000	2.759857000	1.222652000
				1	5.195847000	2.373610000	0.490032000
				1	5.115045000	2.586924000	2.240348000
				6	1.974901000	2.280243000	1.469082000
				1	1.604624000	1.328968000	1.815339000
				6	1.746594000	4.318161000	0.633809000
				1	1.289043000	5.200603000	0.215929000
				7	3.060436000	4.044866000	0.698054000
				6	4.126498000	4.934614000	0.241985000
				1	4.823229000	5.132093000	1.058559000
				1	4.659936000	4.477508000	-0.593892000
				1	3.679093000	5.871970000	-0.086486000
				8	4.543738000	0.726188000	3.892430000
				6	4.017361000	0.354914000	5.189672000
				1	4.604837000	0.921749000	5.909155000
				1	2.960467000	0.619751000	5.251776000
				1	4.138357000	-0.718223000	5.346727000
				6	-0.860247000	-2.881461000	0.777328000
				8	-0.752675000	-3.899496000	0.078735000
				8	-0.384052000	-2.757390000	2.035764000
				6	0.491799000	-3.776851000	2.631263000
				6	1.767717000	-3.916884000	1.796354000
				1	1.548251000	-4.319085000	0.806346000
				1	2.257440000	-2.943954000	1.698162000
				1	2.460695000	-4.596420000	2.303284000
				6	0.811617000	-3.178208000	4.001566000
				1	-0.107120000	-3.039556000	4.579440000
				1	1.471690000	-3.854386000	4.554137000

Table 12. Cartesian coordinates for complex 1_2c.

Atom	X	Y	Z
1	1.621038000	-0.139334000	-1.325213000
6	2.133684000	-1.093302000	-1.479655000
6	2.099872000	-3.262739000	-2.734644000
6	4.295193000	-2.251874000	-2.030107000
6	3.574857000	-3.059336000	-3.124382000
6	3.610979000	-0.867907000	-1.862397000
6	1.404614000	-1.896891000	-2.582094000
1	2.030455000	-3.817318000	-1.789852000
1	5.347989000	-2.106654000	-2.294951000
1	2.047844000	-1.675033000	-0.553453000
1	1.579188000	-3.851120000	-3.499687000
1	4.264118000	-2.793609000	-1.076287000

6	-0.258118000	-5.102323000	2.781520000
1	-0.480845000	-5.542895000	1.809721000
1	0.355604000	-5.801332000	3.359518000
1	-1.196223000	-4.943421000	3.322708000
7	-1.193641000	2.512483000	-0.802469000
1	-1.118137000	1.566748000	-1.182264000
6	-2.878936000	3.681212000	0.615933000
1	-3.049502000	3.947412000	1.661197000
1	-2.577996000	4.598587000	0.101039000
6	-2.115178000	1.629918000	2.799108000
1	-1.323007000	1.564327000	3.553242000
1	-2.716827000	0.719477000	2.892092000
1	-2.750578000	2.487555000	3.025610000
6	-0.671227000	3.515940000	-1.536583000
8	-0.563453000	4.688015000	-1.114156000
6	-0.228370000	3.157928000	-2.940997000
1	-0.221443000	2.082524000	-3.120709000
1	-0.908557000	3.634827000	-3.655477000
1	1.309756000	-2.212786000	3.888632000
1	0.767972000	3.575152000	-3.113999000
7	1.084556000	3.265884000	1.100770000
1	0.039325000	3.169057000	1.096392000
6	-1.472251000	1.660565000	1.422783000
6	-1.752325000	2.670019000	0.510099000
8	-0.612653000	0.723313000	1.181981000
6	-4.530355000	-1.159443000	-0.377347000
6	-4.530605000	-1.128159000	1.160525000
6	-5.904287000	-1.515265000	1.725592000
6	-6.359823000	-2.886003000	1.206774000
6	-6.349743000	-2.929257000	-0.327770000
6	-4.971489000	-2.542828000	-0.882522000
1	-5.295114000	-0.439104000	-0.699621000
1	-4.253950000	-0.124350000	1.498725000
1	-3.767660000	-1.814482000	1.545920000
1	-5.875985000	-1.513941000	2.822479000
1	-6.641775000	-0.756605000	1.427670000
1	-7.360122000	-3.126126000	1.588105000
1	-5.680202000	-3.660228000	1.591317000
1	-6.635854000	-3.926992000	-0.682705000
1	-7.103320000	-2.227431000	-0.713379000
1	-4.985233000	-2.555207000	-1.980675000
1	-4.243595000	-3.302502000	-0.565833000
6	-4.168072000	3.158741000	0.010170000
6	-4.359267000	3.170253000	-1.379916000
6	-5.178735000	2.611648000	0.813576000
6	-5.518916000	2.640668000	-1.950375000
6	-6.345942000	2.092567000	0.249441000
6	-6.519277000	2.100255000	-1.137124000
1	-3.590299000	3.596262000	-2.016984000
1	-5.047920000	2.590050000	1.892146000
1	-5.643860000	2.654537000	-3.029543000
1	-7.116372000	1.676072000	0.891773000
1	-7.422911000	1.690307000	-1.578441000

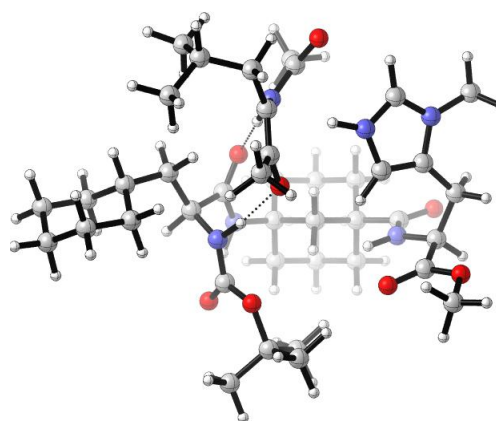
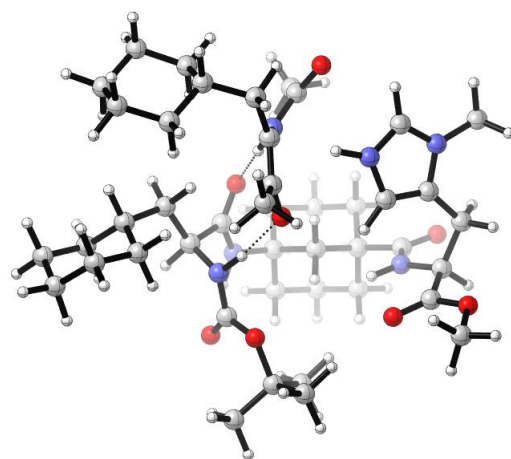


Table 13. Cartesian coordinates for complex 1_2d.

Atom	X	Y	Z
1	1.365143000	-0.396495000	-1.317036000
6	1.735514000	-1.425375000	-1.350097000
6	1.394547000	-3.699292000	-2.344786000
6	3.710918000	-2.937500000	-1.717045000
6	2.884711000	-3.756268000	-2.724487000
6	3.232528000	-1.459918000	-1.724596000
6	0.902805000	-2.239660000	-2.367937000
1	1.240738000	-4.121320000	-1.343175000
1	4.774363000	-2.976227000	-1.976626000
1	1.561519000	-1.875091000	-0.364597000
1	0.798114000	-4.293746000	-3.047257000
1	3.600857000	-3.354996000	-0.708203000
1	3.222170000	-4.799042000	-2.699293000
6	3.079431000	-3.176295000	-4.136782000
1	2.519372000	-3.772187000	-4.868125000
1	4.138668000	-3.224099000	-4.418723000
6	3.399646000	-0.885010000	-3.150350000
1	4.460309000	-0.884519000	-3.415478000
1	3.059186000	0.157949000	-3.163344000
6	1.094965000	-1.668585000	-3.784762000
1	0.499839000	-2.261463000	-4.489752000
1	0.722894000	-0.643402000	-3.817706000
6	2.586912000	-1.718658000	-4.156510000
1	2.721318000	-1.296129000	-5.159169000
6	4.124468000	-0.676567000	-0.758669000
8	5.258860000	-0.294787000	-1.071466000
7	-0.507803000	-2.236326000	-1.952710000
1	-0.791771000	-3.016486000	-1.360954000
7	-1.914594000	-1.344433000	0.518143000
6	-2.453960000	-1.300359000	-0.840732000
6	-1.256456000	-1.115436000	-1.793086000
8	-0.980482000	-0.021809000	-2.301717000
1	-1.545070000	-0.444164000	0.894479000
1	-2.908968000	-2.273329000	-1.042440000
6	-3.481312000	-0.178687000	-1.001275000
1	-3.562816000	0.044242000	-2.070630000
1	-3.082491000	0.725872000	-0.533627000
7	3.628002000	-0.448395000	0.484952000
6	4.390343000	0.239948000	1.503075000
6	3.702406000	0.008016000	2.843280000
8	2.684440000	-0.642497000	2.980846000

1	2.711509000	-0.783241000	0.747779000
1	5.391461000	-0.202631000	1.566840000
6	4.600091000	1.738130000	1.190264000
6	3.329674000	2.495851000	0.978992000
1	5.207987000	1.778581000	0.282231000
1	5.187968000	2.182939000	2.000605000
6	2.014750000	2.196547000	1.225270000
1	1.519696000	1.325778000	1.622344000
6	2.063118000	4.195035000	0.272505000
1	1.728365000	5.099343000	-0.209056000
7	3.329424000	3.760242000	0.380256000
6	4.508772000	4.479259000	-0.096215000
1	5.206301000	4.639438000	0.727955000
1	4.999171000	3.906554000	-0.885962000
1	4.190756000	5.442146000	-0.494276000
8	4.356513000	0.607604000	3.842093000
6	3.774247000	0.461274000	5.160339000
1	4.431036000	1.017754000	5.825953000
1	2.765161000	0.876856000	5.168515000
1	3.740963000	-0.593639000	5.437692000
6	-1.453840000	-2.502195000	1.035991000
8	-1.498218000	-3.600561000	0.461978000
8	-0.949622000	-2.301178000	2.273873000
6	-0.254821000	-3.370670000	3.004590000
6	0.986673000	-3.808300000	2.222155000
1	0.709523000	-4.279662000	1.278058000
1	1.627592000	-2.943951000	2.027161000
1	1.558090000	-4.527896000	2.817661000
6	0.146615000	-2.676028000	4.306312000
1	-0.742650000	-2.328117000	4.840425000
1	0.685445000	-3.379694000	4.948797000
6	-1.209566000	-4.533331000	3.285667000
1	-1.496256000	-5.040396000	2.364625000
1	-0.719622000	-5.250498000	3.952679000
1	-2.112200000	-4.165502000	3.783893000
7	-1.070556000	2.723837000	-1.130995000
1	-1.132236000	1.740107000	-1.397345000
6	-2.491015000	4.346489000	0.157304000
1	-2.543026000	4.734556000	1.180178000
1	-1.986205000	5.116921000	-0.433886000
6	-3.942316000	4.210067000	-0.377998000
6	-4.814291000	3.319846000	0.514572000
6	-3.989384000	3.734728000	-1.836481000
1	-4.408210000	2.306156000	0.568414000
1	-3.629783000	2.705983000	-1.928290000
1	-4.366346000	5.225622000	-0.349806000
1	-4.870487000	3.710075000	1.536894000
1	-3.363924000	4.363926000	-2.479435000
6	-2.160651000	2.343158000	2.507636000
1	-1.395381000	2.217163000	3.281807000
1	-2.901743000	1.550809000	2.664584000
1	-2.656665000	3.304888000	2.644379000
6	-0.354321000	3.530508000	-1.939856000
8	-0.043869000	4.705779000	-1.644892000
6	0.059435000	2.939190000	-3.273196000
1	-0.146953000	1.870968000	-3.346466000
1	-0.478256000	3.464056000	-4.070396000
1	0.793319000	-1.820860000	4.098899000
1	1.127105000	3.124867000	-3.424622000
7	1.264793000	3.264789000	0.783118000

1	0.218656000	3.305809000	0.763670000
6	-1.512534000	2.153254000	1.147300000
6	-1.637271000	3.098133000	0.137506000
8	-0.801831000	1.074845000	1.009894000
6	-4.891332000	-0.460033000	-0.455100000
6	-4.947127000	-0.699284000	1.063225000
6	-6.394510000	-0.846376000	1.550829000
6	-7.120659000	-1.972939000	0.802410000
6	-7.055809000	-1.765010000	-0.717159000
6	-5.606891000	-1.601492000	-1.198506000
1	-5.468309000	0.456163000	-0.654442000
1	-4.447208000	0.122012000	1.589499000
1	-4.386305000	-1.608055000	1.311729000
1	-6.411808000	-1.035496000	2.631151000
1	-6.929763000	0.100401000	1.387673000
1	-8.164643000	-2.041255000	1.132162000
1	-6.646264000	-2.932749000	1.053395000
1	-7.535462000	-2.603300000	-1.237075000
1	-7.625226000	-0.862294000	-0.981683000
1	-5.584927000	-1.412617000	-2.279724000
1	-5.070557000	-2.546213000	-1.031453000
1	-5.835768000	3.250368000	0.123299000
1	-5.015477000	3.768332000	-2.221178000

Table 14. Cartesian coordinates for complex **1_2e**.

Atom	X	Y	Z
1	-1.630991000	-0.048619000	1.380730000
6	-2.191786000	-0.970854000	1.559820000
6	-2.257285000	-3.115364000	2.856693000
6	-4.404553000	-2.001747000	2.165287000
6	-3.711931000	-2.825594000	3.264880000
6	-3.649637000	-0.659910000	1.959675000
6	-1.490894000	-1.792958000	2.666830000
1	-2.232815000	-3.690222000	1.921868000
1	-5.443549000	-1.794037000	2.443038000
1	-2.148289000	-1.571911000	0.643172000
1	-1.756137000	-3.716345000	3.624949000
1	-4.419059000	-2.563426000	1.222710000
1	-4.246473000	-3.774332000	3.391542000

Unpublished Results

6	-3.728810000	-2.033438000	4.584498000	1	0.067033000	-5.656320000	-1.668094000
1	-3.265598000	-2.624946000	5.383937000	1	-0.797350000	-5.921785000	-3.201031000
1	-4.763813000	-1.829939000	4.886296000	1	0.787098000	-5.125476000	-3.204256000
6	-3.640274000	0.122124000	3.293296000	7	1.258995000	2.477474000	0.708240000
1	-4.668403000	0.366710000	3.573312000	1	1.163931000	1.539757000	1.100654000
1	-3.104955000	1.069747000	3.154785000	6	2.880203000	3.657907000	-0.807503000
6	-1.505018000	-1.010679000	3.992832000	1	2.992966000	3.851540000	-1.879191000
1	-1.006310000	-1.609694000	4.764348000	1	2.509470000	4.589305000	-0.367058000
1	-0.939112000	-0.084823000	3.876070000	6	4.288669000	3.384465000	-0.221061000
6	-2.961324000	-0.713701000	4.392472000	6	5.707524000	3.055394000	1.861214000
1	-2.967016000	-0.142876000	5.328404000	6	6.399226000	1.955828000	-0.315772000
6	-4.418694000	0.143401000	0.908182000	6	6.403262000	1.849670000	1.215987000
8	-5.434953000	0.791053000	1.187537000	6	4.986571000	2.182416000	-0.873434000
7	-0.128725000	-2.131434000	2.228075000	6	4.286666000	3.227991000	1.309103000
1	-0.038451000	-3.024834000	1.745226000	1	6.291754000	3.964577000	1.656312000
7	1.286040000	-1.896435000	-0.384173000	1	7.042884000	2.795722000	-0.615226000
6	1.896031000	-1.783765000	0.939924000	1	5.875031000	0.934966000	1.518377000
6	0.818056000	-1.220578000	1.886675000	1	4.376969000	1.288591000	-0.702153000
8	0.795797000	-0.034704000	2.237767000	1	3.687624000	2.350613000	1.580389000
1	1.096835000	-1.000149000	-0.881451000	1	4.890004000	4.279862000	-0.452205000
1	2.144968000	-2.795203000	1.270167000	1	5.679978000	2.937872000	2.951709000
6	3.147974000	-0.908126000	0.914381000	1	6.837311000	1.052542000	-0.759115000
1	3.394031000	-0.662666000	1.953918000	1	7.431876000	1.754223000	1.585692000
1	2.902665000	0.041089000	0.429768000	1	5.033886000	2.321012000	-1.960951000
7	-3.960407000	0.076544000	-0.368555000	1	3.797228000	4.095135000	1.769901000
6	-4.632371000	0.737539000	-1.465355000	6	2.139802000	1.450515000	-2.861508000
6	-4.060420000	0.184947000	-2.765622000	1	1.331462000	1.424812000	-3.601615000
8	-3.186432000	-0.658715000	-2.818559000	1	2.679192000	0.501456000	-2.951422000
1	-3.142661000	-0.470886000	-0.598839000	1	2.826981000	2.259546000	-3.111387000
1	-5.699281000	0.484807000	-1.443400000	6	0.729835000	3.493994000	1.418832000
6	-4.552305000	2.277582000	-1.384720000	8	0.615561000	4.659429000	0.979384000
6	-3.157448000	2.807398000	-1.304893000	6	0.286269000	3.157121000	2.828911000
1	-5.106876000	2.566867000	-0.487923000	1	0.269261000	2.084094000	3.022744000
1	-5.078956000	2.697326000	-2.248641000	1	0.975573000	3.634469000	3.534441000
6	-1.929103000	2.233785000	-1.509188000	1	-1.614043000	-2.316153000	-3.821546000
1	-1.615622000	1.235717000	-1.768177000	1	-0.704978000	3.586603000	3.000581000
6	-1.576478000	4.328026000	-0.882619000	7	-0.980659000	3.198500000	-1.245640000
1	-1.066452000	5.217543000	-0.550770000	1	0.057775000	3.043811000	-1.234284000
7	-2.904203000	4.126737000	-0.914712000	6	1.528305000	1.542401000	-1.473896000
6	-3.915025000	5.120689000	-0.561092000	6	1.835904000	2.582316000	-0.605389000
1	-4.583973000	5.289679000	-1.407105000	8	0.659906000	0.623322000	-1.181124000
1	-4.491426000	4.775198000	0.299369000	6	4.395693000	-1.517387000	0.250946000
1	-3.411653000	6.052504000	-0.306320000	6	4.284046000	-1.711246000	-1.270811000
8	-4.638449000	0.741433000	-3.833825000	6	5.621356000	-2.168307000	-1.868253000
6	-4.154952000	0.291749000	-5.123038000	6	6.118812000	-3.456319000	-1.197040000
1	-4.726316000	0.858083000	-5.855755000	6	6.206080000	-3.293238000	0.327015000
1	-3.087479000	0.500384000	-5.212566000	6	4.868719000	-2.821853000	0.915971000
1	-4.332025000	-0.779367000	-5.233888000	1	5.195837000	-0.780054000	0.409883000
6	0.579371000	-2.995642000	-0.721230000	1	3.958465000	-0.776516000	-1.739413000
8	0.427348000	-3.987312000	0.007550000	1	3.509976000	-2.454150000	-1.492953000
8	0.074539000	-2.873743000	-1.968814000	1	5.520878000	-2.318006000	-2.950249000
6	-0.846295000	-3.875105000	-2.526545000	1	6.370030000	-1.374923000	-1.727713000
6	-2.116823000	-3.943080000	-1.674469000	1	7.094336000	-3.748926000	-1.604486000
1	-1.900813000	-4.327132000	-0.676528000	1	5.420363000	-4.273155000	-1.429654000
1	-2.566823000	-2.949467000	-1.597122000	1	6.514039000	-4.236839000	0.793660000
1	-2.841706000	-4.608106000	-2.155363000	1	6.983599000	-2.553583000	0.566611000
6	-1.157511000	-3.304124000	-3.910523000	1	4.960797000	-2.677785000	2.000635000
1	-0.240759000	-3.220607000	-4.501987000	1	4.118103000	-3.609589000	0.762727000
1	-1.851118000	-3.968632000	-4.435581000				
6	-0.149896000	-5.232656000	-2.648544000				

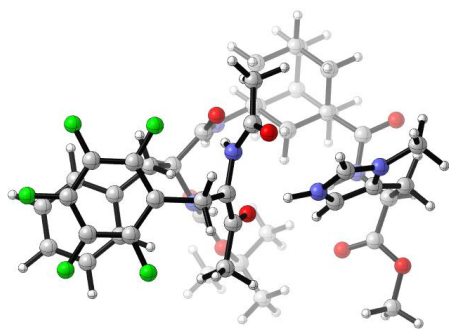


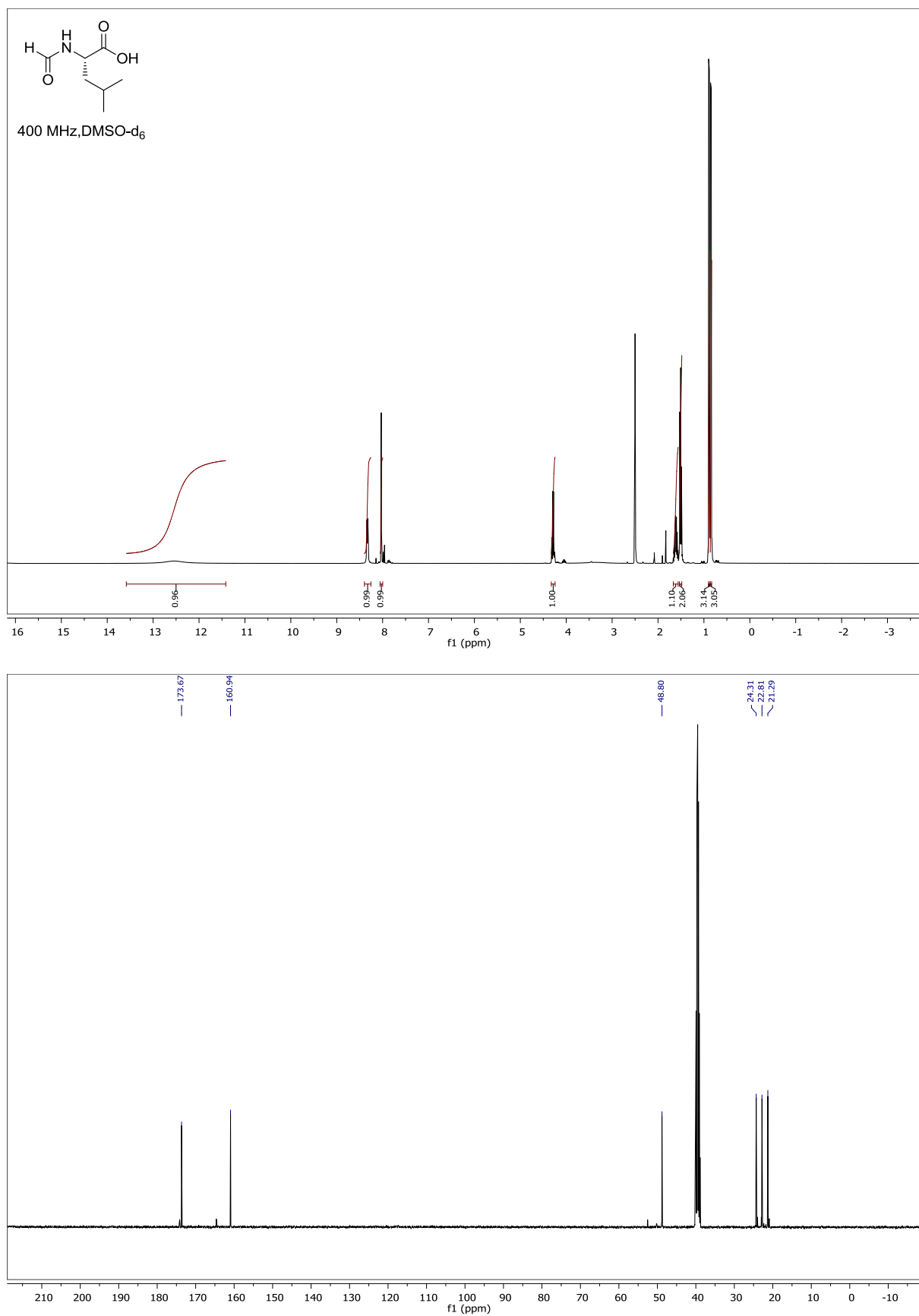
Table 15. Cartesian coordinates for the complex of protonated **3** with the enolate of **5**.

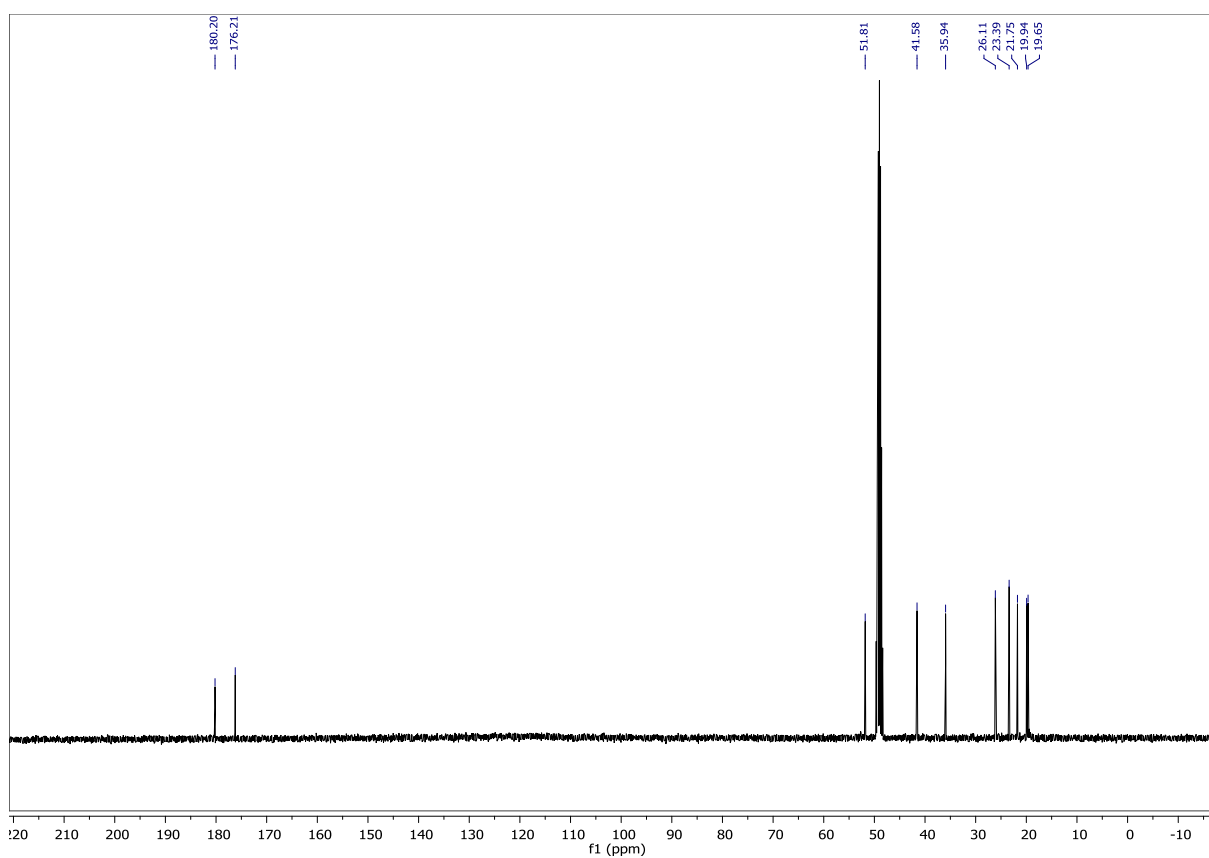
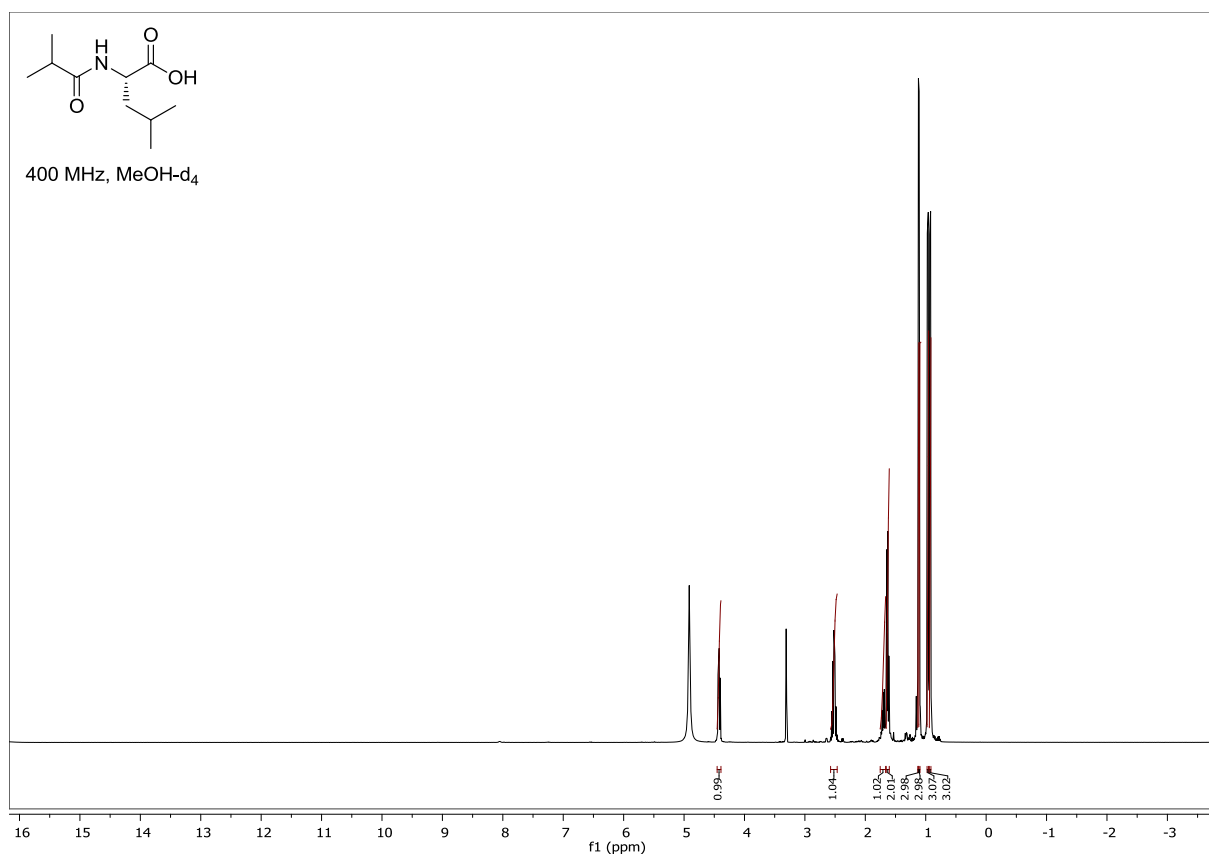
Atom	X	Y	Z
1	2.205275000	-0.258728000	-1.327402000
6	2.833441000	-1.152611000	-1.282474000
6	3.120153000	-3.504484000	-2.096212000
6	5.141793000	-2.112056000	-1.533189000
6	4.579778000	-3.195072000	-2.471723000
6	4.292043000	-0.818547000	-1.657482000
6	2.263664000	-2.232028000	-2.232025000
1	3.064520000	-3.876123000	-1.065158000
1	6.182943000	-1.889164000	-1.790031000
1	2.768362000	-1.558561000	-0.265608000
1	2.714994000	-4.286633000	-2.749474000
1	5.124322000	-2.464940000	-0.494181000
1	5.179353000	-4.106464000	-2.364499000
6	4.641236000	-2.694879000	-3.926023000
1	4.273131000	-3.472375000	-4.606829000
1	5.680341000	-2.481001000	-4.205474000
6	4.328422000	-0.332073000	-3.125477000
1	5.356821000	-0.073395000	-3.391444000
1	3.726010000	0.580067000	-3.220731000
6	2.322281000	-1.739648000	-3.689331000
1	1.914649000	-2.518717000	-4.344633000
1	1.694498000	-0.852972000	-3.797922000
6	3.782254000	-1.425031000	-4.060593000
1	3.819425000	-1.060742000	-5.093892000
6	4.924389000	0.250355000	-0.763409000
8	5.932634000	0.880403000	-1.105045000
7	0.894527000	-2.571789000	-1.813441000
1	0.809998000	-3.380494000	-1.198484000
7	-0.717813000	-1.983880000	0.629059000
6	-1.230453000	-2.117522000	-0.731639000
6	-0.112842000	-1.673746000	-1.695175000
8	-0.120011000	-0.563961000	-2.244229000
1	-0.549056000	-1.013531000	0.962878000
1	-1.451102000	-3.175487000	-0.899006000
6	-2.504604000	-1.283795000	-0.925167000
1	-2.730113000	-1.253744000	-1.994733000
1	-2.304145000	-0.256625000	-0.616499000
7	4.345844000	0.462704000	0.447469000
6	4.883631000	1.412252000	1.396180000
6	4.277045000	1.107991000	2.761635000
8	3.497639000	0.198619000	2.971102000
1	3.549286000	-0.081782000	0.748402000
1	5.966873000	1.264172000	1.479541000
6	4.682743000	2.879437000	0.955868000
6	3.253656000	3.246374000	0.718627000
1	5.255123000	3.002876000	0.032153000
1	5.130957000	3.534620000	1.710747000
6	2.075649000	2.621406000	1.033361000
1	1.841542000	1.684430000	1.512217000
6	1.560605000	4.469431000	-0.075759000
1	0.983304000	5.211822000	-0.603101000
7	2.899179000	4.406993000	0.022859000
6	3.832077000	5.381572000	-0.539745000
1	4.465535000	5.788776000	0.250291000
1	4.454319000	4.904689000	-1.299502000
1	3.259857000	6.188367000	-0.995941000
8	4.712236000	1.960864000	3.693473000
6	4.193019000	1.760078000	5.030808000
1	4.645605000	2.544933000	5.633497000
1	3.105366000	1.849141000	5.024632000
1	4.479919000	0.772928000	5.396981000
6	0.029399000	-2.969430000	1.181349000
8	0.274182000	-4.055710000	0.640890000
8	0.462835000	-2.599006000	2.404011000
6	1.462084000	-3.389617000	3.140087000
6	2.756428000	-3.471101000	2.326656000
1	2.607394000	-4.033651000	1.403968000
1	3.112698000	-2.464357000	2.089843000
1	3.527477000	-3.973156000	2.919930000
6	1.675994000	-2.557355000	4.404644000
1	0.737117000	-2.458151000	4.957620000
1	2.409272000	-3.051054000	5.050200000
6	0.899067000	-4.769294000	3.487457000
1	0.755317000	-5.375554000	2.593140000
1	1.593282000	-5.283191000	4.160623000
1	-0.061205000	-4.664024000	4.001826000
7	-1.075316000	1.989433000	-1.138920000
1	-0.809309000	1.039735000	-1.404795000
6	-2.976132000	2.984837000	0.143050000
1	-3.121997000	3.503752000	1.090213000
1	-2.925654000	3.754376000	-0.630800000
6	-1.772672000	1.562100000	2.599885000
1	-0.956098000	1.775519000	3.298385000
1	-2.193014000	0.596083000	2.900663000
1	-2.547172000	2.319953000	2.711136000
6	-0.765218000	2.979729000	-2.001477000
8	-0.891391000	4.190112000	-1.716832000
6	-0.264036000	2.546890000	-3.362797000
1	-0.015925000	1.485484000	-3.402907000
1	-1.044696000	2.755206000	-4.102407000
1	2.044728000	-1.561226000	4.149162000
1	0.609039000	3.149635000	-3.628349000
7	1.055665000	3.403232000	0.535082000
1	0.043798000	3.156850000	0.564365000
6	-1.182511000	1.453409000	1.205106000
6	-1.671511000	2.209200000	0.146641000
8	-0.167209000	0.662082000	1.080148000
6	-4.197736000	2.108564000	-0.109280000
6	-4.492376000	1.582260000	-1.370026000
6	-5.091675000	1.766628000	0.906712000
9	-3.714679000	1.891572000	-2.430468000
9	-4.913526000	2.253771000	2.157748000
6	-5.580642000	0.749112000	-1.603862000
6	-6.197478000	0.946307000	0.703804000
9	-5.810174000	0.255398000	-2.834392000

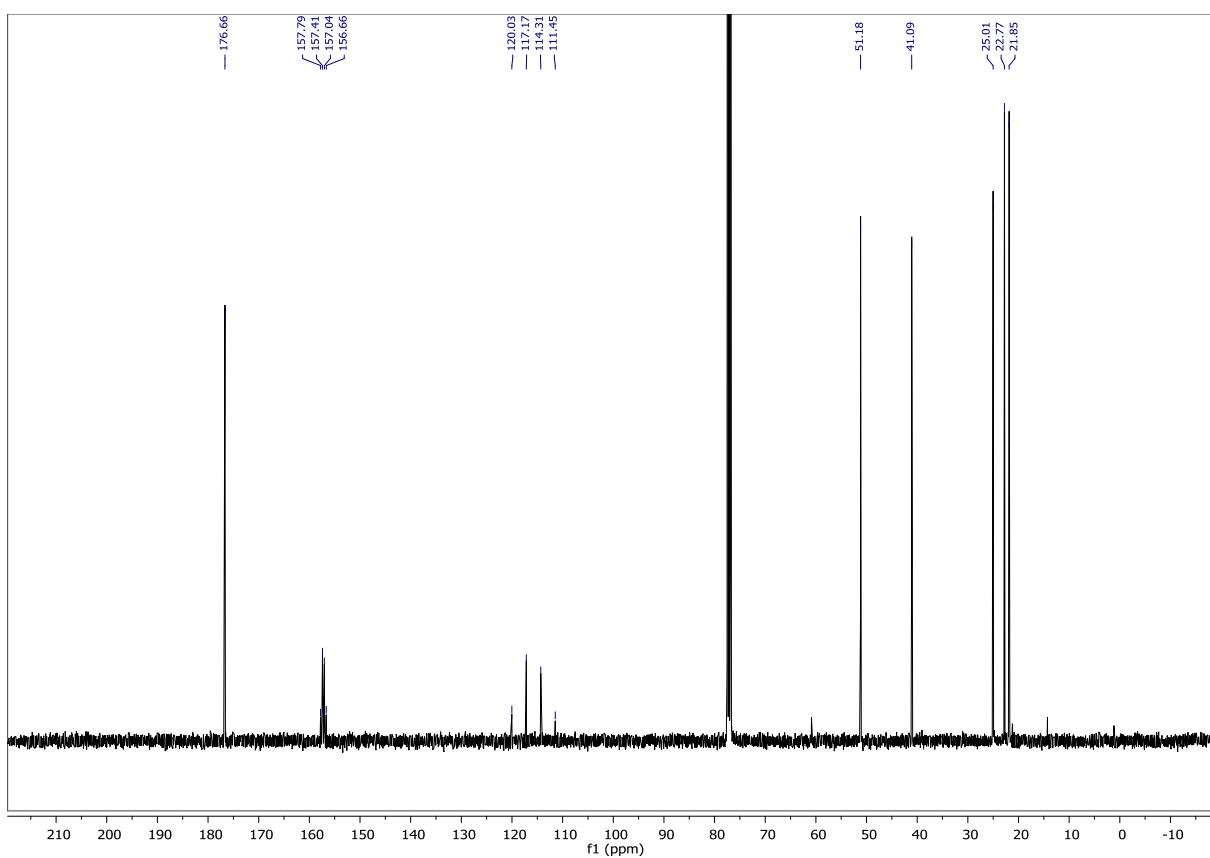
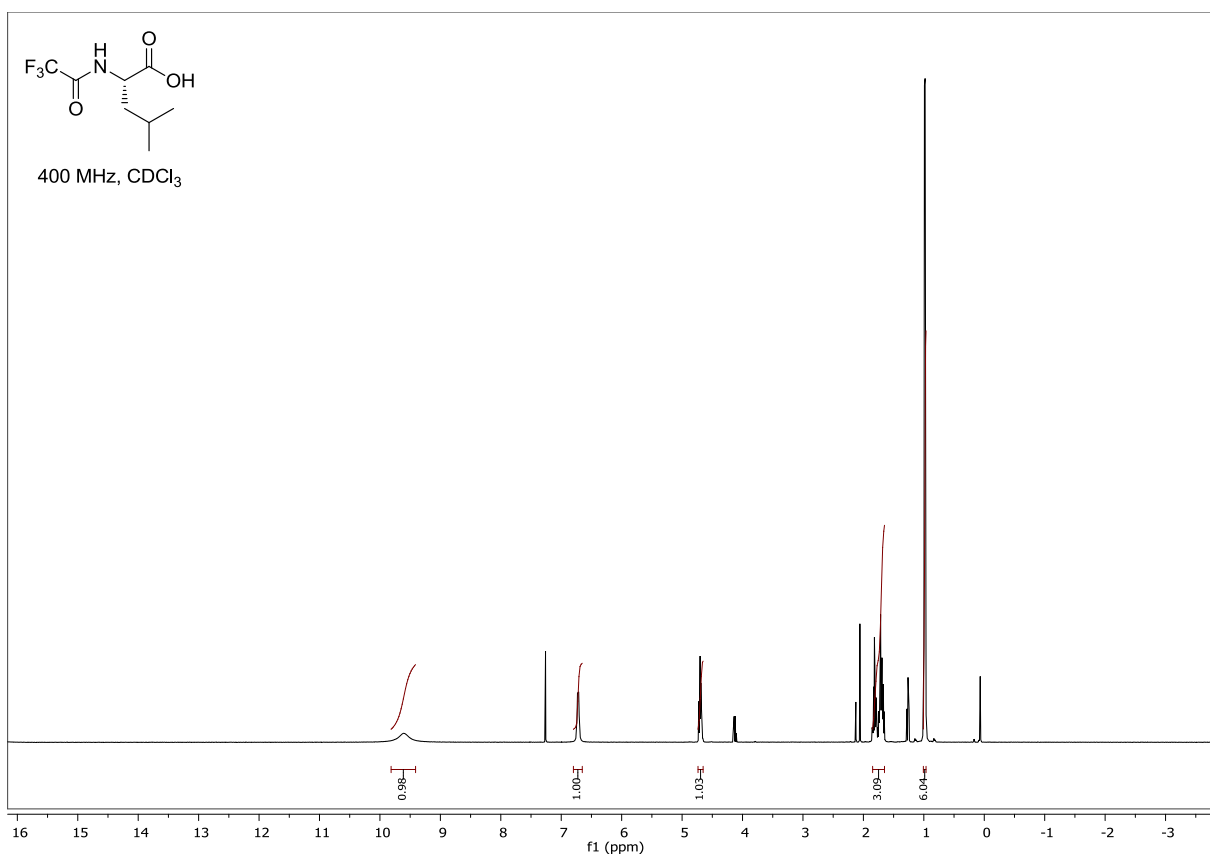
9	-7.028421000	0.658563000	1.720979000
6	-6.444390000	0.429862000	-0.561325000
9	-7.507839000	-0.357997000	-0.780207000
6	-3.689582000	-1.818681000	-0.161634000
6	-4.660435000	-2.599954000	-0.802059000
6	-3.849162000	-1.540009000	1.202328000
1	-4.558652000	-2.811362000	-1.863547000
1	-3.108966000	-0.932040000	1.708414000
6	-5.765020000	-3.088987000	-0.100690000
6	-4.950081000	-2.026735000	1.908323000
1	-6.515398000	-3.678488000	-0.618824000
1	-5.062263000	-1.788049000	2.961789000
6	-5.913832000	-2.802560000	1.258495000
1	-6.778635000	-3.168963000	1.803043000

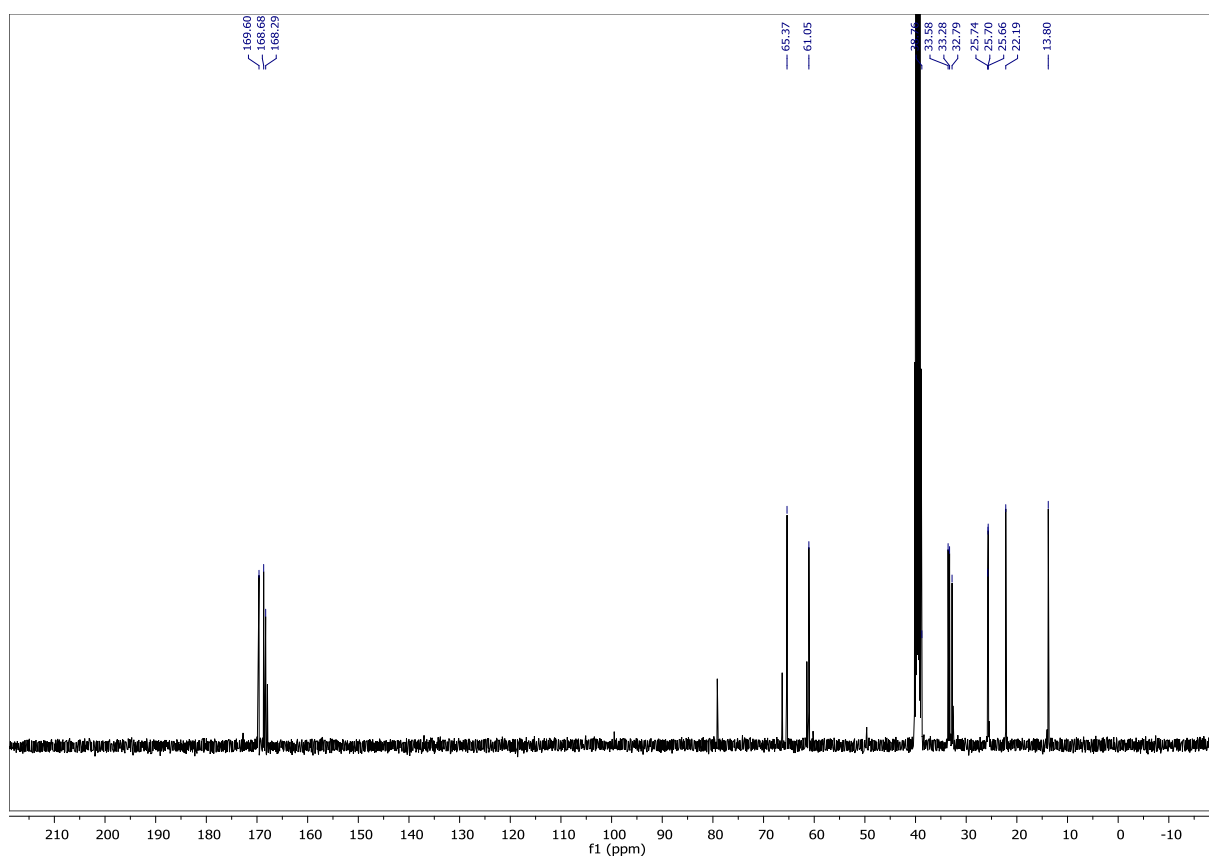
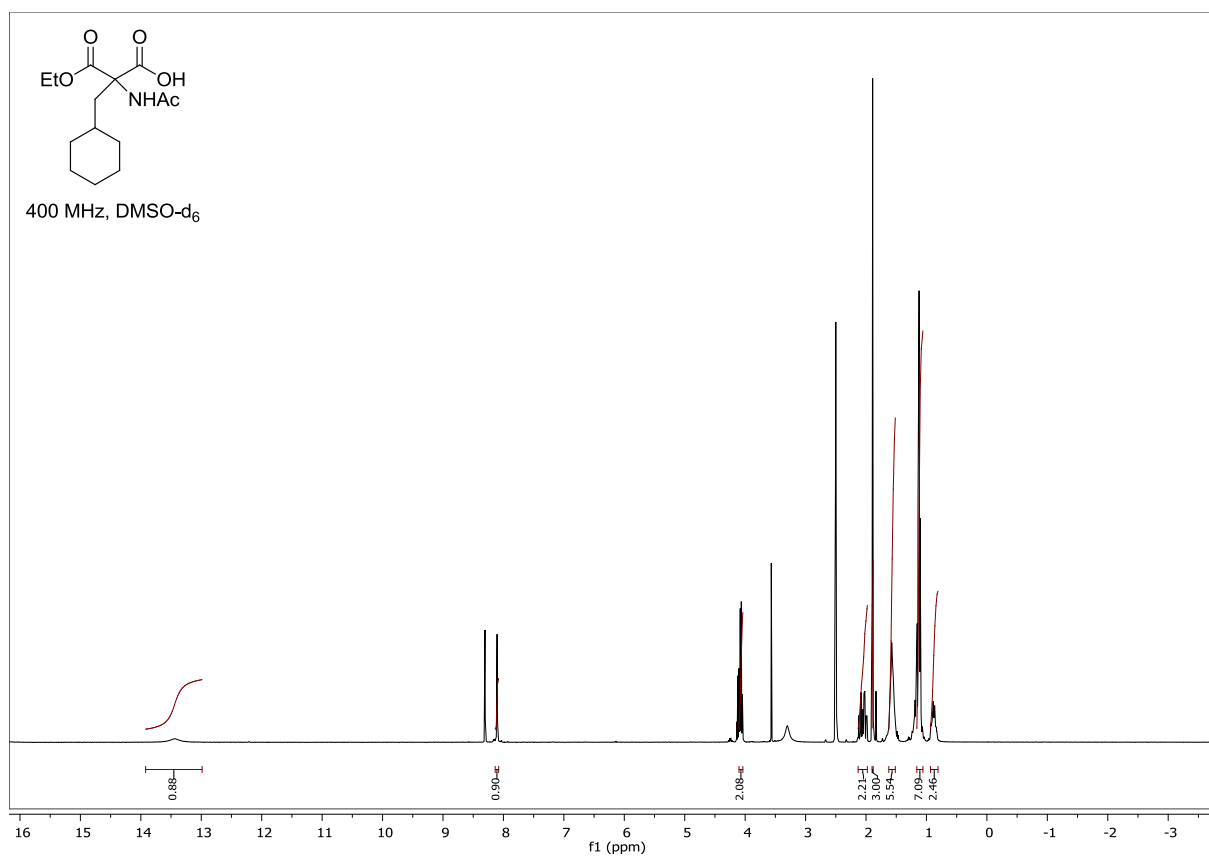
6.8 NMR Spectra

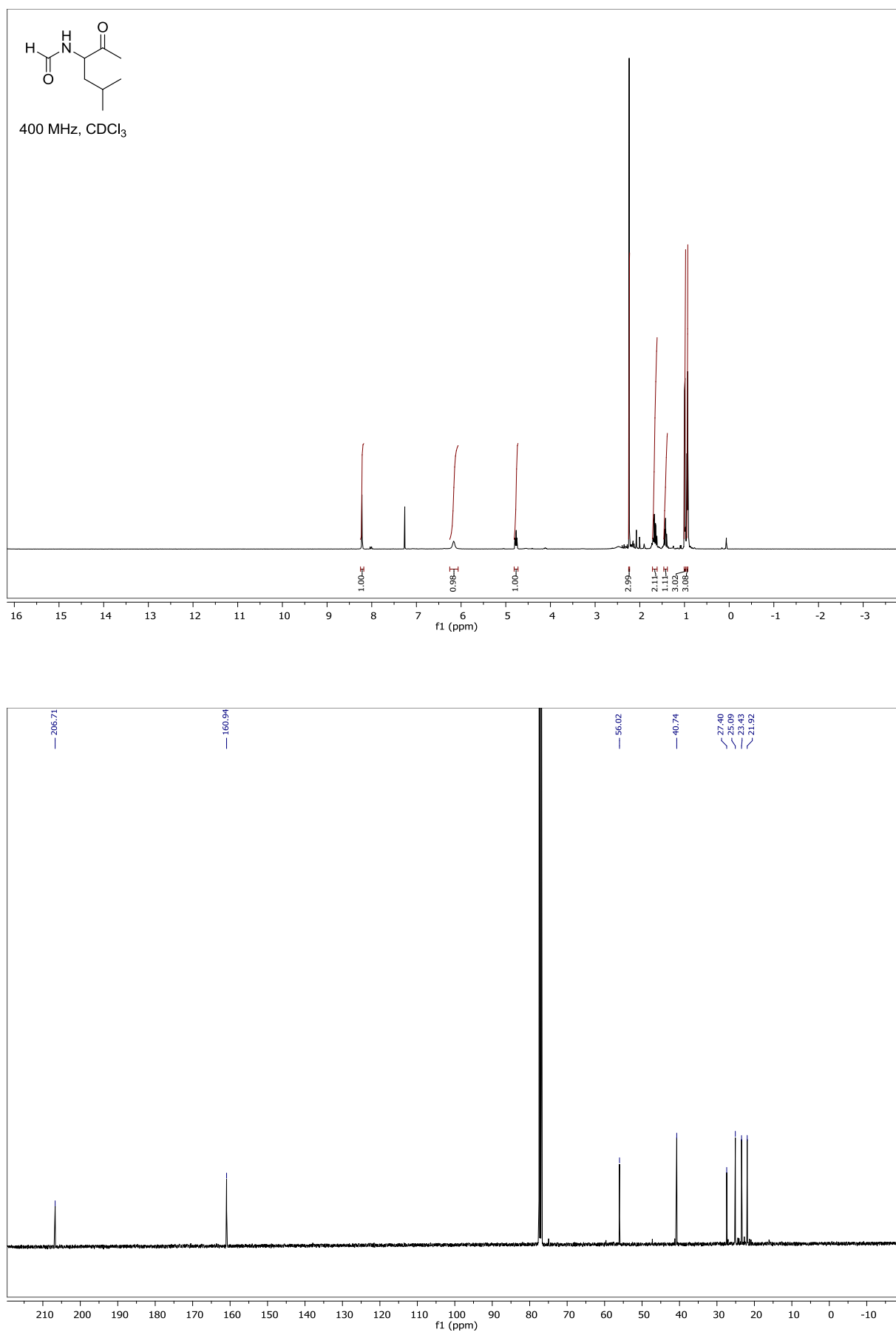
(*S*)-2-formamido-4-methylpentanoic acid (6b)

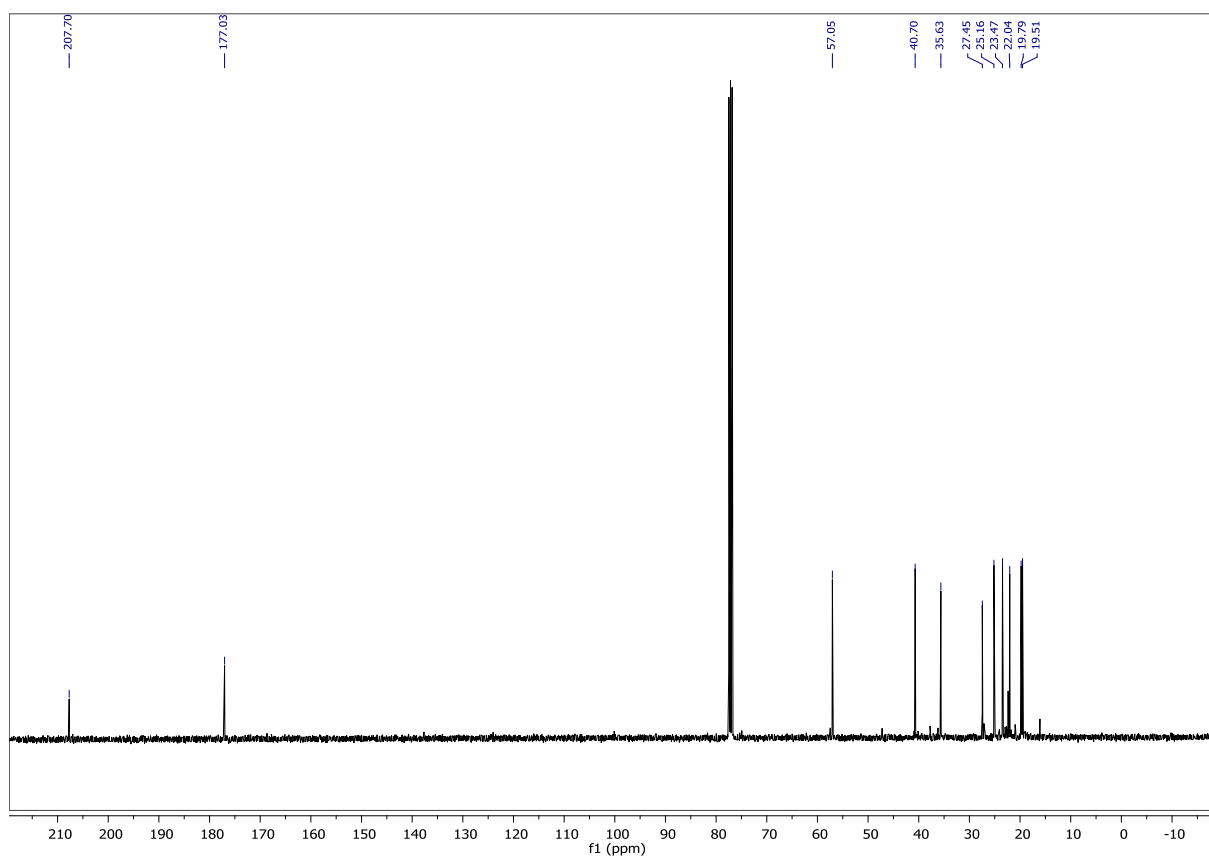
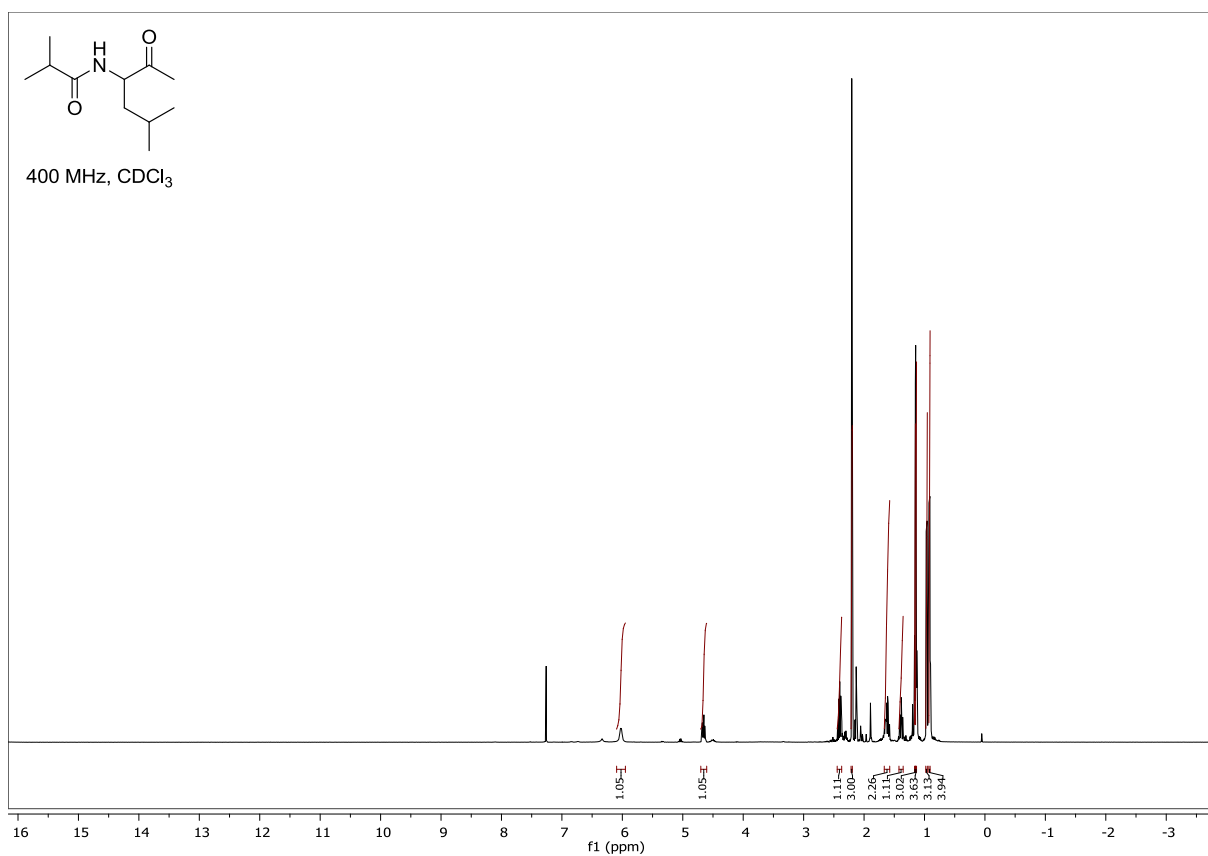


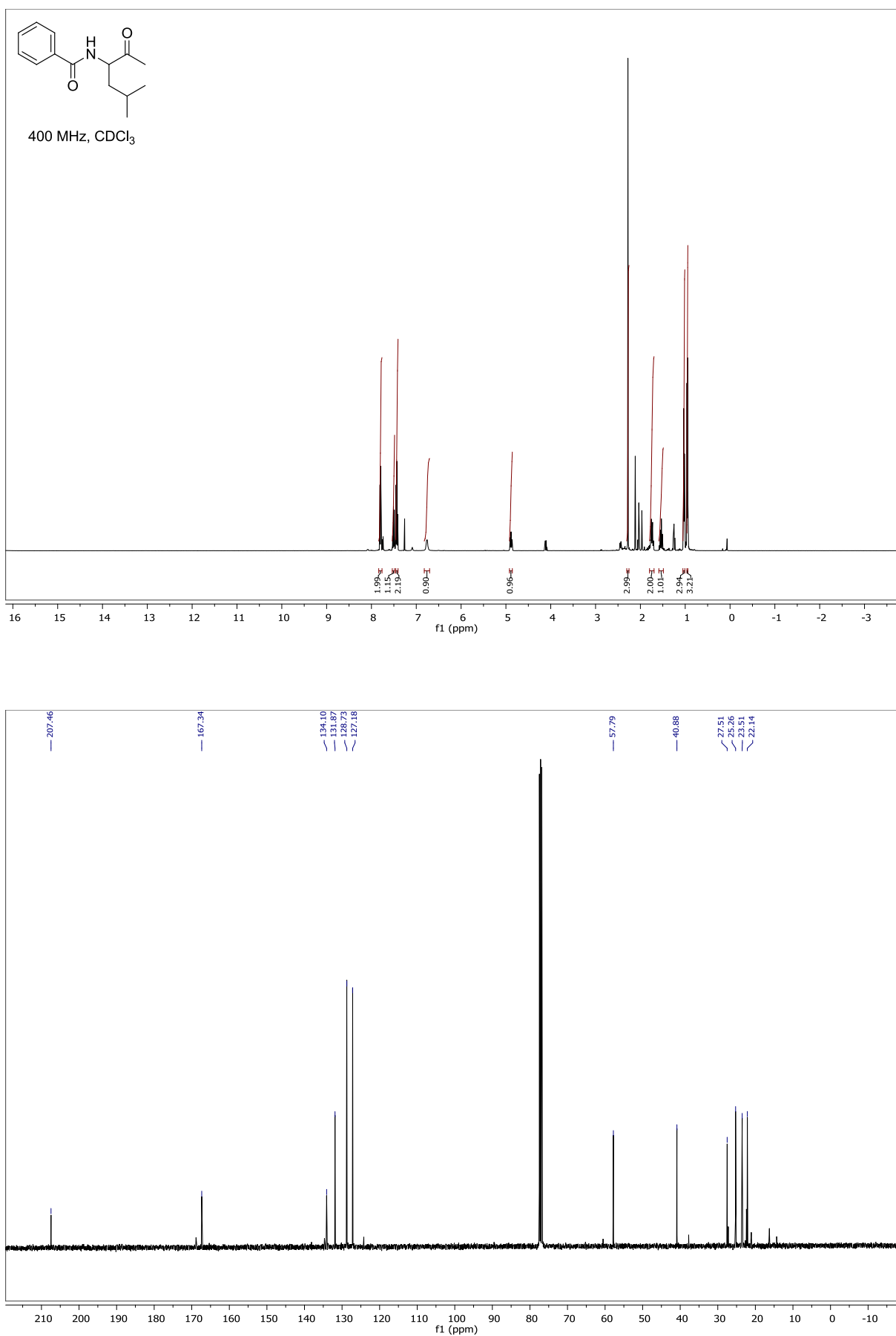
(S)-2-isobutyramido-4-methylpentanoic acid (6c)

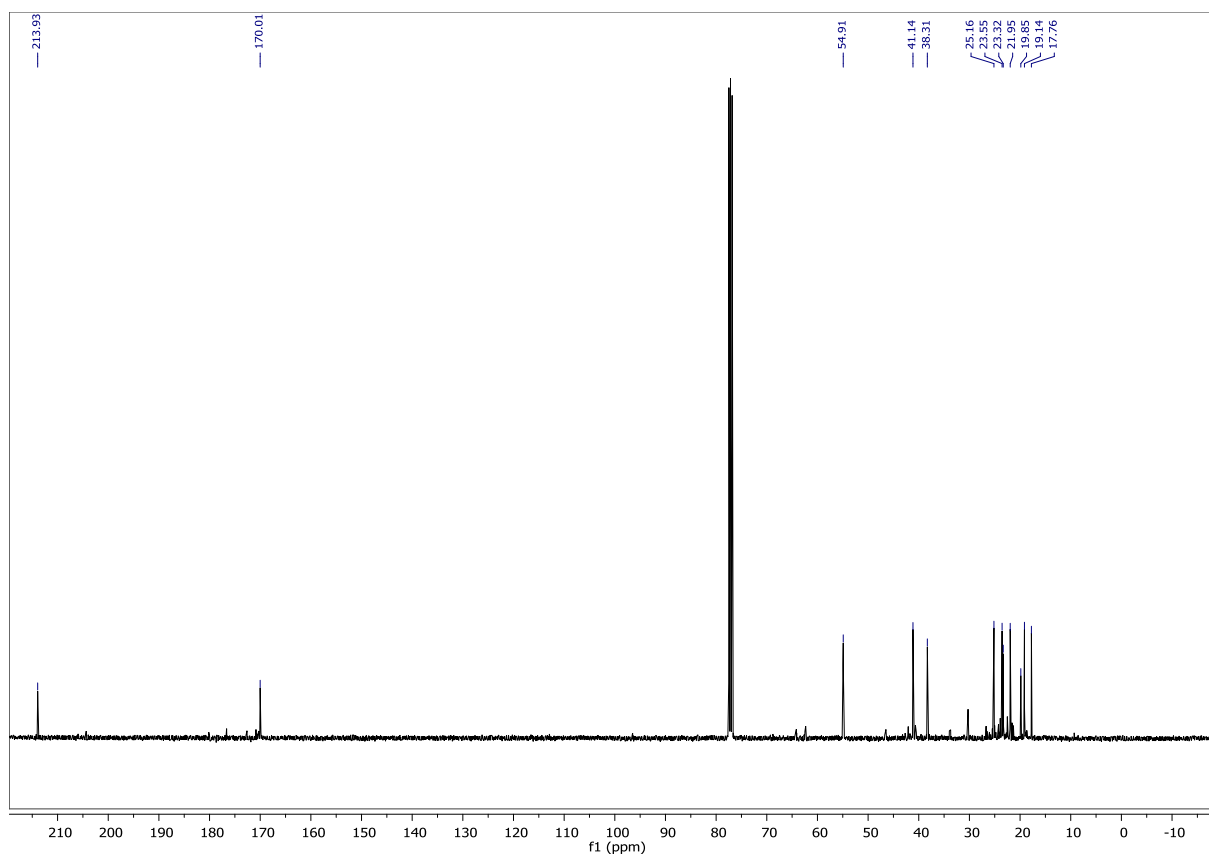
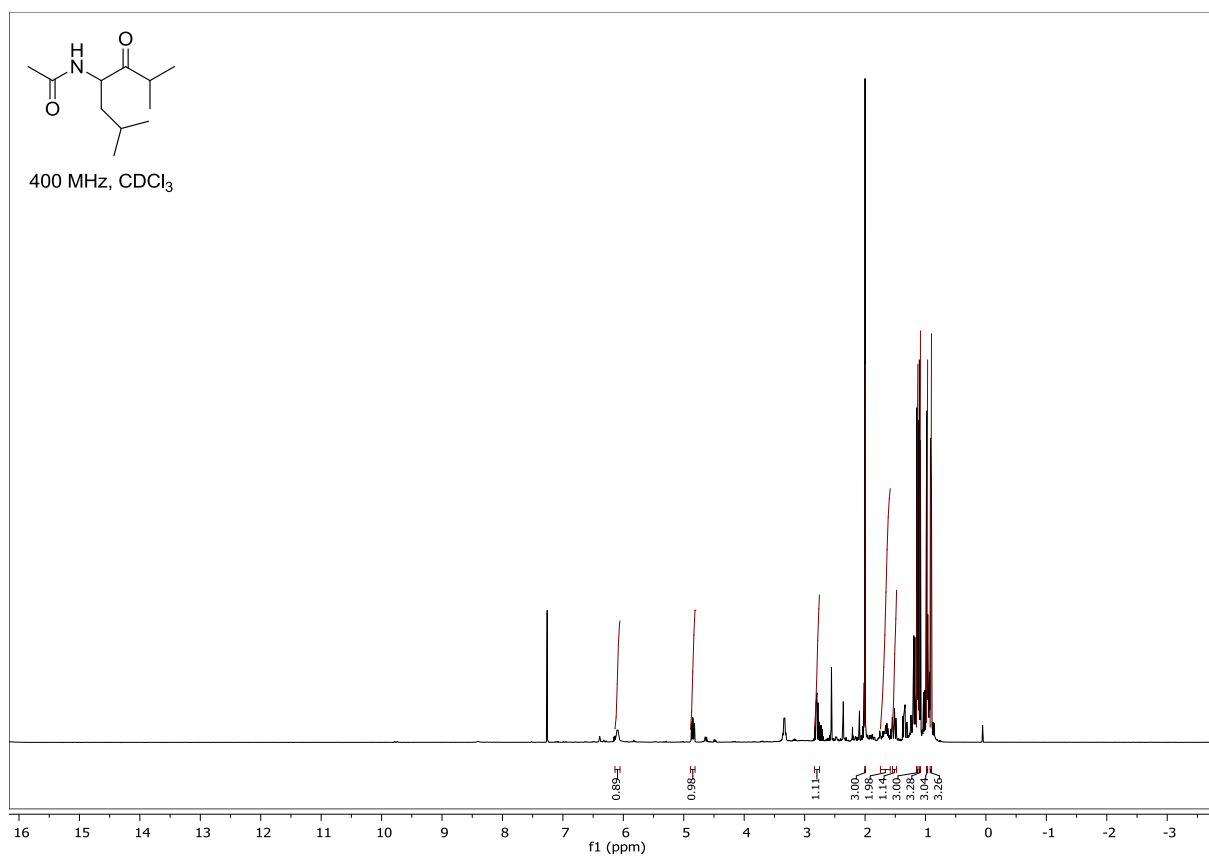
(S)-4-methyl-2-(2,2,2-trifluoroacetamido)pentanoic acid (6e)

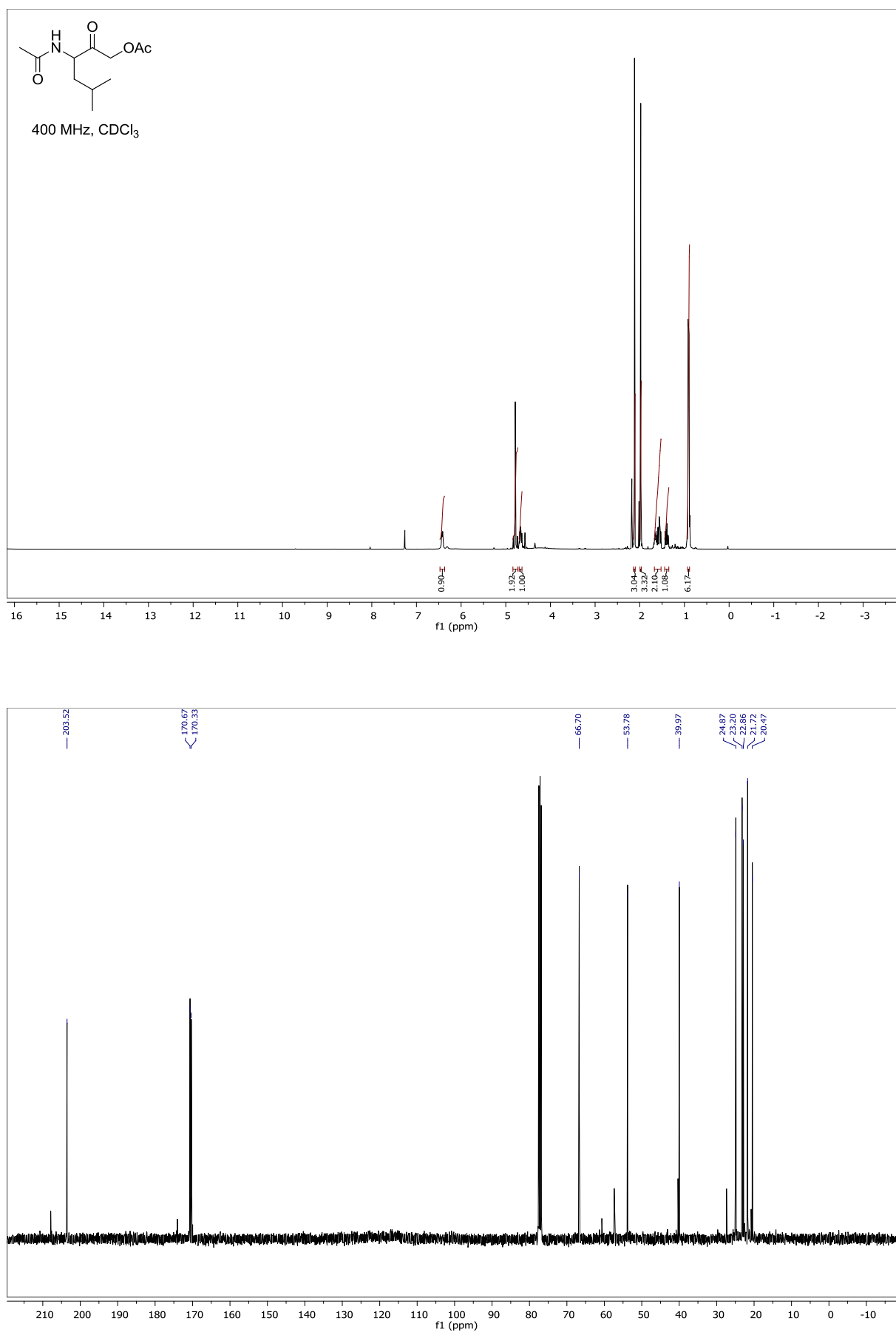
2-Acetamido-2-(cyclohexylmethyl)-3-ethoxy-3-oxopropanoic acid (12)

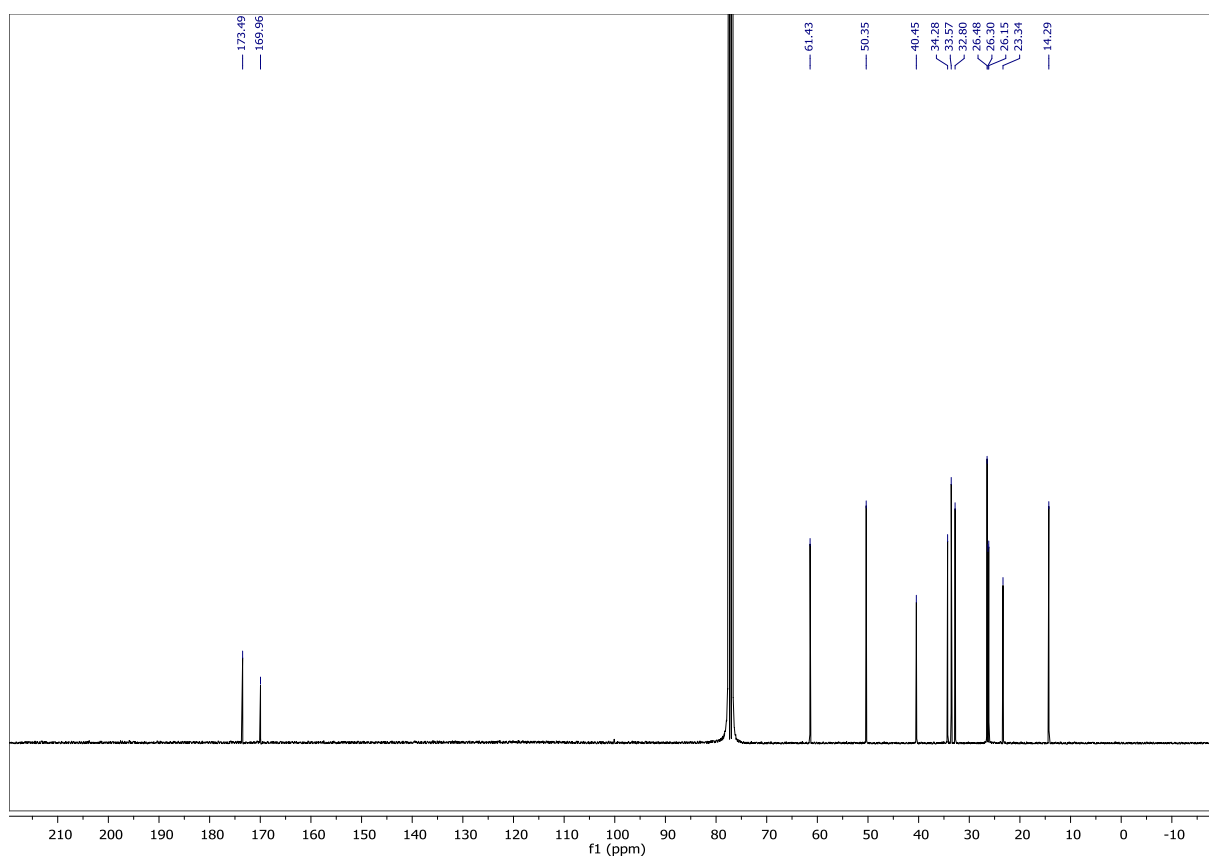
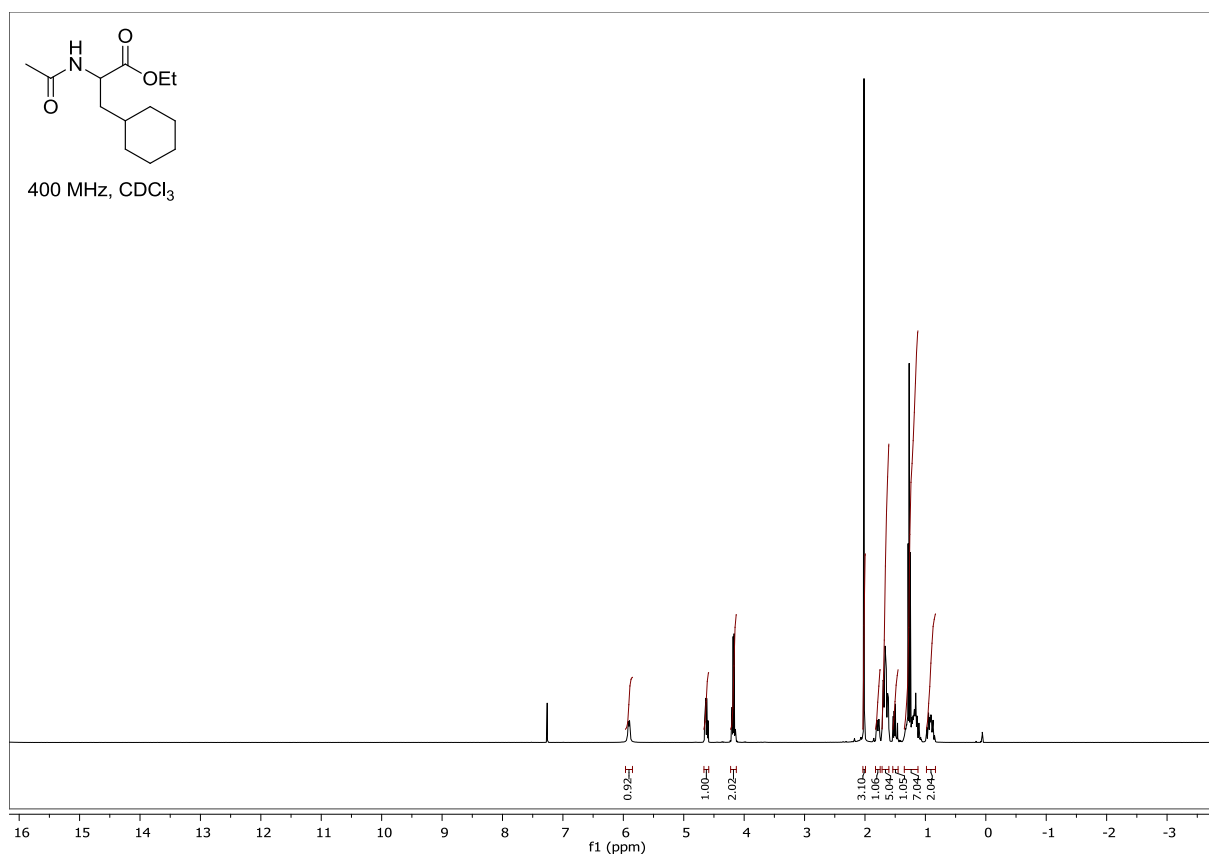
***N*-(5-methyl-2-oxohexan-3-yl)formamide (7b)**

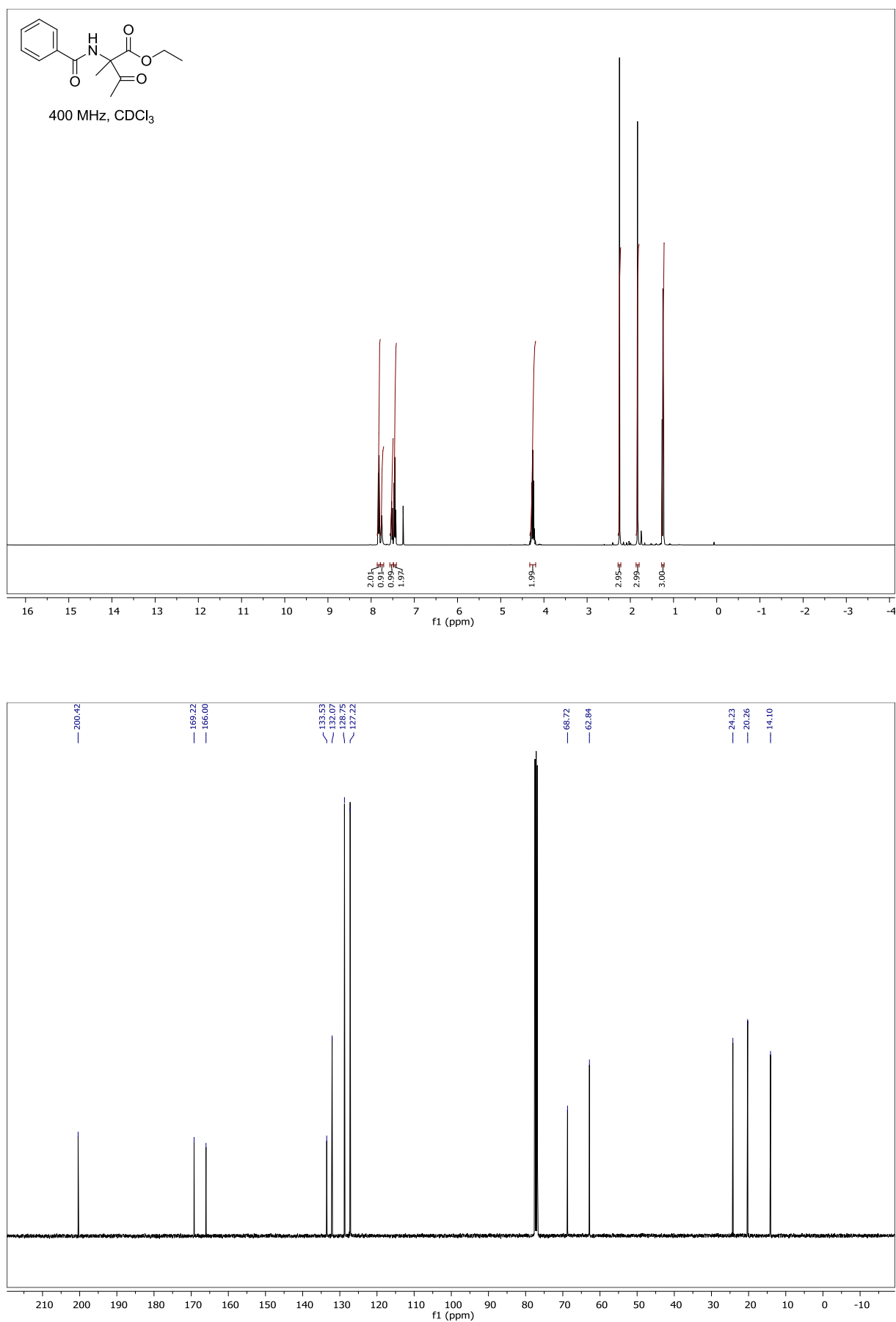
***N*-(5-methyl-2-oxohexan-3-yl)isobutyramide (7c)**

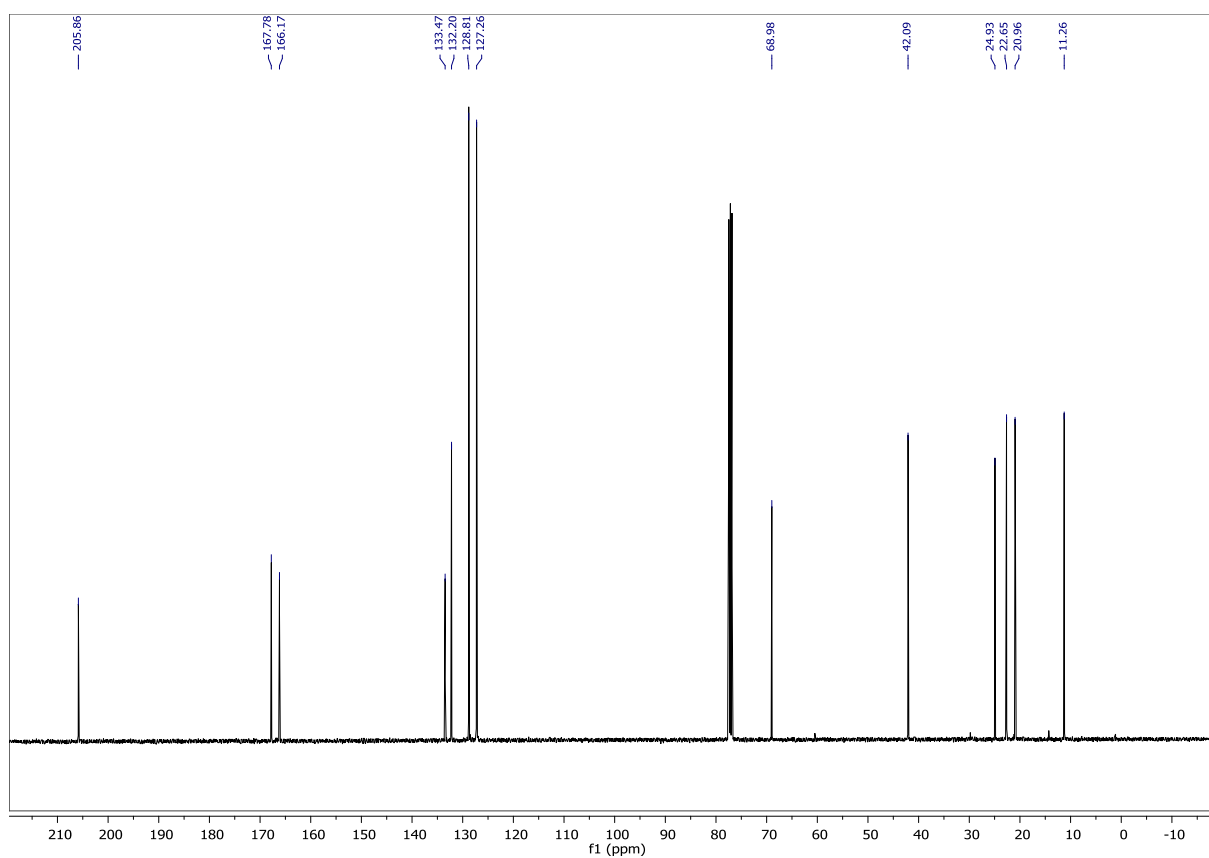
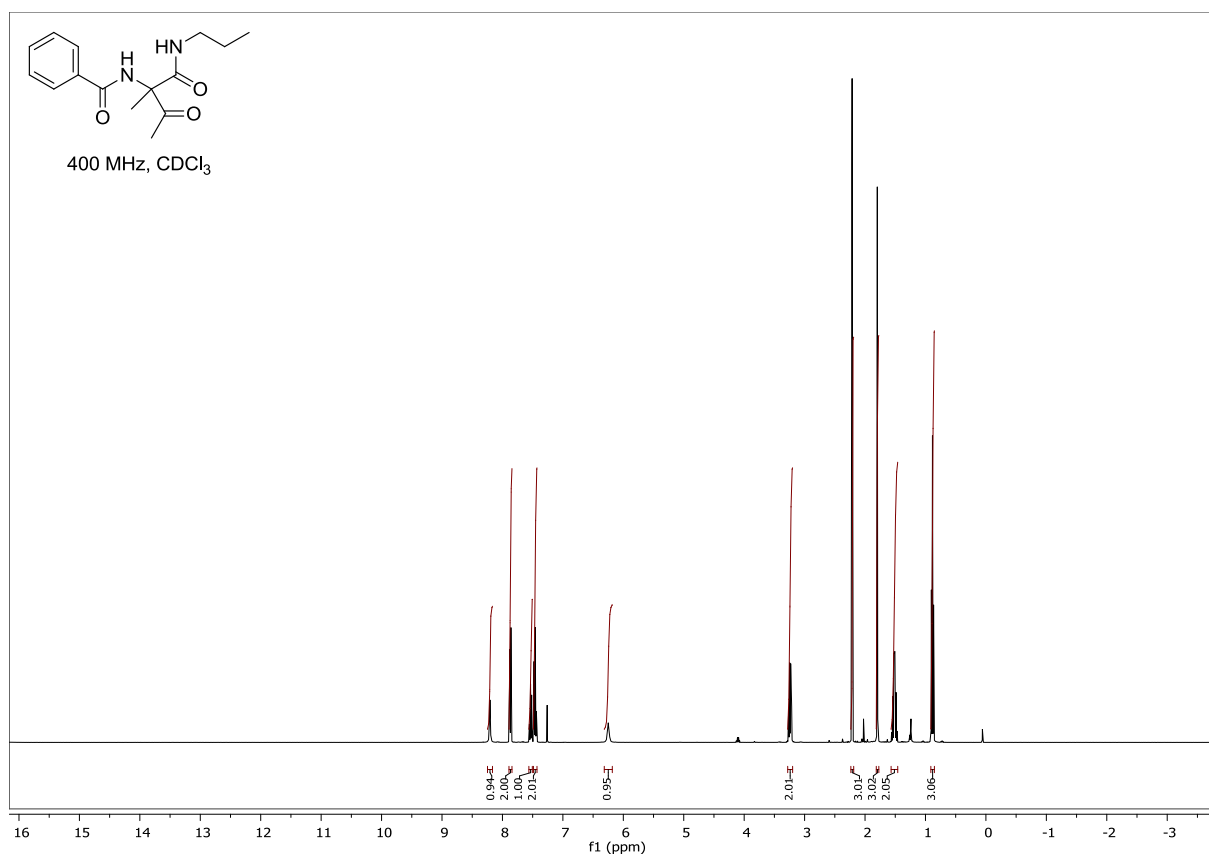
***N*-(5-methyl-2-oxohexan-3-yl)benzamide (7d)**

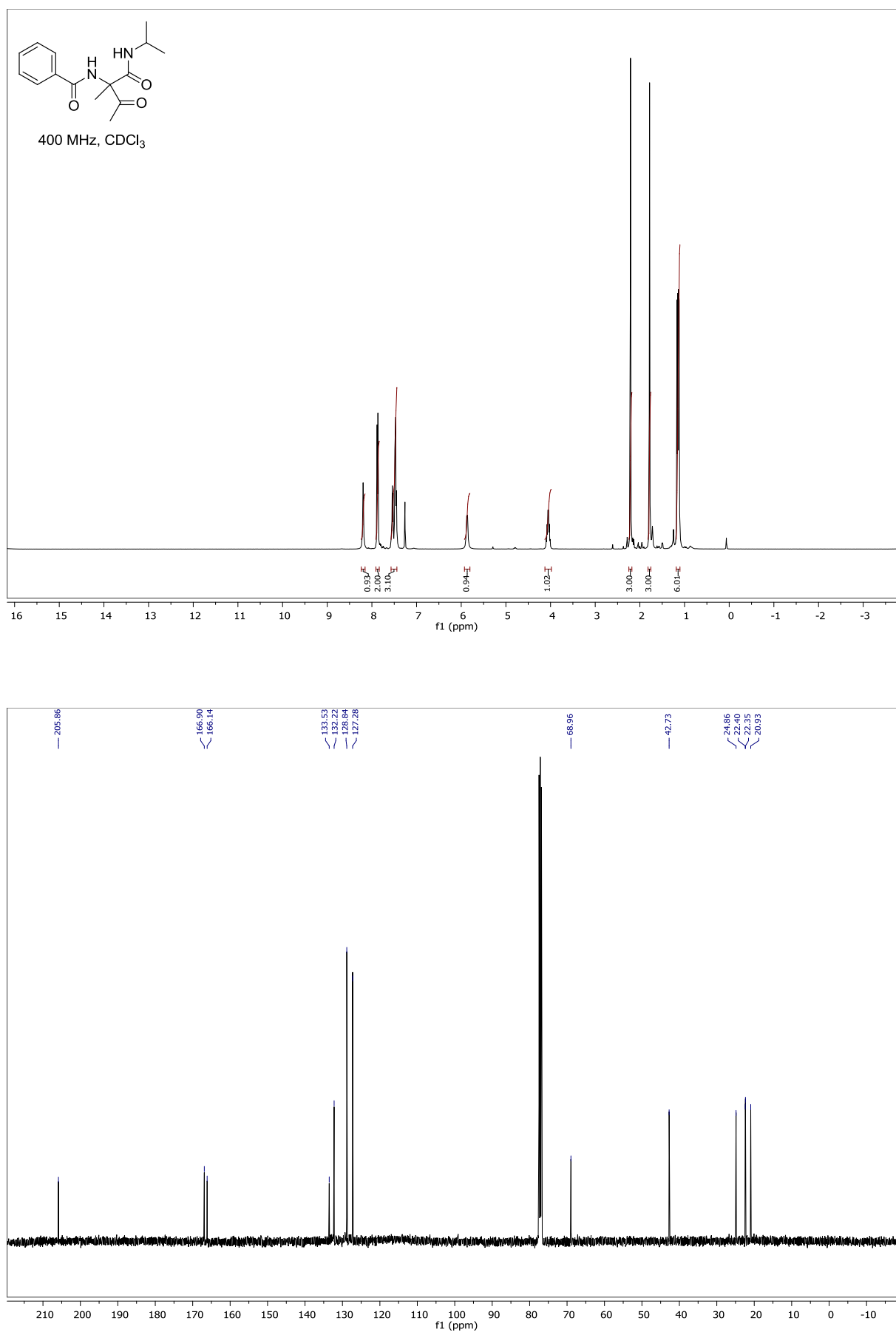
***N*-(2,6-dimethyl-3-oxoheptan-4-yl)acetamide (7f)**

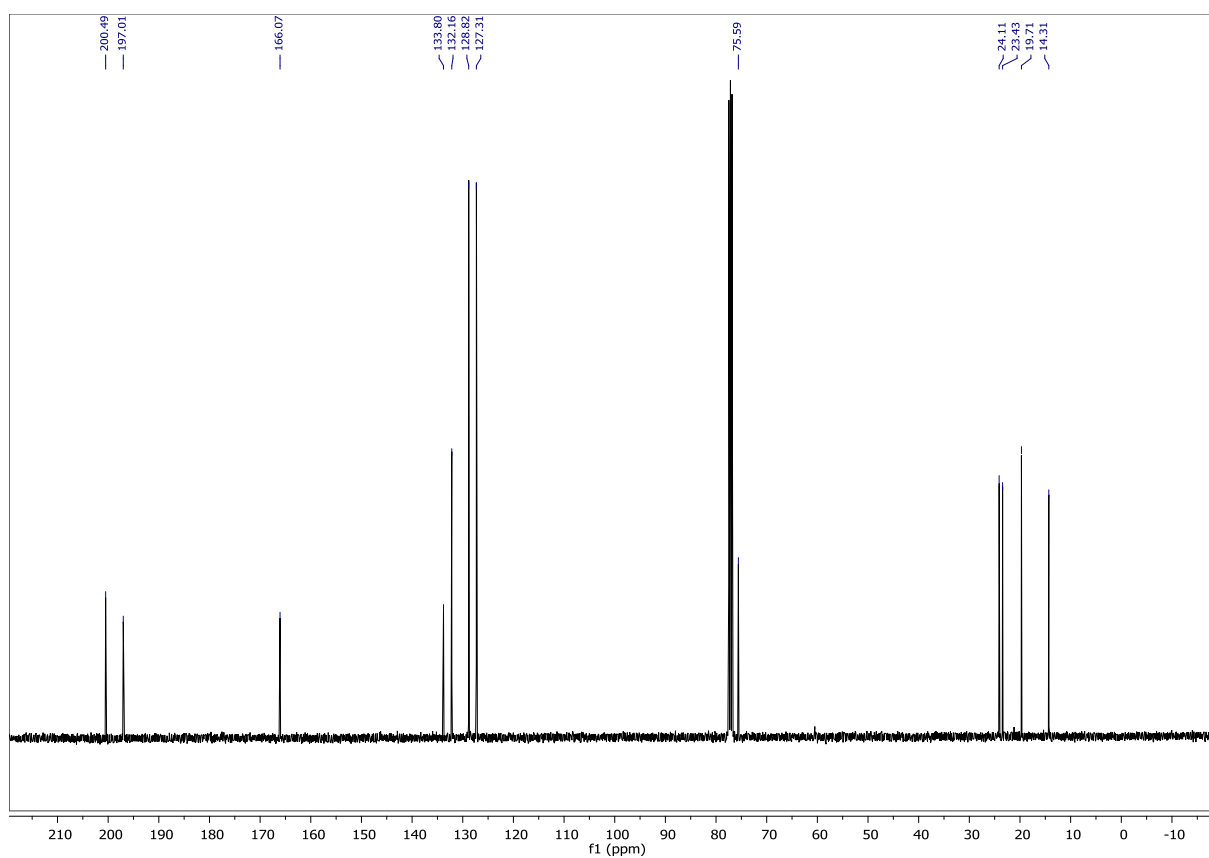
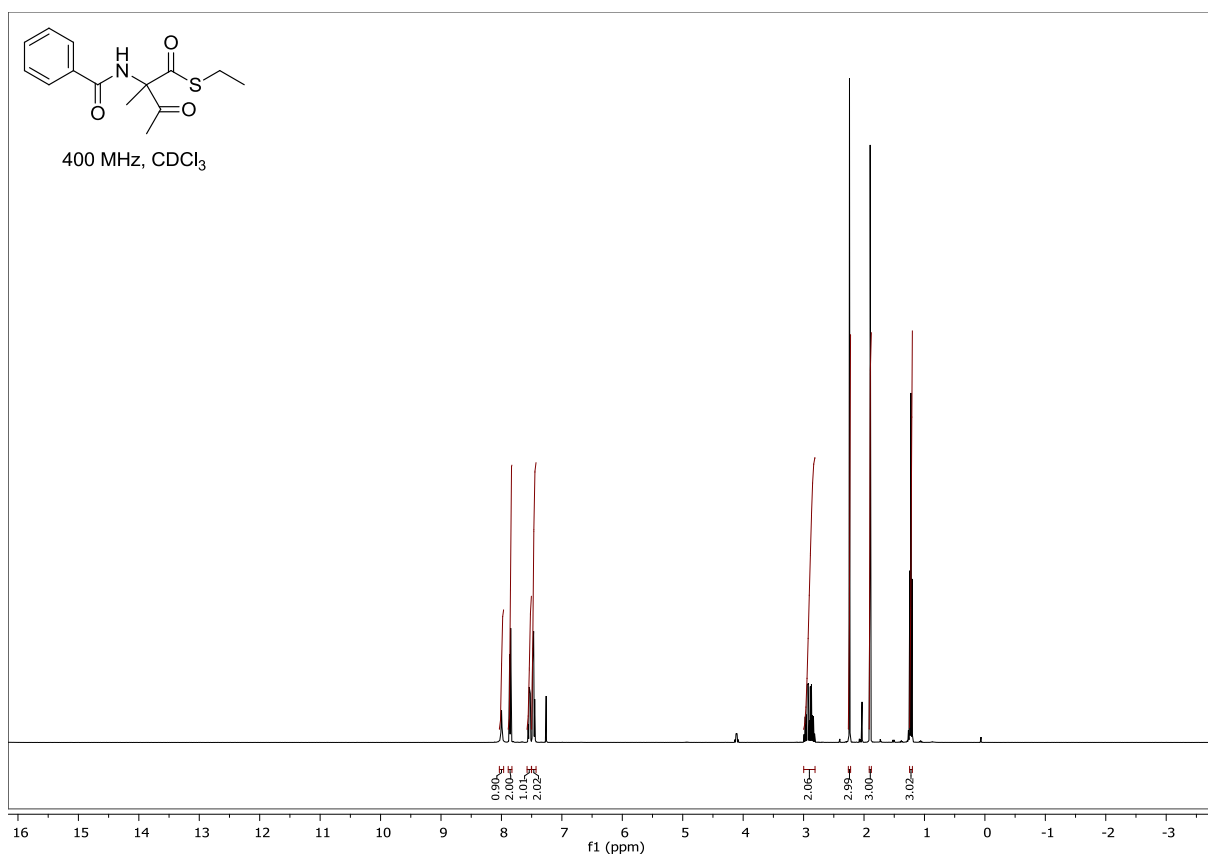
3-Acetamido-5-methyl-2-oxohexyl acetate (7i)

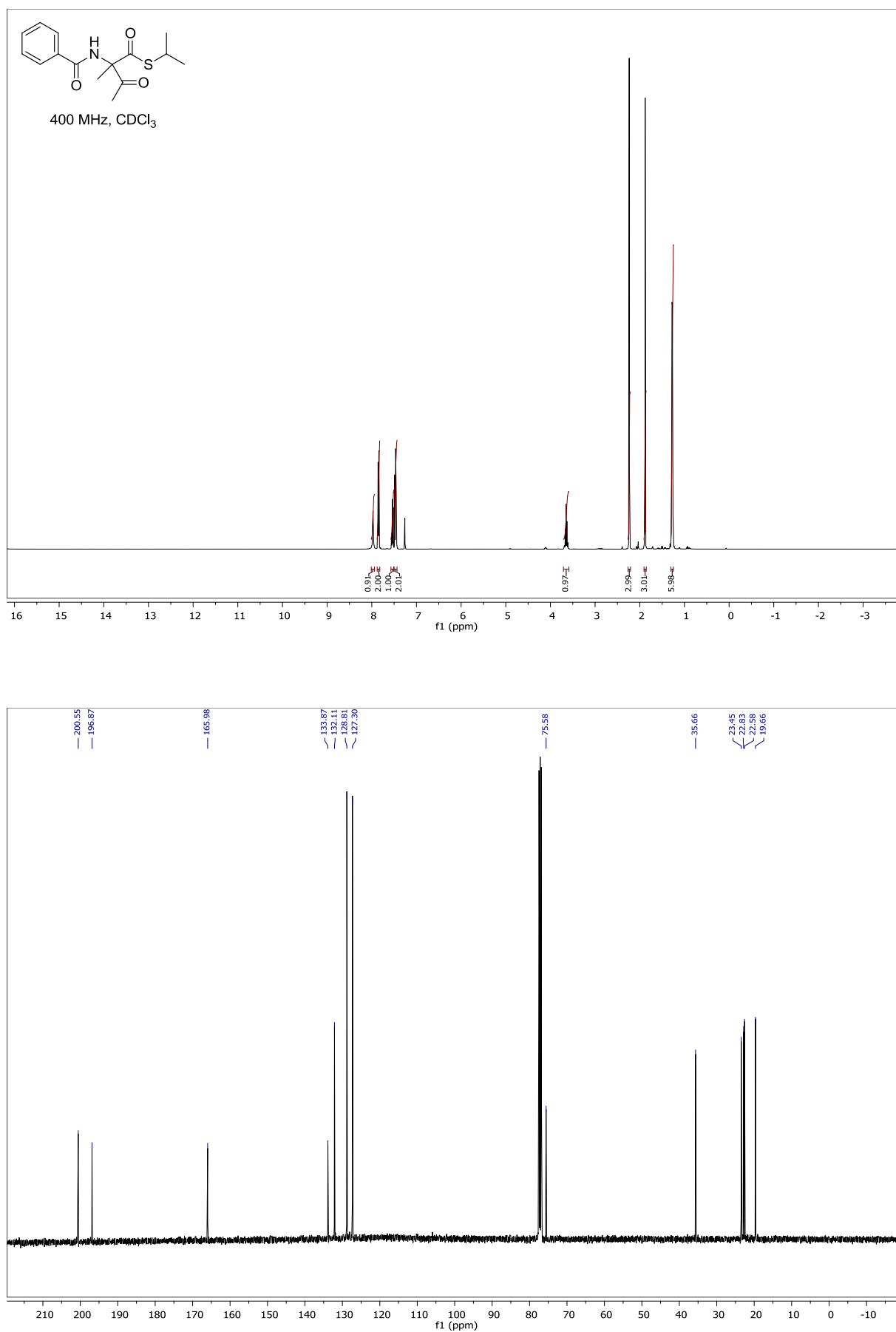
Ethyl 2-acetamido-3-cyclohexylpropanoate (13)

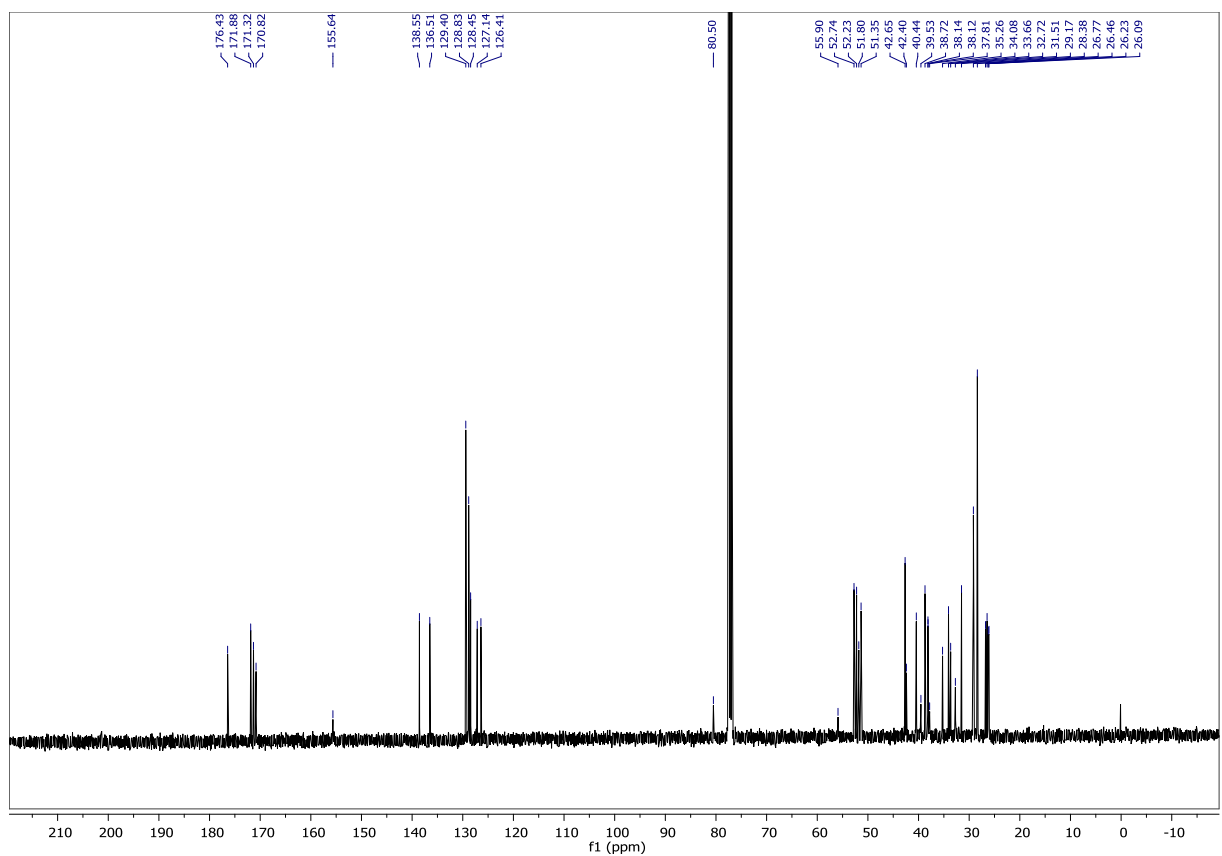
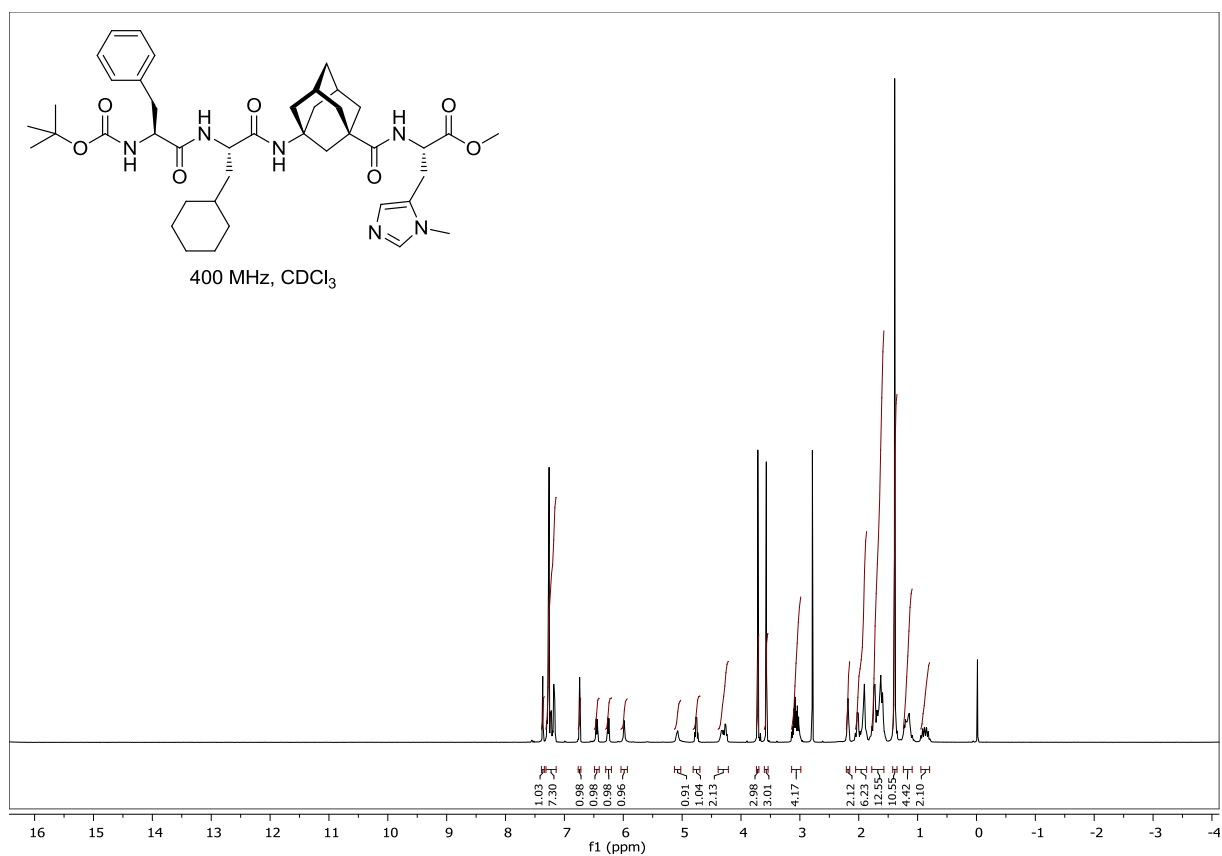
Ethyl 2-benzamido-2-methyl-3-oxobutanoate (23b)

***N*-(2-methyl-1,3-dioxo-1-(propylamino)butan-2-yl)benzamide (23e)**

***N*-(1-(isopropylamino)-2-methyl-1,3-dioxobutan-2-yl)benzamide (23f)**

S-Ethyl 2-benzamido-2-methyl-3-oxobutanethioate (23g)

S-Isopropyl 2-benzamido-2-methyl-3-oxobutanethioate (23h)

Boc-L-Phe-L-Cha^AGly-L-Pmh-OMe (11)

7. References

- [1] R. C. Wende, A. Seitz, D. Niedek, S. M. M. Schuler, C. Hofmann, J. Becker, P. R. Schreiner, *Angew. Chem. Int. Ed.* **2016**, *55*, 2719–2723.
- [2] J. P. Wagner, P. R. Schreiner, *Angew. Chem. Int. Ed.* **2015**, *54*, 12274–12296.
- [3] a) A. D. Becke, *J. Chem. Phys.* **1993**, *98*, 5648–5652; b) C. Lee, W. Yang, R. G. Parr, *Phys. Rev. B* **1988**, *37*, 785–789.
- [4] S. Grimme, J. Antony, S. Ehrlich, H. Krieg, *J. Chem. Phys.* **2010**, *132*, 154104–154122.
- [5] S. Grimme, S. Ehrlich, L. Goerigk, *J. Comput. Chem.* **2011**, *32*, 1456–1465.
- [6] J. Tomasi, B. Mennucci, R. Cammi, *Chem. Rev.* **2005**, *105*, 2999–3094.
- [7] V. Barone, M. Cossi, J. Tomasi, *J. Chem. Phys.* **1997**, *107*, 3210–3221.
- [8] Gaussian 09, Revision D.01, M. J. Frisch, G. W. Trucks, H. B. Schlegel, G. E. Scuseria, M. A. Robb, J. R. Cheeseman, G. Scalmani, V. Barone, B. Mennucci, G. A. Petersson, H. Nakatsuji, M. Caricato, X. Li, H. P. Hratchian, A. F. Izmaylov, J. Bloino, G. Zheng, J. L. Sonnenberg, M. Hada, M. Ehara, K. Toyota, R. Fukuda, J. Hasegawa, M. Ishida, T. Nakajima, Y. Honda, O. Kitao, H. Nakai, T. Vreven, J. A. Montgomery, Jr., J. E. Peralta, F. Ogliaro, M. Bearpark, J. J. Heyd, E. Brothers, K. N. Kudin, V. N. Staroverov, T. Keith, R. Kobayashi, J. Normand, K. Raghavachari, A. Rendell, J. C. Burant, S. S. Iyengar, J. Tomasi, M. Cossi, N. Rega, J. M. Millam, M. Klene, J. E. Knox, J. B. Cross, V. Bakken, C. Adamo, J. Jaramillo, R. Gomperts, R. E. Stratmann, O. Yazyev, A. J. Austin, R. Cammi, C. Pomelli, J. W. Ochterski, R. L. Martin, K. Morokuma, V. G. Zakrzewski, G. A. Voth, P. Salvador, J. J. Dannenberg, S. Dapprich, A. D. Daniels, O. Farkas, J. B. Foresman, J. V. Ortiz, J. Cioslowski, D. J. Fox, Gaussian, Inc., Wallingford CT, **2013**.
- [9] C. Y. Legault, CYLview 1.0b, Université de Sherbrooke; <http://www.cylview.org>, **2009**.
- [10] S. Tsuzuki, T. Uchimaru, M. Mikami, *J. Phys. Chem. A* **2006**, *110*, 2027–2033.
- [11] W. Steglich, G. Höfle, *Angew. Chem. Int. Ed.* **1969**, *8*, 981–981.
- [12] a) E. Baltazzi, *Q. Rev. Chem. Soc.* **1955**, *9*, 150–173; b) J. S. Fisk, R. A. Mosey, J. J. Tepe, *Chem. Soc. Rev.* **2007**, *36*, 1432–1440; c) A.-N. R. Alba, R. Rios, *Chem.-Asian J.* **2011**, *6*, 720–734.
- [13] a) W. Steglich, G. Höfle, *Chem. Ber.* **1969**, *102*, 883–898; b) W. Steglich, G. Höfle, *Chem. Ber.* **1969**, *102*, 899–903; c) W. Steglich, G. Höfle, *Chem. Ber.* **1969**, *102*, 1129–1147; d) W. Steglich, P. Gruber, G. Höfle, W. König, *Angew. Chem. Int. Ed.* **1971**, *10*, 653–654.
- [14] a) J. T. Mohr, A. Y. Hong, B. M. Stoltz, *Nat. Chem.* **2009**, *1*, 359–369; b) Y. Pan, C.-H. Tan, *Synthesis* **2011**, 2044–2053; c) S. Nakamura, *Org. Biomol. Chem.* **2014**, *12*, 394–405; d) S. Oudeyer, J.-F. Brière, V. Levacher, *Eur. J. Org. Chem.* **2014**, 6103–6119.
- [15] H. Brunner, Markus A. Baur, *Eur. J. Org. Chem.* **2003**, 2854–2862.
- [16] J. C. Powers, J. L. Asgian, Ö. D. Ekici, K. E. James, *Chem. Rev.* **2002**, *102*, 4639–4750.
- [17] a) M. Kolb, J. Barth, B. Neises, *Tetrahedron Lett.* **1986**, *27*, 1579–1582; b) M. Kolb, B. Neises, F. Gerhart, *Liebigs Ann. Chem.* **1990**, 1–6; c) T. T. Curran, *J. Fluorine Chem.* **1995**, *74*, 107–112; d) A. G. Godfrey, D. A. Brooks, L. A. Hay, M. Peters, J. R. McCarthy, D. Mitchell, *J. Org. Chem.* **2003**, *68*, 2623–2632.
- [18] J. Blanchet, J. Baudoux, M. Amere, M.-C. Lasne, J. Rouden, *Eur. J. Org. Chem.* **2008**, 5493–5506.
- [19] a) W. Steglich, G. Höfle, *Angew. Chem. Int. Ed.* **1968**, *7*, 61; b) W. Steglich, G. Höfle, *Tetrahedron Lett.* **1970**, *11*, 4727–4730.
- [20] a) J. C. Ruble, G. C. Fu, *J. Am. Chem. Soc.* **1998**, *120*, 11532–11533; b) S. A. Shaw, P. Aleman, E. Vedejs, *J. Am. Chem. Soc.* **2003**, *125*, 13368–13369; c) E. Busto, V. Gotor-Fernández, V. Gotor, *Adv. Synth. Catal.* **2006**, *348*, 2626–2632; d) H. V. Nguyen, D. C. D. Butler, C. J. Richards, *Org. Lett.* **2006**, *8*, 769–772; e) S. A. Shaw, P. Aleman, J. Christy, J. W. Kampf, P. Va, E. Vedejs, *J. Am. Chem. Soc.* **2006**, *128*, 925–934; f) C. Joannesse, C. P. Johnston, C. Concellón, C. Simal, D. Philp, A. D. Smith, *Angew. Chem. Int. Ed.* **2009**, *48*, 8914–8918; g) D. Uraguchi, K. Koshimoto, S. Miyake, T. Ooi, *Angew. Chem. Int. Ed.* **2010**, *49*, 5567–5569; h) Z. Zhang, F. Xie, J. Jia, W. Zhang, *J. Am. Chem. Soc.* **2010**, *132*, 15939–15941; i) C. D. Campbell, C. J. Collett, J. E. Thomson, A. M. Z. Slawin, A. D. Smith, *Org. Biomol. Chem.* **2011**, *9*, 4205–4218; j) C. D. Campbell, C. Concellón, A. D. Smith, *Tetrahedron: Asymmetry* **2011**, *22*, 797–811; k) C. K. De, N. Mittal, D. Seidel, *J. Am. Chem. Soc.* **2011**, *133*, 16802–16805; l) B. Viswambharan, T. Okimura, S. Suzuki, S. Okamoto, *J. Org. Chem.* **2011**, *76*, 6678–6685; m)

- C. Joannesse, C. P. Johnston, L. C. Morrill, P. A. Woods, M. Kieffer, T. A. Nigst, H. Mayr, T. Lebl, D. Philp, R. A. Bragg, A. D. Smith, *Chem.–Eur. J.* **2012**, *18*, 2398–2408; n) H. Mandai, T. Fujiwara, K. Noda, K. Fujii, K. Mitsudo, T. Korenaga, S. Suga, *Org. Lett.* **2015**, *17*, 4436–4439.
- [21] a) F. R. Dietz, H. Gröger, *Synlett* **2008**, 663–666; b) F. R. Dietz, H. Gröger, *Synthesis* **2009**, 4208–4218.
- [22] a) C. M. Harris, H. Kopecka, T. M. Harris, *J. Am. Chem. Soc.* **1983**, *105*, 6915–6922; b) D. H. Williams, *Acc. Chem. Res.* **1984**, *17*, 364–369; c) R. Chênevert, S. Thiboutot, *Synthesis* **1989**, 444–446.
- [23] R. G. Pearson, *J. Am. Chem. Soc.* **1963**, *85*, 3533–3539.
- [24] G. R. Fulmer, A. J. M. Miller, N. H. Sherden, H. E. Gottlieb, A. Nudelman, B. M. Stoltz, J. E. Bercaw, K. I. Goldberg, *Organometallics* **2010**, *29*, 2176–2179.
- [25] P.-Y. Yang, K. Liu, M. H. Ngai, M. J. Lear, M. R. Wenk, S. Q. Yao, *J. Am. Chem. Soc.* **2010**, *132*, 656–666.
- [26] G. Naturale, M. Lamblin, C. Commandeur, F.-X. Felpin, J. Dessolin, *Eur. J. Org. Chem.* **2012**, 5774–5788.
- [27] A. Varnavas, L. Lassiani, V. Valenta, L. Mennuni, F. Makovec, D. Hadjipavlou-Litina, *Eur. J. Med. Chem.* **2005**, *40*, 563–581.
- [28] M. Weber, S. Jautze, W. Frey, R. Peters, *J. Am. Chem. Soc.* **2010**, *132*, 12222–12225.
- [29] J. S. Davies, W. A. Thomas, *J. Chem. Soc., Perkin Trans. 2* **1978**, 1157–1163.
- [30] A. D. Melhado, M. Luparia, F. D. Toste, *J. Am. Chem. Soc.* **2007**, *129*, 12638–12639.
- [31] J. Li, Y. Sha, *Molecules* **2008**, *13*, 1111–1119.
- [32] V. Denniel, P. Bauchat, B. Carboni, D. Danion, R. Danion-Bougot, *Tetrahedron Lett.* **1995**, *36*, 6875–6878.

Acknowledgement

Zurückblickend wird mir bewusst, dass unglaublich viele Menschen einen wesentlich Beitrag zum Gelingen dieser Arbeit beigetragen haben. An dieser Stelle möchte ich mich dafür bedanken.

Mein herzlichster Dank gilt Herrn Prof. Dr. Peter R. Schreiner, Ph.D. für die Aufnahme in seine Arbeitsgruppe, für seine immerwährende Unterstützung und sein Engagement. Ich möchte Herrn Schreiner auch für die mir entgegengebrachte Geduld und die vielen Möglichkeiten danken, die er mir eröffnet hat.

Ein großer Dank geht an die vielen derzeitigen und ehemaligen Mitarbeiterinnen und Mitarbeiter des Instituts, ganz besonders Dr. Erwin Röcker, Dr. Heike Hausmann, Dr. Hans P. Reisenauer, Anika und Stefan Bernhardt, Steffen Wagner, Rainer Schmidt, Edgar Reitz, Dr. Jörg Neudert, Brigitte Weinl-Boulakhrouf, Gertrud Stammer, Antonie Pospiech, Beatrix Toth, Eike Santowski, Doris Verch und Michaela Krekel, für das Messen zahlreicher Elementaranalysen, NMR- und IR-Spektren, HPLC-Reinigungen und -Trennungen, kompetente Hilfe bei allen analytischen Fragestellungen, den Nachschub an Chemikalien, die Hilfe bei technischen Problemen, die Organisation der Praktika, die Hilfe bei allen formellen Angelegenheiten, die Unterhaltungen abseits der Chemie,... Kurzum: Ohne die erwähnten Personen wäre diese Arbeit nicht möglich gewesen!

Herrn Prof. Dr. Richard Göttlich danke ich für die Bereitschaft das Zweitgutachten zu dieser Arbeit zu übernehmen.

Mein Dank gilt auch allen Kooperationspartnern für die gute Zusammenarbeit im Rahmen zahlreicher unterschiedlicher Projekte.

Des Weiteren danke ich Alexander Seitz, Fabian Metz, Stefanie Dobitz, Lindsay Coby, Stefanie Pleik, Florian Lotz, Mahjabeen Ahmad und Weike S. Newe für die helfenden Hände und den Beitrag, den sie zu dieser Arbeit geleistet haben.

Ein besonderer Dank geht an alle Kolleginnen und Kollegen, die ich in den letzten Jahren kennen und schätzen gelernt habe. Ganz speziell möchte ich mich bei Dr. Christian E. Müller, Dr. Radim Hrdina, Dr. Dennis Gerbig (danke für das Versorgen mit Kaffee an so einigem Samstagmorgen), Dr. Christine Hofmann, Dr. Katharina M. Lippert, Dr. Daniela Zell, Dr. Mareike M. Machuy, Sören M. M. Schuler, Dominik Niedek, Alexander Seitz, Jan-Philipp Berndt, Christian Eschmann, Jan M. Schümann, Cesare Sevarino und Jan Philipp Wagner bedanken. Ich danke euch für die schöne Zeit und die zahlreichen anregenden Gespräche und

Diskussionen, die nicht selten zu neuen Ideen und Erkenntnissen geführt haben. Ein großes Dankeschön an den ganzen großen Rest der Arbeits-gruppe Schreiner für das angenehme Arbeitsklima, das Aushelfen mit Chemikalien und die netten Gespräche zwischendurch.

Ich danke meiner Familie, ganz besonders meinen Eltern und meinem Bruder Matthäus, und meinen Freunden für die fortwährende Unterstützung und dafür, dass sie immer an mich geglaubt haben.

Das Beste kommt bekanntlich zum Schluss. Aus diesem Grund möchte ich abschließend meiner wunderbaren Frau Lena und unseren großartigen Kindern Nele, Carlotta und Janne danken. Gerade in den letzten Wochen der Fertigstellung dieser Arbeit musste ich mir von meinem zweieinhalb Jahre alten Sohn häufiger die Frage „Papa, wann bist du endlich fertig mit deiner Doktorarbeit?“ anhören. Jetzt! Und das habe ich zu einem großen Teil auch euch zu verdanken. Ich danke euch für euer Vertrauen, dass ihr jederzeit in mich gesetzt habt, für die Geduld, die ihr aufbringen musstet und das Verständnis, dass ich so oft keine Zeit für euch hatte. Ich danke euch für die liebevolle Unterstützung auf diesem langen Weg. Ich liebe euch!